GEORGIA INSTITUTE OF TECHNOLOGY — OFFICE OF CONTRACT ADMINISTRATION

PROJECT ADMINISTRATION DATA SHEET

[x] ORIGINAL [ ] REVISION NO. _____

Project No. E-16-612 DATE 10/23/81

Project Director: G. A. Pierce School/Lab Aerospace Engineering

Sponsor: NASA - Langley Research Center; Hampton, VA

Type Agreement: Contract No. NAS1 - 16817

Award Period: From 9/21/81 To 8/5/82 (Performance) _____ (Reports)

Sponsor Amount: $20,331 Contracted through:

Cost Sharing: $5,122 (E-16-356) GTRI/GIT

Title: Helicopter Rotor Loads Using a Matched Asymptotic Expansion Technique Study

ADMINISTRATIVE DATA

OCA Contact Leamon R. Scott

1) Sponsor Technical Contact:

Capt. John Berry
NASA Langley Research Center
Hampton, VA 23665

2) Sponsor Admin/Contractual Matters:

Ms. Sharon De Berry
Mail Stop 126
NASA - Langley Research Center
Hampton, VA 23665
804/827-2002

Defense Priority Rating: N/A

Security Classification: N/A

RESTRICTIONS

See Attached Government Supplemental Information Sheet for Additional Requirements.

Travel: Foreign travel must have prior approval – Contact OCA in each case. Domestic travel requires sponsor approval where total will exceed greater of $500 or 125% of approved proposal budget category.

Equipment: Title vests with none proposed

COMMENTS:

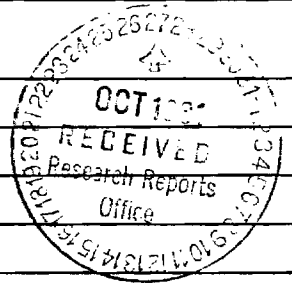

COPIES TO:

Administrative Coordinator	Research Security Services	EES Public Relations (2)
Research Property Management	Reports Coordinator (OCA) ✓	Computer Input
Accounting	Legal Services (OCA)	Project File
Procurement/EES Supply Services	Library	Other

FORM OCA 4:781

GEORGIA INSTITUTE OF TECHNOLOGY OFFICE OF CONTRACT ADMINISTRATION

SPONSORED PROJECT TERMINATION SHEET

Date 6/29/83

Project Title: Helicopter Rotor Loads Using a Matched Asymptotic Expansion Technique Study

Project No: E-16-612

Project Director: G. A. Pierce

Sponsor: NASA - Langley Research Center; Hampton, VA

Effective Termination Date: 12/31/82

Clearance of Accounting Charges: --

Grant/Contract Closeout Actions Remaining:

- [X] Final Invoice and Closing Documents
- [X] Final Fiscal Report (FCTR Form 272)
- [X] Final Report of Inventions
- [X] Govt. Property Inventory & Related Certificate
- [ ] Classified Material Certificate
- [ ] Other _____

Assigned to: Aerospace Engineering (School/Laboratory)

COPIES TO:

Administrative Coordinator	Research Security Services	EES Public Relations (2)
Research Property Management	Reports Coordinator (OCA) ✓	Computer Input
Accounting	Legal Services (OCA)	Project File
Procurement/EES Supply Services	Library	Other _____

FORM OCA 10-78

Technical Progress Report
NASA Contract NAS1-16817
for the Period September 21-October 31, 1981

This program is intended to study the possible simplification of the computational scheme for an asymptotic method (Ref. 1) of calculating the unsteady, three-dimensional airloads on a helicopter rotor blade. The original computational scheme was used to generate numerical results (Ref. 2) but the computation time was found to be large for conditions of low forward speed and large number of blades. The unknown doublet strength distribution on the blade is determined, as a continuous function of blade spanwise location and azimuth, by satisfying the normal velocity boundary condition which requires integration of the normal gradient of the blade pressure field. This function is too complicated to be integrated analytically, due to a) the continuous variation of the unknown strength and b) the helical motion of the freesteam fluid particle with respect to the blade. Consequently, numerical integration must be used and this leads to significant computational times. The same is true of a vortex lifting-line model with a continuous wake representation. However, such a model can be approximated by one with a finite number of discrete wake and bound vortex elements, which results in considerable reduction of computation. It is possible to consider similar simplications for the scheme of Ref. 1.

Work Accomplished during the Report Period

The following simplifications of the computational model are considered: a) the blade radial and azimuth intervals are broken up into a finite number of segments and the continuous variation of the unknown doublet strength distribution is replaced by a piecewise constant or piecewise linear variation over each segment b) the helical trajectory of the freestream fluid particle is approximated by a succession of straight line segments.

The blade pressure field consists of the sum of a far field, a near field and a common part. The development of Ref. 1 derives the far field in prolate spheroidal coordinates and the near field in plane elliptic coordinates. In this form, the above simplifications are not of any help. Hence the expressions are re-derived, in Cartesian coordinates with the far field as the spanwise integral of a three-dimensional doublet distribution and the near field as the chordwise integral of a two-dimensional doublet distribution. In this form, the above simplifications can be introduced and the entire integration for the velocity induced by the blade pressure field reduces to a double summation over radial and azimuth segments. Each element of the summation is an integral that can be expressed in terms of more elementary integrals which can be found in any table of indefinite integrals (eg. Ref. 3). These expressions have been derived for both piecewise constant and piecewise linear variations assumed over each segment.

The extent of approximation involved in replacing the continuous doublet strenght distibution by piecewise constant or linear variations can be tested by some simple calculations.

a) For the chordwise integral, the problem considered is that of a two-dimensional airfoil in steady flow, with a fluid particle passing at various vertical distances parallel to the chord. The vertical velocity induced on the particle by the two dimensional pressure field is calculated with both the exact chordwise pressure distribution (using numerical integration) and the piecewise constant approximation. It is found that very nearly identical numbers are obtained, even with just 5 chordwise segments.

b) For the spanwise integral, the model problem is that of a finite wing with a spanwise doublet distribution of the form $y^2 (1-y^2)^{1/2}$ (y is the spanwise coordinate) and a fluid particle travelling at various vertical distances from the wing at various spanwise locations. The velocity induced is calculated using the exact spanwise linear approximations. It is found that, with 6 spanwise segments, the approximations are quite close to the exact result for vertical distances down to about 3% of the wing span. For distances smaller than this, there are significant deviations but in such cases the basic linear theory is itself expected to be invalid.

Work to be Accomplished During the Next Report Period

The computer program developed in Ref. 2 will be re-written to incoporate the induced velocity expressions derived using the above approximations. The new program will be checked out and applied to selected cases for comparison.

References

1. Van Holten, Th., "The Computaion of Aerodynamic Loads on Helicopter Blades in Forward Flight, Using the Method of the Acceleration Potential," Delft Institute of Technology, Report VTH-189, March 1975.
2. Pierce, G. A. and Vaidyanathan, A. R. "Helicopter Rotor Loads Using a Matched Asymptotic Expansion Technique", Prepared for NASA Langley Research Center under Contract NAS1-16222, Georgia Institute of Technology, 1981.
3. Gradshteyn, I. S. and Ryzhik, I. M., "Table of Integrals, Series and Products," Academic Press, 1980.

Technical Progress Report
NASA Contract NAS1 - 16817
for the Period November 1 - November 30, 1981

This program is intended to study the possible simplification of the computational scheme for an asymptotic method (Ref. 1) of calculating the unsteady airloads on a helicopter rotor blade in forward flight.

As described in the last progress report, the blade doublet strength distribution is approximated by a piecewise constant or piecewise linear variation and the helical trajectory is approximated by a series of straight line segments. These simplifications eliminate the need for numerical integration. Expressions have been derived for the velocity induced by the blade pressure field, using the above approximations.

Work Accomplished during the Report Period

The original computational scheme described by Van Holten in Ref. 1 was programmed as part of the work undertaken in Ref. 2. This program has been re-written with a scheme using the expressions derived for a piecewise constant variation of the doublet strength distribution. In the basic asymptotic method, the sum of the far field, near field and common part contributions to the induced velocity is required to vary smoothly over the flow field. This is an important feature of the method and must be verified for the approximate analytical expressions derived here. The integrated expressions have been studied in the vicinity of the blade, with the singular and non-singular contributions separated out. It has been verified that the singular portions of the far field and common part contributions cancel out exactly, as they should. The correctness of the analytical integration has also been confirmed by comparison with numerical integration of the same integrands.

The blade span is divided into 5 segments over each of which the doublet strength is assumed to have a constant value. The variation in the azimuth direction also occurs in convenient steps, with a constant value over each step. The program has been checked out and applied to the conditions corresponding to Case 1 of Ref. 2 (two-bladed, teetering, model rotor of aspect ratio 5.4, tested in a wind tunnel). The results are compared with the

measured values for the azimuth variation of the total blade lift as well as with the results from the original computational scheme (Ref. 2). The present program was used with azimuth steps of 0.5 (about 28.6^{o}) and 0.25.

At an advance ratio (μ) of 0.29, the results of the present program are close to the original computational results for both azimuth steps, with the results for $\Delta\Psi = 0.25$ being closer than those for 0.5, which is to be expected. However, for lower advance ratios (0.15 and 0.08), the results for $\Delta\Psi = 0.5$ show a fair amount of deviation from the original computation whereas the results for $\Delta\Psi = 0.25$ remain close. It is anticipated that, as the azimuth step size is decreased, the results of the present program will approach the original results, the penalty being increased computation time. For example, in the above computation for $\mu = 0.29$, the present program with $\Delta\Psi = 0.5$ required about 28 seconds to execute on the CDC Cyber 75 computer, while the computation with $\Delta\Psi = 0.25$ required about 50 seconds and the original computation about 200 seconds. It is possible that better results may be obtained with an improved representation of the azimuth variation, expecially in the vicinity of the blade, since the near field behavior in this region is important. One way of achieving this is to replace the piecewise constant variation with a piecewise linear variation.

Work to be Accomplished during the next Report Period

The computer program will be applied to conditions corresponding to Cases 2 and 3 of Ref. 2 and the results will be discussed for the total lift distribution as well as the spanwise lift variation. The expressions derived for a piecewise linear variation will be checked out and a new program developed to incorporate these expressions.

References

1. Van Holten, Th., "The Computation of Aerodynamic Loads on Helicopter Blades in Forward Flight, Using the Method of the Acceleration Potential," Delft Institute of Technology, Netherlands, Report VTH-189, March 1975.

2. Pierce, G. A. and Vaidyanathan, A. R., "Helicopter Rotor Loads Using a Matched Asymptotic Expansion Technique," Prepared for NASA Langley Research Center under Contract NAS1-16222, Georgia Institute of Technology, 1981.

LIBRARY DOES NOT HAVE

Technical Progress Report, December 1 - December 31, 1981

Technical Progress Report
NASA Contract NAS1-16817
for the Period January 1 - January 31, 1982

This program is intended to study the possibility of simplifying the computational scheme for an asymptotic method (Ref. 1) of calculating the unsteady airloads on a helicopter rotor blade in forward flight.

Work Accomplished during the Report Period

As described in previous progress reports, a scheme with a piecewise constant representation for the dipole strength has been set up, incorporating a routine to locate the points of closest approach to a blade along the particle trajectory so that shorter azimuth intervals can be used around these locations. This program has now also been applied to Case 2 of Ref. 2 (a four-bladed, articulated full-scale rotor). The results are somewhat different from the results obtained for Case 1 where the simplified scheme yielded results close to the original computations. For μ = 0.29 (μ is the forward speed ratio) of Case 2, the piecewise constant scheme deviates from the original results on the advancing blade region of the disk. For μ = 0.13, the original results show considerable oscillations which are not seen in the results of the simplified scheme. These discrepancies are perhaps to be expected since the larger number of blades in this case leads to flows with stronger blade/wake interactions. It appears that agreement between the original computations and the piecewise constant representation will be worse in flight conditions involving significant interaction effects.

An abstract of the work performed under Contract NAS1-16222 (Ref. 2) has been accepted for presentation at the Aerodynamics Session of the 38th Annual AHS Forum to be held in May 1982. The material for the paper has been prepared and contains mainly a condensation of the results and conclusions of Ref. 2. In addition, the simplifying computational scheme (the subject of the current contract) has been discussed together with results for Cases 1 and 2 with the constant representation.

Work to be Accomplished during the next Report Period

The simplified scheme will be used with a piecewise linear representation to study possible improvement over the piecewise constant representation, expecially under the conditions of Case 2.

References

1. Van Holten, Th., "The Computation of the Aerodynamic Loads on Helicopter Blades in Forward Flight, Using the Method of the Acceleration Potential", Delft Institute of Technology, Netherlands, Report VTH-189, March 1975.
2. Pierce, G.A. and Vaidyanathan, A.R., "Helicopter Rotor Loads Using a Matched Asymptotic Expansion Technique", Prepared for NASA Langley Research Center under Contract NAS1-16222, Georgia Institute of Technology, 1981.

E 16-612

Technical Progress Report
NASA Contract NAS1-16817
for the Period February 1 - February 28, 1982

This program is intended to study the possibility of simplifying the computational scheme for an asymptotic method (Ref. 1) of calculating the unsteady airloads on a helicopter rotor blade in forward flight.

Work Accomplished during the Report Period

It was stated in the last progress report that the simplified scheme would be tested with a piecewise linear representation of the unknown doublet strength along the blade span. This approach has been found to involve certain problems. The piecewise linear representation can be set up in basically two ways. (1) The blade span is divided into n segments and the functional values at the ends of the segments are considered unknown, with the variation being linear between successive values. Since the strength is required to go to zero at the root and tip of the blade, this leaves (n-1) unknowns for n segments and an equal number of equations can be generated only by locating the collocation points at the same (n-1) points as the unknowns. However, the location of a collocation point at the discontinuous joint between two segments leads to non-cancellation of the far field and common part expressions close to the blade, which is a violation of a basic feature of the asymptotic method. (2) Alternatively, the value at the center of each segment can be considered unknown, so that there are as many unknowns as segments and an equal number of equations obtained with a collocation point at the center of each segment. However, in this case, it is not possible in general to achieve zero values at both the root and the tip. If the tip value is made zero, for instance, the value at the root is determined by the unknowns and cannot be fixed in advance. In spite of this, such a representation was used in the computational scheme. However, acceptable results were not obtained with this program. At the present time, it has not been established whether these discrepancies are due to programming technique, numerical instabilities or the actual representation.

Work to be Accomplished during the next Report Period

It appears that a second-degree curve can be used to approximate the strength variation in each segment of the span. This representation will be studied and incorporated into the computational scheme if possible. The linear scheme described above will be studied in greater detail in order to ascertain the reasons for the bad results from the program.

References

1. Van Holten, Th., "The Computation of the Aerodynamic Loads on Hellcopter Blades in Forward Flight, Using the Method of the Acceleration Potential", Delft Institute of Technology, Netherlands, Report VTH-189, March 1975.

Technical Progress Report
NASA Contract NAS1-16817
for the Period March 1 - March 31, 1982

This program is intended to study the possibility of simplifying the computational scheme for an asymptotic method (Ref. 1) of calculating the unsteady airloads on a helicopter rotor blade in forward flight.

Work Accomplished during the Report Period

It has been found possible to approximate the spanwise blade doublet strength distribution by a variation made up of piecewise curves of second degree. The expressions for the induced velocity due to the blade pressure field with such a variation have been obtained and verified to ensure that the contributions from the far field and common part cancel out properly in the vicinity of the blade. The piecewise representation is set up as follows, for n segments along the span. Each second degree curve requires three constants, so that there are (3 n) unknowns. Each curve is required to pass through the doublet strength value at its mid-point. At the boundary between two segments, the curves are required to have equal value and equal slope. In addition, the end segments are required to go to zero at the root and the tip. This yields a total of (3 n) equations to solve for the (3 n) unknowns and the resulting curve segments are then known in terms of the doublet strength at their mid-points.

The program has been adapted to use the new expressions and has been run for Cases 1 and 2 (two-bladed model rotor and four-bladed full-scale rotor, respectively). The results have been compared with the results from the piecewise constant representation and the original computational scheme. For all three forward speeds of Case 1, the total blade lift variations for the second-degree representation lie close to the original results (as also the results from the piecewise constant representation). For Case 2, there is a slight improvement over the piecewise constant results. The spanwise lift distributions from the piecewise constant representation do not compare well with the original results in the blade tip region. This drawback is improved with the second degree representation, which is to be expected since the second degree curve provides a better approximation to the rapid fall-off near the tip.

For comparison, the computation times for the original asymptotic method, the piecewise constant representation and the piecewise second-degree representation are given below for a typical case, viz. the two-bladed rotors of Case 1 (Ref. 2), at a forward speed ratio of 0.29. The programs were executed on the Cyber 760 system at the Georgia Tech Computing Center, but the execution times supplied are all normalized to the old CDC 6400 computational rate.

Original computational scheme	350 secs.
Piecewise constant representation	35 secs.
Piecewise second-degree repesentation	65 secs.

Work to be Accomplished during the Next Report Period

The programs with piecewise constant and piecewise second-degree representations will be applied to Case 3 (Ref. 2), viz. the four-bladed rotor of Case 2 tested in a wind tunnel at higher forward speeds. The programs will also be re-written and documented to conform to the Computer Programming and Documentation Specifications (Exhibit B of this contract).

References

1. Van Holten, Th., "The Computation of the Aerodynamic Loads on Helicopter Rotor Blades in Forward Flight, Using the Method of the Accleration Potential," Delft Institute of Technology, Netherlands, Report VTH-189, March 1975.

2. Pierce, G. Alvin and Vaidyanathan, Anand R., "Helicopter Rotor Loads Using a Matched Asymptotic Expansion Technique", NASA Contractor Report 165742, May 1981.

Technical Progress Report
NASA Contract NAS1-16817
for the Period April 1 - April 30, 1982

This program is intended to study the possibility of simplifying the computational scheme for an asymptotic method (Ref. 1) of calculating the unsteady airloads on a helicopter rotor blade in forward flight.

Work Accomplished during the Report Period

At this stage, two schemes are available for use in the simplified asymptotic method, based on piecewise constant and piecewise quadratic approximations of the spanwise dipole strength variation along the blade. Since the program logic for implementing these schemes is similar, differing mainly in the form of the expressions used for integrating the pressure gradient, the two programs have been combined into one that can be selected to compute according to either scheme. The numerical output from this program has been verified by comparison with the output from the separate programs.

Results have been obtained for Case 3 (Ref. 2). As with the computation for the previous cases, the break-up of the helical trajectory into straight line segments was done with a normal spacing of 30° and a reduced spacing of 7.5°, the latter being used whenever the particle trajectory was judged to be close to a blade (within a distance of one-half of the blade radius). In general, for all 3 forward speeds ($\mu = 0.29, 0.39, 0.45$), both schemes resulted in an overestimation of the blade lift around the 0° azimuth position (downwind) and an underestimation around the 180° position (upwind). As noted in Ref. 2, this could be an effect of the radial flow (along the blade span) component that is present in forward flight. This effect can be expected to be significant around the upwind and downwind positions and to increase with increasing forward speed. Other than this, the piecewise quadratic scheme showed acceptable agreement for all 3 forward speeds. However, the piecewise constant scheme showed strong deviations on the advancing portion of the rotor disk, for $\mu = 0.29$ and 0.39. When the computation was repeated with a uniform azimuth spacing of 6°, some improvement was noted in the above cases but the results on the advancing side continued to compare unfavorably with the piecewise quadratic scheme. This may be an indication that the piecewise constant scheme is not suitable for cases involving significant blade/wake interaction.

Work to be Accomplished during the next Report Period

As with the two cases mentioned above, the other cases that have been computed will also be tested for sensitivity to the azimuth spacing used. The computer programs (the simplified schemes used above and the original computational scheme of Van Holten used in Ref. 2) will be prepared for validation. The numerical results obtained so far will be collected and prepared for presentation in the final report.

References

1. Van Holten, Th., "The Computation of the Aerodynamic Loads on Helicopter Rotor Blades in Forward Flight, using the Method of the Acceleration Potential", Delft Institute of Technology, Netherlands, Report VTH-189, March 1975.
2. Pierce, G. Alvin and Vaidyanathan, Anand R., "Helicopter Rotor Loads using a Matched Asymptotic Expansion Technique", NASA CR 165742, May 1981.

HELICOPTER ROTOR LOADS USING DISCRETIZED MATCHED ASYMPTOTIC EXPANSIONS

By

G. Alvin Pierce

and

Anand R. Vaidyanathan

Prepared by

GEORGIA INSTITUTE OF TECHNOLOGY
SCHOOL OF AEROSPACE ENGINEERING
Atlanta, Georgia 30332

Prepared for

NATIONAL AERONAUTICS AND SPACE ADMINISTRATION
Langley Research Center
Contract NAS1-16817

CONTENTS

	Page
SUMMARY	1
INTRODUCTION	1
SYMBOLS	2
DISCRETIZED ASYMPTOTIC REPRESENTATION	4
DISCUSSION OF RESULTS	6
CONCLUDING REMARKS	10
APPENDIX A Piecewise Continuous Representations	12
APPENDIX B Trajectory Approximation and List of Integrals	15
APPENDIX C Integration of Pressure Field	25
APPENDIX D Evaluation of Chordwise and Spanwise Approximations	37
APPENDIX E Final Equations and Output Quantities	43
REFERENCES	49
FIGURES	50

SUMMARY

This investigation is intended to improve the numerical practicality of a matched asymptotic expansion approach for the computation of unsteady three-dimensional airloads on a helicopter rotor. The original method as suggested by Van Holten has previously been evaluated and proven to be a comprehensive and accurate analysis for flight conditions conducive to linear flow phenomena. This effort to decrease the computational requirements of the original analysis utilizes a discretized representation of the doublet strength distribution and helical streamlines. The continuous variation of the doublet strength has been approximated by piecewise constant or piecewise quadratic distributions, and the helical trajectory of a fluid particle has been approximated by connected straight line segments. As a direct result of these simplified representations the computational time required for the execution of a typical flight condition has been reduced by an order of magnitude with respect to the requirements of the original analysis. Airloads which have been computed using the discretized method for a two-bladed model rotor and a full-scale four-bladed rotor are in close agreement with measured results and airloads from the original asymptotic analysis. For conditions characterized by significant rotor/wake interaction the piecewise constant representation requires a reduced azimuth spacing to maintain acceptable accuracy.

INTRODUCTION

The problem of estimating airloads on helicopter rotor blades can be approached by a variety of approximate methods. One such approach, put forward by Van Holten (refs. 1-4), uses an acceleration potential description of the flow field and a matched asymptotic expansion technique. Under the assumption of incompressible potential flow the unsteady three-dimensional airloads on a rotor blade in forward flight are calculated to a consistent order of approximation in terms of the aspect ratio.

A study has been conducted (ref. 5) to examine the theoretical basis and computational feasibility of the method, and to evaluate its performance and range of validity by numerical comparison with experiment and other approximate methods. The study concluded that, within the restrictions of linear theory (i.e., small disturbances), the Van Holten approach does lead to a valid description of the rotor flow field and a systematic determination of the airloads on the rotor blade. It was also found for flight conditions involving significant blade/wake interaction effects, the agreement between computation and measurement is poorer than in other cases.

The analysis in Van Holten's approach leads to an integral equation for the blade doublet strength distribution (eq. (8), ref. 5). This is solved using a collocation technique, which consists of assuming the unknown function to be made up of a combination of suitable spanwise modes and azimuthal harmonics, and satisfying the integral equation at an equal number of points distributed over the rotor disk. The result is a set of linear, simultaneous algebraic equations. However, setting up the equation at any collocation point requires integration with respect to azimuth of the individual assumed mode combinations. This numerical integration makes up the bulk of the total computation required for the solution. Under conditions of low forward speed and low inflow (when a larger azimuth range must be covered with a finer integration step) and/or a larger number of blades, the computation time is significantly increased.

As an example, for a two-bladed rotor at an advance ratio of 0.3, the computer program takes about 250 seconds to execute on a CDC 6400 computer. For other conditions, the time would vary approximately in direct proportion to the number of blades and in inverse proportion to the forward speed (advance ratio). In addition, when interaction effects are judged to be significant (possible even at moderate to high forward speeds), a smaller integration step will have to be used.

It would therefore be desirable to seek a simplified computational scheme for the basic asymptotic approach that would lead to significantly lower computation time without sacrificing any of the essential features of the asymptotic method. One possibility is to consider the analogous situation in the vortex representation of rotor wakes. In the vortex approach, the continuously varying bound circulation of the induced velocity due to such a wake would require double integration over the wake surface, which can be time-consuming. In practice, this problem is often overcome by assuming that the variation of the blade bound circulation over the span and the azimuth takes place in discrete, finite steps. This results in a wake of discrete trailing and shed vortex elements. Since the velocity induced by a straight vortex element can be analytically expressed, the induced velocity due to the entire wake can be written as a summation of analytical expressions representing the contribution of individual trailing and shed vortex elements. This results in considerable reduction of computational time over the exact numerical integration.

It appears that a similar simplification could be achieved by approximating the continuous variation of the doublet strength distribution in the asymptotic approach. It is the purpose of the current study to develop a discretized representation for the asymptotic method and compare its performance with the original computational scheme and its results with measured data for the flight conditions considered in reference 5. This report describes the details of the simplified scheme and discusses the computational results. Detailed analytical expressions are presented as Appendices.

SYMBOLS

A	aspect ratio
a_o	coning angle
a_1, b_1	blade flapping coefficients
B	number of blades
b, c	semi-chord and chord, repsectively
c_{1j}, c_{2j}, c_{3j}	coefficient of piecewise quadratic representation (eq. (A1))
d	distance between fluid particle and collocation point
d_0, d_1, d_2	coefficients of quadratic expression for d^2 in terms of θ
d_n	distance between fluid particle and point on the chord at the same spanwise location
d_{n0}, d_{n1}, d_{n2}	coefficients of quadratic expression for d_n^2 in terms of θ
F_2, F_3	terms appearing in the regualr part of the near field solution (eq. (E 5))

$G_j^o, G_{jn}^c, G_{jn}^s$	harmonic coefficients in the Fourier expansion of g in terms of Ψ_b (eq. (E 1))
g	function representing the doublet strength distribution along the blade, and the basic unknown in the problem
g_j	value of g at the beginning of the j^{th} spanwise segment
I_i^c	i^{th} integral expression for the common part, Appendix B
I_i^f	i^{th} integral expression for the far field, Appendix B
I_i^n	i^{th} integral expression for the near field, Appendix B
L	total lift on one blade (eq. (E 10))
ℓ	lift per unit span, sectional lift, (eq. (E 7))
M	moment of lift distribtuion about the rotor hub (eq. (E 11))
m	sectional pitching moment about quarter-chord, positive nose-down (eq. (E 8))
p	perturbation pressure
R_0, R_1	root and tip radius of blade, respectively
R_i, R_s	coefficients of linear expression for r_b in terms of θ (eq. (B 2))
r	radial distance between fluid particle and collocation point, $\sqrt{x_b^2 + y_b^2}$
r_b	spanwise location of fluid particle
r_{bo}	spanwise location of collocation point
r_0, r_1, r_2	coefficients of quadratic expression for r^2 in terms of θ
r_j	midpoint of j^{th} spanwise segment
s	blade spanwise coordinate
s_j	spanwise location of the beginning of the j^{th} spanwise segment
Δs_j	length of j^{th} spanwise segment
U_T	local effective freestream speed
v_{io}	simple momentum induced velocity
w	induced velocity component in the z direction
Δw	incremental contribution to w
x,y,z x_b, y_b, z_b	rotor coordinate systems (fig. 1)

x_{cp}	chordwise location of center of pressure (eq. (E 9))
X_i, X_s	coefficients of linear expression for x_b in terms of θ (eq. (B 2))
Y_i, Y_s	coefficients of linear expression for y_b in terms of θ (eq. (B 2))
γ	blade inertia coefficient for flapping (Lock number)
ϵ	linear blade twist, root pitch angle-tip pitch angle
θ	azimuth position with respect to reference blade, ($\Psi_b - \Psi_{bo}$)
θ_o	collective pitch angle at blade root
λ	nondimensional rotor inflow, $\mu\alpha_r + v_{io}$
μ	nondimensional rotor forward speed
ξ	R_0, R_1
ρ	air density
ϕ , η	plane elliptic coordinates
χ	meridional angle in cylindrical coordinates
Ψ_b	azimuth position with respect to downwind reference line
Ψ_{bo}	azimuth position of collocation point
$\Delta \Psi_j$	azimuth separation of j^{th} blade from reference blade
Ω	rotor angular velocity

DISCRETIZED ASYMPTOTIC REPRESENTATION

The essential features of the asymptotic approach are retained in the discretized representation, i.e., the blade pressure field is obtained in composite form as the sum of far field, near field and common part expressions in such a way that the composite field reduces to the near and far field solutions in the near and far field regions, respectively. In view of the approximations being considered, it is not known if it would be consistent to retain the terms of $O(1/A^2)$ that are present in Van Holten's analysis (ref. 1). For the sake of simplicity in computation these terms are dropped in the present study,so that the discretized representation is of $O(1/A)$, comparable to standard lifting-line formulations.

The approximations to be introduced are:

(1) The continuous variation of the unknown blade doublet strength distribution over the range of blade span and azimuth is replaced by simple, piecewise continuous functions over suitable subintervals of span and azimuth.

(2) The helical trajectory of a freestream fluid particle relative to the blade is replaced by a series of connected straight line segments.

Over the azimuth, the doublet strength variation is assumed to be piecewise constant, i.e., its value is constant over each subinterval of azimuth. Over the span, it is approximated by a piecewise constant or a piecewise quadratic variation, the latter providing a more accurate spanwise representation at the cost of more complicated algebra. Appendix A describes the manner in which these representations are

formulated, while typical representations are illustrated in figures 2(a) and 2(b).

The basic problem is the calculation of the vertical velocity induced on the blade by its pressure field, as given by the relation

$$w = -\int_{-\infty}^{\Psi_{bo}} \frac{\partial p}{\partial y_b} \, d\Psi_b \qquad (1)$$

The rotor coordinate systems are shown in figure 1 and Ψ_{bo} is the azimuth position of the reference blade. The blade pressure field is written in composite form as

$$p = p_{far} + p_{near} - p_{common}$$

By appropriate construction and matching (ref. 1), all three components can be expressed in terms of the doublet strength distribution along the lifting line.

In Van Holten's analysis, the far pressure field is the field of a dipole line along the quarter-chord location and is expressed as a series of associated Legendre functions in terms of prolate spheroidal coordinates. The near pressure field is the local two-dimensional field of the section and is expressed in plane elliptic coordinates. The common part corresponds to the behavior of the far field solution in the near field or, equivalently, that of the near field solution in the far field. With the form of the pressure field established, the induced velocity is calculated by numerical integration of the composite pressure gradient, for which purpose the above expressions are convenient. In fact, one of the merits of Van Holten's approach is that the composite pressure field is given by a direct expression free of integrals, so that the induced velocity calculation requires only one numerical integration.

However, these expressions are not convenient for the purpose of applying the proposed approximations. To O(1/A), the far field is the field of a dipole line along the blade midchord location, and can be written as the spanwise integral of a distribution of three-dimensional doublets. If the approximations described above are introduced, it is found that the calculation of the induced velocity due to the far field reduces to a double summation (over spanwise and azimuthal segments) of fairly simple integrals that can be analytically evaluated. Likewise, the near field is written as the integral, over the chord, of a two-dimensional doublet distribution, of strength proportional to the surface pressure differential. The chord is divided into a suitable number of segments over each of which the pressure differential is assumed constant, at its average value on that segment. With this simplification, the induced velocity due to the near field also becomes a double summation (over chordwise and azimuthal segments) of analytical expressions. The contribution of the common part, which is the field of a single two-dimensional dipole, presents no problems. The complete details of the various steps pertaining to the above calculations are presented in Appendices B and C. Appendix B describes the result of approximating the trajectory and also presents a list of integral expressions to be used for the induced velocity calculation. Appendix C derives the summation expressions for the induced velocity due to the far field, common part, and near field, for both the piecewise constant and the piecewise quadratic representation of the doublet strength variation along the span. Appendix C also demonstrates that the expressions derived for the far field and the common part correctly cancel in the vicinity of the blade, thus verifying their asymptotic character.

In summary, the effect of the discretized representation on the problem is to reduce the induced velocity integration of equation (1) to a summation of analytical

expressions. The normal velocity boundary condition is then applied by setting this induced velocity equal to the normal velocity on the blade surface due to blade motion. The form of this equation is given in Appendix E (eq. (E 2)). The unknowns to be solved for are the discrete values of the doublet strength at the spanwise segment midpoints, at discrete azimuth locations. However, for final presentation as output, the discrete variation with azimuth would have to be fitted by an interpolation curve. This is accomplished by substituting into equation (E 2), for the azimuth variation of each midpoint value, a harmonic interpolation formula given by (E 3). It must be noted that this does not imply a continuous azimuthal variation in the induced velocity calculation, since the doublet strength is still held constant over each azimuth segment. The advantage of the substitution is that the interpolation coefficients are obtained directly and available for calculation of output data at desired azimuth locations. Expressions for the various quantities calculated for presentation as output are given in Appendix E.

Examination of equation (E 2) shows that the near field induced velocity contains a contribution from the regular solution, proportional to the blade motion parameters. If these parameters are considered known, this contribution should be taken together with the blade normal velocity term. However, if any or all of the blade motion parameters (collective pitch, coning angle, cyclic pitch coefficients) are considered unknown, additional equations must be generated to solve for them. This can be done by using the following conditions:

(1) Azimuth average of the total lift due to all blades should equal the known rotor thrust.

(2) Flapping moment equilibrium should exist about the rotor hub.

If only first harmonic flapping is considered, the second condition yields three equations (zeroth harmonic, first harmonic cosine and first harmonic sine components). These additional equations are also listed in Appendix E, for the piecewise constant and piecewise quadratic representations.

DISCUSSION OF RESULTS

The discretized representations which have been incorporated in the analysis have been numerically evaluated to ascertain their potential accuracy. All analytical details of this evaluation are presented in Appendix D. Figure 2 illustrates the piecewise constant and quadratic representations of the spanwise distribution of doublet strength for a typical condition.

For the near field chordwise approximation, an airfoil with a steady two-dimensional pressure distribution is considered. The induced vleocity of a fluid particle travelling parallel to the chord is calculated for various vertical distances from the airfoil. The calculation is performed using both the exact solution and the approximation. The results are tabulated in Appendix D (table D1) and plotted in figure 3. It can be seen that the approximations with three segments and five segments across the chord are acceptably close to the exact solution, even at very small vertical distances. This simple example shows that, as far as the induced velocity calculation is concerned, even a relatively crude representation of the surface pressure distribution is sufficient.

For the spanwise approximations of the far field solution, a finite wing is considered with a spanwise distribution of a form which is typical of a rotor blade distribution. The induced velocity due to this distribution is calculated for a fluid particle travelling parallel to the chord, at various spanwise locations and vertical distances. The calculation is performed using the exact solution as well as the piecewise constant and piecewise quadratic approximations with three and five

spanwise segments. The results are tabulated in Appendix D (tables D2 and D3) and plotted in figure 4. With the three segment model, it can be seen that both approximations deviate from the exact solution when close to the wing, the deviations being more marked near the loaded tip and generally greater for the piecewise constant representation. With five segments, the piecewise quadratic representation is nearly identical to the exact solution while the piecewise constant results still show significant deviation very close to the wing. It may be noted that the exact and approximate results tend to merge with increasing distance from the wing, as is to be expected. It may also be noted that the results for different spanwise locations tend to merge with increasing vertical distance.

Airload computations have been carried out for the same experimental cases considered in reference 5, viz, (1) a two-bladed teetering model rotor at forward speed/tip speed ratios (μ) of 0.08, 0.15, 0.29 (ref. 6), (2) a four-bladed articulated full-scale rotor tested in flight, at μ =0.06, 0.13, 0.29 (ref. 7), and (3) the same four-bladed rotor tested in a wind tunnel at μ = 0.29, 0.39, 0.45 (ref. 8). The geometric and flight conditions are listed in table 1, which is reproduced from reference 5. The measured results are compared with computations using the piecewise constant (p.c.) and piecewise quadratic (p.q.) representations, as well as Van Holten's computational scheme. Before proceeding with a discussion of these comparisons, some comments regarding the computations are in order. In the original scheme, the numerical integration is carried out with a 5-point Gauss-Chebyschev rule over a suitable subinterval of azimuth, to be properly chosen for accurate computation. In the discretized representation, there is no numerical integration but a choice has to be made with regard to a suitable azimuth subinterval over which the trajectory is straightened. In both cases, the smaller the azimuth subinterval chosen, the more exact are the computations. In order to keep the computation economical and at the same time achieve some of the accuracy of small azimuth spacing, the procedure adopted is to use a "normal" spacing whenever the fluid particle is not close to the blade and a "reduced" spacing whenever it is close to a blade. Reference to figure 1 shows that the trajectory locations at which the fluid particle is directly over a blade are characterized by $x_b = 0$. For each collocation point (r_{bo}, Ψ_{bo}) these azimuth positions are determined in advance using equation (B 1). During the azimuth integration (or summation), a reduced spacing is used in the vicinity of these locations. In the computations carried out here (unless otherwise mentioned) the normal and reduced azimuth intervals used were 15^o and 5^o for the Van Holten scheme and 30^o and 10^o for the discretized representation. Although results of computing with the original scheme were reported in reference 5, these results were recomputed for the present study using normal and reduced spacing as above, and with spanwise collocation points at r/R_1 = 0.30, 0.55, 0.75, 0.85, 0.95. Due to these changes, some differences will be noted between the curves presented here and the corresponding ones in reference 5, but the differences are generally small with one exception which will be pointed out later on. For the discretized representation five spanwise segments were used, with end points at $r/R_1 = R_0/R_1$, 0.5, 0.7, 0.8, 0.9, 1.0, and five chordwise segments with end points at x/b = - 1.0, -0.9, - 0.6, 0.0, 0.5, 1.0.

Results for the variation of total blade lift as a function of azimuth position for Case 1 are shown in figure 5. It can be seen that for all three forward speeds, the results of the discretized representation are quite close to the original scheme, with the p.q. representation being generally a little closer than the p.c. representation.

For Case 2, the results are illustrated in figure 6 and, as may be anticipated from the computations reported in reference 5, there is greater variation here, mainly for μ = 0.13 and μ = 0.29. At μ = 0.13, the original scheme results in a considerably wavy

TABLE I. - GEOMETRIC AND FLIGHT CONDITIONS FOR THE EXPERIMENTAL CASES

Case	Aspect ratio, A	Number of blades, B	Root Ratio, R_o/R_1	Linear twist, ϵ, deg.	Rotor angle, α_r, deg.	Thrust coefficient, C_T	Lock number, γ	Advance Ratio, μ	Wake Spacing, $\frac{2\pi w_r}{\Omega B R_1}$
1 (ref.21)	5.4	2	0.17	0	0	0.00367	-	0.08	0.069
					2.0	0.00482	-	0.15	0.067
					6.7	0.00394	-	0.29	0.128
2 (ref. 22)	17.2	4	0.16	8	0	0.00499	11.4	0.06	0.055
					0.6	0.00501	11.4	0.13	0.032
					6.1	0.00571	9.6	0.29	0.064
3 (ref. 23)	17.2	4	0.16	8	5.0	0.00357	10.0	0.29	0.049
					4.0	0.00366	9.9	0.39	0.050
					4.8	0.00334	10.1	0.45	0.065

distribution which is not seen in the results of the discretized scheme, especially with the p.q. representation which remains close to the measured curve except near the advancing blade position. At $\mu = 0.29$, there is once again a deviation near the advancing blade position, with the p.c. results being particularly bad in this region. The p.q. results are generally close to the original ones. However, both results from the discretized scheme tend to overestimate the lift in the disk trailing edge region (around $\Psi_b = 0^o$).

The results for Case 3 are presented in figure 7. It was observed in reference 5 that the original results showed a tendency to overestimate the lift near the downwind azimuth position and correspondingly underestimate it near the upwind position. This tendency is also present in the results from the discretized representations. This may be due to the increasingly important effect of radial flow (along the blade span) in these regions at moderate to high forward speeds. The influence of radial flow is primarily on the spanwise development of the blade boundary layer, increasing with forward speed, and must be accounted for empirically. Otherwise, the p.q. results are acceptable and show the same trend as the measured curves. However, the p.c. results show particularly significant deviations for $\mu = 0.29$ and $\mu = 0.39$, near the advancing blade position and in the disk trailing edge region. It was noted earlier that the changes made in the original scheme produced only small variations with one exception. This exception is $\mu = 0.39$ of Case 3. Comparison of figure 19 of reference 5 with figure 7(b) of the present study reveals that the latter variation is much better, particularly in the absence of the large peak near the disk trailing edge that is present in the former. This difference is surprising, at first glance, because the changes made do not seem that important. Apart from using a constant azimuth spacing, the original version of the computational scheme also used spanwise collocation points at $r/R_1 = 0.40, 0.55, 0.75, 0.85, 0.95$, differing from the present version only in the innermost point. Both programs use the zero lift condition instead of the normal velocity boundary condition at a collocation point whenever the local effective freestream speed $U_T < 0.1$. However, if $r/R_1 = 0.4$ is used, there is a collocation point near the retreating blade position that has $U_T = 0.105$, which is small yet large enough to escape the zero lift condition. It is apparently this particular point that is the source of the trouble, for when it is replaced by another collocation point with $U_T > 0.2$, the resulting distribution is quite regular (like figure 7(b) of the present study). This situation does point out the need to use care in the choice of collocation points (avoiding those points with small positive values of U_T) and use of close azimuth spacing in those cases where interference effects are significant.

Spanwise distributions of sectional lift, at various azimuth positions, are plotted in figure 8 for $\mu = 0.29$ of Case 1, and in figure 9 for $\mu = 0.29$ of Case 2. General comments on these curves are much the same as those made for the original scheme in reference 5. Agreement is acceptable as long as the measured curves do not show any sharp variations, as in the case of close interaction with a tip vortex. When sharp variations do occur, they are not evident in the computed curves. There is also general deviation from the measured curves in the tip region. In addition, the falloff to zero at the tip is better with the piecewise quadratic represenation, presumably because it provides a better approximation to the actual curve than the piecewise constant representation.

In discussing the total lift variations it was noticed that the p.c. representation led to particularly significant deviations for three flight conditions , viz, $\mu = 0.29$ of Case 2, $\mu = 0.29$ and $\mu = 0.39$ of Case 3. To test the possibility of improvement with smaller azimuth spacing, these three cases were computed again with a constant

azimuth subinterval of 5° and the results are shown plotted in figures 10 to 12. It can be seen that there is considerable improvement in the results for the p.c. representation, while the p.q. results are only slightly changed. This is a clear indication that, for flight conditions involving significant interaction effects, the results from the p.c. representation are sensitive to the azimuth spacing used and should be calculated with a small spacing.

Since the primary objective of this investigation is to improve the numerical practicality of the original asymptotic execution time requirements, it is essential that these requirements be examined. Table 2 presents results suitable for comparison of the different representations for two typical rotor configurations. In addition to the original continuous representation suggested by Van Holten and the piecewise constant and quadratic representations of this study, there is also presented data for the segmented lifting line model with a discrete vortex wake. This was the only linear method considered in reference 5 which provided airloads of an accuracy which could be compared with the asymptotic method. It can be observed from table 2 that the piecewise constant representation reduces the execution time requirement of the original continuous representation by a factor of seven. A reduction to almost one fifth is attained for the piecewise quadratic simulation. As indicated in the table, these figures are based on computational azimuth intervals of 30° normal and 10° reduced spacing. In cases where much shorter intervals are required for the piecewise constant representation the computational requirements are proportionately increased as illustrated in table 2. It should be noted that the computational efficiency of the piecewise constant representation is equivalent to the less comprehensive segmented lifting line with a discrete vortex wake when the azimuth intervals are the same.

TABLE 2. - COMPARATIVE COMPUTER EXECUTION TIMES FOR TYPICAL CONDITIONS

Computational azimuth intervals, normal/reduced	Method of analysis	CDC 6400 execution time, sec
	Case 1 $\mu = 0.29$	
$15^{\circ}/5^{\circ}$	Original continuous	231
$30^{\circ}/10^{\circ}$	Discrete vortex wake	30
	Piecewsie constant	33
	Piecewise quadratic	49
	Case 2 $\mu = 0.29$	
$15^{\circ}/5^{\circ}$	Original continuous	467
$30^{\circ}/10^{\circ}$	Discrete vortex wake	60
	Piecewise constant	65
	Piecewise quadratic	100
$5^{\circ}/5^{\circ}$	Discrete vortex wake	265
	Piecewise constant	265
	Piecewise quadratic	415

CONCLUDING REMARKS

The asymptotic approach developed by Van Holten is a suitable method for rotor airload calculation, within the scope of linear theory. However, in spite of the fact that only a single numerical integration is required to calculate the induced velocity, significant computation times may be required under certain conditions. It is possible to reduce the computation time by making two approximations, viz, replacing the continuous variation of the doublet strength distribtuion along the blade span by a piecewise continuous variation, and replacing the continuous helical trajectory of a fluid particle by a succession of connected straight line segments.

In the present study, such a discretized representation has been developed for the asymptotic method, using either a piecewise constant or piecewise quadratic variation of the doublet strength along the span. Computations have been carried out for the case of a two-bladed, teetering model rotor and a four-bladed, articulated full-scale rotor, and the results compared with both measurement and the original computational scheme. In general, when interaction effects are not significant, the simplified scheme agrees well with the original results, with the piecewise quadratic representation being slightly better. When interaction effects are significant, the piecewise constant scheme yields poor results but is found to improve upon using smaller azimuth spacing, while the piecewise quadratic scheme continues to compare well with the original results. Computationally, the discretized representation shows considerable improvement over the original scheme; under conditions where interaction effects are not significant, the piecewise constant scheme requires only about one-seventh and the piecewise quadratic scheme about one-fifth of the computation time required for the original scheme.

APPENDIX A

PIECEWISE CONTINUOUS REPRESENTATIONS

The continuous variation of the dipole strength function, g, over the blade span is approximated by dividing the span into J segments and replacing the actual curve by a series of simpler curves, continuous over each segment but discontinuous at the segment boundaries. The points marking the spanwise division are labeled s_j, $j = 1,2,\ldots(J+1)$ with s_1 being the root and s_{J+1} the tip of the blade. Points r_j, $j = 1,2,\ldots J$ denote the midpoints of the segments, where the boundary condition of normal velocity is applied. The length of a segment is Δs_j, $j = 1,2,\ldots J$ and this is allowed to vary along the span, generally being chosen smaller near the tip to achieve a better representation of the rapid variation of blade loading.

The simplest representation is a constant value over each segment and this is shown in figure 2. The spanwise variation can be represented much better with a second-degree curve over each segment as illustrated in figure 2. However, setting up such a piecewise quadratic representation involves more complicated algebra, the details of which are given below.

The quadratic curve is constructed to satisfy the following requirements: (1) at the midpoint, r_j, it must have the actual functional value, $g(r_j)$, (2) at its end points, s_j and s_{j+1}, it must equal the values on the adjacent segments, (3) at its end points, it must also equal the slopes of the adjacent segments. It must be noted that, for the segments at the ends of the blade, the curve is allowed to go to zero at the root and the tip, without any constraint on the slope at these points. Since each curve requires 3 constants for its definition, a total of 3 J constants must be determined from the available conditions, which are listed below.

Number of equations for midpoint values	=	J
Number of equations for end point values (including zero values at root and tip)	=	J + 1
Number of equations for end point slopes (excluding root and tip)	=	J - 1

This adds up to a total of 3 J equations, so that it is possible to set up a piecewise quadratic approximation which is completely determinate.

The curves will have to be determined in terms of the midpoint values and segment locations. To begin with, the slope conditions are ignored and the end point values assumed known. If C_{1j}, C_{2j}, C_{3j} denote the constants for the j^{th} curve, the conditions to be satisfied are

$$C_{1j} + C_{2j}\, s_j + C_{3j}\, s_j^2 = g_j$$

$$C_{1j} + C_{2j}\, r_j + C_{3j}\, r_j^2 = g(r_j)$$

$$C_{1j} + C_{2j}\, s_{j+1} + C_{3j}\, s_{j+1}^2 = g_{j+1}$$

which can be solved to give

$$C_{1j} = 2\left[r_j s_j g_{j+1} + r_j s_{j+1} g_j - 2 s_j s_{j+1} g(r_j)\right] / \Delta s_j^2$$

$$C_{2j} = -2\left[(r_j + s_j) g_{j+1} + (r_j + s_{j+1}) g_j - 4 r_j g(r_j)\right] / \Delta s_j^2 \qquad \text{(A 1)}$$

$$C_{3j} = 2\left[g_{j+1} + g_j - 2 g(r_j)\right] / \Delta s_j^2$$

Now the slope conditions can be used to elimate the end point values g_j, $j = 1,2. \ . \ . (J+1)$. At any end point, say s_{j+1}, the equality of slopes leads to

$$C_{2j} + 2 C_{3j} s_{j+1} = C_{2,j+1} + 2 C_{3,j+1} s_{j+1}$$

which, on substitution, becomes

$$(1/\Delta s_j) g_j + 3(1/\Delta s_j + 1/\Delta s_{j+1}) g_{j+1} + (1/\Delta s_{j+1}) g_{j+2} = 4\left[g(r_j)/\Delta s_j + g(r_{j+1})/\Delta s_{j+1}\right]$$

$$\text{for } j = 1,2. \ . \ . (J-1) \qquad \text{(A 2)}$$

This tridiagonal system of (J-1) equations can be solved by the following recursive scheme, which consists basically of the forward elimination and back substitution of the Gaussian elimination method.

$$\left.\begin{aligned} \beta_2 &= 3(1/\Delta s_1 + 1/\Delta s_2) \\ \gamma_2 &= 4\left[g(r_1)/\Delta s_1 + g(r_2)/\Delta s_2\right] \\ \beta_j &= 3(1/\Delta s_{j-1} + 1/\Delta s_{j-2}) - 1/\Delta s_{j-1}^2 \, \beta_{j-1} \\ \gamma_j &= \left\{4\left[g(r_{j-1})/\Delta s_{j-1} + g(r_j)/\Delta s_j\right]\right. \\ &\quad \left. - \gamma_{j-1}/\Delta s_{j-1}\right\} / \beta_j \qquad (j = 3, 4. \ . \ . \ , J-1) \end{aligned}\right\} \qquad \text{(A 3)}$$

$$g_J = \gamma_J$$

$$g_j = \gamma_j - g_{j+1}/\beta_j \Delta s_j \qquad (j = J-1, J-2. \ . \ . 2)$$

This determines the (J-1) end point values in terms of the J midpoint values, so that the quadratic components C_{1j}, C_{2j}, C_{3j} are completely defined. Within a segment, the function can be written as

$$g = C_{1j} + C_{2j}\, s + C_{3j}\, s^2$$

$$= 2\Big[(s - s_{j+1})(s - r_j)\, g_j + (s - s_j)(s - r_j)\, g_{j+1}$$

$$- 2(s - s_j)(s - s_{j+1})\, g(r_j)\Big] \;/\Delta\, s_j^2 \qquad \text{(A 4)}$$

Calculation of the total blade lift and the moment about the hub requires the spanwise integral of g and its moment about the hub. These integrals are given below.

Piecewise constant representation:

$$\int_{\xi}^{1} g(s)\, ds = \sum_{j=1}^{J} g(r_j)\, \Delta s_j$$

$$\int_{\xi}^{1} g(s)\, s\, ds = \sum_{j=1}^{J} g(r_j)\, r_j \Delta\, s_j \qquad \text{(A 5)}$$

Piecewise quadratic representation:

$$\int_{\xi}^{1} g(s)\, ds = \sum_{j=1}^{J} \Big[g_j + g_{j+1} + 4g(r_j)\Big]\, \Delta s_j \;/\; 6$$

$$\int_{\xi}^{1} g(s)\, s\, ds = \sum_{j=1}^{J} \Big[s_j\, g_j + s_{j+1}\, g_{j+1} + 4r_j\, g(r_j)\Big] \Delta\, s_j \;/\; 6 \qquad \text{(A 6)}$$

APPENDIX B

TRAJECTORY APPROXIMATION AND LIST OF INTEGRALS

The helical trajectory of a freestream fluid particle, ending at a collocation point $(r_{bo}/R_1, \Psi_{bo})$ on a reference blade, relative to the axes fixed to the j^{th} blade, is given by the following equations.

$$\left.\begin{aligned} x_b/R_1 &= (r_{bo}/R_1 \sin(\theta + \Delta\Psi_j) + \mu\theta \sin(\theta + \Psi_{bo} + \Delta\Psi_j) \\ y_b/R_1 &= \lambda\theta \\ r_b/R_1 &= (r_{bo}/R_1)\cos(\theta + \Delta\Psi_j) + \mu\theta \cos(\theta + \Psi_{bo} + \Delta\Psi_j) \end{aligned}\right\} \quad (B\ 1)$$

where $\theta = (\Psi_b - \Psi_{bo})$ is the azimuth relative to the reference blade position and $\Delta\Psi_j$ is the azimuth separation of the j^{th} blade from the first (reference) blade. For uniformly separated blades,

$$\Delta\Psi_j = 2\pi(j-1)/B$$

The approximation used here divides the continuous helical trajectory into a succession of straight-line segments, each connecting the initial and final points of the helical path over a subinterval of azimuth. The coordinates of each of these trajectory segments can be written as

$$\left.\begin{aligned} x_b/R_1 &= X_i + X_s\,\theta \\ y_b/R_1 &= Y_i + Y_s\,\theta \\ r_b/R_1 &= R_i + R_s\,\theta \end{aligned}\right\} \quad (B\ 2)$$

If θ_1 and θ_2 are the ends of the azimuth interval, the intercepts and slopes are given by

$$\left.\begin{aligned} X_i &= (x_{b1} - R_1 X_s\,\theta_1)/R_1 \\ X_s &= (x_{b2} - x_{b1})/R_1(\theta_2 - \theta_1) \\ Y_i &= 0 \\ Y_s &= \lambda \\ R_i &= (r_{b1} - R_1 R_s\,\theta_1)/R_1 \\ R_s &= (r_{b2} - r_{b1})/R_1(\theta_2 - \theta_1) \end{aligned}\right\} \quad (B\ 3)$$

The integrals along the fluid particle trajectories which appear in Appendix C contain the following expressions which are written in terms of the straight-line notation as

$$r^2 = x_b^2 + y_b^2 = (r_o + 2r_1\theta + r_2\theta^2)\, R_1^2$$

where

$$r_o = X_i^2$$

$$r_1 = X_i X_s$$

$$r_2 = X_s^2 + Y_s^2$$

Letting $u = (s - r_b)$

$$d^2 = r^2 + u^2 = (d_o + 2d_1\theta + d_2\theta^2)\, R_1^2$$

where

$$d_o = X_i^2 + (s - R_i)^2$$

$$d_1 = X_i X_s - (s - R_i)\, R_s$$

$$d_2 = X_s^2 + \lambda^2 + R_s^2$$

$$d_n^2 = (x - x_b)^2 + y_b^2 = (d_{no} + 2d_{n1}\theta + d_{n2}\theta^2)\, R_1^2$$

where

$$d_{n0} = (x - X_i)^2$$

$$d_{n1} = -(x - X_i)\, X_s$$

$$d_{n2} = X_s^2 + Y_s^2$$

The primary advantage which has been achieved by introduction of the straight-line segment approximation for the particle trajectories is evident in the above "distance" expressions. It can be noted that they are all quadratic expressions in θ. As a direct result the integrals of the pressure gradient which are described in Appendix C can be analytically evaluated. These integral expressions are listed below as determined from reference 9. The symbolic parameter, t, is defined as

$$t \equiv d_1 + d_2\theta + d\sqrt{d_2}$$

Far field integrals:

$$I_1^f = \int \frac{d\theta}{d} = \frac{\ell n\ t}{\sqrt{d_2}}$$

$$I_2^f = \int \frac{\theta\, d\theta}{d} = \frac{d - d_1 I_1^f}{d_2}$$

$$I_3^f = \int \frac{d\ \theta}{d(d-u)} - \int \frac{d\,\theta}{d(d+u)}$$

$$= \frac{2}{|X_i\ \lambda|}\left[\tan^{-1}\left\{\frac{t + (R_s d - u\sqrt{d_2})}{|X_i\ \lambda\ |}\right\}\right.$$

$$\left. - \tan^{-1}\left\{\frac{t - (R_s d - u\sqrt{d_2})}{|\ X_i\ \lambda\ |}\right\}\right]$$

$$I_4^f = I_3^f \Big|_{y_b = y_o + \lambda\theta}$$

$$I_5^f = \int \frac{\theta\, d\,\theta}{d(d-u)} - \int \frac{\theta\ d\,\theta}{d(d+u)}$$

$$= \frac{1}{r_2}\left[\ell n\left\{\frac{d-u}{d+u}\right\} - 2R_s\, I_1^f - r_1\, I_3^f\right]$$

$$I_6^f = I_5^f \Big|_{y_b = y_o + \lambda\theta}$$

$$I_7^f = \frac{\partial\, I_4^f}{\partial\, y_o}\Bigg|_{y_o \to 0}$$

$$= \frac{2\lambda(R_s d - u\sqrt{d_2})}{t r_2\, r^2} - \frac{X_s\, I_3^f}{X_i \lambda} - \frac{2 y_b u}{t d r^2}$$

$$+ \frac{2X_s(R_s d - u\sqrt{d_2})\ (X_s\, x_b + \lambda\, y_b)}{X_i\, \lambda\, t r_2 r^2}$$

$$I_8^f = \left.\frac{\partial I_6^f}{\partial y_o}\right|_{y_o \to 0}$$

$$= \left[\frac{2R_s(\lambda d + y_b\sqrt{d_2})}{td\sqrt{d_2}} - \frac{2y_b u}{dr^2}\right.$$

$$\left. + \lambda I_3^f - r_1 I_7^f\right]\frac{1}{r_2}$$

$$I_9^f = \int \frac{\theta^2 d\theta}{d(d-u)} - \int \frac{\theta^2 d\theta}{d(d+u)}$$

$$= \left[2(s - R_i) I_1^f - 2R_s I_2^f - r_o I_3^f - 2r_1 I_5^f\right] / r_2$$

$$I_{10}^f = \int \frac{d\theta}{d(d-u)^2} + \int \frac{d\theta}{d(d+u)^2}$$

$$= \frac{1}{r^2 t X_i^2 \lambda^2 \sqrt{d_2}} \left\{2(d_1^2 - d_0 d_2)(d\sqrt{d_2} - R_s u)\right.$$

$$\left. + t(2u + r^2 I_3^f \sqrt{d_2})\left[r_1 R_s + r_2 (s - R_i)\right]\right\}$$

$$I_{11}^f = \int \frac{\theta\, d\theta}{d(d-u)^2} + \int \frac{\theta\, d\theta}{d(d+u)^2}$$

$$= -(2d/r^2 + r_1 I_{10}^f + R_s I_3^f) / r_2$$

$$I_{12}^{f} = \int \frac{\theta^2 d\theta}{d(d-u)^2} + \int \frac{\theta^2 d\theta}{d(d+u)^2}$$

$$= \left[2I_1^{f} + 2(s - R_i) I_3^{f} - 2R_s I_5^{f} \right.$$

$$\left. - r_0 I_{10}^{f} - 2r_1 I_{11}^{f} \right] / r_2$$

$$I_{13}^{f} = \int \frac{\theta^3 d\theta}{d(d-u)^2} + \int \frac{\theta^3 d\theta}{d(d+u)^2}$$

$$= \left[2I_2^{f} + 2(s - R_i) I_5^{f} - 2R_s I_9^{f} \right.$$

$$\left. - r_o I_{11}^{f} - 2r_1 I_{12}^{f} \right] / r_2$$

$$I_{14}^{f} = \int \frac{\theta d\theta}{d(d+u)}$$

$$= \frac{\ell n[2d_2 t (d+u)]}{r_2} - \frac{\ell n\, t}{\sqrt{d_2}(\sqrt{d_2} + R_s)}$$

$$- \frac{2r_1}{r_2 |X_i \lambda|} \tan^{-1} \left\{ \frac{t - (R_s d - u\sqrt{d_2})}{|X_i \lambda|} \right\}$$

$$I_{15}^{f} = \int \frac{\theta^2 d\theta}{d(d+u)}$$

$$= \left[\theta + \frac{2X_i^2(X_s^2 - Y_s^2)}{r_2 |X_i \lambda|} \tan^{-1} \left\{ \frac{t - (R_s d - u\sqrt{d_2})}{|X_i \lambda|} \right\} \right.$$

$$+ \frac{2r_1 d_2 - (\sqrt{d_2} + R_s)[r_1 R_s + r_2(s - R_i)]}{\sqrt{d_2}\, d_2 (\sqrt{d_2} + R_s)} \ln t$$

$$\left. - \frac{2r_1}{r_2} \ln \left\{ 2d_2\, t(d+u) \right\} \right] \frac{1}{r_2}$$

$$I_{16}^{f} = \int \frac{d\theta}{d-u} + \int \frac{d\theta}{d+u}$$

$$= 2I_1^{f} + (s - R_i) I_3^{f} - R_s I_5^{f}$$

$$I_{17}^{f} = \int \frac{\theta\, d\theta}{d-u} + \int \frac{\theta\, d\theta}{d+u}$$

$$= 2I_2^{f} + (s - R_i) I_5^{f} - R_s I_9^{f}$$

$$I_{18}^{f} = \int \frac{\partial}{\partial y_b} \left[y_b \ln(d+u) \right] d\theta$$

$$= \theta \ln(d+u) + R_s I_2^{f} - r_1 I_{14}^{f} - X_s^2 I_{15}^{f}$$

Some of the above integrals are not valid for the trajectory segment which ends at the collocation point for which $X_i = 0$. For this circumstance the following integrals are used.

$$I_{19}^{f} = \int \frac{\partial}{\partial y_b}\left[\frac{y_b d}{r^2}\right] d\theta \Big|_{X_i = 0}$$

$$= \frac{\lambda^2 \ell n\, t}{r_2\sqrt{d_2}} + \frac{X_s^2 - Y_s^2}{r_2^2}\left[\sqrt{d_2}\,\ell n\, t - \frac{d}{\theta}\right.$$

$$\left. - \frac{R_s(s - R_i)}{|s - R_i|}\,\ell n\left\{\frac{d_2\theta + \sqrt{d_2}(d - |s - R_i|)}{d_2\theta + \sqrt{d_2}(d + |s - R_i|)}\right\}\right]$$

$$I_{20}^{f} = \int \frac{\partial}{\partial y_b}\left[\frac{y_b d}{r^2}\right] \theta\, d\theta \Big|_{X_i = 0}$$

$$= \frac{\lambda^2}{r_2 d_2}\left[d + \frac{(s - R_i) R_s\, \ell n\, t}{\sqrt{d_2}}\right] + \frac{X_s^2 - Y_s^2}{r_2^2}\left[d\right.$$

$$\left. + |s - R_i|\ell n\left\{\frac{d_2\theta + \sqrt{d_2}\,(d - |s - R_i|)}{d_2\theta + \sqrt{d_2}(d + |s - R_i|)}\right\} - \frac{2(s - R_i) R_s \ell n\, t}{\sqrt{d_2}}\right]$$

$$I_{21}^{f} = \int \frac{\partial}{\partial y_b}\left[\frac{y_b u}{r^2 d}\right] d\theta \Big|_{X_i = 0}$$

$$= \frac{d(X_s^2 - Y_s^2)}{r_2^2 \theta\, |s - R_i|} + \frac{\lambda^2 \theta}{r_2 d(s - R_i)}$$

Common part integrals

$$I_1^c = \int \frac{d\theta}{r^2}$$

$$= \frac{1}{|X_i \lambda|} \tan^{-1} \left\{ \frac{r_1 + r_2 \theta}{|X_i \lambda|} \right\}$$

$$I_2^c = \int \frac{d\theta}{r^4}$$

$$= (r_1 + r_2\theta + r_2 r^2 I_1^c) / 2X_i^2 \lambda^2$$

$$I_3^c = \int \frac{\theta d\theta}{r^4}$$

$$= -(1 + 2r_1 r^2 I_2^c) / 2r_2 r^2$$

$$I_4^c = \int \frac{\theta^2 d\theta}{r^4}$$

$$= (r_o r^2 I_2^c - \theta) / r_2 r^2$$

$$I_5^c = \int \frac{\theta^3 d\theta}{r^4}$$

$$= (\ell n\, r - r_1 I_1^c - r_o r_2 I_3^c - 2r_1 r_2 I_4^c) / r_2^2$$

$$I_6^c = \int \frac{\theta^4 d\theta}{r^4}$$

$$= (\theta^3 - 3r_o r^2 I_4^c - 4r_1 r^2 I_5^c) / r_2 r^2$$

For the special case where $X_i = 0$

$$I_2^c \Big|_{X_i = 0} = -1 / 3r_2^2\theta^3$$

$$I_3^c \Big|_{X_i = 0} = -1 / 2r_2^2\theta^2$$

$$I_4^c \Big|_{X_i = 0} = -1 / r_2^2\theta$$

$$I_5^c \Big|_{X_i = 0} = \ell n\, \theta / r_2^2$$

$$I_6^c \Big|_{X_i = 0} = \theta / r_2^2$$

Near field integrals:

$$I_1^n = \int \frac{d\theta}{d_n^2}$$

$$= \frac{1}{\lambda |x - X_i|} \tan^{-1}\left\{ \frac{d_{n1} + d_{n2}\theta}{\lambda |x - X_i|} \right\}$$

$$I_2^n = \int \frac{\theta d\theta}{d_n^2}$$

$$= (\ell n\, d_n - d_{n1}\, I_1^n) / d_{n2}$$

$$I_3^n = \int \frac{\theta^2 d\theta}{d_n^2}$$

$$= (\theta - d_{no}\, I_1^n - 2d_{n1}\, I_2^n) / d_{n2}$$

$$I_4^n = \int \frac{\theta^3 d\theta}{d_n^2}$$

$$= (\theta^2 - 2d_{no}\, I_2^n - 4d_{n1}\, I_3^n) / 2d_{n2}$$

APPENDIX C

INTEGRATION OF PRESSURE FIELD

The composite pressure field of the blade, to O(1/A), can be written from equations (6) and (7) of reference 5 as

$$\frac{p}{\rho\Omega^2R_1^2} = \left[\frac{p_{dip}}{\rho\Omega^2R_1^2}\right] + \left[\frac{(1-\xi)}{2A}\ \frac{g}{\rho\Omega^2R_1^2}\ \frac{\sin\chi}{r/R_1}\right] + \left[-\frac{g}{\rho\Omega^2R_1^2}\ \frac{\sin\phi}{\cosh\eta + \cos\phi}\right.$$

$$\left. + \frac{(1-\xi)}{2A}\left(F_2 + (r_b/R_1)\,F_3\right)e^{-\eta}\sin\phi\right]$$

for points within the blade span, and for points outside the span

$$\frac{p}{\rho\Omega^2R_1^2} = \frac{p_{dip}}{\rho\Omega^2R_1^2} \qquad \text{(C 1)}$$

The corresponding sectional lift is

$$\frac{\ell}{\rho\Omega^2R_1^3} = -\frac{\pi(1-\xi)}{A}\left[\frac{g}{\rho\Omega^2R_1^2} - \frac{(1-\xi)}{4A}\left(F_2 + (r_b/R_1)\,F_3\right)\right] \qquad \text{(C 2)}$$

The integration of the far field, common part and near field terms (bracketed separately on the right hand side of equation (C 1) above) will be discussed for the piecewise constant and piecewise quadratic schemes.

Far Field

To O(1/A), this is the field of a dipole line located along the blade midchord and can be expressed as the integral of point dipoles distributed along the line.

$$\frac{p_{dip}}{\rho\Omega^2R_1^2} = \frac{y_b/R_1}{4\pi}\int_{\xi}^{1}\frac{\ell}{\rho\Omega^2R_1^3}\,\frac{d(s/R_1)}{(d/R_1)^3}$$

$$= -\frac{(1-\xi)}{4A}\,(y_b/R_1)\int_{\xi}^{1}\frac{g}{\rho\Omega^2R_1^2}\,\frac{d(s/R_1)}{(d/R_1)^3} \qquad \text{(C 3)}$$

where $d^2 = x_b^2 + y_b^2 + (s - r_b)^2$. Using integration by parts, this can also be written as

$$\frac{p_{dip}}{\rho \Omega^2 R_1^2} = \frac{(1-\xi)}{4A} \frac{(y_b/R_1)}{(r/R_1)^2} \int_{\xi}^{1} \frac{\partial}{\partial s} \left(\frac{g}{\rho \Omega^2 R_1^2} \right) \frac{(s - r_b) ds}{d} \qquad \text{(C 4)}$$

provided g goes to zero at the root and tip. The azimuth variation of g is approximated by a piecewise constant variation over each sub-interval of azimuth, while the spanwise variation is represented by a piecewise constant or a piecewise quadratic variation, as discussed in Appendix A.

Piecewise constant representation. -

$$p_{far} = -\frac{(y_b/R_1)}{4A} (1-\xi) \sum_{j=1}^{J} g_j \int_{s_j/R_1}^{s_{j+1}/R_1} \frac{d(s/R_1)}{(d/R_1)^3}$$

$$= -\frac{(y_b/R_1)}{4A} \frac{(1-\xi)}{(r/R_1)^2} \sum_{j=1}^{J} g_j \left[\frac{s - r_b}{d} \right]_{s=s_j}^{s=s_{j+1}}$$

The function g_j which varies with azimuth will have a constant value over the i^{th} azimuth subinterval that will be denoted by g_{ij}. The velocity induced by the far field is given by

$$\frac{w_{far}}{\Omega R_1} = \frac{(1-\xi)}{4A} \sum_i \sum_j g_{ij} \int_{\theta_{i+1}}^{\theta_i} \frac{\partial}{\partial (y_b/R_1)} \left[\frac{(y_b u)/R_1^2}{(r^2 d)/R_1^3} \right] d\theta \Bigg|_{s_j}^{s_{j+1}} \qquad \text{(C 5)}$$

where $u = s - r_b$. The integration will be easier if the derivative can be taken out of the integral and this is done as,

$$\frac{w_{far}}{\Omega R_1} = -\frac{(1-\xi)}{4A} \lim_{y_o \to 0} \frac{\partial}{\partial (y_o/R_1)} \sum_i \sum_j g_{ij} \int_{\theta_{i+1}}^{\theta_i} \frac{(y_b - y_o)\, u/R_1^2}{(r^2 d)/R_1^3} d\theta \Bigg|_{s_j}^{s_{j+1}}$$

where now $d^2 = x_b^2 + (y_b - y_o)^2 + u^2$. Noting that

$$\frac{u}{r^2 d} = \frac{1}{2} \left[\frac{1}{d(d-u)} - \frac{1}{d(d+u)} \right]$$

the integration can now be evaluated using the integrals listed in Appendix B with $y_b/R_1 = \lambda\theta$, where λ is the inflow ratio.

$$\int_{\theta_{i+1}}^{\theta_i} \frac{(y_b - y_o)\, u/R_1^2}{(r^2 d)/R_1^3}\, d\theta = -\frac{y_o}{R_1} I_4^f + \lambda I_6^f \Bigg|_{\theta_{i+1}}^{\theta_i}$$

Carrying out the differentiation and letting $y_o \to 0$, the induced velocity is obtained as

$$\frac{w_{far}}{\Omega R_1} = \sum_i \sum_j (\Delta w_{far})_{ij}^{p.c.}\, g_{ij} \qquad (C\ 6)$$

where, for $i \neq 1$,

$$(\Delta w_{far})_{ij}^{p.c.} = -\frac{(1-\xi)}{4A}\left(-I_4^f + \lambda I_8^f\right)\Bigg|_{\theta_{i+1}}^{\theta_i}\Bigg|_{s_j}^{s_{j+1}}$$

Here, the azimuth index i is set up so that $\theta_1 = 0$ is the collocation point on the blade and the trajectory ranges over $-\infty < \theta \leq 0$. For $i = 1$, the trajectory segment has one end on the blade and the unit induced velocity is expressed as

$$(\Delta w_{far})_{ij}^{p.c.} = \frac{(1-\xi)}{4A} I_{21}^f \Bigg|_{\theta_2}^{\theta_1}\Bigg|_{s_j}^{s_{j+1}}$$

Piecewise quadratic representation. - For this case, it is more convenient to express the field of the dipole line in its second form (eq. (C 4)). Using the representation of Appendix A as

$$\frac{\partial}{\partial(s/R_1)}\left(\frac{g}{\rho\,\Omega^2 R_1^2}\right) = C_{2j} + 2C_{3j}(s/R_1)$$

$$\frac{p_{far}}{\rho\,\Omega^2 R_1^2} = \frac{(1-\xi)}{4A}\,\frac{y_b/R_1}{(r/R_1)^2}\sum_{j=1}^{J}\int_{s_j}^{s_{j+1}}\left\{C_{2j} + 2C_{3j}(s/R_1)\right\}\frac{u\,ds/R_1^2}{d/R_1}$$

$$\frac{p_{far}}{\rho \Omega^2 R_1^2} = \frac{(1-\xi)}{4A} \sum_{j=1}^{J} \left[\left\{ C_{2j} + C_{3j} (r_b + s)/R_1 \right\} \frac{y_b d}{r^2} \right.$$

$$\left. - C_{3j} (y_b/R_1) \ell n \left\{ (u + d)/R_1 \right\} \right]_{s_j}^{s_{j+1}}$$

The induced velocity can then be written as

$$\frac{w_{far}}{\Omega R_1} = -\frac{(1-\xi)}{4A} \sum_i \sum_j \left[(C_{2j} + C_{3j} R_i + C_{3j} s/R_1)_i \int_{\theta_{i+1}}^{\theta_i} \frac{\partial}{\partial (y_b/R_1)} \left[\frac{y_b d/R_1^2}{(r/R_1)^2} \right] d\theta \right.$$

$$+ (C_{3j} R_s)_i \int_{\theta_{i+1}}^{\theta_i} \theta \frac{\partial}{\partial (y_b/R_1)} \left[\frac{y_b d/R_1^2}{(r/R_1)^2} \right] d\theta$$

$$\left. - (C_{3j})_i \int_{\theta_{i+1}}^{\theta_i} \frac{\partial}{\partial (y_b/R_1)} \left[(y_b/R_1) \ell n \left\{ (u + d)/R_1 \right\} \right] d\theta \right]_{s_j}^{s_{j+1}} \qquad \text{(C 7)}$$

It may be noted that

$$\frac{\partial}{\partial y_b} (y_b d/r^2) = (x_b^2 - y_b^2)\, d/r^4 + y_b^2 / r^2 d$$

$$= \frac{1}{2} \left[\frac{1}{d+u} + \frac{1}{d-u} - \frac{y_b^2}{d(d+u)^2} - \frac{y_b^2}{d(d-u)^2} \right]$$

Using this relation, and consulting the integrals listed in Appendix B, the induced velocity can be expressed as

$$\frac{w_{far}}{\Omega R_1} = \sum_i \sum_j (\Delta w_{far})_{ij}^{p.q.} g_i(r_j) \qquad \text{(C 8)}$$

where $g_i(r_j)$ is the midpoint value of the j^{th} spanwise segment within the i^{th} azimuth interval. In terms of the quadratic coefficients, equation (C 7) can be written for $i \neq 1$ as

$$\frac{w_{far}}{\Omega R_1} = -\frac{(1-\xi)}{4A} \sum_i \sum_j \Big[(C_{2j} + C_{3j} R_i + C_{3j} s/R_1)_i$$

$$\times (I^f_{16} - \lambda^2 I^f_{12})/2 + (C_{3j} R_s)_i (I^f_{17} - \lambda^2 I^f_{13})/2$$

$$- (C_{3j})_i I^f_{18} \Big] \Bigg|_{\theta_{i+1}}^{\theta_i} \Bigg|_{s_j}^{s_{j+1}}$$

and for $i = 1$ as

$$\Delta \left(\frac{w_{far}}{\Omega R_1} \right)_{i=1} = -\frac{(1-\xi)}{4A} \sum_j \Big[(C_{2j} + C_{3j} R_i + C_{3j} s/R_1)_1 I^f_{19}$$

$$+ (C_{3j} R_s)_1 I^f_{20} - (C_{3j})_1 I^f_{21} \Big] \Bigg|_{\theta_2}^{\theta_1} \Bigg|_{s_j}^{s_{j+1}}$$

The quadratic coefficients can be expressed in terms of the midpoint and end point values. In turn, the end point values can be expressed in terms of the midpoint values, as shown in Appendix A, to obtain a final expression for the unit induced velocity of equation (C 8). The expression is lengthy and will not be reproduced here.

Common Part

The common part is the pressure field to which the far field tends at points very close to the dipole line, when it behaves essentially as a two-dimensional dipole corresponding to the doublet strength at that spanwise location.

$$\frac{p_{common}}{\rho \Omega^2 R_1^2} = -\frac{(1-\xi)}{2A} \frac{y_b/R_1}{(r/R_1)^2} \frac{g(r_b,\theta)}{\rho \Omega^2 R_1^2}$$

The induced velocity due to the common part is calculated as

$$\frac{w_{common}}{\Omega R_1} = \int_{\infty}^{0} \frac{\partial}{\partial(y_b/R_1)} \left(\frac{P_{common}}{\rho \Omega^2 R_1^2}\right) d\theta \qquad (C\ 9)$$

Piecewise constant representation. - Noting that

$$\frac{\partial}{\partial y_b} (y_b/r^2) = (x_b^2 - y_b^2)/r^4$$

equation (C 9) becomes

$$\frac{w_{common}}{\Omega R_1} = -\frac{(1-\xi)}{2A} \sum_i g_{ij} \left[X_i^2 \int_{\theta_{i+1}}^{\theta_i} \frac{d\theta}{(r/R_1)^4} + 2X_i X_s \int_{\theta_{i+1}}^{\theta_i} \frac{\theta\, d\theta}{(r/R_1)^4} + (X_s^2 - \lambda^2) \int_{\theta_{i+1}}^{\theta_i} \frac{\theta^2 d\theta}{(r/R_1)^4} \right]$$

The index j represents the spanwise segment within which the i^{th} trajectory segment lies; in general, the trajectory segment may range over more than one spanwise segment, in which case the azimuth interval must be subdivided so that each of the subintervals lies entirely within one spanwise segment.

$$\frac{w_{common}}{\Omega R_1} = \sum_i (\Delta w_{common})_i^{p.c.} g_{ij} \qquad (C\ 10)$$

where, from Appendix B,

$$(\Delta w_{common})_i^{p.c.} = -\frac{(1-\xi)}{2A} \left[X_i^2 I_2^c + 2X_i X_s I_3^c + (X_s^2 - \lambda^2) I_4^c \right] \Bigg|_{\theta_{i+1}}^{\theta_i}$$

Piecewise quadratic representation. - The spanwise variation of g is given by equation (A 4) of Appendix A. The induced velocity is given by

$$\frac{w_{common}}{\Omega R_1} = -\frac{(1-\xi)}{2A} \sum_i \frac{2}{\Delta s_j^2} \left[g_{ij} \left\{ (R_i - s_{j+1})(R_i - r_j) C_1 \right.\right.$$

$$\left. + R_s(2R_i - r_j - s_{j+1}) C_2 + R_s^2 C_3 \right\} + g_{i,j+1} \left\{ (R_i - s_j)(R_i - r_j) C_1 \right.$$

$$\left. + R_s(2R_i - r_j - s_j) C_2 + R_s^2 C_3 \right\} - 2g_i(r_j) \left\{ (R_i - s_j)(R_i - s_{j+1}) C_1 \right.$$

$$\left.\left. + R_s(2R_i - s_j - s_{j+1}) C_2 + R_s^2 C_3 \right\} \right]$$

where

$$C_1 = \left[X_i^2 I_2^c + 2X_i X_s I_3^c + (X_s^2 - \lambda^2) I_4^c \right] \Big|_{\theta_{i+1}}^{\theta_i}$$

$$C_2 = \left[X_i^2 I_3^c + 2X_i X_s I_4^c + (X_s^2 - \lambda^2) I_5^c \right] \Big|_{\theta_{i+1}}^{\theta_i}$$

$$C_3 = \left[X_i^2 I_4^c + 2X_i X_s I_5^c + (X_s^2 - \lambda^2) I_6^c \right] \Big|_{\theta_{i+1}}^{\theta_i}$$

Both g_{ij} and $g_{i,j+1}$ can be expressed in terms of the midpoint values, and the induced velocity can be finally written as

$$\frac{w_{common}}{\Omega R_1} = \sum_i (\Delta w_{common})_i^{p.q.} g_i(r_j) \qquad \text{(C 11)}$$

Near Field

The near field is a distribution of two-dimensional dipoles along the chord, of intensity proportional to the surface pressure differential.

$$\frac{p_{near}}{\rho \Omega^2 R_1^2} = \frac{y_b}{\pi R_1} \int_{-1}^{1} \frac{-\frac{g}{\rho \Omega^2 R_1^2} \sqrt{\frac{1-x}{1+x}} + \frac{(1-\xi)}{2A} \left(F_2 + (r_b/R_1) F_3 \right) \sqrt{1-x^2}}{(x - x_b R_1/b)^2 + (y_b R_1/b)^2} \, dx$$

where b is the semi-chord.

To make analytical integration possible, the chord is divided into K segments and the factors $\sqrt{1-x/1+x}$ and $\sqrt{1-x^2}$ are replaced by an average value over each segment. The chordwise integration can then be carried out, resulting in

$$\frac{\partial}{\partial(y_b/R_1)}\left(\frac{P_{near}}{\rho\,\Omega^2 R_1^2}\right) = -\sum_{k=1}^{K}\frac{f_k}{\pi}\left[\frac{\left(\frac{1-\xi}{2A}\,x - x_b\right)/R_1}{\left\{\left(\frac{1-\xi}{2A}\,x - x_b\right)^2 + y_b^2\right\}/R_1^2}\right]_{x_k}^{x_{k+1}}$$

where $f_k = \frac{g}{\rho\,\Omega^2 R_1^2}\,a_k - \frac{(1-\xi)}{2A}\left[F_2 + (r_b/R_1)\,F_3\right]b_k$

$$a_k = \left.\frac{\phi - \sin\phi}{x_k}\right|_{\phi_k}^{\phi_{k+1}}$$

$$b_k = \left.\frac{\phi/2 - (\sin 2\phi)/4}{\Delta x_k}\right|_{\phi_k}^{\phi_{k+1}}$$

$$x_k = \cos\phi_k \;;\quad \Delta x_k = x_{k+1} - x_k$$

Piecewise constant representation. -

$$\frac{w_{near}}{\Omega R_1} = -\int_{-\infty}^{0}\frac{\partial}{\partial(y_b/R_1)}\left(\frac{P_{near}}{\rho\,\Omega^2 R_1^2}\right)d\theta$$

$$= \sum_i\sum_k\frac{f_{ik}}{\pi}\int_{\theta_{i+1}}^{\theta_i}\frac{\left(\frac{1-\xi}{2AR_1}\,x - X_i\right) - X_s\theta}{d_n^2/R_1^2}\,d\theta\Bigg|_{x_k}^{x_{k+1}} \qquad \text{(C 12)}$$

Here, the factor $[F_2 + (r_b/R_1) F_3]$ is taken to be a constant for each azimuth interval i. Using the integrals listed in Appendix A, the induced velocity can be written as

$$\frac{w_{near}}{\Omega R_1} = \sum_i \sum_k \left[\left(\Delta w^{I}_{near} \right)^{p.c}_{ik} g_{ij} + \left(\Delta w^{II}_{near} \right)^{p.c.}_{ik} \right] \qquad (C\ 13)$$

where

$$\left(\Delta w^{I}_{near} \right)^{p.c.}_{ik} = \frac{a_k}{\pi} \left[\left(\frac{1-\xi}{2A} \frac{x}{R_1} - X_i \right) I_1^n - X_s I_2^n \right] \Bigg|_{\theta_{i+1}}^{\theta_i} \Bigg|_{x_k}^{x_{k+1}}$$

$$\left(\Delta w^{II}_{near} \right)^{p.c.}_{ik} = - \frac{(1-\xi)}{2A} \frac{b_k}{\pi} \left[F_2 + (r_b/R_1) F_3 \right]_i$$

$$x \left[\left(\frac{1-\xi}{2A} \frac{x}{R_1} - X_i \right) I_1^n - X_s I_2^n \right] \Bigg|_{\theta_{i+1}}^{\theta_i} \Bigg|_{x_k}^{x_{k+1}}$$

F_2 and F_3 contain terms proportional to blade motion, namely, θ_o, a_o, a_1, b_1 and the twist ε.

Piecewise quadratic representation. - Here, the quadratic expression for the variation of g over a spanwise segment is used and the induced velocity becomes

$$\frac{w_{near}}{\Omega R_1} = \sum_i \sum_k \frac{2a_k}{\pi \Delta s_j^2} \Big[g_{ij} \left\{ (R_i - s_{j+1})(R_i - r_j) n_o \right.$$

$$\left. + R_s (2R_i - r_j - s_{j+1}) n_1 + R_s^2 n_2 \right\} + g_{i,j+1} \left\{ (R_i - s_j)(R_i - r_j) n_o \right.$$

$$\left. + R_s (2R_i - r_j - s_j) n_1 + R_s^2 n_2 \right\}$$

$$- 2 g_i(r_j) \left\{ (R_i - s_j)(R_i - s_{j+1}) n_o + R_s (2R_i - s_j - s_{j+1}) n_1 \right.$$

$$\left. + R_s^2 n_2 \right\} \Big] + \sum_i \sum_k \frac{2b_k}{\pi \Delta s_j^2} \left[F_2 + (r_b/R_1) F_3 \right]_i n_o$$

where

$$n_o = \left[\left(\frac{1-\xi}{2A}\,\frac{x}{R_1} - X_i\right) I_1^n - X_s I_2^n\right] \Bigg|_{\theta_{i+1}}^{\theta_i} \Bigg|_{x_k}^{x_{k+1}}$$

$$n_1 = \left[\left(\frac{1-\xi}{2A}\,\frac{x}{R_1} - X_i\right) I_2^n - X_s I_3^n\right] \Bigg|_{\theta_{i+1}}^{\theta_i} \Bigg|_{x_k}^{x_{k+1}}$$

$$n_2 = \left[\left(\frac{1-\xi}{2A}\,\frac{x}{R_1} - X_i\right) I_3^n - X_s I_4^n\right] \Bigg|_{\theta_{i+1}}^{\theta_i} \Bigg|_{x_k}^{x_{k+1}}$$

As before, the induced velocity expression can be symbolically written as

$$\frac{w_{near}}{\Omega R_1} = \sum_i \sum_k \left[\left(\Delta w_{near}^{I}\right)_{ik}^{p.q.} g_{ij} + \left(\Delta w_{near}^{II}\right)_{ik}^{p.q.}\right] \qquad \text{(C 14)}$$

Limiting Behavior

The behavior of the expressions for the far field and the common part, in the vicinity of the lifting line, will be studied for both piecewise representations.

Piecewise constant representation. - It is sufficient to look at the expressions used for the trajectory segment immediately adjacent to the collocation point on the blade, viz, the segment with i = 1. Let the collocation point be located at the center of spanwise segment m. The unit induced velocity for the far field can be written out in full as below, for i = 1 (see eq. (C 6)).

$$\left(\Delta w_{far}\right)_{1j}^{p.c.} = -\frac{(1-\xi)}{4A}\left[\frac{(X_s^2 - \lambda^2)}{r_2^2}\left(\frac{d}{\frac{s}{R_1} - R_i}\right)\theta + \frac{\lambda^2}{r^2}\left(\frac{\theta}{\frac{s}{R_1} - R_i}\right) d\right] \Bigg|_{\theta_2}^{\theta_1} \Bigg|_{s_j}^{s_{j+1}}$$

$$\text{As } \theta \to 0, \quad d \to \left|\frac{s}{R_1} - R_i\right| - R_s \frac{\left(\frac{s}{R_1} - R_i\right)}{\left|\frac{s}{R_1} - R_i\right|}\theta \; \ldots ,$$

indicating that the first term in the expansion for d will give rise to a singular term, which can be separated out.

$$\lim_{\theta \to 0} \left[\sum_{j=1}^{J} \left(\Delta w_{far} \right)_{1j}^{p.c.} g_{1j} \right]_{sing}$$

$$= - \frac{(1-\xi)}{4A} \frac{(X_s^2 - \lambda^2)}{r_2^2} \frac{1}{\theta} \sum_{j=1}^{J} \frac{\left| \frac{s}{R_1} - R_i \right|}{\left(\frac{s}{R_1} - R_i \right)} \Bigg|_{s_j}^{s_{j+1}} g_{1j}$$

$$= - \frac{(1-\xi)}{2A} \frac{(X_s^2 - \lambda^2)}{r_2^2} \frac{1}{\theta} g_{1m}$$

since $R_i = r_m$. Similarly, by looking at the behavior of the common part expression for $i = 1$, it is found that (see eq. (C 10))

$$\lim_{\theta \to 0} \left(\Delta w_{common} \right)_1^{p.c.} = - \frac{(1-\xi)}{2A} (X_s^2 - \lambda^2) \left(- \frac{1}{r_2^2 \theta} \right) g_{1m}$$

since $X_i = 0$. It can be seen that the two terms cancel each other exactly.

Piecewise quadratic representation. - In a manner similar to that above, the singular part of the far field expression (eq. (C 8)) can be separated out.

$$\lim_{\theta \to 0} \left[\Delta \left(\frac{w_{far}}{\Omega R_1} \right)_{i=1} \right]_{sing}$$

$$= - \frac{(1-\xi)}{4A} \frac{(X_s^2 - \lambda^2)}{r_2^2} \sum_j \left[(C_{2j} + C_{3j} R_i + C_{3j} s/R_1) \left\{ - \frac{\left| \frac{s}{R_1} - R_i \right|}{\theta} \right.\right.$$

$$\left.\left. - R_s \frac{\left(\frac{s}{R_1} - R_i \right)}{\left| \frac{s}{R_1} - R_i \right|} \ln \theta \right\} + C_{3j} R_s \left| \frac{s}{R_1} - R_i \right| \ln \theta \right] \Bigg|_{s_j}^{s_{j+1}}$$

Now, $C_{2j} = g'(r_j) - 2(r_j/R_1) C_{3j}$

Using this relation and carrying out the summation with j, it can be shown that the above limiting expression simplifies to

$$\lim_{\theta \to 0} \left[\Delta \left(\frac{w_{far}}{\Omega R_1} \right)_{i=1} \right]_{sing}$$

$$= - \frac{(1 - \xi)}{4A} \frac{(X_s^2 - \lambda^2)}{r_2^2} \left[2g(r_m) \frac{1}{\theta} - 2R_s \, g'(r_m) \ell n \, \theta \right]$$

The limiting value for the common part (eg. (C 11)) can be shown to be

$$\lim_{\theta \to 0} \left[\Delta \left(\frac{w_{common}}{\Omega R_1} \right)_{i=1} \right]$$

$$= - \frac{(1 - \xi)}{2A} \frac{(X_s^2 - \lambda^2)}{r_2^2} \left[\frac{R_s}{\Delta s_m} (g_{i,m+1} - g_{im}) \ell n \, \theta - g(r_m) \frac{1}{\theta} \right]$$

Since

$$g'(r_m) = (g_{i,m+1} - g_{im}) / \Delta s_m$$

it can be seen that the singularities in the far field and common part cancel exactly.

APPENDIX D

EVALUATION OF CHORDWISE AND SPANWISE APPROXIMATIONS

To facilitate the analytical integration of the pressure field in calculating the velocity induced on the blade, approximations are used for chordwise and spanwise variations, as outlined in Appendices A and C. This Appendix attempts to evaluate the accuracy of these approximations.

Chordwise Approximation

This consists of replacing the factors $\sqrt{1-x/1+x}$ and $\sqrt{1-x^2}$ by their average values over each chordwise segment. Since the first factor is the significant portion of the chordwise pressure distribution, the following problem is considered. Calculate the velocity induced by a steady, two-dimensional pressure distribution (proportional to $\sqrt{1-x/1+x}$ on a fluid particle travelling parallel to the chord, using both the exact and approximate pressure distributions.

The (x, y) axes are centered at the midchord with the x-axis being parallel to the chord. The exact nondimensional pressure field of the airfoil is given by

$$p_e(x, y) = \frac{y}{2\pi} \int_{-1}^{1} \sqrt{\frac{1-x'}{1+x'}} \frac{dx'}{(x' - x)^2 + y^2}$$

$$= \frac{1}{2} \frac{\sin \phi}{\cosh \eta + \cos \phi}$$

where (η, ϕ) is an elliptic coordinate system with

$$x = \cosh \eta \cos \phi$$
$$y = \sinh \eta \sin \phi$$

If the trajectory considered extends from x = - 2 to x = 2 at a constant distance y, the nondimensional induced velocity is given by

$$v = - \int_{-2}^{2} \frac{\partial p_e}{\partial y} dx$$

$$= - \frac{1}{2} \int_{-2}^{2} \frac{\sinh \eta \cos \phi + \sinh \eta \cosh \eta \cos 2\phi}{(\cosh^2 \eta - \cos^2 \phi)(\cosh \eta + \cos \phi)^2} dx \qquad \text{(D 1)}$$

This integral can be evaluated by numerical integration.

Using the approximation, the average value of the pressure distribution over the k^{th} chordwise segment is given by

$$\bar{p}_k = \frac{1}{x_{k+1} - x_k} \int_{x_k}^{x_{k+1}} \sqrt{\frac{1-x}{1+x}}\, dx$$

$$= -\frac{1}{x_{k+1} - x_k} \left[\theta_{k+1} - \theta_k - \sin \theta_{k+1} + \sin \theta_k\right]$$

where $x_k = \cos \theta_k$.

$$p_e(x, y) = \frac{y}{2\pi} \sum_{k=1}^{K} \bar{p}_k \int_{x_k}^{x_{k+1}} \frac{dx'}{(x' - x)^2 + y^2}$$

$$\frac{\partial p_e}{\partial y} = -\sum_{k=1}^{K} \frac{\bar{p}_k}{2\pi} \frac{(x' - x)}{(x' - x)^2 + y^2} \Bigg|_{x_k}^{x_{k+1}}$$

$$v = \sum_{k=1}^{K} \frac{\bar{p}_k}{4\pi} \ln \left\{\frac{(x_{k+1} - x)^2 + y^2}{(x_k - x)^2 + y^2}\right\} \Bigg|_{x=-2}^{x=2} \qquad \text{(D 2)}$$

Two approximations are considered: (1) three segments along the chord, $\Delta x_k = 0.1, 0.9, 1.0$; and (2) five segments along the chord, $\Delta x_k = 0.1, 0.4, 0.5, 0.5, 0.5$. The results for the induced velocity are listed in table D 1. These results are also plotted in figure 3 and it can be seen that the approximate results are quite close to the exact results, even down to a vertical distance of 1% of the semi-chord.

TABLE D 1. - COMPARATIVE EVALUATION OF CHORDWISE APPROXIMATION

Vertical distance, y	Exact	Three segments	Five segments
.01	.5773	.5708	.5738
.05	.5766	.5702	.5731
.10	.5745	.5681	.5711
.20	.5661	.5602	.5629
.30	.5529	.5476	.5501
.40	.5357	.5313	.5335
.50	.5157	.5121	.5139
.60	.4938	.4910	.4925
.70	.4709	.4689	.4700
.80	.4476	.4464	.4472
.90	.4246	.4241	.4245
1.00	.4022	.4022	.4024

Spanwise Approximation

As discussed elsewhere, the span is divided into J segments, over each of which the variation of the function g is replaced by a piecewise constant or piecewise quadratic function. To evaluate this approximation, the following problem is considered. Calculate the velocity induced by a finite wing on a fluid particle travelling with the freestream flow past the wing, at various vertical and spanwise locations. The nondimensional loading along the wing span is taken to be

$$g_e = z^2\sqrt{1 - z^2}$$

with the z axis originating at one tip of the wing so that z = 1 represents the other tip. This type of loading has resemblance to the typical loading on a helicopter rotor blade.

For a particle travelling with constant velocity in the x direction, at constant values of y and z, the nondimensional vertical velocity induced by the wing may be written as

$$v = \frac{1}{4A}\int_{x_1}^{x_2}\left\{\frac{\partial}{\partial y}\, y \int_0^1 \frac{\zeta^2\sqrt{1-\zeta^2}\, d\zeta}{\left[x^2 + y^2 + (z-\zeta)^2\right]^{3/2}}\right\} dx$$

$$4Av = \int_{x_1}^{x_2} dx \int_0^1 \zeta^2\sqrt{1-\zeta^2}\, d\zeta \left[\frac{1}{\left[x^2 + y^2 + (z-\zeta)^2\right]^{3/2}} - \frac{3y^2}{\left[x^2 + y^2 + (z-\zeta)^2\right]^{5/2}}\right]$$

$$4Av = \int_0^1 \zeta^2 \sqrt{1-\zeta^2}\, d\zeta \left[\frac{x}{(y^2 + (z-\zeta)^2)_d} + \frac{y^2}{xd^3} \right.$$

$$\left. - \frac{y^2 d}{\left[y^2 + (z-\zeta)^2\right]^2 x} - \frac{y^2 x}{\left[y^2 + (z-\zeta)^2\right]^2 d} \right] \Bigg|_{x=x_1}^{x=x_2} \qquad \text{(D 3)}$$

where $d = \left[x^2 + y^2 (z-\zeta)^2\right]^{1/2}$

The integral with respect to ζ can be numerically evaluated. The induced velocity can also be calculated with a piecewise constant or piecewise quadratic approximation to g, using integrals similar to those listed in Appendix B, but the details of these expressions will not be written out here. For the calculation, $x_1 = -1$ and $x_2 = 1$, while the spanwise division for the approximations was done with 2 models: (1) three segments along the span, with $\Delta\zeta_j = 0.5, 0.3, 0.2$; and, (2) five segments along the span, with $\Delta\zeta_j = 0.5, 0.2, 0.1, 0.1, 0.1$. The results of the calculations are shown in tables D 2 and D 3 where the abbreviations p.c. and p.q. represent the piecewise constant and piecewise quadratic schemes. These induced velocity comparisons are also plotted in figure 4.

TABLE D 2. INDUCED VELOCITY COMPARISON FOR THREE-SEGMENT SPANWISE APPROXIMATIONS

Vertical distance, y	Spanwise location, z = 0.25			Spanwise location, z = 0.65			Spanwise location, z = 0.9		
	Exact	p.c.	p.q.	Exact	p.c.	p.q.	Exact	p.c.	p.q.
0.01	1.144	-0.603	-1.071	5.147	5.426	4.772	11.454	9.247	12.468
0.02	-1.050	-0.596	-0.987	5.037	5.381	4.735	10.455	9.024	11.017
0.05	-0.791	-0.548	-0.755	4.693	5.094	4.565	7.831	7.762	7.773
0.10	-0.440	-0.401	-0.430	4.099	4.343	4.128	5.007	5.391	4.849
0.20	0.026	-0.042	0.018	3.012	2.963	3.086	2.692	2.881	2.644
0.40	0.375	0.334	0.369	1.605	1.522	1.625	1.311	1.351	1.302
0.60	0.394	0.373	0.392	0.924	0.884	0.927	0.786	0.793	0.781
0.80	0.327	0.316	0.326	0.574	0.555	0.573	0.509	0.508	0.505
1.00	0.253	0.247	0.252	0.377	0.368	0.376	0.344	0.343	0.342

TABLE D 3. INDUCED VELOCITY COMPARISON FOR FIVE-SEGMENT SPANWISE APPROXIMATIONS

Vertical distance, y	Spanwise location, z = 0.25			Spanwise location, z = 0.60			Spanwise location, z = 0.95		
	Exact	p.c.	p.q.	Exact	p.c.	p.q.	Exact	p.c.	p.q.
0.01	-1.144	-0.518	-1.101	4.037	5.206	4.125	11.708	9.139	12.651
0.02	-1.050	-0.512	-1.013	3.975	5.120	4.048	9.481	8.404	9.495
0.05	-0.791	-0.470	-0.770	3.771	4.626	3.813	5.274	5.711	5.057
0.10	-0.440	-0.341	-0.432	3.393	3.661	3.406	2.963	3.386	2.876
0.20	0.026	-0.022	0.025	2.629	2.464	2.624	1.845	2.011	1.823
0.40	0.375	0.324	0.372	1.502	1.365	1.496	1.093	1.117	1.085
0.60	0.394	0.363	0.392	0.892	0.824	0.887	0.706	0.700	0.702
0.80	0.327	0.308	0.326	0.562	0.527	0.559	0.474	0.462	0.471
1.00	0.253	0.241	0.252	0.372	0.352	0.370	0.327	0.317	0.325

APPENDIX E

FINAL EQUATIONS AND OUTPUT QUANTITIES

The basic solution is for the spanwise and azimuthwise variation of the dipole strength function, g. With the span divided into J segments, the value at the midpoint of each segment is given the following harmonic representation over the azimuth.

$$\frac{g(r_j)}{\rho \Omega^2 R_1^2} = G_j^o + \sum_{n=1}^{N_h} \left[G_{jn}^c \cos(n\Psi_b) + G_{jn}^s \sin(n\Psi_b) \right] \qquad \text{(E 1)}$$

In the present calculation, the above formula serves only as an interpolation.

The boundary condition to be satisfied states that the normal velocity induced at a point on the blade by the combined pressure field of all the blades is equal to the normal velocity due to blade motion. If w_b denotes the normal velocity due to blade motion, the boundary condition can be symbolically written as

$$\frac{w_b}{\Omega R_1}(r_{bo}, \Psi_{bo}) = \sum_{\substack{\text{no. of} \\ \text{blades}}} \left\{ \sum_i \sum_j (\Delta w_{far})_{ij} \frac{g_i(r_j)}{\rho \Omega^2 R_1^2} \right.$$

$$+ \sum_i (\Delta w_{common})_i \frac{g_i(r_{j'})}{\rho \Omega^2 R_1^2}$$

$$\left. + \sum_i \sum_k \left[(\Delta w_{near}^{I})_{ik} \frac{g_i(r_{j'})}{\rho \Omega^2 R_1^2} + (\Delta w_{near}^{II})_{ik} \right] \right\} \qquad \text{(E 2)}$$

The contributions Δw can be calculated with either the piecewise constant or piecewise quadratic spanwise representation, as described in Appendix C. The index j' refers to the spanwise segment within which the i^{th} trajectory segment is located (if the i^{th} trajectory segment ranges over more than one spanwise segment, Δw must be summed over these segments as well).

$$\frac{g_i(r_j)}{\rho \Omega^2 R_1^2} = G_j^o + \sum_{n=1}^{N_h} \left[G_{jn}^c \cos(n\Psi_{bi}) + G_{jn}^s \sin(n\Psi_{bi}) \right] \qquad \text{(E 3)}$$

where Ψ_{bi} is any typical point of the i^{th} azimuth interval (e.g., either end or the midpoint). It must be noted that the collective pitch, coning angle and the cyclic pitch coefficients are contained both in w_b and in the near field contribution (Δw_{near}), which is proportional to the functions F_2 and F_3. These are defined below

$$\frac{w_b}{\Omega R_1} = \left[\left\{\theta_o - \epsilon \frac{r_b - R_o}{R_1 - R_o}\right\} \frac{r_b}{R_1} - \mu\alpha_r - \mu \frac{a_1}{2}\right]$$

$$+ \left[b_1 \frac{r_b}{R_1} - \mu a_o\right] \cos\Psi_b + \left[-a_1 \frac{r_b}{R_1} + \mu \left\{\theta_o\right.\right.$$

$$\left.\left. - \epsilon \frac{r_b - R_o}{R_1 - R_o}\right\}\right] \sin\Psi_b + \left[\mu \frac{a_1}{2}\right] \cos 2\Psi_b$$

$$+ \left[\mu \frac{b_1}{2}\right] \sin 2\Psi_b \qquad \text{(E 4)}$$

$$F_2 = \left[2\mu\theta_o + 2\mu\epsilon \frac{R_o}{R_1 - R_o}\right] \cos\Psi_b + \left[2\mu a_o\right] \sin\Psi_b$$

$$+ \left[2\mu b_1\right] \cos 2\Psi_b + \left[-2\mu a_1 - \mu^2 \epsilon \frac{R_1}{R_1 - R_o}\right] \sin 2\Psi_b \qquad \text{(E 5)}$$

$$F_3 = a_o + \left[-2a_1 - 4\mu\epsilon \frac{R_1}{R_1 - R_o}\right] \cos\Psi_b + \left[-2b_1\right] \sin\Psi_b$$

For presentation as output, the following quantities are calculated:

(1) azimuthwise variations of total lift per blade, aerodynamic moment about the hub and spanwise center of lift location,

(2) spanwise and azimuthwise variations of sectional lift, pitching moment about quarter-chord and center of pressure location,

(3) chordwise, spanwise and azimuthwise variations of surface pressure differential. The expressions for these quantities are presented below.

Surface pressure differential,

$$\frac{\Delta p}{\rho \Omega^2 R_1^2} = 2\left[- \frac{g}{\rho \Omega^2 R_1^2} \sqrt{\frac{1-x}{1+x}} + \frac{(1-\xi)}{2A} \left(F_2 + \frac{r_b}{R_1} F_3\right) \sqrt{1-x^2} \right] \quad \text{(E 6)}$$

where x is nondimensional with respect to the semi-chord.

Sectional lift,

$$\frac{\ell}{\rho \Omega^2 R_1^3} = - \frac{\pi}{A} (1-\xi) \left[\frac{g}{\rho \Omega^2 R_1^2} - \frac{(1-\xi)}{4A} \left(F_2 + \frac{r_b}{R_1} F_3\right) \right] \quad \text{(E 7)}$$

Pitching moment about quarter-chord,

$$\frac{m}{\rho \Omega^2 R_1^4} = - \frac{\pi}{16 A^3} (1-\xi)^3 \left(F_2 + \frac{r_b}{R_1} F_3\right) \quad \text{(E 8)}$$

Center of pressure location (from leading edge), as a fraction of the chord,

$$\frac{x_{cp}}{c} = 0.25 + \frac{A}{(1-\xi)} \frac{m}{R_1 \ell} \quad \text{(E 9)}$$

Total lift per blade,

$$\begin{aligned} \frac{L}{\rho \Omega^2 R_1^4} = & - \frac{\pi}{A} (1-\xi) \int_{\xi}^{1} \frac{g}{\rho \Omega^2 R_1^2} \, d\left(\frac{r_b}{R_1}\right) \\ & + \frac{\pi (1-\xi)^2}{4A^2} \left\{ \frac{(1-\xi^2)}{2} a_o + \left[2\mu\theta_o (1-\xi) - a_1 (1-\xi^2) - 2\mu\epsilon \right] \cos \Psi_b \right. \\ & + \left[2\mu a_o (1-\xi) - b_1 (1-\xi^2) \right] \sin \Psi_b + \left[2\mu b_1 (1-\xi) \right] \cos 2\Psi_b \\ & \left. + \left[- 2\mu a_1 (1-\xi) - \mu^2 \epsilon \right] \sin 2\Psi_b \right\} \end{aligned} \quad \text{(E 10)}$$

Aerodynamic moment about hub,

$$\frac{M}{\rho \Omega^2 R_1^5} = -\frac{\pi}{A}(1-\xi)\int_{\xi}^{1} \frac{g}{\rho \Omega^2 R_1^2}\frac{r_b}{R_1}\, d\left(\frac{r_b}{R_1}\right)$$

$$+ \frac{\pi(1-\xi)^2}{A^2}\left\{\frac{(1-\xi^3)}{3}a_o + \left[\mu\theta_o(1-\xi^2) - \frac{2a_1}{3}(1-\xi^3)\right.\right.$$

$$\left. + \frac{\mu\epsilon}{3}(-4-\xi-\xi^2)\right]\cos\Psi_b$$

$$+ \left[\mu a_o(1-\xi^2) - \frac{2b_1}{3}(1-\xi^3)\right]\sin\Psi_b + \left[\mu b_1(1-\xi^2)\right]\cos 2\Psi_b$$

$$\left. + \left[-\mu a_1(1-\xi^2) - \frac{\mu^2\epsilon}{2}(1+\xi)\right]\sin 2\Psi_b\right\} \qquad \text{(E 11)}$$

Spanwise center of lift location,

$$\frac{r_L}{R_1} = \frac{M}{R_1 L} \qquad \text{(E 12)}$$

The spanwise integrals of g, required in some of the expressions above, are given in Appendix A.

If the collective pitch, coning angle and cyclic pitch coefficients are considered unknown, additional equations are necessary. These equations are given below.

Piecewise Constant Representation

$$-\sum_{j=1}^{J} G_j^o \Delta s_j + \left[\frac{1}{8A}(1-\xi)(1-\xi^2)\right]a_o = \frac{A}{(1-\xi)}\frac{C_T}{B}$$

$$- \sum_{j=1}^{J} G_j^o \, r_j \Delta s_j + \left[\frac{1}{12A} (1 - \xi)(1 - \xi^3) - \frac{2}{\gamma} \right] a_o = 0$$

$$- \sum_{j=1}^{J} G_{j1}^c \, r_j \Delta s_j + \left[\frac{\mu}{4A} (1 - \xi)(1 - \xi^2) \right] \theta_o - \left[\frac{1}{6A} (1 - \xi)(1 - \xi^3) \right] a_1$$

$$= - \frac{\epsilon}{12A} \mu (-4 + 3\xi + \xi^3)$$

$$- \sum_{j=1}^{J} G_{j1}^s \, r_j \Delta s_j + \left[\frac{\mu}{4A} (1 - \xi)(1 - \xi^2) \right] a_o - \left[\frac{1}{6A} (1 - \xi)(1 - \xi^3) \right] b_1 = 0$$

Piecewise Quadratic Representation

In this case, the equations will also involve the values of g at the ends of spanwise segments; however, these can be related to the central values, as described in Appendix A. Let this relation be written symbolically as,

$$\frac{g(s_i)}{\rho \Omega^2 R_1^2} = \sum_{j=1}^{J} h_{ij} \frac{g(r_j)/\rho \Omega^2 R_1^2}{\Delta s_j}$$

Then the equations are as follows.

$$- \sum_{i=1}^{J} \left[4 G_i^o + \sum_{j=1}^{J} (h_{ij} + h_{i+1,j}) \frac{G_j^o}{\Delta s_j} \right] \frac{\Delta s_i}{6}$$

$$+ \left[\frac{1}{8A} (1 - \xi)(1 - \xi^2) \right] a_o = \frac{A}{(1 - \xi)} \frac{C_T}{B}$$

$$- \sum_{i=1}^{J} \left[4 r_i \, G_i^o + \sum_{j=1}^{J} (s_i \, h_{ij} + s_{i+1} \, h_{i+1,j}) \frac{G_j^o}{\Delta s_j} \right] \frac{\Delta s_i}{6}$$

$$+ \left[\frac{1}{12A} (1 - \xi)(1 - \xi^3) - \frac{2}{\gamma} \right] a_o = 0$$

$$- \sum_{i=1}^{J} \left[4r_i \, G_{i1}^{c} + \sum_{j=1}^{J} (s_i \, h_{ij} + s_{i+1} \, h_{i+1,j}) \, \frac{G_{j1}^{c}}{\Delta s_j} \right] \frac{\Delta s_i}{6}$$

$$+ \left[\frac{\mu}{4A} (1 - \xi)(1 - \xi^2) \right] \theta_o - \left[\frac{1}{6A} (1 - \xi)(1 - \xi^3) \right] a_1$$

$$= - \frac{\varepsilon}{12A} \mu (-4 + 3\xi + \xi^3)$$

$$- \sum_{i=1}^{J} \left[4r_i \, G_{i1}^{s} + \sum_{j=1}^{J} (s_i \, h_{ij} + s_{i+1} \, h_{i+1,j}) \, \frac{G_{j1}^{s}}{\Delta s_j} \right] \frac{\Delta s_i}{6}$$

$$+ \left[\frac{\mu}{4A} (1 - \xi)(1 - \xi^2) \right] a_o - \left[\frac{1}{6A} (1 - \xi)(1 - \xi^3) \right] b_1 = 0$$

REFERENCES

1. Van Holten, Th.: The Computation of Aerodynamic Loads on Helicopter Blades in Forward Flight, Using the Method of the Acceleration Potential. Rep. VTH-189, Technische Hogeschool Delft, Netherlands, March 1975.

2. Van Holten, Th.: Computation of Aerodynamic Loads on Helicopter Rotor Blades in Forward Flight, Using the Method of the Acceleration Potential. Presented at the 9th Congress of the International Congress of the Aeronautical Sciences, ICAS Paper No. 74-54, Haifa, 1974.

3. Van Holten, Th.: On the Validity of Lifting Line Concepts in Rotor Analysis. Vertica, vol. 1, 1977, pp. 239-254.

4. Van Holten, Th.: Some Notes on Unsteady Lifting Line Theory. Journal of Fluid Mechanics, vol. 77, Part 3, 1976, pp. 561-579.

5. Pierce, G. Alvin; and Vaidyanathan, Anand R.: Helicopter Rotor Loads Using a Matched Asymptotic Expansion Technique. NASA CR 165742, May 1981.

6. Rabbott, J. P., Jr; and Churchill, G. B.: Experimental Investigation of the Aerodynamic Loading on a Helicopter Rotor Blade in Forward Flight. NACA RM L56I07, October 1956.

7. Scheiman, J.: A Tabulation of Helicopter Rotor Blade Differential Pressures, Stresses and Motions as Measured in Flight. NASA TM X-952, March 1964.

8. Rabbott, J. P., Jr,; Lizak, A. A.; and Paglino, V. M.: A Presentation of Measured and Calculated Full-Scale Rotor Blade Aerodynamic and Structural Loads. USAAVLABS Tech. Rep. 66-31, July 1966.

9. Gradshteyn, I. S.; and Ryzhik, I. M.: Table of Integrals, Series and Products. Academic Press, 1980.

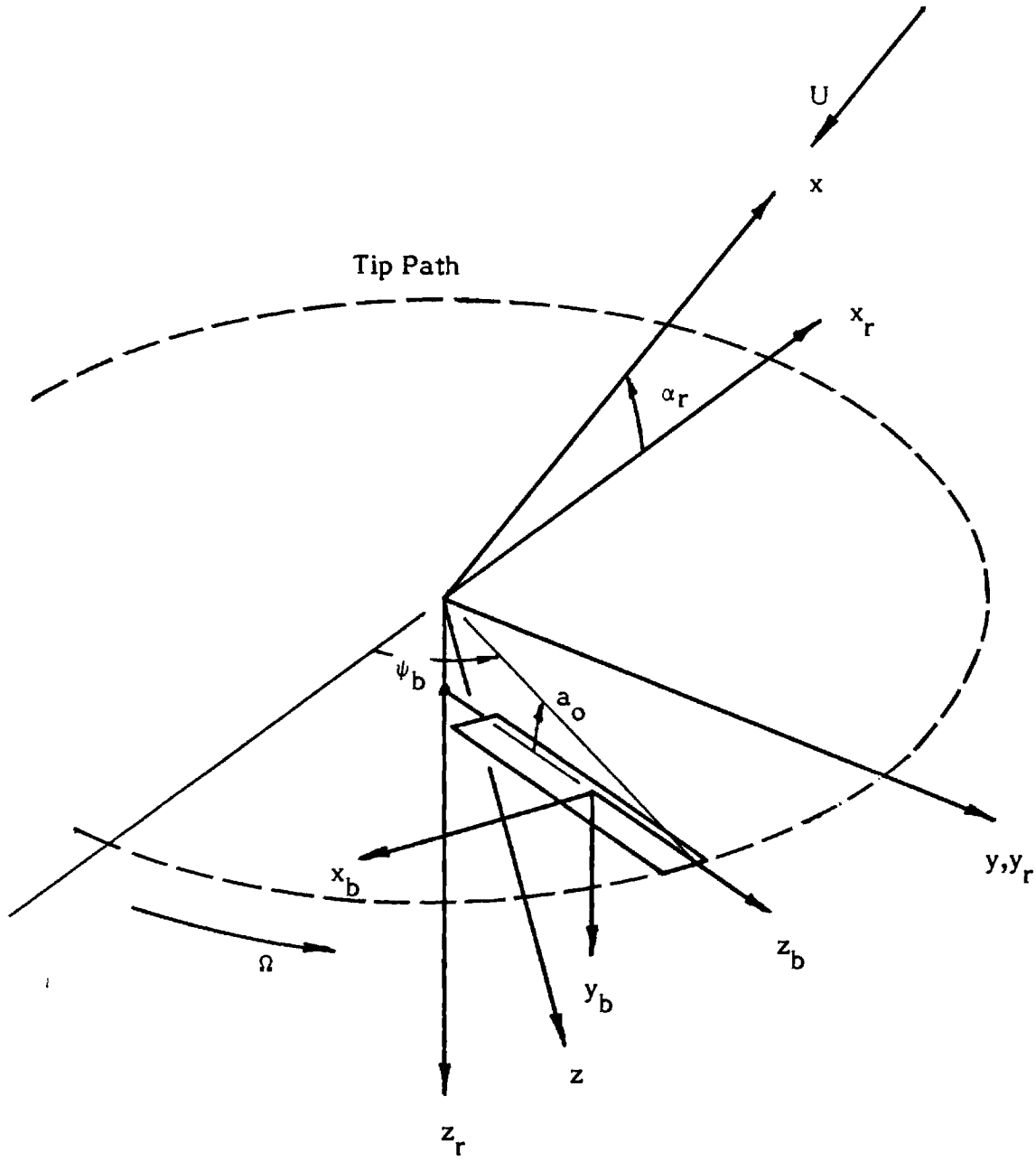

Figure 1. - Rotor coordinate systems.

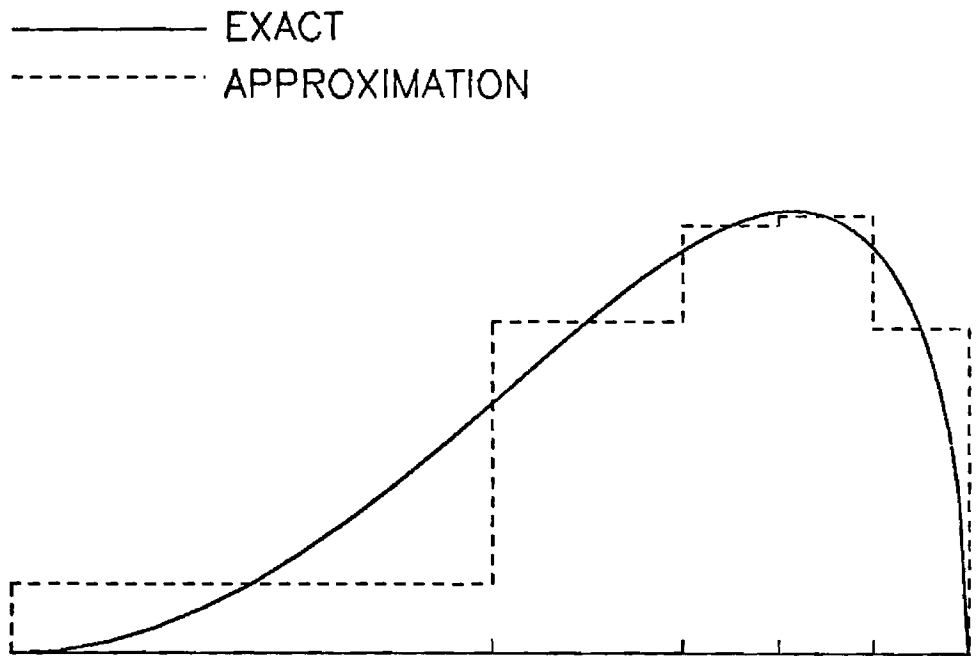

(a) Piecewise constant.

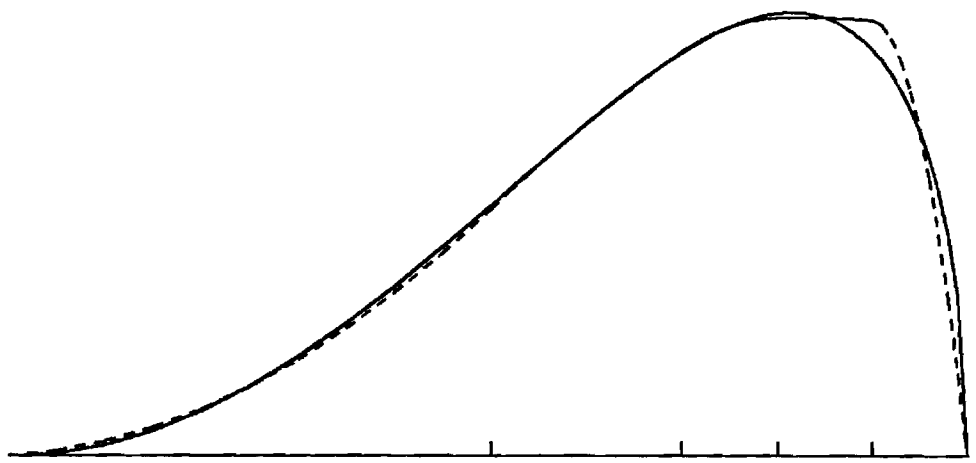

(b) Piecewise quadratic.

Figure 2. - Piecewise continuous representations of the spanwise distribution of doublet strength.

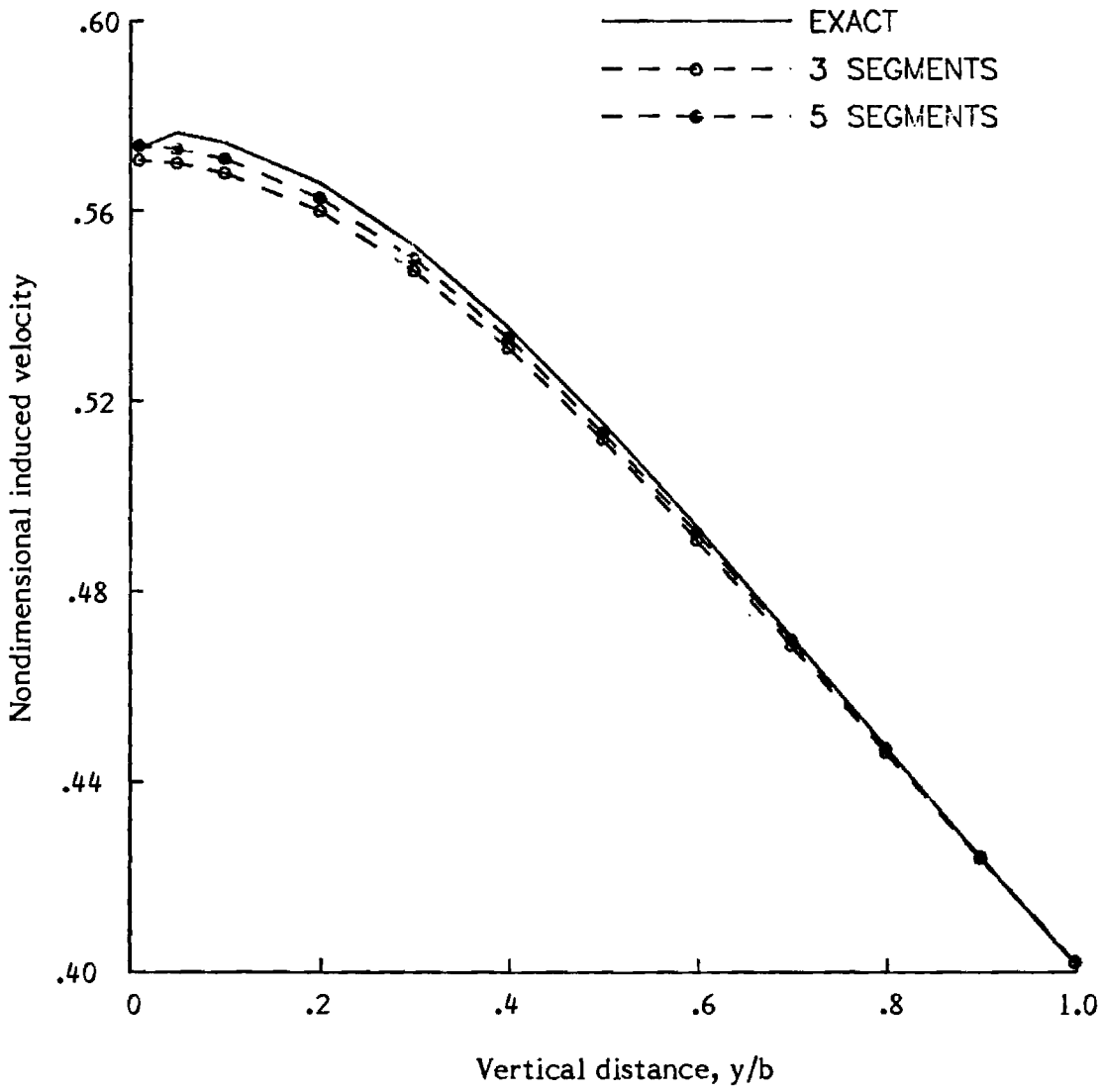

Figure 3. - Induced velocity comparison for piecewise constant chorwise pressure distribution.

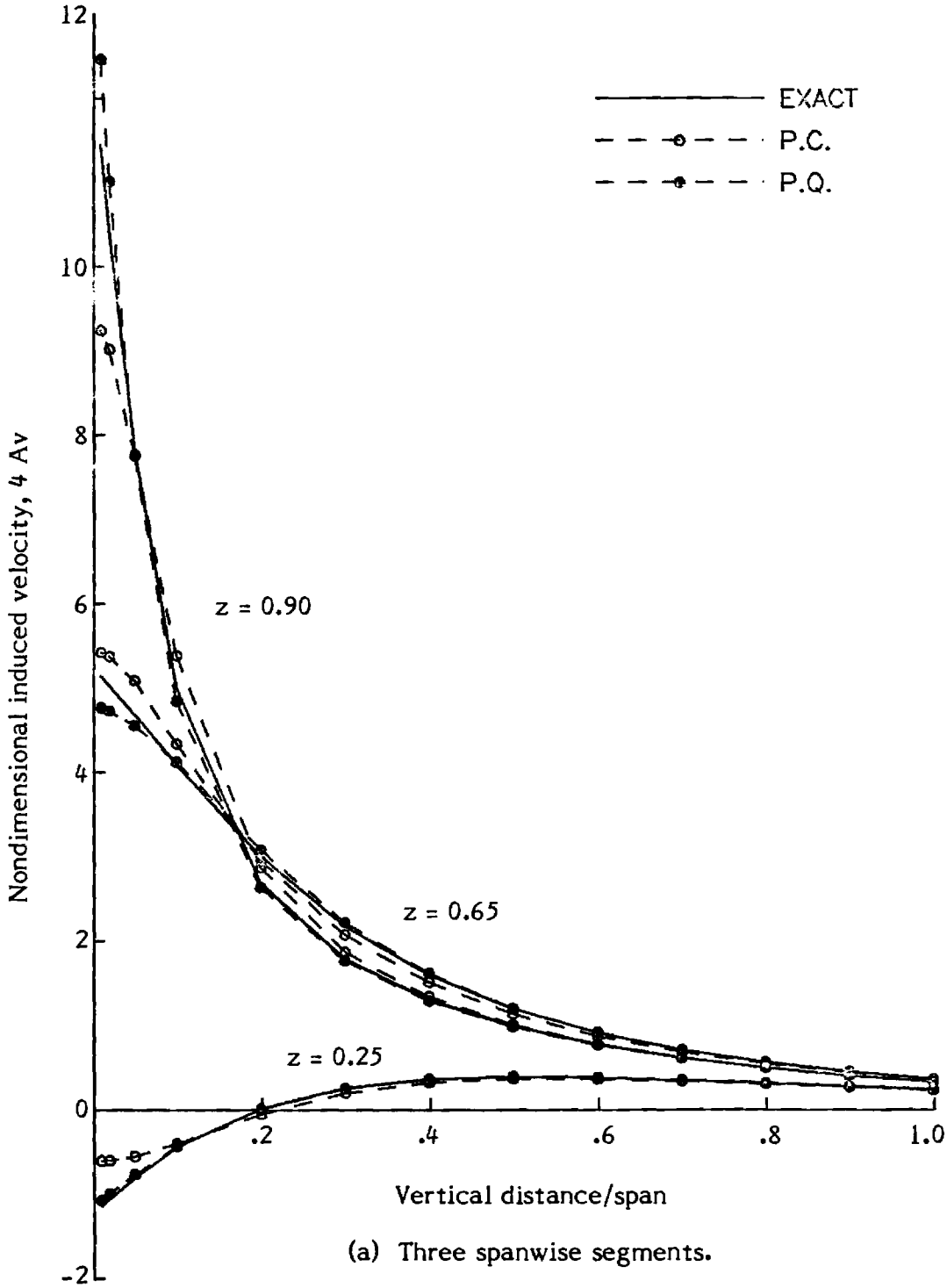

(a) Three spanwise segments.

Figure 4. - Induced velocity comparison for for spanwise approximations.

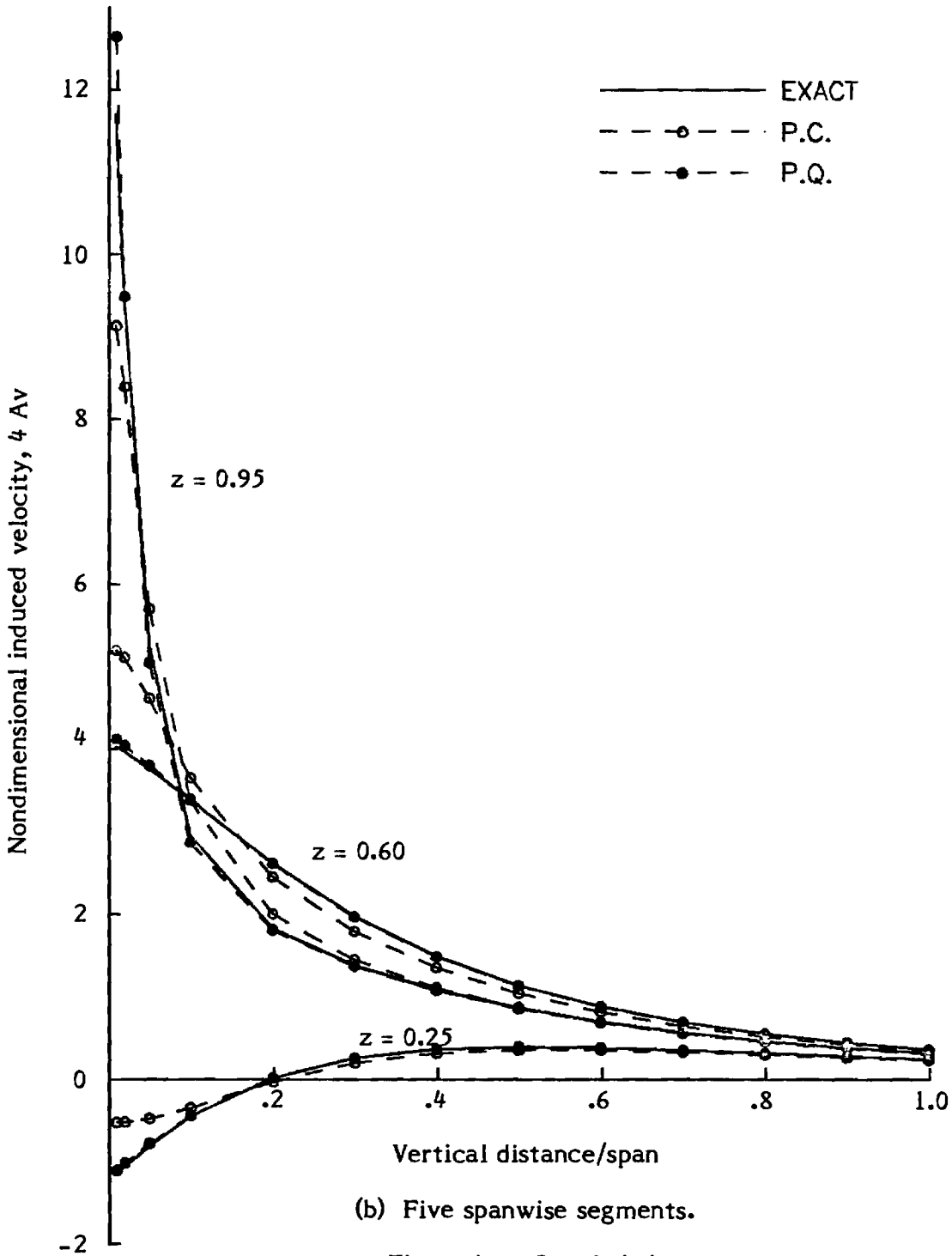

(b) Five spanwise segments.

Figure 4. - Concluded.

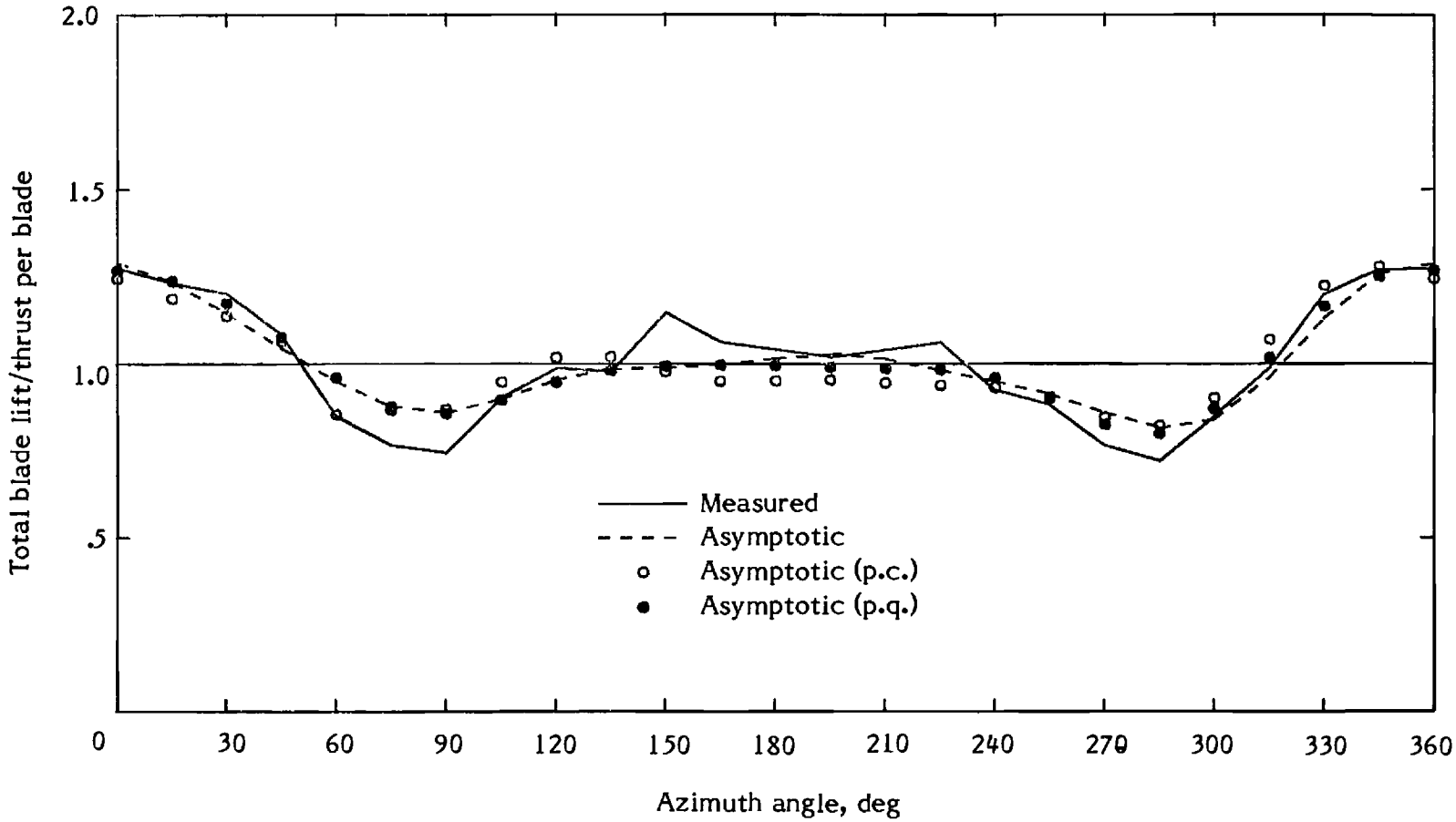

(a) μ = 0.08.

Figure 5. - Total blade lift versus azimuth for Case 1.

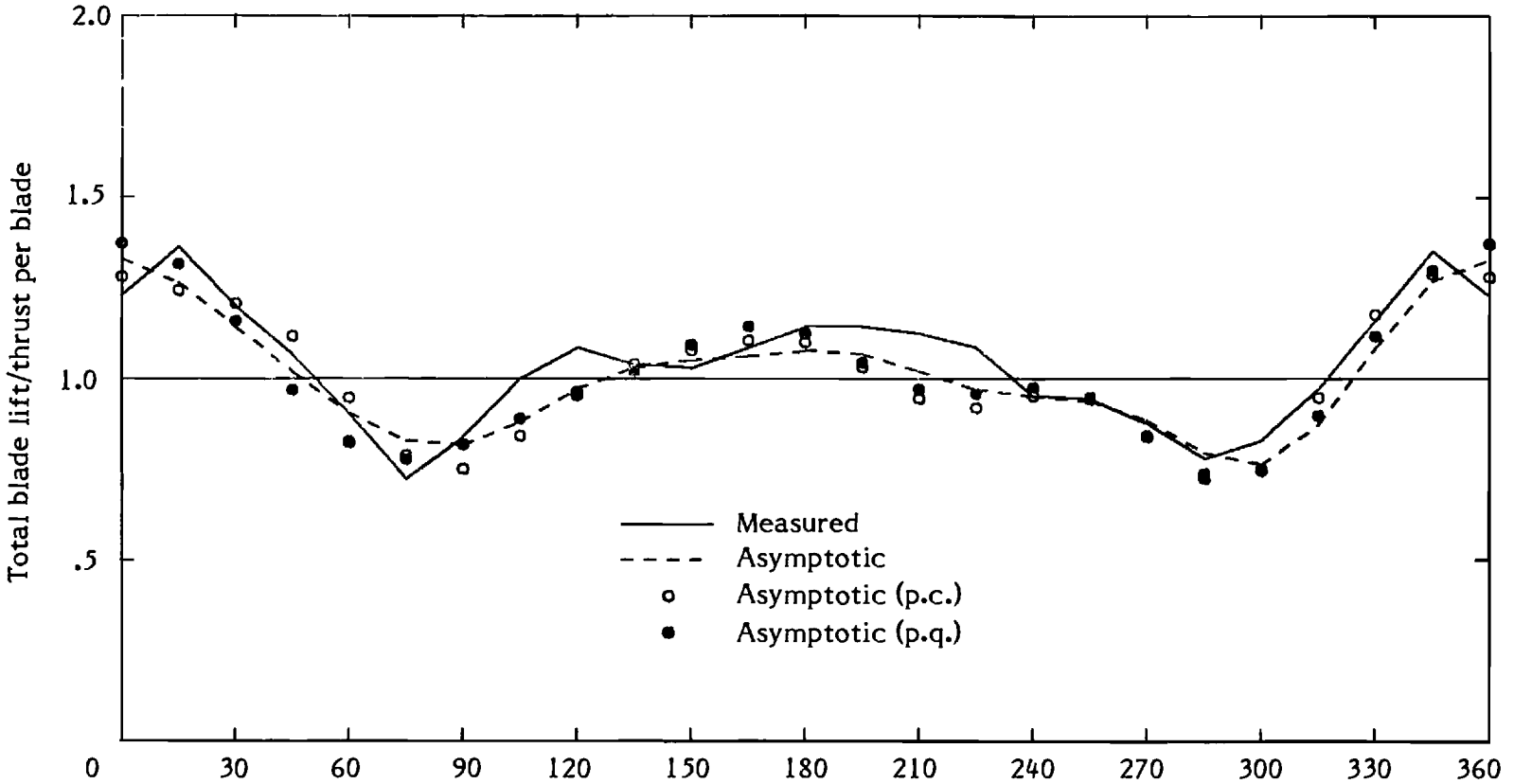

(b) $\mu = 0.15$.

Figure 5. - Continued.

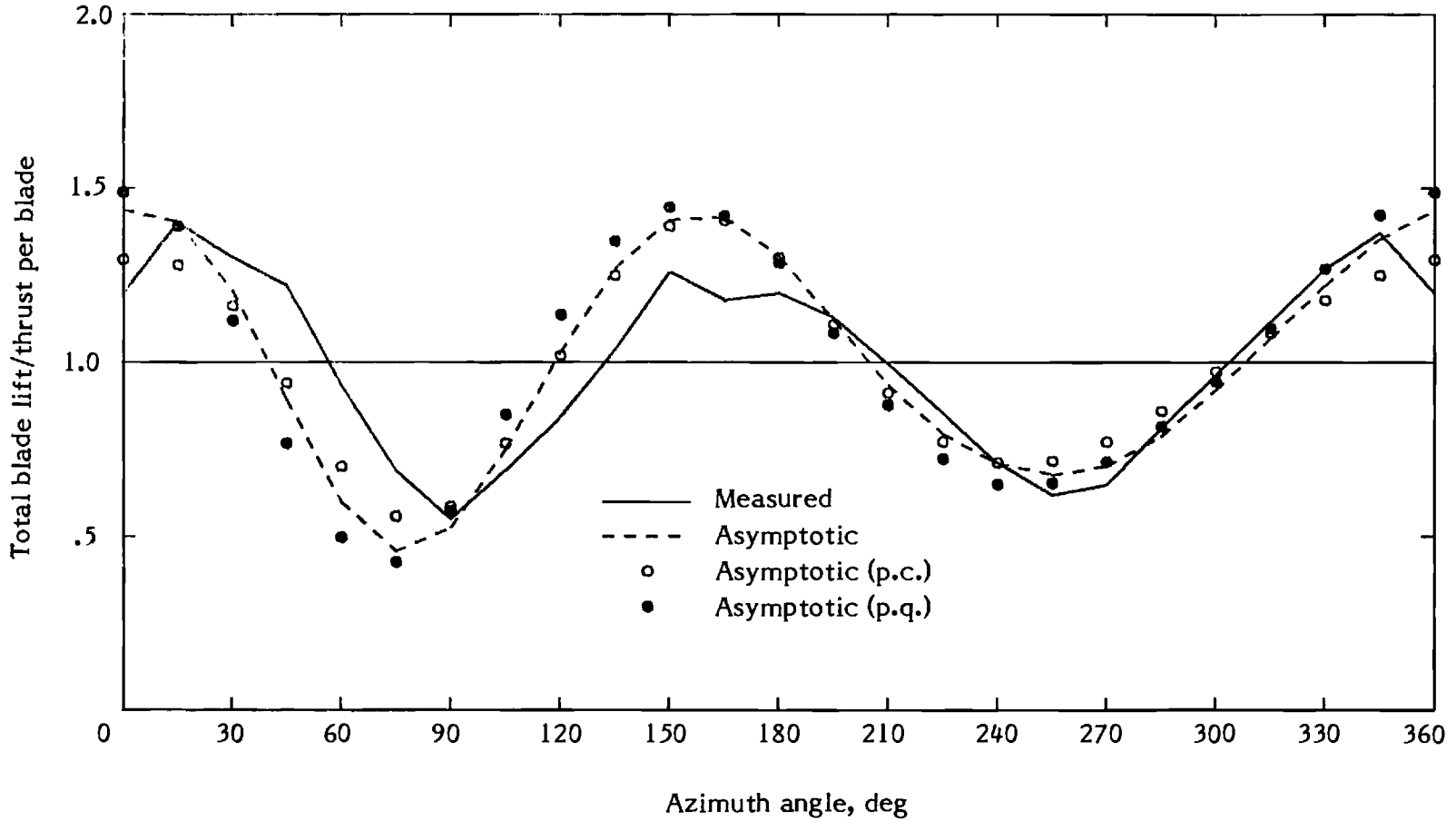

(c) $\mu = 0.29$.

Figure 5. - Concluded.

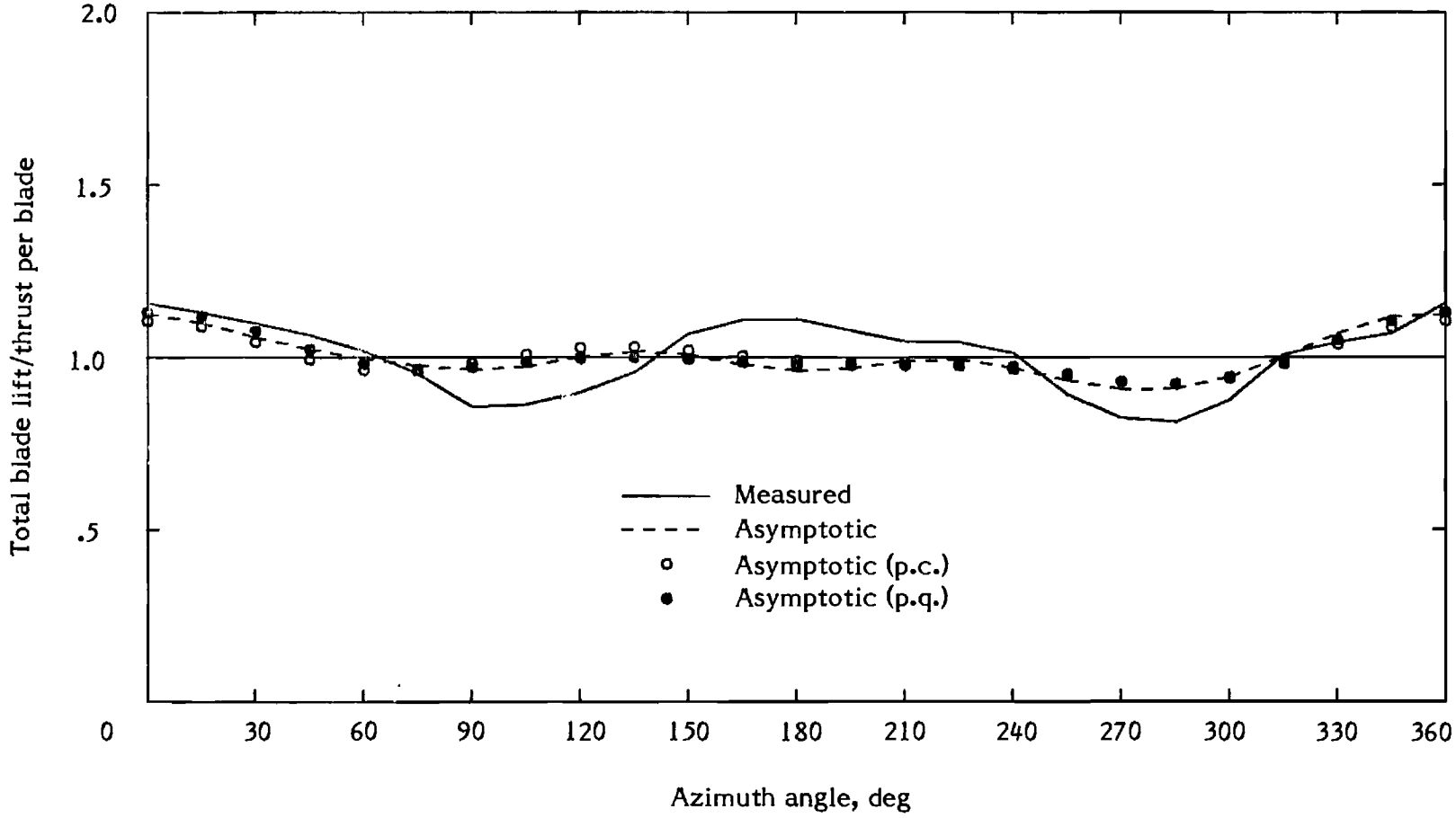

(a) $\mu = 0.06$.

Figure 6. - Total blade lift versus azimuth for Case 2.

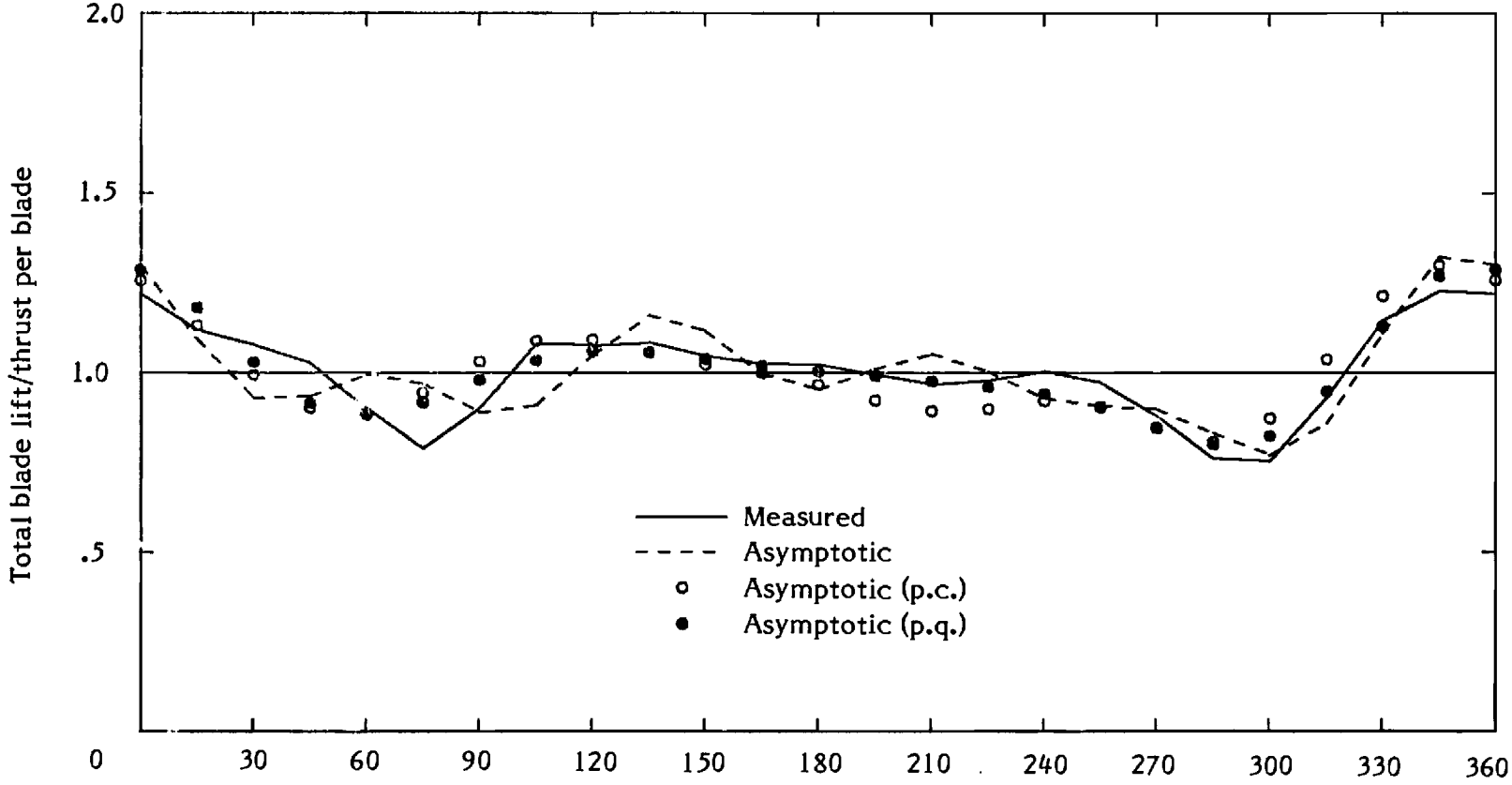

(b) $\mu = 0.13$.

Figure 6. – Continued.

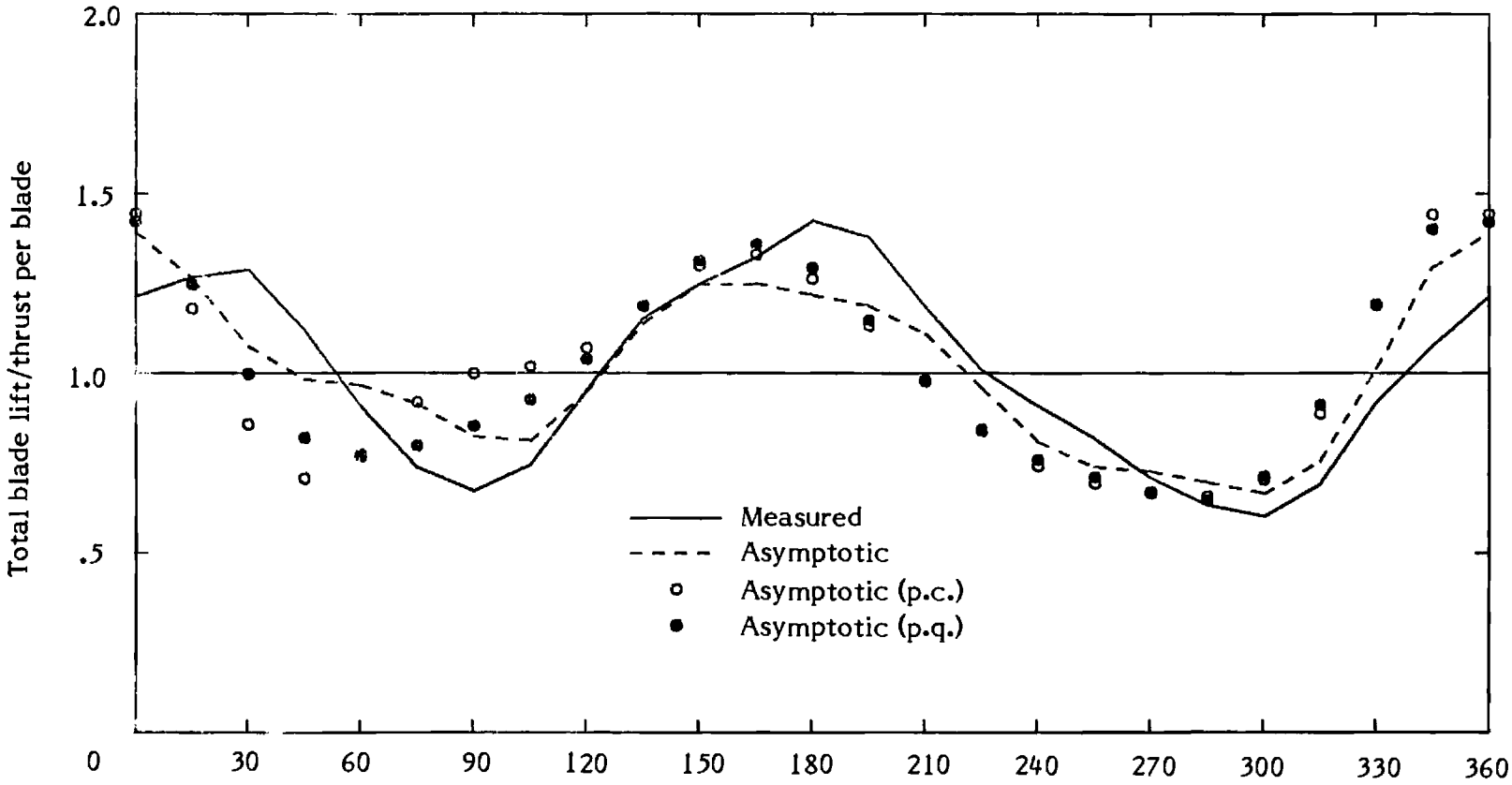

(c) $\mu = 0.29$.

Figure 6. - Concluded.

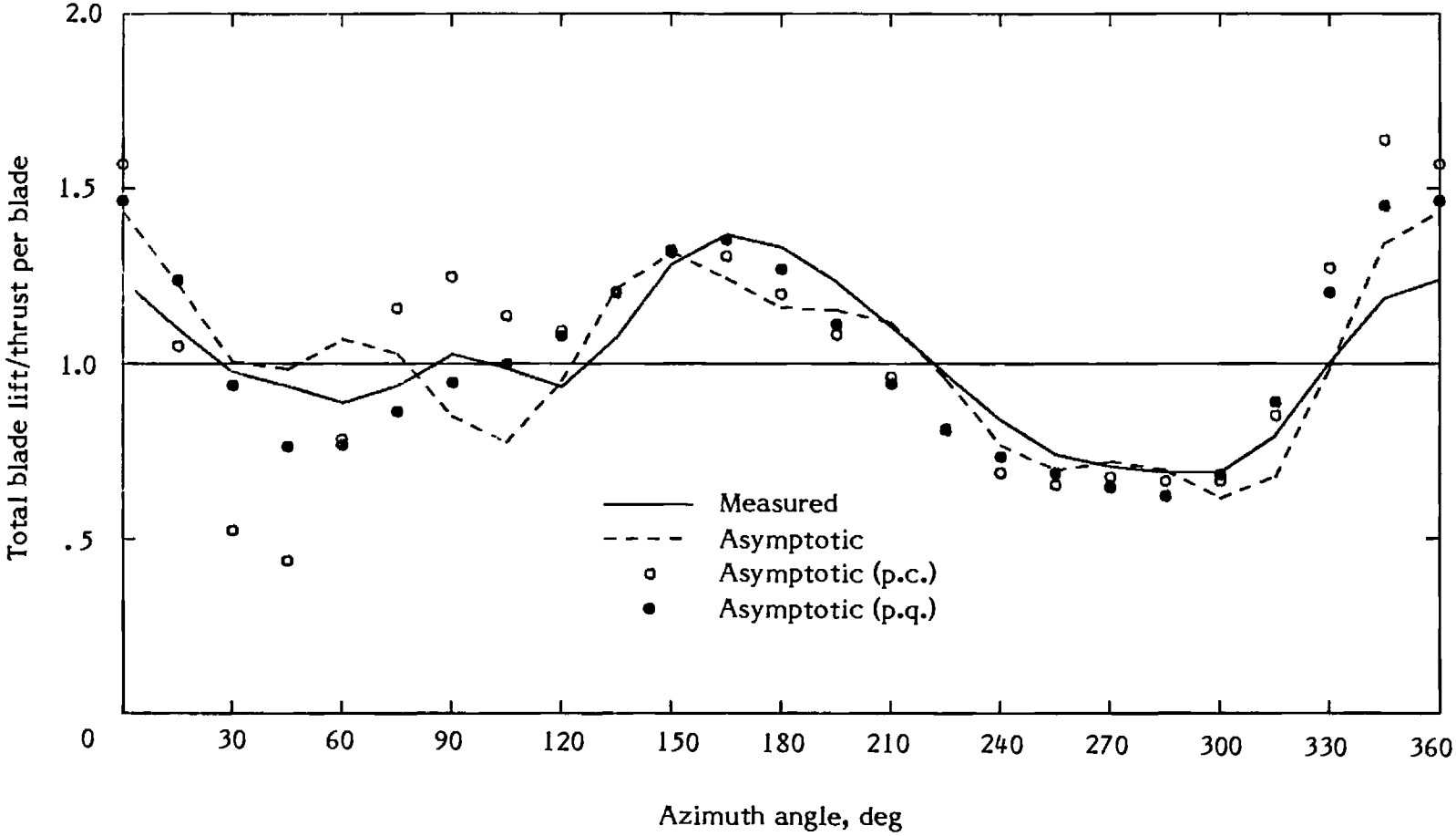

(a) $\mu = 0.29$

Figure 7. - Total blade lift versus azimuth for Case 3.

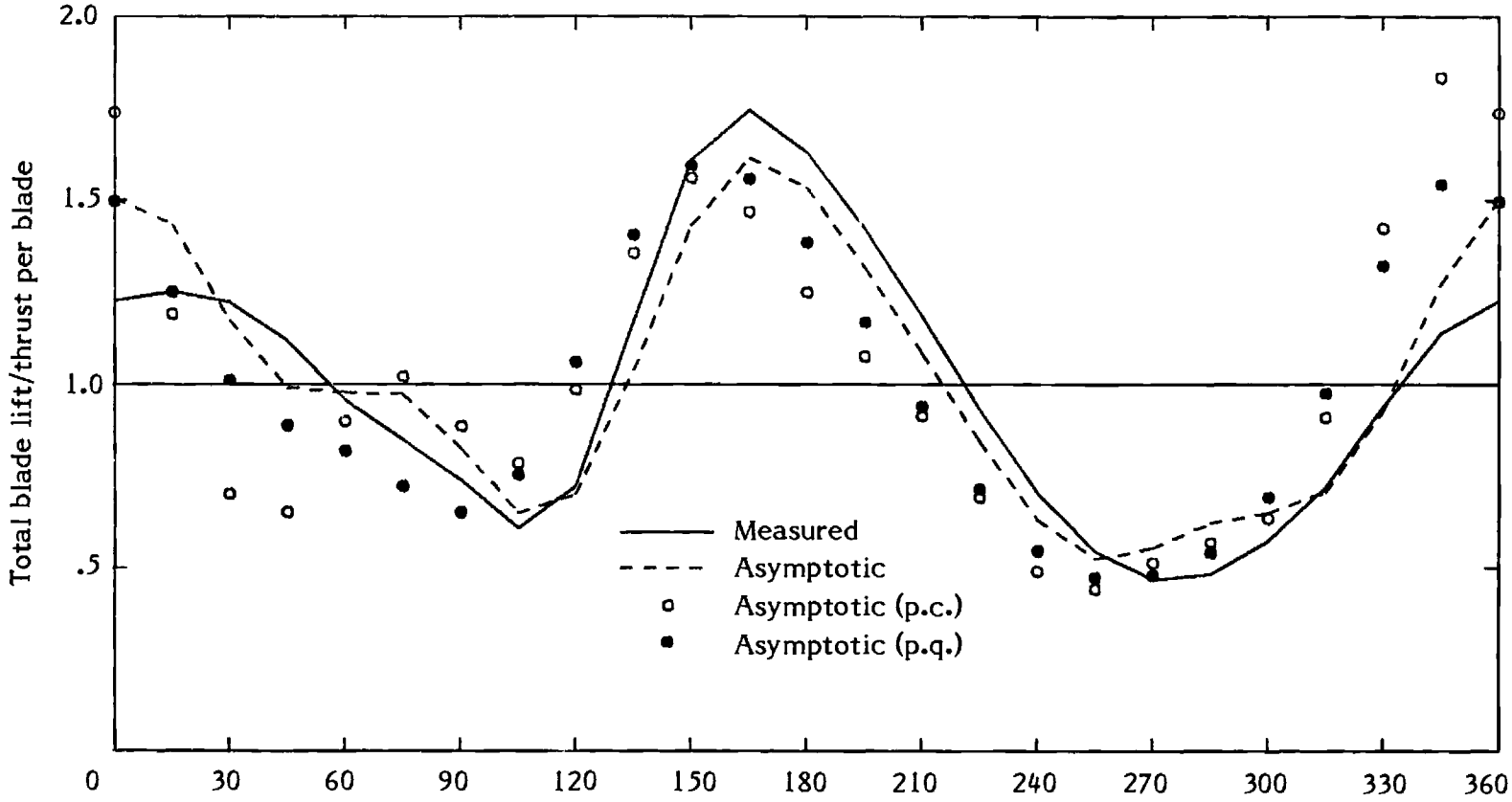

(b) $\mu = 0.39$.

Figure 7. - Continued.

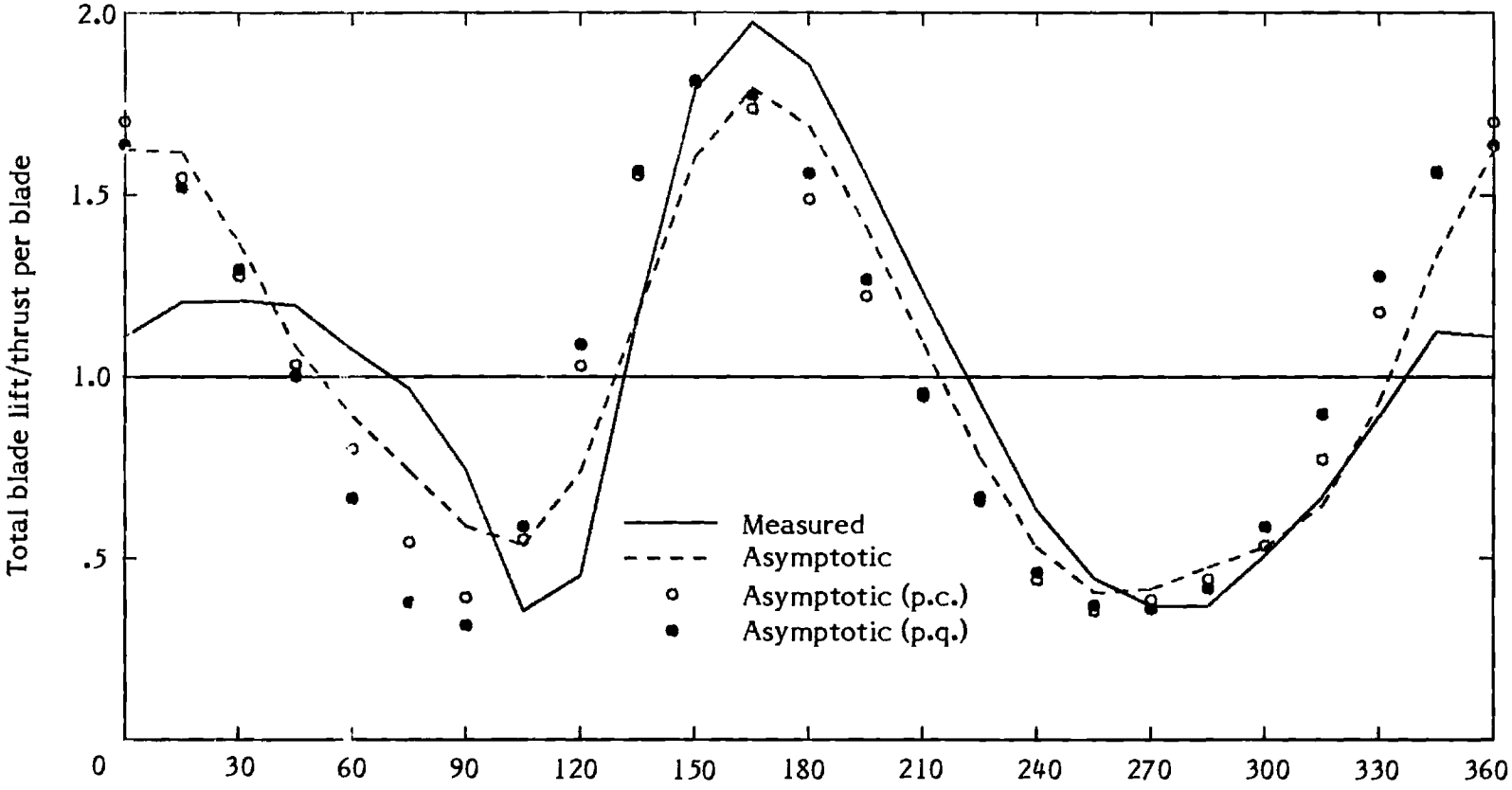

(c) $\mu = 0.45$.

Figure 7. - Concluded.

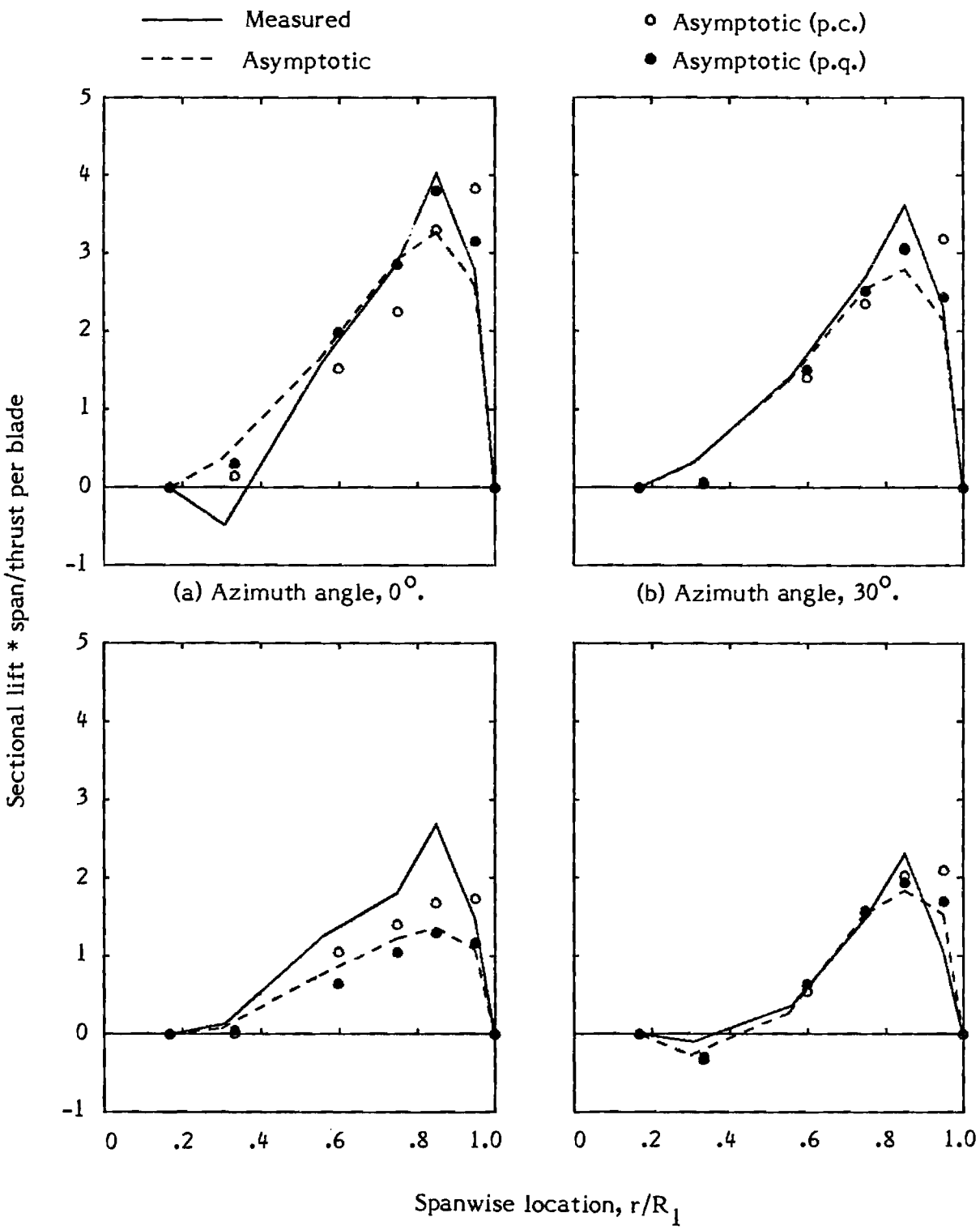

Figure 8. - Sectional lift versus spanwise location for Case 1, $\mu = 0.29$.

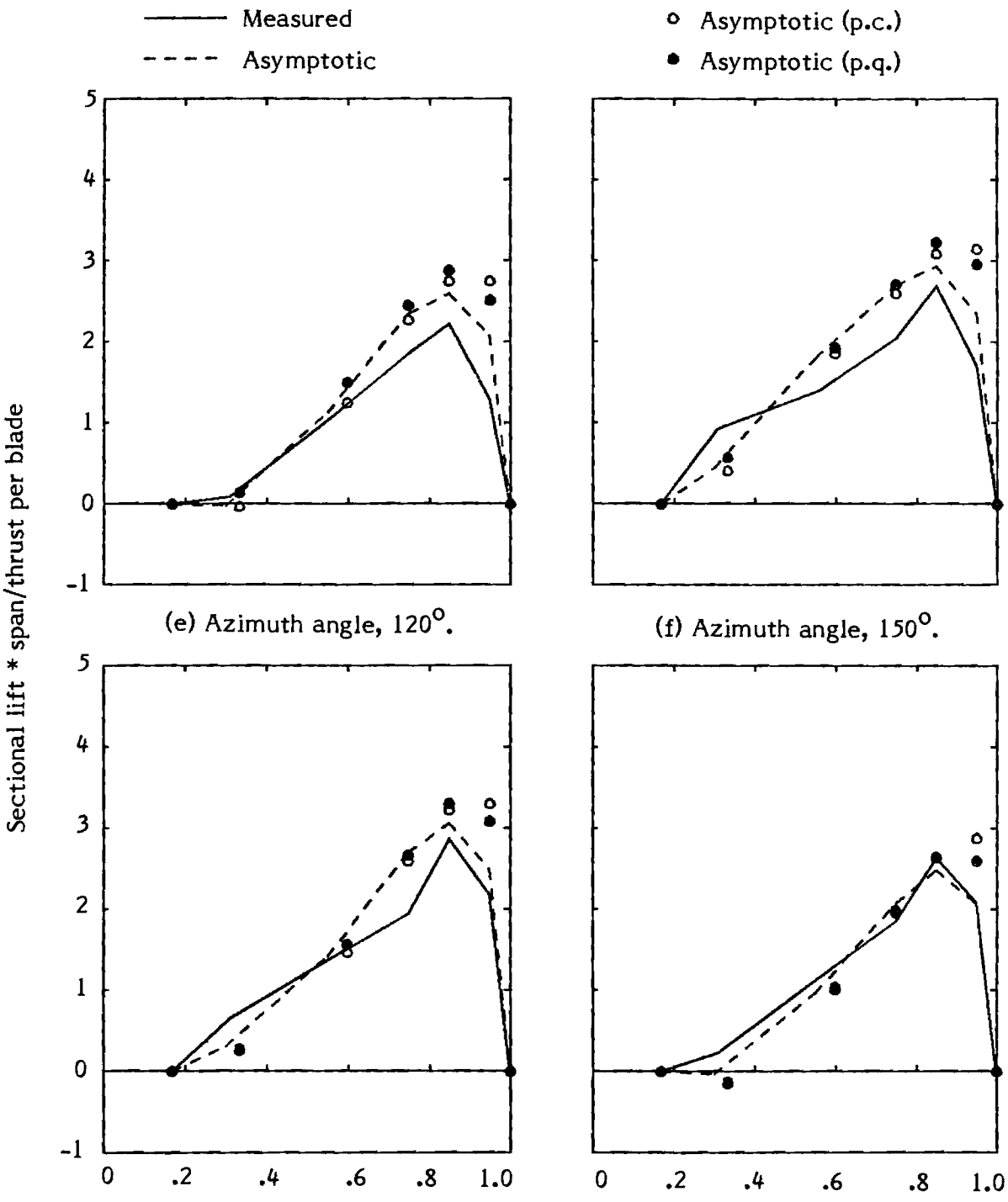

(e) Azimuth angle, 120°.

(f) Azimuth angle, 150°.

(g) Azimuth angle, 180°.

(h) Azimuth angle, 210°.

Figure 8. - Continued.

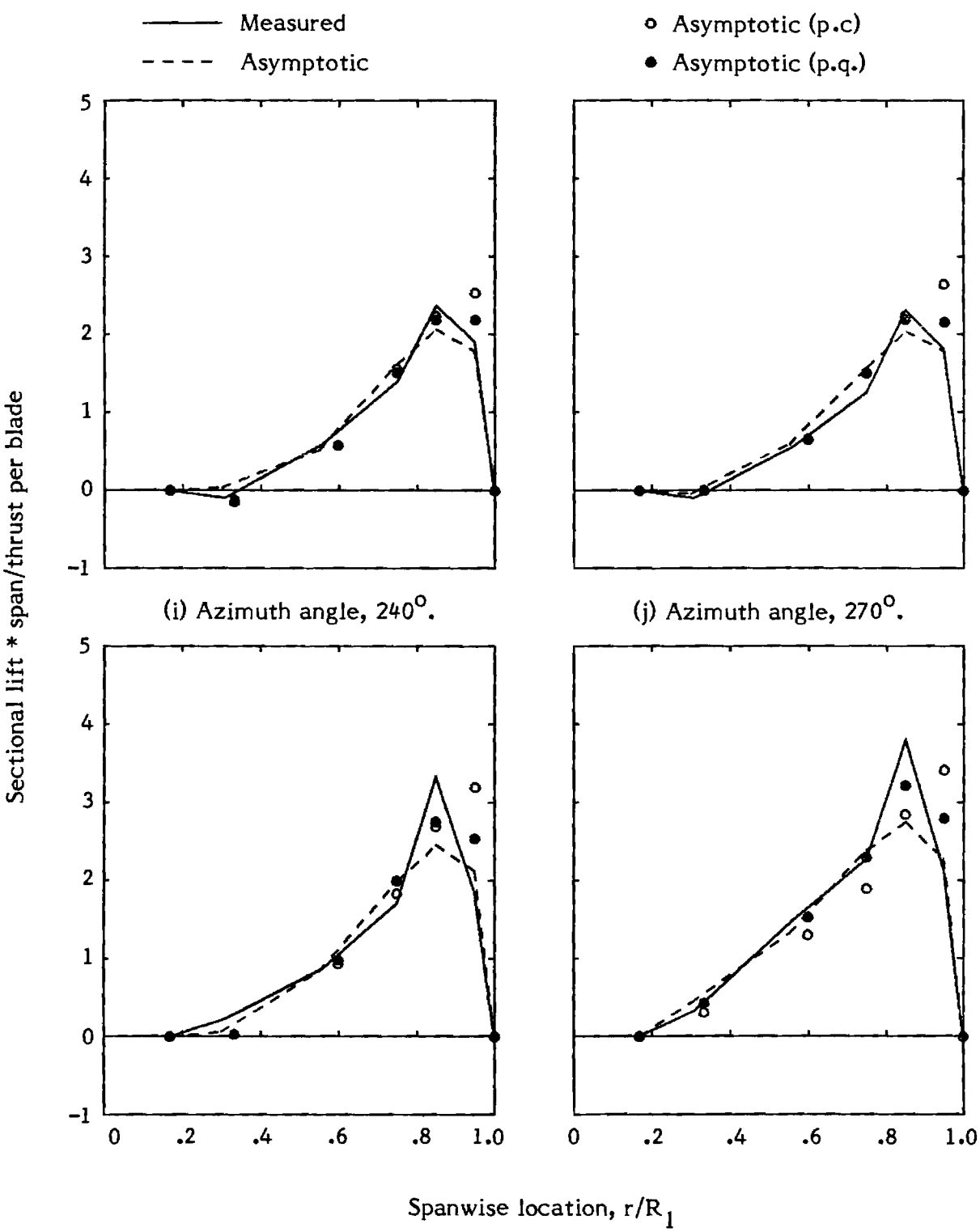

(i) Azimuth angle, 240°.

(j) Azimuth angle, 270°.

(k) Azimuth angle, 300°.

(l) Azimuth angle, 330°.

Figure 8. - Concluded.

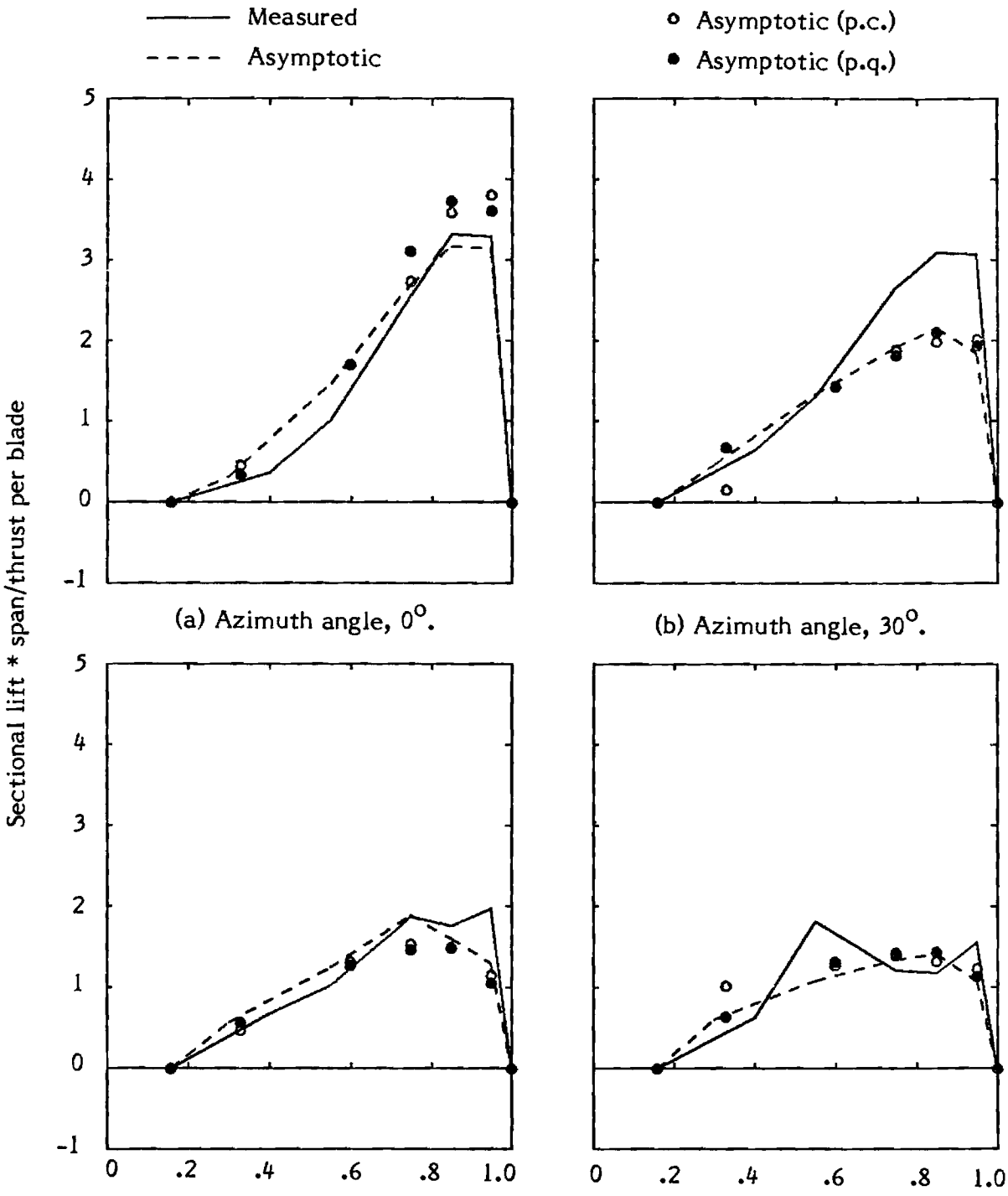

Figure 9. - Sectional lift versus spanwise location for Case 2, $\mu = 0.29$.

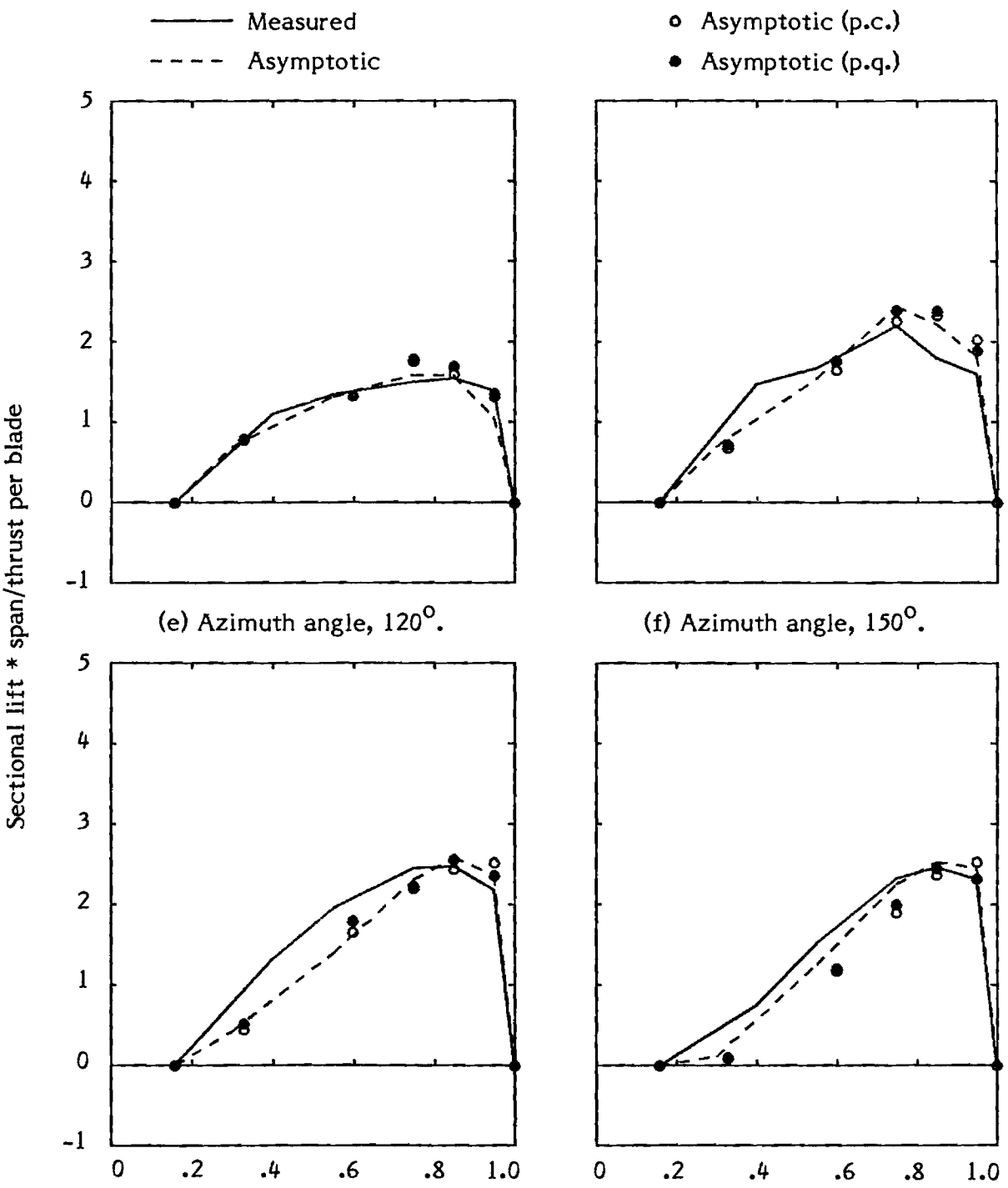

(e) Azimuth angle, 120°.

(f) Azimuth angle, 150°.

(g) Azimuth angle, 180°.

(h) Azimuth angle, 210°.

Figure 9. - Continued.

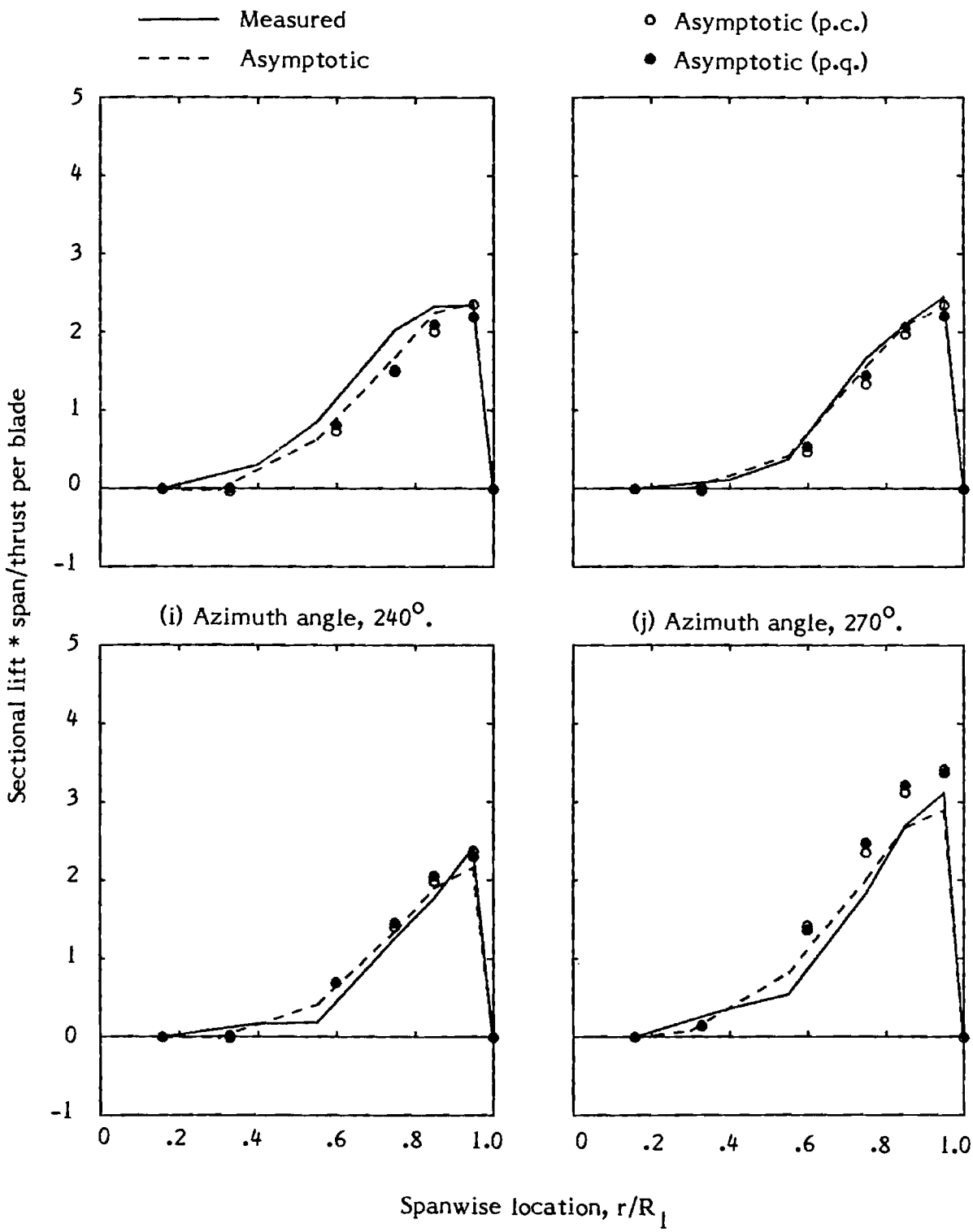

(i) Azimuth angle, 240°.

(j) Azimuth angle, 270°.

(k) Azimuth angle, 300°.

(l) Azimuth angle, 330°.

Figure 9. - Concluded.

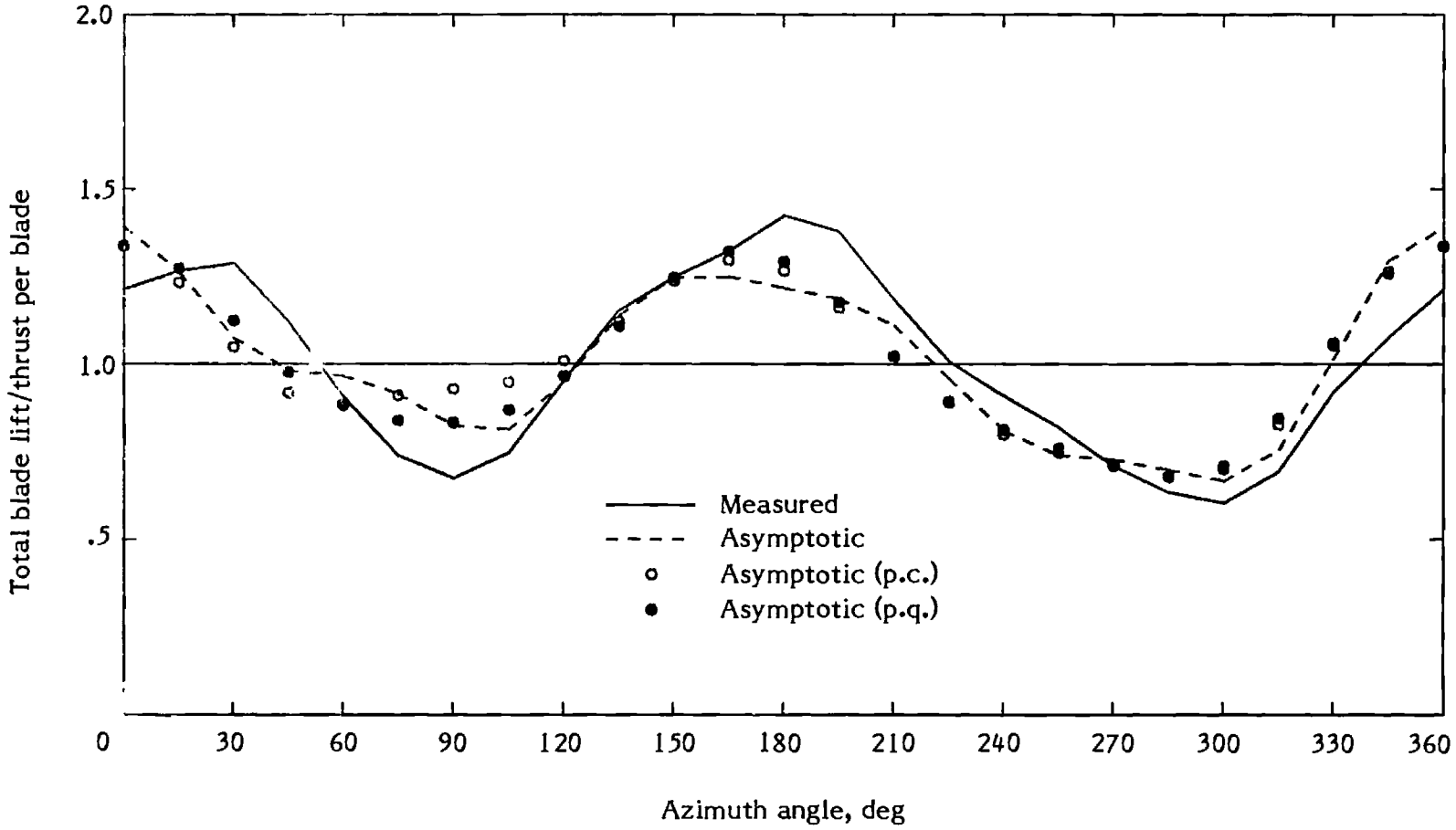

Figure 10. - Computation with constant azimuth spacing of 5^{o}, Case 2, $\mu = 0.29$.

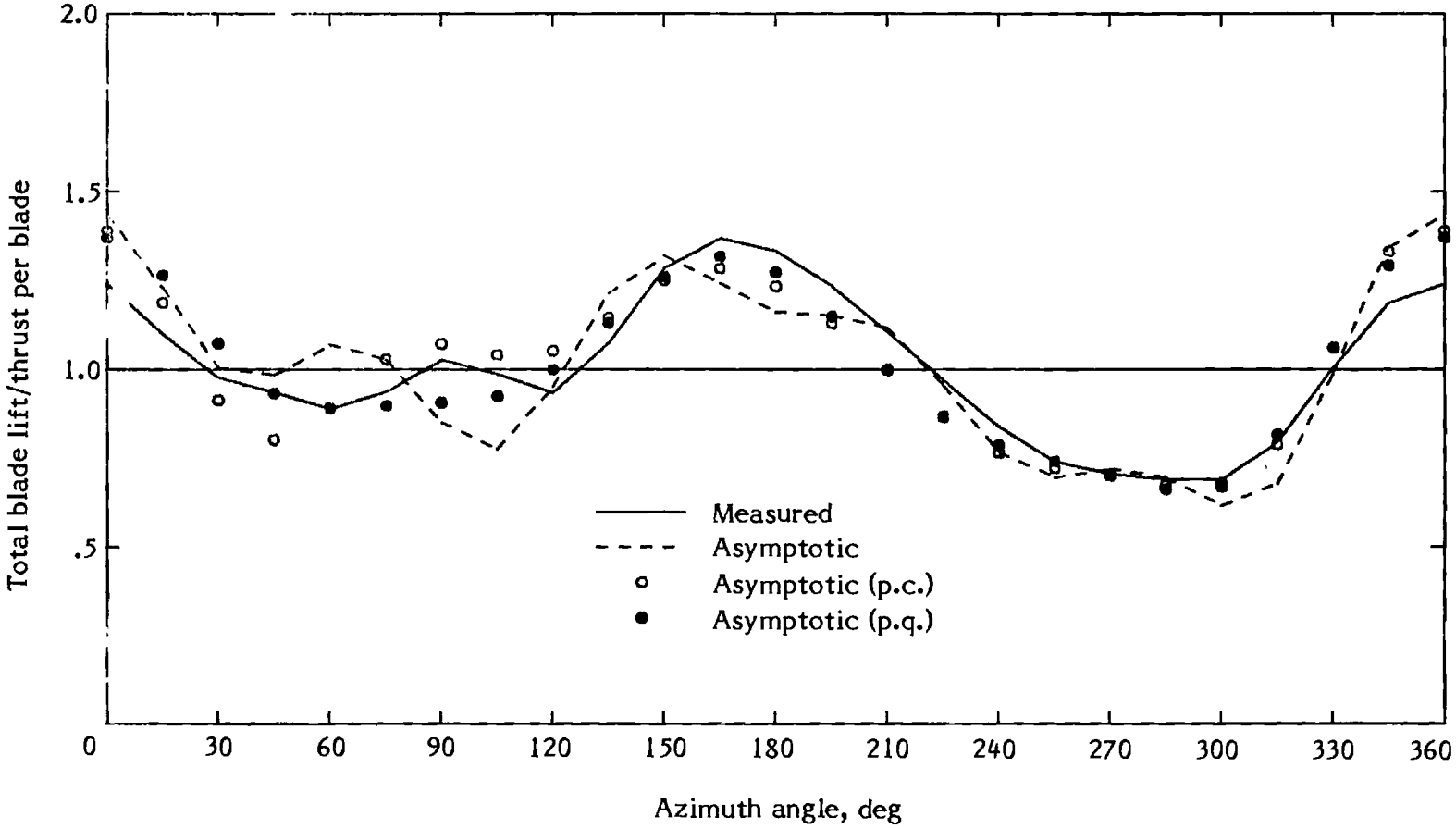

Figure 11. - Computation with constant azimuth spacing of 5^{o}, Case 3, $\mu = 0.29$.

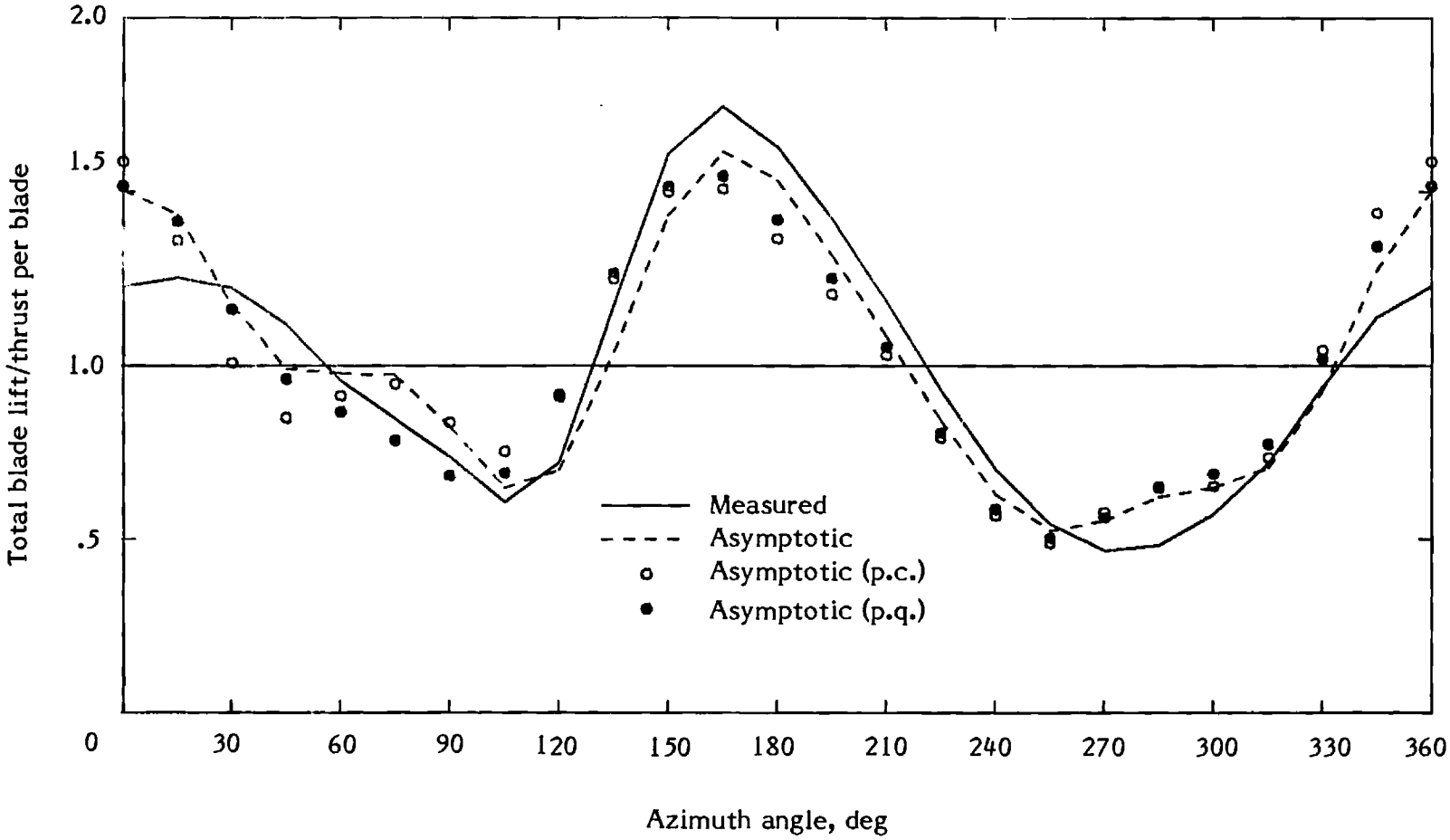

Figure 12. - Computation with constant azimuth spacing of 5^{o}, Case 3, $\mu = 0.39$.

E-16-612

NASA Contractor Report 166092

HELICOPTER ROTOR LOADS USING DISCRETIZED MATCHED ASYMPTOTIC EXPANSIONS

G. Alvin Pierce and
Anand R. Vaidyanathan

Georgia Institute of Technology
A Unit of the University System of Georgia
School of Aerospace Engineering
Atlanta, GA 30332

CONTRACT NAS1-16817

May 1983

National Aeronautics and
Space Administration

Langley Research Center
Hampton, Virginia 23665

HELICOPTER ROTOR LOADS USING DISCRETIZED MATCHED ASYMPTOTIC EXPANSIONS

By

G. Alvin Pierce

and

Anand R. Vaidyanathan

Prepared by

GEORGIA INSTITUTE OF TECHNOLOGY
SCHOOL OF AEROSPACE ENGINEERING
Atlanta, Georgia 30332

Prepared for

NATIONAL AERONAUTICS AND SPACE ADMINISTRATION
Langley Research Center
Contract NAS1-16817

CONTENTS

	Page
SUMMARY	1
INTRODUCTION	1
SYMBOLS	2
DISCRETIZED ASYMPTOTIC REPRESENTATION	4
DISCUSSION OF RESULTS	6
CONCLUDING REMARKS	10
APPENDIX A Piecewise Continuous Representations	12
APPENDIX B Trajectory Approximation and List of Integrals	15
APPENDIX C Integration of Pressure Field	25
APPENDIX D Evaluation of Chordwise and Spanwise Approximations	37
APPENDIX E Final Equations and Output Quantities	43
REFERENCES	49
FIGURES	50

SUMMARY

This investigation is intended to improve the numerical practicality of a matched asymptotic expansion approach for the computation of unsteady three-dimensional airloads on a helicopter rotor. The original method as suggested by Van Holten has previously been evaluated and proven to be a comprehensive and accurate analysis for flight conditions conducive to linear flow phenomena. This effort to decrease the computational requirements of the original analysis utilizes a discretized representation of the doublet strength distribution and helical streamlines. The continuous variation of the doublet strength has been approximated by piecewise constant or piecewise quadratic distributions, and the helical trajectory of a fluid particle has been approximated by connected straight line segments. As a direct result of these simplified representations the computational time required for the execution of a typical flight condition has been reduced by an order of magnitude with respect to the requirements of the original analysis. Airloads which have been computed using the discretized method for a two-bladed model rotor and a full-scale four-bladed rotor are in close agreement with measured results and airloads from the original asymptotic analysis. For conditions characterized by significant rotor/wake interaction the piecewise constant representation requires a reduced azimuth spacing to maintain acceptable accuracy.

INTRODUCTION

The problem of estimating airloads on helicopter rotor blades can be approached by a variety of approximate methods. One such approach, put forward by Van Holten (refs. 1-4), uses an acceleration potential description of the flow field and a matched asymptotic expansion technique. Under the assumption of incompressible potential flow the unsteady three-dimensional airloads on a rotor blade in forward flight are calculated to a consistent order of approximation in terms of the aspect ratio.

A study has been conducted (ref. 5) to examine the theoretical basis and computational feasibility of the method, and to evaluate its performance and range of validity by numerical comparison with experiment and other approximate methods. The study concluded that, within the restrictions of linear theory (i.e., small disturbances), the Van Holten approach does lead to a valid description of the rotor flow field and a systematic determination of the airloads on the rotor blade. It was also found for flight conditions involving significant blade/wake interaction effects, the agreement between computation and measurement is poorer than in other cases.

The analysis in Van Holten's approach leads to an integral equation for the blade doublet strength distribution (eq. (8), ref. 5). This is solved using a collocation technique, which consists of assuming the unknown function to be made up of a combination of suitable spanwise modes and azimuthal harmonics, and satisfying the integral equation at an equal number of points distributed over the rotor disk. The result is a set of linear, simultaneous algebraic equations. However, setting up the equation at any collocation point requires integration with respect to azimuth of the individual assumed mode combinations. This numerical integration makes up the bulk of the total computation required for the solution. Under conditions of low forward speed and low inflow (when a larger azimuth range must be covered with a finer integration step) and/or a larger number of blades, the computation time is significantly increased. As an example, for a two-bladed rotor at an advance ratio of 0.3, the computer program

takes about 250 seconds to execute on a CDC 6400 computer. For other conditions, the time would vary approximately in direct proportion to the number of blades and in inverse proportion to the forward speed (advance ratio). In addition, when interaction effects are judged to be significant (possible even at moderate to high forward speeds), a smaller integration step will have to be used.

It would therefore be desirable to seek a simplified computational scheme for the basic asymptotic approach that would lead to significantly lower computation time without sacrificing any of the essential features of the asymptotic method. One possibility is to consider the analogous situation in the vortex representation of rotor wakes. In the vortex approach, the continuously varying bound circulation on the blade generates a wake in the form of a helical vortex sheet of continuously distributed trailing and shed vorticity. Calculation of the induced velocity due to such a wake would require double integration over the wake surface, which can be time-consuming. In practice, this problem is often overcome by assuming that the variation of the blade bound circulation over the span and the azimuth takes place in discrete, finite steps. This results in a wake of discrete trailing and shed vortex elements. Since the velocity induced by a straight vortex element can be analytically expressed, the induced velocity due to the entire wake can be written as a summation of analytical expressions representing the contribution of individual trailing and shed vortex elements. This results in considerable reduction of computational time over the exact numerical integration.

It appears that a similar simplification could be achieved by approximating the continuous variation of the doublet strength distribution in the asymptotic approach. It is the purpose of the current study to develop a discretized representation for the asymptotic method and compare its performance with the original computational scheme and its results with measured data for the flight conditions considered in reference 5. This report describes the details of the simplified scheme and discusses the computational results. Detailed analytical expressions are presented as Appendices.

SYMBOLS

A	aspect ratio
a_o	coning angle
a_1, b_1	blade flapping coefficients
B	number of blades
b, c	semi-chord and chord, repsectively
c_{1j}, c_{2j}, c_{3j}	coefficient of piecewise quadratic representation (eq. (A1))
d	distance between fluid particle and collocation point
d_0, d_1, d_2	coefficients of quadratic expression for d^2 in terms of θ
d_n	distance between fluid particle and point on the chord at the same spanwise location
d_{n0}, d_{n1}, d_{n2}	coefficients of quadratic expression for d_n^2 in terms of θ
F_2, F_3	terms appearing in the regular part of the near field solution (eq. (E 5))

$G_j^o, G_{jn}^c, G_{jn}^s$	harmonic coefficients in the Fourier expansion of g in terms of ψ_b (eq. (E 1))
g	function representing the doublet strength distribution along the blade, and the basic unknown in the problem
g_j	value of g at the beginning of the j^{th} spanwise segment
I_i^c	i^{th} integral expression for the common part, Appendix B
I_i^f	i^{th} integral expression for the far field, Appendix B
I_i^n	i^{th} integral expression for the near field, Appendix B
L	total lift on one blade (eq. (E 10))
ℓ	lift per unit span, sectional lift, (eq. (E 7))
M	moment of lift distribtuion about the rotor hub (eq. (E 11))
m	sectional pitching moment about quarter-chord, positive nose-down (eq. (E 8))
p	perturbation pressure
R_0, R_1	root and tip radius of blade, respectively
R_i, R_s	coefficients of linear expression for r_b in terms of θ (eq. (B 2))
r	radial distance between fluid particle and collocation point, $\sqrt{x_b^2 + y_b^2}$
r_b	spanwise location of fluid particle
r_{bo}	spanwise location of collocation point
r_0, r_1, r_2	coefficients of quadratic expression for r^2 in terms of θ
r_j	midpoint of j^{th} spanwise segment
s	blade spanwise coordinate
s_j	spanwise location of the beginning of the j^{th} spanwise segment
Δs_j	length of j^{th} spanwise segment
U_T	local effective freestream speed
v_{io}	simple momentum induced velocity
w	induced velocity component in the z direction
Δw	incremental contribution to w
x,y,z x_b, y_b, z_b	rotor coordinate systems (fig. 1)

x_{cp}	chordwise location of center of pressure (eq. (E 9))
X_i, X_s	coefficients of linear expression for x_b in terms of θ (eq. (B 2))
Y_i, Y_s	coefficients of linear expression for y_b in terms of θ (eq. (B 2))
γ	blade inertia coefficient for flapping (Lock number)
ϵ	linear blade twist, root pitch angle-tip pitch angle
θ	azimuth position with respect to reference blade, ($\Psi_b - \Psi_{bo}$)
θ_o	collective pitch angle at blade root
λ	nondimensional rotor inflow, $\mu\alpha_r + v_{io}$
μ	nondimensional rotor forward speed
ξ	R_0, R_1
ρ	air density
ϕ , η	plane elliptic coordinates
χ	meridional angle in cylindrical coordinates
Ψ_b	azimuth position with respect to downwind reference line
Ψ_{bo}	azimuth position of collocation point
$\Delta \Psi_j$	azimuth separation of j^{th} blade from reference blade
Ω	rotor angular velocity

DISCRETIZED ASYMPTOTIC REPRESENTATION

The essential features of the asymptotic approach are retained in the discretized representation, i.e., the blade pressure field is obtained in composite form as the sum of far field, near field and common part expressions in such a way that the composite field reduces to the near and far field solutions in the near and far field regions, respectively. In view of the approximations being considered, it is not known if it would be consistent to retain the terms of $O(1/A^2)$ that are present in Van Holten's analysis (ref. 1). For the sake of simplicity in computation these terms are dropped in the present study,so that the discretized representation is of $O(1/A)$, comparable to standard lifting-line formulations.

The approximations to be introduced are:

(1) The continuous variation of the unknown blade doublet strength distribution over the range of blade span and azimuth is replaced by simple, piecewise continuous functions over suitable subintervals of span and azimuth.

(2) The helical trajectory of a freestream fluid particle relative to the blade is replaced by a series of connected straight line segments.

Over the azimuth, the doublet strength variation is assumed to be piecewise constant, i.e., its value is constant over each subinterval of azimuth. Over the span, it is approximated by a piecewise constant or a piecewise quadratic variation, the latter providing a more accurate spanwise representation at the cost of more complicated algebra. Appendix A describes the manner in which these representations are

formulated, while typical representations are illustrated in figures 2(a) and 2(b).

The basic problem is the calculation of the vertical velocity induced on the blade by its pressure field, as given by the relation

$$w = -\int_{-\infty}^{\Psi_{bo}} \frac{\partial p}{\partial y_b} \, d\Psi_b \qquad (1)$$

The rotor coordinate systems are shown in figure 1 and Ψ_{bo} is the azimuth position of the reference blade. The blade pressure field is written in composite form as

$$p = p_{far} + p_{near} - p_{common}$$

By appropriate construction and matching (ref. 1), all three components can be expressed in terms of the doublet strength distribution along the lifting line.

In Van Holten's analysis, the far pressure field is the field of a dipole line along the quarter-chord location and is expressed as a series of associated Legendre functions in terms of prolate spheroidal coordinates. The near pressure field is the local two-dimensional field of the section and is expressed in plane elliptic coordinates. The common part corresponds to the behavior of the far field solution in the near field or, equivalently, that of the near field solution in the far field. With the form of the pressure field established, the induced velocity is calculated by numerical integration of the composite pressure gradient, for which purpose the above expressions are convenient. In fact, one of the merits of Van Holten's approach is that the composite pressure field is given by a direct expression free of integrals, so that the induced velocity calculation requires only one numerical integration.

However, these expressions are not convenient for the purpose of applying the proposed approximations. To O(1/A), the far field is the field of a dipole line along the blade midchord location, and can be written as the spanwise integral of a distribution of three-dimensional doublets. If the approximations described above are introduced, it is found that the calculation of the induced velocity due to the far field reduces to a double summation (over spanwise and azimuthal segments) of fairly simple integrals that can be analytically evaluated. Likewise, the near field is written as the integral, over the chord, of a two-dimensional doublet distribution, of strength proportional to the surface pressure differential. The chord is divided into a suitable number of segments over each of which the pressure differential is assumed constant, at its average value on that segment. With this simplification, the induced velocity due to the near field also becomes a double summation (over chordwise and azimuthal segments) of analytical expressions. The contribution of the common part, which is the field of a single two-dimensional dipole, presents no problems. The complete details of the various steps pertaining to the above calculations are presented in Appendices B and C. Appendix B describes the result of approximating the trajectory and also presents a list of integral expressions to be used for the induced velocity calculation. Appendix C derives the summation expressions for the induced velocity due to the far field, common part, and near field, for both the piecewise constant and the piecewise quadratic representation of the doublet strength variation along the span. Appendix C also demonstrates that the expressions derived for the far field and the common part correctly cancel in the vicinity of the blade, thus verifying their asymptotic character.

In summary, the effect of the discretized representation on the problem is to reduce the induced velocity integration of equation (1) to a summation of analytical

expressions. The normal velocity boundary condition is then applied by setting this induced velocity equal to the normal velocity on the blade surface due to blade motion. The form of this equation is given in Appendix E (eq. (E 2)). The unknowns to be solved for are the discrete values of the doublet strength at the spanwise segment midpoints, at discrete azimuth locations. However, for final presentation as output, the discrete variation with azimuth would have to be fitted by an interpolation curve. This is accomplished by substituting into equation (E 2), for the azimuth variation of each midpoint value, a harmonic interpolation formula given by (E 3). It must be noted that this does not imply a continuous azimuthal variation in the induced velocity calculation, since the doublet strength is still held constant over each azimuth segment. The advantage of the substitution is that the interpolation coefficients are obtained directly and available for calculation of output data at desired azimuth locations. Expressions for the various quantities calculated for presentation as output are given in Appendix E.

Examination of equation (E 2) shows that the near field induced velocity contains a contribution from the regular solution, proportional to the blade motion parameters. If these parameters are considered known, this contribution should be taken together with the blade normal velocity term. However, if any or all of the blade motion parameters (collective pitch, coning angle, cyclic pitch coefficients) are considered unknown, additional equations must be generated to solve for them. This can be done by using the following conditions:

(1) Azimuth average of the total lift due to all blades should equal the known rotor thrust.

(2) Flapping moment equilibrium should exist about the rotor hub.

If only first harmonic flapping is considered, the second condition yields three equations (zeroth harmonic, first harmonic cosine and first harmonic sine components). These additional equations are also listed in Appendix E, for the piecewise constant and piecewise quadratic representations.

DISCUSSION OF RESULTS

The discretized representations which have been incorporated in the analysis have been numerically evaluated to ascertain their potential accuracy. All analytical details of this evaluation are presented in Appendix D. Figure 2 illustrates the piecewise constant and quadratic representations of the spanwise distribution of doublet strength for a typical condition.

For the near field chordwise approximation, an airfoil with a steady two-dimensional pressure distribution is considered. The induced vleocity of a fluid particle travelling parallel to the chord is calculated for various vertical distances from the airfoil. The calculation is performed using both the exact solution and the approximation. The results are tabulated in Appendix D (table D1) and plotted in figure 3. It can be seen that the approximations with three segments and five segments across the chord are acceptably close to the exact solution, even at very small vertical distances. This simple example shows that, as far as the induced velocity calculation is concerned, even a relatively crude representation of the surface pressure distribution is sufficient.

For the spanwise approximations of the far field solution, a finite wing is considered with a spanwise distribution of a form which is typical of a rotor blade distribution. The induced velocity due to this distribution is calculated for a fluid particle travelling parallel to the chord, at various spanwise locations and vertical distances. The calculation is performed using the exact solution as well as the piecewise constant and piecewise quadratic approximations with three and five

spanwise segments. The results are tabulated in Appendix D (tables D2 and D3) and plotted in figure 4. With the three segment model, it can be seen that both approximations deviate from the exact solution when close to the wing, the deviations being more marked near the loaded tip and generally greater for the piecewise constant representation. With five segments, the piecewise quadratic representation is nearly identical to the exact solution while the piecewise constant results still show significant deviation very close to the wing. It may be noted that the exact and approximate results tend to merge with increasing distance from the wing, as is to be expected. It may also be noted that the results for different spanwise locations tend to merge with increasing vertical distance.

Airload computations have been carried out for the same experimental cases considered in reference 5, viz, (1) a two-bladed teetering model rotor at forward speed/tip speed ratios (μ) of 0.08, 0.15, 0.29 (ref. 6), (2) a four-bladed articulated full-scale rotor tested in flight, at μ =0.06, 0.13, 0.29 (ref. 7), and (3) the same four-bladed rotor tested in a wind tunnel at μ = 0.29, 0.39, 0.45 (ref. 8). The geometric and flight conditions are listed in table 1, which is reproduced from reference 5. The measured results are compared with computations using the piecewise constant (p.c.) and piecewise quadratic (p.q.) representations, as well as Van Holten's computational scheme. Before proceeding with a discussion of these comparisons, some comments regarding the computations are in order. In the original scheme, the numerical integration is carried out with a 5-point Gauss-Chebyschev rule over a suitable subinterval of azimuth, to be properly chosen for accurate computation. In the discretized representation, there is no numerical integration but a choice has to be made with regard to a suitable azimuth subinterval over which the trajectory is straightened. In both cases, the smaller the azimuth subinterval chosen, the more exact are the computations. In order to keep the computation economical and at the same time achieve some of the accuracy of small azimuth spacing, the procedure adopted is to use a "normal" spacing whenever the fluid particle is not close to the blade and a "reduced" spacing whenever it is close to a blade. Reference to figure 1 shows that the trajectory locations at which the fluid particle is directly over a blade are characterized by $x_b = 0$. For each collocation point (r_{bo}, Ψ_{bo}) these azimuth positions are determined in advance using equation (B 1). During the azimuth integration (or summation), a reduced spacing is used in the vicinity of these locations. In the computations carried out here (unless otherwise mentioned) the normal and reduced azimuth intervals used were 15^o and 5^o for the Van Holten scheme and 30^o and 10^o for the discretized representation. Although results of computing with the original scheme were reported in reference 5, these results were recomputed for the present study using normal and reduced spacing as above, and with spanwise collocation points at r/R_1 = 0.30, 0.55, 0.75, 0.85, 0.95. Due to these changes, some differences will be noted between the curves presented here and the corresponding ones in reference 5, but the differences are generally small with one exception which will be pointed out later on. For the discretized representation five spanwise segments were used, with end points at $r/R_1 = R_0/R_1$, 0.5, 0.7, 0.8, 0.9, 1.0, and five chordwise segments with end points at x/b = - 1.0, - 0.9, - 0.6, 0.0, 0.5, 1.0.

Results for the variation of total blade lift as a function of azimuth position for Case 1 are shown in figure 5. It can be seen that for all three forward speeds, the results of the discretized representation are quite close to the original scheme, with the p.q. representation being generally a little closer than the p.c. representation.

For Case 2, the results are illustrated in figure 6 and, as may be anticipated from the computations reported in reference 5, there is greater variation here, mainly for μ = 0.13 and μ = 0.29. At μ = 0.13, the original scheme results in a considerably wavy

TABLE I. - GEOMETRIC AND FLIGHT CONDITIONS FOR THE EXPERIMENTAL CASES

Case	Aspect ratio, A	Number of blades, B	Root Ratio, R_o/R_1	Linear twist, ε, deg.	Rotor angle, α_r, deg.	Thrust coefficient, C_T	Lock number, γ	Advance Ratio, μ	Wake Spacing, $\frac{2\pi w_r}{\Omega B R_1}$
1 (ref.21)	5.4	2	0.17	0	0	0.00367	-	0.08	0.069
					2.0	0.00482	-	0.15	0.067
					6.7	0.00394	-	0.29	0.128
2 (ref. 22)	17.2	4	0.16	8	0	0.00499	11.4	0.06	0.055
					0.6	0.00501	11.4	0.13	0.032
					6.1	0.00571	9.6	0.29	0.064
3 (ref. 23)	17.2	4	0.16	8	5.0	0.00357	10.0	0.29	0.049
					4.0	0.00366	9.9	0.39	0.050
					4.8	0.00334	10.1	0.45	0.065

distribution which is not seen in the results of the discretized scheme, especially with the p.q. representation which remains close to the measured curve except near the advancing blade position. At $\mu = 0.29$, there is once again a deviation near the advancing blade position, with the p.c. results being particularly bad in this region. The p.q. results are generally close to the original ones. However, both results from the discretized scheme tend to overestimate the lift in the disk trailing edge region (around $\Psi_b = 0^o$).

The results for Case 3 are presented in figure 7. It was observed in reference 5 that the original results showed a tendency to overestimate the lift near the downwind azimuth position and correspondingly underestimate it near the upwind position. This tendency is also present in the results from the discretized representations. This may be due to the increasingly important effect of radial flow (along the blade span) in these regions at moderate to high forward speeds. The influence of radial flow is primarily on the spanwise development of the blade boundary layer, increasing with forward speed, and must be accounted for empirically. Otherwise, the p.q. results are acceptable and show the same trend as the measured curves. However, the p.c. results show particularly significant deviations for $\mu = 0.29$ and $\mu = 0.39$, near the advancing blade position and in the disk trailing edge region. It was noted earlier that the changes made in the original scheme produced only small variations with one exception. This exception is $\mu = 0.39$ of Case 3. Comparison of figure 19 of reference 5 with figure 7(b) of the present study reveals that the latter variation is much better, particularly in the absence of the large peak near the disk trailing edge that is present in the former. This difference is surprising, at first glance, because the changes made do not seem that important. Apart from using a constant azimuth spacing, the original version of the computational scheme also used spanwise collocation points at $r/R_1 = 0.40, 0.55, 0.75, 0.85, 0.95$, differing from the present version only in the innermost point. Both programs use the zero lift condition instead of the normal velocity boundary condition at a collocation point whenever the local effective freestream speed $U_T < 0.1$. However, if $r/R_1 = 0.4$ is used, there is a collocation point near the retreating blade position that has $U_T = 0.105$, which is small yet large enough to escape the zero lift condition. It is apparently this particular point that is the source of the trouble, for when it is replaced by another collocation point with $U_T > 0.2$, the resulting distribution is quite regular (like figure 7(b) of the present study). This situation does point out the need to use care in the choice of collocation points (avoiding those points with small positive values of U_T) and use of close azimuth spacing in those cases where interference effects are significant.

Spanwise distributions of sectional lift, at various azimuth positions, are plotted in figure 8 for $\mu = 0.29$ of Case 1, and in figure 9 for $\mu = 0.29$ of Case 2. General comments on these curves are much the same as those made for the original scheme in reference 5. Agreement is acceptable as long as the measured curves do not show any sharp variations, as in the case of close interaction with a tip vortex. When sharp variations do occur, they are not evident in the computed curves. There is also general deviation from the measured curves in the tip region. In addition, the falloff to zero at the tip is better with the piecewise quadratic represenation, presumably because it provides a better approximation to the actual curve than the piecewise constant representation.

In discussing the total lift variations it was noticed that the p.c. representation led to particularly significant deviations for three flight conditions , viz, $\mu = 0.29$ of Case 2, $\mu = 0.29$ and $\mu = 0.39$ of Case 3. To test the possibility of improvement with smaller azimuth spacing, these three cases were computed again with a constant

azimuth subinterval of 5° and the results are shown plotted in figures 10 to 12. It can be seen that there is considerable improvement in the results for the p.c. representation, while the p.q. results are only slightly changed. This is a clear indication that, for flight conditions involving significant interaction effects, the results from the p.c. representation are sensitive to the azimuth spacing used and should be calculated with a small spacing.

Since the primary objective of this investigation is to improve the numerical practicality of the original asymptotic execution time requirements, it is essential that these requirements be examined. Table 2 presents results suitable for comparison of the different representations for two typical rotor configurations. In addition to the original continuous representation suggested by Van Holten and the piecewise constant and quadratic representations of this study, there is also presented data for the segmented lifting line model with a discrete vortex wake. This was the only linear method considered in reference 5 which provided airloads of an accuracy which could be compared with the asymptotic method. It can be observed from table 2 that the piecewise constant representation reduces the execution time requirement of the original continuous representation by a factor of seven. A reduction to almost one fifth is attained for the piecewise quadratic simulation. As indicated in the table, these figures are based on computational azimuth intervals of 30° normal and 10° reduced spacing. In cases where much shorter intervals are required for the piecewise constant representation the computational requirements are proportionately increased as illustrated in Table 2. It should be noted that the computational efficiency of the piecewise constant representation is equivalent to the less comprehensive segmented lifting line with a discrete vortex wake when the azimuth intervals are the same.

TABLE 2. - COMPARATIVE COMPUTER EXECUTION TIMES FOR TYPICAL CONDITIONS

Computational azimuth intervals, normal/reduced	Method of analysis	CDC 6400 execution time, sec
Case 1 $\mu = 0.29$		
$15^{\circ}/5^{\circ}$	Original continuous	231
$30^{\circ}/10^{\circ}$	Discrete vortex wake Piecewise constant Piecewise quadratic	30 33 49
Case 2 $\mu = 0.29$		
$15^{\circ}/5^{\circ}$	Original continuous	467
$30^{\circ}/10^{\circ}$	Discrete vortex wake Piecewise constant Piecewise quadratic	60 65 100
$5^{\circ}/5^{\circ}$	Discrete vortex wake Piecewise constant Piecewise quadratic	265 265 415

CONCLUDING REMARKS

The asymptotic approach developed by Van Holten is a suitable method for rotor airload calculation, within the scope of linear theory. However, in spite of the fact that only a single numerical integration is required to calculate the induced velocity, significant computation times may be required under certain conditions. It is possible to reduce the computation time by making two approximations, viz, replacing the continuous variation of the doublet strength distribtuion along the blade span by a piecewise continuous variation, and replacing the continuous helical trajectory of a fluid particle by a succession of connected straight line segments.

In the present study, such a discretized representation has been developed for the asymptotic method, using either a piecewise constant or piecewise quadratic variation of the doublet strength along the span. Computations have been carried out for the case of a two-bladed, teetering model rotor and a four-bladed, articulated full-scale rotor, and the results compared with both measurement and the original computational scheme. In general, when interaction effects are not significant, the simplified scheme agrees well with the original results, with the piecewise quadratic representation being slightly better. When interaction effects are significant, the piecewise constant scheme yields poor results but is found to improve upon using smaller azimuth spacing, while the piecewise quadratic scheme continues to compare well with the original results. Computationally, the discretized representation shows considerable improvement over the original scheme; under conditions where interaction effects are not significant, the piecewise constant scheme requires only about one-seventh and the piecewise quadratic scheme about one-fifth of the computation time required for the original scheme.

APPENDIX A

PIECEWISE CONTINUOUS REPRESENTATIONS

The continuous variation of the dipole strength function, g, over the blade span is approximated by dividing the span into J segments and replacing the actual curve by a series of simpler curves, continuous over each segment but discontinuous at the segment boundaries. The points marking the spanwise division are labeled s_j, $j = 1,2,\ldots(J+1)$ with s_1 being the root and s_{J+1} the tip of the blade. Points r_j, $j = 1,2,\ldots J$ denote the midpoints of the segments, where the boundary condition of normal velocity is applied. The length of a segment is Δs_j, $j = 1,2,\ldots J$ and this is allowed to vary along the span, generally being chosen smaller near the tip to achieve a better representation of the rapid variation of blade loading.

The simplest representation is a constant value over each segment and this is shown in figure 2. The spanwise variation can be represented much better with a second-degree curve over each segment as illustrated in figure 2. However, setting up such a piecewise quadratic representation involves more complicated algebra, the details of which are given below.

The quadratic curve is constructed to satisfy the following requirements: (1) at the midpoint, r_j, it must have the actual functional value, $g(r_j)$, (2) at its end points, s_j and s_{j+1}, it must equal the values on the adjacent segments, (3) at its end points, it must also equal the slopes of the adjacent segments. It must be noted that, for the segments at the ends of the blade, the curve is allowed to go to zero at the root and the tip, without any constraint on the slope at these points. Since each curve requires 3 constants for its definition, a total of 3 J constants must be determined from the available conditions, which are listed below.

Number of equations for midpoint values	=	J
Number of equations for end point values (including zero values at root and tip)	=	J + 1
Number of equations for end point slopes (excluding root and tip)	=	J - 1

This adds up to a total of 3 J equations, so that it is possible to set up a piecewise quadratic approximation which is completely determinate.

The curves will have to be determined in terms of the midpoint values and segment locations. To begin with, the slope conditions are ignored and the end point values assumed known. If C_{1j}, C_{2j}, C_{3j} denote the constants for the j^{th} curve, the conditions to be satisfied are

$$C_{1j} + C_{2j}\, s_j + C_{3j}\, s_j^2 = g_j$$

$$C_{1j} + C_{2j}\, r_j + C_{3j}\, r_j^2 = g(r_j)$$

$$C_{1j} + C_{2j}\, s_{j+1} + C_{3j}\, s_{j+1}^2 = g_{j+1}$$

which can be solved to give

$$C_{1j} = 2\left[r_j s_j g_{j+1} + r_j s_{j+1} g_j - 2 s_j s_{j+1} g(r_j)\right] / \Delta s_j^2$$

$$C_{2j} = -2\left[(r_j + s_j) g_{j+1} + (r_j + s_{j+1}) g_j - 4 r_j g(r_j)\right] / \Delta s_j^2 \qquad \text{(A 1)}$$

$$C_{3j} = 2\left[g_{j+1} + g_j - 2 g(r_j)\right] / \Delta s_j^2$$

Now the slope conditions can be used to elimate the end point values g_j, $j = 1,2. \ . \ .(J+1)$. At any end point, say s_{j+1}, the equality of slopes leads to

$$C_{2j} + 2 C_{3j} s_{j+1} = C_{2,j+1} + 2 C_{3,j+1} s_{j+1}$$

which, on substitution, becomes

$$(1/\Delta s_j) g_j + 3(1/\Delta s_j + 1/\Delta s_{j+1}) g_{j+1} + (1/\Delta s_{j+1}) g_{j+2} = 4\left[g(r_j)/\Delta s_j + g(r_{j+1})/\Delta s_{j+1}\right]$$

$$\text{for } j = 1,2. \ . \ .(J-1) \qquad \text{(A 2)}$$

This tridiagonal system of (J-1) equations can be solved by the following recursive scheme, which consists basically of the forward elimination and back substitution of the Gaussian elimination method.

$$\left.\begin{aligned}
\beta_2 &= 3(1/\Delta s_1 + 1/\Delta s_2) \\
\gamma_2 &= 4\left[g(r_1)/\Delta s_1 + g(r_2)/\Delta s_2\right] \\
\beta_j &= 3(1/\Delta s_{j-1} + 1/\Delta s_{j-2}) - 1/\Delta s_{j-1}^2 \, \beta_{j-1} \\
\gamma_j &= \left\{4\left[g(r_{j-1})/\Delta s_{j-1} + g(r_j)/\Delta s_j\right]\right. \\
&\quad \left. - \gamma_{j-1}/\Delta s_{j-1}\right\} / \beta_j \qquad (j = 3, 4. \ . \ . \ , J-1)
\end{aligned}\right\} \qquad \text{(A 3)}$$

$$g_J = \gamma_J$$

$$g_j = \gamma_j - g_{j+1}/\beta_j \Delta s_j \qquad (j = J-1, J-2. \ . \ 2)$$

This determines the (J-1) end point values in terms of the J midpoint values, so that the quadratic components C_{1j}, C_{2j}, C_{3j} are completely defined. Within a segment, the function can be written as

$$\begin{aligned} g &= C_{1j} + C_{2j}\, s + C_{3j}\, s^2 \\ &= 2\Big[(s - s_{j+1})(s - r_j)\, g_j + (s - s_j)(s - r_j)\, g_{j+1} \\ &\quad - 2(s - s_j)(s - s_{j+1})\, g(r_j)\Big] \;/\Delta s_j^2 \end{aligned} \tag{A 4}$$

Calculation of the total blade lift and the moment about the hub requires the spanwise integral of g and its moment about the hub. These integrals are given below.

Piecewise constant representation:

$$\begin{aligned} \int_{\xi}^{1} g(s)\, ds &= \sum_{j=1}^{J} g(r_j)\, \Delta s_j \\ \int_{\xi}^{1} g(s)\, s\, ds &= \sum_{j=1}^{J} g(r_j)\, r_j \Delta s_j \end{aligned} \tag{A 5}$$

Piecewise quadratic representation:

$$\begin{aligned} \int_{\xi}^{1} g(s)\, ds &= \sum_{j=1}^{J} \Big[g_j + g_{j+1} + 4g(r_j)\Big] \Delta s_j \;/\; 6 \\ \int_{\xi}^{1} g(s)\, s\, ds &= \sum_{j=1}^{J} \Big[s_j\, g_j + s_{j+1}\, g_{j+1} + 4 r_j\, g(r_j)\Big] \Delta s_j \;/\; 6 \end{aligned} \tag{A 6}$$

APPENDIX B

TRAJECTORY APPROXIMATION AND LIST OF INTEGRALS

The helical trajectory of a freestream fluid particle, ending at a collocation point $(r_{bo}/R_1, \Psi_{bo})$ on a reference blade, relative to the axes fixed to the j^{th} blade, is given by the following equations.

$$\left.\begin{aligned} x_b/R_1 &= (r_{bo}/R_1 \sin(\theta + \Delta\Psi_j) + \mu\theta \sin(\theta + \Psi_{bo} + \Delta\Psi_j) \\ y_b/R_1 &= \lambda\theta \\ r_b/R_1 &= (r_{bo}/R_1) \cos(\theta + \Delta\Psi_j) + \mu\theta \cos(\theta + \Psi_{bo} + \Delta\Psi_j) \end{aligned}\right\} \quad (B\ 1)$$

where $\theta = (\Psi_b - \Psi_{bo})$ is the azimuth relative to the reference blade position and $\Delta\Psi_j$ is the azimuth separation of the j^{th} blade from the first (reference) blade. For uniformly separated blades,

$$\Delta\Psi_j = 2\pi(j - 1)/B$$

The approximation used here divides the continuous helical trajectory into a succession of straight-line segments, each connecting the initial and final points of the helical path over a subinterval of azimuth. The coordinates of each of these trajectory segments can be written as

$$\left.\begin{aligned} x_b/R_1 &= X_i + X_s\,\theta \\ y_b/R_1 &= Y_i + Y_s\,\theta \\ r_b/R_1 &= R_i + R_s\,\theta \end{aligned}\right\} \quad (B\ 2)$$

If θ_1 and θ_2 are the ends of the azimuth interval, the intercepts and slopes are given by

$$\left.\begin{aligned} X_i &= (x_{b1} - R_1 X_s\,\theta_1)/R_1 \\ X_s &= (x_{b2} - x_{b1})/R_1(\theta_2 - \theta_1) \\ Y_i &= 0 \\ Y_s &= \lambda \\ R_i &= (r_{b1} - R_1 R_s\,\theta_1)/R_1 \\ R_s &= (r_{b2} - r_{b1})/R_1(\theta_2 - \theta_1) \end{aligned}\right\} \quad (B\ 3)$$

The integrals along the fluid particle trajectories which appear in Appendix C contain the following expressions which are written in terms of the straight-line notation as

$$r^2 = x_b^2 + y_b^2 = (r_o + 2r_1\theta + r_2\theta^2) R_1^2$$

where

$$r_o = X_i^2$$

$$r_1 = X_i X_s$$

$$r_2 = X_s^2 + Y_s^2$$

Letting $u = (s - r_b)$

$$d^2 = r^2 + u^2 = (d_o + 2d_1\theta + d_2\theta^2) R_1^2$$

where

$$d_o = X_i^2 + (s - R_i)^2$$

$$d_1 = X_i X_s - (s - R_i) R_s$$

$$d_2 = X_s^2 + \lambda^2 + R_s^2$$

$$d_n^2 = (x - x_b)^2 + y_b^2 = (d_{no} + 2d_{n1}\theta + d_{n2}\theta^2) R_1^2$$

where

$$d_{n0} = (x - X_i)^2$$

$$d_{n1} = -(x - X_i) X_s$$

$$d_{n2} = X_s^2 + Y_s^2$$

The primary advantage which has been achieved by introduction of the straight-line segment approximation for the particle trajectories is evident in the above "distance" expressions. It can be noted that they are all quadratic expressions in θ. As a direct result the integrals of the pressure gradient which are described in Appendix C can be analytically evaluated. These integral expressions are listed below as determined from reference 9. The symbolic parameter, t, is defined as

$$t \equiv d_1 + d_2\theta + d\sqrt{d_2}$$

Far field integrals:

$$I_1^f = \int \frac{d\theta}{d} = \frac{\ell n\ t}{\sqrt{d_2}}$$

$$I_2^f = \int \frac{\theta\, d\theta}{d} = \frac{d - d_1 I_1^f}{d_2}$$

$$I_3^f = \int \frac{d\ \theta}{d(d-u)} - \int \frac{d\,\theta}{d(d+u)}$$

$$= \frac{2}{|X_i\ \lambda|}\left[\tan^{-1}\left\{\frac{t + (R_s d - u\sqrt{d_2})}{|X_i\ \lambda\ |}\right\}\right.$$

$$\left. - \tan^{-1}\left\{\frac{t - (R_s d - u\sqrt{d_2})}{|\ X_i\ \lambda\ |}\right\}\right]$$

$$I_4^f = I_3^f \Big|_{y_b = y_o + \lambda\theta}$$

$$I_5^f = \int \frac{\theta\, d\,\theta}{d(d-u)} - \int \frac{\theta\ d\,\theta}{d(d+u)}$$

$$= \frac{1}{r_2}\left[\ell n\left\{\frac{d-u}{d+u}\right\} - 2R_s\, I_1^f - r_1\, I_3^f\right]$$

$$I_6^f = I_5^f \Big|_{y_b = y_o + \lambda\theta}$$

$$I_7^f = \frac{\partial\, I_4^f}{\partial\, y_o}\Bigg|_{y_o \to 0}$$

$$= \frac{2\lambda(R_s d - u\sqrt{d_2})}{t r_2\, r^2} - \frac{X_s\, I_3^f}{X_i \lambda} - \frac{2 y_b u}{t d r^2}$$

$$+ \frac{2X_s(R_s d - u\sqrt{d_2})\,(X_s\, x_b + \lambda\, y_b)}{X_i\, \lambda\, t r_2 r^2}$$

$$I_8^f = \left.\frac{\partial I_6^f}{\partial y_o}\right|_{y_o \to 0}$$

$$= \left[\frac{2R_s(\lambda d + y_b\sqrt{d_2})}{td\sqrt{d_2}} - \frac{2y_b u}{dr^2}\right.$$

$$\left. + \lambda I_3^f - r_1 I_7^f\right]\frac{1}{r_2}$$

$$I_9^f = \int \frac{\theta^2 d\theta}{d(d-u)} - \int \frac{\theta^2 d\theta}{d(d+u)}$$

$$= \left[2(s - R_i) I_1^f - 2R_s I_2^f - r_o I_3^f - 2r_1 I_5^f\right] / r_2$$

$$I_{10}^f = \int \frac{d\theta}{d(d-u)^2} + \int \frac{d\theta}{d(d+u)^2}$$

$$= \frac{1}{r^2 t X_i^2 \lambda^2 \sqrt{d_2}} \left\{2(d_1^2 - d_0 d_2)(d\sqrt{d_2} - R_s u)\right.$$

$$\left. + t(2u + r^2 I_3^f \sqrt{d_2})\left[r_1 R_s + r_2 (s - R_i)\right]\right\}$$

$$I_{11}^f = \int \frac{\theta\, d\theta}{d(d-u)^2} + \int \frac{\theta\, d\theta}{d(d+u)^2}$$

$$= -(2d/r^2 + r_1 I_{10}^f + R_s I_3^f) / r_2$$

$$I_{12}^{f} = \int \frac{\theta^2 d\theta}{d(d-u)^2} + \int \frac{\theta^2 d\theta}{d(d+u)^2}$$

$$= \left[2I_1^{f} + 2(s - R_i) I_3^{f} - 2R_s I_5^{f} \right.$$

$$\left. - r_0 I_{10}^{f} - 2r_1 I_{11}^{f} \right] / r_2$$

$$I_{13}^{f} = \int \frac{\theta^3 d\theta}{d(d-u)^2} + \int \frac{\theta^3 d\theta}{d(d+u)^2}$$

$$= \left[2I_2^{f} + 2(s - R_i) I_5^{f} - 2R_s I_9^{f} \right.$$

$$\left. - r_o I_{11}^{f} - 2r_1 I_{12}^{f} \right] / r_2$$

$$I_{14}^{f} = \int \frac{\theta \, d\theta}{d(d+u)}$$

$$= \frac{\ell n[2d_2 t\,(d+u)]}{r_2} - \frac{\ell n\, t}{\sqrt{d_2}\,(\sqrt{d_2} + R_s)}$$

$$- \frac{2r_1}{r_2 |X_i \lambda|} \tan^{-1} \left\{ \frac{t - (R_s d - u\sqrt{d_2})}{|X_i \lambda|} \right\}$$

$$I_{15}^{f} = \int \frac{\theta^2 d\theta}{d(d+u)}$$

$$= \left[\theta + \frac{2X_i^2(X_s^2 - Y_s^2)}{r_2 |X_i \lambda|} \tan^{-1} \left\{ \frac{t - (R_s d - u\sqrt{d_2})}{|X_i \lambda|} \right\} \right.$$

$$+ \frac{2r_1 d_2 - (\sqrt{d_2} + R_s)[r_1 R_s + r_2(s - R_i)]}{\sqrt{d_2}\, d_2 (\sqrt{d_2} + R_s)} \ell n\, t$$

$$\left. - \frac{2r_1}{r_2} \ell n \left\{ 2d_2\, t(d+u) \right\} \right] \frac{1}{r_2}$$

$$I_{16}^{f} = \int \frac{d\theta}{d-u} + \int \frac{d\theta}{d+u}$$

$$= 2I_1^{f} + (s - R_i) I_3^{f} - R_s I_5^{f}$$

$$I_{17}^{f} = \int \frac{\theta d\theta}{d-u} + \int \frac{\theta d\theta}{d+u}$$

$$= 2I_2^{f} + (s - R_i) I_5^{f} - R_s I_9^{f}$$

$$I_{18}^{f} = \int \frac{\partial}{\partial y_b} \left[y_b \ell n(d+u) \right] d\theta$$

$$= \theta \ell n(d+u) + R_s I_2^{f} - r_1 I_{14}^{f} - X_s^2 I_{15}^{f}$$

Some of the above integrals are not valid for the trajectory segment which ends at the collocation point for which $X_i = 0$. For this circumstance the following integrals are used.

$$I_{19}^{f} = \int \frac{\partial}{\partial y_b}\left[\frac{y_b d}{r^2}\right] d\theta \Big|_{X_i = 0}$$

$$= \frac{\lambda^2 \ell n\, t}{r_2\sqrt{d_2}} + \frac{X_s^2 - Y_s^2}{r_2^2}\left[\sqrt{d_2}\,\ell n\, t - \frac{d}{\theta}\right.$$

$$\left. - \frac{R_s(s - R_i)}{|s - R_i|}\,\ell n\left\{\frac{d_2\theta + \sqrt{d_2}(d - |s - R_i|)}{d_2\theta + \sqrt{d_2}(d + |s - R_i|)}\right\}\right]$$

$$I_{20}^{f} = \int \frac{\partial}{\partial y_b}\left[\frac{y_b d}{r^2}\right] \theta d\theta \Big|_{X_i = 0}$$

$$= \frac{\lambda^2}{r_2 d_2}\left[d + \frac{(s - R_i) R_s\, \ell n\, t}{\sqrt{d_2}}\right] + \frac{X_s^2 - Y_s^2}{r_2^2}\left[d\right.$$

$$\left. + |s - R_i|\,\ell n\left\{\frac{d_2\theta + \sqrt{d_2}\,(d - |s - R_i|)}{d_2\theta + \sqrt{d_2}(d + |s - R_i|)}\right\} - \frac{2(s - R_i) R_s\, \ell n\, t}{\sqrt{d_2}}\right]$$

$$I_{21}^{f} = \int \frac{\partial}{\partial y_b}\left[\frac{y_b u}{r^2 d}\right] d\theta \Big|_{X_i = 0}$$

$$= \frac{d(X_s^2 - Y_s^2)}{r_2^2 \theta\, |s - R_i|} + \frac{\lambda^2 \theta}{r_2 d(s - R_i)}$$

Common part integrals

$$I_1^C = \int \frac{d\theta}{r^2}$$

$$= \frac{1}{|X_i \lambda|} \tan^{-1} \left\{ \frac{r_1 + r_2 \theta}{|X_i \lambda|} \right\}$$

$$I_2^C = \int \frac{d\theta}{r^4}$$

$$= (r_1 + r_2\theta + r_2 r^2 I_1^C) / 2X_i^2 \lambda^2 r^2$$

$$I_3^C = \int \frac{\theta d\theta}{r^4}$$

$$= -(1 + 2r_1 r^2 I_2^C) / 2r_2 r^2$$

$$I_4^C = \int \frac{\theta^2 d\theta}{r^4}$$

$$= (r_o r^2 I_2^C - \theta) / r_2 r^2$$

$$I_5^C = \int \frac{\theta^3 d\theta}{r^4}$$

$$= (\ell n\, r - r_1 I_1^C - r_o r_2 I_3^C - 2r_1 r_2 I_4^C) / r_2^2$$

$$I_6^c = \int \frac{\theta^4 d\theta}{r^4}$$

$$= (\theta^3 - 3r_o r^2 I_4^c - 4r_1 r^2 I_5^c) / r_2 r^2$$

For the special case where $X_i = 0$

$$I_2^c \Big|_{X_i = 0} = -1 / 3r_2^2\theta^3$$

$$I_3^c \Big|_{X_i = 0} = -1 / 2r_2^2\theta^2$$

$$I_4^c \Big|_{X_i = 0} = -1 / r_2^2\theta$$

$$I_5^c \Big|_{X_i = 0} = \ell n\, \theta / r_2^2$$

$$I_6^c \Big|_{X_i = 0} = \theta / r_2^2$$

Near field integrals:

$$I_1^n = \int \frac{d\theta}{d_n^2}$$

$$= \frac{1}{\lambda |x - X_i|} \tan^{-1}\left\{\frac{d_{n1} + d_{n2}\theta}{\lambda |x - X_i|}\right\}$$

$$I_2^n = \int \frac{\theta \, d\theta}{d_n^2}$$

$$= (\ell n \, d_n - d_{n1} \, I_1^n) / d_{n2}$$

$$I_3^n = \int \frac{\theta^2 d\theta}{d_n^2}$$

$$= (\theta - d_{no} \, I_1^n - 2d_{n1} \, I_2^n) / d_{n2}$$

$$I_4^n = \int \frac{\theta^3 d\theta}{d_n^2}$$

$$= (\theta^2 - 2d_{no} \, I_2^n - 4d_{n1} \, I_3^n) / 2d_{n2}$$

APPENDIX C

INTEGRATION OF PRESSURE FIELD

The composite pressure field of the blade, to O(1/A), can be written from equations (6) and (7) of reference 5 as

$$\frac{p}{\rho\Omega^2R_1^2} = \left[\frac{P_{dip}}{\rho\Omega^2R_1^2}\right] + \left[\frac{(1-\xi)}{2A}\,\frac{g}{\rho\Omega^2R_1^2}\,\frac{\sin\chi}{r/R_1}\right] + \left[-\frac{g}{\rho\Omega^2R_1^2}\,\frac{\sin\phi}{\cosh\eta+\cos\phi} + \frac{(1-\xi)}{2A}\left(F_2 + (r_b/R_1)\,F_3\right)e^{-\eta}\sin\phi\right]$$

for points within the blade span, and for points outside the span

$$\frac{p}{\rho\Omega^2R_1^2} = \frac{P_{dip}}{\rho\Omega^2R_1^2} \qquad \text{(C 1)}$$

The corresponding sectional lift is

$$\frac{\ell}{\rho\Omega^2R_1^3} = -\frac{\pi(1-\xi)}{A}\left[\frac{g}{\rho\Omega^2R_1^2} - \frac{(1-\xi)}{4A}\left(F_2 + (r_b/R_1)\,F_3\right)\right] \qquad \text{(C 2)}$$

The integration of the far field, common part and near field terms (bracketed separately on the right hand side of equation (C 1) above) will be discussed for the piecewise constant and piecewise quadratic schemes.

Far Field

To O(1/A), this is the field of a dipole line located along the blade midchord and can be expressed as the integral of point dipoles distributed along the line.

$$\frac{P_{dip}}{\rho\Omega^2R_1^2} = \frac{y_b/R_1}{4\pi}\int_{\xi}^{1}\frac{\ell}{\rho\Omega^2R_1^3}\,\frac{d(s/R_1)}{(d/R_1)^3}$$

$$= -\frac{(1-\xi)}{4A}\,(y_b/R_1)\int_{\xi}^{1}\frac{g}{\rho\Omega^2R_1^2}\,\frac{d(s/R_1)}{(d/R_1)^3} \qquad \text{(C 3)}$$

where $d^2 = x_b^2 + y_b^2 + (s - r_b)^2$. Using integration by parts, this can also be written as

$$\frac{p_{dip}}{\rho \Omega^2 R_1^2} = \frac{(1-\xi)}{4A} \frac{(y_b/R_1)}{(r/R_1)^2} \int_{\xi}^{1} \frac{\partial}{\partial s} \left(\frac{g}{\rho \Omega^2 R_1^2} \right) \frac{(s - r_b)ds}{d} \qquad \text{(C 4)}$$

provided g goes to zero at the root and tip. The azimuth variation of g is approximated by a piecewise constant variation over each sub-interval of azimuth, while the spanwise variation is represented by a piecewise constant or a piecewise quadratic variation, as discussed in Appendix A.

Piecewise constant representation. -

$$p_{far} = -\frac{(y_b/R_1)}{4A} (1-\xi) \sum_{j=1}^{J} g_j \int_{s_j/R_1}^{s_{j+1}/R_1} \frac{d(s/R_1)}{(d/R_1)^3}$$

$$= -\frac{(y_b/R_1)}{4A} \frac{(1-\xi)}{(r/R_1)^2} \sum_{j=1}^{J} g_j \left[\frac{s - r_b}{d} \right]_{s=s_j}^{s=s_{j+1}}$$

The function g_j which varies with azimuth will have a constant value over the i^{th} azimuth subinterval that will be denoted by g_{ij}. The velocity induced by the far field is given by

$$\frac{w_{far}}{\Omega R_1} = \frac{(1-\xi)}{4A} \sum_i \sum_j g_{ij} \int_{\theta_{i+1}}^{\theta_i} \frac{\partial}{\partial(y_b/R_1)} \left[\frac{(y_b u)/R_1^2}{(r^2 d)/R_1^3} \right] d\theta \Bigg|_{s_j}^{s_{j+1}} \qquad \text{(C 5)}$$

where $u = s - r_b$. The integration will be easier if the derivative can be taken out of the integral and this is done as,

$$\frac{w_{far}}{\Omega R_1} = -\frac{(1-\xi)}{4A} \lim_{y_o \to 0} \frac{\partial}{\partial(y_o/R_1)} \sum_i \sum_j g_{ij} \int_{\theta_{i+1}}^{\theta_i} \frac{(y_b - y_o)\, u/R_1^2}{(r^2 d)/R_1^3} d\theta \Bigg|_{s_j}^{s_{j+1}}$$

where now $d^2 = x_b^2 + (y_b - y_o)^2 + u^2$. Noting that

$$\frac{u}{r^2 d} = \frac{1}{2} \left[\frac{1}{d(d-u)} - \frac{1}{d(d+u)} \right]$$

the integration can now be evaluated using the integrals listed in Appendix B with $y_b/R_1 = \lambda\theta$, where λ is the inflow ratio.

$$\int_{\theta_{i+1}}^{\theta_i} \frac{(y_b - y_o)\, u/R_1^2}{(r^2 d)/R_1^3}\, d\theta = -\frac{y_o}{R_1} I_4^f + \lambda I_6^f \Bigg|_{\theta_{i+1}}^{\theta_i}$$

Carrying out the differentiation and letting $y_o \to 0$, the induced velocity is obtained as

$$\frac{w_{far}}{\Omega R_1} = \sum_i \sum_j (\Delta w_{far})_{ij}^{p.c.}\, g_{ij} \qquad (C\ 6)$$

where, for $i \neq 1$,

$$(\Delta w_{far})_{ij}^{p.c.} = -\frac{(1-\xi)}{4A}\left(-I_4^f + \lambda I_8^f\right)\Bigg|_{\theta_{i+1}}^{\theta_i}\Bigg|_{s_j}^{s_{j+1}}$$

Here, the azimuth index i is set up so that $\theta_1 = 0$ is the collocation point on the blade and the trajectory ranges over $-\infty < \theta \leq 0$. For $i = 1$, the trajectory segment has one end on the blade and the unit induced velocity is expressed as

$$(\Delta w_{far})_{ij}^{p.c.} = \frac{(1-\xi)}{4A} I_{21}^f \Bigg|_{\theta_2}^{\theta_1}\Bigg|_{s_j}^{s_{j+1}}$$

Piecewise quadratic representation. - For this case, it is more convenient to express the field of the dipole line in its second form (eq. (C 4)). Using the representation of Appendix A as

$$\frac{\partial}{\partial(s/R_1)}\left(\frac{g}{\rho\,\Omega^2 R_1^2}\right) = C_{2j} + 2C_{3j}(s/R_1)$$

$$\frac{p_{far}}{\rho\,\Omega^2 R_1^2} = \frac{(1-\xi)}{4A}\,\frac{y_b/R_1}{(r/R_1)^2}\sum_{j=1}^{J}\int_{s_j}^{s_{j+1}}\left\{C_{2j} + 2C_{3j}(s/R_1)\right\}\frac{uds/R_1^2}{d/R_1}$$

$$\frac{p_{far}}{\rho \Omega^2 R_1^2} = \frac{(1-\xi)}{4A} \sum_{j=1}^{J} \left[\left\{ C_{2j} + C_{3j} (r_b + s)/R_1 \right\} \frac{y_b d}{r^2} \right.$$

$$\left. - C_{3j} (y_b/R_1) \ell n \left\{ (u + d)/R_1 \right\} \right]_{s_j}^{s_{j+1}}$$

The induced velocity can then be written as

$$\frac{w_{far}}{\Omega R_1} = -\frac{(1-\xi)}{4A} \sum_i \sum_j \left[(C_{2j} + C_{3j} R_i + C_{3j} s/R_1)_i \int_{\theta_{i+1}}^{\theta_i} \frac{\partial}{\partial (y_b/R_1)} \left[\frac{y_b d/R_1^2}{(r/R_1)^2} \right] d\theta \right.$$

$$+ (C_{3j} R_s)_i \int_{\theta_{i+1}}^{\theta_i} \theta \frac{\partial}{\partial (y_b/R_1)} \left[\frac{y_b d/R_1^2}{(r/R_1)^2} \right] d\theta$$

$$\left. - (C_{3j})_i \int_{\theta_{i+1}}^{\theta_i} \frac{\partial}{\partial (y_b/R_1)} \left[(y_b/R_1) \ell n \left\{ (u + d)/R_1 \right\} \right] d\theta \right]_{s_j}^{s_{j+1}} \qquad (C\ 7)$$

It may be noted that

$$\frac{\partial}{\partial y_b} (y_b d/r^2) = (x_b^2 - y_b^2)\, d/r^4 + y_b^2 / r^2 d$$

$$= \frac{1}{2} \left[\frac{1}{d+u} + \frac{1}{d-u} - \frac{y_b^2}{d(d+u)^2} - \frac{y_b^2}{d(d-u)^2} \right]$$

Using this relation, and consulting the integrals listed in Appendix B, the induced velocity can be expressed as

$$\frac{w_{far}}{\Omega R_1} = \sum_i \sum_j (\Delta w_{far})_{ij}^{p.q.} g_i(r_j) \qquad (C\ 8)$$

where $g_i(r_j)$ is the midpoint value of the j^{th} spanwise segment within the i^{th} azimuth interval. In terms of the quadratic coefficients, equation (C 7) can be written for $i \neq 1$ as

$$\frac{w_{far}}{\Omega R_1} = -\frac{(1-\xi)}{4A}\sum_i \sum_j \Big[(C_{2j} + C_{3j} R_i + C_{3j} s/R_1)_i$$

$$\times (I^f_{16} - \lambda^2 I^f_{12})/2 + (C_{3j} R_s)_i (I^f_{17} - \lambda^2 I^f_{13})/2$$

$$- (C_{3j})_i I^f_{18}\Big] \Bigg|_{\theta_{i+1}}^{\theta_i} \Bigg|_{s_j}^{s_{j+1}}$$

and for $i = 1$ as

$$\Delta\left(\frac{w_{far}}{\Omega R_1}\right)_{i=1} = -\frac{(1-\xi)}{4A} \sum_j \Big[(C_{2j} + C_{3j} R_i + C_{3j} s/R_1)_1 I^f_{19}$$

$$+ (C_{3j} R_s)_1 I^f_{20} - (C_{3j})_1 I^f_{21}\Big] \Bigg|_{\theta_2}^{\theta_1} \Bigg|_{s_j}^{s_{j+1}}$$

The quadratic coefficients can be expressed in terms of the midpoint and end point values. In turn, the end point values can be expressed in terms of the midpoint values, as shown in Appendix A, to obtain a final expression for the unit induced velocity of equation (C 8). The expression is lengthy and will not be reproduced here.

Common Part

The common part is the pressure field to which the far field tends at points very close to the dipole line, when it behaves essentially as a two-dimensional dipole corresponding to the doublet strength at that spanwise location.

$$\frac{p_{common}}{\rho \Omega^2 R_1^2} = -\frac{(1-\xi)}{2A} \frac{y_b/R_1}{(r/R_1)^2} \frac{g(r_b,\theta)}{\rho \Omega^2 R_1^2}$$

The induced velocity due to the common part is calculated as

$$\frac{w_{common}}{\Omega R_1} = \int_{\infty}^{0} \frac{\partial}{\partial(y_b/R_1)} \left(\frac{P_{common}}{\rho \Omega^2 R_1^2}\right) d\theta \qquad (C\ 9)$$

Piecewise constant representation. - Noting that

$$\frac{\partial}{\partial y_b} (y_b/r^2) = (x_b^2 - y_b^2)/r^4$$

equation (C 9) becomes

$$\frac{w_{common}}{\Omega R_1} = -\frac{(1-\xi)}{2A} \sum_i g_{ij} \left[X_i^2 \int_{\theta_{i+1}}^{\theta_i} \frac{d\theta}{(r/R_1)^4} + 2X_i X_s \int_{\theta_{i+1}}^{\theta_i} \frac{\theta\, d\theta}{(r/R_1)^4} + (X_s^2 - \lambda^2) \int_{\theta_{i+1}}^{\theta_i} \frac{\theta^2 d\theta}{(r/R_1)^4} \right]$$

The index j represents the spanwise segment within which the i^{th} trajectory segment lies; in general, the trajectory segment may range over more than one spanwise segment, in which case the azimuth interval must be subdivided so that each of the subintervals lies entirely within one spanwise segment.

$$\frac{w_{common}}{\Omega R_1} = \sum_i (\Delta w_{common})_i^{p.c.} g_{ij} \qquad (C\ 10)$$

where, from Appendix B,

$$(\Delta w_{common})_i^{p.c.} = -\frac{(1-\xi)}{2A} \left[X_i^2 I_2^c + 2X_i X_s I_3^c + (X_s^2 - \lambda^2) I_4^c \right] \Bigg|_{\theta_{i+1}}^{\theta_i}$$

Piecewise quadratic representation. - The spanwise variation of g is given by equation (A 4) of Appendix A. The induced velocity is given by

$$\frac{w_{common}}{\Omega R_1} = -\frac{(1-\xi)}{2A}\sum_i \frac{2}{\Delta s_j^2}\Big[g_{ij}\Big\{(R_i - s_{j+1})(R_i - r_j)C_1$$

$$+ R_s(2R_i - r_j - s_{j+1})C_2 + R_s^2 C_3\Big\} + g_{i,j+1}\Big\{(R_i - s_j)(R_i - r_j)C_1$$

$$+ R_s(2R_i - r_j - s_j)C_2 + R_s^2 C_3\Big\} - 2g_i(r_j)\Big\{(R_i - s_j)(R_i - s_{j+1})C_1$$

$$+ R_s(2R_i - s_j - s_{j+1})C_2 + R_s^2 C_3\Big\}\Big]$$

where

$$C_1 = \Big[X_i^2 I_2^c + 2X_i X_s I_3^c + (X_s^2 - \lambda^2) I_4^c\Big]\Big|_{\theta_{i+1}}^{\theta_i}$$

$$C_2 = \Big[X_i^2 I_3^c + 2X_i X_s I_4^c + (X_s^2 - \lambda^2) I_5^c\Big]\Big|_{\theta_{i+1}}^{\theta_i}$$

$$C_3 = \Big[X_i^2 I_4^c + 2X_i X_s I_5^c + (X_s^2 - \lambda^2) I_6^c\Big]\Big|_{\theta_{i+1}}^{\theta_i}$$

Both g_{ij} and $g_{i,j+1}$ can be expressed in terms of the midpoint values, and the induced velocity can be finally written as

$$\frac{w_{common}}{\Omega R_1} = \sum_i (\Delta w_{common})_i^{p.q.} g_i(r_j) \qquad (C\ 11)$$

Near Field

The near field is a distribution of two-dimensional dipoles along the chord, of intensity proportional to the surface pressure differential.

$$\frac{p_{near}}{\rho \Omega^2 R_1^2} = \frac{y_b}{\pi R_1}\int_{-1}^{1} \frac{-\frac{g}{\rho \Omega^2 R_1^2}\sqrt{\frac{1-x}{1+x}} + \frac{(1-\xi)}{2A}\left(F_2 + (r_b/R_1)F_3\right)\sqrt{1-x^2}}{(x - x_b R_1/b)^2 + (y_b R_1/b)^2}\,dx$$

where b is the semi-chord.

To make analytical integration possible, the chord is divided into K segments and the factors $\sqrt{1-x/1+x}$ and $\sqrt{1-x^2}$ are replaced by an average value over each segment. The chordwise integration can then be carried out, resulting in

$$\frac{\partial}{\partial(y_b/R_1)}\left(\frac{p_{near}}{\rho\,\Omega^2 R_1^2}\right) = -\sum_{k=1}^{K}\frac{f_k}{\pi}\left[\frac{\left(\frac{1-\xi}{2A}\,x - x_b\right)/R_1}{\left\{\left(\frac{1-\xi}{2A}\,x - x_b\right)^2 + y_b^2\right\}/R_1^2}\right]_{x_k}^{x_{k+1}}$$

where $f_k = \frac{g}{\rho\,\Omega^2 R_1^2}\,a_k - \frac{(1-\xi)}{2A}\left[F_2 + (r_b/R_1)\,F_3\right]b_k$

$$a_k = \left.\frac{\phi - \sin\phi}{x_k}\right|_{\phi_k}^{\phi_{k+1}}$$

$$b_k = \left.\frac{\phi/2 - (\sin 2\phi)/4}{\Delta x_k}\right|_{\phi_k}^{\phi_{k+1}}$$

$$x_k = \cos\phi_k \quad ; \quad \Delta x_k = x_{k+1} - x_k$$

Piecewise constant representation. -

$$\frac{w_{near}}{\Omega R_1} = -\int_{-\infty}^{0}\frac{\partial}{\partial(y_b/R_1)}\left(\frac{p_{near}}{\rho\,\Omega^2 R_1^2}\right)d\theta$$

$$= \sum_i\sum_k\frac{f_{ik}}{\pi}\int_{\theta_{i+1}}^{\theta_i}\frac{\left(\frac{1-\xi}{2AR_1}\,x - X_i\right) - X_s\theta}{d_n^2/R_1^2}\,d\theta\Bigg|_{x_k}^{x_{k+1}} \qquad \text{(C 12)}$$

Here, the factor $[F_2 + (r_b/R_1) F_3]$ is taken to be a constant for each azimuth interval i. Using the integrals listed in Appendix A, the induced velocity can be written as

$$\frac{w_{near}}{\Omega R_1} = \sum_i \sum_k \left[\left(\Delta w^{I}_{near} \right)^{p.c}_{ik} g_{ij} + \left(\Delta w^{II}_{near} \right)^{p.c.}_{ik} \right] \qquad (C\ 13)$$

where

$$\left(\Delta w^{I}_{near} \right)^{p.c.}_{ik} = \frac{a_k}{\pi} \left[\left(\frac{1-\xi}{2A} \frac{x}{R_1} - X_i \right) I_1^n - X_s I_2^n \right] \Bigg|_{\theta_{i+1}}^{\theta_i} \Bigg|_{x_k}^{x_{k+1}}$$

$$\left(\Delta w^{II}_{near} \right)^{p.c.}_{ik} = - \frac{(1-\xi)}{2A} \frac{b_k}{\pi} \left[F_2 + (r_b/R_1) F_3 \right]_i$$

$$x \left[\left(\frac{1-\xi}{2A} \frac{x}{R_1} - X_i \right) I_1^n - X_s I_2^n \right] \Bigg|_{\theta_{i+1}}^{\theta_i} \Bigg|_{x_k}^{x_{k+1}}$$

F_2 and F_3 contain terms proportional to blade motion, namely, θ_o, a_o, a_1, b_1 and the twist ε.

Piecewise quadratic representation. - Here, the quadratic expression for the variation of g over a spanwise segment is used and the induced velocity becomes

$$\begin{aligned}
\frac{w_{near}}{\Omega R_1} = \sum_i \sum_k \frac{2a_k}{\pi \Delta s_j^2} \Big[& g_{ij} \Big\{ (R_i - s_{j+1})(R_i - r_j) n_o \\
& + R_s (2R_i - r_j - s_{j+1}) n_1 + R_s^2 n_2 \Big\} + g_{i,j+1} \Big\{ (R_i - s_j)(R_i - r_j) n_o \\
& + R_s (2R_i - r_j - s_j) n_1 + R_s^2 n_2 \Big\} \\
& - 2 g_i(r_j) \Big\{ (R_i - s_j)(R_i - s_{j+1}) n_o + R_s (2R_i - s_j - s_{j+1}) n_1 \\
& + R_s^2 n_2 \Big\} \Big] + \sum_i \sum_k \frac{2b_k}{\pi \Delta s_j^2} \left[F_2 + (r_b/R_1) F_3 \right]_i n_o
\end{aligned}$$

where

$$n_o = \left[\left(\frac{1-\xi}{2A}\,\frac{x}{R_1} - X_i\right) I_1^n - X_s\, I_2^n\right] \Bigg|_{\theta_{i+1}}^{\theta_i} \Bigg|_{x_k}^{x_{k+1}}$$

$$n_1 = \left[\left(\frac{1-\xi}{2A}\,\frac{x}{R_1} - X_i\right) I_2^n - X_s\, I_3^n\right] \Bigg|_{\theta_{i+1}}^{\theta_i} \Bigg|_{x_k}^{x_{k+1}}$$

$$n_2 = \left[\left(\frac{1-\xi}{2A}\,\frac{x}{R_1} - X_i\right) I_3^n - X_s\, I_4^n\right] \Bigg|_{\theta_{i+1}}^{\theta_i} \Bigg|_{x_k}^{x_{k+1}}$$

As before, the induced velocity expression can be symbolically written as

$$\frac{w_{near}}{\Omega R_1} = \sum_i \sum_k \left[\left(\Delta w_{near}^{I}\right)_{ik}^{p.q.} g_{ij} + \left(\Delta w_{near}^{II}\right)_{ik}^{p.q.}\right] \qquad (C\ 14)$$

Limiting Behavior

The behavior of the expressions for the far field and the common part, in the vicinity of the lifting line, will be studied for both piecewise representations.

Piecewise constant representation. - It is sufficient to look at the expressions used for the trajectory segment immediately adjacent to the collocation point on the blade, viz, the segment with i = 1. Let the collocation point be located at the center of spanwise segment m. The unit induced velocity for the far field can be written out in full as below, for i = 1 (see eq. (C 6)).

$$\left(\Delta w_{far}\right)_{1j}^{p.c.} = -\frac{(1-\xi)}{4A}\left[\frac{(X_s^2 - \lambda^2)}{r_2^2}\,\frac{d}{\left(\frac{s}{R_1} - R_i\right)\theta} + \frac{\lambda^2}{r^2}\,\frac{\theta}{\left(\frac{s}{R_1} - R_i\right)}\,d\right]\Bigg|_{\theta_2}^{\theta_1} \Bigg|_{s_j}^{s_{j+1}}$$

$$\text{As } \theta \to 0, \quad d \to \left|\frac{s}{R_1} - R_i\right| - R_s\,\frac{\left(\frac{s}{R_1} - R_i\right)}{\left|\frac{s}{R_1} - R_i\right|}\,\theta \ \ldots,$$

indicating that the first term in the expansion for d will give rise to a singular term, which can be separated out.

$$\lim_{\theta \to 0} \left[\sum_{j=1}^{J} \left(\Delta w_{far} \right)_{1j}^{p.c.} g_{1j} \right]_{sing}$$

$$= - \frac{(1-\xi)}{4A} \frac{(X_s^2 - \lambda^2)}{r_2^2} \frac{1}{\theta} \sum_{j=1}^{J} \frac{\left| \frac{s}{R_1} - R_i \right|}{\left(\frac{s}{R_1} - R_i \right)} \Bigg|_{s_j}^{s_{j+1}} g_{1j}$$

$$= - \frac{(1-\xi)}{2A} \frac{(X_s^2 - \lambda^2)}{r_2^2} \frac{1}{\theta} g_{1m}$$

since $R_i = r_m$. Similarly, by looking at the behavior of the common part expression for $i = 1$, it is found that (see eq. (C 10))

$$\lim_{\theta \to 0} \left(\Delta w_{common} \right)_1^{p.c.} = - \frac{(1-\xi)}{2A} (X_s^2 - \lambda^2) \left(- \frac{1}{r_2^2 \theta} \right) g_{1m}$$

since $X_j = 0$. It can be seen that the two terms cancel each other exactly.

Piecewise quadratic representation. - In a manner similar to that above, the singular part of the far field expression (eq. (C 8)) can be separated out.

$$\lim_{\theta \to 0} \left[\Delta \left(\frac{w_{far}}{\Omega R_1} \right)_{i=1} \right]_{sing}$$

$$= - \frac{(1-\xi)}{4A} \frac{(X_s^2 - \lambda^2)}{r_2^2} \sum_j \left[(C_{2j} + C_{3j} R_i + C_{3j} s/R_1) \left\{ - \frac{\left| \frac{s}{R_1} - R_i \right|}{\theta} \right.\right.$$

$$\left.\left. - R_s \frac{\left(\frac{s}{R_1} - R_i \right)}{\left| \frac{s}{R_1} - R_i \right|} \ln \theta \right\} + C_{3j} R_s \left| \frac{s}{R_1} - R_i \right| \ln \theta \right] \Bigg|_{s_j}^{s_{j+1}}$$

Now, $C_{2j} = g'(r_j) - 2(r_j/R_1) C_{3j}$

Using this relation and carrying out the summation with j, it can be shown that the above limiting expression simplifies to

$$\lim_{\theta \to 0} \left[\Delta \left(\frac{w_{far}}{\Omega R_1} \right)_{i=1} \right]_{sing}$$

$$= - \frac{(1 - \xi)}{4A} \frac{(X_s^2 - \lambda^2)}{r_2^2} \left[2g(r_m) \frac{1}{\theta} - 2R_s g'(r_m) \ell n \, \theta \right]$$

The limiting value for the common part (eq. (C 11)) can be shown to be

$$\lim_{\theta \to 0} \left[\Delta \left(\frac{w_{common}}{\Omega R_1} \right)_{i=1} \right]$$

$$= - \frac{(1 - \xi)}{2A} \frac{(X_s^2 - \lambda^2)}{r_2^2} \left[\frac{R_s}{\Delta s_m} (g_{i,m+1} - g_{im}) \ell n \, \theta - g(r_m) \frac{1}{\theta} \right]$$

Since

$$g'(r_m) = (g_{i,m+1} - g_{im}) / \Delta s_m$$

it can be seen that the singularities in the far field and common part cancel exactly.

APPENDIX D

EVALUATION OF CHORDWISE AND SPANWISE APPROXIMATIONS

To facilitate the analytical integration of the pressure field in calculating the velocity induced on the blade, approximations are used for chordwise and spanwise variations, as outlined in Appendices A and C. This Appendix attempts to evaluate the accuracy of these approximations.

Chordwise Approximation

This consists of replacing the factors $\sqrt{1-x/1+x}$ and $\sqrt{1-x^2}$ by their average values over each chordwise segment. Since the first factor is the significant portion of the chordwise pressure distribution, the following problem is considered. Calculate the velocity induced by a steady, two-dimensional pressure distribution (proportional to $\sqrt{1-x/1+x}$) on a fluid particle travelling parallel to the chord, using both the exact and approximate pressure distributions.

The (x, y) axes are centered at the midchord with the x-axis being parallel to the chord. The exact nondimensional pressure field of the airfoil is given by

$$p_e(x, y) = \frac{y}{2\pi} \int_{-1}^{1} \sqrt{\frac{1-x'}{1+x'}} \frac{dx'}{(x' - x)^2 + y^2}$$

$$= \frac{1}{2} \frac{\sin \phi}{\cosh \eta + \cos \phi}$$

where (η, ϕ) is an elliptic coordinate system with

$$x = \cosh \eta \cos \phi$$

$$y = \sinh \eta \sin \phi$$

If the trajectory considered extends from x = - 2 to x = 2 at a constant distance y, the nondimensional induced velocity is given by

$$v = - \int_{-2}^{2} \frac{\partial p_e}{\partial y} dx$$

$$= - \frac{1}{2} \int_{-2}^{2} \frac{\sinh \eta \cos \phi + \sinh \eta \cosh \eta \cos 2 \phi}{(\cosh^2 \eta - \cos^2 \phi)(\cosh \eta + \cos \phi)^2} dx \qquad \text{(D 1)}$$

This integral can be evaluated by numerical integration.

Using the approximation, the average value of the pressure distribution over the k^{th} chordwise segment is given by

$$\bar{p}_k = \frac{1}{x_{k+1} - x_k} \int_{x_k}^{x_{k+1}} \sqrt{\frac{1-x}{1+x}}\, dx$$

$$= -\frac{1}{x_{k+1} - x_k} \left[\theta_{k+1} - \theta_k - \sin \theta_{k+1} + \sin \theta_k\right]$$

where $x_k = \cos \theta_k$.

$$p_e(x, y) = \frac{y}{2\pi} \sum_{k=1}^{K} \bar{p}_k \int_{x_k}^{x_{k+1}} \frac{dx'}{(x' - x)^2 + y^2}$$

$$\frac{\partial p_e}{\partial y} = -\sum_{k=1}^{K} \frac{\bar{p}_k}{2\pi} \frac{(x' - x)}{(x' - x)^2 + y^2} \Bigg|_{x_k}^{x_{k+1}}$$

$$v = \sum_{k=1}^{K} \frac{\bar{p}_k}{4\pi} \ln \left\{\frac{(x_{k+1} - x)^2 + y^2}{(x_k - x)^2 + y^2}\right\} \Bigg|_{x=-2}^{x=2} \qquad \text{(D 2)}$$

Two approximations are considered: (1) three segments along the chord, $\Delta x_k = 0.1, 0.9, 1.0$; and (2) five segments along the chord, $\Delta x_k = 0.1, 0.4, 0.5, 0.5, 0.5$. The results for the induced velocity are listed in table D 1. These results are also plotted in figure 3 and it can be seen that the approximate results are quite close to the exact results, even down to a vertical distance of 1% of the semi-chord.

TABLE D 1. - COMPARATIVE EVALUATION OF CHORDWISE APPROXIMATION

Vertical distance, y	Exact	Three segments	Five segments
.01	.5773	.5708	.5738
.05	.5766	.5702	.5731
.10	.5745	.5681	.5711
.20	.5661	.5602	.5629
.30	.5529	.5476	.5501
.40	.5357	.5313	.5335
.50	.5157	.5121	.5139
.60	.4938	.4910	.4925
.70	.4709	.4689	.4700
.80	.4476	.4464	.4472
.90	.4246	.4241	.4245
1.00	.4022	.4022	.4024

Spanwise Approximation

As discussed elsewhere, the span is divided into J segments, over each of which the variation of the function g is replaced by a piecewise constant or piecewise quadratic function. To evaluate this approximation, the following problem is considered. Calculate the velocity induced by a finite wing on a fluid particle travelling with the freestream flow past the wing, at various vertical and spanwise locations. The nondimensional loading along the wing span is taken to be

$$g_e = z^2\sqrt{1 - z^2}$$

with the z axis originating at one tip of the wing so that z = 1 represents the other tip. This type of loading has resemblance to the typical loading on a helicopter rotor blade.

For a particle travelling with constant velocity in the x direction, at constant values of y and z, the nondimensional vertical velocity induced by the wing may be written as

$$v = \frac{1}{4A}\int_{x_1}^{x_2}\left\{\frac{\partial}{\partial y}\, y \int_0^1 \frac{\zeta^2\sqrt{1-\zeta^2}\,d\zeta}{\left[x^2 + y^2 + (z-\zeta)^2\right]^{3/2}}\right\} dx$$

$$4Av = \int_{x_1}^{x_2} dx \int_0^1 \zeta^2\sqrt{1-\zeta^2}\; d\zeta \left[\frac{1}{\left[x^2 + y^2 + (z-\zeta)^2\right]^{3/2}} - \frac{3y^2}{\left[x^2 + y^2 + (z-\zeta)^2\right]^{5/2}}\right]$$

$$4Av = \int_0^1 \zeta^2 \sqrt{1-\zeta^2}\, d\zeta \left[\frac{x}{(y^2 + (z-\zeta)^2)_d} + \frac{y^2}{xd^3} \right.$$

$$\left. - \frac{y^2 d}{\left[y^2 + (z-\zeta)^2\right]^2 x} - \frac{y^2 x}{\left[y^2 + (z-\zeta)^2\right]^2 d} \right] \Bigg|_{x=x_1}^{x=x_2} \qquad \text{(D 3)}$$

where $d = \left[x^2 + y^2 (z-\zeta)^2\right]^{1/2}$

The integral with respect to ζ can be numerically evaluated. The induced velocity can also be calculated with a piecewise constant or piecewise quadratic approximation to g, using integrals similar to those listed in Appendix B, but the details of these expressions will not be written out here. For the calculation, $x_1 = -1$ and $x_2 = 1$, while the spanwise division for the approximations was done with 2 models: (1) three segments along the span, with $\Delta\zeta_j = 0.5, 0.3, 0.2$; and, (2) five segments along the span, with $\Delta\zeta_j = 0.5, 0.2, 0.1, 0.1, 0.1$. The results of the calculations are shown in tables D 2 and D 3 where the abbreviations p.c. and p.q. represent the piecewise constant and piecewise quadratic schemes. These induced velocity comparisons are also plotted in figure 4.

TABLE D 2. INDUCED VELOCITY COMPARISON FOR THREE-SEGMENT SPANWISE APPROXIMATIONS

Vertical distance, y	Spanwise location, z = 0.25			Spanwise location, z = 0.65			Spanwise location, z = 0.9		
	Exact	p.c.	p.q.	Exact	p.c.	p.q.	Exact	p.c.	p.q.
0.01	1.144	-0.603	-1.071	5.147	5.426	4.772	11.454	9.247	12.468
0.02	-1.050	-0.596	-0.987	5.037	5.381	4.735	10.455	9.024	11.017
0.05	-0.791	-0.548	-0.755	4.693	5.094	4.565	7.831	7.762	7.773
0.10	-0.440	-0.401	-0.430	4.099	4.343	4.128	5.007	5.391	4.849
0.20	0.026	-0.042	0.018	3.012	2.963	3.086	2.692	2.881	2.644
0.40	0.375	0.334	0.369	1.605	1.522	1.625	1.311	1.351	1.302
0.60	0.394	0.373	0.392	0.924	0.884	0.927	0.786	0.793	0.781
0.80	0.327	0.316	0.326	0.574	0.555	0.573	0.509	0.508	0.505
1.00	0.253	0.247	0.252	0.377	0.368	0.376	0.344	0.343	0.342

TABLE D 3. INDUCED VELOCITY COMPARISON FOR FIVE-SEGMENT SPANWISE APPROXIMATIONS

Vertical distance, y	Spanwise location, z = 0.25			Spanwise location, z = 0.60			Spanwise location, z = 0.95		
	Exact	p.c.	p.q.	Exact	p.c.	p.q.	Exact	p.c.	p.q.
0.01	-1.144	-0.518	-1.101	4.037	5.206	4.125	11.708	9.139	12.651
0.02	-1.050	-0.512	-1.013	3.975	5.120	4.048	9.481	8.404	9.495
0.05	-0.791	-0.470	-0.770	3.771	4.626	3.813	5.274	5.711	5.057
0.10	-0.440	-0.341	-0.432	3.393	3.661	3.406	2.963	3.386	2.876
0.20	0.026	-0.022	0.025	2.629	2.464	2.624	1.845	2.011	1.823
0.40	0.375	0.324	0.372	1.502	1.365	1.496	1.093	1.117	1.085
0.60	0.394	0.363	0.392	0.892	0.824	0.887	0.706	0.700	0.702
0.80	0.327	0.308	0.326	0.562	0.527	0.559	0.474	0.462	0.471
1.00	0.253	0.241	0.252	0.372	0.352	0.370	0.327	0.317	0.325

APPENDIX E

FINAL EQUATIONS AND OUTPUT QUANTITIES

The basic solution is for the spanwise and azimuthwise variation of the dipole strength function, g. With the span divided into J segments, the value at the midpoint of each segment is given the following harmonic representation over the azimuth.

$$\frac{g(r_j)}{\rho \Omega^2 R_1^2} = G_j^o + \sum_{n=1}^{N_h} \left[G_{jn}^c \cos(n\Psi_b) + G_{jn}^s \sin(n\Psi_b) \right] \qquad \text{(E 1)}$$

In the present calculation, the above formula serves only as an interpolation.

The boundary condition to be satisfied states that the normal velocity induced at a point on the blade by the combined pressure field of all the blades is equal to the normal velocity due to blade motion. If w_b denotes the normal velocity due to blade motion, the boundary condition can be symbolically written as

$$\frac{w_b}{\Omega R_1}(r_{bo}, \Psi_{bo}) = \sum_{\substack{\text{no. of} \\ \text{blades}}} \left\{ \sum_i \sum_j (\Delta w_{far})_{ij} \frac{g_i(r_j)}{\rho \Omega^2 R_1^2} \right.$$

$$+ \sum_i (\Delta w_{common})_i \frac{g_i(r_{j'})}{\rho \Omega^2 R_1^2}$$

$$\left. + \sum_i \sum_k \left[(\Delta w_{near}^{I})_{ik} \frac{g_i(r_{j'})}{\rho \Omega^2 R_1^2} + (\Delta w_{near}^{II})_{ik} \right] \right\} \qquad \text{(E 2)}$$

The contributions Δw can be calculated with either the piecewise constant or piecewise quadratic spanwise representation, as described in Appendix C. The index j' refers to the spanwise segment within which the i^{th} trajectory segment is located (if the i^{th} trajectory segment ranges over more than one spanwise segment, Δw must be summed over these segments as well).

$$\frac{g_i(r_j)}{\rho \Omega^2 R_1^2} = G_j^o + \sum_{n=1}^{N_h} \left[G_{jn}^c \cos(n\Psi_{bi}) + G_{jn}^s \sin(n\Psi_{bi}) \right] \qquad \text{(E 3)}$$

where Ψ_{bi} is any typical point of the i^{th} azimuth interval (e.g., either end or the midpoint). It must be noted that the collective pitch, coning angle and the cyclic pitch coefficients are contained both in w_b and in the near field contribution (Δw_{near}), which is proportional to the functions F_2 and F_3. These are defined below

$$\frac{w_b}{\Omega R_1} = \left[\left\{\theta_o - \epsilon \frac{r_b - R_o}{R_1 - R_o}\right\} \frac{r_b}{R_1} - \mu\alpha_r - \mu \frac{a_1}{2}\right]$$

$$+ \left[b_1 \frac{r_b}{R_1} - \mu a_o\right] \cos\Psi_b + \left[-a_1 \frac{r_b}{R_1} + \mu \left\{\theta_o \right.\right.$$

$$\left.\left. - \epsilon \frac{r_b - R_o}{R_1 - R_o}\right\}\right] \sin\Psi_b + \left[\mu \frac{a_1}{2}\right] \cos 2\Psi_b$$

$$+ \left[\mu \frac{b_1}{2}\right] \sin 2\Psi_b \qquad \text{(E 4)}$$

$$\left.\begin{aligned} F_2 &= \left[2\mu\theta_o + 2\mu\epsilon \frac{R_o}{R_1 - R_o}\right] \cos\Psi_b + \left[2\mu a_o\right] \sin\Psi_b \\ &+ \left[2\mu b_1\right] \cos 2\Psi_b + \left[-2\mu a_1 - \mu^2 \epsilon \frac{R_1}{R_1 - R_o}\right] \sin 2\Psi_b \\ F_3 &= a_o + \left[-2a_1 - 4\mu\epsilon \frac{R_1}{R_1 - R_o}\right] \cos\Psi_b + \left[-2b_1\right] \sin\Psi_b \end{aligned}\right\} \qquad \text{(E 5)}$$

For presentation as output, the following quantities are calculated:

(1) azimuthwise variations of total lift per blade, aerodynamic moment about the hub and spanwise center of lift location,

(2) spanwise and azimuthwise variations of sectional lift, pitching moment about quarter-chord and center of pressure location,

(3) chordwise, spanwise and azimuthwise variations of surface pressure differential. The expressions for these quantities are presented below.

Surface pressure differential,

$$\frac{\Delta p}{\rho \Omega^2 R_1^2} = 2\left[- \frac{g}{\rho \Omega^2 R_1^2} \sqrt{\frac{1-x}{1+x}} + \frac{(1-\xi)}{2A} (F_2 + \frac{r_b}{R_1} F_3) \sqrt{1-x^2} \right] \quad \text{(E 6)}$$

where x is nondimensional with respect to the semi-chord.

Sectional lift,

$$\frac{\ell}{\rho \Omega^2 R_1^3} = - \frac{\pi}{A} (1-\xi) \left[\frac{g}{\rho \Omega^2 R_1^2} - \frac{(1-\xi)}{4A} (F_2 + \frac{r_b}{R_1} F_3) \right] \quad \text{(E 7)}$$

Pitching moment about quarter-chord,

$$\frac{m}{\rho \Omega^2 R_1^4} = - \frac{\pi}{16 A^3} (1-\xi)^3 (F_2 + \frac{r_b}{R_1} F_3) \quad \text{(E 8)}$$

Center of pressure location (from leading edge), as a fraction of the chord,

$$\frac{x_{cp}}{c} = 0.25 + \frac{A}{(1-\xi)} \frac{m}{R_1 \ell} \quad \text{(E 9)}$$

Total lift per blade,

$$\frac{L}{\rho \Omega^2 R_1^4} = - \frac{\pi}{A} (1-\xi) \int_{\xi}^{1} \frac{g}{\rho \Omega^2 R_1^2} d\left(\frac{r_b}{R_1}\right)$$

$$+ \frac{\pi (1-\xi)^2}{4A^2} \left\{ \frac{(1-\xi^2)}{2} a_o + \left[2\mu\theta_o (1-\xi) - a_1 (1-\xi^2) - 2\mu\epsilon \right] \cos \Psi_b \right.$$

$$+ \left[2\mu a_o (1-\xi) - b_1 (1-\xi^2) \right] \sin \Psi_b + \left[2\mu b_1 (1-\xi) \right] \cos 2\Psi_b$$

$$\left. + \left[- 2\mu a_1 (1-\xi) - \mu^2 \epsilon \right] \sin 2\Psi_b \right\} \quad \text{(E 10)}$$

Aerodynamic moment about hub,

$$\frac{M}{\rho \Omega^2 R_1^5} = -\frac{\pi}{A}(1-\xi)\int_{\xi}^{1} \frac{g}{\rho \Omega^2 R_1^2}\frac{r_b}{R_1}\, d\left(\frac{r_b}{R_1}\right)$$

$$+ \frac{\pi(1-\xi)^2}{A^2}\left\{\frac{(1-\xi^3)}{3}a_o + \left[\mu\theta_o(1-\xi^2) - \frac{2a_1}{3}(1-\xi^3)\right.\right.$$

$$\left. + \frac{\mu\varepsilon}{3}(-4-\xi-\xi^2)\right]\cos\psi_b$$

$$+ \left[\mu a_o(1-\xi^2) - \frac{2b_1}{3}(1-\xi^3)\right]\sin\psi_b + \left[\mu b_1(1-\xi^2)\right]\cos 2\psi_b$$

$$\left. + \left[-\mu a_1(1-\xi^2) - \frac{\mu^2\varepsilon}{2}(1+\xi)\right]\sin 2\psi_b\right\} \qquad \text{(E 11)}$$

Spanwise center of lift location,

$$\frac{r_L}{R_1} = \frac{M}{R_1 L} \qquad \text{(E 12)}$$

The spanwise integrals of g, required in some of the expressions above, are given in Appendix A.

If the collective pitch, coning angle and cyclic pitch coefficients are considered unknown, additional equations are necessary. These equations are given below.

Piecewise Constant Representation

$$-\sum_{j=1}^{J} G_j^o \Delta s_j + \left[\frac{1}{8A}(1-\xi)(1-\xi^2)\right]a_o = \frac{A}{(1-\xi)}\frac{C_T}{B}$$

$$- \sum_{j=1}^{J} G_j^o \, r_j \Delta s_j + \left[\frac{1}{12A} (1 - \xi)(1 - \xi^3) - \frac{2}{\gamma} \right] a_o = 0$$

$$- \sum_{j=1}^{J} G_{j1}^c \, r_j \Delta s_j + \left[\frac{\mu}{4A} (1 - \xi)(1 - \xi^2) \right] \theta_o - \left[\frac{1}{6A} (1 - \xi)(1 - \xi^3) \right] a_1$$

$$= - \frac{\epsilon}{12A} \mu (-4 + 3\xi + \xi^3)$$

$$- \sum_{j=1}^{J} G_{j1}^s \, r_j \Delta s_j + \left[\frac{\mu}{4A} (1 - \xi)(1 - \xi^2) \right] a_o - \left[\frac{1}{6A} (1 - \xi)(1 - \xi^3) \right] b_1 = 0$$

Piecewise Quadratic Representation

In this case, the equations will also involve the values of g at the ends of spanwise segments; however, these can be related to the central values, as described in Appendix A. Let this relation be written symbolically as,

$$\frac{g(s_i)}{\rho \Omega^2 R_1^2} = \sum_{j=1}^{J} h_{ij} \frac{g(r_j)/\rho \Omega^2 R_1^2}{\Delta s_j}$$

Then the equations are as follows.

$$- \sum_{i=1}^{J} \left[4G_i^o + \sum_{j=1}^{J} (h_{ij} + h_{i+1,j}) \frac{G_j^o}{\Delta s_j} \right] \frac{\Delta s_i}{6}$$

$$+ \left[\frac{1}{8A} (1 - \xi)(1 - \xi^2) \right] a_o = \frac{A}{(1 - \xi)} \frac{C_T}{B}$$

$$- \sum_{i=1}^{J} \left[4r_i \, G_i^o + \sum_{j=1}^{J} (s_i \, h_{ij} + s_{i+1} \, h_{i+1,j}) \frac{G_j^o}{\Delta s_j} \right] \frac{\Delta s_i}{6}$$

$$+ \left[\frac{1}{12A} (1 - \xi)(1 - \xi^3) - \frac{2}{\gamma} \right] a_o = 0$$

$$- \sum_{i=1}^{J} \left[4r_i \, G_{i1}^{c} + \sum_{j=1}^{J} (s_i \, h_{ij} + s_{i+1} \, h_{i+1,j}) \, \frac{G_{j1}^{c}}{\Delta s_j} \right] \frac{\Delta s_i}{6}$$

$$+ \left[\frac{\mu}{4A} (1 - \xi)(1 - \xi^2) \right] \theta_o - \left[\frac{1}{6A} (1 - \xi)(1 - \xi^3) \right] a_1$$

$$= - \frac{\varepsilon}{12A} \mu (-4 + 3\xi + \xi^3)$$

$$- \sum_{i=1}^{J} \left[4r_i \, G_{i1}^{s} + \sum_{j=1}^{J} (s_i \, h_{ij} + s_{i+1} \, h_{i+1,j}) \, \frac{G_{j1}^{s}}{\Delta s_j} \right] \frac{\Delta s_i}{6}$$

$$+ \left[\frac{\mu}{4A} (1 - \xi)(1 - \xi^2) \right] a_o - \left[\frac{1}{6A} (1 - \xi)(1 - \xi^3) \right] b_1 = 0$$

REFERENCES

1. Van Holten, Th.: The Computation of Aerodynamic Loads on Helicopter Blades in Forward Flight, Using the Method of the Acceleration Potential. Rep. VTH-189, Technische Hogeschool Delft, Netherlands, March 1975.

2. Van Holten, Th.: Computation of Aerodynamic Loads on Helicopter Rotor Blades in Forward Flight, Using the Method of the Acceleration Potential. Presented at the 9th Congress of the International Congress of the Aeronautical Sciences, ICAS Paper No. 74-54, Haifa, 1974.

3. Van Holten, Th.: On the Validity of Lifting Line Concepts in Rotor Analysis. Vertica, vol. 1, 1977, pp. 239-254.

4. Van Holten, Th.: Some Notes on Unsteady Lifting Line Theory. Journal of Fluid Mechanics, vol. 77, Part 3, 1976, pp. 561-579.

5. Pierce, G. Alvin; and Vaidyanathan, Anand R.: Helicopter Rotor Loads Using a Matched Asymptotic Expansion Technique. NASA CR-165742, May 1981.

6. Rabbott, J. P., Jr; and Churchill, G. B.: Experimental Investigation of the Aerodynamic Loading on a Helicopter Rotor Blade in Forward Flight. NACA RM L56I07, October 1956.

7. Scheiman, J.: A Tabulation of Helicopter Rotor Blade Differential Pressures, Stresses and Motions as Measured in Flight. NASA TM X-952, March 1964.

8. Rabbott, J. P., Jr,; Lizak, A. A.; and Paglino, V. M.: A Presentation of Measured and Calculated Full-Scale Rotor Blade Aerodynamic and Structural Loads. USAAVLABS Tech. Rep. 66-31, July 1966.

9. Gradshteyn, I. S.; and Ryzhik, I. M.: Table of Integrals, Series and Products. Academic Press, 1980.

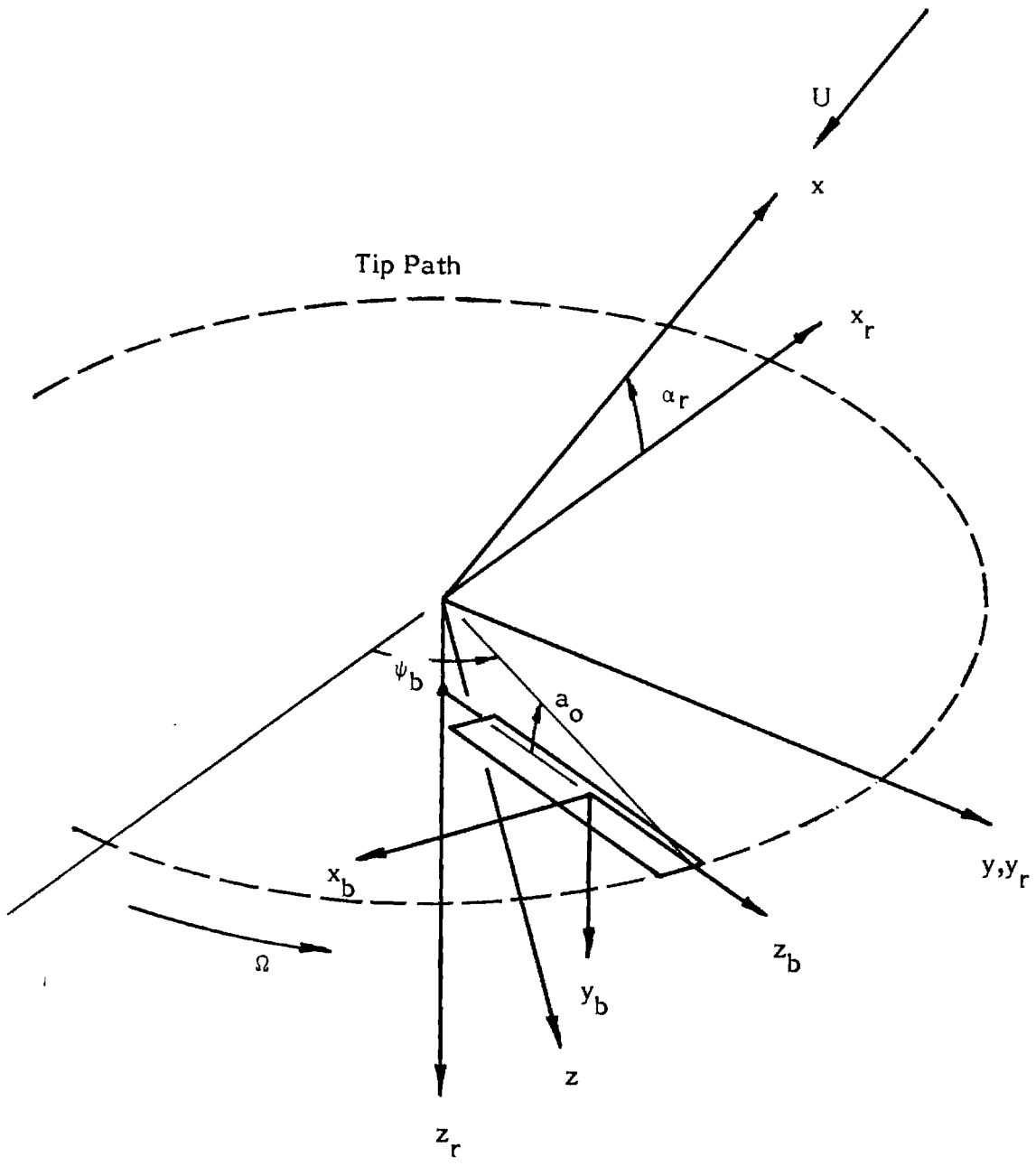

Figure 1. - Rotor coordinate systems.

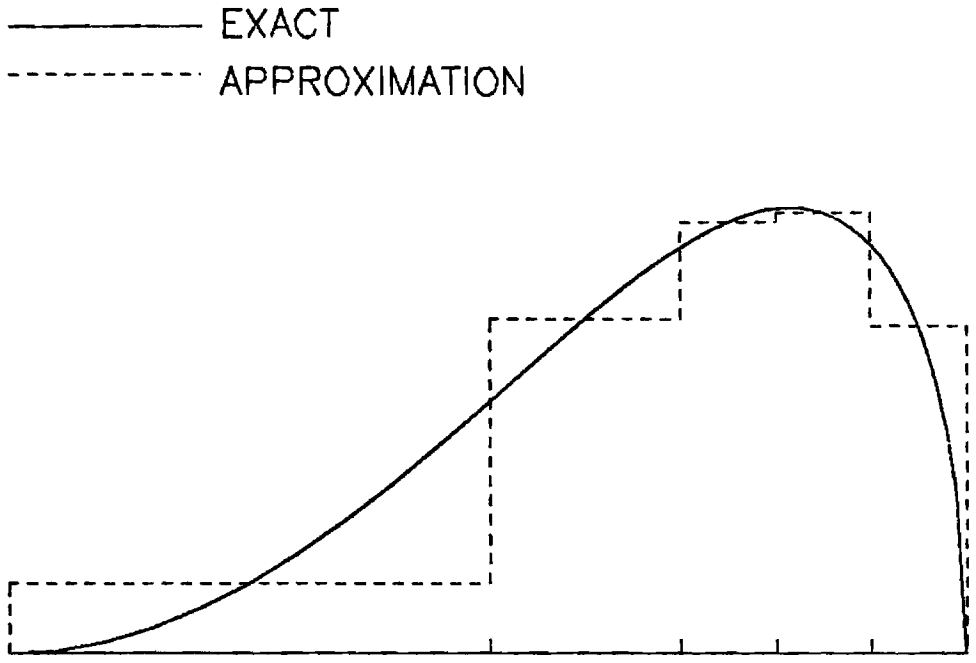

(a) Piecewise constant.

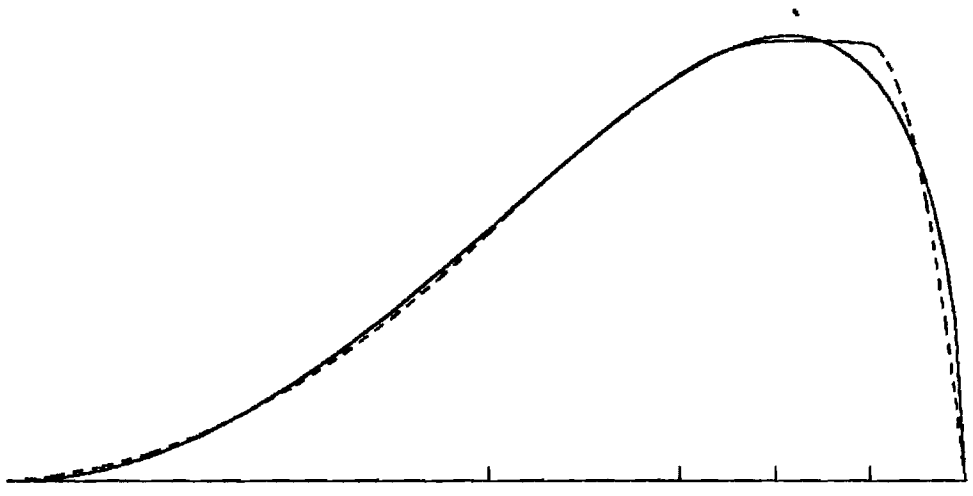

(b) Piecewise quadratic.

Figure 2. - Piecewise continuous representations of the spanwise distribution of doublet strength.

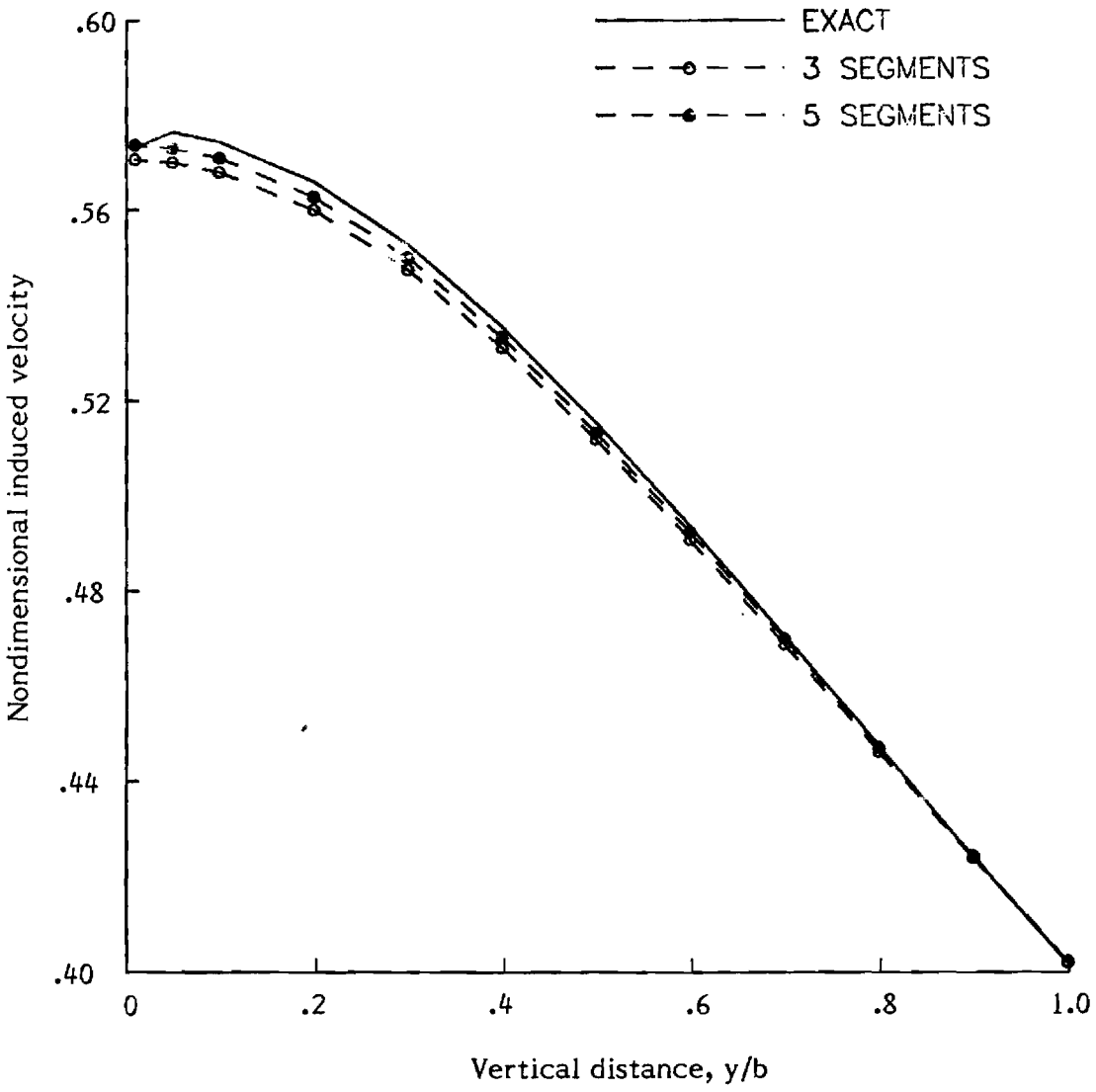

Figure 3. - Induced velocity comparison for piecewise constant chorwise pressure distribution.

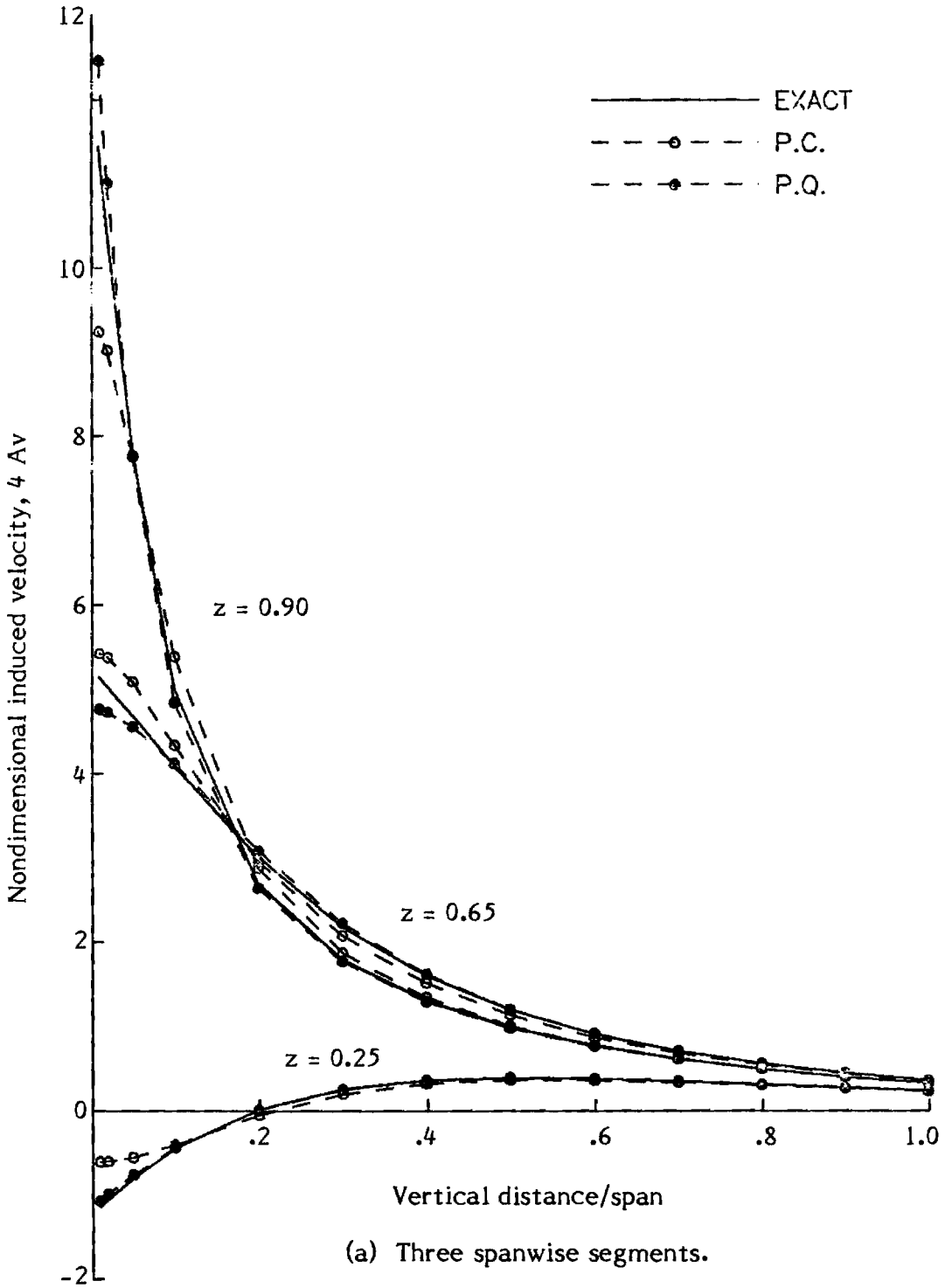

(a) Three spanwise segments.

Figure 4. - Induced velocity comparison for for spanwise approximations.

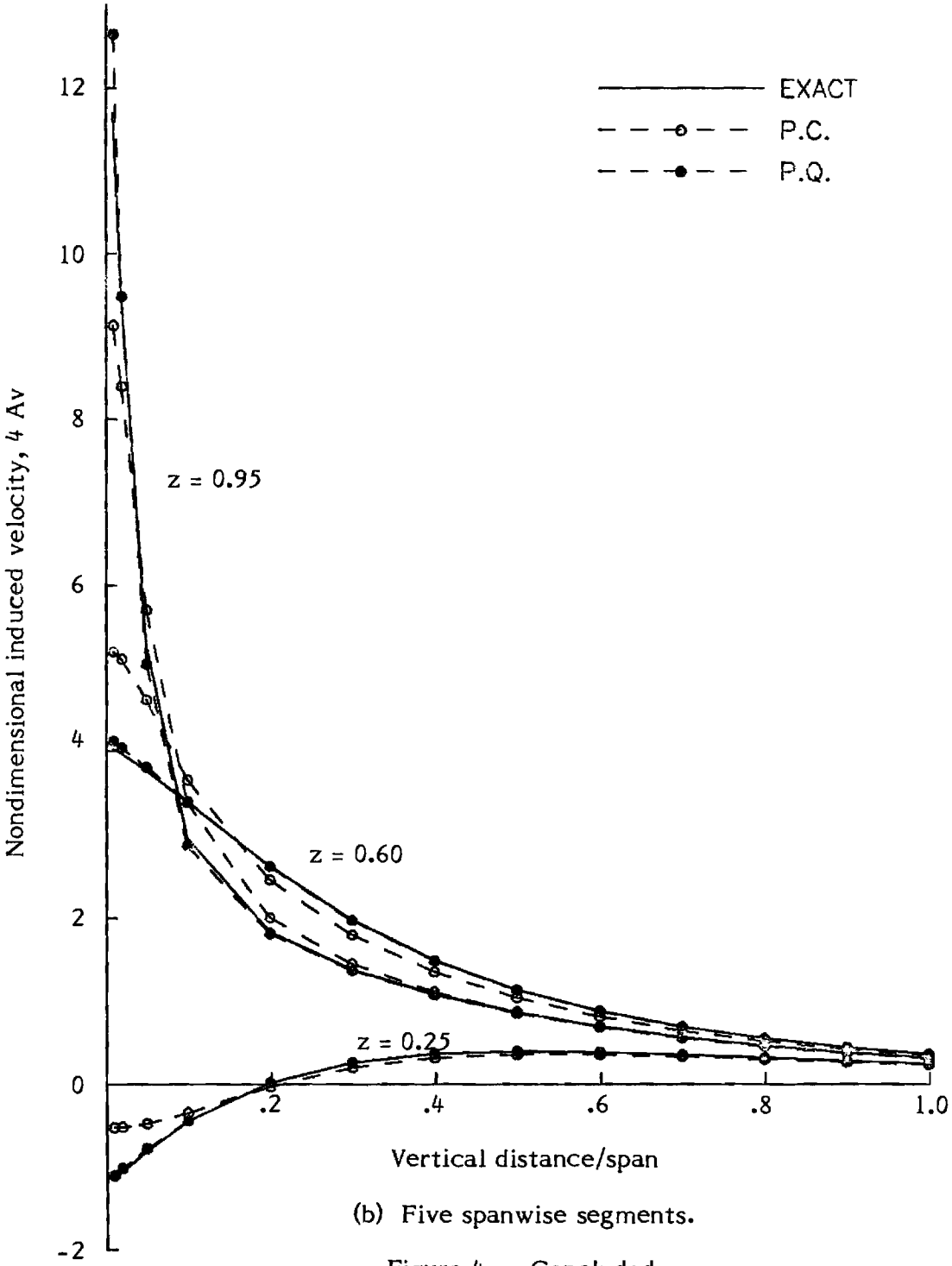

(b) Five spanwise segments.

Figure 4. - Concluded.

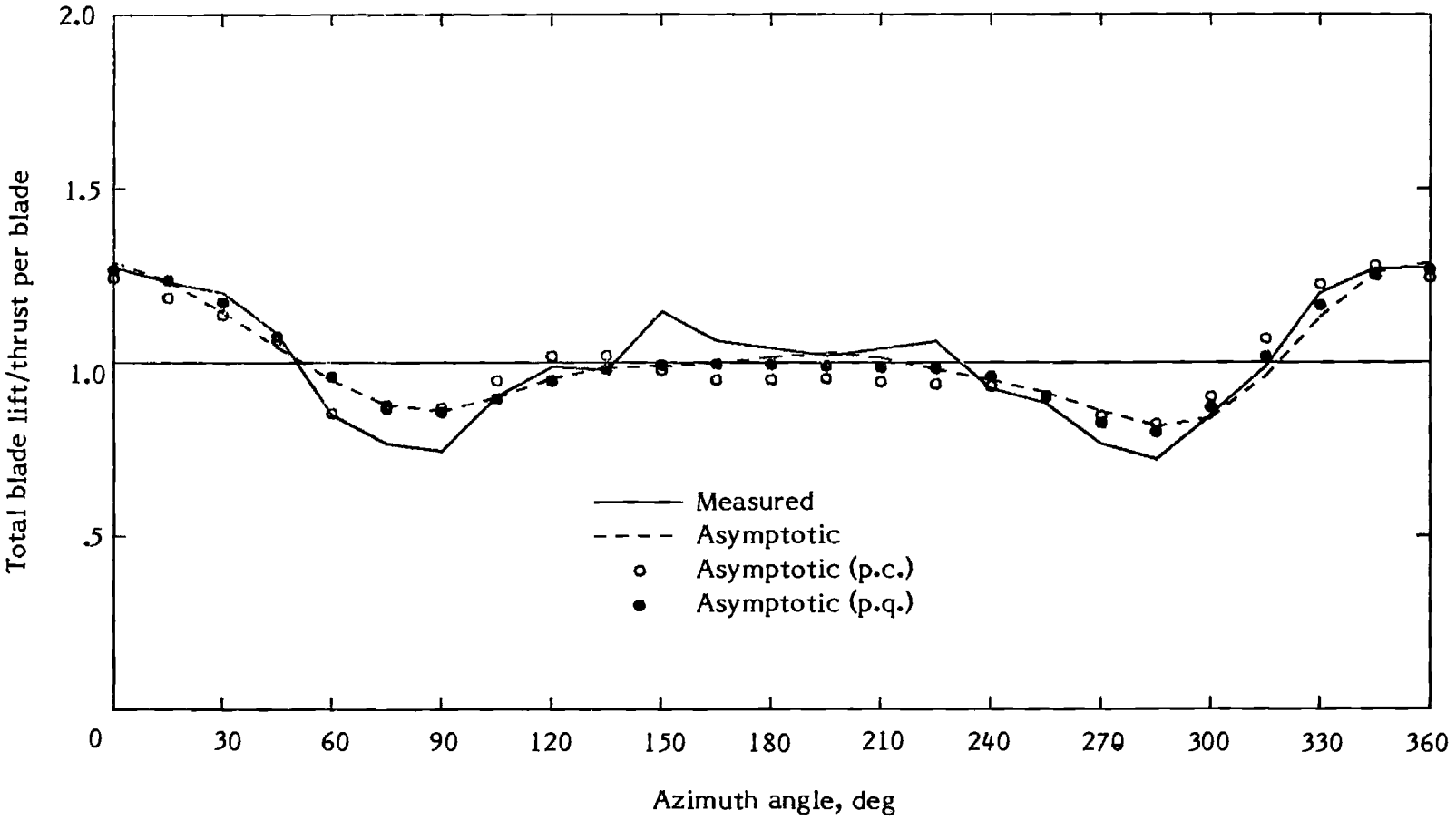

(a) $\mu = 0.08$.

Figure 5. - Total blade lift versus azimuth for Case 1.

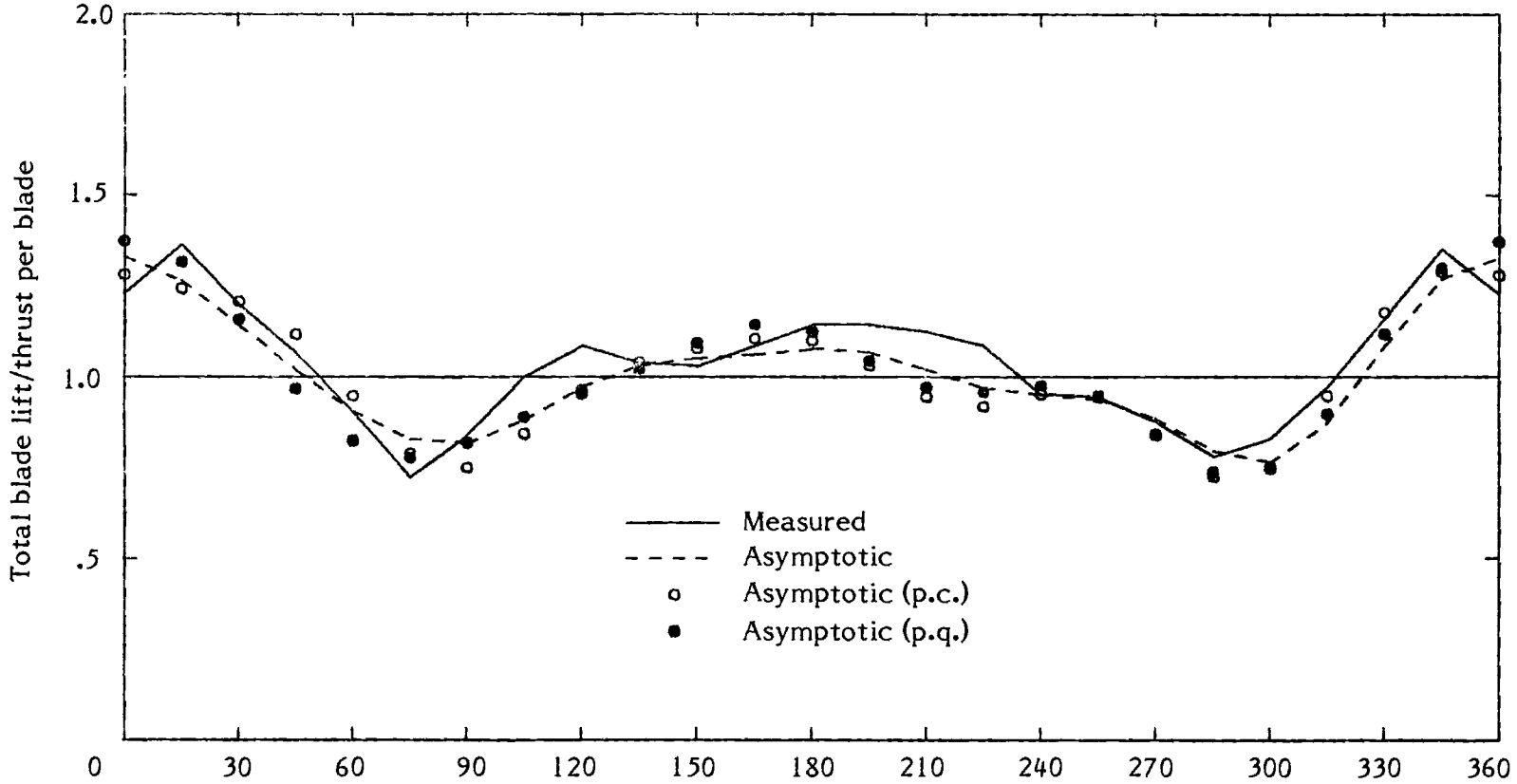

(b) $\mu = 0.15$.

Figure 5. - Continued.

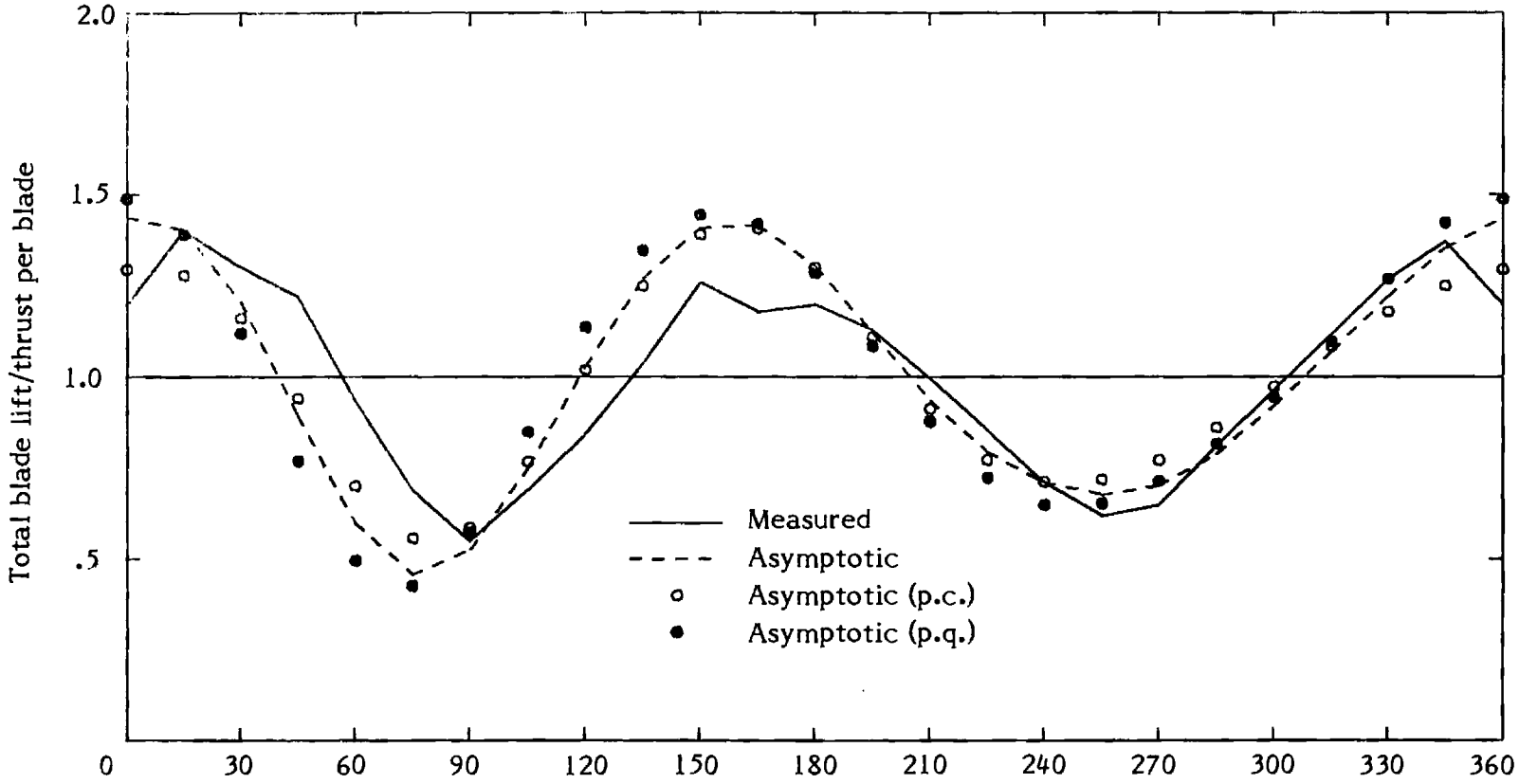

(c) $\mu = 0.29$.

Figure 5. - Concluded.

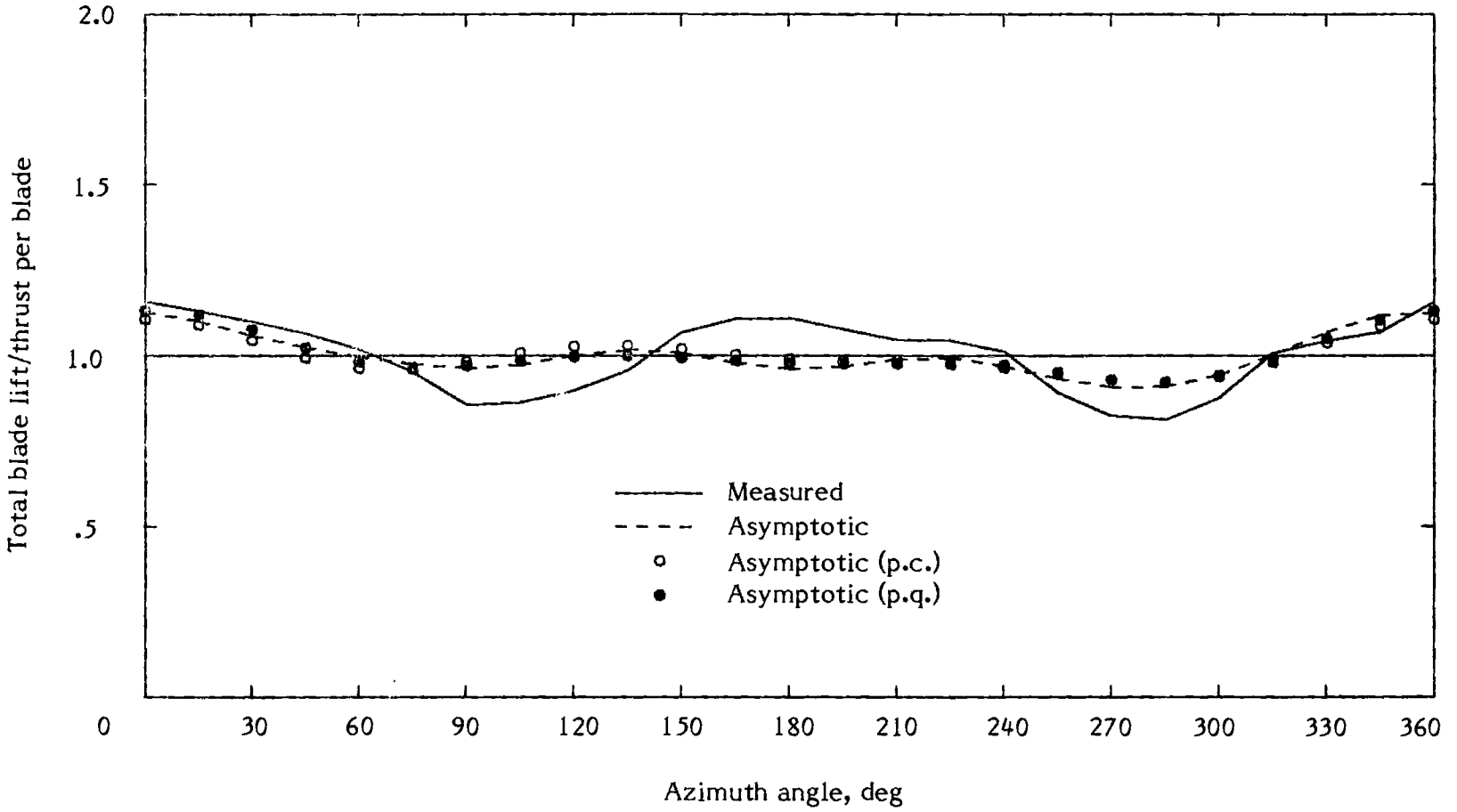

(a) $\mu = 0.06$.

Figure 6. - Total blade lift versus azimuth for Case 2.

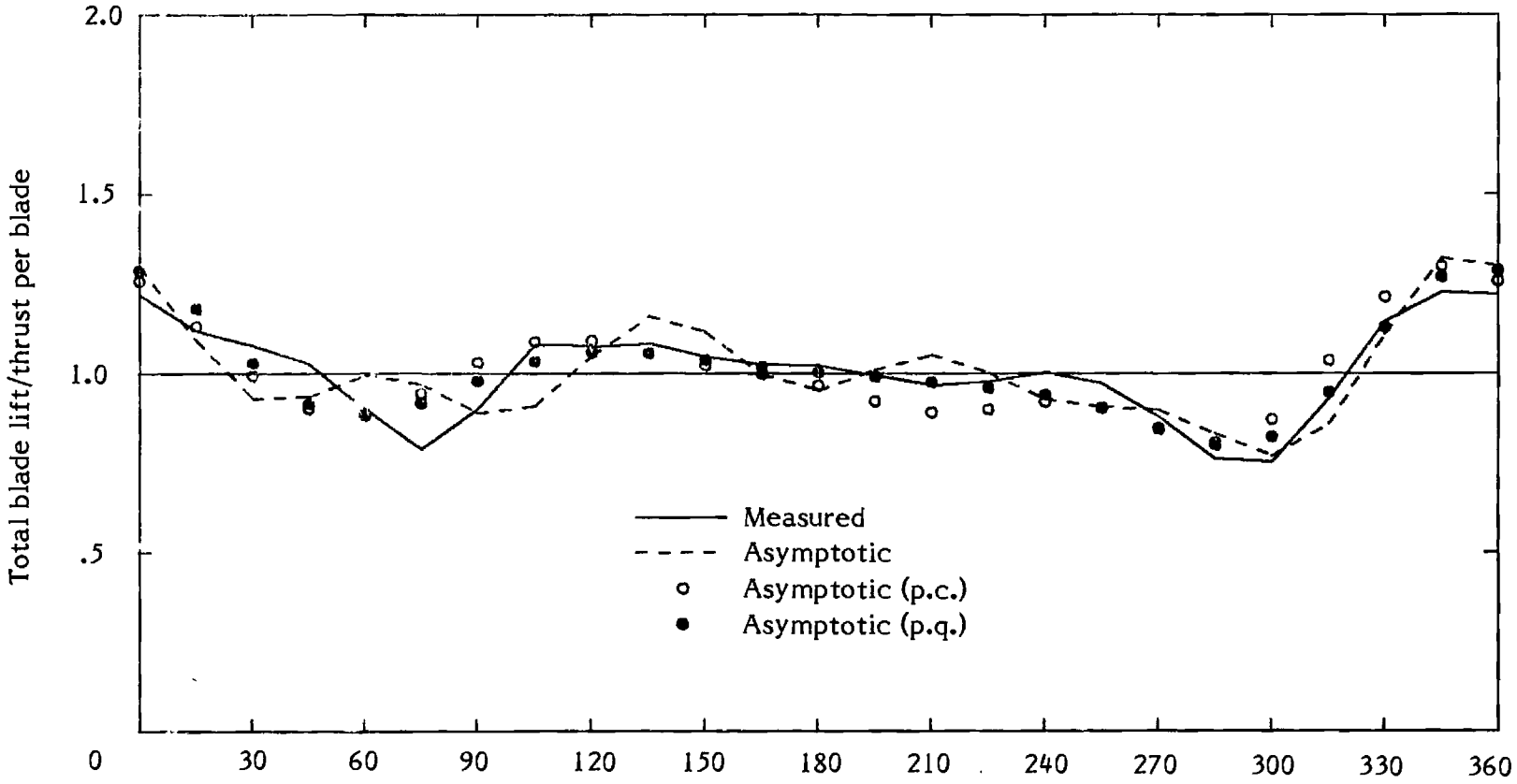

(b) $\mu = 0.13$.

Figure 6. – Continued.

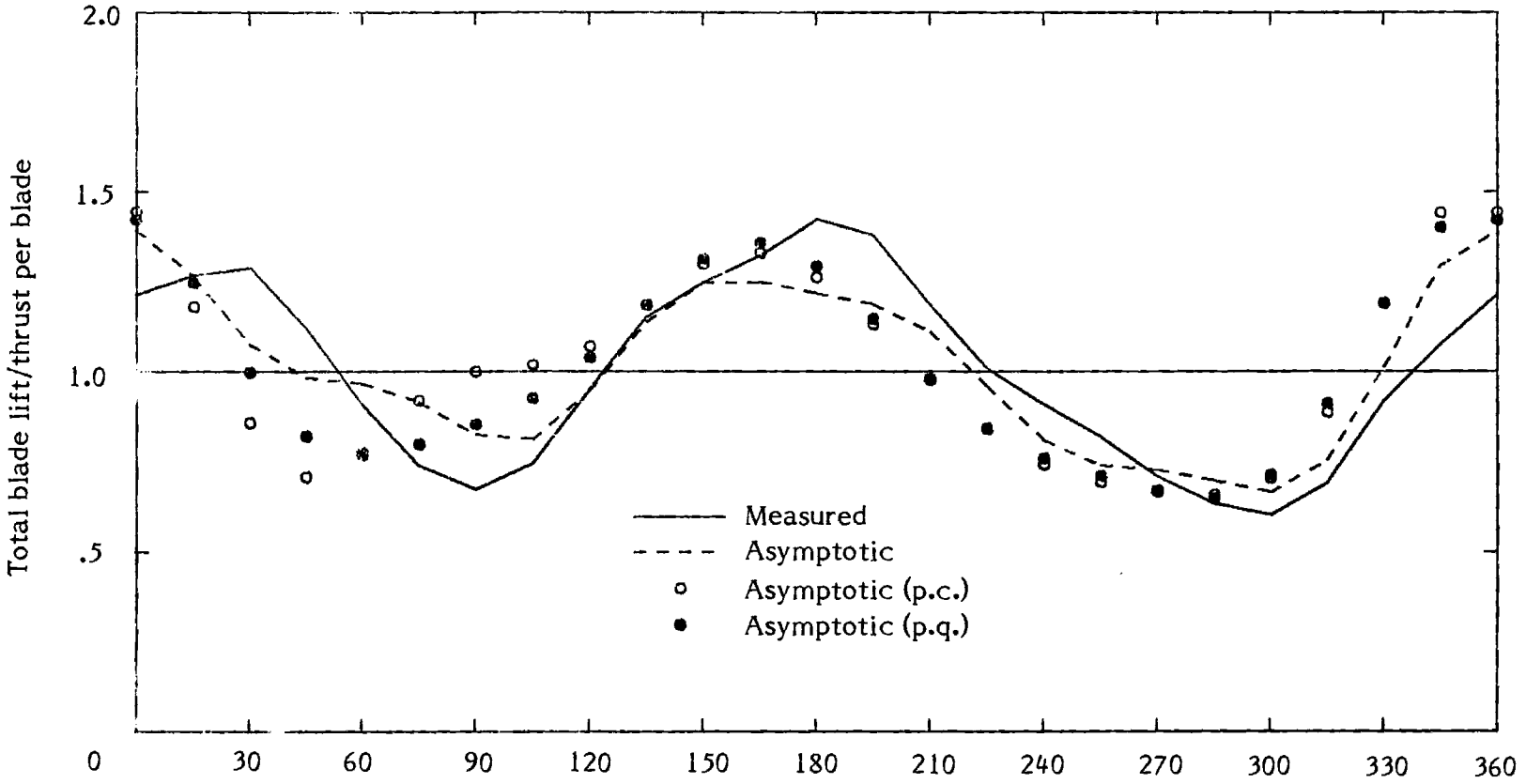

(c) $\mu = 0.29$.

Figure 6. - Concluded.

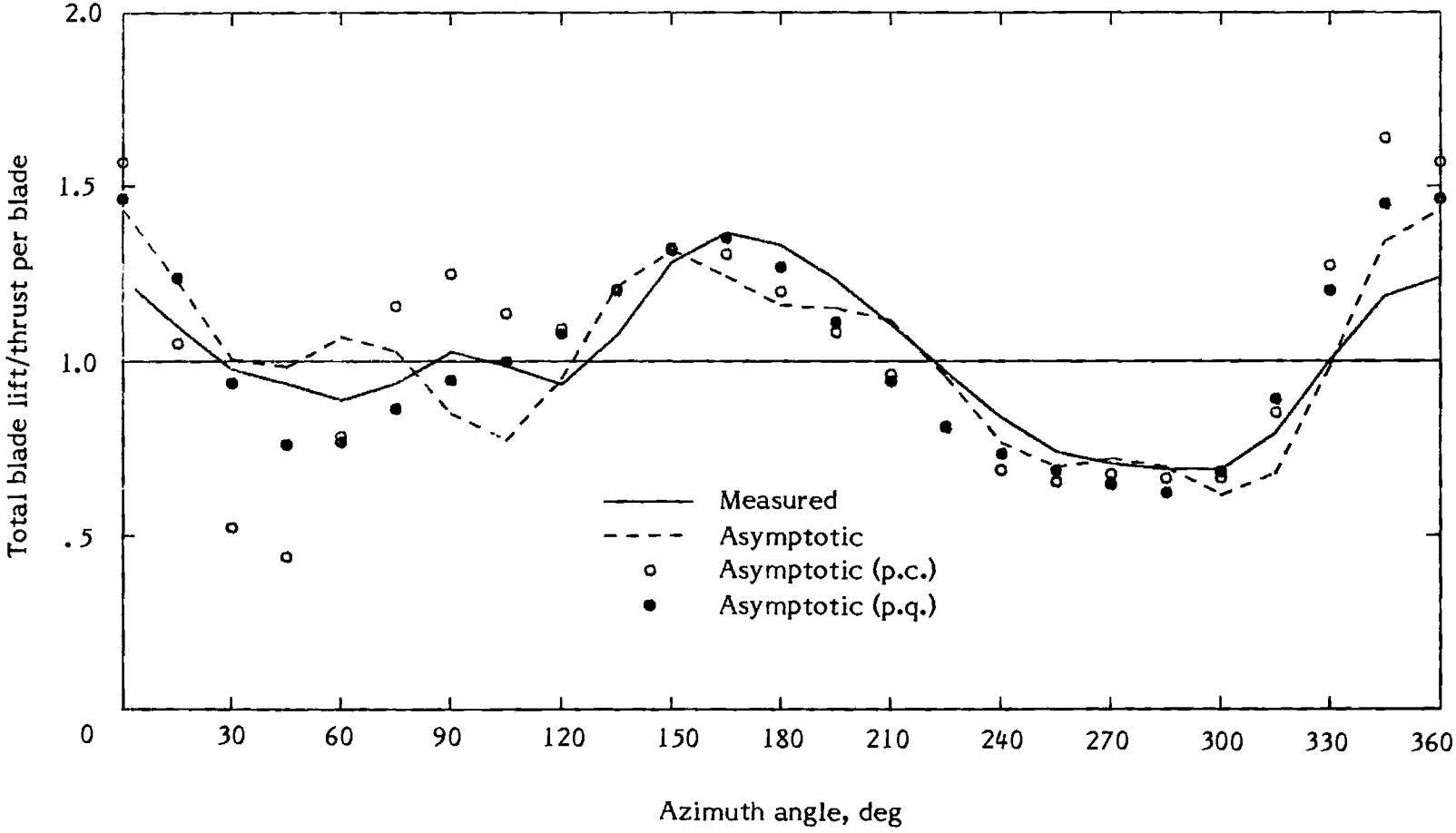

(a) $\mu = 0.29$

Figure 7. - Total blade lift versus azimuth for Case 3.

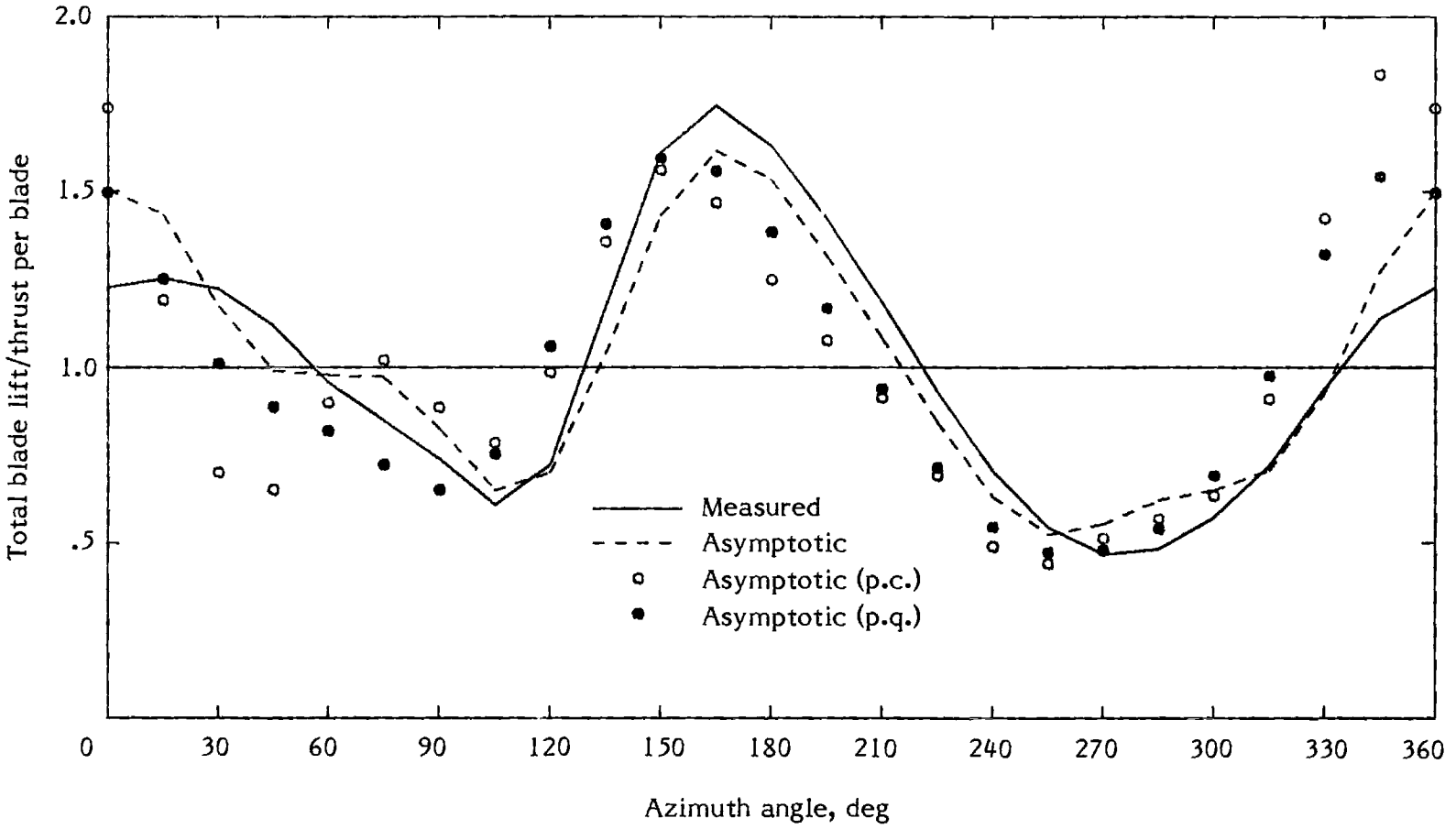

(b) $\mu = 0.39$.

Figure 7. - Continued.

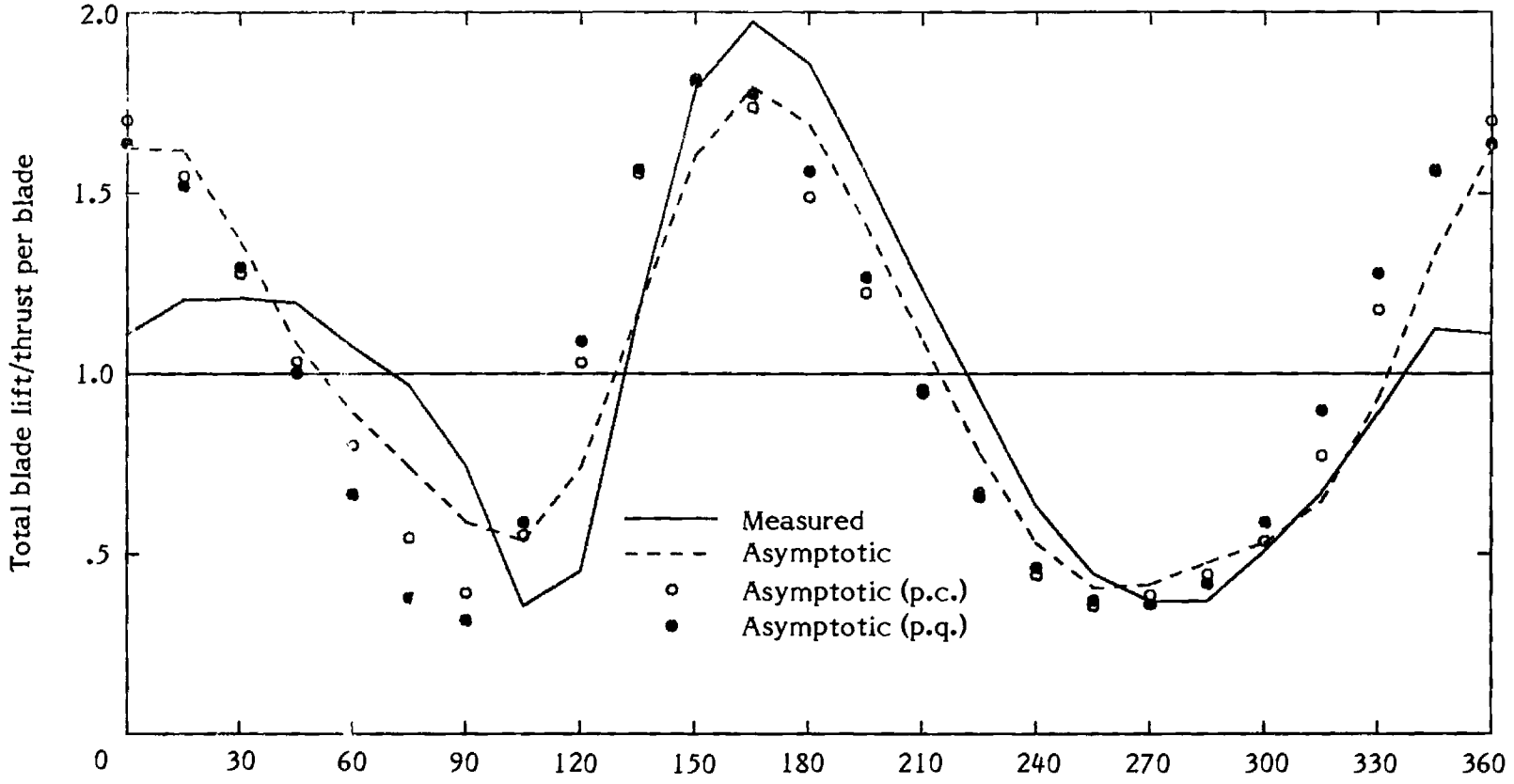

(c) $\mu = 0.45$.

Figure 7. - Concluded.

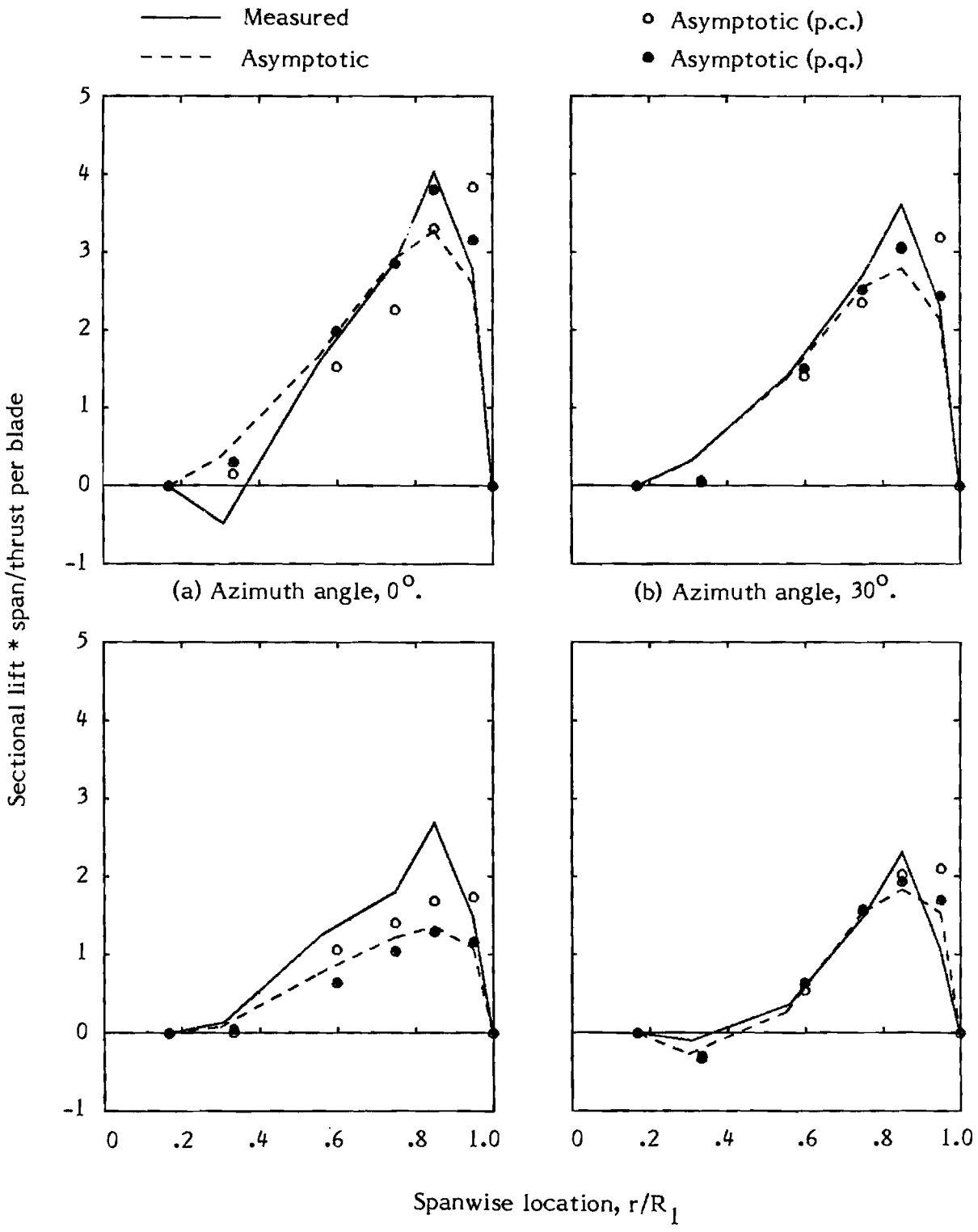

Figure 8. - Sectional lift versus spanwise location for Case 1, $\mu = 0.29$.

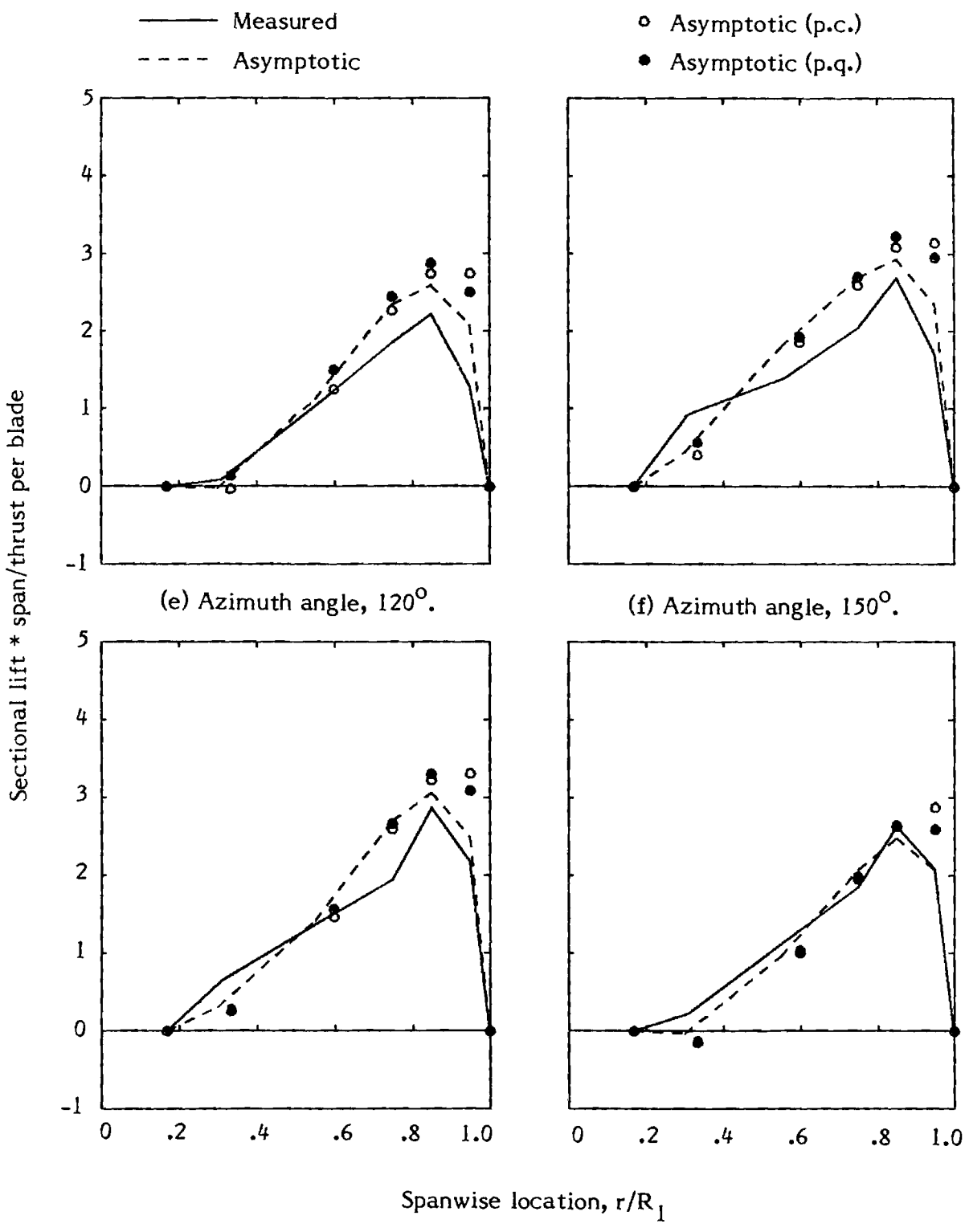

(e) Azimuth angle, 120°.

(f) Azimuth angle, 150°.

(g) Azimuth angle, 180°.

(h) Azimuth angle, 210°.

Figure 8. - Continued.

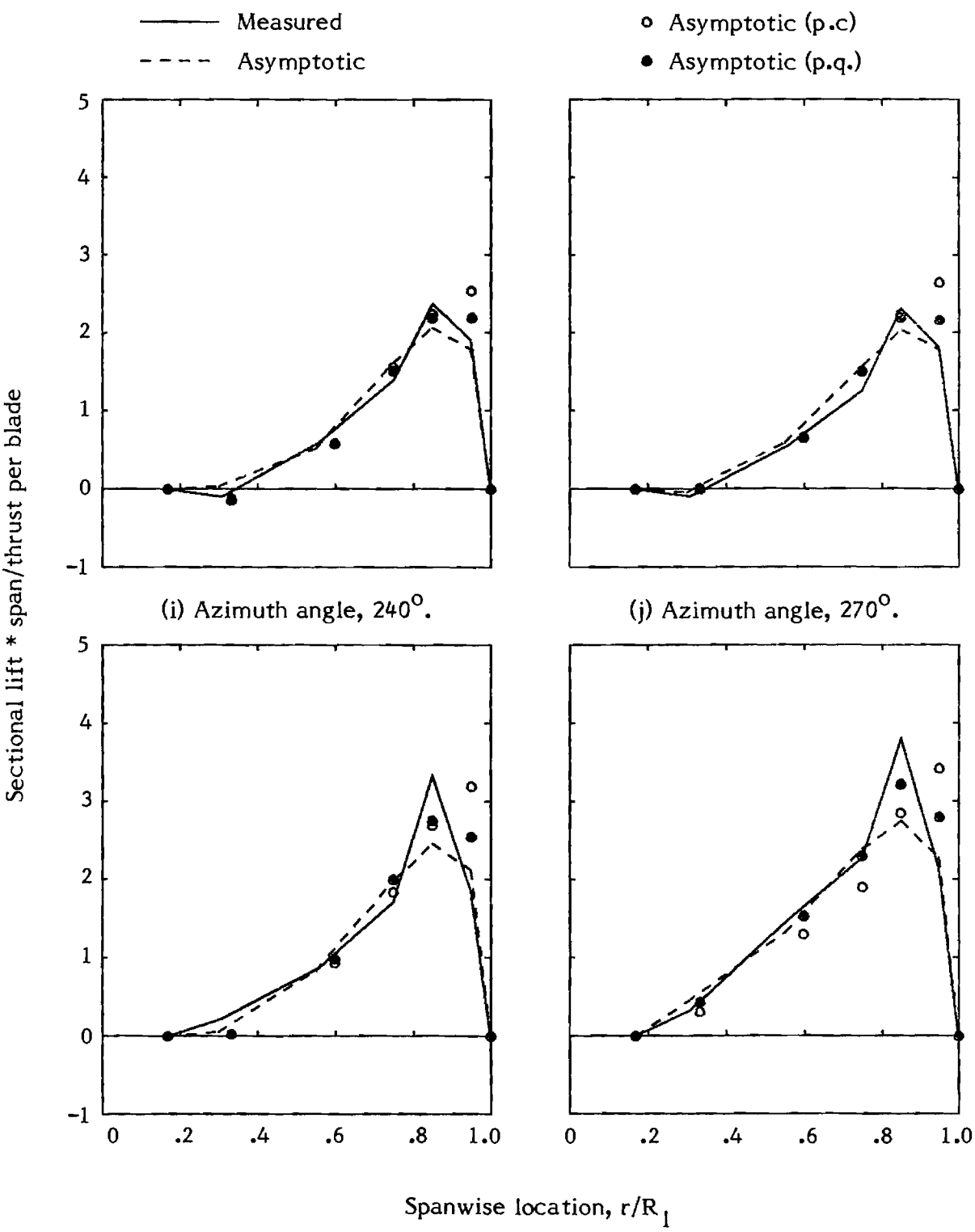

(i) Azimuth angle, 240°.

(j) Azimuth angle, 270°.

(k) Azimuth angle, 300°.

(l) Azimuth angle, 330°.

Figure 8. - Concluded.

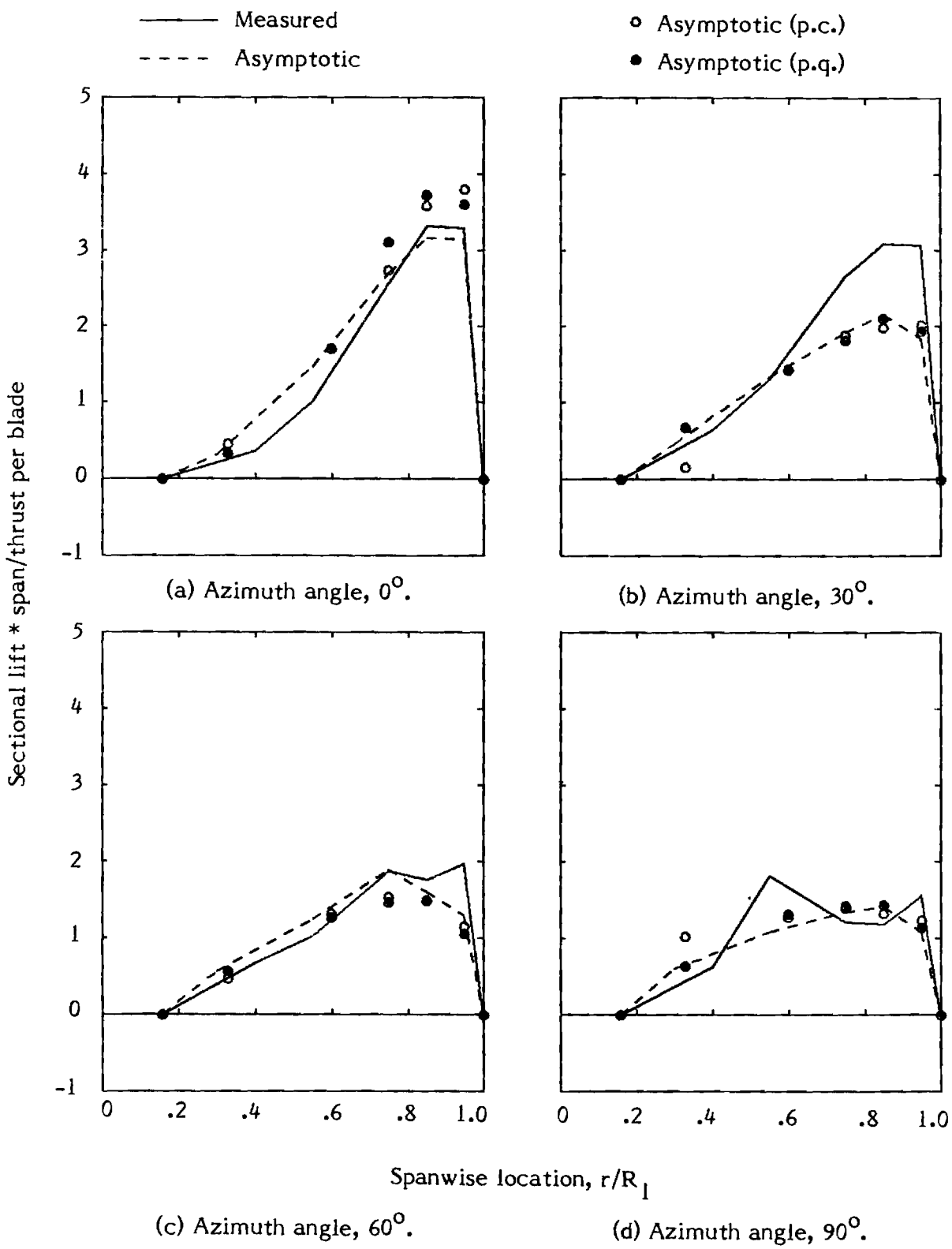

Figure 9. - Sectional lift versus spanwise location for Case 2, $\mu = 0.29$.

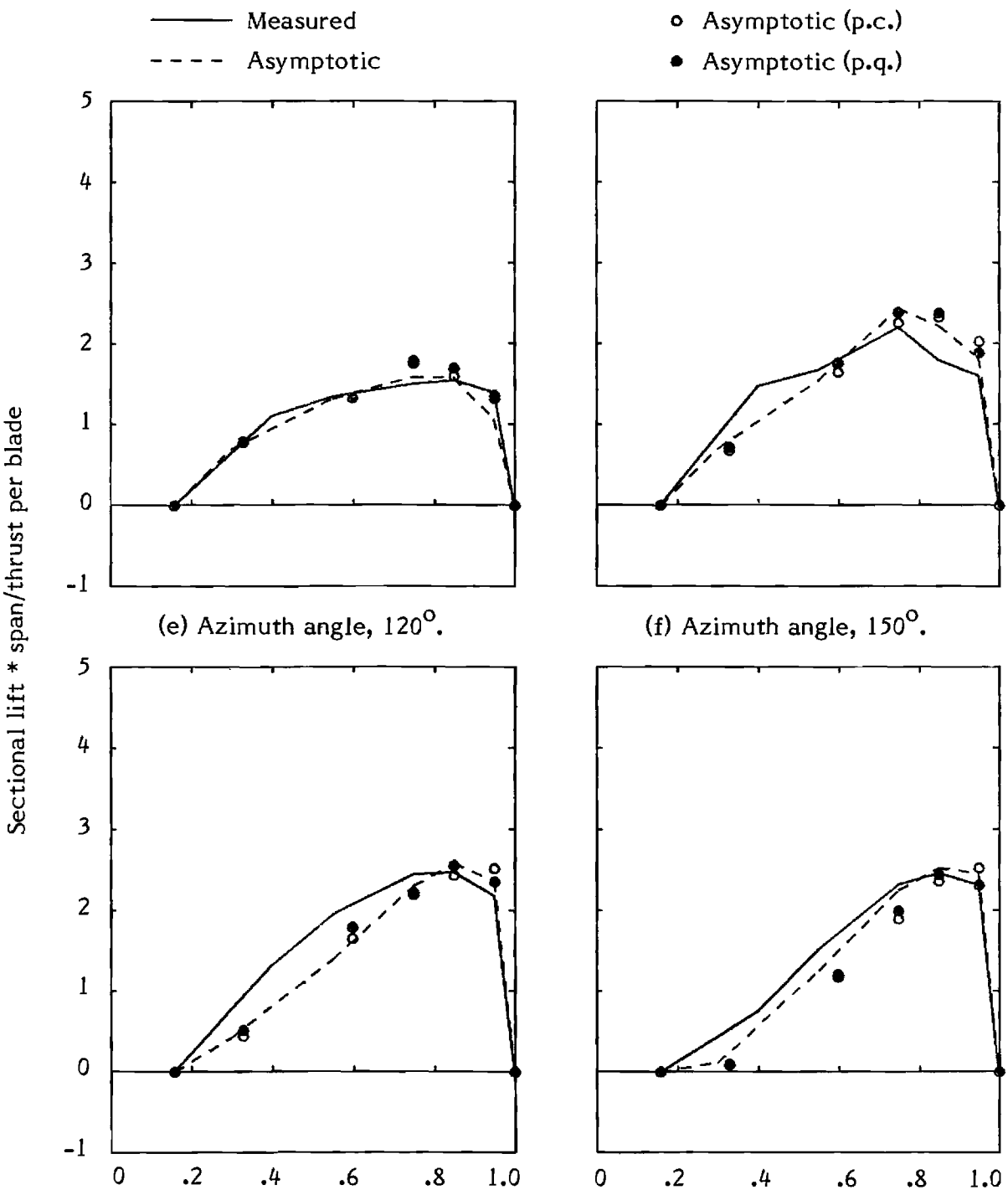

(e) Azimuth angle, 120°.

(f) Azimuth angle, 150°.

(g) Azimuth angle, 180°.

(h) Azimuth angle, 210°.

Figure 9. - Continued.

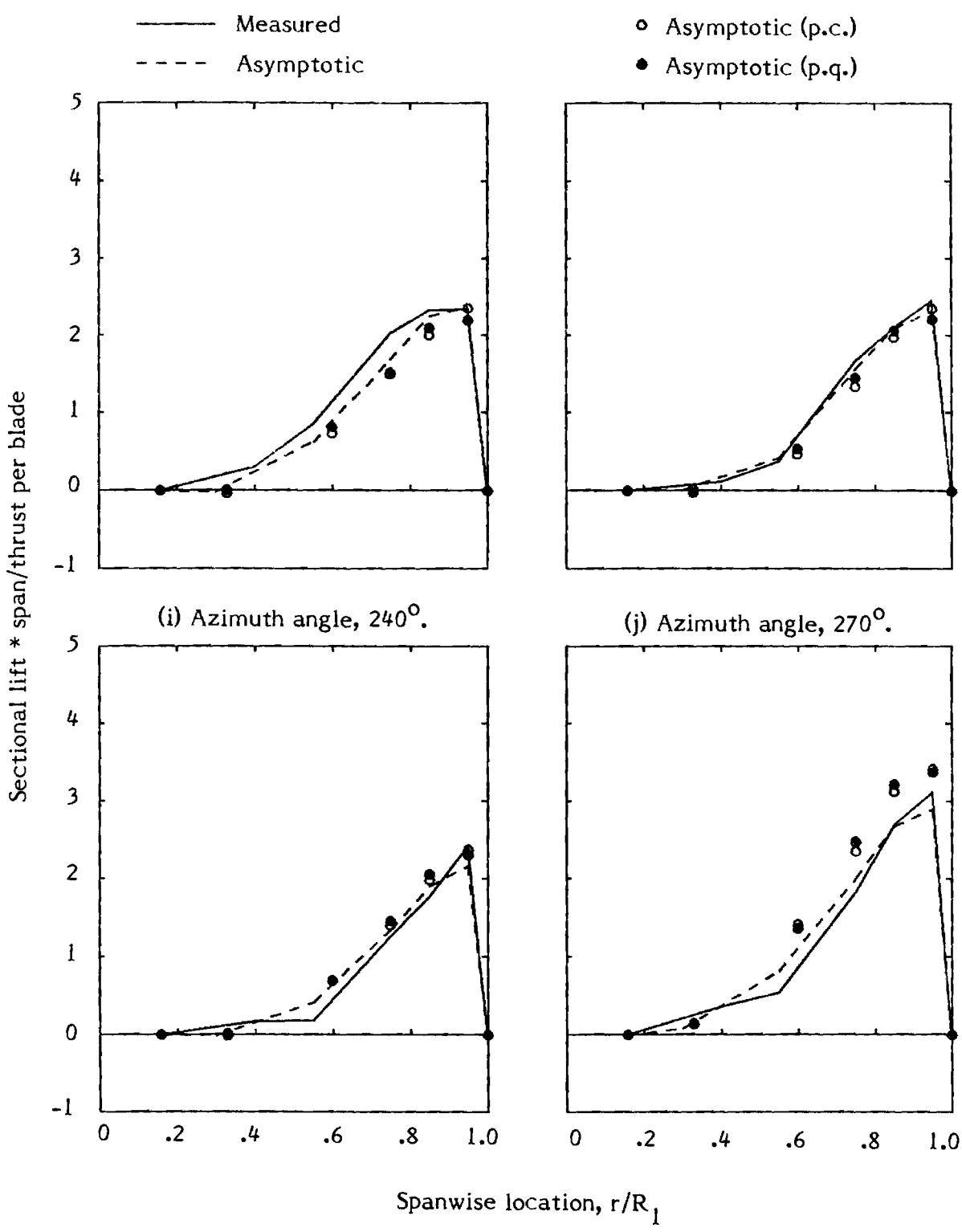

(i) Azimuth angle, 240°.

(j) Azimuth angle, 270°.

(k) Azimuth angle, 300°.

(l) Azimuth angle, 330°.

Figure 9. - Concluded.

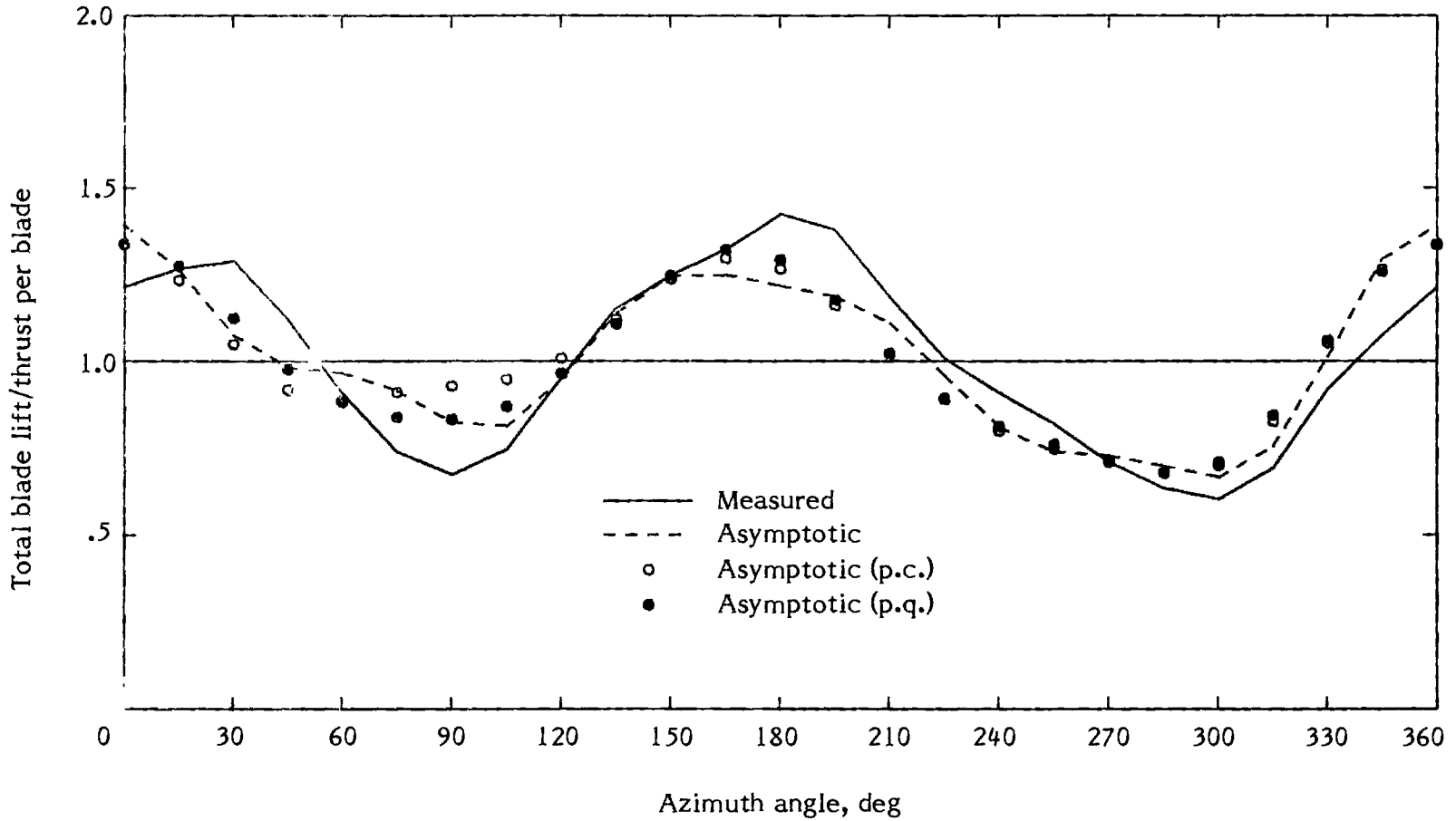

Figure 10. - Computation with constant azimuth spacing of 5^{o}, Case 2, $\mu = 0.29$.

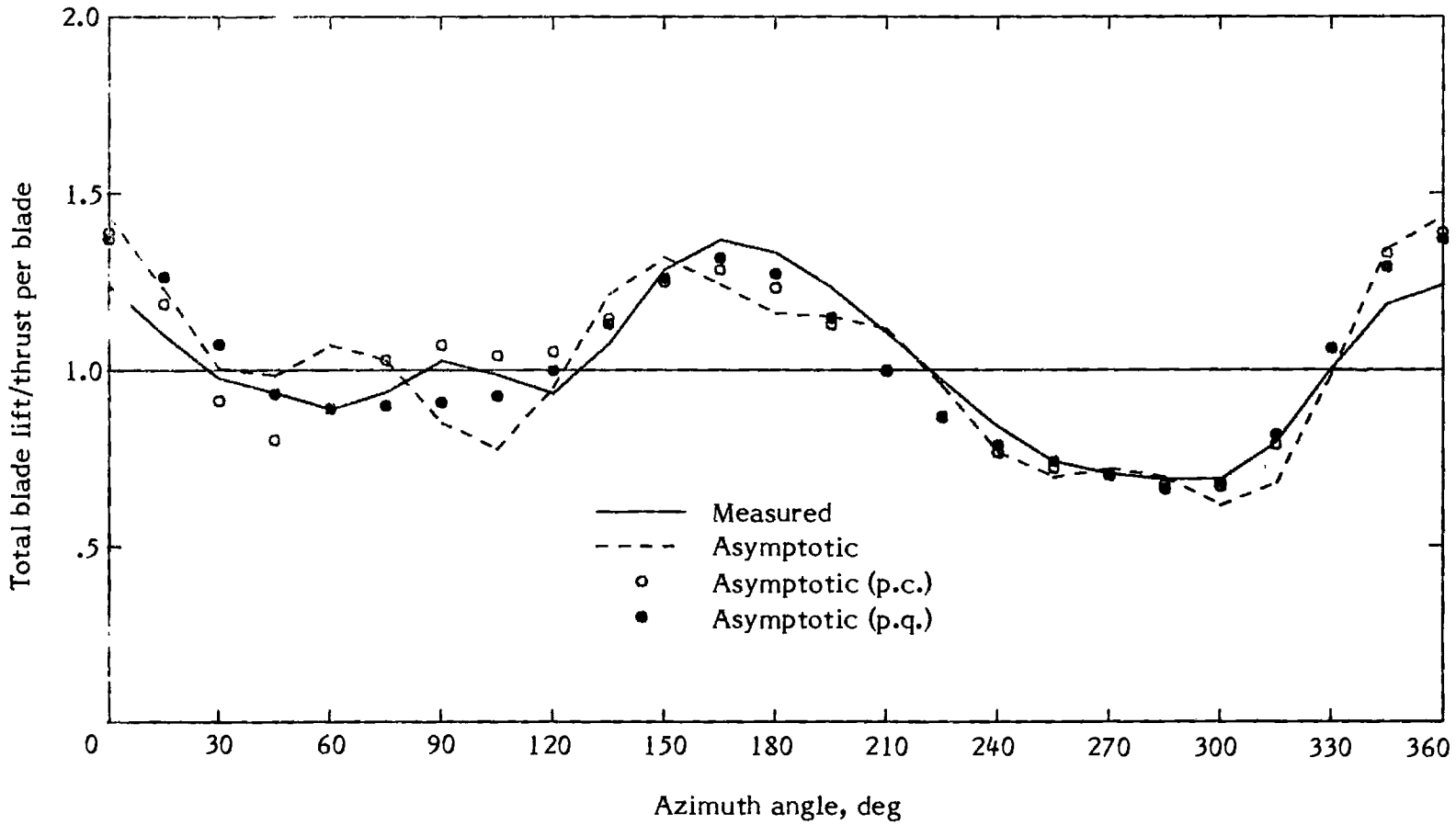

Figure 11. - Computation with constant azimuth spacing of 5^{o}, Case 3, $\mu = 0.29$.

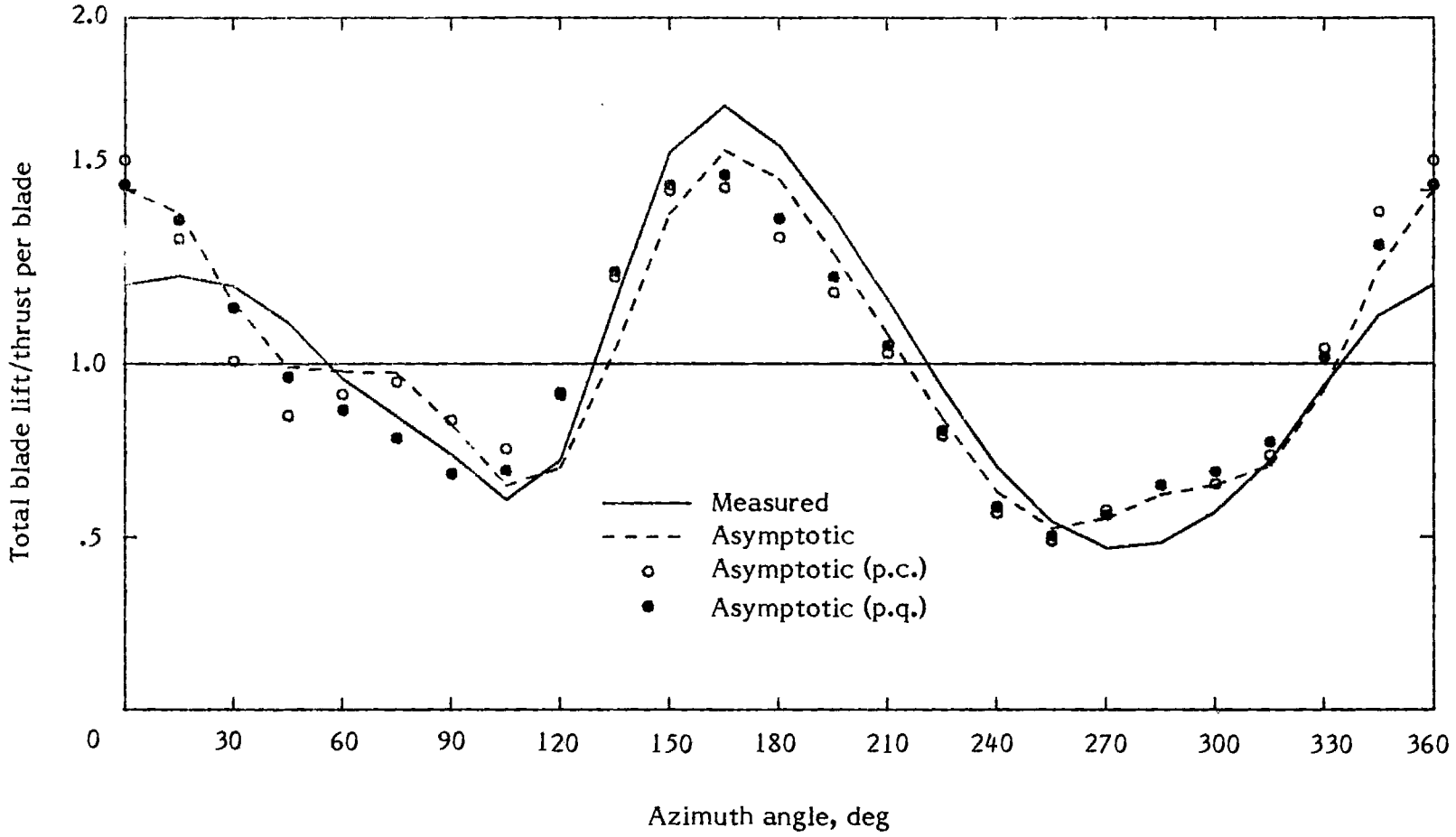

Figure 12. - Computation with constant azimuth spacing of 5^{o}, Case 3, $\mu = 0.39$.

1. Report No.	2. Government Accession No.	3. Recipient's Catalog No.
NASA CR-166092		

4. Title and Subtitle	5. Report Date
HELICOPTER ROTOR LOADS USING DISCRETIZED MATCHED ASYMPTOTIC EXPANSIONS	May 1983
	6. Performing Organization Code
7. Author(s)	8. Performing Organization Report No.
G. Alvin Pierce and Anand R. Vaidyanathan	
	10. Work Unit No.
9. Performing Organization Name and Address	
Georgia Institute of Technology School of Aerospace Engineering Atlanta, Georgia 30332	11. Contract or Grant No. NAS1-16817
	13. Type of Report and Period Covered
12. Sponsoring Agency Name and Address	Final Report
National Aeronautics and Space Administration Washington, DC 20546	14. Sponsoring Agency Code

15. Supplementary Notes

The contract research effort which led to the results in this report was financially supported by the Structures Laboratory, USARTL (AVRADCOM).
Langley Technical Monitor: John D. Berry Final Report

16. Abstract

This investigation is intended to improve the numerical practicality of a matched asymptotic expansion approach for the computation of unsteady three-dimensional airloads on a helicopter rotor. The original method as suggested by Van Holten has previously been evaluated and proven to be a comprehensive and accurate analysis for flight conditions conducive to linear flow phenomena. This effort to decrease the computational requirements of the original analysis utilizes a discretized representation of the doublet strength distribution and helical streamlines. The continuous variation of the doublet strength has been approximated by piecewise constant or piecewise quadratic distributions, and the helical trajectory of a fluid particle has been approximated by connected straight line segments. As a direct result of these simplified representations the computational time required for the execution of a typical flight condition has been reduced by an order of magnitude with respect to the requirements of the original analysis. Airloads which have been computed using the discretized method for a two-bladed model rotor and a full-scale four-bladed rotor are in close agreement with measured results and airloads from the original asymptotic analysis. For conditions characterized by significant rotor/wake interaction the piecewise constant representation requires a reduced azimuth spacing to maintain acceptable accuracy.

17. Key Words (Suggested by Author(s))	18. Distribution Statement
Unsteady airloads, Helicopter rotor, Potential flow, Asymptotic expansion	Unclassified - Unlimited Subject Category 02

19. Security Classif. (of this report)	20. Security Classif. (of this page)	21. No. of Pages	22. Price
Unclassified	Unclassified	76	

For sale by the National Technical Information Service, Springfield, Virginia 22161

HELICOPTER ROTOR LOADS USING MATCHED ASYMPTOTIC EXPANSIONS: USER'S MANUAL

By

G. Alvin Pierce
and
Anand R. Vaidyanathan

Prepared by

GEORGIA INSTITUTE OF TECHNOLOGY
SCHOOL OF AEROSPACE ENGINEERING
Atlanta, Georgia 30332

Prepared for

NATIONAL AERONAUTICS AND SPACE ADMINISTRATION

Langley Research Center
Contract NAS1-16817

CONTENTS

	Page
SUMMARY	1
INTRODUCTION	1
PROGRAM OUTLINE	3
DESCRIPTION OF INPUT	9
DESCRIPTION OF OUTPUT	12
EXAMPLES OF JOB ENTRY, INPUT DATA AND OUTPUT	13
REFERENCES	48
APPENDIX A Listing of Program ASYMP1	49
APPENDIX B Listing of Program ASYMP2	69

SUMMARY

Computer programs have been developed to implement the computational scheme arising from Van Holten's asymptotic method for calculating airloads on a helicopter rotor blade in forward flight, and a similar technique which is based on a discretized version of the method. The basic outlines of the two programs are presented, followed by separate descriptions of the input requirements and output format. Two examples illustrating job entry with appropriate input data and corresponding output are included. Appendices contain a sample table of lift coefficient data for the NACA 0012 airfoil and listings of the two programs.

INTRODUCTION

The computer programs described in this report were developed during the course of an evaluation of Van Holten's asymptotic method (ref. 1) for the calculation of airloads on a helicopter rotor blade in forward flight. The validity and computational feasibility of the approach were investigated (ref. 2), and numerical results for specific flight conditions were compared with corresponding experimental data and computations based on other analytical methods. Program ASYMP1 was written to implement the computational scheme of reference 1 (the relevant equations and expressions are given in ref. 2). As an extension of this investigation, the above computational scheme was made more efficient by discretizing the variation of the doublet strength distribution, $g(r_b, \Psi_b)$, utilizing both piecewise constant and piecewise quadratic representations for the spanwise variation. The details of the discretized scheme are presented in reference 3 and the corresponding computational method is applied in Program ASYMP2.

The general organization is similar for both programs, since the two schemes differ only in the manner in which the velocity induced by the blade pressure field is calculated. The basic unknown to be determined is the doublet strength function, $g(r_b, \Psi_b)$. Its solution is effected by a collocation technique. In the original scheme (ref. 1) this unknown function appears as a continuous modal representation for the spanwise variation and a finite Fourier series for the azimuth variation. In the discretized scheme the unknowns are the values of g at the midpoints of the spanwise segments, with a finite Fourier series for the azimuth variation of each. In either case, the solution reduces to the determination of the coefficients in the collocation representations, which is accomplished by setting up a system of simultaneous equations.

The main programs and the various subprograms will be discussed in the next section, but the general sequence of program steps is as below.

(1) Read and write input; define auxiliary parameters required for the computation.

(2) Start loop for collocation points.

(3) Test the tangential velocity U_T; if $U_T \leq (U_T)_{min}$, set up the condition for zero lift and go to the end of the collocation loop.

(4) If airfoil data tables are used, determine the lift curve slope for the current collocation point.

(5) Start loop for the number of blades and define the first azimuth interval.

(6) Compute the induced velocity contributions for the current interval and add to the corresponding coefficient matrix elements in the system of equations.

(7) Increment the azimuth interval; if the azimuth limit has been reached, go to the the next step; if not, go to Step 6.

(8) End loop for number of blades.

(9) End loop for collocation points.

(10) Set up the extra equations for the blade motion parameters.

(11) Solve system of equations and write solution.

(12) Compute and write output.

Some mention must be made of the way in which the airfoil data are used in the computational scheme. The basic equation to be set up at any collocation point is of the form

$$w_b(r_{bo}, \Psi_{bo}) = w_{ind} \tag{1}$$

where w_{ind} is the velocity induced by the pressure fields of all the blades and w_b the normal velocity due to blade motion at a collocation point (r_{bo}, Ψ_{bo}). This is rewritten as

$$\begin{aligned} w_b(r_{bo}, \Psi_{bo}) &= (w_{ind})^{2D} + \left[w_{ind} - (w_{ind})^{2D}\right] \\ &= (w_{ind})^{2D} + \Delta w \end{aligned} \tag{2}$$

where $(w_{ind})^{2D}$ is the induced velocity corresponding to a steady, two-dimensional flow. Accordingly, corrections based on airfoil data are only applied to this term and, after modification, equation (2) becomes

$$\begin{aligned} w_b(r_{bo}, \Psi_{bo}) &= (w_{ind})^{2D}_{mod} + \Delta w \\ &= \left[(w_{ind})^{2D}_{mod} - (w_{ind})^{2D}\right] + w_{ind} \end{aligned} \tag{3}$$

For steady, locally two-dimensional flow,

$$(w_{ind})^{2D} = - g(r_{bo}, \Psi_{bo}) / \rho U_T \tag{4}$$

At the local incidence and Mach number corresponding to the collocation point, the airfoil data are interpolated in the form of a locally linear relation given by

$$C_\ell = a\alpha + C_{\ell o}$$

To account for such a relation, the expression in equation (4) is modified as

$$(w_{ind})^{2D}_{mod} = -\frac{2\pi}{a}\,\frac{g(r_{bo},\,\psi_{bo})}{\rho U_T} - U_T\,\frac{C_{\ell o}}{a} \qquad (5)$$

Using equations (4) and (5) in equation (3), the modified form of the boundary condition is obtained as

$$w_b(r_{bo},\,\psi_{bo}) = \left[-\frac{(2\pi - a)}{a}\,\frac{g(r_{bo},\,\psi_{bo})}{\rho U_T} - U_T\,\frac{C_{\ell o}}{a}\right] + w_{ind} \qquad (6)$$

Comparing equations (1) and (6), it can be seen that the modification due to the airfoil data is purely an additive term that is easily incorporated into the basic computational scheme.

The next section presents an outline of the main program and the various subprograms for ASYMP1 and ASYMP2, listing the input and output of each subprogram along with a brief description of its function. The sections following this deal with descriptions of the input and output for the two programs, and samples of job entry with the corresponding output.

PROGRAM OUTLINE

Program ASYMP1

Main Program. - The program steps listed in the previous section will now be discussed in more detail.

(1) The details regarding input data and the format in which they are to be entered are given in the next section. The data include parameters describing rotor geometry, the flight condition and blade motion. Specification of the blade motion parameters (collective pitch, coning angle and the two first harmonic flapping coefficients) is optional. If they are not specified, they will be calculated as part of the solution by generating additional equilibrium equations. The input also includes the five spanwise locations of the collocation points, the normal and reduced azimuth intervals to be used for the numerical integration, the minimum value of the local onset velocity below which the zero lift condition is to be used and an integer specifying whether airfoil data are to be used. The program then writes the input data as part of the output and defines auxiliary quantities such as the induced velocity from simple momentum theory and certain factors occurring in the induced velocity contribution from the trajectory segment immediately adjacent to the collocation point.

(2) The collocation loop consists of an outer loop for the eleven equally spaced azimuth locations and an inner loop for the five spanwise locations.

(3) For the current collocation point, the local onset velocity (UT) is compared with the specified minimum value (UTMIN). If UT> UTMIN, the next step is executed. If not, the zero lift condition is set up and the next collocation point is taken up.

(4) If airfoil data are not used, this step is skipped. If they are used, the local values of $a/2\pi$ and C_{ℓ_o} are interpolated from the tables. The local values of Mach number (MLOC) and incidence (ALOC) are first defined. Subroutine TABSCH is called to find the position of MLOC and ALOC in the arrays MCL and ACL that were read as part of the input. The required values of $a/2\pi$ (SLCR) and C_{ℓ_o} (CLØ) are then determined by linear interpolation.

(5) As mentioned in reference 2, the near field has a square root singularity

corresponding to the leading edge, and this is dealt with by stopping the numerical integration just in front of the leading edge and accounting for the remainder analytically. Before starting the numerical integration, therefore, this contribution is entered into the coefficient matrix, A. The system of equations is of the form

$$Ax = B$$

where x is the array of unknown coefficients (A_{ij}, B_{ij}, eq. (9) of ref. 2). If UT <UTMIN, the zero lift condition is set up at this point.

In order to start the numerical integration, a loop for the number of blades is set up. For the current blade, Subroutine DMIN is called to determine the positions along the fluid particle trajectory at which it is directly over the blade, within a distance DMAX. Around these locations (stored in array PMIN), the reduced azimuth interval DP2 will be used. The first azimuth interval is defined with its ends at PB1 and PB2.

(6) For the current azimuth interval, a loop is set up for the 5-point Gauss-Chebyschev integration (p. 12 of ref. 2). With 55 unknown coefficients, 4 blade motion parameters and one right-hand side, there are 60 integrations to be carried out over each interval of azimuth. The corresponding functional values are sequentially obtained from function FUN2.

(7) PB1 and PB2 are incremented for the next azimuth interval. If the azimuth limit PLIM has been reached, the integration is stopped and the next blade is taken up. If not, the interval is tested to check if it includes one of the "close" locations stored in PMIN. If it does, the reduced azimuth interval is used.

(8) At the end of the loop for the number of blades, the terms in the blade normal velocity, $w_b(r_{bo}, \Psi_{bo})$, are entered in the corresponding coefficient matrix elements.

(9) At the end of the loop for the collocation points, certain spanwise integrals required for the total blade lift and the moment about the hub due to the lift are calculated (p. 42 of ref. 2).

(10) To close the system of equations, four additional equations are set up (eqs. (E8), (E9), (E10), (E11) of ref. 2). If the four blade motion parameters are specified in the input, these equations are replaced by equations of the form

$$\theta_o = (\theta_o)_{input}$$

$$a_o = (a_o)_{input}, \text{ etc.}$$

(11) The completed system of equations is solved by calling Subroutine GELIM. This is a library-supplied routine that uses the LU decomposition. The solution is overwritten on the vector B and the program prints out the values of the collocation coefficients and the blade motion parameters.

(12) With the basic solution complete, the program computes and prints out various output quantities in tabular form. The output format is described separately in a later section.

Subroutine DMIN. -

Input: MU(μ), LAM(λ), DB($\Delta\Psi_j$), RBØ(r_{bo}), PBØ(Ψ_{bo}), PLIM, DMAX

Output: I, P

Comments: This subroutine locates those azimuth positions along the fluid particle trajectory at which the particle is "close" to the j^{th} blade. The x_b axis is fixed to the blade and rotates with it (fig. 1 of ref. 2) so that the x_b coordinate along the trajectory periodically goes to zero whenever there is an intersection with the z_b axis. At some of these locations the particle may be too close to the blade (within a specified distance DMAX). These are the locations (I in number) that are returned in the array P. The routine locates the positions by scanning the trajectory with small azimuth increments checking for a change in sign of the x_b coordinate. When such a position is located, the distance from the blade is compared with DMAX.

Subroutine TRAJ. -

Input: RØ(R_o/R_1), AR(A), MU, LAM, RBØ, PBØ, DB, PB(Ψ_b)

Output: R(r), SX(sin χ), CX(cos χ), SHP(sinh Ψ), CHP(cosh Ψ),
ST(sin θ), CT(cos θ), SHE(sinh η), CHE(cosh η),
SP(sin ϕ), CP(cos ϕ) - returned through common block TRAJ1
ZS(z_b/s)

Comments: Given a point Ψ_b on the trajectory relative to the j^{th} blade, the corresponding coordinates in various coordinate systems are calculated. The coordinates (r,χ, z_b), (Ψ,θ,χ) and (η,ϕ) are respectively of the point in cylindrical, prolate spheriodal and plane elliptic coordinate systems.

Function FUN1. -

Input: RØ, AR, I
N(n), PI(π) - through common block MAIN1
R, SX, CX, SHP, CHP, ST, CT, SHE, CHE, SP, CP - through common block TRAJ1

Comments: The values of various functions required in FUN2 are calculated. Specifically, the six derivative expressions D_1 to D_6 (Appendix C of ref. 2) are returned for values of I from 1 to 6 in the input.

Function FUN2. -

Input: RØ, AR, TW(ϵ), MU, LAM, RBØ, PBØ, DP($\Delta\Psi_b$), DB,
X(Ψ_{bi}, p. 12, ref. 2), I
N, PI - through common block MAIN1

Comments: As described in Step 6 of the main program, the coefficient matrix elements corresponding to the various unknowns and the right-hand side require numerical integration, for which the necessary functional values are returned by function FUN2. Given the azimuth position X, Subroutine TRAJ and Function FUN1 are used to set up the relevant expressions. The value, I = 1, corresponds to the function multiplying A_{oo} (eq. (9) of ref. 2). The value, I = 2, corresponds to the function

multiplying A_{no} (n = 1,2,3,4). The values, I = 3,4,5,6,7, respectively correspond to the functions multiplying θ_o, a_o, a_1, b_1 and the right-hand side. The forms of these integrands are given in Appendix C of reference 2 as induced velocity coefficients. The nonintegral parts of these expressions are the result of analytical integration of the near field over a small interval $\Delta\Psi_b$ adjacent to the collocation point and are defined in the main program (Step 5). Over this interval, therefore, the near field contribution is skipped in Function FUN2.

Function FUN3. -

Input: RØ, AR, X, I

N, PI - through common block MAIN1

Comments: The expressions for the total blade lift and the moment about the hub due to the lift involve certain spanwise integrals (I_o^1, I_o^2, I_n^1, I_n^2 (n = 1,2,3,4) see p. 42 of ref.2) and the corresponding integrands are set up in FUN3. The radial position, r_b/R_1, is X. The notation, I = 1,2,3,4, corresponds respectively to the integrals I_o^1, I_o^2, I_n^1, I_n^2.

Function PNM. -

Input: N(n), M(m), X(x)

Comments: This function generates the associated Legendre function $P_n^m(x)$ over the ranges $0 \le n \le 4$, $0 \le m \le 3$, $|x|<1$. Although the relevant recursive relations could be used, the function defines P_n^m explicitly in terms of x for all the above values of n and m (Appendix D of ref. 2).

Function QNM. -

Input: N, M, X

Comments: The associated Legendre function $Q_n^m(x)$ is calculated over the ranges $1 \le n \le 4$, $1 \le m \le 2$, $|x| > 1$. As listed in Appendix D of reference 2, the exact definitions are used for $|x| \le 3$ and asymptotic expansions are used for $|x| > 3$ to avoid the accumulation of roundoff error.

Subroutine TABSCH. -

Input: X, N, XT

Output: I1,I2, INT

Comments: This routine searches an array X, of dimension N, for the position of a value XT. If XT lies between X(I1) and X(I2), INT = 0. If XT is outside the range of X, the subroutine returns INT = -1 for XT< X(1) and INT = 1 for XT >X(N) (it is assumed that the elements in X are arranged in increasing order).

Program ASYMP2

Main Program. - Here again the previously listed program steps will be discussed

in more detail.

(1) This step is similar to Step 1 of Program ASYMP1. There are some changes in the entry of input data (described in the next section). Instead of spanwise collocation point locations, the program reads the spanwise locations at which the blade is divided into segments for discretization. Collocation points are located at the center of each segment. The integer, ISEL, specifies whether a piecewise constant or piecewise quadratic representation is to be used for the computation. Following the reading and writing of input data, some arrays that will be required later are set up. Arrays FX1 and FX2 contain the average values of the factors

$$\sqrt{\frac{1-x}{1+x}} \quad \text{and} \quad \left\{ \frac{(R_1 - R_0)}{2R_1} \quad \frac{\sqrt{1-x^2}}{A} \right\}$$

over each chordwise segment. These values will be used in the near field calculation. Array GF relates the endpoint and midpoint values for the spanwise segments in the piecewise quadratic representation. If $\rho_j (j = 1,\ldots 6)$ represent the ends of the 5 spanwise segments ($\rho_1 = R_0$, $\rho_6 = R_1$) and $r_j (j = 1,\ldots 5)$ the midpoints, then

$$g(\rho_i) = \sum_{j=1}^{5} (GF)_{ij}\, g(r_j) \qquad (i = 2,3,4,5)$$

(2-5) These steps are generally the same as the corresponding steps in Program ASYMP1.

(6) For the current azimuth interval, the slopes and intercepts for the linear approximations to $x_b(\Psi_b)$, $y_b(\Psi_b)$ and $r_b(\Psi_b)$ are defined as XBI, XBS, YBS, RBI, RBS. The far field contribution is computed using Subroutine FFINT. For computing the common part and near field contributions (which are both dependent on the local spanwise dipole strength) it is necessary to divide that part of the interval (PB1, PB2) which has the trajectory within the blade span into subintervals such that each subinterval has a trajectory wholly within one spanwise segment. This is done by calling Subroutine SUBIVL. The common part and near field contributions are then computed respectively by calling Subroutines CPINT and NFINT, summing the contributions over each subinterval.

(7-12) Comments on these steps are the same as for Program ASYMP1.

Subroutine SUBIVL. -

Input: RB1(r_{b1}), RB2(r_{b2}), PB1(Ψ_{b1}), PB2(Ψ_{b2}), R(ρ_j;j = 1,. . .6)

Output: I, P1, P2

Comments: As explained in Step 6 for the main program, the azimuth interval must be subdivided so that the trajectory segments within each subinterval lie completely within one spanwise segment. This is done by comparing the endpoints for each segment (ρ_j, ρ_{j+1} for the j^{th} segment) successively with the spanwise coordinates at the ends of the interval, r_{b1} and r_{b2}. The terms I, P1 and P2 are all arrays of dimension 5, corresponding to the number of spanwise segments. For the segment J, I(J) = 1 or 0 depending on whether a portion of the trajectory does or does not lie within that

segment. If I(J) = 1, the azimuth positions corresponding to the ends of that portion of the trajectory segment are stored in P1(J) and P2(J).

Subroutine NFINT. -

Input: P1, P2, X, ISEL

XI, XS, YS, RI, RS - through common block MAIN1

Output: T1, T2, T3

Comments: This subroutine computes various integral terms required for the near field contribution over the azimuth interval (P1, P2), with X being the chordwise location of a segment over which the surface pressure has been averaged. The terms T1, T2, T3 correspond to the terms n_0, n_1, n_2 in Appendix C of reference 3. For the piecewise constant representation, ISEL = 0, only T1 is used.

Subroutine CPINT. -

Input: P1, P2, ISEL

XI, XS, YS, RI, RS - through common block MAIN1

Output: T1, T2, T3

Comments: The terms required to set up the common part contribution over the azimuth interval (P1, P2) are calculated. The terms T1, T2, T3 correspond to C_1, C_2, C_3 in Appendix C of reference 3. For the case ISEL = 0, only the term T1 is relevant. The common part is singular at the collocation point, although the complete pressure field is regular due to the singularities in the far field and common part cancelling out in the limit. Since this has been established, when P2 = 0 (corresponding to the collocation point) the routine sets all the terms to zero.

Subroutine FFINT. -

Input: P1, P2, R, ISEL

XI, XS, YS, RI, RS - through common block MAIN1

Output: T1, T2, T3

Comments: This routine calculates the terms required for the far field contribution over the azimuth interval (P1, P2) with R being a boundary of one of the spanwise segments (ρ_j, j = 1, . . .6). The expressions for T1, T2, T3 are derived in Appendix C of reference 3. As pointed out above, the singularity in the far field gets cancelled out in the limit. However, unlike the common part, there is a finite residue left over after cancellation.

In addition to the subroutines listed in this section, both programs make use of Subroutine GELIM to solve the system of simultaneous equations. This routine uses direct Gaussian elimination with pivoting and details can be found in the Langley Computer Programming Manual.

DESCRIPTION OF INPUT

The input data required for the programs can be divided into two parts. The first consists of data pertaining to rotor geometry, flight condition, blade motion and some additional parameters relevant to the computational scheme. These are assumed to be a part of the INPUT file; that is, they must be entered after the job control statements when the job is submitted for execution. The second part consists of airfoil data (if required) and these are assumed to reside in a file called AFDATA which must therefore be available (if the data are to be used) when the job is executed. The format for the airfoil data is described separately following descriptions of the basic input for the two programs.

Program ASYMPI

The READ statements for the first part of the input are given below, followed by explanations of the data items.

```
READ (5,*) R , AR, NB, TW, MU, ALR, CT, MINF
READ (5,*) N1, N2, N3, N4
IF (N1. EQ. 1) READ (5,*) THC
IF (N2. EQ. 0) READ (5,*) GAMA
IF (N2. EQ. 1) READ (5,*) AØ
IF (N3. EQ. 1) READ (5,*) A1
IF (N4. EQ. 1) READ (5,*) B1
READ (5,*) (RBØ(I), I = 1, NSP)
READ (5,*) DP1D, DP2D, UTMIN, NAFD
```

Each READ statement corresponds to a line of data input. It may be noted that all the above statements specify free format for the data entry so that the different items in a single line of data can be entered in any convenient format, separated by commas.

RØ	=	root radius/tip radius
AR	=	aspect ratio
NB	=	number of blades (integer)
TW	=	built-in linear twist (ϵ , ref. 2)
	=	pitch angle at root minus pitch angle at tip
MU	=	forward speed/tip speed (floating point)
ALR	=	inclination of tip path plane to flight path, in degrees (forward tilt positive)
CT	=	rotor thrust coefficient = $T/\rho\,(\pi R_1^2)\,(\Omega R_1)^2$

MINF = Mach number corresponding to forward speed (note: this is used only for interpolating from airfoil data; if airfoil data are not used, this item is not needed and can be set to zero)

N1,N2,N3,N4 = integers associated with the four blade motion parameters (THC, AØ, A1, B1 respectively) - if a blade motion parameter is to be specified in the data, the corresponding integer is set to 1; if it is to be calculated by the program, the integer is set to 0.

THC = pitch angle at blade root in degrees

GAMA = coefficient representing blade flapping inertia

= 2π(air density) (chord) R_1^4/(mass moment of inertia of blade about flapping hinge), to be specified if the coning angle is to be calculated

AØ = blade coning angle

A1 = first harmonic longitudinal flapping coefficient

B1 = first harmonic lateral flapping coefficient

Note: Flapping angle = $A\emptyset - A1 \cos \Psi_b - B1 \sin \Psi_b$

RBØ = array (of dimension 5) containing the spanwise locations of the collocation points, as fractions of the tip radius, e.g., 0.3, 0.5, 0.75, 0.85, 0.95

DP1D, DP2D = normal and reduced azimuth intervals to be used for the numerical integration (step 6 of the main program) in degrees, e.g., 15.0, 5.0

UTMIN = minimum value of local onset velocity at a collocation point for using the normal velocity boundary condition (see step 3), as a fraction of the tip speed

Note: Local onset velocity at $(r_{bo}, \Psi_{bo}) = (r_{bo}/R_1 + \mu \sin \Psi_{bo})$

NAFD = integer related to use of airfoil data:
NAFD = 1 - airfoil data used
NAFD = 0 - airfoil data not used

Program ASYMP2

Much of the input is identical to that for ASYMP1, as can be seen from the READ statements below.

```
READ (5,*) RØ, AR, NB, TW, MU, ALR, CT, MINF
READ (5,*) N1, N2, N3, N4
IF (N1. EQ. 1) READ (5,*) THC
IF (N2. EQ. 0) READ (5,*) GAMA
IF (N2. EQ. 1) READ (5,*) AØ
IF (N3. EQ. 1) READ (5,*) A1
```

IF (N4. EQ. 1) READ (5,*) B1

READ (5,*) (R (I), I = 2, 6)

READ (5,*) DP1D, DP2D, UTMIN, ISEL, NAFD

R = array (of dimension 6) containing the spanwise locations (as fractions of the tip radius) marking the division into 5 spanwise segments

(R (1) = RØ, R (6) = 1.0)

e.g., R (I), I = 2, 6 ⟶ 0.5, 0.7, 0.8, 0.9, 1.0

ISEL = integer specifying choice of piecewise representation:

ISEL = 0 - piecewise constant representation

ISEL = 1 - piecewise quadratic representation

DP1D and DP2D are the normal and reduced azimuth intervals, in degrees, over which the induced velocity contributions are summed. Typical values are 30.0 and 10.0, respectively.

Airfoil Data

The data used in this case (if NAFD = 1) consist of lift coefficients, over a range of incidences and Mach numbers.

NXL = number of Mach numbers in the table

NZL = number of incidences in the table

MCL = array containing the NXL Mach numbers (ascending order)

ACL = array containing the NZL incidences (ascending order)

CL = two-dimensional array (of dimension at least (NZL, NXL)) containing the lift coefficients

The format for data entry is as below.

Line 1: NXL, NZL (30X, 2I2 format)

Col 31 - 32 NXL

33 - 34 NZL

Lines 2(a),(b),. . . MCL (I), I = 1, NXL (7X, 9F7.0 format)

Col	8 - 14	MCL (1)
	15 - 21	MCL (2)
	.	
	.	
	.	
	64 - 70	MCL (9)

If NXL is greater than 9, additional lines are entered with the same format until all NXL entries have been made.

Lines 3(a), (b) . . . ACL (1), CL (1, I), I = 1, NXL (F7.0, 9F7.0 format)

Col	1 - 7	ACL (1)
	8 - 14	CL (1, 1)
	15 - 21	CL (1, 2)
	.	
	.	
	.	
	64 - 70	CL (1, 9)

If NXL is greater than 9, additional lines are entered as below (7X, 9F7.0 format).

Col	8 - 4	CL (1, 10)
	15 - 21	CL (1, 11)
	.	
	.	
	.	
	64 - 70	CL (1, 18)

Lines 4, 5, 6 . . . are identical in format to line 3 and contain the data with ACL (2), ACL (3) . . . ACL (NZL).

DESCRIPTION OF OUTPUT

The presentation of output is basically the same for Programs ASYMP1 and ASYMP2. Each page of output is formatted to fit within letter paper size (11" x 8.5"). Given below is a page-by-page description of the output.

Page 1 contains the input data and some auxiliary parameters, as well as the locations of the collocation points at which the normal velocity condition has been replaced by the zero lift condition. Page 2 contains the basic solution for the collocation coefficients used to express the variation of the dipole strength function $g(r_b, \Psi_b)$. These are 55 in number, corresponding to the coefficients in equation (9) of reference 2 for ASYMP1 and to the coefficients in equation (E3) of reference 3 for ASYMP2. Also presented on this page are the blade motion parameters (θ_o, a_o, a_1, b_1)

and the computed values of the rotor thrust coefficient and the moment coefficients about the rotor X - and Y - axes. Page 3 contains the distribution of sectional lift $/(\rho \Omega^2 R_1^3)$ in tabular form, at 5 radial and 24 azimuth locations. Page 4 contains a similar table of sectional lift$*R_1$/thrust per blade. Pages 5 and 6 contain tables of sectional pitching moment$/(\rho \Omega^2 R_1^4)$ and the center of pressure locations. Page 7 presents the variation with azimuth of the total blade lift, the moment due to lift about the hub and the radial location of the center of lift. Pages 8 - 15 present the distribution of surface pressure differential$/(\rho \Omega^2 R_1^2)$ at 5 spanwise and 10 chordwise locations, for every 15 degrees of azimuth.

EXAMPLES OF JOB ENTRY, INPUT DATA AND OUTPUT

The current versions of ASYMP1 and ASYMP2, written in Fortran IV, are intended to be run on the Cyber network at the Langley Research Center inasmuch as they use subroutine GELIM which is to be accessed from the subroutine library FTNMLIB. With appropriate changes, therefore, they can be run on any other system with a Fortran IV compiler. In order to compile and execute the programs, the basic sequence of job control statements would be as follows.

```
GET, ASYMP1 (or ASYMP2).
GET, AFDATA = airfoil datafile name. (if airfoil data are used)
MAP, OFF. (if load map is not required)
FTN, I = ASYMP1 (or ASYMP2), L = 0.
ATTACH, FTNMLIB/UN = LIBRARY.
LIBRARY, FTNMLIB.
LGO.
```

The control statements must be followed by the relevant input data. Examples are given below for two conditions: (A) data for program ASYMP1, applied to Case 1, $\mu = 0.29$ (see p. 16 of ref. 2) and (B) data for program ASYMP2, applied to Case 2, $\mu = 0.29$ using the piecewise quadratic representation. In each case the input data is followed by the corresponding output listing.

Example A

```
Line 1:  0.17, 5.43, 2, 0., 0.29, 6.7, 0.00394, 0.
Line 2:  0, 1, 0, 0
Line 3:  0.
Line 4:  0.3, 0.5, 0.75, 0.85, 0.95
Line 5:  15.0, 5.0, 0.1, 0
```

In the first line MINF has been set to zero since airfoil data are not going to be

used. The second line specifies that θ_o, a_1 and b_1 are to be computed while a_o will be input. Since this example involves a teetering rotor with no coning angle, the third line specifies $a_o = 0$.

```
ROOT RADIUS/TIP RADIUS=     .17000
ASPECT RATIO=    5.43000
NUMBER OF BLADES= 2
LINEAR TWIST(ROOT TO TIP)=    0.00000 DEGREES
FORWARD SPEED/TIP SPEED=     .29000
ROTOR INCIDENCE(FORWARD TILT POSITIVE)=    5.70000 DEGREES
FREESTREAM MACH NUMBER=    0.00000
THRUST COEFFICIENT=     .00394
CONING ANGLE=    0.00000 DEGREES
TOTAL INFLOW RATIO=     .04070
MINIMUM UT=     .10000(ZERO LIFT CONDITION APPLIED BELOW THIS VALUE)
NORMAL AZIMUTH INTERVAL=  15.00000 DEGREES
REDUCED AZIMUTH INTERVAL=    5.00000 DEGREES
AIRFOIL DATA TABLES NOT USED
R=     .300 PSI= 229.091DEGREES UT=     .081 ZERO LIFT CONDITION APPLIED
R=     .300 PSI= 261.818DEGREES UT=     .018 ZERO LIFT CONDITION APPLIED
R=     .300 PSI= 294.545DEGREES UT=     .036 ZERO LIFT CONDITION APPLIED
```

```
SOLUTION FOR COEFFICIENTS
-------------------------

(GO(I),I=1,NSP)
-.2656E-02 -.4578E-02 -.7425E-02 -.1972E-02 -.4996E-03

(GC(I,J),J=1,NHM),I=1,NSP)

-.3422E-03 -.4419E-03 -.1377E-03 -.1375E-03  .6416E-04
 .2011E-02 -.8356E-02 -.4901E-03  .1343E-02 -.2670E-03
-.4199E-05 -.1021E-02 -.3515E-03 -.4874E-03 -.9597E-04
 .2913E-03 -.5772E-03 -.1844E-03 -.1949E-03  .3887E-03
 .1011E-03 -.3411E-03  .1142E-03  .3015E-03 -.4662E-03

(GS(I,J),J=1,NHM),I=1,NSP)

 .2957E-03  .1249E-03  .1927E-04 -.1278E-03 -.1251E-03
-.2556E-02  .8103E-03 -.3014E-02  .3499E-03  .7783E-03
-.4435E-03  .1160E-02 -.1548E-03 -.1594E-02 -.2098E-03
 .9283E-03 -.3151E-03 -.1013E-03  .2088E-04 -.4070E-03
 .8503E-03  .2049E-03 -.4271E-03 -.2013E-05  .3877E-03

PITCH ANGLE AT BLADE ROOT=   7.69346DEGREES
CONING ANGLE=   0.00000 DEGREES
FLAPPING COEFFICIENT, A1=   4.27211 DEGREES
FLAPPING COEFFICIENT, B1=    .03698 DEGREES
COMPUTED THRUST COEFFICIENT= .3940E-02
COMPUTED MOMENT COEFFICIENT ABOUT ROTOR X-AXIS=-.3092E-16
COMPUTED MOMENT COEFFICIENT ABOUT ROTOR Y-AXIS= .3313E-17
```

TABLE 1 - SECTIONAL LIFT/(RHO)*(OMEGA**2)*(R1**3))

R/R1=	.3000E+00	.5000E+00	.7500E+00	.8500E+00	.9500E+00
PSI					
0.0	.2249E-02	.6022E-02	.1818E-01	.2045E-01	.1620E-01
15.0	.1969E-02	.7424E-02	.1634E-01	.2047E-01	.1589E-01
30.0	.1864E-02	.6600E-02	.1565E-01	.1767E-01	.1319E-01
45.0	.1456E-02	.5512E-02	.1109E-01	.1213E-01	.9265E-02
60.0	.4532E-03	.3671E-02	.7971E-02	.8453E-02	.6733E-02
75.0	-.7856E-03	.1429E-02	.7249E-02	.8486E-02	.7113E-02
90.0	-.1522E-02	.4076E-03	.9650E-02	.1130E-01	.9429E-02
105.0	-.1247E-02	.1773E-02	.1257E-01	.1425E-01	.1159E-01
120.0	-.2901E-04	.3473E-02	.1491E-01	.1593E-01	.1270E-01
135.0	.1562E-02	.8581E-02	.1565E-01	.1692E-01	.1343E-01
150.0	.2731E-02	.9514E-02	.1663E-01	.1811E-01	.1448E-01
165.0	.2853E-02	.9504E-02	.1724E-01	.1914E-01	.1544E-01
180.0	.1906E-02	.6951E-02	.1672E-01	.1897E-01	.1542E-01
195.0	.5907E-03	.3053E-02	.1501E-01	.1744E-01	.1432E-01
210.0	-.1817E-03	.4394E-02	.1289E-01	.1548E-01	.1293E-01
225.0	-.1070E-03	.2997E-02	.1116E-01	.1392E-01	.1186E-01
240.0	.2586E-03	.1975E-02	.1005E-01	.1290E-01	.1118E-01
255.0	.1985E-03	.1867E-02	.9528E-02	.1240E-01	.1088E-01
270.0	-.2695E-03	.2456E-02	.9805E-02	.1274E-01	.1121E-01
285.0	-.3925E-03	.3135E-02	.1094E-01	.1397E-01	.1220E-01
300.0	.3837E-03	.3823E-02	.1244E-01	.1541E-01	.1328E-01
315.0	.1687E-02	.4955E-02	.1370E-01	.1633E-01	.1386E-01
330.0	.2600E-02	.5543E-02	.1485E-01	.1720E-01	.1426E-01
345.0	.2660E-02	.7798E-02	.1647E-01	.1869E-01	.1515E-01

TABLE 2 - SECTIONAL LIFT*R1/THRUST PER BLADE

R/R1:	.3000E+00	.5000E+00	.7500E+00	.8500E+00	.9500E+00
PSI					
0.0	.3635E+00	.1295E+01	.2937E+01	.3304E+01	.2617E+01
15.0	.3162E+00	.1200E+01	.2963E+01	.3308E+01	.2567E+01
30.0	.2011E+00	.1055E+01	.2528E+01	.2790E+01	.2131E+01
45.0	.2352E+00	.8907E+00	.1792E+01	.1960E+01	.1497E+01
60.0	.7322E-01	.5931E+00	.1223E+01	.1366E+01	.1088E+01
75.0	-.1269E+00	.2309E+00	.1171E+01	.1371E+01	.1149E+01
90.0	-.2494E+00	.6586E-01	.1559E+01	.1826E+01	.1523E+01
105.0	-.2016E+00	.3188E+00	.2031E+01	.2303E+01	.1873E+01
120.0	-.4668E-02	.8843E+00	.2345E+01	.2573E+01	.2052E+01
135.0	.2524E+00	.1387E+01	.2529E+01	.2733E+01	.2170E+01
150.0	.4412E+00	.1537E+01	.2687E+01	.2927E+01	.2340E+01
165.0	.4609E+00	.1374E+01	.2785E+01	.3092E+01	.2495E+01
180.0	.3080E+00	.1123E+01	.2702E+01	.3064E+01	.2491E+01
195.0	.9544E-01	.9134E+00	.2425E+01	.2819E+01	.2314E+01
210.0	-.2936E-01	.7100E+00	.2082E+01	.2502E+01	.2089E+01
225.0	-.1729E-01	.4843E+00	.1804E+01	.2250E+01	.1917E+01
240.0	.4179E-01	.3191E+00	.1624E+01	.2084E+01	.1807E+01
255.0	.3207E-01	.3017E+00	.1540E+01	.2004E+01	.1758E+01
270.0	-.4355E-01	.3968E+00	.1584E+01	.2058E+01	.1811E+01
285.0	-.6342E-01	.5066E+00	.1769E+01	.2257E+01	.1971E+01
300.0	.6200E-01	.6135E+00	.2010E+01	.2490E+01	.2146E+01
315.0	.2726E+00	.8023E+00	.2213E+01	.2646E+01	.2243E+01
330.0	.4202E+00	.1053E+01	.2400E+01	.2779E+01	.2307E+01
345.0	.4298E+00	.1260E+01	.2660E+01	.3020E+01	.2448E+01

TABLE 3 - SECTIONAL PITCHING MOMENT/(RHO*(OMEGA**2)*(R1**4))

(ABOUT QUARTER-CHORD)

R/R1	.3000E+00	.5000E+00	.7500E+00	.8500E+00	.9500E+00
PSI					
0.0	.3551E-04	.2542E-05	-.5538E-04	-.1002E-03	-.2298E-03
15.0	.1672E-04	-.7630E-05	-.7253E-04	-.1155E-03	-.2375E-03
30.0	.7246E-05	-.1980E-04	-.7620E-04	-.1124E-03	-.2154E-03
45.0	-.7096E-05	-.3303E-04	-.8516E-04	-.9244E-04	-.1738E-03
60.0	-.5719E-05	-.2723E-04	-.4886E-04	-.6794E-04	-.1352E-03
75.0	.1632E-05	-.7376E-05	-.3588E-04	-.4907E-04	-.1120E-03
90.0	.1282E-04	.1792E-04	-.2463E-04	-.3469E-04	-.9739E-04
105.0	.2607E-04	.3153E-04	-.4036E-05	-.1921E-04	-.8011E-04
120.0	.3549E-04	.2903E-04	.1265E-04	-.2037E-05	-.6118E-04
135.0	.3279E-04	.2079E-04	.2701E-04	.8561E-05	-.5242E-04
150.0	.1603E-04	.1620E-04	.2583E-04	.5792E-05	-.6087E-04
165.0	-.5481E-05	.1209E-04	.1147E-04	-.8223E-05	-.8076E-04
180.0	-.2433E-04	.2639E-06	-.5972E-05	-.2559E-04	-.1013E-03
195.0	-.3545E-04	-.1797E-04	-.1975E-04	-.4064E-04	-.1175E-03
210.0	-.4468E-04	-.3135E-04	-.2998E-04	-.5221E-04	-.1298E-03
225.0	-.5260E-04	-.3211E-04	-.3742E-04	-.5977E-04	-.1381E-03
240.0	-.5087E-04	-.2389E-04	-.3902E-04	-.6153E-04	-.1412E-03
255.0	-.3203E-04	-.1409E-04	-.3229E-04	-.5747E-04	-.1411E-03
270.0	-.1019E-05	-.3647E-05	-.2095E-04	-.5139E-04	-.1433E-03
285.0	.2748E-04	.1047E-04	-.1238E-04	-.4766E-04	-.1499E-03
300.0	.4311E-04	.2554E-04	-.1033E-04	-.4746E-04	-.1580E-03
315.0	.4753E-04	.3258E-04	-.1348E-04	-.5064E-04	-.1662E-03
330.0	.4733E-04	.2698E-04	-.2109E-04	-.5965E-04	-.1800E-03
345.0	.4383E-04	.1436E-04	-.3533E-04	-.7747E-04	-.2041E-03

TABLE 4 - CENTER OF PRESSURE LOCATION FROM LEADING EDGE(FRACTION OF CHORD)

R/R1:	.3000E+00	.5000E+00	.7500E+00	.8500E+00	.9500E+00
PSI					
0.0	.3475E+00	.2522E+00	.2301E+00	.2179E+00	.1572E+00
15.0	.3056E+00	.2433E+00	.2241E+00	.2131E+00	.1522E+00
30.0	.2625E+00	.2334E+00	.2181E+00	.2074E+00	.1432E+00
45.0	.2181E+00	.2144E+00	.2116E+00	.2001E+00	.1273E+00
60.0	.1674E+00	.2014E+00	.2078E+00	.1974E+00	.1186E+00
75.0	.2304E+00	.2162E+00	.2176E+00	.2122E+00	.1470E+00
90.0	.1949E+00	.2376E+00	.2334E+00	.2293E+00	.1924E+00
105.0	.1133E+00	.3545E+00	.2458E+00	.2412E+00	.2048E+00
120.0	-.7753E+01	.2847E+00	.2557E+00	.2492E+00	.2185E+00
135.0	.3873E+00	.2658E+00	.2613E+00	.2533E+00	.2245E+00
150.0	.2884E+00	.2611E+00	.2602E+00	.2521E+00	.2225E+00
165.0	.2391E+00	.2593E+00	.2544E+00	.2472E+00	.2158E+00
180.0	.1655E+00	.2502E+00	.2477E+00	.2412E+00	.2070E+00
195.0	-.1426E+00	.2392E+00	.2414E+00	.2348E+00	.1963E+00
210.0	.1859E+01	.2033E+00	.2348E+00	.2279E+00	.1843E+00
225.0	.3456E+01	.1799E+00	.2281E+00	.2219E+00	.1738E+00
240.0	-.1037E+01	.1708E+00	.2246E+00	.2188E+00	.1674E+00
255.0	-.8056E+00	.2006E+00	.2278E+00	.2197E+00	.1651E+00
270.0	.2747E+00	.2403E+00	.2360E+00	.2236E+00	.1664E+00
285.0	-.2080E+00	.2713E+00	.2426E+00	.2277E+00	.1696E+00
300.0	.9851E+00	.2936E+00	.2446E+00	.2298E+00	.1722E+00
315.0	.4343E+00	.2929E+00	.2436E+00	.2298E+00	.1717E+00
330.0	.3691E+00	.2770E+00	.2407E+00	.2273E+00	.1675E+00
345.0	.3578E+00	.2520E+00	.2360E+00	.2229E+00	.1619E+00

TABLE 5 - TOTAL BLADE LIFT, MOMENT ABOUT HUB AND RADIAL CENTER OF LIFT

TOTAL BLADE LIFT/(RHO*(OMEGA**2)*(R1**4))
TOTAL BLADE LIFT/THRUST PER BLADE
MOMENT ABOUT HUB/(RHO*(OMEGA**2)*(R1**5))
RADIAL CENTER OF LIFT/R1

PSI	TOTAL BLADE LIFT		MOMENT ABOUT HUB	CENTER OF LIFT
0.0	.6859E-02	.1431E+01	.6376E-02	.7198E+00
15.0	.6557E-02	.1399E+01	.6261E-02	.7256E+00
30.0	.7424E-02	.1530E+01	.5353E-02	.7210E+00
45.0	.5458E-02	.8819E+00	.3385E-02	.7118E+00
60.0	.3642E-02	.5385E+00	.2553E-02	.7283E+00
75.0	.2858E-02	.4513E+00	.2300E-02	.8049E+00
90.0	.3379E-02	.5451E+00	.2862E-02	.8466E+00
105.0	.4807E-02	.7757E+00	.3876E-02	.8063E+00
120.0	.6483E-02	.1048E+01	.4870E-02	.7512E+00
135.0	.7860E-02	.1273E+01	.5636E-02	.7152E+00
150.0	.8598E-02	.1403E+01	.6113E-02	.7043E+00
165.0	.8721E-02	.1409E+01	.6215E-02	.7126E+00
180.0	.8036E-02	.1298E+01	.5875E-02	.7311E+00
195.0	.6911E-02	.1117E+01	.5202E-02	.7526E+00
210.0	.5764E-02	.9313E+00	.4449E-02	.7720E+00
225.0	.4838E-02	.7898E+00	.3833E-02	.7842E+00
240.0	.4362E-02	.7047E+00	.3436E-02	.7879E+00
255.0	.4175E-02	.6746E+00	.3291E-02	.7882E+00
270.0	.4359E-02	.7044E+00	.3437E-02	.7884E+00
285.0	.4925E-02	.7959E+00	.3848E-02	.7812E+00
300.0	.5752E-02	.9295E+00	.4373E-02	.7602E+00
315.0	.6652E-02	.1075E+01	.4875E-02	.7328E+00
330.0	.7527E-02	.1216E+01	.5370E-02	.7135E+00
345.0	.8334E-02	.1347E+01	.5927E-02	.7112E+00

TABLE 6 -SURFACE PRESSURE DIFFERENTIAL/(RHO*(OMEGA**2)*(R1**2))

AZIMUTH ANGLE= 0.0 DEGREES

R/R1: / X/C	.3000E+00	.5000E+00	.7500E+00	.8500E+00	.9500E+00
.05000	.2681E-01	.1438E+00	.3514E+00	.4115E+00	.3868E+00
.10000	.2088E-01	.9940E-01	.2336E+00	.2772E+00	.2519E+00
.20000	.1598E-01	.6073E-01	.1547E+00	.1769E+00	.1493E+00
.30000	.1319E-01	.5121E-01	.1148E+00	.1291E+00	.9999E-01
.40000	.1390E-01	.4120E-01	.8925E-01	.9852E-01	.6887E-01
.50000	.1271E-01	.3370E-01	.7054E-01	.7644E-01	.4685E-01
.70000	.1008E-01	.2209E-01	.4296E-01	.4436E-01	.1775E-01
.90000	.6102E-02	.1126E-01	.2004E-01	.1922E-01	.1503E-02
.95000	.4398E-02	.7755E-02	.1344E-01	.1253E-01	-.5220E-03
.99000	.2016E-02	.3415E-02	.5745E-02	.5183E-02	-.9029E-03

AZIMUTH ANGLE= 15.0 DEGREES

R/R1: / X/C	.3000E+00	.5000E+00	.7500E+00	.8500E+00	.9500E+00
.05000	.2838E-01	.1366E+00	.3013E+00	.4182E+00	.3839E+00
.10000	.2079E-01	.9370E-01	.2442E+00	.2807E+00	.2493E+00
.20000	.1540E-01	.6183E-01	.1569E+00	.1778E+00	.1468E+00
.30000	.1286E-01	.4672E-01	.1154E+00	.1283E+00	.9742E-01
.40000	.1113E-01	.3598E-01	.8864E-01	.9760E-01	.6633E-01
.50000	.9739E-02	.2978E-01	.6950E-01	.7497E-01	.4440E-01
.70000	.7220E-02	.1845E-01	.4134E-01	.4256E-01	.1572E-01
.90000	.4166E-02	.9437E-02	.1671E-01	.1786E-01	.3215E-03
.95000	.2980E-02	.5487E-02	.1242E-01	.1150E-01	-.1345E-02
.99000	.1360E-02	.2800E-02	.5257E-02	.4699E-02	-.1259E-02

AZIMUTH ANGLE= 30.0 DEGREES

R/R1: / X/C	.3000E+00	.5000E+00	.7500E+00	.8500E+00	.9500E+00
.05000	.3292E-01	.1265E+00	.3139E+00	.3585E+00	.3257E+00
.10000	.2281E-01	.8587E-01	.2112E+00	.2397E+00	.2105E+00
.20000	.1532E-01	.5554E-01	.1345E+00	.1506E+00	.1226E+00
.30000	.1174E-01	.4106E-01	.9792E-01	.1081E+00	.8019E-01
.40000	.9406E-02	.3179E-01	.7463E-01	.8106E-01	.5352E-01
.50000	.7561E-02	.2503E-01	.5773E-01	.6156E-01	.3481E-01
.70000	.4987E-02	.1517E-01	.3345E-01	.3396E-01	.1068E-01
.90000	.2565E-02	.7177E-02	.1463E-01	.1366E-01	-.1452E-02
.95000	.1786E-02	.4670E-02	.9612E-02	.8663E-02	-.2384E-02
.99000	.7998E-03	.2122E-02	.4027E-02	.3482E-02	-.1530E-02

AZIMUTH ANGLE= 45.0 DEGREES

R/R1:	.3000E+00	.5000E+00	.7500E+00	.8500E+00	.9500E+00
X/C					
.05000	.2851E-01	.1113E+00	.2265E+00	.2567E+00	.2376E+00
.10000	.1426E-01	.7471E-01	.1517E+00	.1708E+00	.1525E+00
.20000	.1221E-01	.4724E-01	.9564E-01	.1062E+00	.9719E-01
.30000	.8804E-02	.3410E-01	.6883E-01	.7526E-01	.5569E-01
.40000	.6627E-02	.2574E-01	.5179E-01	.5565E-01	.3591E-01
.50000	.5054E-02	.1970E-01	.3950E-01	.4158E-01	.2212E-01
.70000	.2559E-02	.1115E-01	.2214E-01	.2200E-01	.4709E-02
.90000	.1278E-02	.4790E-02	.9294E-02	.8295E-02	-.3110E-02
.95000	.8563E-03	.3143E-02	.6034E-02	.5143E-02	-.3237E-02
.99000	.3843E-03	.1327E-02	.2506E-02	.2021E-02	-.1877E-02

AZIMUTH ANGLE= 60.0 DEGREES

R/R1:	.3000E+00	.5000E+00	.7500E+00	.8500E+00	.9500E+00
X/C					
.05000	.9764E-02	.7709E-01	.1562E+00	.1800E+00	.1757E+00
.10000	.6312E-02	.5129E-01	.1043E+00	.1195E+00	.1123E+00
.20000	.3800E-02	.3195E-01	.6592E-01	.7393E-01	.6347E-01
.30000	.2264E-02	.2253E-01	.4668E-01	.5210E-01	.3987E-01
.40000	.1417E-02	.1563E-01	.3485E-01	.3826E-01	.2508E-01
.50000	.9398E-03	.1240E-01	.2634E-01	.2837E-01	.1481E-01
.70000	.1872E-03	.5503E-02	.1446E-01	.1473E-01	.2082E-02
.90000	.2469E-05	.2530E-02	.5916E-02	.5420E-02	-.3143E-02
.95000	.1257E-04	.1597E-02	.3815E-02	.3339E-02	-.2979E-02
.99000	.2280E-04	.6471E-03	.1578E-02	.1308E-02	-.1637E-02

AZIMUTH ANGLE= 75.0 DEGREES

R/R1:	.3000E+00	.5000E+00	.7500E+00	.8500E+00	.9500E+00
X/C					
.05000	-.1566E-01	.2824E-01	.1499E+00	.1736E+00	.1725E+00
.10000	-.1075E-01	.1889E-01	.9809E-01	.1163E+00	.1115E+00
.20000	-.7196E-02	.1183E-01	.6236E-01	.7341E-01	.6467E-01
.30000	-.5548E-02	.8430E-02	.4535E-01	.5296E-01	.4207E-01
.40000	-.4489E-02	.6277E-02	.3454E-01	.3997E-01	.2787E-01
.50000	-.3682E-02	.4745E-02	.2670E-01	.3060E-01	.1796E-01
.70000	-.2351E-02	.2665E-02	.1547E-01	.1728E-01	.5415E-02
.90000	-.1040E-02	.1219E-02	.6765E-02	.7270E-02	-.5903E-03
.95000	-.6535E-03	.8392E-03	.4437E-02	.4702E-02	-.1016E-02
.99000	-.2468E-03	.3796E-03	.1854E-02	.1935E-02	-.6767E-03

AZIMUTH ANGLE= 90.0 DEGREES

R/R1:	.3000E+00	.5000E+00	.7500E+00	.8500E+00	.9500E+00
X/C					
.05000	-.3343E-01	-.7037E-03	.1859E+00	.2400E+00	.2085E+00
.10000	-.2228E-01	.5513E-03	.1264E+00	.1492E+00	.1371E+00
.20000	-.1395E-01	.1543E-02	.8239E-01	.9668E-01	.8295E-01
.30000	-.1000E-01	.2179E-02	.6153E-01	.7179E-01	.5691E-01
.40000	-.7494E-02	.2490E-02	.4624E-01	.5593E-01	.4046E-01
.50000	-.5568E-02	.2567E-02	.3847E-01	.4432E-01	.2582E-01
.70000	-.3018E-02	.2711E-02	.2387E-01	.2711E-01	.1334E-01
.90000	-.1027E-02	.2034E-02	.1128E-01	.1261E-01	.3937E-02
.95000	-.5757E-03	.1615E-02	.7550E-02	.8404E-02	.2207E-02
.99000	-.1947E-03	.6001E-03	.3203E-02	.3552E-02	.7842E-03

AZIMUTH ANGLE=105.0 DEGREES

R/R1:	.3000E+00	.5000E+00	.7500E+00	.8500E+00	.9500E+00
X/C					
.05000	-.3381E-01	.2258E-01	.2329E+00	.2682E+00	.2424E+00
.10000	-.2168E-01	.1743E-01	.1599E+00	.1835E+00	.1617E+00
.20000	-.1245E-01	.1414E-01	.1052E+00	.1210E+00	.1011E+00
.30000	-.8024E-02	.1254E-01	.8083E-01	.9152E-01	.7213E-01
.40000	-.5242E-02	.1152E-01	.6462E-01	.7267E-01	.5378E-01
.50000	-.3287E-02	.1072E-01	.5258E-01	.5873E-01	.4056E-01
.70000	-.7219E-03	.8759E-02	.3405E-01	.3747E-01	.2208E-01
.90000	.9616E-03	.5948E-02	.1691E-01	.1826E-01	.8734E-02
.95000	.6030E-03	.4862E-02	.1150E-01	.1234E-01	.5516E-02
.99000	.3684E-03	.1893E-02	.4951E-02	.5278E-02	.2211E-02

AZIMUTH ANGLE=120.0 DEGREES

R/R1:	.3000E+00	.5000E+00	.7500E+00	.8500E+00	.9500E+00
X/C					
.05000	-.1558E-01	.5798E-01	.2597E+00	.2920E+00	.2578E+00
.10000	-.8907E-02	.6244E-01	.1797E+00	.2010E+00	.1737E+00
.20000	-.2659E-02	.4410E-01	.1211E+00	.1343E+00	.1112E+00
.30000	-.1047E-03	.3556E-01	.9351E-01	.1028E+00	.8162E-01
.40000	.1573E-02	.3001E-01	.7581E-01	.8267E-01	.6279E-01
.50000	.2662E-02	.2574E-01	.6256E-01	.6764E-01	.4903E-01
.70000	.3686E-02	.1848E-01	.4173E-01	.4428E-01	.2881E-01
.90000	.3100E-02	.1029E-01	.2148E-01	.2221E-01	.1239E-01
.95000	.2412E-02	.7250E-02	.1478E-01	.1513E-01	.7960E-02
.99000	.1168E-02	.3242E-02	.6450E-02	.6528E-02	.3203E-02

AZIMUTH ANGLE=135.0 DEGREES

R/R1:	.3000E+00	.5000E+00	.7500E+00	.8500E+00	.9500E+00
X/C					
.05000	.1446E-01	.1433E+00	.2742E+00	.3059E+00	.2696E+00
.10000	.1205E-01	.1035E+00	.1906E+00	.2113E+00	.1827E+00
.20000	.1070E-01	.7098E-01	.1295E+00	.1421E+00	.1184E+00
.30000	.1014E-01	.5572E-01	.1008E+00	.1095E+00	.8808E-01
.40000	.9681E-02	.4587E-01	.8236E-01	.8859E-01	.6876E-01
.50000	.9185E-02	.3841E-01	.6847E-01	.7293E-01	.5451E-01
.70000	.7794E-02	.2634E-01	.4636E-01	.4832E-01	.3298E-01
.90000	.5069E-02	.1393E-01	.2432E-01	.2456E-01	.1449E-01
.95000	.3736E-02	.9653E-02	.1684E-01	.1681E-01	.9813E-02
.99000	.1753E-02	.4242E-02	.7407E-02	.7281E-02	.3717E-02

AZIMUTH ANGLE=150.0 DEGREES

R/R1:	.3000E+00	.5000E+00	.7500E+00	.8500E+00	.9500E+00
X/C					
.05000	.4265E-01	.1567E+00	.2922E+00	.3287E+00	.2923E+00
.10000	.3048E-01	.1150E+00	.2030E+00	.2269E+00	.1978E+00
.20000	.2173E-01	.7893E-01	.1379E+00	.1523E+00	.1279E+00
.30000	.1761E-01	.6149E-01	.1071E+00	.1172E+00	.9490E-01
.40000	.1490E-01	.5125E-01	.8730E-01	.9468E-01	.7385E-01
.50000	.1279E-01	.4177E-01	.7245E-01	.7731E-01	.5835E-01
.70000	.9211E-02	.2824E-01	.4887E-01	.5134E-01	.3501E-01
.90000	.5168E-02	.1478E-01	.2554E-01	.2597E-01	.1519E-01
.95000	.3682E-02	.1020E-01	.1758E-01	.1774E-01	.9724E-02
.99000	.1656E-02	.4473E-02	.7770E-02	.7678E-02	.3962E-02

AZIMUTH ANGLE=165.0 DEGREES

R/R1:	.3000E+00	.5000E+00	.7500E+00	.8500E+00	.9500E+00
X/C					
.05000	.5396E-01	.1492E+00	.3090E+00	.3529E+00	.3165E+00
.10000	.3692E-01	.1036E+00	.2137E+00	.2427E+00	.2132E+00
.20000	.2426E-01	.7029E-01	.1438E+00	.1618E+00	.1364E+00
.30000	.1821E-01	.5454E-01	.1108E+00	.1236E+00	.9996E-01
.40000	.1429E-01	.4436E-01	.8953E-01	.9913E-01	.7676E-01
.50000	.1138E-01	.3571E-01	.7376E-01	.8086E-01	.5978E-01
.70000	.7010E-02	.2463E-01	.4891E-01	.5253E-01	.3475E-01
.90000	.3300E-02	.1235E-01	.2506E-01	.2610E-01	.1454E-01
.95000	.2221E-02	.6912E-02	.1724E-01	.1773E-01	.9209E-02
.99000	.9555E-03	.3934E-02	.7534E-02	.7631E-02	.3628E-02

AZIMUTH ANGLE=180.0 DEGREES

r/R1:	.3000E+00	.5000E+00	.7500E+00	.8500E+00	.9500E+00
x/C					
.05000	.4347E-01	.1250E+00	.3064E+00	.3554E+00	.3234E+00
.10000	.2662E-01	.8830E-01	.2108E+00	.2441E+00	.2167E+00
.20000	.1727E-01	.5773E-01	.1405E+00	.1613E+00	.1369E+00
.30000	.1172E-01	.4414E-01	.1072E+00	.1222E+00	.9899E-01
.40000	.8168E-02	.3430E-01	.8586E-01	.9706E-01	.7485E-01
.50000	.5604E-02	.2380E-01	.6994E-01	.7843E-01	.5729E-01
.70000	.2179E-02	.1873E-01	.4839E-01	.4992E-01	.3190E-01
.90000	.2841E-03	.9517E-02	.2271E-01	.2421E-01	.1249E-01
.95000	.4670E-04	.5170E-02	.1321E-01	.1653E-01	.7714E-02
.99000	-.3237E-04	.2405E-02	.6737E-02	.6930E-02	.2949E-02

AZIMUTH ANGLE=195.0 DEGREES

r/R1:	.3000E+00	.5000E+00	.7500E+00	.8500E+00	.9500E+00
x/C					
.05000	.2331E-01	.1085E+00	.2800E+00	.3341E+00	.3099E+00
.10000	.1407E-01	.7382E-01	.1919E+00	.2279E+00	.2064E+00
.20000	.6612E-02	.4795E-01	.1267E+00	.1492E+00	.1289E+00
.30000	.2817E-02	.3554E-01	.9577E-01	.1120E+00	.9186E-01
.40000	.3849E-03	.2754E-01	.7391E-01	.8605E-01	.6834E-01
.50000	-.1276E-02	.2156E-01	.5818E-01	.7040E-01	.5130E-01
.70000	-.3009E-02	.1299E-01	.3993E-01	.4877E-01	.2704E-01
.90000	-.2664E-02	.5022E-02	.1897E-01	.2063E-01	.9476E-02
.95000	-.2020E-02	.4038E-02	.1288E-01	.1360E-01	.5526E-02
.99000	-.9423E-03	.1745E-02	.5508E-02	.5849E-02	.1944E-02

AZIMUTH ANGLE=210.0 DEGREES

r/R1:	.3000E+00	.5000E+00	.7500E+00	.8500E+00	.9500E+00
x/C					
.05000	.1200E-01	.9074E-01	.2450E+00	.3026E+00	.2892E+00
.10000	.6164E-02	.5083E-01	.1672E+00	.2055E+00	.1914E+00
.20000	.5031E-03	.3824E-01	.1094E+00	.1333E+00	.1179E+00
.30000	-.2363E-02	.2730E-01	.8183E-01	.9901E-01	.8271E-01
.40000	-.4259E-02	.2025E-01	.6415E-01	.7703E-01	.6038E-01
.50000	-.5460E-02	.1513E-01	.5111E-01	.6086E-01	.4428E-01
.70000	-.6321E-02	.7942E-02	.3150E-01	.3682E-01	.2172E-01
.90000	-.4639E-02	.2993E-02	.1500E-01	.1677E-01	.6369E-02
.95000	-.3426E-02	.1883E-02	.1011E-01	.1109E-01	.3315E-02
.99000	-.1573E-02	.7699E-03	.4347E-02	.4652E-02	.9490E-03

AZIMUTH ANGLE=225.0 DEGREES

R/R1:	.3000E+00	.5000E+00	.7500E+00	.8500E+00	.9500E+00
X/C					
.05000	.1736E-01	.6925E-01	.2155E+00	.2769E+00	.2721E+00
.10000	.9027E-02	.4328E-01	.1471E+00	.1873E+00	.1791E+00
.20000	.1984E-02	.2649E-01	.9543E-01	.1206E+00	.1089E+00
.30000	-.1708E-02	.1824E-01	.7073E-01	.8880E-01	.7515E-01
.40000	-.4058E-02	.1292E-01	.5487E-01	.6843E-01	.5375E-01
.50000	-.5516E-02	.9079E-02	.4320E-01	.5349E-01	.3841E-01
.70000	-.6861E-02	.3884E-02	.2598E-01	.3153E-01	.1733E-01
.90000	-.5233E-02	.9216E-03	.1189E-01	.1385E-01	.3975E-02
.95000	-.3913E-02	.4695E-03	.7928E-02	.9048E-02	.1675E-02
.99000	-.1824E-02	.1519E-03	.3375E-02	.3749E-02	.2516E-03

AZIMUTH ANGLE=240.0 DEGREES

R/R1:	.3000E+00	.5000E+00	.7500E+00	.8500E+00	.9500E+00
X/C					
.05000	.2374E-01	.4811E-01	.1969E+00	.2587E+00	.2599E+00
.10000	.1362E-01	.2951E-01	.1336E+00	.1748E+00	.1705E+00
.20000	.5343E-02	.1740E-01	.8634E-01	.1121E+00	.1027E+00
.30000	.1089E-02	.1181E-01	.6373E-01	.8221E-01	.7011E-01
.40000	-.1548E-02	.8149E-02	.4920E-01	.6305E-01	.4941E-01
.50000	-.3514E-02	.5495E-02	.3851E-01	.4902E-01	.3462E-01
.70000	-.5379E-02	.1980E-02	.2281E-01	.2848E-01	.1461E-01
.90000	-.4509E-02	.2151E-03	.1019E-01	.1223E-01	.2600E-02
.95000	-.3442E-02	.4432E-04	.6740E-02	.7930E-02	.7710E-03
.99000	-.1638E-02	.5244E-05	.2846E-02	.3259E-02	-.1080E-03

AZIMUTH ANGLE=255.0 DEGREES

R/R1:	.3000E+00	.5000E+00	.7500E+00	.8500E+00	.9500E+00
X/C					
.05000	.1521E-01	.3763E-01	.1847E+00	.2480E+00	.2544E+00
.10000	.8996E-02	.2544E-01	.1256E+00	.1677E+00	.1668E+00
.20000	.3893E-02	.1621E-01	.8164E-01	.1078E+00	.1003E+00
.30000	.1210E-02	.1159E-01	.6036E-01	.7914E-01	.6827E-01
.40000	-.5749E-03	.8529E-02	.4702E-01	.6079E-01	.4796E-01
.50000	-.1842E-02	.6247E-02	.3701E-01	.4733E-01	.3345E-01
.70000	-.3233E-02	.3027E-02	.2219E-01	.2758E-01	.1384E-01
.90000	-.2852E-02	.1003E-02	.1008E-01	.1190E-01	.2185E-02
.95000	-.2195E-02	.0235E-03	.6702E-02	.7730E-02	.4779E-03
.99000	-.1049E-02	.2590E-03	.2847E-02	.3184E-02	-.2406E-03

AZIMUTH ANGLE=270.0 DEGREES

R/R1: X/C	.3000E+00	.5000E+00	.7500E+00	.8500E+00	.9500E+00
.05000	-.5900E-02	.4472E-01	.1851E+00	.2517E+00	.2621E+00
.10000	-.3552E-02	.3112E-01	.1266E+00	.1706E+00	.1720E+00
.20000	-.1909E-02	.2101E-01	.8325E-01	.1102E+00	.1038E+00
.30000	-.1301E-02	.1605E-01	.6252E-01	.8142E-01	.7100E-01
.40000	-.1055E-02	.1274E-01	.4913E-01	.6293E-01	.5019E-01
.50000	-.9711E-03	.1019E-01	.3920E-01	.4932E-01	.3528E-01
.70000	-.9386E-03	.6227E-02	.2425E-01	.2963E-01	.1496E-01
.90000	-.6851E-03	.2669E-02	.1149E-01	.1292E-01	.2566E-02
.95000	-.4964E-03	.1928E-02	.7750E-02	.8471E-02	.6641E-03
.99000	-.2146E-03	.9363E-03	.3339E-02	.3524E-02	-.2071E-03

AZIMUTH ANGLE=285.0 DEGREES

R/R1: X/C	.3000E+00	.5000E+00	.7500E+00	.8500E+00	.9500E+00
.05000	-.1952E-01	.9190E-01	.2025E+00	.2726E+00	.2833E+00
.10000	-.1111E-01	.3699E-01	.1391E+00	.1852E+00	.1862E+00
.20000	-.4583E-02	.2017E-01	.9231E-01	.1203E+00	.1128E+00
.30000	-.1557E-02	.2097E-01	.6999E-01	.8937E-01	.7752E-01
.40000	.1710E-03	.1747E-01	.5557E-01	.6951E-01	.5515E-01
.50000	.1210E-02	.1469E-01	.4482E-01	.5487E-01	.3911E-01
.70000	.2091E-02	.9990E-02	.2842E-01	.3308E-01	.1712E-01
.90000	.1762E-02	.5175E-02	.1486E-01	.1499E-01	.3403E-02
.95000	.1368E-02	.3573E-02	.9439E-02	.9963E-02	.1169E-02
.99000	.6780E-03	.1573E-02	.4097E-02	.4157E-02	-.2384E-04

AZIMUTH ANGLE=300.0 DEGREES

R/R1: X/C	.3000E+00	.5000E+00	.7500E+00	.8500E+00	.9500E+00
.05000	-.1118E-01	.5853E-01	.2292E+00	.2989E+00	.3055E+00
.10000	-.4376E-02	.4249E-01	.1576E+00	.2033E+00	.2009E+00
.20000	.1265E-02	.3103E-01	.1048E+00	.1324E+00	.1217E+00
.30000	.3950E-02	.2565E-01	.7973E-01	.9861E-01	.8372E-01
.40000	.5445E-02	.2138E-01	.6352E-01	.7695E-01	.5961E-01
.50000	.6214E-02	.1900E-01	.5143E-01	.6097E-01	.4234E-01
.70000	.6277E-02	.1367E-01	.3289E-01	.3710E-01	.1876E-01
.90000	.4342E-02	.7332E-02	.1619E-01	.1704E-01	.4078E-02
.95000	.3216E-02	.5290E-02	.1103E-01	.1131E-01	.1629E-02
.99000	.1510E-02	.2365E-02	.4784E-02	.4766E-02	.1869E-03

AZIMUTH ANGLE=315.0 DEGREES

R/R1:	.3000E+00	.5000E+00	.7500E+00	.8500E+00	.9500E+00
X/C					
.05000	.1138E-01	.7637E-01	.2536E+00	.3178E+00	.3188E+00
.10000	.1139E-01	.5515E-01	.1742E+00	.2191E+00	.2094E+00
.20000	.1219E-01	.4004E-01	.1156E+00	.1406E+00	.1265E+00
.30000	.1266E-01	.3293E-01	.8775E-01	.1046E+00	.8561E-01
.40000	.1271E-01	.2912E-01	.6982E-01	.8161E-01	.6134E-01
.50000	.1239E-01	.2631E-01	.5647E-01	.6463E-01	.4331E-01
.70000	.1061E-01	.1755E-01	.3604E-01	.3934E-01	.1891E-01
.90000	.5542E-02	.9750E-02	.1769E-01	.1810E-01	.4038E-02
.95000	.4796E-02	.6877E-02	.1203E-01	.1203E-01	.1618E-02
.99000	.2191E-02	.3083E-02	.5207E-02	.5075E-02	.2055E-03

AZIMUTH ANGLE=330.0 DEGREES

R/R1:	.3000E+00	.5000E+00	.7500E+00	.8500E+00	.9500E+00
X/C					
.05000	.2618E-01	.1075E+00	.2776E+00	.3362E+00	.3313E+00
.10000	.2292E-01	.7618E-01	.1901E+00	.2291E+00	.2171E+00
.20000	.1981E-01	.5333E-01	.1255E+00	.1477E+00	.1303E+00
.30000	.1845E-01	.4283E-01	.9478E-01	.1095E+00	.8860E-01
.40000	.1735E-01	.3583E-01	.7503E-01	.8497E-01	.6220E-01
.50000	.1618E-01	.3035E-01	.6039E-01	.6699E-01	.4341E-01
.70000	.1311E-01	.2122E-01	.3826E-01	.4039E-01	.1821E-01
.90000	.7921E-02	.1147E-01	.1659E-01	.1840E-01	.3305E-02
.95000	.5674E-02	.8019E-02	.1262E-01	.1220E-01	.1048E-02
.99000	.2572E-02	.3558E-02	.5454E-02	.5137E-02	-.6754E-04

AZIMUTH ANGLE=345.0 DEGREES

R/R1:	.3000E+00	.5000E+00	.7500E+00	.8500E+00	.9500E+00
X/C					
.05000	.3043E-01	.1353E+00	.3123E+00	.3704E+00	.3573E+00
.10000	.2414E-01	.9443E-01	.2131E+00	.2504E+00	.2333E+00
.20000	.2018E-01	.6456E-01	.1395E+00	.1619E+00	.1391E+00
.30000	.1841E-01	.5041E-01	.1044E+00	.1164E+00	.9387E-01
.40000	.1707E-01	.4122E-01	.8201E-01	.9121E-01	.6525E-01
.50000	.1577E-01	.3425E-01	.6547E-01	.7133E-01	.4495E-01
.70000	.1266E-01	.2310E-01	.4074E-01	.4225E-01	.1791E-01
.90000	.7653E-02	.1206E-01	.1950E-01	.1884E-01	.2378E-02
.95000	.5497E-02	.8355E-02	.1318E-01	.1240E-01	.2410E-03
.99000	.2504E-02	.3635E-02	.5677E-02	.5187E-02	-.4990E-03

Example B

Line 1: 0.16, 17.2, 4, 7., 0.29, 6.1, 0.0057, 0.

Line 2: 0, 0, 0, 0

Line 3: 9.6

Line 4: 0.5, 0.7, 0.8, 0.9, 1.0

Line 5: 30.0, 10.0, 0.1, 1, 0

```
ROOT RADIUS/TIP RADIUS= RO/R1 =     .16000

ASPECT RATIO=  17.20000

NUMBER OF BLADES= 4

LINEAR TWIST (ROOT TO TIP) =    7.00000 DEGREES

FORWARD SPEED/TIP SPEED=     .24000

ROTOR INCIDENCE (FORWARD TILT POSITIVE) =    6.10000 DEGREES

FREESTREAM MACH NUMBER=    0.00000

THRUST COEFFICIENT=     .00570

FLAPPING INERTIA COEFFICIENT=    9.60000

TOTAL INFLOW RATIO=     .04070

MINIMUM UT=     .10000(ZERO LIFT CONDITION APPLIED BELOW THIS VALUE)

NORMAL AZIMUTH SPACING=  30.00000 DEGREES

REDUCED AZIMUTH SPACING=  10.00000 DEGREES

PIECEWISE QUADRATIC APPROXIMATION OF SPANWISE DIPOLE STRENGTH VARIATION
**********************************************************************

AIRFOIL DATA TABLES NOT USED

R=     .330 PSI= 261.81800EGREES UT=     .043 ZERO LIFT CONDITION APPLIED

R=     .330 PSI= 294.54500EGREES UT=     .066 ZERO LIFT CONDITION APPLIED
```

SOLUTION FOR COEFFICIENTS

(GC(I),I=1,NSP)

-.1030E-01 -.3620E-01 -.3546E-01 -.6559E-01 -.6185E-01

((GC(I,J),J=1,NHM),I=1,NSP)

.2862E-02 -.1508E-02 -.1917E-03 .6273E-04 .1313E-02

.3552E-02 -.1179E-01 -.3967E-03 -.2030E-02 .3674E-03

-.7279E-03 -.1748E-01 -.6217E-02 -.3336E-02 -.3559E-02

-.4620E-02 -.1986E-01 -.6934E-02 -.4791E-02 -.2886E-02

-.9964E-02 -.1894E-01 -.7201E-02 -.5393E-02 -.9666E-03

((GS(I,J),J=1,NHM),I=1,NSP)

-.1085E-01 .1015E-02 -.2382E-02 -.5882E-03 -.4870E-03

-.9381E-02 .1593E-02 .6553E-03 .2258E-02 -.8259E-03

-.3426E-03 .5535E-02 .3046E-03 .3133E-02 .2034E-02

.9840E-02 .5338E-02 .2388E-02 .3525E-02 .1809E-02

.1839E-01 .6391E-02 .4011E-02 .2664E-02 .6377E-03

PITCH ANGLE AT BLADE ROOT= 15.36381 DEGREES

CONING ANGLE= 5.82643 DEGREES

FLAPPING COEFFICIENT, A1= 6.28243 DEGREES

FLAPPING COEFFICIENT, B1= 1.79994 DEGREES

COMPUTED THRUST COEFFICIENT= .5700E-02

COMPUTED MOMENT COEFFICIENT ABOUT ROTOR X-AXIS=-.1988E-16

COMPUTED MOMENT COEFFICIENT ABOUT ROTOR Y-AXIS= .3755E-16

TABLE 1 - SECTIONAL LIFT/(RHO*(OMEGA**2)*(R1**3))

R/R1=	.3300E+00	.5000E+00	.7500E+00	.8500E+00	.9300E+00
PSI					
0.0	.1364E-02	.7153E-02	.1326E-01	.1599E-01	.1583E-01
15.0	.2196E-02	.6746E-02	.1068E-01	.1269E-01	.1238E-01
30.0	.2733E-02	.5973E-02	.7605E-02	.8833E-02	.8190E-02
45.0	.2654E-02	.5331E-02	.6193E-02	.6638E-02	.5290E-02
60.0	.2307E-02	.5305E-02	.6192E-02	.6257E-02	.4364E-02
75.0	.2311E-02	.5699E-02	.6376E-02	.6428E-02	.4689E-02
90.0	.2814E-02	.5844E-02	.6333E-02	.6463E-02	.5267E-02
105.0	.3383E-02	.5924E-02	.6890E-02	.6887E-02	.5779E-02
120.0	.3602E-02	.6213E-02	.8553E-02	.8250E-02	.6504E-02
135.0	.3519E-02	.7100E-02	.1040E-01	.1008E-01	.7670E-02
150.0	.3371E-02	.8295E-02	.1136E-01	.1144E-01	.9094E-02
165.0	.3100E-02	.8950E-02	.1110E-01	.1199E-01	.1033E-01
180.0	.2436E-02	.8483E-02	.1050E-01	.1208E-01	.1101E-01
195.0	.1394E-02	.7107E-02	.1001E-01	.1192E-01	.1102E-01
210.0	.4668E-03	.5525E-02	.9294E-02	.1135E-01	.1059E-01
225.0	.5559E-04	.4559E-02	.8104E-02	.1041E-01	.1015E-01
240.0	.5088E-04	.3506E-02	.6999E-02	.9638E-02	.9987E-02
255.0	.5183E-04	.3070E-02	.6574E-02	.9385E-02	.9998E-02
270.0	-.7825E-04	.2429E-02	.6561E-02	.9284E-02	.9878E-02
285.0	-.1126E-03	.2313E-02	.6379E-02	.8974E-02	.9737E-02
300.0	.1002E-03	.3333E-02	.6406E-02	.9100E-02	.1032E-01
315.0	.3520E-03	.4386E-02	.7803E-02	.1081E-01	.1226E-01
330.0	.5496E-03	.5841E-02	.1070E-01	.1394E-01	.1499E-01
345.0	.7773E-03	.6667E-02	.1325E-01	.1642E-01	.1673E-01

TABLE 2 - SECTIONAL LIFT*R1/THRUST PER BLADE

R/R1:	.3300E+00	.6000E+00	.7500E+00	.8500E+00	.9500E+00
PSI					
0.0	.3048E+00	.1500E+01	.2963E+01	.3572E+01	.3537E+01
15.0	.4906E+00	.1507E+01	.2386E+01	.2834E+01	.2765E+01
30.0	.6105E+00	.1334E+01	.1712E+01	.1973E+01	.1830E+01
45.0	.5929E+00	.1202E+01	.1383E+01	.1483E+01	.1182E+01
60.0	.5154E+00	.1139E+01	.1383E+01	.1398E+01	.9748E+00
75.0	.5161E+00	.1251E+01	.1425E+01	.1436E+01	.1047E+01
90.0	.6286E+00	.1306E+01	.1415E+01	.1444E+01	.1177E+01
105.0	.7557E+00	.1323E+01	.1539E+01	.1588E+01	.1291E+01
120.0	.8046E+00	.1383E+01	.1911E+01	.1643E+01	.1453E+01
135.0	.7860E+00	.1586E+01	.2036E+01	.2253E+01	.1713E+01
150.0	.7529E+00	.1853E+01	.2537E+01	.2556E+01	.2031E+01
165.0	.6925E+00	.2001E+01	.2479E+01	.2679E+01	.2308E+01
180.0	.5435E+00	.1895E+01	.2345E+01	.2699E+01	.2459E+01
195.0	.3124E+00	.1588E+01	.2237E+01	.2664E+01	.2462E+01
210.0	.1047E+00	.1256E+01	.2076E+01	.2535E+01	.2366E+01
225.0	.1242E-01	.1019E+01	.1810E+01	.2325E+01	.2267E+01
240.0	.1137E-01	.8502E+00	.1563E+01	.2153E+01	.2231E+01
255.0	.1158E-01	.8858E+00	.1468E+01	.2096E+01	.2233E+01
270.0	-.1748E-01	.5425E+00	.1466E+01	.2074E+01	.2206E+01
285.0	-.2514E-01	.5177E+00	.1425E+01	.2005E+01	.2175E+01
300.0	.2239E-01	.6773E+00	.1431E+01	.2033E+01	.2305E+01
315.0	.5533E-01	.9797E+00	.1743E+01	.2414E+01	.2738E+01
330.0	.1228E+00	.1305E+01	.2390E+01	.3115E+01	.3349E+01
345.0	.1736E+00	.1734E+01	.2959E+01	.3867E+01	.3737E+01

TABLE 3 - SECTIONAL PITCHING MOMENT/(RHO*(OMEGA**2)*(R1**4))

(ABOUT QUARTER-CHORD)

R/R1:	.3300E+00	.6000E+00	.7500E+00	.8500E+00	.9500E+00
PSI					
0.0	-.2121E-05	-.3533E-06	.6289E-06	.1284E-05	.1939E-05
15.0	-.1393E-05	.3939E-06	.1387E-05	.2048E-05	.2710E-05
30.0	-.7230E-06	.9181E-06	.1830E-05	.2436E-05	.3045E-05
45.0	-.3145E-06	.1329E-05	.1771E-05	.2268E-05	.2764E-05
60.0	-.2834E-06	.6227E-06	.1126E-05	.1462E-05	.1797E-05
75.0	-.6270E-06	-.2630E-06	-.5615E-07	.7975E-07	.2157E-06
90.0	-.1226E-05	-.1465E-05	-.1599E-05	-.1688E-05	-.1777E-05
105.0	-.1876E-05	-.2749E-05	-.3235E-05	-.3556E-05	-.3882E-05
120.0	-.2350E-05	-.3840E-05	-.4658E-05	-.5220E-05	-.5771E-05
135.0	-.2458E-05	-.4505E-05	-.5543E-05	-.6402E-05	-.7160E-05
150.0	-.2103E-05	-.4612E-05	-.6006E-05	-.6936E-05	-.7865E-05
165.0	-.1317E-05	-.4159E-05	-.5737E-05	-.6790E-05	-.7843E-05
180.0	-.2470E-06	-.3271E-05	-.4951E-05	-.6071E-05	-.7191E-05
195.0	.8704E-06	-.2172E-05	-.3863E-05	-.4990E-05	-.6117E-05
210.0	.1775E-05	-.1122E-05	-.2731E-05	-.3804E-05	-.4877E-05
225.0	.2248E-05	-.3485E-06	-.1791E-05	-.2753E-05	-.3714E-05
240.0	.2169E-05	.6938E-08	-.1194E-05	-.1995E-05	-.2796E-05
255.0	.1548E-05	-.7483E-07	-.9764E-06	-.1577E-05	-.2179E-05
270.0	.5240E-06	-.4920E-06	-.1056E-05	-.1433E-05	-.1809E-05
285.0	-.6714E-06	-.1054E-05	-.1266E-05	-.1408E-05	-.1550E-05
300.0	-.1772E-05	-.1538E-05	-.1408E-05	-.1321E-05	-.1235E-05
315.0	-.2546E-05	-.1734E-05	-.1314E-05	-.1021E-05	-.7274E-06
330.0	-.2852E-05	-.1593E-05	-.9028E-06	-.4387E-06	.2540E-07
345.0	-.2674E-05	-.1088E-05	-.2073E-06	.3802E-06	.9576E-06

TABLE 4 - CENTER OF PRESSURE LOCATION FROM LEADING EDGE(FRACTION OF CHORD)

X/C=	.3300E+00	.6000E+00	.7500E+00	.8500E+00	.9500E+00
PSI					
0.0	.2182E+00	.2490E+00	.2510E+00	.2515E+00	.2525E+00
15.0	.2370E+00	.2512E+00	.2527E+00	.2533E+00	.2545E+00
30.0	.2466E+00	.2531E+00	.2549E+00	.2557E+00	.2576E+00
45.0	.2476E+00	.2539E+00	.2559E+00	.2570E+00	.2607E+00
60.0	.2475E+00	.2524E+00	.2537E+00	.2548E+00	.2584E+00
75.0	.2444E+00	.2490E+00	.2498E+00	.2503E+00	.2509E+00
90.0	.2411E+00	.2449E+00	.2448E+00	.2447E+00	.2431E+00
105.0	.2386E+00	.2405E+00	.2404E+00	.2394E+00	.2362E+00
120.0	.2366E+00	.2374E+00	.2382E+00	.2370E+00	.2316E+00
135.0	.2357E+00	.2370E+00	.2390E+00	.2370E+00	.2309E+00
150.0	.2372E+00	.2385E+00	.2392E+00	.2376E+00	.2323E+00
165.0	.2413E+00	.2405E+00	.2394E+00	.2384E+00	.2345E+00
180.0	.2479E+00	.2421E+00	.2403E+00	.2397E+00	.2366E+00
195.0	.2627E+00	.2437E+00	.2421E+00	.2414E+00	.2386E+00
210.0	.3275E+00	.2459E+00	.2440E+00	.2431E+00	.2406E+00
225.0	.1078E+01	.2484E+00	.2455E+00	.2446E+00	.2425E+00
240.0	.1123E+01	.2500E+00	.2465E+00	.2458E+00	.2443E+00
255.0	.8615E+00	.2495E+00	.2470E+00	.2466E+00	.2455E+00
270.0	.1129E+00	.2459E+00	.2467E+00	.2468E+00	.2463E+00
285.0	.3721E+00	.2407E+00	.2459E+00	.2468E+00	.2467E+00
300.0	-.1121E+00	.2396E+00	.2455E+00	.2470E+00	.2476E+00
315.0	.1135E+00	.2413E+00	.2466E+00	.2481E+00	.2488E+00
330.0	.1437E+00	.2444E+00	.2483E+00	.2494E+00	.2506E+00
345.0	.1795E+00	.2468E+00	.2497E+00	.2505E+00	.2512E+00

TABLE 5 - TOTAL BLADE LIFT, MOMENT ABOUT HUB AND RADIAL CENTER OF LIFT

TOTAL BLADE LIFT/(RHO*(OMEGA**2)*(R1**4))
TOTAL BLADE LIFT/THRUST PER BLADE
MOMENT ABOUT HUB/(RHO*(OMEGA**2)*(R1**5))
RADIAL CENTER OF LIFT/R1

PSI	TOTAL BLADE LIFT		MOMENT ABOUT HUB	CENTER OF LIFT
0.0	.6342E-02	.1417E+01	.4785E-02	.7545E+00
15.0	.5555E-02	.1243E+01	.4034E-02	.7258E+00
30.0	.4464E-02	.9971E+00	.3067E-02	.6871E+00
45.0	.3682E-02	.8223E+00	.2439E-02	.6625E+00
60.0	.3453E-02	.7713E+00	.2289E-02	.6630E+00
75.0	.3585E-02	.8007E+00	.2335E-02	.6652E+00
90.0	.3825E-02	.8546E+00	.2512E-02	.6567E+00
105.0	.4146E-02	.9262E+00	.2703E-02	.6519E+00
120.0	.4644E-02	.1038E+01	.3076E-02	.6626E+00
135.0	.5310E-02	.1186E+01	.3590E-02	.6761E+00
150.0	.5886E-02	.1315E+01	.4033E-02	.6853E+00
165.0	.6089E-02	.1360E+01	.4213E-02	.6926E+00
180.0	.5804E-02	.1296E+01	.4106E-02	.7075E+00
195.0	.5152E-02	.1151E+01	.3780E-02	.7337E+00
210.0	.4401E-02	.9832E+00	.3360E-02	.7633E+00
225.0	.3794E-02	.8476E+00	.2970E-02	.7827E+00
240.0	.3419E-02	.7638E+00	.2703E-02	.7907E+00
255.0	.3192E-02	.7129E+00	.2555E-02	.8004E+00
270.0	.2999E-02	.6699E+00	.2442E-02	.8142E+00
285.0	.2908E-02	.6496E+00	.2372E-02	.8155E+00
300.0	.3193E-02	.7133E+00	.2543E-02	.7963E+00
315.0	.4058E-02	.9064E+00	.3159E-02	.7786E+00
330.0	.5285E-02	.1180E+01	.4088E-02	.7736E+00
345.0	.6241E-02	.1394E+01	.4801E-02	.7693E+00

TABLE 6 - SURFACE PRESSURE DIFFERENTIAL/(RHO*(OMEGA**2)*(R1**2))

AZIMUTH ANGLE= 0.0 DEGREES

R/R1:	.3300E+00	.6000E+00	.7500E+00	.8500E+00	.9500E+00
X/C					
.05000	.6963E-01	.4057E+00	.7561E+00	.9133E+00	.9069E+00
.10000	.4928E-01	.2734E+00	.5200E+00	.6278E+00	.6229E+00
.20000	.3467E-01	.1865E+00	.3461E+00	.4174E+00	.4136E+00
.30000	.2766E-01	.1427E+00	.2639E+00	.3180E+00	.3146E+00
.40000	.2345E-01	.1146E+00	.2113E+00	.2543E+00	.2513E+00
.50000	.2005E-01	.9374E-01	.1722E+00	.2071E+00	.2043E+00
.70000	.1431E-01	.6157E-01	.1124E+00	.1348E+00	.1327E+00
.90000	.7892E-02	.3145E-01	.5706E-01	.6829E-01	.6700E-01
.95000	.5535E-02	.2166E-01	.3924E-01	.4694E-01	.4602E-01
.99000	.2461E-02	.4496E-02	.1718E-01	.2054E-01	.2013E-01

AZIMUTH ANGLE= 15.0 DEGREES

R/R1:	.3300E+00	.6000E+00	.7500E+00	.8500E+00	.9500E+00
X/C					
.05000	.1196E+00	.3848E+00	.6122E+00	.7286E+00	.7135E+00
.10000	.8321E-01	.2646E+00	.4205E+00	.5001E+00	.4893E+00
.20000	.5866E-01	.1751E+00	.2791E+00	.3317E+00	.3239E+00
.30000	.4419E-01	.1342E+00	.2123E+00	.2520E+00	.2456E+00
.40000	.3616E-01	.1074E+00	.1695E+00	.2010E+00	.1955E+00
.50000	.3012E-01	.8752E-01	.1378E+00	.1632E+00	.1585E+00
.70000	.2049E-01	.5708E-01	.8943E-01	.1057E+00	.1022E+00
.90000	.1083E-01	.2895E-01	.4514E-01	.5324E-01	.5128E-01
.95000	.7523E-02	.1990E-01	.3100E-01	.3654E-01	.3516E-01
.99000	.3320E-02	.8713E-02	.1356E-01	.1597E-01	.1536E-01

AZIMUTH ANGLE= 30.0 DEGREES

R/R1:	.3300E+00	.6000E+00	.7500E+00	.8500E+00	.9500E+00
X/C					
.05000	.1526E+00	.3423E+00	.4423E+00	.5110E+00	.4767E+00
.10000	.1055E+00	.2354E+00	.3033E+00	.3501E+00	.3262E+00
.20000	.7094E-01	.1561E+00	.2006E+00	.2313E+00	.2148E+00
.30000	.5465E-01	.1186E+00	.1520E+00	.1751E+00	.1621E+00
.40000	.4420E-01	.9454E-01	.1209E+00	.1391E+00	.1284E+00
.50000	.3640E-01	.7698E-01	.9796E-01	.1125E+00	.1035E+00
.70000	.2423E-01	.4982E-01	.6311E-01	.7231E-01	.6606E-01
.90000	.1254E-01	.2511E-01	.3161E-01	.3613E-01	.3277E-01
.95000	.8659E-02	.1723E-01	.2167E-01	.2474E-01	.2241E-01
.99000	.3810E-02	.7534E-02	.9460E-02	.1080E-01	.9763E-02

AZIMUTH ANGLE= 45.0 DEGREES

R/R1:	.3300E+00	.6000E+00	.7500E+00	.8500E+00	.9500E+00
X/C					
.05000	.1496E+00	.3096E+00	.3985E+00	.3856E+00	.3109E+00
.10000	.1032E+00	.2124E+00	.2456E+00	.2640E+00	.2122E+00
.20000	.6906E-01	.1407E+00	.1622E+00	.1740E+00	.1391E+00
.30000	.5295E-01	.1068E+00	.1227E+00	.1314E+00	.1044E+00
.40000	.4262E-01	.8611E-01	.9748E-01	.1042E+00	.8229E-01
.50000	.3493E-01	.6905E-01	.7884E-01	.8411E-01	.6601E-01
.70000	.2305E-01	.4453E-01	.5062E-01	.5360E-01	.4167E-01
.90000	.1182E-01	.2243E-01	.2527E-01	.2675E-01	.2043E-01
.95000	.8153E-02	.1539E-01	.1731E-01	.1830E-01	.1392E-01
.99000	.3577E-02	.6724E-02	.7551E-02	.7977E-02	.6053E-02

AZIMUTH ANGLE= 60.0 DEGREES

R/R1:	.3300E+00	.6000E+00	.7500E+00	.8500E+00	.9500E+00
X/C					
.05000	.1300E+00	.3038E+00	.3950E+00	.3810E+00	.2547E+00
.10000	.8968E-01	.2087E+00	.2443E+00	.2475E+00	.1741E+00
.20000	.6003E-01	.1386E+00	.1619E+00	.1637E+00	.1145E+00
.30000	.4603E-01	.1055E+00	.1229E+00	.1241E+00	.8631E-01
.40000	.3700E-01	.8422E-01	.9797E-01	.9874E-01	.6826E-01
.50000	.3038E-01	.6850E-01	.7951E-01	.8000E-01	.5497E-01
.70000	.2005E-01	.4450E-01	.5142E-01	.5156E-01	.3498E-01
.90000	.1029E-01	.2248E-01	.2586E-01	.2583E-01	.1730E-01
.95000	.7094E-02	.1544E-01	.1775E-01	.1771E-01	.1182E-01
.99000	.3113E-02	.6754E-02	.7755E-02	.7733E-02	.5147E-02

AZIMUTH ANGLE= 75.0 DEGREES

R/R1:	.3300E+00	.6000E+00	.7500E+00	.8500E+00	.9500E+00
X/C					
.05000	.1290E+00	.3172E+00	.3622E+00	.3655E+00	.2672E+00
.10000	.8916E-01	.2194E+00	.2493E+00	.2515E+00	.1838E+00
.20000	.5997E-01	.1459E+00	.1662E+00	.1676E+00	.1223E+00
.30000	.4621E-01	.1116E+00	.1270E+00	.1280E+00	.9329E-01
.40000	.3738E-01	.8959E-01	.1019E+00	.1026E+00	.7468E-01
.50000	.3079E-01	.7326E-01	.8319E-01	.8371E-01	.6089E-01
.70000	.2051E-01	.4811E-01	.5450E-01	.5475E-01	.3974E-01
.90000	.1062E-01	.2457E-01	.2776E-01	.2786E-01	.2017E-01
.95000	.7340E-02	.1692E-01	.1911E-01	.1917E-01	.1387E-01
.99000	.3226E-02	.7418E-02	.8373E-02	.8396E-02	.6074E-02

AZIMUTH ANGLE= 90.0 DEGREES

R/R1:	.3300E+00	.6000E+00	.7500E+00	.8500E+00	.9500E+00
X/C					
.05000	.1553E+00	.3265E+00	.3539E+00	.3609E+00	.2927E+00
.10000	.1077E+00	.2257E+00	.2446E+00	.2495E+00	.2026E+00
.20000	.7284E-01	.1517E+00	.1644E+00	.1678E+00	.1366E+00
.30000	.5643E-01	.1159E+00	.1256E+00	.1282E+00	.1055E+00
.40000	.4689E-01	.9446E-01	.1024E+00	.1045E+00	.8549E-01
.50000	.3799E-01	.7779E-01	.8426E-01	.8605E-01	.7056E-01
.70000	.2556E-01	.5172E-01	.5606E-01	.5728E-01	.4718E-01
.90000	.1336E-01	.2679E-01	.2900E-01	.2964E-01	.2453E-01
.95000	.9256E-02	.1848E-01	.2004E-01	.2049E-01	.1697E-01
.99000	.4076E-02	.8122E-02	.8805E-02	.9003E-02	.7465E-02

AZIMUTH ANGLE=105.0 DEGREES

R/R1:	.3300E+00	.6000E+00	.7500E+00	.8500E+00	.9500E+00
X/C					
.05000	.1852E+00	.3264E+00	.3795E+00	.3781E+00	.3139E+00
.10000	.1287E+00	.2264E+00	.2632E+00	.2625E+00	.2185E+00
.20000	.8740E-01	.1533E+00	.1782E+00	.1780E+00	.1490E+00
.30000	.6798E-01	.1189E+00	.1383E+00	.1383E+00	.1163E+00
.40000	.5548E-01	.9574E-01	.1125E+00	.1128E+00	.9531E-01
.50000	.4610E-01	.8015E-01	.9327E-01	.9358E-01	.7948E-01
.70000	.3123E-01	.5401E-01	.6287E-01	.6325E-01	.5420E-01
.90000	.1644E-01	.2829E-01	.3293E-01	.3322E-01	.2870E-01
.95000	.1140E-01	.1960E-01	.2282E-01	.2304E-01	.1994E-01
.99000	.5026E-02	.8635E-02	.1005E-01	.1015E-01	.8804E-02

AZIMUTH ANGLE=120.0 DEGREES

R/R1:	.3300E+00	.6000E+00	.7500E+00	.8500E+00	.9500E+00
X/C					
.05000	.1959E+00	.3390E+00	.4686E+00	.4493E+00	.3480E+00
.10000	.1363E+00	.2358E+00	.3255E+00	.3126E+00	.2432E+00
.20000	.9290E-01	.1605E+00	.2210E+00	.2128E+00	.1671E+00
.30000	.7249E-01	.1251E+00	.1718E+00	.1660E+00	.1314E+00
.40000	.5935E-01	.1023E+00	.1402E+00	.1358E+00	.1084E+00
.50000	.4946E-01	.8515E-01	.1165E+00	.1131E+00	.9094E-01
.70000	.3369E-01	.5789E-01	.7886E-01	.7697E-01	.6276E-01
.90000	.1782E-01	.3057E-01	.4148E-01	.4068E-01	.3360E-01
.95000	.1238E-01	.2123E-01	.2878E-01	.2825E-01	.2341E-01
.99000	.5465E-02	.9366E-02	.1269E-01	.1247E-01	.1035E-01

AZIMUTH ANGLE=135.0 DEGREES

R/R1:	.3300E+00	.6000E+00	.7500E+00	.8500E+00	.9500E+00
X/C					
.05000	.1906E+00	.3867E+00	.5733E+00	.5492E+00	.4092E+00
.10000	.1329E+00	.2690E+00	.3982E+00	.3821E+00	.2862E+00
.20000	.9068E-01	.1832E+00	.2703E+00	.2602E+00	.1969E+00
.30000	.7066E-01	.1428E+00	.2101E+00	.2029E+00	.1551E+00
.40000	.5810E-01	.1159E+00	.1714E+00	.1660E+00	.1281E+00
.50000	.4849E-01	.9736E-01	.1424E+00	.1383E+00	.1076E+00
.70000	.3312E-01	.6625E-01	.9636E-01	.9411E-01	.7447E-01
.90000	.1756E-01	.3502E-01	.5067E-01	.4974E-01	.3995E-01
.95000	.1221E-01	.2432E-01	.3515E-01	.3455E-01	.2785E-01
.99000	.5340E-02	.1073E-01	.1550E-01	.1524E-01	.1232E-01

AZIMUTH ANGLE=150.0 DEGREES

R/R1:	.3300E+00	.6000E+00	.7500E+00	.8500E+00	.9500E+00
X/C					
.05000	.1837E+00	.4542E+00	.6231E+00	.6243E+00	.4875E+00
.10000	.1278E+00	.3156E+00	.4327E+00	.4341E+00	.3405E+00
.20000	.8698E-01	.2143E+00	.2938E+00	.2953E+00	.2337E+00
.30000	.6781E-01	.1667E+00	.2282E+00	.2301E+00	.1837E+00
.40000	.5547E-01	.1361E+00	.1861E+00	.1881E+00	.1514E+00
.50000	.4619E-01	.1131E+00	.1545E+00	.1566E+00	.1269E+00
.70000	.3141E-01	.7660E-01	.1045E+00	.1064E+00	.8751E-01
.90000	.1659E-01	.4032E-01	.5492E-01	.5614E-01	.4679E-01
.95000	.1152E-01	.2797E-01	.3809E-01	.3899E-01	.3259E-01
.99000	.5054E-02	.1233E-01	.1679E-01	.1719E-01	.1441E-01

AZIMUTH ANGLE=165.0 DEGREES

R/R1:	.3300E+00	.6000E+00	.7500E+00	.8500E+00	.9500E+00
X/C					
.05000	.1713E+00	.4936E+00	.6093E+00	.6561E+00	.5579E+00
.10000	.1187E+00	.3424E+00	.4230E+00	.4559E+00	.3690E+00
.20000	.8026E-01	.2318E+00	.2869E+00	.3098E+00	.2560E+00
.30000	.6216E-01	.1798E+00	.2229E+00	.2410E+00	.2083E+00
.40000	.5053E-01	.1463E+00	.1817E+00	.1968E+00	.1711E+00
.50000	.4162E-01	.1212E+00	.1508E+00	.1636E+00	.1431E+00
.70000	.2811E-01	.8169E-01	.1019E+00	.1109E+00	.9804E-01
.90000	.1469E-01	.4273E-01	.5354E-01	.5839E-01	.5215E-01
.95000	.1017E-01	.2965E-01	.3713E-01	.4052E-01	.3628E-01
.99000	.4480E-02	.1306E-01	.1636E-01	.1787E-01	.1603E-01

AZIMUTH ANGLE=180.0 DEGREES

R/R1: X/C	.3300E+00	.6000E+00	.7500E+00	.8500E+00	.9500E+00
.05000	.1373E+00	.4698E+00	.5780E+00	.6639E+00	.5988E+00
.10000	.9408E-01	.3254E+00	.4009E+00	.4608E+00	.4167E+00
.20000	.6333E-01	.2198E+00	.2715E+00	.3124E+00	.2840E+00
.30000	.4853E-01	.1700E+00	.2106E+00	.2425E+00	.2216E+00
.40000	.3904E-01	.1390E+00	.1715E+00	.1976E+00	.1814E+00
.50000	.3196E-01	.1141E+00	.1421E+00	.1640E+00	.1512E+00
.70000	.2108E-01	.7550E-01	.9380E-01	.1107E+00	.1030E+00
.90000	.1080E-01	.3983E-01	.5019E-01	.5811E-01	.5449E-01
.95000	.7446E-02	.2761E-01	.3478E-01	.4029E-01	.3786E-01
.99000	.3266E-02	.1215E-01	.1532E-01	.1776E-01	.1671E-01

AZIMUTH ANGLE=195.0 DEGREES

R/R1: X/C	.3300E+00	.6000E+00	.7500E+00	.8500E+00	.9500E+00
.05000	.8270E-01	.3957E+00	.5546E+00	.6590E+00	.6036E+00
.10000	.5636E-01	.2738E+00	.3842E+00	.4567E+00	.4193E+00
.20000	.3683E-01	.1844E+00	.2594E+00	.3088E+00	.2848E+00
.30000	.2756E-01	.1422E+00	.2007E+00	.2391E+00	.2215E+00
.40000	.2164E-01	.1152E+00	.1629E+00	.1943E+00	.1808E+00
.50000	.1730E-01	.9496E-01	.1347E+00	.1608E+00	.1502E+00
.70000	.1084E-01	.6038E-01	.9031E-01	.1080E+00	.1018E+00
.90000	.5271E-02	.3289E-01	.4708E-01	.5643E-01	.5356E-01
.95000	.3585E-02	.2274E-01	.3260E-01	.3909E-01	.3716E-01
.99000	.1556E-02	.1000E-01	.1435E-01	.1721E-01	.1638E-01

AZIMUTH ANGLE=210.0 DEGREES

R/R1: X/C	.3300E+00	.6000E+00	.7500E+00	.8500E+00	.9500E+00
.05000	.3325E-01	.3154E+00	.5179E+00	.6308E+00	.5838E+00
.10000	.2174E-01	.2178E+00	.3582E+00	.4366E+00	.4049E+00
.20000	.1298E-01	.1452E+00	.2411E+00	.2943E+00	.2741E+00
.30000	.8756E-02	.1124E+00	.1860E+00	.2272E+00	.2125E+00
.40000	.6092E-02	.9068E-01	.1505E+00	.1842E+00	.1730E+00
.50000	.4216E-02	.7452E-01	.1241E+00	.1520E+00	.1433E+00
.70000	.1767E-02	.4941E-01	.8275E-01	.1016E+00	.9654E-01
.90000	.3945E-03	.2548E-01	.4291E-01	.5284E-01	.5055E-01
.95000	.1845E-03	.1759E-01	.2967E-01	.3655E-01	.3503E-01
.99000	.5036E-04	.7726E-02	.1304E-01	.1608E-01	.1543E-01

AZIMUTH ANGLE=225.0 DEGREES

R/R1:	.3300E+00	.6000E+00	.7500E+00	.8500E+00	.9500E+00
X/C					
.05000	.1153E-01	.2578E+00	.4538E+00	.5811E+00	.5429E+00
.10000	.6494E-02	.1776E+00	.3135E+00	.4017E+00	.3898E+00
.20000	.2409E-02	.1187E+00	.2105E+00	.2702E+00	.2630E+00
.30000	.3737E-03	.9089E-01	.1620E+00	.2081E+00	.2033E+00
.40000	-.8762E-03	.7306E-01	.1308E+00	.1683E+00	.1650E+00
.50000	-.1575E-02	.5980E-01	.1076E+00	.1386E+00	.1363E+00
.70000	-.2354E-02	.3934E-01	.7141E-01	.9228E-01	.9129E-01
.90000	-.1839E-02	.2013E-01	.3687E-01	.4777E-01	.4754E-01
.95000	-.1376E-02	.1387E-01	.2547E-01	.3301E-01	.3290E-01
.99000	-.6412E-03	.6084E-02	.1119E-01	.1451E-01	.1446E-01

AZIMUTH ANGLE=240.0 DEGREES

R/R1:	.3300E+00	.6000E+00	.7500E+00	.8500E+00	.9500E+00
X/C					
.05000	.1097E-01	.2153E+00	.3932E+00	.5402E+00	.5571E+00
.10000	.6158E-02	.1489E+00	.2714E+00	.3731E+00	.3852E+00
.20000	.2258E-02	.9924E-01	.1820E+00	.2504E+00	.2592E+00
.30000	.3058E-03	.7579E-01	.1398E+00	.1926E+00	.1998E+00
.40000	-.8693E-03	.6076E-01	.1127E+00	.1554E+00	.1616E+00
.50000	-.1652E-02	.4951E-01	.9251E-01	.1278E+00	.1332E+00
.70000	-.2295E-02	.3247E-01	.6123E-01	.8476E-01	.8874E-01
.90000	-.1796E-02	.1653E-01	.3152E-01	.4372E-01	.4598E-01
.95000	-.1335E-02	.1138E-01	.2175E-01	.3019E-01	.3178E-01
.99000	-.6222E-03	.4985E-02	.9549E-02	.1326E-01	.1397E-01

AZIMUTH ANGLE=255.0 DEGREES

R/R1:	.3300E+00	.6000E+00	.7500E+00	.8500E+00	.9500E+00
X/C					
.05000	.8709E-02	.1742E+00	.3699E+00	.5274E+00	.5600E+00
.10000	.5002E-02	.1199E+00	.2552E+00	.3640E+00	.3868E+00
.20000	.2012E-02	.8002E-01	.1710E+00	.2440E+00	.2597E+00
.30000	.5272E-03	.6116E-01	.1312E+00	.1874E+00	.1998E+00
.40000	-.3870E-03	.4939E-01	.1057E+00	.1511E+00	.1613E+00
.50000	-.9771E-03	.4010E-01	.8674E-01	.1240E+00	.1327E+00
.70000	-.1505E-02	.2630E-01	.5733E-01	.8207E-01	.8806E-01
.90000	-.1207E-02	.1341E-01	.2947E-01	.4224E-01	.4546E-01
.95000	-.9067E-03	.9233E-02	.2033E-01	.2915E-01	.3139E-01
.99000	-.4238E-03	.4046E-02	.8923E-02	.1280E-01	.1379E-01

AZIMUTH ANGLE=270.0 DEGREES

R/R1:	.3300E+00	.6000E+00	.7500E+00	.8500E+00	.9500E+00
X/C					
.05000	-.2495E-02	.1362E+00	.3689E+00	.5222E+00	.5545E+00
.10000	-.2053E-02	.9403E-01	.2545E+00	.3603E+00	.3828E+00
.20000	-.1816E-02	.6311E-01	.1706E+00	.2414E+00	.2568E+00
.30000	-.1729E-02	.4852E-01	.1310E+00	.1853E+00	.1973E+00
.40000	-.1660E-02	.3916E-01	.1056E+00	.1493E+00	.1591E+00
.50000	-.1579E-02	.3218E-01	.8706E-01	.1225E+00	.1307E+00
.70000	-.1327E-02	.2134E-01	.5732E-01	.8103E-01	.8657E-01
.90000	-.9248E-03	.1101E-01	.2944E-01	.4166E-01	.4460E-01
.95000	-.5934E-03	.7600E-02	.2034E-01	.2875E-01	.3078E-01
.99000	-.2689E-03	.3333E-02	.8931E-02	.1262E-01	.1352E-01

AZIMUTH ANGLE=285.0 DEGREES

R/R1:	.3300E+00	.6000E+00	.7500E+00	.8500E+00	.9500E+00
X/C					
.05000	-.3895E-02	.1273E+00	.3577E+00	.5047E+00	.5475E+00
.10000	-.3092E-02	.8861E-01	.2470E+00	.3482E+00	.3778E+00
.20000	-.3221E-02	.5997E-01	.1655E+00	.2334E+00	.2532E+00
.30000	-.2022E-02	.4549E-01	.1274E+00	.1791E+00	.1944E+00
.40000	-.1670E-02	.3733E-01	.1028E+00	.1444E+00	.1567E+00
.50000	-.7504E-03	.3134E-01	.8650E-01	.1185E+00	.1286E+00
.70000	-.1158E-03	.2110E-01	.5603E-01	.7835E-01	.8504E-01
.90000	.1322E-03	.1105E-01	.2884E-01	.4030E-01	.4374E-01
.95000	.1239E-03	.7654E-02	.1994E-01	.2780E-01	.3018E-01
.99000	.6579E-04	.3371E-02	.8759E-02	.1220E-01	.1325E-01

AZIMUTH ANGLE=300.0 DEGREES

R/R1:	.3300E+00	.6000E+00	.7500E+00	.8500E+00	.9500E+00
X/C					
.05000	-.9034E-03	.1330E+00	.3588E+00	.5122E+00	.5818E+00
.10000	.5135E-03	.1150E+00	.2478E+00	.3534E+00	.4012E+00
.20000	.1656E-02	.7841E-01	.1664E+00	.2367E+00	.2685E+00
.30000	.2574E-02	.6089E-01	.1280E+00	.1816E+00	.2059E+00
.40000	.2990E-02	.4963E-01	.1034E+00	.1463E+00	.1657E+00
.50000	.3198E-02	.4118E-01	.8501E-01	.1200E+00	.1359E+00
.70000	.3085E-02	.2782E-01	.5644E-01	.7932E-01	.8963E-01
.90000	.2075E-02	.1460E-01	.2914E-01	.4077E-01	.4599E-01
.95000	.1515E-02	.1012E-01	.2012E-01	.2812E-01	.3171E-01
.99000	.6942E-03	.4462E-02	.8840E-02	.1234E-01	.1391E-01

AZIMUTH ANGLE=315.0 DEGREES

R/R1: X/C	.3300E+00	.6000E+00	.7500E+00	.8500E+00	.9500E+00
.05000	.1223E-01	.2427E+00	.4395E+00	.6102E+00	.6939E+00
.10000	.1005E-01	.1681E+00	.3026E+00	.4206E+00	.4780E+00
.20000	.8672E-02	.1136E+00	.2029E+00	.2813E+00	.3193E+00
.30000	.8437E-02	.8790E-01	.1558E+00	.2155E+00	.2443E+00
.40000	.8096E-02	.7140E-01	.1256E+00	.1733E+00	.1963E+00
.50000	.7698E-02	.5904E-01	.1031E+00	.1420E+00	.1606E+00
.70000	.6463E-02	.3953E-01	.6824E-01	.9350E-01	.1055E+00
.90000	.4016E-02	.2064E-01	.3512E-01	.4790E-01	.5394E-01
.95000	.2889E-02	.1432E-01	.2424E-01	.3302E-01	.3716E-01
.99000	.1509E-02	.6303E-02	.1054E-01	.1448E-01	.1629E-01

AZIMUTH ANGLE=330.0 DEGREES

R/R1: X/C	.3300E+00	.6000E+00	.7500E+00	.8500E+00	.9500E+00
.05000	.2661E-01	.3259E+00	.5045E+00	.7037E+00	.8521E+00
.10000	.1601E-01	.2253E+00	.4167E+00	.5445E+00	.5864E+00
.20000	.1311E-01	.1515E+00	.2785E+00	.3633E+00	.3909E+00
.30000	.1187E-01	.1153E+00	.2133E+00	.2778E+00	.2986E+00
.40000	.1101E-01	.9451E-01	.1715E+00	.2230E+00	.2394E+00
.50000	.1021E-01	.7785E-01	.1404E+00	.1822E+00	.1954E+00
.70000	.8279E-02	.5186E-01	.9244E-01	.1195E+00	.1279E+00
.90000	.5027E-02	.2886E-01	.4732E-01	.6099E-01	.6513E-01
.95000	.3600E-02	.1956E-01	.3261E-01	.4200E-01	.4482E-01
.99000	.1626E-02	.8160E-02	.1430E-01	.1841E-01	.1964E-01

AZIMUTH ANGLE=345.0 DEGREES

R/R1: X/C	.3300E+00	.6000E+00	.7500E+00	.8500E+00	.9500E+00
.05000	.3421E-01	.3861E+00	.7519E+00	.9342E+00	.9542E+00
.10000	.2526E-01	.2664E+00	.5176E+00	.6427E+00	.6561E+00
.20000	.1912E-01	.1736E+00	.3453E+00	.4281E+00	.4366E+00
.30000	.1635E-01	.1371E+00	.2638E+00	.3269E+00	.3328E+00
.40000	.1451E-01	.1109E+00	.2116E+00	.2618E+00	.2663E+00
.50000	.1299E-01	.9067E-01	.1729E+00	.2136E+00	.2170E+00
.70000	.9998E-02	.5997E-01	.1133E+00	.1396E+00	.1416E+00
.90000	.5852E-02	.3084E-01	.5775E-01	.7098E-01	.7180E-01
.95000	.4159E-02	.2128E-01	.3976E-01	.4883E-01	.4937E-01
.99000	.1868E-02	.9342E-02	.1742E-01	.2139E-01	.2161E-01

Sample Airfoil Data

Printed below is a sample print of typical airfoil data to illustrate the previously described input format.

1127

	0.	.2	.3	.4	.5	.6	.7	.75	.8
	.9	1.							
-39.	-1.18	-1.18	-1.18	-1.18	-1.18	-1.18	-1.18	-1.18	-1.18
	-1.18	-1.18							
-21.	-.8	-.8	-.81	-.83	-.85	-.85	-.85	-.71	-.68
	-.64	-.64							
-16.5	-1.007	-1.007	-.944	-.960	-.965	-.965	-.965	-.795	-.760
	-.70	-.70							
-15.	-1.19	-1.19	-1.09	-1.055	-.99	-.98	-.98	-.83	-.79
	-.72	-.72							
-14.	-1.333	-1.333	-1.22	-1.096	-1.	-.97	-.97	-.84	-.805
	-.73	-.73							
-13.	-1.334	-1.334	-1.28	-1.12	-1.	-.96	-.96	-.85	-.815
	-.735	-.735							
-12.	-1.255	-1.255	-1.26	-1.13	-1.	-.947	-.94	-.85	-.82
	-.74	-.74							
-11.	-1.161	-1.161	-1.19	-1.12	-.994	-.930	-.923	-.85	-.81
	-.74	-.74							
-10.	-1.055	-1.055	-1.01	-1.082	-.985	-.910	-.900	-.845	-.805
	-.73	-.73							
-8.	-.844	-.844	-.88	-.907	-.922	-.87	-.84	-.82	-.77
	-.695	-.695							
-6.	-.633	-.633	-.66	-.684	-.741	-.77	-.75	-.77	-.72
	-.593	-.593							
-4.	-.46	-.46	-.46	-.4805	-.52	-.5657	-.6401	-.7244	-.53
	-.396	-.396							
-2.	-.25	-.25	-.25	-.2399	-.27	-.282	-.3274	-.3605	-.3469
	-.1399	-.1399							
0.	0.	0.	0.	0.	0.	0.	0.	0.	0.
	0.	0.							
2.	.23	.23	.23	.2403	.25	.271	.3245	.3417	.3676
	.1245	.1245							
4.	.45	.45	.45	.4916	.51	.5731	.6252	.6368	.5428
	.45	.45							
6.	.70	.70	.70	.7224	.75	.7967	.7367	.7169	.6430
	.593	.593							
8.	.89	.89	.89	.9416	.89	.8711	.7513	.7071	.70
	.695	.695							
10.	1.08	1.08	1.08	1.0333	.93	.8802	.8600	.845	.805
	.73	.73							
11.	1.161	1.161	1.19	1.1200	.994	.93	.923	.85	.81
	.74	.74							
12.	1.255	1.255	1.26	1.1305	1.0000	.947	.940	.85	.82
	.74	.74							
13.	1.334	1.334	1.28	1.12	1.	.96	.96	.85	.815
	.735	.735							
14.	1.33	1.33	1.22	1.096	1.	.97	.97	.84	.805
	.73	.73							
15.	1.19	1.19	1.09	1.055	.99	.98	.98	.83	.79
	.72	.72							
16.5	1.007	1.007	.944	.96	.965	.965	.965	.795	.76
	.7	.7							
21.	.8	.8	.81	.83	.85	.85	.85	.71	.68
	.64	.64							
39.	1.18	1.18	1.18	1.18	1.18	1.18	1.18	1.18	1.18
	1.18	1.18							

REFERENCES

1. Van Holten, Th.: The Computation of Aerodynamic Loads on Helicopter Blades in Forward Flight, Using the Method of the Acceleration Potential. Report VTH-189, Technische Hogeschool Delft, Netherlands, March 1975.

2. Pierce, G. Alvin and Vaidyanathan, Anand R.: Helicopter Rotor Loads Using a Matched Asymptotic Expansion Technique, NASA CR 165742, May 1981.

3. Pierce, G. Alvin and Vaidyanathan, Anand R.: Helicopter Rotor Loads Using Discretized Matched Asymptotic Expansions. Final Report Prepared for NASA Langley Research Center under Contract NAS1 - 16817.

APPENDIX A

LISTING OF PROGRAM ASYMP1

```
      PROGRAM MAIN(INPUT,OUTPUT,TAPE5=INPUT,TAPE6=OUTPUT,
     1AFDATA,TAPE1=AFDATA)
C
C   CALCULATION OF THE UNSTEADY AIRLOADS ON A HELICOPTER ROTOR BLADE IN
C   FORWARD FLIGHT. THE METHOD USES AN ACCELERATION POTENTIAL DESCRIPTION
C   OF THE FLOW FIELD AND A MATCHED ASYMPTOTIC EXPANSION TECHNIQUE TO
C   OBTAIN A SOLUTION CORRECT TO O(1/(AR*AR)).
C   REF.1 - TH. VAN HOLTEN, REPORT VTH-189,TECHNISCHE HOGESCHOOL,DELFT,
C   NETHERLANDS.
C   REF.2 - G.A.PIERCE ET AL, NASA CR 165742, MAY 1981.
C   FOR IDENTIFICATION OF PROGRAM STEPS, REFER USER'S MANUAL.
C
      REAL MU,LAM,MCL,MINF,MLOC
      DIMENSION RBO(5),XOUT(10),PBOD(24),A(59,59),B(59,1),
     1IPIVOT(59),PMIN(20),FI1(5),FI2(5),GO(5),GC(5,5),GS(5,5),F1(24),
     2F2(24),F3(24),FLT1(24),FLT2(24),FMT(24),COL(24),GST(24,5),WK(59),
     3DGS2(24,5),FL1(24,5),FL2(24,5),FM(24,5),XCP(24,5),
     4POUT(5,10),POIP(24,5)
      DIMENSION CL(50,20),MCL(20),ACL(50)
      COMMON/MAIN1/NL,PI
      YL(XL,XL1,XL2,YL1,YL2)=YL1+(XL-XL1)*(YL2-YL1)/(XL2-XL1)
      DATA NSP,NHM,NAZ,NCOF,NCOFP,OMAX/5,5,11,59,60,0.5/
      DATA XOUT/.05,.1,.2,.3,.4,.5,.7,.9,.95,.99/
      PI=4.*ATAN(1.)
C
C   PROGRAM STEP 1.
C   READ AND WRITE INPUT DATA AND ASSOCIATED QUANTITIES.
C
      READ(5,*)RO,AR,NB,TW,MU,ALR,CT,MINF
      READ(5,*)N1,N2,N3,N4
      IF(N1 .EQ. 1)READ(5,*)THC
      IF(N2 .EQ. 0)READ(5,*)GAMA
      IF(N2 .EQ. 1)READ(5,*)A0
      IF(N3 .EQ. 1)READ(5,*)A1
      IF(N4 .EQ. 1)READ(5,*)B1
      READ(5,*)(RBO(I),I=1,NSP)
      READ(5,*)DP1D,DP2D,UTMIN,NAFD
C
C   NAFD=0 -- AIRFOIL TABLES NOT USED.
C   NAFD=1 -- AIRFOIL TABLES USED.
C
      IF(NAFD .EQ. 0)GO TO 8
      READ(1,1)NXL,NZL
    1 FORMAT(30X,2I2)
      READ(1,2)(MCL(I),I=1,NXL)
    2 FORMAT(7X,9F7.0)
      NL1=NXL/9
      NL2=NL1+1
      DO 3 I=1,NZL
      DO 3 J=1,NL2
      J1=(J-1)*9+1
      J2=J*9
      IF(J1 .GT. NXL)GO TO 3
      IF(J2 .GT. NXL)J2=NXL
      IF(J .EQ. 1)READ(1,4)ACL(I),(CL(I,J3),J3=J1,J2)
    4 FORMAT(F7.0,9F7.0)
      IF(J .GT. 1)READ(1,5)(CL(I,J3),J3=J1,J2)
    5 FORMAT(7X,9F7.0)
    3 CONTINUE
```

```
    8  CONTINUE
       DP1=DP1D*PI/180.
       DP2=DP2D*PI/180.
       WRITE(6,10)
   10  FORMAT(1H1)
       WRITE(6,20)RO,AR,NB,TW,MU,ALR,MINF
   20  FORMAT(//6X,"ROOT RADIUS/TIP RADIUS=",F10.5//6X,"ASPECT RATIO=",
      1F10.5//6X,"NUMBER OF BLADES=",I2//6X,
      2"LINEAR TWIST(ROOT TO TIP)=",F10.5,1X,"DEGREES"//6X,
      3"FORWARD SPEED/TIP SPEED=",F10.5//6X,
      4"ROTOR INCIDENCE(FORWARD TILT POSITIVE)=",F10.5,1X,"DEGREES"//6X,
      5"FREESTREAM MACH NUMBER=",F10.5)
       TW=TW*PI/180.
       ALR=ALR*PI/180.
       IF(N1 .EQ. 0)THC=0.
       IF(N2 .EQ. 0)A0=0.
       IF(N3 .EQ. 0)A1=0.
       IF(N4 .EQ. 0)B1=0.
       WRITE(6,30)CT
   30  FORMAT(//6X,"THRUST COEFFICIENT=",F10.5)
       IF(N1 .EQ. 1)WRITE(6,40)THC
   40  FORMAT(//6X,"PITCH ANGLE AT BLADE ROOT=",F10.5,1X,"DEGREES")
       IF(N2 .EQ. 0)WRITE(6,50)GAMA
   50  FORMAT(//6X,"FLAPPING INERTIA COEFFICIENT=",F10.5)
       IF(N2 .EQ. 1)WRITE(6,60)A0
   60  FORMAT(//6X,"CONING ANGLE=",F10.5,1X,"DEGREES")
       IF(N3 .EQ. 1)WRITE(6,70)A1
   70  FORMAT(//6X,"FLAPPING COEFFICIENT, A1=",F10.5,1X,"DEGREES")
       IF(N4 .EQ. 1)WRITE(6,80)B1
   80  FORMAT(//6X,"FLAPPING COEFFICIENT, B1=",F10.5,1X,"DEGREES")
       THC=THC*PI/180.
       A0=A0*PI/180.
       A1=A1*PI/180.
       B1=B1*PI/180.
       LAM=MU*ALR+SQRT(.5*(-MU*MU+SQRT(MU*MU*MU*MU+CT*CT)))
       WRITE(6,90)LAM,UTMIN,DP1D,DP2D
   90  FORMAT(//6X,"TOTAL INFLOW RATIO=",F10.5//6X,"MINIMUM UT=",F10.5,
      1"(ZERO LIFT CONDITION APPLIED BELOW THIS VALUE)"//6X,
      2"NORMAL AZIMUTH INTERVAL=",F10.5,1X,"DEGREES"//6X,
      3"REDUCED AZIMUTH INTERVAL=",F10.5,1X,"DEGREES")
       SLOR=1.
       CL0=0.
       IF(NAFD .EQ. 0)WRITE(6,91)
   91  FORMAT(//6X,"AIRFOIL DATA TABLES NOT USED")
       IF(NAFD .EQ. 1)WRITE(6,92)
   92  FORMAT(//6X,"AIRFOIL DATA TABLES USED")
C
C  CALCULATE QUANTITIES NEEDED FOR TRAJECTORY SEGMENT ADJACENT TO THE
C  COLLOCATION POINT.
C
       ETA1P=ALOG((3.+SQRT(5.))/2.)
       CF1=COSH(.5*ETA1P)/SINH(.5*ETA1P)
       CF2=.5*CF1-ETA1P
       CF3=.25*CF1-SINH(ETA1P)
       EX1=EXP(-ETA1P)
       CF4=.5-EX1
       CF5=-.5*ETA1P-.5*EX1+.25*EX1*EX1+3./8.
       L=1
C
C  PROGRAM STEP 2.
```

```
C  START OUTER LOOP FOR COLLOCATION. THIS LOOP SETS THE CURRENT AZIMUTH
C  STATION.
C
      DO 100 J=1,NAZ
      PBO=2.*J*PI/NAZ
      PBO(J)=360.*J/NAZ
      CP1=COS(PBO)
      SP1=SIN(PBO)
      CP2=COS(2.*PBO)
      SP2=SIN(2.*PBO)
C
C  START INNER LOOP FOR COLLOCATION. THIS LOOP SETS THE CURRENT RADIAL
C  LOCATION.
C
      DO 100 I=1,NSP
      DO 110 M=1,NCOF
      A(L,M)=0.
 110  CONTINUE
      B(L,1)=0.
      ZBO=2.*(RBO(I)-.5*(1.+RO))/(1.-RO)
      SQZ=SQRT(1.-ZBO*ZBO)
      UT=RBO(I)+MU*SP1
C
C  PROGRAM STEP 3.
C  TEST THE TANGENTIAL VELOCITY AT THE COLLOCATION POINT, TO DECIDE
C  WHETHER NORMAL VELOCITY BOUNDARY CONDITION OR ZERO LIFT CONDITION
C  SHOULD BE APPLIED.
C
      IF(UT .GT. UTMIN)GO TO 120
      WRITE(6,130)RBO(I),PBO(J),UT
 130  FORMAT(/6X,"R=",F8.3,1X,"PSI=",F8.3,"DEGREES",1X,"UT=",
     1F8.3,1X,"ZERO LIFT CONDITION APPLIED")
      GO TO 140
 120  DP=(1.-RO)/(2.*AR*UT)
      PLIM=PBO-(2.*RBO(I)*CP1)/SQRT(MU*MU+LAM*LAM)
      IF(NAFO .EQ. 0)GO TO 133
C
C  PROGRAM STEP 4.
C  CALCULATE LIFT CURVE SLOPE FROM DATA TABLES FOR THE CURRENT
C  COLLOCATION POINT, USING THE LOCAL INCIDENCE AND MACH NUMBER.
C
      MLOC=UT*MINF/MU
      ALOC=THC-TW*(RBO(I)-RO)/(1.-RO)+B1*CP1-A1*SP1
     1-(MU*AO*CP1+LAM)/UT
      ALOC=ALOC*180./PI
      CALL TABSCH(MCL,NXL,MLOC,IMCL1,IMCL2,INT)
      IF(INT .EQ. -1)IMCL1=IMCL2=1
      IF(INT .EQ. 1)IMCL1=IMCL2=NXL
      CALL TABSCH(ACL,NZL,ALOC,IACL1,IACL2,INT)
      IF(INT .EQ. 0)GO TO 131
      IF(INT .EQ. -1)GO TO 132
      IACL1=NXL-1
      IACL2=NXL
      GO TO 131
 132  IACL1=1
      IACL2=2
 131  SLC1=(CL(IACL2,IMCL1)-CL(IACL1,IMCL1))/(ACL(IACL2)
     1-ACL(IACL1))
      CLO1=CL(IACL1,IMCL1)-SLC1*ACL(IACL1)
      SLC1=SLC1*180./PI
```

```
      SLC2=(CL(IACL2,IMCL2)-CL(IACL1,IMCL2))/(ACL(IACL2)
     1-ACL(IACL1))
      CLO2=CL(IACL1,IMCL2)-SLC2*ACL(IACL1)
      SLC2=SLC2*180./PI
      IF(IMCL1 .EQ. IMCL2)SLCR=SLC1/(2.*PI)
      IF(IMCL1 .NE. IMCL2)SLCR=YL(MLOC,MCL(IMCL1),MCL(IMCL2),
     1SLC1,SLC2)/(2.*PI)
      IF(IMCL1 .EQ. IMCL2)CLO=CLO1
      IF(IMCL1 .NE. IMCL2)CLO=YL(MLOC,MCL(IMCL1),MCL(IMCL2),
     1CLO1,CLO2)
  133 CONTINUE
C
C   CALCULATE THE CONTRIBUTION TO THE INDUCED VELOCITY FROM THE
C   TRAJECTORY SEGMENT ADJACENT TO THE COLLOCATION POINT, AND ADD TO
C   COEFFICIENT MATRIX ELEMENT. ALTERNATIVELY, SET UP THE ZERO LIFT
C   CONDITION.
C
  140 DO 150 I1=1,NSP
      IF(I1 .GT. 1)GO TO 160
      IF(UT .LE. UTMIN)GO TO 170
      IF(SLCR .EQ. 0.)GO TO 151
      W1=-AR*(1.+ZBO)*CF1/UT+MU*CP1*CF2/(UT*UT)-(2.*AR*(1.+ZBO)-
     1FUN3(RO,AR,RBO(I),1))/UT
      W2=(1.-RO)*(1.+ZBO)*CF2/(2.*UT*UT)-(1.-RO)*MU*CP1*CF3/(2.*AR*
     1UT*UT*UT)
      W3=(1.-RO)*(1.-RO)*(1.+ZBO)*CF3/(8.*AR*UT*UT*UT)
      W1=W1-AR*(1.+ZBO)*(1.-SLCR)/(SLCR*UT)
      GO TO 180
  151 W1=AR*(1.+ZBO)
      W2=W3=0.
      GO TO 180
  170 W1=AR*(1.+ZBO)-FUN3(RO,AR,RBO(I),1)
      W2=0.
      W3=0.
      GO TO 180
  160 NL=I1-1
      IF(UT .LE. UTMIN)GO TO 190
      POS=PNM(I1-1,0,ZBO)
      P1S=PNM(I1-1,1,ZBO)
      PO=FUN3(RO,AR,RBO(I),3)
      IF(SLCR .EQ. 0.)GO TO 152
      W1=-AR*SQZ*P1S*CF1/(2.*PI*UT)-MU*CP1*NL*(NL+1.)*POS*CF2/(2.*PI
     1*UT*UT)+MU*MU*CP1*CP1*NL*(NL+1.)*P1S*CF3/(4.*PI*AR*SQZ*UT
     2*UT*UT)-(AR*SQZ*P1S+PO/2.)/(PI*UT)
      W2=(1.-RO)*SQZ*P1S*CF2/(4.*PI*UT*UT)+(1.-RO)*MU*CP1*NL*(NL+1.)
     1*POS*CF3/(4.*PI*AR*UT*UT*UT)
      W3=(1.-RO)*(1.-RO)*SQZ*P1S*CF3/(16.*PI*AR*UT*UT*UT)
      W1=W1-AR*SQZ*P1S*(1.-SLCR)/(2.*PI*SLCR*UT)
      GO TO 180
  152 W1=AR*SQZ*P1S/(2.*PI)
      W2=W3=0.
      GO TO 180
  190 W1=(AR*SQZ*PNM(I1-1,1,ZBO)+FUN3(RO,AR,RBO(I),3))/(2.*PI)
      W2=0.
      W3=0.
  180 M=(I1-1)*NAZ+1
      A(L,M)=A(L,M)+W1
      DO 150 I2=1,NHM
      M=M+1
      A(L,M)=A(L,M)+(W1+I2*I2*W3)*COS(I2*PBO)-I2*W2*SIN(I2*PBO)
```

```
      M=M+1
      A(L,M)=A(L,M)+(W1+I2*I2*W3)*SIN(I2*PBO)+I2*W2*COS(I2*PBO)
  150 CONTINUE
      IF(UT .GT. UTMIN)GO TO 200
      M=NSP*NAZ+1
      A(L,M)=A(L,M)+(1.-RO)*(2.*MU*CP1)/(4.*AR)+(1.-RO)*(1.-RO)
     1*(-1.)/(16.*AR*AR)
      M=M+1
      A(L,M)=A(L,M)+(1.-RO)*(2.*MU*SP1+RBO(I))/(4.*AR)
      M=M+1
      A(L,M)=A(L,M)+(1.-RO)*(-2.*MU*SP2-2.*RBO(I)*CP1)/(4.*AR)+(1.-RO)
     1*(1.-RO)*(2.*SP1)/(16.*AR*AR)
      M=M+1
      A(L,M)=A(L,M)+(1.-RO)*(2.*MU*CP2-2.*RBO(I)*SP1)/(4.*AR)+(1.-RO)
     1*(1.-RO)*(-2.*CP1)/(16.*AR*AR)
      B(L,1)=B(L,1)-TW*(2.*MU*RO*CP1-MU*MU*SP2-4.*MU*RBO(I)*CP1)/(4.*AR)
     1-(1.-RO)*(-RO+4.*RBO(I)+4.*MU*SP1)*TW/(16.*AR*AR)
      L=L+1
      GO TO 100
  200 CONTINUE
      IF(SLCR .NE. 0.)GO TO 201
      B(L,1)=B(L,1)-UT*UT*CLO/(2.*PI)
      L=L+1
      GO TO 100
  201 B(L,1)=B(L,1)+UT*CLO/(2.*PI*SLCR)
C
C   PROGRAM STEP 5.
C   START CALCULATION OF THE INDUCED VELOCITY CONTRIBUTION THAT REQUIRES
C   INTEGRATION WITH AZIMUTH.
C   START LOOP FOR NUMBER OF BLADES.
C
      DO 210 IBL=1,NB
      DB=2.*PI*(IBL-1)/NB
C
C   CALL SUBROUTINE TO DETERMINE AZIMUTH POSITIONS AT WHICH TRAJECTORY
C   IS CLOSE TO A BLADE.
C
      IF(DP1 .NE. DP2)CALL DMIN(MU,LAM,DB,RBO(I),PBO,PLIM,DMAX,IMIN,
     1PMIN)
      J1=1
      K1=0
C
C   SET LOWER AND UPPER LIMITS FOR AZIMUTH SUB-INTERVAL.
C
      PB2=PBO
      IF(IBL .EQ. 1)PB1=PBO-DP
      IF(IBL .GT. 1)PB1=PBO-DP1
  220 CONTINUE
      G1=.5*(PB2+PB1)
      G2=.5*(PB2-PB1)
C
C   PROGRAM STEP 6.
C   START LOOP FOR 5-POINT GAUSS-CHEBYSCHEV INTEGRATION.
C
      DO 230 I1=1,5
      G=G1+G2*COS((2.*I1-1.)*PI/10.)
      FACT=SQRT((G-PB1)*(PB2-G))
      DO 230 M=1,NCOEP
      M1=(M-1)/NAZ+1
      M2=M-(M1-1)*NAZ
```

```
      IF(M1 .GT. NSP)GO TO 240
      M3=M2/2
      M4=M2-M3*2
      IF(M1 .GT. 1)GO TO 250
      IF(M2 .EQ. 1)FN=FUN2(RO,AR,TW,MU,LAM,RBO(I),PBO,DP,DB,G,1)
      GO TO 260
  250 NL=M1-1
      IF(M2 .EQ. 1)FN=FUN2(RO,AR,TW,MU,LAM,RBO(I),PBO,DP,DB,G,2)
  260 IF(M2 .EQ. 1)A(L,M)=A(L,M)+FN*FACT*PI/5.
      IF(M2 .GT. 1 .AND. M4 .EQ. 0)A(L,M)=A(L,M)+FN*COS(M3*(G+DB))
     1*FACT*PI/5.
      IF(M2 .GT. 1 .AND. M4 .GT. 0)A(L,M)=A(L,M)+FN*SIN(M3*(G+DB))
     1*FACT*PI/5.
      GO TO 230
  240 I2=M+2-(NSP*NAZ)
      FN=FUN2(RO,AR,TW,MU,LAM,RBO(I),PBO,DP,DB,G,I2)
      IF(M .LE. NCOF)A(L,M)=A(L,M)+FN*FACT*PI/5.
      IF(M .EQ. NCOFP)B(L,1)=B(L,1)+FN*FACT*PI/5.
  230 CONTINUE
C
C   PROGRAM STEP 7.
C   END OF LOOP FOR GAUSS-CHEBYSCHEV INTEGRATION.
C   REDEFINE UPPER AND LOWER LIMITS FOR THE NEXT AZIMUTH SUB-INTERVAL.
C   TEST TO SEE IF THE AZIMUTH LIMIT HAS BEEN REACHED. ALSO TEST TO SEE
C   IF THE TRAJECTORY IN THE NEXT SEGMENT IS CLOSE TO A BLADE, IN WHICH
C   CASE REDUCED SPACING MUST BE USED.
C
      PB2=PB1
      IF(PB2 .LE. PLIM)GO TO 210
      IF(DP1 .EQ. DP2)GO TO 270
      IF(J1 .GT. IMIN)GO TO 270
      IF(K1 .EQ. 0 .AND. PB2 .LE. (PMIN(J1)+PI/6.))GO TO 280
      IF(K1 .EQ. 1 .AND. PB2 .GT. (PMIN(J1)-PI/6.))GO TO 280
      IF(K1 .EQ. 1 .AND. PB2 .LE. (PMIN(J1)-PI/6.))GO TO 290
      IF(PB2 .GT. (PBO-PI/6.) .AND. IBL .EQ. 1)PB1=PB1-DP2
      IF(PB2 .LE. (PBO-PI/6.) .OR. IBL .GT. 1)PB1=PB1-DP1
      IF(K1 .EQ. 0 .AND. PB1 .LT. (PMIN(J1)+DP1))PB1=PMIN(J1)+DP1
      GO TO 220
  270 PB1=PB1-DP1
      GO TO 220
  280 PB1=PB1-DP2
      K1=1
      GO TO 220
  290 PB1=PB1-DP1
      K1=0
      J1=J1+1
      GO TO 220
  210 CONTINUE
C
C   PROGRAM STEP 8.
C   END OF LOOP FOR NUMBER OF BLADES.
C   SET UP THE COEFFICIENT MATRIX ELEMENTS CORRESPONDING TO THE
C   4 AUXILIARY UNKNOWNS, AND THE RIGHT HAND SIDE.
C
      M=NSP*NAZ+1
      A(L,M)=A(L,M)-UT-(1.-RO)*(2.*MU*CP1)*CF4/(2.*AR*UT)-
     1(1.-RO)*(1.-RO)*(-2.*MU*SP1)*CF5/(4.*AR*AR*UT*UT)
      M=M+1
      A(L,M)=A(L,M)+MU*CP1-(1.-RO)*(2.*MU*SP1+RBO(I))*CF4/(2.*AR*UT)
     1-(1.-RO)*(1.-RO)*(3.*MU*CP1)*CF5/(4.*AR*AR*UT*UT)
```

```
      M=M+1
      A(L,M)=A(L,M)+.5*MU*(1.-CP2)+RBO(I)*SP1-(1.-RO)*(-2.*MU*SP2
     1-2.*RBO(I)*CP1)*CF4/(2.*AR*UT)-(1.-RO)*(1.-RO)*(-4.*MU*CP2
     2+2.*RBO(I)*SP1-2.*MU*CP1*CP1)*CF5/(4.*AR*AR*UT*UT)
      M=M+1
      A(L,M)=A(L,M)-RBO(I)*CP1-.5*MU*SP2-(1.-RO)*(2.*MU*CP2-2.*RBO(I)
     1*SP1)*CF4/(2.*AR*UT)-(1.-RO)*(1.-RO)*(-4.*MU*SP2-2.*RBO(I)
     2*CP1-2.*MU*CP1*SP1)*CF5/(4.*AR*AR*UT*UT)
      B(L,1)=B(L,1)-MU*ALR-TW*(RBO(I)-RO)*UT/(1.-RO)-TW*(-2.*MU*RO*CP1
     1+MU*MU*SP2+4.*MU*RBO(I)*CP1)*CF4/(2.*AR*UT)-(1.-RO)*TW*
     2(2.*MU*RO*SP1+2.*MU*MU*CP2-4.*MU*RBO(I)*SP1+4.*MU*MU
     3*CP1*CP1)*CF5/(4.*AR*AR*UT*UT)
      L=L+1
  100 CONTINUE
C
C   PROGRAM STEP 9.
C   END OF COLLOCATION LOOP.
C   CALCULATE SPANWISE INTEGRALS NEEDED IN SUBSEQUENT STEPS.
C
      DO 300 I=1,NSP
      FI1(I)=0.
      FI2(I)=0.
  300 CONTINUE
      G1=.5*(1.+RO)
      G2=.5*(1.-RO)
      DO 310 I=1,10
      G=G1+G2*COS((2.*I-1.)*PI/20.)
      FACT=SQRT((G-RO)*(1.-G))
      DO 310 I1=1,NSP
      NL=I1-1
      IF(I1 .GT. 1)GO TO 320
      FI1(I1)=FI1(I1)+FACT*FUN3(RO,AR,G,1)*PI/10.
      FI2(I1)=FI2(I1)+FACT*FUN3(RO,AR,G,2)*PI/10.
      GO TO 310
  320 FI1(I1)=FI1(I1)+FACT*FUN3(RO,AR,G,3)*PI/10.
      FI2(I1)=FI2(I1)+FACT*FUN3(RO,AR,G,4)*PI/10.
  310 CONTINUE
C
C   PROGRAM STEP 10.
C   SET UP THE EXTRA 4 EQUATIONS NEEDED TO CLOSE THE SYSTEM.
C
      DO 330 I=1,4
      DO 340 M=1,NCOF
      A(L,M)=0.
  340 CONTINUE
      B(L,1)=0.
      IF(I .EQ. 1 .AND. N1 .EQ. 1)GO TO 350
      IF(I .EQ. 2 .AND. N2 .EQ. 1)GO TO 360
      IF(I .EQ. 3 .AND. N3 .EQ. 1)GO TO 370
      IF(I .EQ. 4 .AND. N4 .EQ. 1)GO TO 380
      IF(I .LE. 2)I1=1
      IF(I .GT. 2)I1=I-1
      IF(I .GT. 1)GO TO 390
C
C   THE FOLLOWING EQUATION SETS THE TOTAL BLADE LIFT,AVERAGED OVER
C   THE AZIMUTH, EQUAL TO THE THRUST COEFFICIENT.
C
      M=1
      A(L,M)=A(L,M)+(1.-RO)*(1.-RO)-(1.-RO)*FI1(1)/AR
      M=M+NAZ
```

```
      A(L,M)=A(L,M)+(1.-RO)*(1.-RO)/(3.*PI)
      DO 400 I2=2,NSP
      M=(I2-1)*NAZ+I1
      A(L,M)=A(L,M)+(1.-RO)*FI1(I2)/(2.*PI*AR)
 400  CONTINUE
      M=NSP*NAZ+1
      A(L,M)=A(L,M)-(1.-RO)*(1.-RO)*(1.-RO)*(1.-RO)/(16.*AR*AR*AR)
      M=M+1
      A(L,M)=A(L,M)+(1.-RO)*(1.-RO)*(1.-RO)*(1.+RO)/(8.*AR*AR)
      B(L,1)=B(L,1)+CT/NB-(1.-RO)*(1.-RO)*(1.-RO)*(2.+RO)*TW/(16.*AR*AR*
     1AR)
      L=L+1
      GO TO 330
C
C  THE NEXT THREE EQUATIONS (I=2,3,4) REPRESENT MOMENT EQUILIBRIUM
C  ABOUT THE HUB (ZEROTH HARMONIC, FIRST HARMONIC COSINE AND FIRST
C  HARMONIC SINE COMPONENTS).
 390  M=I1
      A(L,M)=A(L,M)-FI2(I)+AR*(.5*(1.-RO*RO)+(1.-RO)*(1.-RO)/6.)
      M=M+NAZ
      A(L,M)=A(L,M)+AR*(1.-RO*RO)/(6.*PI)
      M=M+NAZ
      A(L,M)=A(L,M)+AR*(1.-RO)*(1.-RO)/(10.*PI)
      DO 410 I2=2,NSP
      M=(I2-1)*NAZ+I1
      A(L,M)=A(L,M)+FI2(I2)/(2.*PI)
 410  CONTINUE
      M=NSP*NAZ+1
      IF(I .EQ. 2)A(L,M)=A(L,M)-(1.-RO)*(1.-RO)*(1.-RO)*(1.+RO)/(32.*
     1AR*AR)
      IF(I .EQ. 3)A(L,M)=A(L,M)+MU*(1.-RO)*(1.-RO*RO)/(4.*AR)
      M=M+1
      IF(I .EQ. 2)A(L,M)=A(L,M)+(1.-RO)*(1.-RO*RO*RO)/(12.*AR)
     1-2./GAMA
      IF(I .EQ. 4)A(L,M)=A(L,M)+(1.-RO)*(1.-RO*RO)*MU/(4.*AR)
      M=M+1
      IF(I .EQ. 3)A(L,M)=A(L,M)-(1.-RO)*(1.-RO*RO*RO)/(6.*AR)
      IF(I .EQ. 4)A(L,M)=A(L,M)+(1.-RO)*(1.-RO)*(1.-RO*RO)/(16.*AR*AR)
      M=M+1
      IF(I .EQ. 3)A(L,M)=A(L,M)-(1.-RO)*(1.-RO)*(1.-RO*RO)/(16.*AR*AR)
      IF(I .EQ. 4)A(L,M)=A(L,M)-(1.-RO)*(1.-RO*RO*RO)/(6.*AR)
      IF(I .EQ. 2)B(L,1)=B(L,1)-(1.-RO)*(1.-RO)*(1.-RO)*(1.-RO)*TW/(12.
     1*AR*AR)+RO*(1.-RO)*(1.-RO)*(1.+RO)*TW/(32.*AR*AR)
      IF(I .EQ. 3)B(L,1)=B(L,1)+MU*TW*(-RO*(1.-RO*RO)/4.+(1.-RO*RO*RO)/
     13.)/AR
      IF(I .EQ. 4)B(L,1)=B(L,1)-MU*TW*(1.-RO)*(1.-RO*RO)/(8.*AR*AR)
      L=L+1
      GO TO 330
C
C  THE FOLLOWING EQUATION SETS THE COLLECTIVE PITCH EQUAL TO THE
C  GIVEN VALUE.
C
 350  M=NSP*NAZ+1
      A(L,M)=1.
      B(L,1)=THC
      L=L+1
      GO TO 330
C
C  THE FOLLOWING EQUATION SETS THE CONING ANGLE EQUAL TO THE GIVEN
C  VALUE.
```

```
C
 360  M=NSP*NAZ+2
      A(L,M)=1.
      B(L,1)=A0
      L=L+1
      GO TO 330
C
C   THE FOLLOWING EQUATION SETS THE CYCLIC PITCH COEFFICIENT, A1,EQUAL
C   TO THE GIVEN VALUE.
C
 370  M=NSP*NAZ+3
      A(L,M)=1.
      B(L,1)=A1
      L=L+1
      GO TO 330
C
C   THE FOLLOWING EQUATION SETS THE CYCLIC PITCH COEFFICIENT, B1, EQUAL
C   TO THE GIVEN VALUE.
C
 380  M=NSP*NAZ+4
      A(L,M)=1.
      B(L,1)=B1
      L=L+1
 330  CONTINUE
C
C   PROGRAM STEP 11.
C   SOLVE THE SYSTEM OF SIMULTANEOUS EQUATIONS AND PRINT THE SOLUTION.
C
      CALL GELIM(NCOF,NCOF,A,1,B,IPIVOT,D,WK,IERR)
      IF(IERR .EQ. 1)GO TO 420
      L=1
      DO 430 I1=1,NSP
      GO(I1)=B(L,1)
      L=L+1
      DO 430 I2=1,NHM
      GC(I1,I2)=B(L,1)
      L=L+1
      GS(I1,I2)=B(L,1)
      L=L+1
 430  CONTINUE
      THC=B(NSP*NAZ+1,1)
      THCD=THC*180./PI
      A0=B(NSP*NAZ+2,1)
      A0D=A0*180./PI
      A1=B(NSP*NAZ+3,1)
      A1D=A1*180./PI
      B1=B(NSP*NAZ+4,1)
      B1D=B1*180./PI
      WRITE(6,10)
      WRITE(6,440)
 440  FORMAT(//6X,"SOLUTION FOR COEFFICIENTS"/6X,25(1H-)//6X,
     1"(GO(I),I=1,NSP)")
      WRITE(6,450)(GO(I),I=1,NSP)
 450  FORMAT(/6X,5(E10.4,1X))
      WRITE(6,460)
 460  FORMAT(//5X,"(GC(I,J),J=1,NHM),I=1,NSP)"//)
      DO 470 I=1,NSP
      WRITE(6,450)(GC(I,J),J=1,NHM)
 470  CONTINUE
      WRITE(6,480)
```

```
 480  FORMAT(//6X,"(GS(I,J),J=1,NHM),I=1,NSP)"//)
      DO 490 I=1,NSP
      WRITE(6,450)(GS(I,J),J=1,NHM)
 490  CONTINUE
      WRITE(6,500)THCD,A0D,A1D,B1D
 500  FORMAT(//6X,"PITCH ANGLE AT BLADE ROOT=",F10.5,"DEGREES"//6X,
     1"CONING ANGLE=",F10.5,1X,"DEGREES"//6X,
     2"FLAPPING COEFFICIENT, A1=",F10.5,1X,"DEGREES"//6X,
     3"FLAPPING COEFFICIENT, B1=",F10.5,1X,"DEGREES")
C
C  PROGRAM STEP 12.
C  START LOOP FOR AZIMUTH STATIONS AT WHICH OUTPUT QUANTITIES ARE
C  CALCULATED.
C
      CTCAL=0.
      CMXCAL=0.
      CMYCAL=0.
      DO 510 I=1,24
      PSID(I)=15.*(I-1.)
      PSI=(I-1.)*PI/12.
      CP1=COS(PSI)
      SP1=SIN(PSI)
      CP2=COS(2.*PSI)
      SP2=SIN(2.*PSI)
      F1(I)=-THC-TW*RO/(1.-RO)-2.*B1*CP1+(2.*A1+4.*MU*TW/(1.-RO))*SP1
      F2(I)=CP1*(2.*MU*TW*RO/(1.-RO)+2.*MU*THC)+2.*MU*A0*SP1
     1+2.*MU*B1*CP2-(2.*MU*A1+MU*MU*TW/(1.-RO))*SP2
      F3(I)=A0-CP1*(4.*MU*TW/(1.-RO)+2.*A1)-2.*B1*SP1
      FG1=G0(1)
      FG2=G0(2)
      FG3=G0(3)
      FN1=0.
      FN2=0.
      DO 520 I1=2,5
      FN1=FN1+FI1(I1)*G0(I1)
      FN2=FN2+FI2(I1)*G0(I1)
      DO 520 I2=1,NHM
      CI2=COS(I2*PSI)
      SI2=SIN(I2*PSI)
      IF(I1 .GT. 2)GO TO 530
      FG1=FG1+GC(1,I2)*CI2+GS(1,I2)*SI2
      FG2=FG2+GC(2,I2)*CI2+GS(2,I2)*SI2
      FG3=FG3+GC(3,I2)*CI2+GS(3,I2)*SI2
 530  FN1=FN1+FI1(I1)*(GC(I1,I2)*CI2+GS(I1,I2)*SI2)
      FN2=FN2+FI2(I1)*(GC(I1,I2)*CI2+GS(I1,I2)*SI2)
 520  CONTINUE
      FLT1(I)=-PI*(1.-RO)*FI1(1)*FG1/AR+PI*(1.-RO)*(1.-RO)*FG1+(1.-RO)*
     1(1.-RO)*FG2/3.+(1.-RO)*FN1/(2.*AR)+PI*(1.-RO)*(1.-RO)*(1.-RO)
     2*F2(I)/(4.*AR*AR)+PI*(1.-RO)*(1.-RO)*(1.-RO*RO)*F3(I)/(8.*
     3AR*AR)+PI*(1.-RO)*(1.-RO)*(1.-RO)*(1.-RO)*(F1(I)+2.*TW*(1.+RO)
     4/(1.-RO))/(16.*AR*AR*AR)
      FLT2(I)=FLT1(I)/(CT*PI/NB)
      FMT(I)=-PI*(1.-RO)*FI2(1)*FG1/AR+PI*(1.-RO)*(.5*(1.-RO*RO)+(1.-RO)
     1*(1.-RO)/6.)*FG1+(1.-RO)*(1.-RO*RO)*FG2/6.+(1.-RO)*(1.-RO)
     2*(1.-RO)*FG3/10.+(1.-RO)*FN2/(2.*AR)+PI*(1.-RO)*(1.-RO)*
     3(1.-RO*RO)*F2(I)/(8.*AR*AR)+PI*(1.-RO)*(1.-RO)*(1.-RO)*(1.-RO*RO*RO)
     4*F3(I)/(12.*AR*AR)+PI*(1.-RO)*(1.-RO)*(1.-RO)*(1.-RO*RO)*F1(I)
     5/(32.*AR*AR*AR)+PI*TW*(1.-RO)*(1.-RO)*(1.-RO*RO*RO)/(12.*AR
     6*AR*AR)
      COL(I)=FMT(I)/FLT1(I)
```

```
      CTCAL=CTCAL+FLT1(I)/24.
      CMXCAL=CMXCAL+FMT(I)*SP1/24.
      CMYCAL=CMYCAL-FMT(I)*CP1/24.
C
C  START LOOP FOR RADIAL STATIONS AT WHICH OUTPUT QUANTITIES ARE
C  CALCULATED.
C
      DO 510 I1=1,NSP
      F23=F2(I)+RBO(I1)*F3(I)
      Z8=2.*(RBO(I1)-.5*(1.+RO))/(1.-RO)
      UT=RBO(I1)+MU*SP1
      SQZ=SQRT(1.-Z8*Z8)
      FN0=FUN3(RO,AR,RBO(I1),1)
      FN1=0.
      FN2=0.
      FN3=0.
      DO 540 I2=2,5
      NL=I2-1
      PN1=PNM(I2-1,1,Z8)
      PN2=FUN3(RO,AR,RBO(I1),3)
      FN1=FN1+GC(I2)*PN1
      FN2=FN2+GO(I2)*PN2
      FN3=FN3+GC(I2)*NL*(NL+1.)*PN1
      DO 540 I3=1,NHM
      CI3=COS(I3*PBO)
      SI3=SIN(I3*PBO)
      FN1=FN1+PN1*(GC(I2,I3)*CI3+GS(I2,I3)*SI3)
      FN2=FN2+PN2*(GC(I2,I3)*CI3+GS(I2,I3)*SI3)
      FN3=FN3+NL*(NL+1.)*PN1*(GC(I2,I3)*CI3+GS(I2,I3)*SI3)
 540  CONTINUE
      GST(I,I1)=AR*((1.+Z8)*FG1+SQZ*FN1/(2.*PI))
      PDIP(I,I1)=-FNC*FG1+FN2/(2.*PI)
      DGS2(I,I1)=-AR*FN3/(2.*PI*SQZ)
      FL1(I,I1)=(1.-RO)*PI*(PDIP(I,I1)+GST(I,I1)+(1.-RO)*F23/
     1(4.*AR)+(1.-RO)*(1.-RO)*(F1(I)+4.*TW*RBO(I1)/(1.-RO)))/
     2(16.*AR*AR))/AR
      FL2(I,I1)=FL1(I,I1)/(CT*PI/NB)
      FM(I,I1)=GST(I,I1)+(2.*DGS2(I,I1)+(1.-RO)*(1.-RO)*(F1(I)+4.*TW
     1*RBO(I1)/(1.-RO)))/(32.*AR*AR)
      FM(I,I1)=FM(I,I1)*PI*(1.-RO)*(1.-RO)/(4.*AR*AR)
      FM(I,I1)=FM(I,I1)+(1.-RO)*FL1(I,I1)/(4.*AR)
      XCP(I,I1)=.25+FM(I,I1)*AR/(FL1(I,I1)*(1.-RO))
 510  CONTINUE
      CTCAL=CTCAL*NB/PI
      CMXCAL=CMXCAL*NB/PI
      CMYCAL=CMYCAL*NB/PI
      WRITE(6,541)CTCAL,CMXCAL,CMYCAL
 541  FORMAT(//6X,"COMPUTED THRUST COEFFICIENT=",E10.4//6X,
     1"COMPUTED MOMENT COEFFICIENT ABOUT ROTOR X-AXIS=",E10.4//6X,
     2"COMPUTED MOMENT COEFFICIENT ABOUT ROTOR Y-AXIS=",E10.4)
C
C  PRINT OUTPUT IN TABULAR FORM.
C
      WRITE(6,10)
      WRITE(6,550)
 550  FORMAT(//6X,"TABLE 1 - SECTIONAL LIFT/(RHO*(OMEGA**2)*(R1**3))"/6X
     1,49(1H-)//)
      WRITE(6,560)(RBO(I),I=1,NSP)
 560  FORMAT(/12X,"R/R1=  ",5(E10.4,1X))
      WRITE(6,570)
```

```
570   FORMAT(/7X,"PSI")
      DO 580 I=1,24
      WRITE(6,590)PSOD(I),(FL1(I,I1),I1=1,NSP)
590   FORMAT(/6X,F5.1,8X,5(E10.4,1X))
580   CONTINUE
      WRITE(6,10)
      WRITE(6,600)
600   FORMAT(//6X,"TABLE 2 - SECTIONAL LIFT*R1/THRUST PER BLADE"/6X,
     144(1H-)//)
      WRITE(6,560)(RSO(I),I=1,NSP)
      WRITE(6,570)
      DO 610 I=1,24
      WRITE(6,590)PSOD(I),(FL2(I,I1),I1=1,NSP)
610   CONTINUE
      WRITE(6,10)
      WRITE(6,620)
620   FORMAT(//6X,"TABLE 3 - SECTIONAL PITCHING MOMENT/(RHO*(OMEGA**2)*(
     1R1**4))"/6X,60(1H-)/16X,"(ABOUT QUARTER-CHORD)"//)
      WRITE(6,560)(RSO(I),I=1,NSP)
      WRITE(6,570)
      DO 630 I=1,24
      WRITE(6,590)PSOD(I),(FM(I,I1),I1=1,NSP)
630   CONTINUE
      WRITE(6,10)
      WRITE(6,640)
640   FORMAT(//6X,"TABLE 4 - CENTER OF PRESSURE LOCATION FROM LEADING ED
     1GE(FRACTION OF CHORD)"/6X,74(1H-)//)
      WRITE(6,560)(RSO(I),I=1,NSP)
      WRITE(6,570)
      DO 650 I=1,24
      WRITE(6,590)PSOD(I),(XCP(I,I1),I1=1,NSP)
650   CONTINUE
      WRITE(6,10)
      WRITE(6,660)
660   FORMAT(//6X,"TABLE 5 - TOTAL BLADE LIFT, MOMENT ABOUT HUB AND RADI
     1AL CENTER OF LIFT"/6X,70(1H-)//6X,
     2"TOTAL BLADE LIFT/(RHO*(OMEGA**2)*(R1**4))"/6X,
     3"TOTAL BLADE LIFT/THRUST PER BLADE"/6X,
     4"MOMENT ABOUT HUB/(RHO*(OMEGA**2)*(R1**5))"/6X,
     5"RADIAL CENTER OF LIFT/R1"//7X,"PSI",8X,"TOTAL BLADE LIFT",
     65X,"MOMENT",5X,"CENTER"/38X,"ABOUT HUB",4X,"OF LIFT")
      DO 670 I=1,24
      WRITE(6,680)PSOD(I),FLT1(I),FLT2(I),FMT(I),COL(I)
680   FORMAT(/6X,F5.1,5X,4(E10.4,1X))
670   CONTINUE
      WRITE(6,10)
      WRITE(6,690)
690   FORMAT(//6X,"TABLE 6 -SURFACE PRESSURE DIFFERENTIAL/(RHO*(OMEGA**2
     1)*(R1**2))"/6X,64(1H-)//)
      DO 700 I=1,24
      WRITE(6,710)PSOD(I)
710   FORMAT(/6X,"AZIMUTH ANGLE=",F5.1,1X,"DEGREES"/6X,27(1H-))
      WRITE(6,560)(RSO(I1),I1=1,NSP)
      WRITE(6,720)
720   FORMAT(11X,"X/C")
      DO 730 I1=1,NSP
      F23=F2(I)+RSO(I1)*F3(I)
      DO 740 I2=1,10
      CCH=2.*XOUT(I2)-1.
      SCH=SQRT(1.-CCH*CCH)
```

```
      POUT(I1,I2)=-GST(I,I1)*SCH/(1.+CCH)+2.*SCH*(PDIP(I,I1)+2.*GST
     1(I,I1))+DGS2(I,I1)*SCH*SCH/(4.*AR*AR)+F23*(1.-RJ)*SCH/(2.*AR)
     2+(F1(I)+4.*TW*R30(I1)/(1.-RJ))*(1.-RO)*(1.-RO)*(1.-RO)*
     3SCH*(1.+CCH)/(8.*AR*AR)
      POUT(I1,I2)=2.*POUT(I1,I2)
  740 CONTINUE
  730 CONTINUE
      DO 750 I2=1,10
      WRITE(6,755)XOUT(I2),(POUT(I1,I2),I1=1,NSP)
  755 FORMAT(6X,F8.5,5X,5(E10.4,1X))
  750 CONTINUE
      IPG=3
      IREM=I-(I/IPG)*IPG
      IF(IREM .EQ. 0)WRITE(6,10)
  700 CONTINUE
      STOP
C
C  PRINT ERROR MESSAGE IF COEFFICIENT MATRIX IS SINGULAR.
C
  420 WRITE(6,760)
  760 FORMAT(/6X,"COEFFICIENT MATRIX IS SINGULAR")
      STOP
      END
      SUBROUTINE DMIN(MU,LAM,DB,R30,P80,PLIM,DMAX,I,P)
C
C  CALCULATION OF AZIMUTH POSITIONS AT WHICH TRAJECTORY IS DIRECTLY
C  OVER A BLADE, WITHIN A DISTANCE DMAX.
C
      REAL MU,LAM
      DIMENSION P(20)
      Y(X,X1,X2,Y1,Y2)=Y1+(Y2-Y1)*(X-X1)/(X2-X1)
      I=0
      P1=0.
      X81=0.
      P2=-0.2
   10 X82=R30*SIN(P2+DB)+MU*SIN(P2+P80+DB)*P2
      IF(P1 .NE. 0.)GO TO 20
   30 P1=P2
      IF(P1 .LE. PLIM)RETURN
      P2=P2-0.2
      X81=X82
      GO TO 10
   20 TEST=X81*X82
      IF(TEST .GT. 0.)GO TO 30
      PC=Y(0.,X81,X82,P1,P2)
      XBC=R80*SIN(PC+DB)+MU*SIN(PC+P80+DB)*PC
      RBC=R80*COS(PC+DB)+MU*COS(PC+P80+DB)*PC
      D=SQRT(XBC*XBC+LAM*LAM*PC*PC+(RBC-R80)*(RBC-R80))
      IF(D .GT. DMAX)GO TO 30
      I=I+1
      P(I)=PC
      GO TO 30
      END
      SUBROUTINE TRAJ(RO,AR,MU,LAM,R30,P80,DB,PB,ZS)
C  THIS SUBROUTINE CALCULATES THE PARAMETERS FOR THE LINEARISED
C  TRAJECTORY CORRESPONDING TO A GIVEN COLLOCATION POINT.
      REAL MU,LAM
      COMMON/TRAJ1/R,SX,CX,SHP,CHP,ST,CT,SHE,CHE,SP,CP
      XB=R30*SIN(PB+DB-P80)+MU*(PB-P30)*SIN(PB+DB)
      YB=LAM*(PB-P80)
```

```
      ZB=-.5*(1.+R0)+RB0*COS(P8+D8-P30)+MU*(P8-P80)*COS(P8+D8)
      R=SQRT(XB*XB+YB*YB)
      SX=YB/R
      CX=XB/R
      XS=2.*XB/(1.-R0)
      YS=2.*YB/(1.-R0)
      ZS=2.*ZB/(1.-R0)
      RS=2.*R/(1.-R0)
      R1=SQRT(RS*RS+(1.+ZS)*(1.+ZS))
      R2=SQRT(RS*RS+(1.-ZS)*(1.-ZS))
      CHP=(R1+R2)/2.
      SHP=SQRT(CHP*CHP-1.)
      CT=ZS/CHP
      ST=RS/SHP
      R3=SQRT((XS*AR-1.5)*(XS*AR-1.5)+YS*YS*AR*AR)
      R4=SQRT((XS*AR+.5)*(XS*AR+.5)+YS*YS*AR*AR)
      CHE=(R3+R4)/2.
      IF(CHE .LE. 1.)CHE=ABS((R4-R3)/2.)
      SHE=SQRT(CHE*CHE-1.)
      CP=(XS*AR-.5)/CHE
      SP=AR*YS/SHE
      RETURN
      END
      FUNCTION FUN1(R0,AR,I)
C  THIS SUBPROGRAM RETURNS THE VALUES OF VARIOUS FUNCTIONS REQUIRED
C  IN FUNCTION FUN2.
      COMMON/MAIN1/N,PI
      COMMON/TRAJ1/R,SX,CX,SHP,CHP,ST,CT,SHE,CHE,SP,CP
      GO TO (10,20,30,40,50,60),I
   10 F1=SHP*SHP*(CHP-CT)
      F2=(CHP-CT)*(CHP-CT)
      F3=(CHP-CT)*(CHP+CT)
      F4=(SHP*SHP*CT*CT-CHP*CHP*ST*ST)/F1-ST*ST*(CHP+CT)/F2
      FUN1=-2.*(SX*SX*F4/F3+CX*CX/F1)/(1.-R0)
      RETURN
   20 PN1=PNM(N,1,CT)
      PN2=PNM(N,2,CT)
      QN1=QNM(N,1,CHP)
      QN2=QNM(N,2,CHP)
      F1=1./(ST*SHP)
      F2=SX*SX/(SHP*SHP+ST*ST)
      FUN1=(F1*PN1*QN1+F2*(ST*CHP*PN1*QN2-CT*SHP*PN2*QN1))/(PI*(1.-R0))
      RETURN
   30 F1=SHP*SHP+ST*ST
      F2=F1*SHP*SHP
      F3=CHP/F1-CHP*CHP*CHP*ST*ST/F2
      F3=F3-2.*CHP*ST*ST*(CHP*CHP+CT*CT)/(F1*F1)
      F3=F3*SX*SX/F1
      FUN1=2.*(F3+CX*CX*CHP/F2)/(1.-R0)
      RETURN
   40 FUN1=(1.-R0)*(CX*CX-SX*SX)/(R*R)
      RETURN
   50 F1=SHE*SHE*CP*CP+CHE*CHE*SP*SP
      F2=(CHE+CP)*(CHE+CP)
      FUN1=2.*AR*(SHE*CP+SHE*CHE*(CP*CP-SP*SP))/((1.-R0)*F1*F2)
      RETURN
   60 F1=SHE*SHE*CP*CP+CHE*CHE*SP*SP
      F2=SHE*CP*CP-CHE*SP*SP
      FUN1=2.*AR*(CHE-SHE)*F2/((1.-R0)*F1)
      RETURN
```

```
      END
      FUNCTION FUN2(RO,AR,TW,MU,LAM,RBO,PBO,DP,DB,X,I)
C   THIS SUBPROGRAM SETS UP THE INTEGRAND FOR THE INTEGRATION REQUIRED
C   FOR THE INDUCED VELOCITY IN THE MAIN PROGRAM.
      REAL MU,LAM
      COMMON/MAIN1/N,PI
      COMMON/FUN21/F1,F2,F3,F4,F5,F6,ZBS
      P=X+DB
      IF(I .EQ. 2)GO TO 20
      IF(I .GT. 2)GO TO 40
      CALL TRAJ(RO,AR,MU,LAM,RBO,PBO,DB,X,ZS)
      ZBS=ZS
      F1=FUN1(RO,AR,1)
      F3=FUN1(RO,AR,3)
      F4=FUN1(RO,AR,4)
      F5=FUN1(RO,AR,5)
      F6=FUN1(RO,AR,6)
      FUN2=-F1
      IF(ABS(ZBS) .GT. 1.)GO TO 10
      FUN2=FUN2-(1.+ZBS)*F4/2.
   10 IF(DB .EQ. 0. .AND. X .GT. (PBO-DP))RETURN
      IF(ABS(ZBS) .GT. 1.)RETURN
      FUN2=FUN2+AR*(1.+ZBS)*F5
      RETURN
   20 F2=FUN1(RO,AR,2)
      FUN2=-F2
      IF(ABS(ZBS) .GT. 1.)GO TO 30
      PN1=PNM(N,1,ZBS)
      FUN2=FUN2-PN1*SQRT(1.-ZBS*ZBS)*F4/(4.*PI)
   30 IF(DB .EQ. 0. .AND. X .GT. (PBO-DP))RETURN
      IF(ABS(ZBS) .GT. 1.)RETURN
      FUN2=FUN2+AR*SQRT(1.-ZBS*ZBS)*PN1*F5/(2.*PI)
      RETURN
   40 ITEST=I-2
      ZB=(1.-RO)*ZBS/2.
      RB=ZB+.5*(1.+RO)
      GO TO (50,60,70,80,90),ITEST
   50 FN2=2.*MU*COS(P)
      FN3=0.
      GO TO 100
   60 FN2=2.*MU*SIN(P)
      FN3=1.
      GO TO 100
   70 FN2=-2.*MU*SIN(2.*P)
      FN3=-2.*COS(P)
      GO TO 100
   80 FN2=2.*MU*COS(2.*P)
      FN3=-2.*SIN(P)
      GO TO 100
   90 FN2=-TW*(2.*MU*COS(P)+MU*MU*SIN(2.*P))/(1.-RO)
      FN3=4.*MU*TW*COS(P)/(1.-RO)
  100 FUN2=-(1.-RO)*F3*(FN2+RO*FN3)/(4.*AR*AR)
      FUN2=FUN2+(1.-RO)*(1.-RO)*FN3*F1/(8.*AR*AR)
      IF(ABS(ZBS) .GT. 1.)GO TO 110
      FUN2=FUN2+(1.-RO)*(FN2+RB*FN3)*F4/(8.*AR*AR)
  110 IF(DB .EQ. 0. .AND. X .GT. (PBO-DP))RETURN
      IF(ABS(ZBS) .GT. 1.)RETURN
      FUN2=FUN2-(1.-RO)*(FN2+RB*FN3)*F6/(2.*AR)
      RETURN
      END
```

```
      FUNCTION FUN3(RO,AR,X,I)
C  THIS SUBPROGRAM SETS UP THE INTEGRAND FOR SOME SPANWISE INTEGRALS
C  REQUIRED IN THE MAIN PROGRAM.
      COMMON/MAIN1/N,PI
      ZBS=2.*(X-.5*(1.+RO))/(1.-RO)
      R1=SQRT(1./(16.*AR*AR)+.25*(1.+ZBS)*(1.+ZBS))
      R2=SQRT(1./(16.*AR*AR)+.25*(1.-ZBS)*(1.-ZBS))
      CHP1=R1+R2
      SHP1=SQRT(CHP1*CHP1-1.)
      CT1=ZBS/CHP1
      ST1=1./(2.*AR*SHP1)
      IF(I .LE. 2)GO TO 10
      PN1=PNM(N,1,CT1)
      QN1=QNM(N,1,CHP1)
      GO TO 20
   10 F1=ST1/(SHP1*(CHP1-CT1))
      IF(I .EQ. 1)FUN3=F1
      IF(I .EQ. 2)FUN3=X*F1
      RETURN
   20 F2=PN1*QN1
      IF(I .EQ. 3)FUN3=F2
      IF(I .EQ. 4)FUN3=X*F2
      RETURN
      END
      FUNCTION PNM(N,M,X)
C  CALCULATION OF ASSOCIATED LEGENDRE FUNCTIONS PNM.
C  RANGE: 0 .LE. N .LE. 4, 0 .LE. M .LE. 3, ABS(X) .LT. 1.
      IF(N .LT. 1 .OR. N .GT. 4)GO TO 10
      IF(M .LT. 0 .OR. M .GT. 3)GO TO 20
      IF(ABS(X) .GE. 1.)GO TO 30
      SX=SQRT(1.-X*X)
      IF(M .EQ. 1)GO TO 40
      IF(M .EQ. 2)GO TO 50
      IF(M .EQ. 3)GO TO 190
      GO TO (60,70,80,90),N
   60 PNM=X
      RETURN
   70 PNM=.5*(3.*X*X-1.)
      RETURN
   80 PNM=.5*(5.*X*X*X-3.*X)
      RETURN
   90 PNM=(35.*X*X*X*X-30.*X*X+3.)/8.
      RETURN
   40 GO TO (100,110,120,130),N
  100 PNM=SX
      RETURN
  110 PNM=3.*X*SX
      RETURN
  120 PNM=.5*SX*(15.*X*X-3.)
      RETURN
  130 PNM=.5*SX*(35.*X*X*X-15.*X)
      RETURN
   50 GO TO (140,150,160,170),N
  140 PNM=0.
      RETURN
  150 PNM=3.*SX*SX
      RETURN
  160 PNM=15.*X*SX*SX
      RETURN
  170 PNM=.5*SX*SX*(105.*X*X-15.)
```

```
      RETURN
  160 GO TO (190,200,210,220),N
  190 PNM=0.
      RETURN
  200 PNM=0.
      RETURN
  210 PNM=15.*SX*SX*SX
      RETURN
  220 PNM=105.*X*SX*SX*SX
      RETURN
   10 WRITE(6,11)N
   11 FORMAT(6X,*N=*,I5,1X,*INVALID N IN PNM*)
      STOP
   20 WRITE(6,21)M
   21 FORMAT(6X,*M=*,I5,1X,*INVALID M IN PNM*)
      STOP
   30 WRITE(6,31)X
   31 FORMAT(6X,*X=*,E10.4,1X,*INVALID X IN PNM*)
      STOP
      END
      FUNCTION QNM(N,M,X)
C  CALCULATION OF ASSOCIATED LEGENDRE FUNCTIONS QNM.
C  RANGE: 1 .LE. N .LE. 4, 1 .LE. M .LE. 2, ABS(X) .GT. 1.
C  ASYMPTOTIC EXPANSIONS USED FOR X .GT. 3.
      IF(N .LT. 1 .OR. N .GT. 4)GO TO 10
      IF(M .LT. 1 .OR. M .GT. 2)GO TO 20
      IF(ABS(X) .LE. 1.)GO TO 30
      SX=SQRT(X*X-1.)
      ALX=ALOG((X+1.)/(X-1.))
      X2=X*X
      X3=X2*X
      X4=X3*X
      X5=X4*X
      X6=X5*X
      X7=X6*X
      X8=X7*X
      X9=X8*X
      X10=X9*X
      X11=X10*X
      X12=X11*X
      IF(M .EQ. 2)GO TO 40
      GO TO (50,60,70,80),N
   50 IF(X .GT. 3.)GO TO 51
      QNM=SX*(.5*ALX-X/(SX*SX))
      RETURN
   51 QNM=-SX*(2./(3.*X3)+4./(5.*X5)+6./(7.*X7)+8./(9.*X9))
      RETURN
   60 IF(X .GT. 3.)GO TO 61
      QNM=SX*(1.5*X*ALX-(3.*X2-1.)/(2.*SX*SX)-1.5)
      RETURN
   61 QNM=-SX*(2./(5.*X4)+4./(7.*X6)+2./(3.*X8)+8./(11.*X10))
      RETURN
   70 IF(X .GT. 3.)GO TO 71
      QNM=SX*((15.*X2-3.)*ALX/4.-(5.*X3-3.*X)/(2.*SX*SX)-5.*X)
      RETURN
   71 QNM=-SX*(8./(35.*X5)+8./(21.*X7)+16./(33.*X9)+10./(13.*X11))
      RETURN
   80 IF(X .GT. 3.)GO TO 81
      QNM=SX*((35.*X3-15.*X)*ALX/4.-(35.*X4-30.*X2+3.)/(8.*SX*SX)
     1-105.*X2/8.+55./24.)
```

```
      RETURN
   81 QNM=-SX*(8./(63.*X6)+8./(33.*X8)+48./(143.*X10))
      RETURN
   40 GO TO (90,100,110,120),N
   90 IF(X .GT. 3.)GO TO 91
      QNM=2./(SX*SX)
      RETURN
   91 QNM=SX*SX*(2./X4+4./X6+6./X8+8./X10)
      RETURN
  100 IF(X .GT. 3.)GO TO 101
      QNM=SX*SX*(1.5*ALX-6.*X/(SX*SX)+X*(3.*X2-1.)/(SX*SX*SX*SX))
      RETURN
  101 QNM=SX*SX*(8./(5.*X5)+24./(7.*X7)+16./(3.*X9)+80./(11.*X11))
      RETURN
  110 IF(X .GT. 3.)GO TO 111
      QNM=SX*SX*(15.*X*ALX/2.-(15.*X2-3.)/(SX*SX)+X*(5.*X3-3.*X)
     1/(SX*SX*SX*SX)-5.)
      RETURN
  111 QNM=SX*SX*(8./(7.*X6)+8./(3.*X8)+48./(11.*X10)+110./(13.*X12))
      RETURN
  120 IF(X .GT. 3.)GO TO 121
      QNM=SX*SX*((105.*X2-15.)*ALX/4.-(35.*X3-15.*X)/(SX*SX)
     1+X*(35.*X4-30.*X2+3.)/(4.*SX*SX*SX*SX)-105.*X/4.)
      RETURN
  121 QNM=SX*SX*(16./(21.*X7)+64./(33.*X9)+480./(143.*X11))
      RETURN
   10 WRITE(6,11)N
   11 FORMAT(6X,*N=*,I5,1X,*INVALID N IN QNM*)
      STOP
   20 WRITE(6,21)M
   21 FORMAT(6X,*M=*,I5,1X,*INVALID M IN QNM*)
      STOP
   30 WRITE(6,31)X
   31 FORMAT(6X,*X=*,E10.4,1X,*INVALID X IN QNM*)
      STOP
      END
      SUBROUTINE TABSCH(X,N,XT,I1,I2,INT)
C
C  GIVEN AN ARRAY X, TO LOCATE THE POSITION OF A VALUE XT.
C  IF INT=0, XT LIES BETWEEN X(I1) AND X(I2).
C  IF INT=1, XT IS GREATER THAN X(N).
C  IF INT=-1, XT IS LESS THAN X(1).
C
      DIMENSION X(N)
      I1=0
      I2=0
      NM=N-1
      DO 10 I=1,NM
      IF(XT .GE. X(I) .AND. XT .LE. X(I+1))GO TO 20
   10 CONTINUE
      IF(XT .LT. X(1))GO TO 30
      IF(XT .GT. X(N))GO TO 40
   20 INT=0
      IF(XT .EQ. X(I))GO TO 21
      IF(XT .EQ. X(I+1))GO TO 22
      I1=I
      I2=I+1
      RETURN
   21 I1=I2=I
      RETURN
```

```
22   I1=I2=I+1
     RETURN
30   INT=-1
     RETURN
40   INT=1
     RETURN
     END
```

APPENDIX B

LISTING OF PROGRAM ASYMP2

```
      PROGRAM MAIN(INPUT,OUTPUT,TAPE5=INPUT,TAPE6=OUTPUT,
     1AFDATA,TAPE1=AFDATA)
C
C   COMPUTATION OF THE UNSTEADY AIRLOADS ON A HELICOPTER ROTOR BLADE IN
C   FORWARD FLIGHT, USING A SIMPLIFIED VERSION OF THE ASYMPTOTIC APPROACH
C   PROPOSED BY VAN HOLTEN. THE DIPOLE STRENGTH DISTRIBUTION ALONG THE
C   BLADE IS APPROXIMATED BY A PIECEWISE CONSTANT OR PIECEWISE QUADRATIC
C   REPRESENTATION. THE HELICAL TRAJECTORY OF THE FREESTREAM FLUID
C   PARTICLE RELATIVE TO THE BLADE IS APPROXIMATED BY SUCCESSIVE STRAIGHT
C   LINE SEGMENTS.
C   FOR IDENTIFICATION OF PROGRAM STEPS, REFER USER'S MANUAL.
C
      REAL MU,LAM,MCL,MINF,MLOC
      DIMENSION R(6),RBO(5),DR(5),X(6),FX1(5),FX2(5),P1(5),P2(5),IP(5),
     1FG(5),WK(59),BT(4),GF(4,5),PMIN(20),GO(5),GC(5,5),GS(5,5),G(24,5),
     2A(59,59),B(59,1),IPIVOT(59),PSOO(24),FLT1(24),FLT2(24),
     3FMT(24),COL(24),GL(5),GR(5),FL1(24,5),FL2(24,5),FM(24,5),
     4XCP(24,5),XOUT(10),F23(24,5),POUT(5,10)
      DIMENSION CL(50,20),MCL(20),ACL(50)
      COMMON/MAIN1/XBI,XBS,YBS,RBI,RBS
      YL(XL,XL1,XL2,YL1,YL2)=YL1+(XL-XL1)*(YL2-YL1)/(XL2-XL1)
      DATA X/-1.,-.9,-.6,0.,.5,1./
      DATA NSP,NHM,NAZ,NCOF,DMAX/5,5,11,59,0.5/
      DATA XOUT/.05,.1,.2,.3,.4,.5,.7,.9,.95,.99/
      PI=4.*ATAN(1.)
C
C   PROGRAM STEP 1.
C   READ AND WRITE INPUT DATA AND ASSOCIATED QUANTITIES.
C
      READ(5,*)RO,AR,NB,TW,MU,ALR,CT,MINF
      READ(5,*)N1,N2,N3,N4
      IF(N1 .EQ. 1)READ(5,*)THC
      IF(N2 .EQ. 0)READ(5,*)GAMA
      IF(N2 .EQ. 1)READ(5,*)A0
      IF(N3 .EQ. 1)READ(5,*)A1
      IF(N4 .EQ. 1)B1
      READ(5,*)(R(I),I=2,6)
C
C   ISEL .EQ. 0 -- PIECEWISE CONSTANT REPRESENTATION.
C   ISEL .EQ. 1 -- PIECEWISE QUADRATIC REPRESENTATION.
C
      READ(5,*)DP10,DP20,UTMIN,ISEL,NAFD
C
C   NAFD=0 -- AIRFOIL TABLES NOT USED.
C   NAFD=1 -- AIRFOIL TABLES USED.
C
      IF(NAFD .EQ. 0)GO TO 8
      READ(1,1)NXL,NZL
    1 FORMAT(30X,2I2)
      READ(1,2)(MCL(I),I=1,NXL)
    2 FORMAT(7X,9F7.0)
      NL1=NXL/9
      NL2=NL1+1
      DO 3 I=1,NZL
      DO 3 J=1,NL2
      J1=(J-1)*9+1
      J2=J*9
      IF(J1 .GT. NXL)GO TO 3
      IF(J2 .GT. NXL)J2=NXL
```

```
      IF(J .EQ. 1)READ(1,4)ACL(I),(CL(I,J3),J3=J1,J2)
    4 FORMAT(F7.3,9F7.0)
      IF(J .GT. 1)READ(1,5)(CL(I,J3),J3=J1,J2)
    5 FORMAT(7X,9F7.0)
    3 CONTINUE
    8 CONTINUE
      DP1=DP1D*PI/180.
      DP2=DP2D*PI/180.
      WRITE(6,9)
    9 FORMAT(1H1)
      WRITE(6,10)RO,AR,NB,TW,MU,ALR,MINF
   10 FORMAT(//6X,"ROOT RADIUS/TIP RADIUS= RO/R1 =",F10.5//6X,
     1"ASPECT RATIO=",F10.5//6X,"NUMBER OF BLADES=",I2//6X,
     2"LINEAR TWIST (ROOT TO TIP) =",F10.5,1X,"DEGREES"//6X,
     3"FORWARD SPEED/TIP SPEED=",F10.5//6X,
     4"ROTOR INCIDENCE (FORWARD TILT POSITIVE) =",F10.5,1X,
     5"DEGREES"//6X,"FREESTREAM MACH NUMBER=",F10.5)
      R(1)=RO
      TW=TW*PI/180.
      ALR=ALR*PI/180.
      IF(N1 .EQ. 0)THC=0.
      IF(N2 .EQ. 0)A0=0.
      IF(N3 .EQ. 0)A1=0.
      IF(N4 .EQ. 0)B1=0.
      WRITE(6,11)CT
   11 FORMAT(//6X,"THRUST COEFFICIENT=",F10.5)
      IF(N1 .EQ. 1)WRITE(6,12)THC
   12 FORMAT(//6X,"PITCH ANGLE AT BLADE ROOT=",F10.5,1X,"DEGREES")
      IF(N2 .EQ. 0)WRITE(6,13)GAMA
   13 FORMAT(//6X,"FLAPPING INERTIA COEFFICIENT=",F10.5)
      IF(N2 .EQ. 1)WRITE(6,14)A0
   14 FORMAT(//6X,"CONING ANGLE=",F10.5,1X,"DEGREES")
      IF(N3 .EQ. 1)WRITE(6,15)A1
   15 FORMAT(//6X,"FLAPPING COEFFICIENT, A1=",F10.5,1X,"DEGREES")
      IF(N4 .EQ. 1)WRITE(6,16)B1
   16 FORMAT(//6X,"FLAPPING COEFFICIENT, B1=",F10.5,1X,"DEGREES")
      THC=THC*PI/180.
      A0=A0*PI/180.
      A1=A1*PI/180.
      B1=B1*PI/180.
      LAM=MU*ALR+SQRT(.5*(-MU*MU+SQRT(MU*MU*MU*MU+CT*CT)))
      WRITE(6,20)LAM,UTMIN,DP1D,DP2D
   20 FORMAT(//6X,"TOTAL INFLOW RATIO=",F10.5//6X,
     1"MINIMUM UT=",F10.5,"(ZERO LIFT CONDITION APPLIED BELOW THIS VALUE
     2)"//6X,"NORMAL AZIMUTH SPACING=",F10.5,1X,"DEGREES"//6X,
     3"REDUCED AZIMUTH SPACING=",F10.5,1X,"DEGREES")
      IF(ISEL .EQ. 0)WRITE(6,30)
   30 FORMAT(//6X,"PIECEWISE CONSTANT APPROXIMATION OF SPANWISE DIPOLE ST
     1RENGTH VARIATION"/6X,70(1H*)/)
      IF(ISEL .NE. 0)WRITE(6,40)
   40 FORMAT(//6X,"PIECEWISE QUADRATIC APPROXIMATION OF SPANWISE DIPOLE S
     1TRENGTH VARIATION"/6X,71(1H*)/)
      SLOR=1.
      CL0=0.
      IF(NAFD .EQ. 0)WRITE(6,41)
   41 FORMAT(//6X,"AIRFOIL DATA TABLES NOT USED")
      IF(NAFD .EQ. 1)WRITE(6,42)
   42 FORMAT(//6X,"AIRFOIL DATA TABLES USED")
C
C  CALCULATE QUANTITIES NEEDED FOR TRAJECTORY SEGMENT ADJACENT TO
```

```
      BT(I)=3.*(1./DR(I)+1./DR(I+1))
      IF(I .EQ. 1)GO TO 80
      BT(I)=BT(I)-1./(BT(I-1)*DR(I)*DR(I))
   80 CONTINUE
      DO 90 I=1,NSPM
      DO 90 J=1,NSP
      GF(I,J)=0.
      IF(J .EQ. I .OR. J .EQ. (I+1))GF(I,J)=GF(I,J)+4./BT(I)
      IF(I .EQ. 1)GO TO 90
      GF(I,J)=GF(I,J)-GF(I-1,J)/(BT(I)*DR(I))
   90 CONTINUE
      DO 100 I=2,NSPM
      I1=NSP-I
      DO 100 J=1,NSP
      GF(I1,J)=GF(I1,J)-GF(I1+1,J)/(BT(I1)*DR(I1+1))
  100 CONTINUE
C
C  PROGRAM STEP 2.
C  BEGIN SETTING UP THE SYSTEM OF SIMULTANEOUS EQUATIONS.
C
   70 L=1
      DO 110 J=1,NAZ
C
C  SET THE AZIMUTH STATION FOR THE CURRENT COLLOCATION POINT.
C
      P30=2.*J*PI/NAZ
      PBO(J)=360.*J/NAZ
      CP1=COS(P30)
      SP1=SIN(P30)
      CP2=COS(2.*P30)
      SP2=SIN(2.*P30)
      DO 110 I=1,NSP
C
```

```
C   THE BLADE AT THE COLLOCATION POINT.
C
      ETA1P=ALOG((3.+SQRT(5.))/2.)
      CF1=COSH(.5*ETA1P)/SINH(.5*ETA1P)
      CF2=.5-EXP(-ETA1P)
      CF3=ETA1P-.5*CF1
C
C   CALCULATE QUANTITIES NEEDED FOR NEAR FIELD REPRESENTATION.
C
      DO 50 I=1,5
      T1=ACOS(X(I))
      T2=ACOS(X(I+1))
      FX1(I)=(T2-T1-(SIN(T2)-SIN(T1)))/(X(I+1)-X(I))
      FX2(I)=-((T2-T1)/2.-(SIN(2.*T2)-SIN(2.*T1))/4.)/(X(I+1)-X(I))
      FX2(I)=FX2(I)*(1.-R0)/(2.*AR)
   50 CONTINUE
      DO 60 I=1,NSP
      RBO(I)=(R(I)+R(I+1))/2.
      DR(I)=R(I+1)-R(I)
   60 CONTINUE
      IF(ISEL .EQ. 0)GO TO 70
C
C   FOR PIECEWISE QUADRATIC REPRESENTATION, DETERMINE VALUES AT THE ENDS
C   OF THE SEGMENTS IN TERMS OF THE CENTRAL VALUES.
C
```

```
C   SET THE RADIAL STATION FOR THE CURRENT COLLOCATION POINT.
C
      UT=RBC(I)+MU*SP1
      DO 115 M=1,NCOF
      A(L,M)=0.
  115 CONTINUE
C
C   PROGRAM STEP 3.
C   TEST THE TANGENTIAL VELOCITY AT THE COLLOCATION POINT, TO DECIDE
C   WHETHER NORMAL VELOCITY BOUNDARY CONDITION OR ZERO LIFT CONDITION
C   SHOULD BE APPLIED.
C
      IF(UT .GT. UTMIN)GO TO 120
      WRITE(6,130)RBO(I),PBOO(J),UT
  130 FORMAT(/6X,"R=",F8.3,1X,"PSI=",F8.3,"DEGREES",1X,
     1"UT=",F8.3,1X,"ZERO LIFT CONDITION APPLIED")
      B(L,1)=0.
      GO TO 140
  120 DP=1.5*(1.-RO)/(2.*AR*UT)
      PLIM=-(2.+RBO(I)*CP1)/SQRT(MU*MU+LAM*LAM)
      IF(NAFO .EQ. 0)GO TO 133
C
C   PROGRAM STEP 4.
C   CALCULATE LIFT CURVE SLOPE FROM DATA TABLES FOR THE CURRENT
C   COLLOCATION POINT, USING THE LOCAL INCIDENCE AND MACH NUMBER.
C
      MLOC=UT*MINF/MU
      ALOC=THC-TW*(RBO(I)-RO)/(1.-RO)+B1*CP1-A1*SP1
     1-(MU*AO*CP1+LAM)/UT
      ALOC=ALOC*180./PI
      CALL TABSCH(MCL,NXL,MLOC,IMCL1,IMCL2,INT)
      IF(INT .EQ. -1)IMCL1=IMCL2=1
      IF(INT .EQ. 1)IMCL1=IMCL2=NXL
      CALL TABSCH(ACL,NZL,ALOC,IACL1,IACL2,INT)
      IF(INT .EQ. 0)GO TO 131
      IF(INT .EQ. -1)GO TO 132
      IACL1=NXL-1
      IACL2=NXL
      GO TO 131
  132 IACL1=1
      IACL2=2
  131 SLC1=(CL(IACL2,IMCL1)-CL(IACL1,IMCL1))/(ACL(IACL2)
     1-ACL(IACL1))
      CLO1=CL(IACL1,IMCL1)-SLC1*ACL(IACL1)
      SLC1=SLC1*180./PI
      SLC2=(CL(IACL2,IMCL2)-CL(IACL1,IMCL2))/(ACL(IACL2)
     1-ACL(IACL1))
      CLO2=CL(IACL1,IMCL2)-SLC2*ACL(IACL1)
      SLC2=SLC2*180./PI
      IF(IMCL1 .EQ. IMCL2)SLCR=SLC1/(2.*PI)
      IF(IMCL1 .NE. IMCL2)SLCR=YL(MLOC,MCL(IMCL1),MCL(IMCL2),
     1SLC1,SLC2)/(2.*PI)
      IF(IMCL1 .EQ. IMCL2)CLO=CLO1
      IF(IMCL1 .NE. IMCL2)CLO=YL(MLOC,MCL(IMCL1),MCL(IMCL2),
     1CLO1,CLO2)
  133 CONTINUE
      IF(SLCR .EQ. 0.)GO TO 134
      T1=-(CF1+(1.-SLCR)/SLCR)/UT
      T2=MU*CP1*CF3*(1.-RO)/(2.*AR*UT*UT*DR(I))
      T3=-(1.-RO)*CF3/(2.*AR*UT*UT)
```

```
      B(L,1)=-MU*ALR-UT*TW*(RBO(I)-RO)/(1.-RO)+UT*CLO/(2.*PI*SLCR)
      GO TO 140
  134 T1=1.
      T2=T3=0.
      B(L,1)=-UT*UT*CLO/(2.*PI)
  140 CONTINUE
C
C   SET UP THE CONTRIBUTION TO THE COEFFICIENT MATRIX OF THE TRAJECTORY
C   SEGMENT ADJACENT TO THE BLADE. ALTERNATIVELY, SET UP THE ZERO LIFT
C   CONDITION.
C
      DO 150 M=1,NCOF
      M1=(M-1)/NAZ+1
      M2=M-(M1-1)*NAZ
      IF(M1 .EQ. (NSP+1))GO TO 160
      M3=M2/2
      M4=M2-M3*2
      WT1=0.
      WT2=0.
      WT3=0.
      IF(UT .LE. UTMIN)GO TO 170
      IF(M1 .EQ. I)WT1=T1
      IF(M1 .EQ. I)WT3=T3
      IF(ISEL .EQ. 0)GO TO 180
      IF(I .LT. NSP)WT2=WT2+T2*GF(I,M1)/DR(M1)
      IF(I .GT. 1)WT2=WT2-T2*GF(I-1,M1)/DR(M1)
      GO TO 180
  170 IF(M1 .EQ. I)WT1=1.
  180 IF(M2 .EQ. 1)A(L,M)=WT1+WT2
      IF(M2 .GT. 1 .AND. M4 .EQ. 0)A(L,M)=(WT1+WT2)*COS(M3*PBO)
     1-M3*WT3*SIN(M3*PBO)
      IF(M2 .GT. 1 .AND. M4 .GT. 0)A(L,M)=(WT1+WT2)*SIN(M3*PBO)
     1+M3*WT3*COS(M3*PBO)
      GO TO 150
  160 IF(SLCR .EQ. 0.)GO TO 150
      IF(UT .GT. UTMIN)WT=-(1.-RO)*CF2/(2.*AR*UT)
      IF(UT .LE. UTMIN)WT=-(1.-RO)/(4.*AR)
      IF(M2 .EQ. 1)A(L,M)=WT*(2.*MU*CP1)
      IF(M2 .EQ. 2)A(L,M)=WT*(2.*MU*SP1+RBO(I))
      IF(M2 .EQ. 3)A(L,M)=WT*(-2.*MU*SP2-2.*RBO(I)*CP1)
      IF(M2 .EQ. 4)A(L,M)=WT*(2.*MU*CP2-2.*RBO(I)*SP1)
  150 CONTINUE
      IF(SLCR .EQ. 0.)GO TO 191
      B(L,1)=B(L,1)-WT*TW*(2.*MU*RO*CP1-MU*MU*SP2-4.*MU*CP1*RBO(I))/
     1(1.-RO)
      IF(UT .GT. UTMIN)GO TO 190
  191 L=L+1
      GO TO 110
C
C   PROGRAM STEP 5.
C   START LOOP FOR NUMBER OF BLADES.
C
  190 DO 200 IBL=1,NB
      IBLO=IBL
      DB=2.*PI*(IBL-1)/NB
C
C   CALL SUBROUTINE TO DETERMINE AZIMUTH POSITIONS ALONG THE TRAJECTORY
C   AT WHICH THE TRAJECTORY IS CLOSE TO A BLADE.
C
      IF(DP1 .NE. DP2)CALL DMIN(MU,LAM,DB,RBO(I),PBO,PLIM,DMAX,
```

```
     1IMIN,PMIN)
C
C   DEFINE THE AZIMUTH INTERVAL FOR THE FIRST TRAJECTORY SEGMENT.
C
      J1=1
      K1=0
      PB2=0.
      IF(I9L .EQ. 1)PB1=-DP
      IF(I9L .GT. 1)PB1=-DP1
  210 CONTINUE
      DO 220 I1=1,5
      FG(I1)=0.
  220 CONTINUE
      FCNF=0.
      FTHNF=0.
      FA0NF=0.
      FA1NF=0.
      FB1NF=0.
C
C   PROGRAM STEP 6.
C   CALCULATE SLOPE AND INTERCEPT COMPONENTS FOR CURRENT TRAJECTORY
C   SEGMENT.
C
      XB1=RB0(I)*SIN(PB1+DB)+MU*PB1*SIN(PB1+PB0+DB)
      XB2=RB0(I)*SIN(PB2+DB)+MU*PB2*SIN(PB2+PB0+DB)
      RB1=RB0(I)*COS(PB1+DB)+MU*PB1*COS(PB1+PB0+DB)
      RB2=RB0(I)*COS(PB2+DB)+MU*PB2*COS(PB2+PB0+DB)
      XBS=(XB2-XB1)/(PB2-PB1)
      XBI=XB1-XBS*PB1
      IF(PB2 .EQ. 0. .AND. (DB .EQ. 0. .OR. DB .EQ. PI))XBI=0.
      RBS=(RB2-RB1)/(PB2-PB1)
      RBI=RB1-RBS*PB1
      YBS=LAM
      NSPP=NSP+1
C
C   START CALCULATION OF FAR FIELD CONTRIBUTION.
C
      DO 230 I1=1,NSPP
      I2=I1-1
      CALL FFINT(PB1,PB2,R(I1),ISEL,FG1,FG2,FG3)
      IF(I1 .EQ. 1)GO TO 240
      IF(ISEL .EQ. 0)GO TO 250
      FF1=-(1.-R0)*(FG1-FG1M)/(4.*AR*DR(I2)*DR(I2))
      FF2=-(1.-R0)*(R(I1)*FG1-R(I2)*FG1M)/(4.*AR*DR(I2)*DR(I2))
      FF3=-(1.-R0)*(FG2-FG2M)/(4.*AR*DR(I2)*DR(I2))
      FF4=-(1.-R0)*(FG3-FG3M)/(4.*AR*DR(I2)*DR(I2))
      T1M=(-2.*(RB0(I2)+R(I1))+2.*RBI)*FF1+2.*FF2+2.*RBS*FF3-2.*FF4
      T1=(8.*RB0(I2)-4.*RBI)*FF1-4.*FF2-4.*RBS*FF3+4.*FF4
      T1P=(-2.*(RB0(I2)+R(I2))+2.*RBI)*FF1+2.*FF2+2.*RBS*FF3-2.*FF4
      DO 260 I3=1,NSP
      IF(I2 .NE. 1)FG(I3)=FG(I3)+T1M*GF(I2-1,I3)/DR(I3)
      IF(I3 .EQ. I2)FG(I3)=FG(I3)+T1
      IF(I2 .NE. NSP)FG(I3)=FG(I3)+T1P*GF(I2,I3)/DR(I3)
  260 CONTINUE
      GO TO 240
  250 FG(I2)=FG(I2)-(1.-R0)*(FG1-FG1M)/(4.*AR)
  240 FG1M=FG1
      FG2M=FG2
      FG3M=FG3
  230 CONTINUE
```

```
C
C   END CALCULATION OF FAR FIELD CONTRIBUTION.
C   CALL SUBROUTINE TO DIVIDE CURRENT TRAJECTORY SEGMENT INTO SUB-
C   SEGMENTS ALIGNED WITH SPANWISE SEGMENTS ALONG THE BLADE.
C
      CALL SUBIVL(RB1,RB2,PB1,PB2,R,IP,P1,P2)
      CB1=COS(PB2+PB0+DB)
      CB2=COS(2.*(PB2+PB0+DB))
      SB1=SIN(PB2+PB0+DB)
      SB2=SIN(2.*(PB2+PB0+DB))
      FC=TW*(2.*MU*RO*CB1-MU*MU*SB2-4.*MU*RB2*CB1)/(1.-RO)
      FTH=2.*MU*CB1
      FA0=2.*MU*SB1+RB2
      FA1=-2.*MU*SB2-2.*RB2*CB1
      FB1=2.*MU*CB2-2.*RB2*SB1
C
C   START CALCULATION OF COMMON PART AND NEAR FIELD CONTRIBUTIONS. IN
C   THE FOLLOWING LOOP, THE FIRST PASS CALCULATES THE COMMON PART, AND
C   THE SECOND PASS THE NEAR FIELD.
C
      DO 270 I1=1,2
      IF(I1 .EQ. 2 .AND. IBL .EQ. 1 .AND. PB2 .EQ. 0.)GO TO 290
      DO 270 I2=1,NSP
      FG1=0.
      FG2=0.
      FG3=0.
      FG4=0.
      IF(IP(I2) .EQ. 0)GO TO 270
      IF(I1 .EQ. 2)GO TO 290
      CALL CPINT(P1(I2),P2(I2),ISEL,FG1,FG2,FG3)
      IF(ISEL .EQ. 0)GO TO 300
      FG1=-(1.-RO)*FG1/(2.*AR*DR(I2)*DR(I2))
      FG2=-(1.-RO)*FG2/(2.*AR*DR(I2)*DR(I2))
      FG3=-(1.-RO)*FG3/(2.*AR*DR(I2)*DR(I2))
      GO TO 310
  300 FG(I2)=FG(I2)-(1.-RO)*FG1/(2.*AR)
      GO TO 270
  290 DO 320 I3=1,6
      CALL NFINT(P1(I2),P2(I2),(1.-RO)*X(I3)/(2.*AR),ISEL,FN1,FN2,FN3)
      IF(I3 .EQ. 1)GO TO 330
      FG4=FG4+FX2(I3-1)*(FN1-FN1M)/PI
      IF(ISEL .EQ. 0)GO TO 340
      FG1=FG1+FX1(I3-1)*(FN1-FN1M)/(PI*DR(I2)*DR(I2))
      FG2=FG2+FX1(I3-1)*(FN2-FN2M)/(PI*DR(I2)*DR(I2))
      FG3=FG3+FX1(I3-1)*(FN3-FN3M)/(PI*DR(I2)*DR(I2))
      GO TO 330
  340 FG(I2)=FG(I2)+FX1(I3-1)*(FN1-FN1M)/PI
  330 FN1M=FN1
      FN2M=FN2
      FN3M=FN3
  320 CONTINUE
      IF(ISEL .EQ. 0)GO TO 270
  310 T1M=2.*((RBI-R(I2+1))*(RBI-RB0(I2))*FG1+(2.*RBI-RB0(I2)
     1-R(I2+1))*RBS*FG2+RBS*RBS*FG3)
      T1=-4.*((RBI-R(I2))*(RBI-R(I2+1))*FG1+(2.*RBI-R(I2)-R(I2+1))
     1*RBS*FG2+RBS*RBS*FG3)
      T1P=2.*((RBI-R(I2))*(RBI-RB0(I2))*FG1+(2.*RBI-RB0(I2)-R(I2))
     1*RBS*FG2+RBS*RBS*FG3)
      DO 350 I3=1,NSP
      IF(I2 .GT. 1)FG(I3)=FG(I3)+T1M*GF(I2-1,I3)/DR(I3)
```

```
      IF(I3 .EQ. I2)FG(I3)=FG(I3)+T1
      IF(I2 .NE. NSP)FG(I3)=FG(I3)+T1P*GF(I2,I3)/OK(I3)
 350  CONTINUE
      IF(I1 .EQ. 1)GO TO 270
      FCNF=FCNF+FG4*FC
      FTHNF=FTHNF+FG4*FTH
      FA0NF=FA0NF+FG4*FA0
      FA1NF=FA1NF+FG4*FA1
      FB1NF=FB1NF+FG4*FB1
 270  CONTINUE
 280  CONTINUE
C
C  ADD THE CONTRIBUTIONS, CALCULATED FOR THE CURRENT TRAJECTORY SEGMENT,
C  TO THE COEFFICIENT MATRIX ELEMENTS
C
      DO 360 M=1,NCOF
      M1=(M-1)/NAZ+1
      M2=M-(M1-1)*NAZ
      IF(M1 .EQ. (NSP+1))GO TO 370
      M3=M2/2
      M4=M2-M3*2
      IF(M2 .EQ. 1)A(L,M)=A(L,M)+FG(M1)
      IF(M2 .GT. 1 .AND. M4 .EQ. 0)A(L,M)=A(L,M)+FG(M1)
     1*COS(M3*(PB2+PB0+DB))
      IF(M2 .GT. 1 .AND. M4 .GT. 0)A(L,M)=A(L,M)+FG(M1)
     1*SIN(M3*(PB2+PB0+DB))
      GO TO 360
 370  IF(M2 .EQ. 1)A(L,M)=A(L,M)+FTHNF
      IF(M2 .EQ. 2)A(L,M)=A(L,M)+FA0NF
      IF(M2 .EQ. 3)A(L,M)=A(L,M)+FA1NF
      IF(M2 .EQ. 4)A(L,M)=A(L,M)+FB1NF
 360  CONTINUE
      B(L,1)=B(L,1)-FCNF
C
C  PROGRAM STEP 7.
C  REDEFINE THE AZIMUTH INTERVAL, FOR THE NEXT TRAJECTORY SEGMENT.
C  TEST TO SEE IF THE FINAL SEGMENT HAS BEEN CALCULATED. ALSO TEST
C  TO SEE IF THE NEXT SEGMENT IS CLOSE TO A BLADE, IN WHICH CASE
C  REDUCED SPACING IS TO BE USED.
C
      PB2=PB1
      IF(PB2 .LE. PLIM)GO TO 200
      IF(DP1 .EQ. DP2)GO TO 390
      IF(J1 .GT. IMIN)GO TO 390
      IF(K1 .EQ. 0 .AND. PB2 .LE. (PMIN(J1)+DP1))GO TO 390
      IF(K1 .EQ. 1 .AND. PB2 .GT. (PMIN(J1)-DP1))GO TO 390
      IF(K1 .EQ. 1 .AND. PB2 .LE. (PMIN(J1)-DP1))GO TO 400
      IF(PB2 .GT. (-3.*DP1) .AND. I8L .EQ. 1)PB1=PB1-DP2
      IF(PB2 .LE. (-3.*DP1) .OR. I9L .GT. 1)PB1=PB1-DP1
      IF(K1 .EQ. 0 .AND. PB1 .LT. (PMIN(J1)+DP1))PB1=PMIN(J1)+DP1
      GO TO 210
 380  PB1=PB1-DP1
      GO TO 210
 390  PB1=PB1-DP2
      K1=1
      GO TO 210
 400  PB1=PB1-DP1
      K1=0
      J1=J1+1
      GO TO 210
```

```
C
C   PROGRAM STEP 8. END OF LOOP FOR NUMBER OF BLADES.
C
 200  CONTINUE
C
C   SET UP THE ELEMENTS CORRESPONDING TO THE 4 AUXILIARY UNKNOWNS.
C
      M=NSP*NAZ+1
      A(L,M)=A(L,M)-UT
      M=M+1
      A(L,M)=A(L,M)+MU*CP1
      M=M+1
      A(L,M)=A(L,M)+RBO(I)*SP1+.5*MU*(1.-CP2)
      M=M+1
      A(L,M)=A(L,M)-RBO(I)*CP1-.5*MU*SP2
      L=L+1
C
C   PROGRAM STEP 9. END OF COLLOCATION LOOP.
C
 110  CONTINUE
C
C   PROGRAM STEP 10.
C   SET UP THE EXTRA 4 EQUATIONS NEEDED TO CLOSE THE SYSTEM.
C
      DO 410 I=1,4
      DO 420 M=1,NCOF
      A(L,M)=0.
 420  CONTINUE
      B(L,1)=0.
      IF(I .EQ. 1 .AND. N1 .EQ. 1)GO TO 430
      IF(I .EQ. 2 .AND. N2 .EQ. 1)GO TO 440
      IF(I .EQ. 3 .AND. N3 .EQ. 1)GO TO 450
      IF(I .EQ. 4 .AND. N4 .EQ. 1)GO TO 460
      IF(I .LE. 2)I1=1
      IF(I .GT. 2)I1=I-1
      DO 470 M1=1,NSP
      IF(I .GT. 1)GO TO 480
      DO 490 M2=1,NSP
      M=(M2-1)*NAZ+I1
      IF(ISEL .EQ. 0)GO TO 500
      IF(M1 .NE. 1)A(L,M)=A(L,M)-DR(M1)*GF(M1-1,M2)/(6.*DR(M2))
      IF(M2 .EQ. M1)A(L,M)=A(L,M)-4.*DR(M1)/6.
      IF(M1 .LT. NSP)A(L,M)=A(L,M)-DR(M1)*GF(M1,M2)/(6.*DR(M2))
      GO TO 490
 500  IF(M2 .EQ. M1)A(L,M)=A(L,M)-DR(M1)
 490  CONTINUE
      GO TO 470
 480  DO 510 M2=1,NSP
      M=(M2-1)*NAZ+I1
      IF(ISEL .EQ. 0)GO TO 520
      IF(M1 .NE. 1)A(L,M)=A(L,M)-R(M1)*DR(M1)*GF(M1-1,M2)/(6.*DR(M2))
      IF(M2 .EQ. M1)A(L,M)=A(L,M)-4.*RBO(M1)*DR(M1)/6.
      IF(M1 .LT. NSP)A(L,M)=A(L,M)-R(M1+1)*DR(M1)*GF(M1,M2)/(6.*DR(M2))
      GO TO 510
 520  IF(M2 .EQ. M1)A(L,M)=A(L,M)-RBO(M1)*DR(M1)
 510  CONTINUE
 470  CONTINUE
      GO TO (530,540,550,560),I
 530  M=NSP*NAZ+2
      A(L,M)=(1.-RO)*(1.-RO*RO)/(8.*AR)
```

```
      B(L,1)=AR*CT/(N8*(1.-RO))
C
C   THE ABOVE EQUATION EQUATES THE TOTAL LIFT DUE TO ALL THE BLADES,
C   AVERAGED OVER THE AZIMUTH, TO THE THRUST COEFFICIENT.
C
      L=L+1
      GO TO 410
 430  M=NSP*NAZ+1
      A(L,M)=1.
      B(L,1)=THC
C
C   THE ABOVE EQUATION SETS THE COLLECTIVE PITCH TO THE GIVEN VALUE.
C
      L=L+1
      GO TO 410
 540  M=NSP*NAZ+2
      A(L,M)=(1.-RO)*(1.-RO*RO*RO)/(12.*AR)-2./GAMA
      B(L,1)=0.
C
C   THE ABOVE EQUATION REPRESENTS THE ZEROTH HARMONIC COMPONENT OF
C   MOMENT EQUILIBRIUM ABOUT THE HUB.
C
      L=L+1
      GO TO 410
 440  M=NSP*NAZ+2
      A(L,M)=1.
      B(L,1)=A0
C
C   THE ABOVE EQUATION SETS THE CONING ANGLE TO THE GIVEN VALUE.
C
      L=L+1
      GO TO 410
 550  M=NSP*NAZ+1
      A(L,M)=MU*(1.-RO)*(1.-RO*RO)/(4.*AR)
      M=M+2
      A(L,M)=-(1.-RO)*(1.-RO*RO*RO)/(6.*AR)
      B(L,1)=-TW*MU*(RO*(1.-RO*RO)-4.*(1.-RO*RO*RO)/3.)/(4.*AR)
C
C   THE ABOVE EQUATION REPRESENTS THE FIRST HARMONIC COSINE COMPONENT
C   OF MOMENT EQUILIBRIUM ABOUT THE HUB.
C
      L=L+1
      GO TO 410
 450  M=NSP*NAZ+3
      A(L,M)=1.
      B(L,1)=A1
C
C   THE ABOVE EQUATION SETS THE CYCLIC PITCH COEFFICIENT, A1, TO THE
C   GIVEN VALUE.
C
      L=L+1
      GO TO 410
 560  M=NSP*NAZ+2
      A(L,M)=MU*(1.-RO)*(1.-RO*RO)/(4.*AR)
      M=M+2
      A(L,M)=-(1.-RO)*(1.-RO*RO*RO)/(6.*AR)
      B(L,1)=0.
C
C   THE ABOVE EQUATION REPRESENTS THE FIRST HARMONIC SINE COMPONENT OF
C   MOMENT EQUILIBRIUM ABOUT THE HUB.
```

```
C
      L=L+1
      GO TO 410
 460  M=NSP*NAZ+4
      A(L,M)=1.
      B(L,1)=B1
C
C  THE ABOVE EQUATION SETS THE CYCLIC PITCH COEFFICIENT, B1, TO THE
C  GIVEN VALUE.
C
      L=L+1
 410  CONTINUE
C
C  PROGRAM STEP 11.
C  SOLVE THE SYSTEM OF SIMULTANEOUS EQUATIONS AND PRINT THE SOLUTION.
C
      CALL GELIM(NCOF,NCOF,A,1,B,IPIVOT,0,WK,IERR)
      IF(IERR .EQ. 1)GO TO 570
      L=1
      DO 580 I=1,NSP
      GC(I)=B(L,1)
      L=L+1
      DO 580 J=1,NHM
      GC(I,J)=B(L,1)
      L=L+1
      GS(I,J)=B(L,1)
      L=L+1
 580  CONTINUE
      THC=B(NSP*NAZ+1,1)
      THCD=THC*180./PI
      A0=B(NSP*NAZ+2,1)
      A0D=A0*180./PI
      A1=B(NSP*NAZ+3,1)
      A1D=A1*180./PI
      B1=B(NSP*NAZ+4,1)
      B1D=B1*180./PI
      WRITE(6,9)
      WRITE(6,590)
 590  FORMAT(6X,"SOLUTION FOR COEFFICIENTS"/6X,25(1H-)//6X,
     1"(GO(I),I=1,NSP)")
      WRITE(6,600)(GO(I),I=1,NSP)
 600  FORMAT(//6X,5(E10.4,1X))
      WRITE(6,610)
 610  FORMAT(//6X,"((GC(I,J),J=1,NHM),I=1,NSP)"//)
      DO 620 I=1,NSP
      WRITE(6,600)(GC(I,J),J=1,NHM)
 620  CONTINUE
      WRITE(6,630)
 630  FORMAT(//6X,"((GS(I,J),J=1,NHM),I=1,NSP)"//)
      DO 640 I=1,NSP
      WRITE(6,600)(GS(I,J),J=1,NHM)
 640  CONTINUE
      WRITE(6,650)THCD,A0D,A1D,B1D
 650  FORMAT(//6X,"PITCH ANGLE AT BLADE ROOT=",F10.5,1X,"DEGREES"//6X,
     1"CONING ANGLE=",F10.5,1X,"DEGREES"//6X,
     2"FLAPPING COEFFICIENT, A1=",F10.5,1X,"DEGREES"//6X,
     3"FLAPPING COEFFICIENT, B1=",F10.5,1X,"DEGREES")
C
C  PROGRAM STEP 12.
C  START LOOP FOR AZIMUTH STATIONS AT WHICH OUTPUT QUANTITIES ARE
```

```
C  CALCULATED.
C
      CTCAL=0.
      CMXCAL=0.
      CMYCAL=0.
      DO 670 I=1,24
      PBOD(I)=15.*(I-1)
      PBO=PBOD(I)*PI/180.
      CP1=COS(PBO)
      SP1=SIN(PBO)
      CP2=COS(2.*PBO)
      SP2=SIN(2.*PBO)
      F2=CP1*(2.*MU*TW*RO/(1.-RO)+2.*MU*THC)+2.*MU*AO*SP1+2.*MU*B1*CP2
     1-SP2*(MU*MU*TW/(1.-RO)+2.*MU*A1)
      F3=AO-CP1*(4.*MU*TW/(1.-RO)+2.*A1)-2.*B1*SP1
      GI1=0.
      GI2=0.
      DO 690 I1=1,NSP
      G(I,I1)=GO(I1)
      DO 690 I2=1,NHM
      G(I,I1)=G(I,I1)+GC(I1,I2)*COS(I2*PBO)+GS(I1,I2)*SIN(I2*PBO)
  690 CONTINUE
      DO 700 I1=1,NSP
      IF(ISEL .NE. 0)GO TO 710
      GI1=GI1+DR(I1)*G(I,I1)
      GI2=GI2+DR(I1)*RBO(I1)*G(I,I1)
      GO TO 700
  710 GI1=GI1+4.*DR(I1)*G(I,I1)/6.
      GI2=GI2+4.*DR(I1)*RBO(I1)*G(I,I1)/6.
      IF(I1 .EQ. 1)GL(I1)=0.
      IF(I1 .GT. 1)GL(I1)=GR(I1-1)
      GR(I1)=0.
      IF(I1 .EQ. NSP)GO TO 720
      DO 730 I2=1,NSP
      GR(I1)=GR(I1)+GF(I1,I2)*G(I,I2)/DR(I2)
  730 CONTINUE
  720 GI1=GI1+DR(I1)*(GL(I1)+GR(I1))/6.
      GI2=GI2+DR(I1)*(R(I1)*GL(I1)+R(I1+1)*GR(I1))/6.
  700 CONTINUE
      FLT1(I)=(1.-RO*RO)*AO/2.+CP1*(2.*MU*THC*(1.-RO)-2.*MU*TW
     1-A1*(1.-RO*RO))+SP1*(1.-RO)*(2.*MU*AO-B1*(1.+RO))
     2+2.*MU*B1*(1.-RO)*CP2-SP2*(2.*MU*A1*(1.-RO)+MU*MU*TW)
      FLT1(I)=-FLT1(I)*(1.-RO)/(4.*AR)
      FLT1(I)=-(FLT1(I)+GI1)*PI*(1.-RO)/AR
      FLT2(I)=FLT1(I)/(CT*PI/NB)
      FMT(I)=(1.-RO*RO*RO)*AO/3.+CP1*(MU*THC*(1.-RO*RO)-2.*A1*
     1(1.-RO*RO*RO)/3.+MU*TW*RO*(1.+RO)-4.*MU*TW*(1.+RO+RO*RO)/3.)
     2+SP1*(MU*AO*(1.-RO*RO)-2.*B1*(1.-RO*RO*RO)/3.)+CP2*MU*B1*
     3(1.-RO*RO)-SP2*(MU*A1*(1.-RO*RO)+MU*MU*TW*(1.+RO)/2.)
      FMT(I)=-FMT(I)*(1.-RO)/(4.*AR)
      FMT(I)=-(FMT(I)+GI2)*PI*(1.-RO)/AR
      COL(I)=FMT(I)/FLT1(I)
      CTCAL=CTCAL+FLT1(I)/24.
      CMXCAL=CMXCAL+FMT(I)*SP1/24.
      CMYCAL=CMYCAL-FMT(I)*CP1/24.
C
C  START LOOP FOR RADIAL STATIONS AT WHICH OUTPUT QUANTITIES ARE
C  CALCULATED.
C
      DO 740 I1=1,NSP
```

```
      IF(ISEL .EQ. 0)GO TO 780
      QC=2.*(GR(I1)+GL(I1)-2.*G(I,I1))/(DR(I1)*DR(I1))
      QB=(GR(I1)-GL(I1))/DR(I1)-2.*QC*RBO(I1)
      QA=G(I,I1)-RBO(I1)*QB-RBO(I1)*RBO(I1)*QC
      GOUT=QA+QB*RBO(I1)+QC*RBO(I1)*RBO(I1)
      GO TO 790
  780 GOUT=G(I,I1)
  790 F23(I,I1)=F2+RBO(I1)*F3
      FL1(I,I1)=-PI*(1.-RO)*(GOUT-(1.-RO)*F23(I,I1)/(4.*AR))/AR
      FL2(I,I1)=FL1(I,I1)/(CT*PI/NB)
      FM(I,I1)=-PI*(1.-RO)*(1.-RO)*(1.-RO)*F23(I,I1)/(16.*AR*AR*AR)
      XCP(I,I1)=.25+FM(I,I1)*AR/(FL1(I,I1)*(1.-RO))
  740 CONTINUE
  670 CONTINUE
      CTCAL=CTCAL*NB/PI
      CMXCAL=CMXCAL*NB/PI
      CMYCAL=CMYCAL*NB/PI
      WRITE(6,791)CTCAL,CMXCAL,CMYCAL
  791 FORMAT(//6X,"COMPUTED THRUST COEFFICIENT=",E10.4//6X,
     1"COMPUTED MOMENT COEFFICIENT ABOUT ROTOR X-AXIS=",E10.4//6X,
     2"COMPUTED MOMENT COEFFICIENT ABOUT ROTOR Y-AXIS=",E10.4)
C
C  PRINT ALL OUTPUT QUANTITIES IN TABULAR FORM.
C
      WRITE(6,9)
      WRITE(6,800)
  800 FORMAT(//6X,"TABLE 1 - SECTIONAL LIFT/(RHO*(OMEGA**2)*(R1**3))"/6X
     1,49(1H-)//)
      WRITE(6,810)(RBO(I),I=1,NSP)
  810 FORMAT(/12X,"R/R1:  ",5(E10.4,1X))
      WRITE(6,811)
  811 FORMAT(/7X,"PSI")
      DO 820 I=1,24
      WRITE(6,830)PBOD(I),(FL1(I,I1),I1=1,NSP)
  830 FORMAT(/6X,F5.1,8X,5(E10.4,1X))
  820 CONTINUE
      WRITE(6,9)
      WRITE(6,840)
  840 FORMAT(//6X,"TABLE 2 - SECTIONAL LIFT*R1/THRUST PER BLADE"/6X,
     144(1H-)//)
      WRITE(6,810)(RBO(I),I=1,NSP)
      WRITE(6,811)
      DO 850 I=1,24
      WRITE(6,830)PBOD(I),(FL2(I,I1),I1=1,NSP)
  850 CONTINUE
      WRITE(6,9)
      WRITE(6,860)
  860 FORMAT(//6X,"TABLE 3 - SECTIONAL PITCHING MOMENT/(RHO*(OMEGA**2)*(
     1R1**4))"/6X,60(1H-)/16X,"(ABOUT QUARTER-CHORD)"//)
      WRITE(6,810)(RBO(I),I=1,NSP)
      WRITE(6,811)
      DO 870 I=1,24
      WRITE(6,830)PBOD(I),(FM(I,I1),I1=1,NSP)
  870 CONTINUE
      WRITE(6,9)
      WRITE(6,880)
  880 FORMAT(//6X,"TABLE 4 - CENTER OF PRESSURE LOCATION FROM LEADING ED
     1GE(FRACTION OF CHORD)"/6X,74(1H-)//)
      WRITE(6,810)(RBO(I),I=1,NSP)
      WRITE(6,811)
```

```
      DO 890 I=1,24
      WRITE(6,830)PBOD(I),(XCP(I,I1),I1=1,NSP)
  890 CONTINUE
      WRITE(6,9)
      WRITE(6,900)
  900 FORMAT(//6X,"TABLE 5 - TOTAL BLADE LIFT, MOMENT ABOUT HUB AND RADI
     1AL CENTER OF LIFT"/6X,70(1H-)//6X,
     2"TOTAL BLADE LIFT/(RHO*(OMEGA**2)*(R1**4))"/6X,
     3"TOTAL BLADE LIFT/THRUST PER BLADE"/6X,
     4"MOMENT ABOUT HUB/(RHO*(OMEGA**2)*(R1**5))"/6X,
     5"RADIAL CENTER OF LIFT/R1"//7X,"PSI",8X,"TOTAL BLADE LIFT",
     55X,"MOMENT",5X,"CENTER"/38X,"ABOUT HUB",4X,"OF LIFT")
      DO 910 I=1,24
      WRITE(6,920)PBOD(I),FLT1(I),FLT2(I),FMT(I),COL(I)
  920 FORMAT(/6X,F5.1,5X,4(E10.4,1X))
  910 CONTINUE
      WRITE(6,9)
      WRITE(6,940)
  940 FORMAT(//6X,"TABLE 6 - SURFACE PRESSURE DIFFERENTIAL/(RHO*(OMEGA**
     12)*(R1**2))"/6X,64(1H-)//)
      DO 950 I=1,24
      WRITE(6,960)PBOD(I)
  960 FORMAT(/6X,"AZIMUTH ANGLE=",F5.1,1X,"DEGREES"/6X,27(1H-))
      WRITE(6,810)(RBO(I1),I1=1,NSP)
      WRITE(6,970)
  970 FORMAT(11X,"X/C")
      DO 980 I1=1,NSP
      DO 980 I2=1,10
      CCH=2.*XOUT(I2)-1.
      SCH=SQRT(1.-CCH*CCH)
      POUT(I1,I2)=-G(I,I1)*SCH/(1.+CCH)+F23(I,I1)*(1.-RO)*SCH/(2.*AR)
      POUT(I1,I2)=2.*POUT(I1,I2)
  980 CONTINUE
      DO 990 I2=1,10
      WRITE(6,991)XOUT(I2),(POUT(I1,I2),I1=1,NSP)
  991 FORMAT(6X,F8.5,5X,5(E10.4,1X))
  990 CONTINUE
      IREM=I-(I/3)*3
      IF(IREM .EQ. 0)WRITE(6,9)
  950 CONTINUE
      STOP
C
C  PRINT ERROR MESSAGE IF COEFFICIENT MATRIX IS SINGULAR.
C
  570 WRITE(6,930)
  930 FORMAT(6X,"COEFFICIENT MATRIX SINGULAR")
      STOP
      END
      SUBROUTINE DMIN(MU,LAM,DB,RBO,PBO,PLIM,DMAX,I,P)
C
C  CALCULATION OF AZIMUTH POSITIONS AT WHICH TRAJECTORY IS DIRECTLY
C  OVER A BLADE, WITHIN A DISTANCE DMAX.
C
      REAL MU,LAM
      DIMENSION P(20)
      Y(X,X1,X2,Y1,Y2)=Y1+(Y2-Y1)*(X-X1)/(X2-X1)
      I=0
      P1=0.
      X81=0.
      P2=-0.2
```

```
   10  XB2=RB0*SIN(P2+DB)+MU*SIN(P2+PB0+DB)*P2
       IF(P1 .NE. 0.)GO TO 20
   30  P1=P2
       IF(P1 .LE. PLIM)RETURN
       P2=P2-0.2
       XB1=XB2
       GO TO 10
   20  TEST=XB1*XB2
       IF(TEST .GT. 0.)GO TO 30
       PC=Y(0.,XB1,XB2,P1,P2)
       XBC=RB0*SIN(PC+DB)+MU*SIN(PC+PB0+DB)*PC
       RBC=RB0*COS(PC+DB)+MU*COS(PC+PB0+DB)*PC
       D=SQRT(XBC*XBC+LAM*LAM*PC*PC+(RBC-RB0)*(RBC-RB0))
       IF(D .GT. DMAX)GO TO 30
       I=I+1
       P(I)=PC
       GO TO 30
       END
       SUBROUTINE SUBIVL(RB1,RB2,PB1,PB2,R,I,P1,P2)
C
C  DIVISION OF TRAJECTORY SEGMENT INTO SUB-SEGMENTS ALIGNED WITH BLADE
C  SPANWISE SEGMENTS.
C
       DIMENSION R(6),I(5),P1(5),P2(5)
       Y(X,X1,X2,Y1,Y2)=Y1+(Y2-Y1)*(X-X1)/(X2-X1)
       DO 10 J=1,5
       I(J)=0
       P1(J)=0.
       P2(J)=0.
   10  CONTINUE
       DO 20 J=1,5
       R1=R(J)
       R2=R(J+1)
       IF(RB1 .LE. R1 .AND. RB2 .LE. R1)GO TO 20
       IF(RB1 .GE. R2 .AND. RB2 .GE. R2)GO TO 20
       IF(RB1 .GE. R1 .AND. RB1 .LE. R2 .AND. RB2 .GE. R1
      1.AND. RB2 .LE. R2)GO TO 30
       IF(RB1 .LE. R2 .AND. RB2 .GT. R1)GO TO 40
       IF(RB1 .LT. R2 .AND. RB2 .GE. R2)GO TO 50
       IF(RB1 .GT. R1 .AND. RB2 .LE. R1)GO TO 60
       IF(RB1 .GE. R2 .AND. RB2 .LT. R2)GO TO 70
   30  I(J)=1
       P1(J)=PB1
       P2(J)=PB2
       RETURN
   40  I(J)=1
       P1(J)=Y(R1,RB1,RB2,PB1,PB2)
       IF(RB2 .GT. R2)P2(J)=Y(R2,RB1,RB2,PB1,PB2)
       IF(RB2 .LE. R2)P2(J)=PB2
       GO TO 20
   50  I(J)=1
       P2(J)=Y(R2,RB1,RB2,PB1,PB2)
       IF(RB1 .LT. R1)P1(J)=Y(R1,RB1,RB2,PB1,PB2)
       IF(RB1 .GE. R1)P1(J)=PB1
       GO TO 20
   60  I(J)=1
       P2(J)=Y(R1,RB1,RB2,PB1,PB2)
       IF(RB1 .GT. R2)P1(J)=Y(R2,RB1,RB2,PB1,PB2)
       IF(RB1 .LE. R2)P1(J)=PB1
       GO TO 20
```

```
   70  I(J)=1
       P1(J)=Y(R2,RB1,RB2,PB1,PB2)
       IF(RB2 .LT. R1)P2(J)=Y(R1,RB1,RB2,PB1,PB2)
       IF(RB2 .GE. R1)P2(J)=PB2
   20  CONTINUE
       RETURN
       END
       SUBROUTINE NFINT(P1,P2,X,ISEL,T1,T2,T3)
C
C  INTEGRATION OF NEAR FIELD PRESSURE GRADIENT.
C
       DIMENSION F0(2),F1(2),F2(2),F3(2)
       COMMON/MAIN1/XI,XS,YS,RI,RS
       D0=(X-XI)*(X-XI)
       D1=-2.*(X-XI)*XS
       D2=XS*XS+YS*YS
       Q=4.*D0*D2-D1*D1
       IF(Q .NE. 0.)SQ=SQRT(Q)
       DO 10 I=1,2
       IF(I .EQ. 1)P=P1
       IF(I .EQ. 2)P=P2
       DD=D0+D1*P+D2*P*P
       IF(Q .NE. 0.)F0(I)=2.*ATAN((D1+2.*D2*P)/SQ)/SQ
       IF(Q .EQ. 0.)F0(I)=-1./(D2*P)
       F1(I)=(ALOG(DD)-D1*F0(I))/(2.*D2)
       IF(ISEL .EQ. 0)GO TO 20
       F2(I)=(P-D1*F1(I)-D0*F0(I))/D2
       F3(I)=(P*P/2.-D1*F2(I)-D0*F1(I))/D2
       GO TO 10
   20  F2(I)=0.
       F3(I)=0.
   10  CONTINUE
       T1=(X-XI)*(F0(2)-F0(1))-XS*(F1(2)-F1(1))
       T2=(X-XI)*(F1(2)-F1(1))-XS*(F2(2)-F2(1))
       T3=(X-XI)*(F2(2)-F2(1))-XS*(F3(2)-F3(1))
       RETURN
       END
       SUBROUTINE CPINT(P1,P2,ISEL,T1,T2,T3)
C
C  INTEGRATION OF COMMON PART PRESSURE GRADIENT.
C
       DIMENSION F0(2),F1(2),F2(2),F3(2),F4(2)
       COMMON/MAIN1/XI,XS,YS,RI,RS
       R0=XI*XI
       R1=XI*XS
       R2=XS*XS+YS*YS
       Q=4.*XI*XI*YS*YS
       IF(Q .NE. 0.)SQ=SQRT(Q)
       DO 10 I=1,2
       IF(I .EQ. 1)P=P1
       IF(I .EQ. 2)P=P2
       RR=R0+2.*R1*P+R2*P*P
       IF(Q .EQ. 0. .AND. P .EQ. 0.)GO TO 20
       IF(Q .NE. 0.)T=2.*ATAN((2.*R1+2.*R2*P)/SQ)/SQ
       IF(Q .EQ. 0.)T=0.
       IF(Q .NE. 0.)F0(I)=2.*(R1+R2*P)/(Q*RR)+2.*R2*T/Q
       IF(Q .EQ. 0.)F0(I)=-1./(3.*R2*R2*P*P*P)
       F1(I)=(-1./(2.*RR)-R1*F0(I))/R2
       F2(I)=(-P/RR+R0*F0(I))/R2
       IF(ISEL .EQ. 0)GO TO 30
```

```
      G6=(8.*SD2*FN3*(SD2*D-RS*U)/(T*RR)+8.*SD2*FN2*U/RR
     1+4.*D2*FN2*G3)/Q
      G7=(-2.*D/RR-R1*G6-RS*G3)/R2
      G8=(-R0*G6-2.*R1*G7+2.*G1+2.*(R-RI)*G3-2.*RS*G4)/R2
      G9=(-R0*G7-2.*R1*G8+2.*G2+2.*(R-RI)*G4-2.*RS*G5)/R2
      F1(I)=(2.*G1+(R-RI)*G3-RS*G4-YS*YS*G6)/2.
      F2(I)=(2.*G2+(R-RI)*G4-RS*G5-YS*YS*G9)/2.
      G10=2.*ATAN((2.*(SD2-RS)*T+2.*FN2)/SQ)/SQ
      G11=ALOG(ABS((SD2-RS)*T*T+2.*FN2*T-(SD2+RS)*FN3))
      G12=(-2.*R1*SD2*G10+G11-(SD2-RS)*G1)/R2
      G13=(P+2.*R0*(XS*XS-YS*YS)*SD2*G10/R2-2.*R1*G11/R2
     1+(2.*R1*D2-(SD2+RS)*FN2)*G1/(D2*(SD2+RS))+RS*D/D2)/R2
      F3(I)=P*ALOG(D+U)-R1*G12-XS*XS*G13+RS*G2
      GO TO 10
   40 F1(I)=RS*YS*(YS*D+SD2*YB)/(R2*SD2*T*D)-XS*XB*
     1(RS*D-SD2*U)/(R2*T*RR)-YS*YB*U*(1.-R1/T)/(D*R2*RR)
      F2(I)=0.
      F3(I)=0.
      GO TO 10
   30 IF(ISEL .EQ. 0)GO TO 50
      G14=(T-D1-SD2*ABS(R-RI))/(T-D1+SD2*ABS(R-RI))
      G14=ALOG(G14*G14)/2.
      F1(I)=(XS*XS-YS*YS)*(-D/P+D2*G1+D1*G14/ABS(R-RI))/(R2*R2)
     1+YS*YS*G1/R2
      F2(I)=(XS*XS-YS*YS)*(D+ABS(R-RI)*G14+D1*G1)/(R2*R2)
     1+YS*YS*G2/R2
      G15=(P+RS*D/D2)/R2-(R-RI)*G1/D2
      F3(I)=P*ALOG(D+U)-XS*XS*G15+RS*G2
      GO TO 10
   50 F1(I)=(XS*XS-YS*YS)*D/(R2*R2*(R-RI)*P)
     1+YS*YS*P/(R2*(R-RI)*D)
      F2(I)=0.
      F3(I)=0.
      GO TO 10
   20 IF(ISEL .EQ. 0)GO TO 60
      G16=ALOG(T/(2.*U*U))
      F1(I)=(XS*XS-YS*YS)*(D2*G1-D1*(1.-G16)/ABS(U))/(R2*R2)
     1+YS*YS*G1/R2
      F2(I)=(XS*XS-YS*YS)*(D1*G1+ABS(U)*(1.+G16))/(R2*R2)
     1+YS*YS*G2/R2
      G17=RS*D/(R2*D2)-U*G1/D2
      F3(I)=-XS*XS*G17+RS*G2
      GO TO 10
   60 F1(I)=-(XS*XS-YS*YS)*RS/(R2*R2*ABS(U))
      F2(I)=0.
      F3(I)=0.
   10 CONTINUE
      T1=F1(2)-F1(1)
      T2=F2(2)-F2(1)
      T3=F3(2)-F3(1)
      RETURN
      END
      SUBROUTINE TABSCH(X,N,XT,I1,I2,INT)
C
C  GIVEN AN ARRAY X, TO LOCATE THE POSITION OF A VALUE XT.
C  IF INT=0, XT LIES BETWEEN X(I1) AND X(I2).
C  IF INT=1, XT IS GREATER THAN X(N).
C  IF INT=-1, XT IS LESS THAN X(1).
C
      DIMENSION X(N)
```

```
      F3(I)=(-R0*F1(I)-2.*R1*F2(I))/R2+(ALOG(RR)/2.-R1*T)/(R2*R2)
      IF(Q .EQ. 0.)F3(I)=ALOG(P*P)/(2.*R2*R2)
      F4(I)=(P*P*P/RR-4.*R1*F3(I)-3.*R0*F2(I))/R2
      GO TO 10
   20 F0(I)=0.
      F1(I)=0.
      F2(I)=0.
   30 F3(I)=0.
      F4(I)=0.
   10 CONTINUE
      DF0=F0(2)-F0(1)
      DF1=F1(2)-F1(1)
      DF2=F2(2)-F2(1)
      DF3=F3(2)-F3(1)
      DF4=F4(2)-F4(1)
      T1=R0*DF0+2.*R1*DF1+(XS*XS-YS*YS)*DF2
      T2=R0*DF1+2.*R1*DF2+(XS*XS-YS*YS)*DF3
      T3=R0*DF2+2.*R1*DF3+(XS*XS-YS*YS)*DF4
      RETURN
      END
      SUBROUTINE FFINT(P1,P2,R,ISEL,T1,T2,T3)
C
C  INTEGRATION OF FAR FIELD PRESSURE GRADIENT.
C
      DIMENSION F1(2),F2(2),F3(2)
      COMMON/MAIN1/XI,XS,YS,RI,RS
      R0=XI*XI
      R1=XI*XS
      R2=XS*XS+YS*YS
      D0=R0+(R-RI)*(R-RI)
      D1=R1-(R-RI)*RS
      D2=R2+RS*RS
      SD2=SQRT(D2)
      FN1=ABS(XI*YS)
      FN2=(R-RI)*R2+RS*R1
      FN3=D1*D1-D0*D2
      Q=4.*D2*FN1*FN1
      IF(Q .NE. 0.)SQ=SQRT(Q)
      DO 10 I=1,2
      IF(I .EQ. 1)P=P1
      IF(I .EQ. 2)P=P2
      F1(I)=0.
      F2(I)=0.
      F3(I)=0.
      XB=XI+XS*P
      YB=YS*P
      RB=RI+RS*P
      RR=XB*XB+YB*YB
      U=R-RB
      D=SQRT(RR+U*U)
      T=D1+D2*P+SD2*D
      G1=ALOG(T*T)/(2.*SD2)
      G2=(D-D1*G1)/D2
      IF(XI .EQ. 0. .AND. P .EQ. 0.)GO TO 20
      IF(XI .EQ. 0.)GO TO 30
      IF(ISEL .EQ. 0)GO TO 40
      G3=ATAN(2.*(T*(SD2+RS)-FN2)/SQ)-ATAN(2.*(T*(SD2-RS)+FN2)/SQ)
      G3=4.*SD2*G3/SQ
      G4=(ALOG((D-U)/(D+U))-2.*RS*G1-R1*G3)/R2
      G5=(-R0*G3-2.*R1*G4+2.*(R-RI)*G1-2.*RS*G2)/R2
```

```
      I1=0
      I2=0
      NM=N-1
      DO 10 I=1,NM
      IF(XT .GE. X(I) .AND. XT .LE. X(I+1))GO TO 20
   10 CONTINUE
      IF(XT .LT. X(1))GO TO 30
      IF(XT .GT. X(N))GO TO 40
   20 INT=0
      IF(XT .EQ. X(I))GO TO 21
      IF(XT .EQ. X(I+1))GO TO 22
      I1=I
      I2=I+1
      RETURN
   21 I1=I2=I
      RETURN
   22 I1=I2=I+1
      RETURN
   30 INT=-1
      RETURN
   40 INT=1
      RETURN
      END
```

NASA Contractor Report 166093

HELICOPTER ROTOR LOADS USING MATCHED ASYMPTOTIC EXPANSIONS: USER'S MANUAL

G. Alvin Pierce and
Anand R. Vaidyanathan

Georgia Institute of Technology
A Unit of the University System of Georgia
School of Aerospace Engineering
Atlanta, GA 30332

CONTRACT NAS1-16817

May 1983

National Aeronautics and
Space Administration

Langley Research Center
Hampton, Virginia 23665

HELICOPTER ROTOR LOADS USING MATCHED ASYMPTOTIC EXPANSIONS: USER'S MANUAL

By

G. Alvin Pierce
and
Anand R. Vaidyanathan

Prepared by

GEORGIA INSTITUTE OF TECHNOLOGY
SCHOOL OF AEROSPACE ENGINEERING
Atlanta, Georgia 30332

Prepared for

NATIONAL AERONAUTICS AND SPACE ADMINISTRATION

Langley Research Center
Contract NAS1-16817

CONTENTS

	Page
SUMMARY	1
INTRODUCTION	1
PROGRAM OUTLINE	3
DESCRIPTION OF INPUT	9
DESCRIPTION OF OUTPUT	12
EXAMPLES OF JOB ENTRY, INPUT DATA AND OUTPUT	13
REFERENCES	48
APPENDIX A Listing of Program ASYMP1	49
APPENDIX B Listing of Program ASYMP2	69

SUMMARY

Computer programs have been developed to implement the computational scheme arising from Van Holten's asymptotic method for calculating airloads on a helicopter rotor blade in forward flight, and a similar technique which is based on a discretized version of the method. The basic outlines of the two programs are presented, followed by separate descriptions of the input requirements and output format. Two examples illustrating job entry with appropriate input data and corresponding output are included. Appendices contain a sample table of lift coefficient data for the NACA 0012 airfoil and listings of the two programs.

INTRODUCTION

The computer programs described in this report were developed during the course of an evaluation of Van Holten's asymptotic method (ref. 1) for the calculation of airloads on a helicopter rotor blade in forward flight. The validity and computational feasibility of the approach were investigated (ref. 2), and numerical results for specific flight conditions were compared with corresponding experimental data and computations based on other analytical methods. Program ASYMP1 was written to implement the computational scheme of reference 1 (the relevant equations and expressions are given in ref. 2). As an extension of this investigation, the above computational scheme was made more efficient by discretizing the variation of the doublet strength distribution, $g(r_b, \Psi_b)$, utilizing both piecewise constant and piecewise quadratic representations for the spanwise variation. The details of the discretized scheme are presented in reference 3 and the corresponding computational method is applied in Program ASYMP2.

The general organization is similar for both programs, since the two schemes differ only in the manner in which the velocity induced by the blade pressure field is calculated. The basic unknown to be determined is the doublet strength function, $g(r_b, \Psi_b)$. Its solution is effected by a collocation technique. In the original scheme (ref. 1) this unknown function appears as a continuous modal representation for the spanwise variation and a finite Fourier series for the azimuth variation. In the discretized scheme the unknowns are the values of g at the midpoints of the spanwise segments, with a finite Fourier series for the azimuth variation of each. In either case, the solution reduces to the determination of the coefficients in the collocation representations, which is accomplished by setting up a system of simultaneous equations.

The main programs and the various subprograms will be discussed in the next section, but the general sequence of program steps is as below.

(1) Read and write input; define auxiliary parameters required for the computation.

(2) Start loop for collocation points.

(3) Test the tangential velocity U_T; if $U_T \leq (U_T)_{min}$, set up the condition for zero lift and go to the end of the collocation loop.

(4) If airfoil data tables are used, determine the lift curve slope for the current collocation point.

(5) Start loop for the number of blades and define the first azimuth interval.

(6) Compute the induced velocity contributions for the current interval and add to the corresponding coefficient matrix elements in the system of equations.

(7) Increment the azimuth interval; if the azimuth limit has been reached, go to the the next step; if not, go to Step 6.

(8) End loop for number of blades.

(9) End loop for collocation points.

(10) Set up the extra equations for the blade motion parameters.

(11) Solve system of equations and write solution.

(12) Compute and write output.

Some mention must be made of the way in which the airfoil data are used in the computational scheme. The basic equation to be set up at any collocation point is of the form

$$w_b(r_{bo}, \Psi_{bo}) = w_{ind} \tag{1}$$

where w_{ind} is the velocity induced by the pressure fields of all the blades and w_b the normal velocity due to blade motion at a collocation point (r_{bo}, Ψ_{bo}). This is rewritten as

$$\begin{aligned} w_b(r_{bo}, \Psi_{bo}) &= (w_{ind})^{2D} + \left[w_{ind} - (w_{ind})^{2D}\right] \\ &= (w_{ind})^{2D} + \Delta w \end{aligned} \tag{2}$$

where $(w_{ind})^{2D}$ is the induced velocity corresponding to a steady, two-dimensional flow. Accordingly, corrections based on airfoil data are only applied to this term and, after modification, equation (2) becomes

$$\begin{aligned} w_b(r_{bo}, \Psi_{bo}) &= (w_{ind})^{2D}_{mod} + \Delta w \\ &= \left[(w_{ind})^{2D}_{mod} - (w_{ind})^{2D}\right] + w_{ind} \end{aligned} \tag{3}$$

For steady, locally two-dimensional flow,

$$(w_{ind})^{2D} = -g(r_{bo}, \Psi_{bo}) / \rho U_T \tag{4}$$

At the local incidence and Mach number corresponding to the collocation point, the airfoil data are interpolated in the form of a locally linear relation given by

$$C_\ell = a\alpha + C_{\ell o}$$

To account for such a relation, the expression in equation (4) is modified as

$$(w_{ind})^{2D}_{mod} = -\frac{2\pi}{a}\,\frac{g(r_{bo}, \Psi_{bo})}{\rho U_T} - U_T\,\frac{C_{\ell o}}{a} \qquad (5)$$

Using equations (4) and (5) in equation (3), the modified form of the boundary condition is obtained as

$$w_b(r_{bo}, \Psi_{bo}) = \left[-\frac{(2\pi - a)}{a}\,\frac{g(r_{bo}, \Psi_{bo})}{\rho U_T} - U_T\,\frac{C_{\ell o}}{a}\right] + w_{ind} \qquad (6)$$

Comparing equations (1) and (6), it can be seen that the modification due to the airfoil data is purely an additive term that is easily incorporated into the basic computational scheme.

The next section presents an outline of the main program and the various subprograms for ASYMP1 and ASYMP2, listing the input and output of each subprogram along with a brief description of its function. The sections following this deal with descriptions of the input and output for the two programs, and samples of job entry with the corresponding output.

PROGRAM OUTLINE

Program ASYMP1

Main Program. - The program steps listed in the previous section will now be discussed in more detail.

(1) The details regarding input data and the format in which they are to be entered are given in the next section. The data include parameters describing rotor geometry, the flight condition and blade motion. Specification of the blade motion parameters (collective pitch, coning angle and the two first harmonic flapping coefficients) is optional. If they are not specified, they will be calculated as part of the solution by generating additional equilibrium equations. The input also includes the five spanwise locations of the collocation points, the normal and reduced azimuth intervals to be used for the numerical integration, the minimum value of the local onset velocity below which the zero lift condition is to be used and an integer specifying whether airfoil data are to be used. The program then writes the input data as part of the output and defines auxiliary quantities such as the induced velocity from simple momentum theory and certain factors occurring in the induced velocity contribution from the trajectory segment immediately adjacent to the collocation point.

(2) The collocation loop consists of an outer loop for the eleven equally spaced azimuth locations and an inner loop for the five spanwise locations.

(3) For the current collocation point, the local onset velocity (UT) is compared with the specified minimum value (UTMIN). If UT> UTMIN, the next step is executed. If not, the zero lift condition is set up and the next collocation point is taken up.

(4) If airfoil data are not used, this step is skipped. If they are used, the local values of $a/2\pi$ and C_{ℓ_o} are interpolated from the tables. The local values of Mach number (MLOC) and incidence (ALOC) are first defined. Subroutine TABSCH is called to find the position of MLOC and ALOC in the arrays MCL and ACL that were read as part of the input. The required values of $a/2\pi$ (SLCR) and C_{ℓ_o} (CLØ) are then determined by linear interpolation.

(5) As mentioned in reference 2, the near field has a square root singularity

corresponding to the leading edge, and this is dealt with by stopping the numerical integration just in front of the leading edge and accounting for the remainder analytically. Before starting the numerical integration, therefore, this contribution is entered into the coefficient matrix, A. The system of equations is of the form

$$Ax = B$$

where x is the array of unknown coefficients (A_{ij}, B_{ij}, eq. (9) of ref. 2). If UT <UTMIN, the zero lift condition is set up at this point.

In order to start the numerical integration, a loop for the number of blades is set up. For the current blade, Subroutine DMIN is called to determine the positions along the fluid particle trajectory at which it is directly over the blade, within a distance DMAX. Around these locations (stored in array PMIN), the reduced azimuth interval DP2 will be used. The first azimuth interval is defined with its ends at PB1 and PB2.

(6) For the current azimuth interval, a loop is set up for the 5-point Gauss-Chebyschev integration (p. 12 of ref. 2). With 55 unknown coefficients, 4 blade motion parameters and one right-hand side, there are 60 integrations to be carried out over each interval of azimuth. The corresponding functional values are sequentially obtained from function FUN2.

(7) PB1 and PB2 are incremented for the next azimuth interval. If the azimuth limit PLIM has been reached, the integration is stopped and the next blade is taken up. If not, the interval is tested to check if it includes one of the "close" locations stored in PMIN. If it does, the reduced azimuth interval is used.

(8) At the end of the loop for the number of blades, the terms in the blade normal velocity, $w_b(r_{bo}, \Psi_{bo})$, are entered in the corresponding coefficient matrix elements.

(9) At the end of the loop for the collocation points, certain spanwise integrals required for the total blade lift and the moment about the hub due to the lift are calculated (p. 42 of ref. 2).

(10) To close the system of equations, four additional equations are set up (eqs. (E8), (E9), (E10), (E11) of ref. 2). If the four blade motion parameters are specified in the input, these equations are replaced by equations of the form

$$\theta_o = (\theta_o)_{input}$$

$$a_o = (a_o)_{input}, \text{ etc.}$$

(11) The completed system of equations is solved by calling Subroutine GELIM. This is a library-supplied routine that uses the LU decomposition. The solution is overwritten on the vector B and the program prints out the values of the collocation coefficients and the blade motion parameters.

(12) With the basic solution complete, the program computes and prints out various output quantities in tabular form. The output format is described separately in a later section.

Subroutine DMIN. -

Input: MU(μ), LAM(λ), DB($\Delta\Psi_j$), RBØ(r_{bo}), PBØ(Ψ_{bo}), PLIM, DMAX

Output: I, P

Comments: This subroutine locates those azimuth positions along the fluid particle trajectory at which the particle is "close" to the j^{th} blade. The x_b axis is fixed to the blade and rotates with it (fig. 1 of ref. 2) so that the x_b coordinate along the trajectory periodically goes to zero whenever there is an intersection with the z_b axis. At some of these locations the particle may be too close to the blade (within a specified distance DMAX). These are the locations (I in number) that are returned in the array P. The routine locates the positions by scanning the trajectory with small azimuth increments checking for a change in sign of the x_b coordinate. When such a position is located, the distance from the blade is compared with DMAX.

Subroutine TRAJ. -

Input: RØ(R_o/R_1), AR(A), MU, LAM, RBØ, PBØ, DB, PB(Ψ_b)

Output: R(r), SX(sin χ), CX(cos χ), SHP(sinh Ψ), CHP(cosh Ψ), ST(sin θ), CT(cos θ), SHE(sinh η), CHE(cosh η), SP(sin ϕ), CP(cos ϕ) - returned through common block TRAJ1
ZS(z_b/s)

Comments: Given a point Ψ_b on the trajectory relative to the j^{th} blade, the corresponding coordinates in various coordinate systems are calculated. The coordinates (r,χ, z_b), (Ψ,θ,χ) and (η,ϕ) are respectively of the point in cylindrical, prolate spheriodal and plane elliptic coordinate systems.

Function FUN1. -

Input: RØ, AR, I
N(n), PI(π) - through common block MAIN1
R, SX, CX, SHP, CHP, ST, CT, SHE, CHE, SP, CP - through common block TRAJ1

Comments: The values of various functions required in FUN2 are calculated. Specifically, the six derivative expressions D_1 to D_6 (Appendix C of ref. 2) are returned for values of I from 1 to 6 in the input.

Function FUN2. -

Input: RØ, AR, TW(ϵ), MU, LAM, RBØ, PBØ, DP($\Delta\Psi_b$), DB,
X(Ψ_{bi}, p. 12, ref. 2), I
N, PI - through common block MAIN1

Comments: As described in Step 6 of the main program, the coefficient matrix elements corresponding to the various unknowns and the right-hand side require numerical integration, for which the necessary functional values are returned by function FUN2. Given the azimuth position X, Subroutine TRAJ and Function FUN1 are used to set up the relevant expressions. The value, I = 1, corresponds to the function multiplying A_{oo} (eq. (9) of ref. 2). The value, I = 2, corresponds to the function

multiplying A_{no} (n = 1,2,3,4). The values, I = 3,4,5,6,7, respectively correspond to the functions multiplying θ_o, a_o, a_1, b_1 and the right-hand side. The forms of these integrands are given in Appendix C of reference 2 as induced velocity coefficients. The nonintegral parts of these expressions are the result of analytical integration of the near field over a small interval $\Delta\Psi_b$ adjacent to the collocation point and are defined in the main program (Step 5). Over this interval, therefore, the near field contribution is skipped in Function FUN2.

Function FUN3. -

Input: RØ, AR, X, I

N, PI - through common block MAIN1

Comments: The expressions for the total blade lift and the moment about the hub due to the lift involve certain spanwise integrals (I^1_o, I^2_o, I^1_n, I^2_n (n = 1,2,3,4) see p. 42 of ref.2) and the corresponding integrands are set up in FUN3. The radial position, r_2/R_1, is X. The notation, I = 1,2,3,4, corresponds respectively to the integrals I^1_o, I^2_o, I^1_n, I^2_n.

Function PNM. -

Input: N(n), M(m), X(x)

Comments: This function generates the associated Legendre function $P^m_n(x)$ over the ranges $0 \le n \le 4$, $0 \le m \le 3$, $|x|<1$. Although the relevant recursive relations could be used, the function defines P^m_n explicitly in terms of x for all the above values of n and m (Appendix D of ref. 2).

Function QNM. -

Input: N, M, X

Comments: The associated Legendre function $Q^m_n(x)$ is calculated over the ranges $1 \le n \le 4$, $1 \le m \le 2$, $|x| > 1$. As listed in Appendix D of reference 2, the exact definitions are used for $|x| \le 3$ and asymptotic expansions are used for $|x| > 3$ to avoid the accumulation of roundoff error.

Subroutine TABSCH. -

Input: X, N, XT

Output: I1,I2, INT

Comments: This routine searches an array X, of dimension N, for the position of a value XT. If XT lies between X(I1) and X(I2), INT = 0. If XT is outside the range of X, the subroutine returns INT = -1 for XT < X(1) and INT = 1 for XT > X(N) (it is assumed that the elements in X are arranged in increasing order).

Program ASYMP2

Main Program. - Here again the previously listed program steps will be discussed

in more detail.

(1) This step is similar to Step 1 of Program ASYMP1. There are some changes in the entry of input data (described in the next section). Instead of spanwise collocation point locations, the program reads the spanwise locations at which the blade is divided into segments for discretization. Collocation points are located at the center of each segment. The integer, ISEL, specifies whether a piecewise constant or piecewise quadratic representation is to be used for the computation. Following the reading and writing of input data, some arrays that will be required later are set up. Arrays FX1 and FX2 contain the average values of the factors

$$\sqrt{\frac{1-x}{1+x}} \quad \text{and} \quad \left\{ \frac{(R_1 - R_0)}{2R_1} \quad \frac{\sqrt{1-x^2}}{A} \right\}$$

over each chordwise segment. These values will be used in the near field calculation. Array GF relates the endpoint and midpoint values for the spanwise segments in the piecewise quadratic representation. If $\rho_j (j = 1,\ldots 6)$ represent the ends of the 5 spanwise segments ($\rho_1 = R_o$, $\rho_6 = R_1$) and $r_j (j = 1,\ldots 5)$ the midpoints, then

$$g(\rho_i) = \sum_{j=1}^{5} (GF)_{ij}\, g(r_j) \qquad (i = 2,3,4,5)$$

(2-5) These steps are generally the same as the corresponding steps in Program ASYMP1.

(6) For the current azimuth interval, the slopes and intercepts for the linear approximations to $x_b(\Psi_b)$, $y_b(\Psi_b)$ and $r_b(\Psi_b)$ are defined as XBI, XBS, YBS, RBI, RBS. The far field contribution is computed using Subroutine FFINT. For computing the common part and near field contributions (which are both dependent on the local spanwise dipole strength) it is necessary to divide that part of the interval (PB1, PB2) which has the trajectory within the blade span into subintervals such that each subinterval has a trajectory wholly within one spanwise segment. This is done by calling Subroutine SUBIVL. The common part and near field contributions are then computed respectively by calling Subroutines CPINT and NFINT, summing the contributions over each subinterval.

(7-12) Comments on these steps are the same as for Program ASYMP1.

Subroutine SUBIVL. -

Input: RB1(r_{b1}), RB2(r_{b2}), PB1(Ψ_{b1}), PB2(Ψ_{b2}), R(ρ_j, j = 1,..6)

Output: I, P1, P2

Comments: As explained in Step 6 for the main program, the azimuth interval must be subdivided so that the trajectory segments within each subinterval lie completely within one spanwise segment. This is done by comparing the endpoints for each segment (ρ_j, ρ_{j+1} for the j^{th} segment) successively with the spanwise coordinates at the ends of the interval, r_{b1} and r_{b2}. The terms I, P1 and P2 are all arrays of dimension 5, corresponding to the number of spanwise segments. For the segment J, I(J) = 1 or 0 depending on whether a portion of the trajectory does or does not lie within that

segment. If I(J) = 1, the azimuth positions corresponding to the ends of that portion of the trajectory segment are stored in P1(J) and P2(J).

Subroutine NFINT. -

Input: P1, P2, X, ISEL

XI, XS, YS, RI, RS - through common block MAIN1

Output: T1, T2, T3

Comments: This subroutine computes various integral terms required for the near field contribution over the azimuth interval (P1, P2), with X being the chordwise location of a segment over which the surface pressure has been averaged. The terms T1, T2, T3 correspond to the terms n_0, n_1, n_2 in Appendix C of reference 3. For the piecewise constant representation, ISEL = 0, only T1 is used.

Subroutine CPINT. -

Input: P1, P2, ISEL

XI, XS, YS, RI, RS - through common block MAIN1

Output: T1, T2, T3

Comments: The terms required to set up the common part contribution over the azimuth interval (P1, P2) are calculated. The terms T1, T2, T3 correspond to C_1, C_2, C_3 in Appendix C of reference 3. For the case ISEL = 0, only the term T1 is relevant. The common part is singular at the collocation point, although the complete pressure field is regular due to the singularities in the far field and common part cancelling out in the limit. Since this has been established, when P2 = 0 (corresponding to the collocation point) the routine sets all the terms to zero.

Subroutine FFINT. -

Input: P1, P2, R, ISEL

XI, XS, YS, RI, RS - through common block MAIN1

Output: T1, T2, T3

Comments: This routine calculates the terms required for the far field contribution over the azimuth interval (P1, P2) with R being a boundary of one of the spanwise segments (ρ_j, j = 1, . . .6). The expressions for T1, T2, T3 are derived in Appendix C of reference 3. As pointed out above, the singularity in the far field gets cancelled out in the limit. However, unlike the common part, there is a finite residue left over after cancellation.

In addition to the subroutines listed in this section, both programs make use of Subroutine GELIM to solve the system of simultaneous equations. This routine uses direct Gaussian elimination with pivoting and details can be found in the Langley Computer Programming Manual.

DESCRIPTION OF INPUT

The input data required for the programs can be divided into two parts. The first consists of data pertaining to rotor geometry, flight condition, blade motion and some additional parameters relevant to the computational scheme. These are assumed to be a part of the INPUT file; that is, they must be entered after the job control statements when the job is submitted for execution. The second part consists of airfoil data (if required) and these are assumed to reside in a file called AFDATA which must therefore be available (if the data are to be used) when the job is executed. The format for the airfoil data is described separately following descriptions of the basic input for the two programs.

Program ASYMPI

The READ statements for the first part of the input are given below, followed by explanations of the data items.

```
READ (5,*) R , AR, NB, TW, MU, ALR, CT, MINF
READ (5,*) N1, N2, N3, N4
IF (N1. EQ. 1) READ (5,*) THC
IF (N2. EQ. 0) READ (5,*) GAMA
IF (N2. EQ. 1) READ (5,*) AØ
IF (N3. EQ. 1) READ (5,*) A1
IF (N4. EQ. 1) READ (5,*) B1
READ (5,*) (RBØ(I), I = 1, NSP)
READ (5,*) DP1D, DP2D, UTMIN, NAFD
```

Each READ statement corresponds to a line of data input. It may be noted that all the above statements specify free format for the data entry so that the different items in a single line of data can be entered in any convenient format, separated by commas.

RØ = root radius/tip radius

AR = aspect ratio

NB = number of blades (integer)

TW = built-in linear twist (ϵ , ref. 2)

= pitch angle at root minus pitch angle at tip

MU = forward speed/tip speed (floating point)

ALR = inclination of tip path plane to flight path, in degrees (forward tilt positive)

CT = rotor thrust coefficient = $T/\rho\,(\pi R_1^2)\,(\Omega R_1)^2$

MINF = Mach number corresponding to forward speed (note: this is used only for interpolating from airfoil data; if airfoil data are not used, this item is not needed and can be set to zero)

N1,N2,N3,N4 = integers associated with the four blade motion parameters (THC, AØ, A1, B1 respectively) - if a blade motion parameter is to be specified in the data, the corresponding integer is set to 1; if it is to be calculated by the program, the integer is set to 0.

THC = pitch angle at blade root in degrees

GAMA = coefficient representing blade flapping inertia

= 2π(air density) (chord) R_1^4/(mass moment of inertia of blade about flapping hinge), to be specified if the coning angle is to be calculated

AØ = blade coning angle

A1 = first harmonic longitudinal flapping coefficient

B1 = first harmonic lateral flapping coefficient

Note: Flapping angle = AØ - A1 cos Ψ_b - B1 sin Ψ_b

RBØ = array (of dimension 5) containing the spanwise locations of the collocation points, as fractions of the tip radius, e.g., 0.3, 0.5, 0.75, 0.85, 0.95

DP1D, DP2D = normal and reduced azimuth intervals to be used for the numerical integration (step 6 of the main program) in degrees, e.g., 15.0, 5.0

UTMIN = minimum value of local onset velocity at a collocation point for using the normal velocity boundary condition (see step 3), as a fraction of the tip speed

Note: Local onset velocity at (r_{bo}, Ψ_{bo}) = (r_{bo}/R_1 + μ sin Ψ_{bo})

NAFD = integer related to use of airfoil data:
NAFD = 1 - airfoil data used
NAFD = 0 - airfoil data not used

Program ASYMP2

Much of the input is identical to that for ASYMP1, as can be seen from the READ statements below.

```
READ (5,*) RØ, AR, NB, TW, MU, ALR, CT, MINF
READ (5,*) N1, N2, N3, N4
IF (N1. EQ. 1) READ (5,*) THC
IF (N2. EQ. 0) READ (5,*) GAMA
IF (N2. EQ. 1) READ (5,*) AØ
IF (N3. EQ. 1) READ (5,*) A1
```

```
IF (N4. EQ. 1) READ (5,*) B1
READ (5,*) (R (I), I = 2, 6)
READ (5,*) DP1D, DP2D, UTMIN, ISEL, NAFD
```

R = array (of dimension 6) containing the spanwise locations (as fractions of the tip radius) marking the division into 5 spanwise segments

(R (1) = RØ, R (6) = 1.0)

e.g., R (I), I = 2, 6 ⟶ 0.5, 0.7, 0.8, 0.9, 1.0

ISEL = integer specifying choice of piecewise representation:

ISEL = 0 - piecewise constant representation

ISEL = 1 - piecewise quadratic representation

DP1D and DP2D are the normal and reduced azimuth intervals, in degrees, over which the induced velocity contributions are summed. Typical values are 30.0 and 10.0, respectively.

Airfoil Data

The data used in this case (if NAFD = 1) consist of lift coefficients, over a range of incidences and Mach numbers.

NXL = number of Mach numbers in the table

NZL = number of incidences in the table

MCL = array containing the NXL Mach numbers (ascending order)

ACL = array containing the NZL incidences (ascending order)

CL = two-dimensional array (of dimension at least (NZL, NXL)) containing the lift coefficients

The format for data entry is as below.

Line 1: NXL, NZL (30X, 2I2 format)

Col 31 - 32 NXL

33 - 34 NZL

Lines 2(a),(b),. . . MCL (I), I = 1, NXL (7X, 9F7.0 format)

Col	8 - 14	MCL (1)
	15 - 21	MCL (2)
	.	
	.	
	.	
	64 - 70	MCL (9)

If NXL is greater than 9, additional lines are entered with the same format until all NXL entries have been made.

Lines 3(a), (b) . . . ACL (1), CL (1, I), I = 1, NXL (F7.0, 9F7.0 format)

Col	1 - 7	ACL (1)
	8 - 14	CL (1, 1)
	15 - 21	CL (1, 2)
	.	
	.	
	.	
	64 - 70	CL (1, 9)

If NXL is greater than 9, additional lines are entered as below (7X, 9F7.0 format).

Col	8 - 4	CL (1, 10)
	15 - 21	CL (1, 11)
	.	
	.	
	.	
	64 - 70	CL (1, 18)

Lines 4, 5, 6 . . . are identical in format to line 3 and contain the data with ACL (2), ACL (3) . . . ACL (NZL).

DESCRIPTION OF OUTPUT

The presentation of output is basically the same for Programs ASYMP1 and ASYMP2. Each page of output is formatted to fit within letter paper size (11" x 8.5"). Given below is a page-by-page description of the output.

Page 1 contains the input data and some auxiliary parameters, as well as the locations of the collocation points at which the normal velocity condition has been replaced by the zero lift condition. Page 2 contains the basic solution for the collocation coefficients used to express the variation of the dipole strength function $g(r_b, \Psi_b)$. These are 55 in number, corresponding to the coefficients in equation (9) of reference 2 for ASYMP1 and to the coefficients in equation (E3) of reference 3 for ASYMP2. Also presented on this page are the blade motion parameters (θ_o, a_o, a_1, b_1)

and the computed values of the rotor thrust coefficient and the moment coefficients about the rotor X - and Y - axes. Page 3 contains the distribution of sectional lift $/(\rho \Omega^2 R_1^3)$ in tabular form, at 5 radial and 24 azimuth locations. Page 4 contains a similar table of sectional lift$*R_1$/thrust per blade. Pages 5 and 6 contain tables of sectional pitching moment$/(\rho \Omega^2 R_1^4)$ and the center of pressure locations. Page 7 presents the variation with azimuth of the total blade lift, the moment due to lift about the hub and the radial location of the center of lift. Pages 8 - 15 present the distribution of surface pressure differential$/(\rho \Omega^2 R_1^2)$ at 5 spanwise and 10 chordwise locations, for every 15 degrees of azimuth.

EXAMPLES OF JOB ENTRY, INPUT DATA AND OUTPUT

The current versions of ASYMP1 and ASYMP2, written in Fortran IV, are intended to be run on the Cyber network at the Langley Research Center inasmuch as they use subroutine GELIM which is to be accessed from the subroutine library FTNMLIB. With appropriate changes, therefore, they can be run on any other system with a Fortran IV compiler. In order to compile and execute the programs, the basic sequence of job control statements would be as follows.

```
GET, ASYMP1 (or ASYMP2).
GET, AFDATA = airfoil datafile name. (if airfoil data are used)
MAP, OFF. (if load map is not required)
FTN, I = ASYMP1 (or ASYMP2), L = 0.
ATTACH, FTNMLIB/UN = LIBRARY.
LIBRARY, FTNMLIB.
LGO.
```

The control statements must be followed by the relevant input data. Examples are given below for two conditions: (A) data for program ASYMP1, applied to Case 1, $\mu = 0.29$ (see p. 16 of ref. 2) and (B) data for program ASYMP2, applied to Case 2, $\mu = 0.29$ using the piecewise quadratic representation. In each case the input data is followed by the corresponding output listing.

Example A

```
Line 1:  0.17, 5.43, 2, 0., 0.29, 6.7, 0.00394, 0.
Line 2:  0, 1, 0, 0
Line 3:  0.
Line 4:  0.3, 0.5, 0.75, 0.85, 0.95
Line 5:  15.0, 5.0, 0.1, 0
```

In the first line MINF has been set to zero since airfoil data are not going to be

used. The second line specifies that θ_o, a_1 and b_1 are to be computed while a_o will be input. Since this example involves a teetering rotor with no coning angle, the third line specifies $a_o = 0$.

```
ROOT RADIUS/TIP RADIUS=     .17000
ASPECT RATIO=    5.43000
NUMBER OF BLADES= 2
LINEAR TWIST(ROOT TO TIP)=    0.00000 DEGREES
FORWARD SPEED/TIP SPEED=     .29000
ROTOR INCIDENCE(FORWARD TILT POSITIVE)=    5.70000 DEGREES
FREESTREAM MACH NUMBER=    0.00000
THRUST COEFFICIENT=     .00394
CONING ANGLE=    0.00000 DEGREES
TOTAL INFLOW RATIO=     .04070
MINIMUM UT=     .10000(ZERO LIFT CONDITION APPLIED BELOW THIS VALUE)
NORMAL AZIMUTH INTERVAL=  15.00000 DEGREES
REDUCED AZIMUTH INTERVAL=    5.00000 DEGREES
AIRFOIL DATA TABLES NOT USED
R=     .600 PSI= 229.09100EGREES UT=     .081 ZERO LIFT CONDITION APPLIED
R=     .800 PSI= 261.81800EGREES UT=     .018 ZERO LIFT CONDITION APPLIED
R=     .900 PSI= 294.54500EGREES UT=     .036 ZERO LIFT CONDITION APPLIED
```

```
SOLUTION FOR COEFFICIENTS
-------------------------

(GO(I),I=1,NSP)

-.2o5oE-02 -.4578E-02 -.7425E-02 -.1972E-02 -.4996E-03

(GC(I,J),J=1,NHM),I=1,NSP)


-.2422E-03 -.4419E-03 -.1377E-03 -.1375E-03  .641oE-04
 .2011E-02 -.o358E-02 -.4901E-03  .1343E-02 -.2570E-03
-.4199E-05 -.1021E-02 -.3515E-03 -.4874E-03 -.9597E-04
 .2913E-03 -.5772E-03 -.1344E-03 -.1949E-03  .3887E-03
 .1011E-03 -.3411E-03  .1142E-03  .3015E-03 -.4o62E-03

(GS(I,J),J=1,NHM),I=1,NSP)


 .2957E-03  .1249E-03  .1927E-04 -.1278E-03 -.1251E-03
-.2556E-02  .o1o3E-03 -.3014E-02  .3499E-03  .7783E-03
-.4436E-03  .1166E-02 -.1548E-03 -.1594E-02 -.2o98E-03
 .9263E-03 -.3151E-03 -.1o13E-03  .2088E-04 -.4070E-03
 .3553E-03  .2c49E-03 -.4271E-03 -.2013E-05  .3877E-03

PITCH ANGLE AT BLADE ROOT=   7.69346DEGREES
CONING ANGLE=   0.00000 DEGREES
FLAPPING COEFFICIENT, A1=   4.27211 DEGREES
FLAPPING COEFFICIENT, B1=    .03698 DEGREES
COMPUTED THRUST COEFFICIENT= .3940E-02
COMPUTED MOMENT COEFFICIENT ABOUT ROTOR X-AXIS=-.3092E-16
COMPUTED MOMENT COEFFICIENT ABOUT ROTOR Y-AXIS= .3313E-17
```

TABLE 1 - SECTIONAL LIFT/((RHO)*(OMEGA**2)*(R1**3))

X/R1	.3000E+00	.5000E+00	.7500E+00	.8500E+00	.9500E+00
PSI					
0.0	.2249E-02	.6022E-02	.1818E-01	.2045E-01	.1520E-01
15.0	.1969E-02	.7424E-02	.1634E-01	.2047E-01	.1589E-01
30.0	.1864E-02	.6600E-02	.1565E-01	.1727E-01	.1319E-01
45.0	.1456E-02	.5513E-02	.1109E-01	.1213E-01	.9265E-02
60.0	.4532E-03	.3671E-02	.7571E-02	.8453E-02	.6733E-02
75.0	-.7856E-03	.1423E-02	.7249E-02	.8486E-02	.7113E-02
90.0	-.1522E-02	.4076E-03	.9650E-02	.1130E-01	.9429E-02
105.0	-.1247E-02	.1773E-02	.1257E-01	.1426E-01	.1159E-01
120.0	-.2901E-04	.3473E-02	.1491E-01	.1693E-01	.1270E-01
135.0	.1562E-02	.8581E-02	.1555E-01	.1692E-01	.1343E-01
150.0	.2731E-02	.9514E-02	.1663E-01	.1811E-01	.1448E-01
165.0	.2853E-02	.9504E-02	.1724E-01	.1914E-01	.1544E-01
180.0	.1906E-02	.8351E-02	.1672E-01	.1897E-01	.1542E-01
195.0	.5907E-03	.6853E-02	.1501E-01	.1744E-01	.1432E-01
210.0	-.1817E-03	.4394E-02	.1289E-01	.1548E-01	.1293E-01
225.0	-.1070E-03	.2997E-02	.1116E-01	.1392E-01	.1186E-01
240.0	.2586E-03	.1975E-02	.1005E-01	.1290E-01	.1118E-01
255.0	.1985E-03	.1867E-02	.9528E-02	.1240E-01	.1088E-01
270.0	-.2695E-03	.2456E-02	.9805E-02	.1274E-01	.1121E-01
285.0	-.3425E-03	.3135E-02	.1094E-01	.1397E-01	.1220E-01
300.0	.3837E-03	.3823E-02	.1244E-01	.1541E-01	.1328E-01
315.0	.1667E-02	.4965E-02	.1370E-01	.1633E-01	.1386E-01
330.0	.2600E-02	.6549E-02	.1485E-01	.1720E-01	.1426E-01
345.0	.2660E-02	.7798E-02	.1647E-01	.1869E-01	.1515E-01

TABLE 2 - SECTIONAL LIFT*R1/THRUST PER BLADE

R/R1:	.3000E+00	.5000E+00	.7500E+00	.8500E+00	.9500E+00
PSI					
0.0	.3635E+00	.1296E+01	.2937E+01	.3304E+01	.2617E+01
15.0	.3162E+00	.1200E+01	.2963E+01	.3303E+01	.2567E+01
30.0	.3011E+00	.1056E+01	.2528E+01	.2790E+01	.2131E+01
45.0	.2352E+00	.8907E+00	.1792E+01	.1960E+01	.1497E+01
60.0	.7322E-01	.5931E+00	.1223E+01	.1365E+01	.1088E+01
75.0	-.1269E+00	.2809E+00	.1171E+01	.1371E+01	.1149E+01
90.0	-.2499E+00	.6536E-01	.1559E+01	.1826E+01	.1523E+01
105.0	-.2016E+00	.3188E+00	.2081E+01	.2503E+01	.1873E+01
120.0	-.4668E-02	.8843E+00	.2345E+01	.2573E+01	.2052E+01
135.0	.2524E+00	.1387E+01	.2529E+01	.2736E+01	.2170E+01
150.0	.4412E+00	.1537E+01	.2687E+01	.2927E+01	.2340E+01
165.0	.4609E+00	.1374E+01	.2765E+01	.3092E+01	.2495E+01
180.0	.3080E+00	.1123E+01	.2702E+01	.3064E+01	.2491E+01
195.0	.9544E-01	.9134E+00	.2425E+01	.2819E+01	.2314E+01
210.0	-.2936E-01	.7100E+00	.2082E+01	.2502E+01	.2089E+01
225.0	-.1729E-01	.4843E+00	.1804E+01	.2250E+01	.1917E+01
240.0	.4179E-01	.3191E+00	.1524E+01	.2084E+01	.1807E+01
255.0	.3207E-01	.3017E+00	.1540E+01	.2004E+01	.1758E+01
270.0	-.4355E-01	.3968E+00	.1584E+01	.2058E+01	.1811E+01
285.0	-.6342E-01	.5066E+00	.1769E+01	.2257E+01	.1971E+01
300.0	.6200E-01	.6135E+00	.2010E+01	.2490E+01	.2146E+01
315.0	.2726E+00	.8023E+00	.2213E+01	.2646E+01	.2243E+01
330.0	.4202E+00	.1033E+01	.2400E+01	.2779E+01	.2307E+01
345.0	.4298E+00	.1260E+01	.2660E+01	.3020E+01	.2448E+01

TABLE 3 - SECTIONAL PITCHING MOMENT/(RHO*(OMEGA**2)*(R1**4))

(ABOUT QUARTER-CHORD)

R/R1:	.3000E+00	.5000E+00	.7500E+00	.8500E+00	.9500E+00
PSI					
0.0	.3331E-04	.2542E-05	-.5538E-04	-.1002E-03	-.2298E-03
15.0	.1672E-04	-.7630E-05	-.7253E-04	-.1155E-03	-.2375E-03
30.0	.7246E-05	-.1983E-04	-.7620E-04	-.1124E-03	-.2154E-03
45.0	-.7096E-05	-.3003E-04	-.8516E-04	-.9244E-04	-.1738E-03
60.0	-.5719E-05	-.2723E-04	-.4886E-04	-.6794E-04	-.1352E-03
75.0	.1632E-05	-.7376E-05	-.3588E-04	-.4907E-04	-.1120E-03
90.0	.1282E-04	.1792E-04	-.2453E-04	-.3469E-04	-.9739E-04
105.0	.2607E-04	.3153E-04	-.4036E-05	-.1921E-04	-.8011E-04
120.0	.3549E-04	.2903E-04	.1265E-04	-.2037E-05	-.6118E-04
135.0	.3279E-04	.2079E-04	.2701E-04	.8561E-05	-.5242E-04
150.0	.1503E-04	.1620E-04	.2583E-04	.5792E-05	-.6087E-04
165.0	-.5481E-05	.1209E-04	.1147E-04	-.3223E-05	-.8076E-04
180.0	-.2433E-04	.2639E-05	-.5972E-05	-.2559E-04	-.1013E-03
195.0	-.3545E-04	-.1797E-04	-.1975E-04	-.4064E-04	-.1175E-03
210.0	-.4468E-04	-.3135E-04	-.2998E-04	-.5221E-04	-.1298E-03
225.0	-.5260E-04	-.3211E-04	-.3742E-04	-.5977E-04	-.1381E-03
240.0	-.5087E-04	-.2389E-04	-.3902E-04	-.6153E-04	-.1412E-03
255.0	-.3203E-04	-.1409E-04	-.3229E-04	-.5747E-04	-.1411E-03
270.0	-.1019E-05	-.3647E-05	-.2095E-04	-.5139E-04	-.1433E-03
285.0	.2748E-04	.1047E-04	-.1238E-04	-.4766E-04	-.1499E-03
300.0	.4311E-04	.2554E-04	-.1083E-04	-.4746E-04	-.1580E-03
315.0	.4753E-04	.3238E-04	-.1348E-04	-.5084E-04	-.1662E-03
330.0	.4733E-04	.2698E-04	-.2109E-04	-.5965E-04	-.1800E-03
345.0	.4383E-04	.1435E-04	-.3533E-04	-.7747E-04	-.2041E-03

TABLE 4 - CENTER OF PRESSURE LOCATION FROM LEADING EDGE(FRACTION OF CHORD)

R/R1:	.3000E+00	.5000E+00	.7500E+00	.8500E+00	.9500E+00
PSI					
0.0	.3475E+00	.2522E+00	.2301E+00	.2179E+00	.1572E+00
15.0	.3056E+00	.2433E+00	.2241E+00	.2131E+00	.1522E+00
30.0	.2525E+00	.2304E+00	.2181E+00	.2074E+00	.1432E+00
45.0	.2181E+00	.2144E+00	.2116E+00	.2001E+00	.1473E+00
60.0	.1574E+00	.2014E+00	.2078E+00	.1974E+00	.1136E+00
75.0	.2364E+00	.2162E+00	.2176E+00	.2122E+00	.1470E+00
90.0	.1949E+00	.5376E+00	.2334E+00	.2298E+00	.1824E+00
105.0	.1133E+00	.3545E+00	.2458E+00	.2412E+00	.2048E+00
120.0	-.7755E+01	.2847E+00	.2557E+00	.2492E+00	.2185E+00
135.0	.3873E+00	.2658E+00	.2513E+00	.2533E+00	.2245E+00
150.0	.2884E+00	.2611E+00	.2602E+00	.2521E+00	.2225E+00
165.0	.2391E+00	.2593E+00	.2544E+00	.2472E+00	.2158E+00
180.0	.1655E+00	.2502E+00	.2477E+00	.2412E+00	.2070E+00
195.0	-.1426E+00	.2292E+00	.2414E+00	.2348E+00	.1963E+00
210.0	.1859E+01	.2033E+00	.2348E+00	.2279E+00	.1843E+00
225.0	.3456E+01	.1799E+00	.2281E+00	.2219E+00	.1738E+00
240.0	-.1037E+01	.1708E+00	.2246E+00	.2188E+00	.1674E+00
255.0	-.8056E+00	.2006E+00	.2278E+00	.2197E+00	.1651E+00
270.0	.2747E+00	.2403E+00	.2300E+00	.2236E+00	.1664E+00
285.0	-.2030E+00	.2713E+00	.2426E+00	.2277E+00	.1696E+00
300.0	.9851E+00	.2936E+00	.2446E+00	.2298E+00	.1722E+00
315.0	.4343E+00	.2929E+00	.2436E+00	.2298E+00	.1717E+00
330.0	.3691E+00	.2770E+00	.2407E+00	.2273E+00	.1675E+00
345.0	.3578E+00	.2520E+00	.2300E+00	.2229E+00	.1619E+00

TABLE 5 - TOTAL BLADE LIFT, MOMENT ABOUT HUB AND RADIAL CENTER OF LIFT

TOTAL BLADE LIFT/(RHO*(OMEGA**2)*(R1**4))
TOTAL BLADE LIFT/THRUST PER BLADE
MOMENT ABOUT HUB/(RHO*(OMEGA**2)*(R1**5))
RADIAL CENTER OF LIFT/R1

PSI	TOTAL BLADE LIFT		MOMENT ABOUT HUB	CENTER OF LIFT
0.0	.6859E-02	.1431E+01	.6376E-02	.7198E+00
15.0	.6657E-02	.1389E+01	.6261E-02	.7256E+00
30.0	.7424E-02	.1550E+01	.5353E-02	.7210E+00
45.0	.5458E-02	.8819E+00	.3885E-02	.7118E+00
60.0	.3642E-02	.5685E+00	.2553E-02	.7283E+00
75.0	.2858E-02	.4513E+00	.2300E-02	.8049E+00
90.0	.3379E-02	.5451E+00	.2862E-02	.8468E+00
105.0	.4807E-02	.7757E+00	.3876E-02	.8065E+00
120.0	.6483E-02	.1054E+01	.4870E-02	.7512E+00
135.0	.7800E-02	.1273E+01	.5536E-02	.7152E+00
150.0	.8590E-02	.1403E+01	.6113E-02	.7043E+00
165.0	.8721E-02	.1409E+01	.6215E-02	.7125E+00
180.0	.8036E-02	.1298E+01	.5875E-02	.7311E+00
195.0	.6911E-02	.1117E+01	.5202E-02	.7526E+00
210.0	.5764E-02	.9313E+00	.4449E-02	.7720E+00
225.0	.4888E-02	.7898E+00	.3833E-02	.7842E+00
240.0	.4362E-02	.7047E+00	.3436E-02	.7879E+00
255.0	.4175E-02	.6746E+00	.3291E-02	.7882E+00
270.0	.4359E-02	.7044E+00	.3437E-02	.7884E+00
285.0	.4925E-02	.7959E+00	.3848E-02	.7812E+00
300.0	.5752E-02	.9295E+00	.4373E-02	.7602E+00
315.0	.6652E-02	.1075E+01	.4875E-02	.7328E+00
330.0	.7527E-02	.1216E+01	.5370E-02	.7135E+00
345.0	.8334E-02	.1347E+01	.5927E-02	.7112E+00

TABLE 6 -SURFACE PRESSURE DIFFERENTIAL/(RHO*(OMEGA**2)*(R1**2))

AZIMUTH ANGLE= 0.0 DEGREES

R/R1:	.3000E+00	.5000E+00	.7500E+00	.8500E+00	.9500E+00
X/C					
.05000	.2681E-01	.1438E+00	.3514E+00	.4115E+00	.3868E+00
.10000	.2088E-01	.9940E-01	.2386E+00	.2772E+00	.2519E+00
.20000	.1698E-01	.6073E-01	.1547E+00	.1769E+00	.1493E+00
.30000	.1519E-01	.5121E-01	.1148E+00	.1291E+00	.9999E-01
.40000	.1390E-01	.4120E-01	.8925E-01	.9852E-01	.6887E-01
.50000	.1271E-01	.3370E-01	.7054E-01	.7644E-01	.4585E-01
.70000	.1008E-01	.2209E-01	.4296E-01	.4436E-01	.1775E-01
.90000	.6102E-02	.1126E-01	.2004E-01	.1922E-01	.1503E-02
.95000	.4398E-02	.7765E-02	.1344E-01	.1253E-01	-.5220E-03
.99000	.2016E-02	.3416E-02	.5745E-02	.5183E-02	-.9029E-03

AZIMUTH ANGLE= 15.0 DEGREES

R/R1:	.3000E+00	.5000E+00	.7500E+00	.8500E+00	.9500E+00
X/C					
.05000	.2638E-01	.1366E+00	.3013E+00	.3182E+00	.3939E+00
.10000	.2079E-01	.9370E-01	.2442E+00	.2807E+00	.2493E+00
.20000	.1540E-01	.6138E-01	.1569E+00	.1778E+00	.1468E+00
.30000	.1288E-01	.4972E-01	.1154E+00	.1283E+00	.9742E-01
.40000	.1113E-01	.3998E-01	.8854E-01	.9760E-01	.6633E-01
.50000	.9739E-02	.2978E-01	.6950E-01	.7497E-01	.4440E-01
.70000	.7220E-02	.1845E-01	.4134E-01	.4256E-01	.1572E-01
.90000	.4166E-02	.9437E-02	.1871E-01	.1786E-01	.3215E-03
.95000	.2980E-02	.5487E-02	.1242E-01	.1150E-01	-.1345E-02
.99000	.1360E-02	.2899E-02	.5257E-02	.4699E-02	-.1259E-02

AZIMUTH ANGLE= 30.0 DEGREES

R/R1:	.3000E+00	.5000E+00	.7500E+00	.8500E+00	.9500E+00
X/C					
.05000	.3292E-01	.1265E+00	.3139E+00	.3585E+00	.3257E+00
.10000	.2281E-01	.8587E-01	.2112E+00	.2397E+00	.2105E+00
.20000	.1532E-01	.5554E-01	.1345E+00	.1506E+00	.1226E+00
.30000	.1174E-01	.4106E-01	.9792E-01	.1081E+00	.8019E-01
.40000	.9406E-02	.3179E-01	.7463E-01	.8106E-01	.5352E-01
.50000	.7661E-02	.2503E-01	.5773E-01	.6156E-01	.3481E-01
.70000	.4987E-02	.1517E-01	.3345E-01	.3396E-01	.1068E-01
.90000	.2565E-02	.7177E-02	.1463E-01	.1366E-01	-.1452E-02
.95000	.1786E-02	.4570E-02	.9612E-02	.8663E-02	-.2384E-02
.99000	.7998E-03	.2122E-02	.4027E-02	.3482E-02	-.1530E-02

AZIMUTH ANGLE= 45.0 DEGREES

R/R1:	.3000E+00	.5000E+00	.7500E+00	.8500E+00	.9500E+00
X/C					
.05000	.2651E-01	.1113E+00	.2265E+00	.2567E+00	.2376E+00
.10000	.1426E-01	.7471E-01	.1517E+00	.1708E+00	.1525E+00
.20000	.1221E-01	.4724E-01	.9564E-01	.1062E+00	.9719E-01
.30000	.8804E-02	.3410E-01	.6883E-01	.7526E-01	.5569E-01
.40000	.6627E-02	.2574E-01	.5179E-01	.5565E-01	.3591E-01
.50000	.5054E-02	.1970E-01	.3950E-01	.4158E-01	.2212E-01
.70000	.2559E-02	.1115E-01	.2214E-01	.2200E-01	.4709E-02
.90000	.1278E-02	.4790E-02	.9294E-02	.8295E-02	-.3110E-02
.95000	.8563E-03	.3145E-02	.6034E-02	.5143E-02	-.3237E-02
.99000	.3543E-03	.1327E-02	.2506E-02	.2021E-02	-.1877E-02

AZIMUTH ANGLE= 60.0 DEGREES

R/R1:	.3000E+00	.5000E+00	.7500E+00	.8500E+00	.9500E+00
X/C					
.05000	.9764E-02	.7709E-01	.1502E+00	.1500E+00	.1757E+00
.10000	.5812E-02	.5129E-01	.1043E+00	.1195E+00	.1123E+00
.20000	.3506E-02	.3195E-01	.6542E-01	.7393E-01	.5347E-01
.30000	.2264E-02	.2253E-01	.4658E-01	.5210E-01	.3987E-01
.40000	.1417E-02	.1563E-01	.3485E-01	.3820E-01	.2508E-01
.50000	.5398E-03	.1240E-01	.2634E-01	.2837E-01	.1481E-01
.70000	.1572E-03	.5508E-02	.1446E-01	.1473E-01	.2082E-02
.90000	.2469E-05	.2530E-02	.5916E-02	.5420E-02	-.3143E-02
.95000	.1237E-04	.1597E-02	.3815E-02	.3339E-02	-.2979E-02
.99000	.2250E-04	.5471E-03	.1578E-02	.1308E-02	-.1637E-02

AZIMUTH ANGLE= 75.0 DEGREES

R/R1:	.3000E+00	.5000E+00	.7500E+00	.8500E+00	.9500E+00
X/C					
.05000	-.1506E-01	.2824E-01	.1499E+00	.1736E+00	.1725E+00
.10000	-.1075E-01	.1889E-01	.9809E-01	.1163E+00	.1115E+00
.20000	-.7196E-02	.1183E-01	.6236E-01	.7341E-01	.6457E-01
.30000	-.5548E-02	.8430E-02	.4536E-01	.5296E-01	.4207E-01
.40000	-.4489E-02	.6277E-02	.3454E-01	.3997E-01	.2737E-01
.50000	-.3682E-02	.4745E-02	.2670E-01	.3060E-01	.1796E-01
.70000	-.2351E-02	.2665E-02	.1547E-01	.1728E-01	.5415E-02
.90000	-.1040E-02	.1219E-02	.6765E-02	.7270E-02	-.5903E-03
.95000	-.6535E-03	.8392E-03	.4437E-02	.4702E-02	-.1016E-02
.99000	-.2468E-03	.3796E-03	.1854E-02	.1935E-02	-.6767E-03

AZIMUTH ANGLE= 90.0 DEGREES

R/R1:	.3000E+00	.5000E+00	.7500E+00	.8500E+00	.9500E+00
X/C					
.05000	-.3343E-01	-.7087E-03	.1859E+00	.2200E+00	.2085E+00
.10000	-.2228E-01	.5513E-03	.1264E+00	.1492E+00	.1371E+00
.20000	-.1395E-01	.1543E-02	.8239E-01	.9668E-01	.8295E-01
.30000	-.1000E-01	.2179E-02	.6153E-01	.7179E-01	.5691E-01
.40000	-.7494E-02	.2490E-02	.4624E-01	.5593E-01	.4046E-01
.50000	-.5668E-02	.2667E-02	.3847E-01	.4432E-01	.2982E-01
.70000	-.3018E-02	.2711E-02	.2387E-01	.2711E-01	.1334E-01
.90000	-.1027E-02	.2034E-02	.1128E-01	.1261E-01	.3937E-02
.95000	-.5757E-03	.1613E-02	.7550E-02	.8404E-02	.2207E-02
.99000	-.1847E-03	.6001E-03	.3203E-02	.3552E-02	.7842E-03

AZIMUTH ANGLE=105.0 DEGREES

R/R1:	.3000E+00	.5000E+00	.7500E+00	.8500E+00	.9500E+00
X/C					
.05000	-.3381E-01	.2258E-01	.2329E+00	.2682E+00	.2424E+00
.10000	-.2168E-01	.1748E-01	.1599E+00	.1835E+00	.1617E+00
.20000	-.1245E-01	.1414E-01	.1062E+00	.1210E+00	.1011E+00
.30000	-.8024E-02	.1254E-01	.8083E-01	.9152E-01	.7213E-01
.40000	-.5245E-02	.1152E-01	.6462E-01	.7267E-01	.5378E-01
.50000	-.3287E-02	.1072E-01	.5258E-01	.5873E-01	.4056E-01
.70000	-.7219E-03	.8759E-02	.3405E-01	.3747E-01	.2208E-01
.90000	.5618E-03	.5948E-02	.1691E-01	.1826E-01	.8734E-02
.95000	.6030E-03	.4962E-02	.1150E-01	.1234E-01	.5516E-02
.99000	.3884E-03	.1883E-02	.4951E-02	.5278E-02	.2211E-02

AZIMUTH ANGLE=120.0 DEGREES

R/R1:	.3000E+00	.5000E+00	.7500E+00	.8500E+00	.9500E+00
X/C					
.05000	-.1558E-01	.5798E-01	.2597E+00	.2920E+00	.2578E+00
.10000	-.8507E-02	.6244E-01	.1797E+00	.2010E+00	.1737E+00
.20000	-.2859E-02	.4410E-01	.1211E+00	.1343E+00	.1112E+00
.30000	-.1047E-03	.3559E-01	.9351E-01	.1028E+00	.8162E-01
.40000	.1573E-02	.3001E-01	.7581E-01	.8267E-01	.6279E-01
.50000	.2662E-02	.2574E-01	.6256E-01	.6764E-01	.4903E-01
.70000	.3686E-02	.1848E-01	.4173E-01	.4428E-01	.2881E-01
.90000	.3100E-02	.1029E-01	.2148E-01	.2221E-01	.1239E-01
.95000	.2412E-02	.7250E-02	.1478E-01	.1513E-01	.7960E-02
.99000	.1188E-02	.3242E-02	.6450E-02	.6528E-02	.3203E-02

AZIMUTH ANGLE=135.0 DEGREES

R/R1:	.3000E+00	.5000E+00	.7500E+00	.8500E+00	.9500E+00
X/C					
.05000	.1496E-01	.1488E+00	.2742E+00	.3059E+00	.2696E+00
.10000	.1205E-01	.1035E+00	.1906E+00	.2113E+00	.1827E+00
.20000	.1070E-01	.7098E-01	.1295E+00	.1421E+00	.1184E+00
.30000	.1014E-01	.5572E-01	.1008E+00	.1095E+00	.8806E-01
.40000	.9661E-02	.4587E-01	.8236E-01	.8853E-01	.6976E-01
.50000	.9185E-02	.3841E-01	.6847E-01	.7293E-01	.5451E-01
.70000	.7794E-02	.2634E-01	.4536E-01	.4832E-01	.3298E-01
.90000	.5069E-02	.1393E-01	.2432E-01	.2496E-01	.1449E-01
.95000	.3736E-02	.9653E-02	.1684E-01	.1681E-01	.9313E-02
.99000	.1753E-02	.4242E-02	.7407E-02	.7261E-02	.3717E-02

AZIMUTH ANGLE=150.0 DEGREES

R/R1:	.3000E+00	.5000E+00	.7500E+00	.8500E+00	.9500E+00
X/C					
.05000	.4265E-01	.1567E+00	.2922E+00	.3287E+00	.2923E+00
.10000	.3046E-01	.1150E+00	.2030E+00	.2269E+00	.1978E+00
.20000	.2173E-01	.7893E-01	.1379E+00	.1523E+00	.1279E+00
.30000	.1761E-01	.6149E-01	.1071E+00	.1172E+00	.9490E-01
.40000	.1490E-01	.5125E-01	.8730E-01	.9468E-01	.7385E-01
.50000	.1279E-01	.4177E-01	.7245E-01	.7781E-01	.5835E-01
.70000	.9211E-02	.2924E-01	.4887E-01	.5134E-01	.3501E-01
.90000	.5168E-02	.1473E-01	.2554E-01	.2597E-01	.1519E-01
.95000	.3682E-02	.1020E-01	.1765E-01	.1774E-01	.9724E-02
.99000	.1656E-02	.4478E-02	.7770E-02	.7678E-02	.3862E-02

AZIMUTH ANGLE=165.0 DEGREES

R/R1:	.3000E+00	.5000E+00	.7500E+00	.8500E+00	.9500E+00
X/C					
.05000	.5396E-01	.1492E+00	.3090E+00	.3529E+00	.3165E+00
.10000	.3692E-01	.1036E+00	.2137E+00	.2427E+00	.2132E+00
.20000	.2426E-01	.7029E-01	.1436E+00	.1618E+00	.1364E+00
.30000	.1821E-01	.5454E-01	.1108E+00	.1236E+00	.9996E-01
.40000	.1429E-01	.4436E-01	.8953E-01	.9913E-01	.7576E-01
.50000	.1138E-01	.3671E-01	.7376E-01	.8086E-01	.5978E-01
.70000	.7010E-02	.2463E-01	.4891E-01	.5253E-01	.3475E-01
.90000	.3300E-02	.1235E-01	.2506E-01	.2610E-01	.1454E-01
.95000	.2221E-02	.8912E-02	.1724E-01	.1773E-01	.9209E-02
.99000	.9555E-03	.3934E-02	.7534E-02	.7631E-02	.3628E-02

AZIMUTH ANGLE=180.0 DEGREES

R/R1:	.3000E+00	.5000E+00	.7500E+00	.8500E+00	.9500E+00
X/C					
.05000	.4347E-01	.1250E+00	.3064E+00	.3554E+00	.3234E+00
.10000	.2e62E-01	.8e30E-01	.2108E+00	.2441E+00	.21e7E+00
.20000	.1727E-01	.5773E-01	.1405E+00	.1613E+00	.1369E+00
.30000	.1172E-01	.4414E-01	.1072E+00	.1222E+00	.9899E-01
.40000	.2163E-02	.3536E-01	.8686E-01	.9706E-01	.7485E-01
.50000	.5804E-02	.2880E-01	.6994E-01	.7843E-01	.5729E-01
.70000	.2179E-02	.1873E-01	.4e39E-01	.4992E-01	.3190E-01
.90000	.2841E-03	.9517E-02	.2271E-01	.2421E-01	.1249E-01
.95000	.4670E-04	.5870E-02	.1521E-01	.1633E-01	.7714E-02
.99000	-.3237E-04	.2905E-02	.6737E-02	.6980E-02	.2949E-02

AZIMUTH ANGLE=195.0 DEGREES

R/R1:	.3000E+00	.5000E+00	.7500E+00	.8500E+00	.9500E+00
X/C					
.05000	.2331E-01	.1085E+00	.2e00E+00	.3341E+00	.3099E+00
.10000	.1407E-01	.7382E-01	.1919E+00	.2279E+00	.2064E+00
.20000	.6612E-02	.4773E-01	.1267E+00	.1492E+00	.1289E+00
.30000	.2817E-02	.3254E-01	.9577E-01	.1120E+00	.9186E-01
.40000	.3849E-03	.2754E-01	.7391E-01	.8e06E-01	.6834E-01
.50000	-.1278E-02	.2153E-01	.5118E-01	.7040E-01	.5130E-01
.70000	-.3009E-02	.1299E-01	.3853E-01	.4377E-01	.2704E-01
.90000	-.2564E-02	.5022E-02	.1e97E-01	.2068E-01	.9476E-02
.95000	-.2020E-02	.4038E-02	.1288E-01	.1360E-01	.5526E-02
.99000	-.9423E-03	.1743E-02	.5508E-02	.5849E-02	.1944E-02

AZIMUTH ANGLE=210.0 DEGREES

R/R1:	.3000E+00	.5000E+00	.7500E+00	.8500E+00	.9500E+00
X/C					
.05000	.1260E-01	.9074E-01	.2450E+00	.3026E+00	.2892E+00
.10000	.6164E-02	.5083E-01	.1672E+00	.2055E+00	.1914E+00
.20000	.5031E-03	.3824E-01	.1094E+00	.1336E+00	.1179E+00
.30000	-.2363E-02	.2730E-01	.8183E-01	.9901E-01	.8271E-01
.40000	-.4259E-02	.2025E-01	.6415E-01	.7703E-01	.6038E-01
.50000	-.5460E-02	.1513E-01	.5111E-01	.6086E-01	.4428E-01
.70000	-.6321E-02	.7942E-02	.3150E-01	.3682E-01	.2172E-01
.90000	-.4639E-02	.2993E-02	.1500E-01	.1677E-01	.6369E-02
.95000	-.3426E-02	.1883E-02	.1011E-01	.1109E-01	.3315E-02
.99000	-.1573E-02	.7699E-03	.4347E-02	.4652E-02	.9490E-03

AZIMUTH ANGLE=225.0 DEGREES

R/R1:	.3000E+00	.5000E+00	.7500E+00	.8500E+00	.9500E+00
X/C					
.05000	.1736E-01	.6925E-01	.2155E+00	.2769E+00	.2721E+00
.10000	.9027E-02	.4328E-01	.1471E+00	.1873E+00	.1791E+00
.20000	.1984E-02	.2048E-01	.9543E-01	.1206E+00	.1089E+00
.30000	-.1768E-02	.1324E-01	.7073E-01	.8880E-01	.7515E-01
.40000	-.4068E-02	.1292E-01	.5487E-01	.6643E-01	.5375E-01
.50000	-.5610E-02	.9070E-02	.4320E-01	.5349E-01	.3841E-01
.70000	-.6861E-02	.3889E-02	.2598E-01	.3153E-01	.1733E-01
.90000	-.5233E-02	.9214E-03	.1169E-01	.1385E-01	.3975E-02
.95000	-.3913E-02	.4695E-03	.7928E-02	.9043E-02	.1675E-02
.99000	-.1824E-02	.1619E-03	.3375E-02	.3749E-02	.2516E-03

AZIMUTH ANGLE=240.0 DEGREES

R/R1:	.3000E+00	.5000E+00	.7500E+00	.8500E+00	.9500E+00
X/C					
.05000	.2374E-01	.4811E-01	.1969E+00	.2587E+00	.2599E+00
.10000	.1362E-01	.2861E-01	.1336E+00	.1748E+00	.1705E+00
.20000	.5343E-02	.1740E-01	.8634E-01	.1121E+00	.1027E+00
.30000	.1089E-02	.1181E-01	.6373E-01	.8221E-01	.7011E-01
.40000	-.1548E-02	.9149E-02	.4920E-01	.6305E-01	.4941E-01
.50000	-.3514E-02	.8499E-02	.3851E-01	.4902E-01	.3462E-01
.70000	-.5379E-02	.1980E-02	.2281E-01	.2848E-01	.1461E-01
.90000	-.4509E-02	.2151E-03	.1019E-01	.1223E-01	.2600E-02
.95000	-.3442E-02	.4432E-04	.5740E-02	.7936E-02	.7710E-03
.99000	-.1638E-02	.5244E-05	.2846E-02	.3259E-02	-.1080E-03

AZIMUTH ANGLE=255.0 DEGREES

R/R1:	.3000E+00	.5000E+00	.7500E+00	.8500E+00	.9500E+00
X/C					
.05000	.1321E-01	.3753E-01	.1847E+00	.2480E+00	.2544E+00
.10000	.6996E-02	.2544E-01	.1256E+00	.1677E+00	.1668E+00
.20000	.3893E-02	.1621E-01	.8164E-01	.1078E+00	.1003E+00
.30000	.1210E-02	.1159E-01	.6056E-01	.7914E-01	.6827E-01
.40000	-.5749E-03	.8529E-02	.4702E-01	.6079E-01	.4796E-01
.50000	-.1842E-02	.6247E-02	.3701E-01	.4733E-01	.3345E-01
.70000	-.3233E-02	.3027E-02	.2219E-01	.2758E-01	.1384E-01
.90000	-.2852E-02	.1003E-02	.1008E-01	.1190E-01	.2185E-02
.95000	-.2195E-02	.6236E-03	.6702E-02	.7730E-02	.4779E-03
.99000	-.1049E-02	.2590E-03	.2847E-02	.3184E-02	-.2406E-03

AZIMUTH ANGLE=270.0 DEGREES

R/R1: X/C	.3000E+00	.5000E+00	.7500E+00	.8500E+00	.9500E+00
.05000	-.5900E-02	.4472E-01	.1851E+00	.2517E+00	.2621E+00
.10000	-.3552E-02	.3112E-01	.1266E+00	.1706E+00	.1720E+00
.20000	-.1909E-02	.2101E-01	.8325E-01	.1102E+00	.1038E+00
.30000	-.1301E-02	.1605E-01	.6252E-01	.8142E-01	.7100E-01
.40000	-.1055E-02	.1274E-01	.4913E-01	.6293E-01	.5019E-01
.50000	-.9711E-03	.1019E-01	.3920E-01	.4932E-01	.3528E-01
.70000	-.9386E-03	.6227E-02	.2425E-01	.2963E-01	.1496E-01
.90000	-.6851E-03	.2869E-02	.1149E-01	.1292E-01	.2566E-02
.95000	-.4964E-03	.1928E-02	.7750E-02	.8471E-02	.6641E-03
.99000	-.2146E-03	.8353E-03	.3339E-02	.3524E-02	-.2071E-03

AZIMUTH ANGLE=285.0 DEGREES

R/R1: X/C	.3000E+00	.5000E+00	.7500E+00	.8500E+00	.9500E+00
.05000	-.1952E-01	.5190E-01	.2025E+00	.2726E+00	.2833E+00
.10000	-.1111E-01	.3699E-01	.1391E+00	.1852E+00	.1862E+00
.20000	-.4563E-02	.2417E-01	.9231E-01	.1203E+00	.1128E+00
.30000	-.1557E-02	.2097E-01	.8999E-01	.8937E-01	.7752E-01
.40000	.1710E-03	.1747E-01	.5557E-01	.6951E-01	.5515E-01
.50000	.1210E-02	.1469E-01	.4482E-01	.5437E-01	.3911E-01
.70000	.2091E-02	.9990E-02	.2842E-01	.3308E-01	.1712E-01
.90000	.1762E-02	.5175E-02	.1386E-01	.1499E-01	.3403E-02
.95000	.1368E-02	.3573E-02	.9433E-02	.9903E-02	.1169E-02
.99000	.6780E-03	.1573E-02	.4097E-02	.4157E-02	-.2384E-04

AZIMUTH ANGLE=300.0 DEGREES

R/R1: X/C	.3000E+00	.5000E+00	.7500E+00	.8500E+00	.9500E+00
.05000	-.1118E-01	.5853E-01	.2292E+00	.2989E+00	.3055E+00
.10000	-.4376E-02	.4249E-01	.1576E+00	.2033E+00	.2009E+00
.20000	.1265E-02	.3103E-01	.1048E+00	.1324E+00	.1217E+00
.30000	.3960E-02	.2565E-01	.7973E-01	.9861E-01	.8372E-01
.40000	.5445E-02	.2198E-01	.6352E-01	.7695E-01	.5961E-01
.50000	.6214E-02	.1900E-01	.5143E-01	.6097E-01	.4234E-01
.70000	.6277E-02	.1367E-01	.3289E-01	.3710E-01	.1876E-01
.90000	.4342E-02	.7532E-02	.1619E-01	.1704E-01	.4078E-02
.95000	.3216E-02	.5290E-02	.1103E-01	.1131E-01	.1629E-02
.99000	.1510E-02	.2365E-02	.4784E-02	.4766E-02	.1869E-03

AZIMUTH ANGLE=315.0 DEGREES

R/R1:	.3000E+00	.5000E+00	.7500E+00	.8500E+00	.9500E+00
X/C					
.00000	.1134E-01	.7637E-01	.2536E+00	.3178E+00	.3188E+00
.10000	.1139E-01	.5515E-01	.1742E+00	.2181E+00	.2094E+00
.20000	.1219E-01	.4004E-01	.1156E+00	.1406E+00	.1265E+00
.30000	.1266E-01	.3293E-01	.8775E-01	.1046E+00	.8501E-01
.40000	.1271E-01	.2812E-01	.6982E-01	.8161E-01	.6134E-01
.50000	.1239E-01	.2431E-01	.5647E-01	.6463E-01	.4331E-01
.70000	.1061E-01	.1755E-01	.3604E-01	.3934E-01	.1891E-01
.90000	.6542E-02	.9760E-02	.1769E-01	.1810E-01	.4038E-02
.95000	.4796E-02	.6877E-02	.1203E-01	.1203E-01	.1618E-02
.99000	.2191E-02	.3083E-02	.5207E-02	.5075E-02	.2055E-03

AZIMUTH ANGLE=330.0 DEGREES

R/R1:	.3000E+00	.5000E+00	.7500E+00	.8500E+00	.9500E+00
X/C					
.00000	.2518E-01	.1075E+00	.2776E+00	.3362E+00	.3313E+00
.10000	.2292E-01	.7618E-01	.1901E+00	.2291E+00	.2171E+00
.20000	.1981E-01	.5353E-01	.1259E+00	.1477E+00	.1303E+00
.30000	.1845E-01	.4293E-01	.9478E-01	.1095E+00	.8850E-01
.40000	.1735E-01	.3583E-01	.7503E-01	.8497E-01	.6220E-01
.50000	.1618E-01	.3035E-01	.6039E-01	.6699E-01	.4341E-01
.70000	.1311E-01	.2122E-01	.3826E-01	.4039E-01	.1821E-01
.90000	.7921E-02	.1147E-01	.1859E-01	.1840E-01	.3305E-02
.95000	.5674E-02	.8219E-02	.1262E-01	.1220E-01	.1046E-02
.99000	.2572E-02	.3558E-02	.5454E-02	.5137E-02	-.6754E-04

AZIMUTH ANGLE=345.0 DEGREES

R/R1:	.3000E+00	.5000E+00	.7500E+00	.8500E+00	.9500E+00
X/C					
.00000	.3043E-01	.1353E+00	.3123E+00	.3704E+00	.3573E+00
.10000	.2414E-01	.9443E-01	.2131E+00	.2504E+00	.2333E+00
.20000	.2018E-01	.6456E-01	.1395E+00	.1610E+00	.1391E+00
.30000	.1841E-01	.5041E-01	.1044E+00	.1184E+00	.9387E-01
.40000	.1707E-01	.4122E-01	.8201E-01	.9121E-01	.6525E-01
.50000	.1577E-01	.3429E-01	.6547E-01	.7133E-01	.4495E-01
.70000	.1266E-01	.2310E-01	.4074E-01	.4225E-01	.1791E-01
.90000	.7653E-02	.1206E-01	.1950E-01	.1884E-01	.2578E-02
.95000	.5497E-02	.8355E-02	.1318E-01	.1240E-01	.2410E-03
.99000	.2504E-02	.3685E-02	.5677E-02	.5187E-02	-.4990E-03

Example B

Line 1: 0.16, 17.2, 4, 7., 0.29, 6.1, 0.0057, 0.

Line 2: 0, 0, 0, 0

Line 3: 9.6

Line 4: 0.5, 0.7, 0.8, 0.9, 1.0

Line 5: 30.0, 10.0, 0.1, 1, 0

```
ROOT RADIUS/TIP RADIUS= R0/R1 =     .16000

ASPECT RATIO=  17.20000

NUMBER OF BLADES= 4

LINEAR TWIST (ROOT TO TIP) =    7.00000 DEGREES

FORWARD SPEED/TIP SPEED=     .24000

ROTOR INCIDENCE (FORWARD TILT POSITIVE) =    6.10000 DEGREES

FREESTREAM MACH NUMBER=    0.00000

THRUST COEFFICIENT=     .00570

FLAPPING INERTIA COEFFICIENT=    9.60000

TOTAL INFLOW RATIO=     .0+07)

MINIMUM UT=     .10000(ZERO LIFT CONDITION APPLIED BELOW THIS VALUE)

NORMAL AZIMUTH SPACING=  30.00000 DEGREES

REDUCED AZIMUTH SPACING=  15.00000 DEGREES

PIECEWISE QUADRATIC APPROXIMATION OF SPANWISE DIPOLE STRENGTH VARIATION
**************************************************************************

AIRFOIL DATA TABLES NOT USED

R=     .330 PSI= 261.8160EGREES UT=     .043 ZERO LIFT CONDITION APPLIED

R=     .330 PSI= 294.5430EGREES UT=     .066 ZERO LIFT CONDITION APPLIED
```

```
SOLUTION FOR COEFFICIENTS
-------------------------

(GC(I),I=1,NSP)
-.1080E-01 -.3620E-01 -.3546E-01 -.6555E-01 -.6189E-01

((GC(I,J),J=1,NHM),I=1,NSP)

 .2862E-02 -.1508E-02 -.1917E-03  .6273E-04  .1313E-02
 .3552E-02 -.1179E-01 -.3967E-03 -.2030E-02  .3574E-03
-.7379E-03 -.1748E-01 -.6217E-02 -.3336E-02 -.3559E-02
-.4820E-02 -.1986E-01 -.5994E-02 -.4791E-02 -.2886E-02
-.9984E-02 -.1894E-01 -.7201E-02 -.5393E-02 -.9688E-03

((GS(I,J),J=1,NHM),I=1,NSP)

-.1085E-01  .1015E-02 -.2382E-02 -.5882E-03 -.4870E-03
-.9381E-02  .1593E-02  .6553E-03  .2258E-02 -.8259E-03
-.3426E-03  .5535E-02  .3046E-03  .3133E-02  .2034E-02
 .9840E-02  .5338E-02  .2366E-02  .3525E-02  .1809E-02
 .1839E-01  .6391E-02  .4011E-02  .2664E-02  .6377E-03

PITCH ANGLE AT BLADE ROOT=  15.36381 DEGREES
CONING ANGLE=   5.82643 DEGREES
FLAPPING COEFFICIENT, A1=   6.28243 DEGREES
FLAPPING COEFFICIENT, B1=   1.79994 DEGREES
COMPUTED THRUST COEFFICIENT= .5700E-02
COMPUTED MOMENT COEFFICIENT ABOUT ROTOR X-AXIS=-.1988E-16
COMPUTED MOMENT COEFFICIENT ABOUT ROTOR Y-AXIS= .3755E-16
```

TABLE 1 - SECTIONAL LIFT/(RHO*(OMEGA**2)*(R1**3))

R/R1:	.8300E+00	.9000E+00	.7500E+00	.8500E+00	.9500E+00
PSI					
0.0	.1364E-02	.7153E-02	.1326E-01	.1599E-01	.1583E-01
15.0	.2196E-02	.6746E-02	.1068E-01	.1269E-01	.1238E-01
30.0	.2733E-02	.5973E-02	.7605E-02	.8833E-02	.8190E-02
45.0	.2654E-02	.5331E-02	.6193E-02	.6638E-02	.5290E-02
60.0	.2307E-02	.5305E-02	.5192E-02	.6257E-02	.4364E-02
75.0	.2511E-02	.5599E-02	.5376E-02	.6428E-02	.4689E-02
90.0	.2814E-02	.5844E-02	.5333E-02	.6463E-02	.5267E-02
105.0	.3383E-02	.6924E-02	.6890E-02	.8687E-02	.5779E-02
120.0	.3602E-02	.6213E-02	.8553E-02	.8250E-02	.6504E-02
135.0	.3519E-02	.7100E-02	.1046E-01	.1008E-01	.7670E-02
150.0	.3371E-02	.8296E-02	.1136E-01	.1144E-01	.9094E-02
165.0	.3100E-02	.8950E-02	.1110E-01	.1199E-01	.1033E-01
180.0	.2436E-02	.8483E-02	.1050E-01	.1208E-01	.1101E-01
195.0	.1399E-02	.7107E-02	.1001E-01	.1192E-01	.1102E-01
210.0	.4688E-03	.5625E-02	.9294E-02	.1135E-01	.1059E-01
225.0	.5559E-04	.4559E-02	.8104E-02	.1041E-01	.1015E-01
240.0	.5088E-04	.3806E-02	.6999E-02	.9638E-02	.9987E-02
255.0	.5183E-04	.3070E-02	.6574E-02	.9385E-02	.9998E-02
270.0	-.7825E-04	.2429E-02	.6561E-02	.9284E-02	.9878E-02
285.0	-.1126E-03	.2313E-02	.6379E-02	.8974E-02	.9737E-02
300.0	.1002E-03	.3033E-02	.6406E-02	.9100E-02	.1032E-01
315.0	.3520E-03	.4386E-02	.7803E-02	.1081E-01	.1226E-01
330.0	.5496E-03	.5841E-02	.1070E-01	.1394E-01	.1499E-01
345.0	.7773E-03	.6667E-02	.1325E-01	.1642E-01	.1673E-01

TABLE 2 - SECTIONAL LIFT*R1/THRUST PER BLADE

x/x1:	.3800E+00	.6000E+00	.7500E+00	.8500E+00	.9500E+00
PSI					
0.0	.3048E+00	.1500E+01	.2963E+01	.3572E+01	.3537E+01
15.0	.4906E+00	.1507E+01	.2386E+01	.2824E+01	.2765E+01
30.0	.6105E+00	.1334E+01	.1712E+01	.1973E+01	.1930E+01
45.0	.5929E+00	.1202E+01	.1383E+01	.1483E+01	.1182E+01
60.0	.5154E+00	.1139E+01	.1383E+01	.1393E+01	.9748E+00
75.0	.5161E+00	.1251E+01	.1425E+01	.1436E+01	.1047E+01
90.0	.6286E+00	.1306E+01	.1415E+01	.1444E+01	.1177E+01
105.0	.7557E+00	.1323E+01	.1539E+01	.1588E+01	.1291E+01
120.0	.8046E+00	.1339E+01	.1911E+01	.1843E+01	.1453E+01
135.0	.7860E+00	.1586E+01	.2536E+01	.2263E+01	.1713E+01
150.0	.7529E+00	.1353E+01	.2537E+01	.2556E+01	.2031E+01
165.0	.6925E+00	.2001E+01	.2479E+01	.2679E+01	.2308E+01
180.0	.5435E+00	.1893E+01	.2345E+01	.2699E+01	.2459E+01
195.0	.3124E+00	.1586E+01	.2237E+01	.2664E+01	.2462E+01
210.0	.1047E+00	.1256E+01	.2076E+01	.2535E+01	.2366E+01
225.0	.1242E-01	.1019E+01	.1810E+01	.2325E+01	.2267E+01
240.0	.1137E-01	.8502E+00	.1563E+01	.2153E+01	.2231E+01
255.0	.1158E-01	.6858E+00	.1468E+01	.2096E+01	.2233E+01
270.0	-.1748E-01	.5425E+00	.1466E+01	.2074E+01	.2206E+01
285.0	-.2514E-01	.5177E+00	.1425E+01	.2005E+01	.2175E+01
300.0	.2239E-01	.6775E+00	.1431E+01	.2033E+01	.2305E+01
315.0	.8533E-01	.9797E+00	.1743E+01	.2414E+01	.2736E+01
330.0	.1228E+00	.1305E+01	.2390E+01	.3115E+01	.3349E+01
345.0	.1736E+00	.1734E+01	.2959E+01	.3867E+01	.3737E+01

TABLE 3 - SECTIONAL PITCHING MOMENT/(RHO*(OMEGA**2)*(R1**4))

(ABOUT QUARTER-CHORD)

R/R1:	.3300E+00	.6000E+00	.7500E+00	.8500E+00	.9500E+00
PSI					
0.0	-.2121E-05	-.3533E-06	.6289E-06	.1284E-05	.1939E-05
15.0	-.1393E-05	.3939E-06	.1387E-05	.2048E-05	.2710E-05
30.0	-.7230E-06	.9181E-06	.1830E-05	.2436E-05	.3045E-05
45.0	-.3145E-06	.1325E-05	.1771E-05	.2268E-05	.2764E-05
60.0	-.2534E-06	.6227E-06	.1126E-05	.1462E-05	.1797E-05
75.0	-.6270E-06	-.2530E-06	-.5615E-07	.7975E-07	.2157E-06
90.0	-.1226E-05	-.1465E-05	-.1599E-05	-.1688E-05	-.1777E-05
105.0	-.1976E-05	-.2749E-05	-.3235E-05	-.3556E-05	-.3862E-05
120.0	-.2350E-05	-.3840E-05	-.4668E-05	-.5220E-05	-.5771E-05
135.0	-.2458E-05	-.4505E-05	-.5543E-05	-.6402E-05	-.7160E-05
150.0	-.2103E-05	-.4612E-05	-.6006E-05	-.6936E-05	-.7865E-05
165.0	-.1317E-05	-.4199E-05	-.5737E-05	-.6790E-05	-.7843E-05
180.0	-.2470E-06	-.3271E-05	-.4951E-05	-.6071E-05	-.7191E-05
195.0	.8704E-06	-.2172E-05	-.3863E-05	-.4990E-05	-.6117E-05
210.0	.1775E-05	-.1122E-05	-.2731E-05	-.3804E-05	-.4877E-05
225.0	.2248E-05	-.3485E-06	-.1791E-05	-.2753E-05	-.3714E-05
240.0	.2169E-05	.6953E-08	-.1194E-05	-.1995E-05	-.2796E-05
255.0	.1548E-05	-.7483E-07	-.9764E-06	-.1577E-05	-.2179E-05
270.0	.5240E-06	-.4920E-06	-.1056E-05	-.1433E-05	-.1809E-05
285.0	-.6714E-06	-.1054E-05	-.1266E-05	-.1408E-05	-.1550E-05
300.0	-.1772E-05	-.1538E-05	-.1408E-05	-.1321E-05	-.1235E-05
315.0	-.2546E-05	-.1734E-05	-.1314E-05	-.1021E-05	-.7274E-06
330.0	-.2652E-05	-.1599E-05	-.9028E-06	-.4387E-06	.2540E-07
345.0	-.2674E-05	-.1088E-05	-.2073E-06	.3802E-05	.9576E-06

TABLE 4 - CENTER OF PRESSURE LOCATION FROM LEADING EDGE(FRACTION OF CHORD)

R/R=	.3300E+00	.6000E+00	.7500E+00	.8500E+00	.9500E+00
PSI					
0.0	.2182E+00	.2490E+00	.2510E+00	.2516E+00	.2525E+00
15.0	.2376E+00	.2512E+00	.2527E+00	.2533E+00	.2545E+00
30.0	.2446E+00	.2531E+00	.2549E+00	.2557E+00	.2570E+00
45.0	.2476E+00	.2539E+00	.2559E+00	.2570E+00	.2607E+00
60.0	.2475E+00	.2524E+00	.2537E+00	.2548E+00	.2584E+00
75.0	.2444E+00	.2490E+00	.2498E+00	.2503E+00	.2509E+00
90.0	.2411E+00	.2449E+00	.2448E+00	.2447E+00	.2431E+00
105.0	.2386E+00	.2405E+00	.2404E+00	.2394E+00	.2362E+00
120.0	.2366E+00	.2374E+00	.2388E+00	.2370E+00	.2316E+00
135.0	.2357E+00	.2370E+00	.2390E+00	.2370E+00	.2309E+00
150.0	.2372E+00	.2385E+00	.2392E+00	.2376E+00	.2326E+00
165.0	.2413E+00	.2405E+00	.2394E+00	.2384E+00	.2345E+00
180.0	.2479E+00	.2421E+00	.2403E+00	.2397E+00	.2366E+00
195.0	.2627E+00	.2437E+00	.2421E+00	.2414E+00	.2386E+00
210.0	.3275E+00	.2459E+00	.2440E+00	.2431E+00	.2406E+00
225.0	.1078E+01	.2484E+00	.2455E+00	.2446E+00	.2425E+00
240.0	.1123E+01	.2500E+00	.2465E+00	.2458E+00	.2443E+00
255.0	.8615E+00	.2495E+00	.2470E+00	.2466E+00	.2455E+00
270.0	.1129E+00	.2459E+00	.2467E+00	.2468E+00	.2463E+00
285.0	.3721E+00	.2407E+00	.2459E+00	.2468E+00	.2467E+00
300.0	-.1121E+00	.2396E+00	.2455E+00	.2470E+00	.2476E+00
315.0	.1135E+00	.2413E+00	.2466E+00	.2481E+00	.2488E+00
330.0	.1437E+00	.2444E+00	.2483E+00	.2494E+00	.2500E+00
345.0	.1795E+00	.2469E+00	.2497E+00	.2505E+00	.2512E+00

TABLE 5 - TOTAL BLADE LIFT, MOMENT ABOUT HUB AND RADIAL CENTER OF LIFT

TOTAL BLADE LIFT/(RHO*(OMEGA**2)*(R1**4))
TOTAL BLADE LIFT/THRUST PER BLADE
MOMENT ABOUT HUB/(RHO*(OMEGA**2)*(R1**5))
RADIAL CENTER OF LIFT/R1

PSI	TOTAL BLADE LIFT		MOMENT ABOUT HUB	CENTER OF LIFT
0.0	.6342E-02	.1417E+01	.4785E-02	.7545E+00
15.0	.5555E-02	.1243E+01	.4034E-02	.7258E+00
30.0	.4464E-02	.9971E+00	.3067E-02	.6871E+00
45.0	.3662E-02	.8225E+00	.2439E-02	.6625E+00
60.0	.3413E-02	.7713E+00	.2289E-02	.6630E+00
75.0	.3565E-02	.8007E+00	.2385E-02	.6652E+00
90.0	.3825E-02	.8546E+00	.2512E-02	.6567E+00
105.0	.4146E-02	.9252E+00	.2703E-02	.6519E+00
120.0	.4544E-02	.1038E+01	.3078E-02	.6816E+00
135.0	.5310E-02	.1186E+01	.3590E-02	.6761E+00
150.0	.5836E-02	.1315E+01	.4033E-02	.6853E+00
165.0	.6069E-02	.1360E+01	.4218E-02	.6926E+00
180.0	.5804E-02	.1296E+01	.4106E-02	.7075E+00
195.0	.5152E-02	.1151E+01	.3780E-02	.7337E+00
210.0	.4401E-02	.9832E+00	.3360E-02	.7633E+00
225.0	.3794E-02	.8476E+00	.2970E-02	.7827E+00
240.0	.3419E-02	.7638E+00	.2703E-02	.7907E+00
255.0	.3192E-02	.7129E+00	.2555E-02	.8004E+00
270.0	.2999E-02	.6699E+00	.2442E-02	.8142E+00
285.0	.2906E-02	.6496E+00	.2372E-02	.8155E+00
300.0	.3193E-02	.7133E+00	.2543E-02	.7963E+00
315.0	.4058E-02	.9064E+00	.3159E-02	.7786E+00
330.0	.5285E-02	.1180E+01	.4088E-02	.7736E+00
345.0	.6241E-02	.1394E+01	.4801E-02	.7693E+00

TABLE 6 - SURFACE PRESSURE DIFFERENTIAL/(RHO*(OMEGA**2)*(R1**2))

AZIMUTH ANGLE= 0.0 DEGREES

R/R1:	.3300E+00	.6000E+00	.7500E+00	.8500E+00	.9500E+00
X/C					
.05000	.6963E-01	.4057E+00	.7561E+00	.9133E+00	.9069E+00
.10000	.4928E-01	.2794E+00	.5200E+00	.6278E+00	.6229E+00
.20000	.3467E-01	.1866E+00	.3461E+00	.4174E+00	.4136E+00
.30000	.2766E-01	.1427E+00	.2639E+00	.3180E+00	.3146E+00
.40000	.2345E-01	.1145E+00	.2113E+00	.2543E+00	.2513E+00
.50000	.2005E-01	.9374E-01	.1722E+00	.2071E+00	.2043E+00
.70000	.1431E-01	.6157E-01	.1124E+00	.1348E+00	.1327E+00
.90000	.7892E-02	.3145E-01	.5706E-01	.6829E-01	.6700E-01
.95000	.5535E-02	.2166E-01	.3924E-01	.4694E-01	.4602E-01
.99000	.2461E-02	.9496E-02	.1718E-01	.2054E-01	.2013E-01

AZIMUTH ANGLE= 15.0 DEGREES

R/R1:	.3300E+00	.6000E+00	.7500E+00	.8500E+00	.9500E+00
X/C					
.05000	.1196E+00	.3848E+00	.6122E+00	.7286E+00	.7135E+00
.10000	.8321E-01	.2646E+00	.4205E+00	.5001E+00	.4893E+00
.20000	.5966E-01	.1761E+00	.2791E+00	.3317E+00	.3239E+00
.30000	.4419E-01	.1342E+00	.2123E+00	.2520E+00	.2456E+00
.40000	.3616E-01	.1074E+00	.1695E+00	.2010E+00	.1955E+00
.50000	.3012E-01	.8752E-01	.1378E+00	.1632E+00	.1585E+00
.70000	.2049E-01	.5706E-01	.8943E-01	.1057E+00	.1022E+00
.90000	.1083E-01	.2839E-01	.4514E-01	.5324E-01	.5128E-01
.95000	.7523E-02	.1990E-01	.3100E-01	.3654E-01	.3516E-01
.99000	.3320E-02	.8713E-02	.1356E-01	.1597E-01	.1536E-01

AZIMUTH ANGLE= 30.0 DEGREES

R/R1:	.3300E+00	.6000E+00	.7500E+00	.8500E+00	.9500E+00
X/C					
.05000	.1526E+00	.3423E+00	.4423E+00	.5110E+00	.4767E+00
.10000	.1055E+00	.2354E+00	.3033E+00	.3501E+00	.3262E+00
.20000	.7094E-01	.1561E+00	.2006E+00	.2313E+00	.2148E+00
.30000	.5465E-01	.1185E+00	.1520E+00	.1751E+00	.1621E+00
.40000	.4420E-01	.9454E-01	.1209E+00	.1391E+00	.1284E+00
.50000	.3640E-01	.7688E-01	.9796E-01	.1125E+00	.1035E+00
.70000	.2423E-01	.4982E-01	.6311E-01	.7231E-01	.6606E-01
.90000	.1254E-01	.2511E-01	.3161E-01	.3613E-01	.3277E-01
.95000	.8659E-02	.1723E-01	.2167E-01	.2474E-01	.2241E-01
.99000	.3810E-02	.7534E-02	.9460E-02	.1080E-01	.9763E-02

AZIMUTH ANGLE= 45.0 DEGREES

R/R1:	.3300E+00	.6000E+00	.7500E+00	.8500E+00	.9500E+00
X/C					
.05000	.1496E+00	.3096E+00	.3585E+00	.3656E+00	.3109E+00
.10000	.1032E+00	.2124E+00	.2456E+00	.2540E+00	.2122E+00
.20000	.6906E-01	.1407E+00	.1622E+00	.1740E+00	.1391E+00
.30000	.5295E-01	.1068E+00	.1227E+00	.1314E+00	.1044E+00
.40000	.4262E-01	.8511E-01	.9748E-01	.1042E+00	.8229E-01
.50000	.3493E-01	.6905E-01	.7884E-01	.8411E-01	.6601E-01
.70000	.2305E-01	.4463E-01	.5062E-01	.5360E-01	.4167E-01
.90000	.1182E-01	.2243E-01	.2527E-01	.2675E-01	.2043E-01
.95000	.8153E-02	.1539E-01	.1731E-01	.1830E-01	.1392E-01
.99000	.3577E-02	.6724E-02	.7551E-02	.7977E-02	.6053E-02

AZIMUTH ANGLE= 60.0 DEGREES

R/R1:	.3300E+00	.6000E+00	.7500E+00	.8500E+00	.9500E+00
X/C					
.05000	.1300E+00	.3038E+00	.3550E+00	.3610E+00	.2547E+00
.10000	.8968E-01	.2087E+00	.2443E+00	.2478E+00	.1741E+00
.20000	.6003E-01	.1386E+00	.1619E+00	.1637E+00	.1145E+00
.30000	.4603E-01	.1056E+00	.1229E+00	.1241E+00	.8631E-01
.40000	.3700E-01	.8422E-01	.9797E-01	.9874E-01	.6826E-01
.50000	.3038E-01	.6850E-01	.7951E-01	.8000E-01	.5497E-01
.70000	.2005E-01	.4460E-01	.5142E-01	.5156E-01	.3498E-01
.90000	.1029E-01	.2248E-01	.2586E-01	.2583E-01	.1730E-01
.95000	.7094E-02	.1544E-01	.1775E-01	.1771E-01	.1182E-01
.99000	.3113E-02	.6754E-02	.7755E-02	.7733E-02	.5147E-02

AZIMUTH ANGLE= 75.0 DEGREES

R/R1:	.3300E+00	.6000E+00	.7500E+00	.8500E+00	.9500E+00
X/C					
.05000	.1290E+00	.3172E+00	.3622E+00	.3655E+00	.2672E+00
.10000	.8916E-01	.2184E+00	.2493E+00	.2515E+00	.1838E+00
.20000	.5997E-01	.1459E+00	.1662E+00	.1676E+00	.1223E+00
.30000	.4621E-01	.1116E+00	.1270E+00	.1280E+00	.9329E-01
.40000	.3738E-01	.8959E-01	.1019E+00	.1026E+00	.7468E-01
.50000	.3079E-01	.7326E-01	.8319E-01	.8371E-01	.6089E-01
.70000	.2051E-01	.4811E-01	.5450E-01	.5475E-01	.3974E-01
.90000	.1062E-01	.2457E-01	.2776E-01	.2786E-01	.2017E-01
.95000	.7340E-02	.1692E-01	.1911E-01	.1917E-01	.1387E-01
.99000	.3226E-02	.7418E-02	.8373E-02	.8396E-02	.6074E-02

AZIMUTH ANGLE= 90.0 DEGREES

R/R1:	.3300E+00	.6000E+00	.7500E+00	.8500E+00	.9500E+00
X/C					
.05000	.1553E+00	.3265E+00	.3539E+00	.3609E+00	.2927E+00
.10000	.1077E+00	.2297E+00	.2446E+00	.2495E+00	.2026E+00
.20000	.7284E-01	.1517E+00	.1644E+00	.1678E+00	.1365E+00
.30000	.5643E-01	.1169E+00	.1266E+00	.1292E+00	.1055E+00
.40000	.4589E-01	.9446E-01	.1024E+00	.1045E+00	.8549E-01
.50000	.3799E-01	.7779E-01	.8426E-01	.8605E-01	.7056E-01
.70000	.2556E-01	.5172E-01	.5606E-01	.5728E-01	.4718E-01
.90000	.1336E-01	.2679E-01	.2900E-01	.2964E-01	.2453E-01
.95000	.9256E-02	.1848E-01	.2004E-01	.2049E-01	.1697E-01
.99000	.4076E-02	.8122E-02	.8805E-02	.9003E-02	.7465E-02

AZIMUTH ANGLE=105.0 DEGREES

R/R1:	.3300E+00	.6000E+00	.7500E+00	.8500E+00	.9500E+00
X/C					
.05000	.1852E+00	.3264E+00	.3795E+00	.3781E+00	.3139E+00
.10000	.1287E+00	.2264E+00	.2632E+00	.2625E+00	.2185E+00
.20000	.8740E-01	.1533E+00	.1782E+00	.1780E+00	.1496E+00
.30000	.6798E-01	.1189E+00	.1383E+00	.1383E+00	.1163E+00
.40000	.5548E-01	.9674E-01	.1125E+00	.1128E+00	.9531E-01
.50000	.4610E-01	.8015E-01	.9327E-01	.9358E-01	.7948E-01
.70000	.3123E-01	.5401E-01	.6287E-01	.6325E-01	.5420E-01
.90000	.1644E-01	.2829E-01	.3293E-01	.3322E-01	.2870E-01
.95000	.1140E-01	.1963E-01	.2282E-01	.2304E-01	.1994E-01
.99000	.5026E-02	.8635E-02	.1005E-01	.1015E-01	.8804E-02

AZIMUTH ANGLE=120.0 DEGREES

R/R1:	.3300E+00	.6000E+00	.7500E+00	.8500E+00	.9500E+00
X/C					
.05000	.1959E+00	.3390E+00	.4686E+00	.4493E+00	.3480E+00
.10000	.1363E+00	.2358E+00	.3255E+00	.3126E+00	.2432E+00
.20000	.9290E-01	.1605E+00	.2210E+00	.2128E+00	.1671E+00
.30000	.7249E-01	.1251E+00	.1718E+00	.1660E+00	.1314E+00
.40000	.5935E-01	.1023E+00	.1402E+00	.1359E+00	.1084E+00
.50000	.4946E-01	.8515E-01	.1165E+00	.1131E+00	.9094E-01
.70000	.3369E-01	.5789E-01	.7886E-01	.7697E-01	.6276E-01
.90000	.1782E-01	.3057E-01	.4148E-01	.4068E-01	.3360E-01
.95000	.1238E-01	.2123E-01	.2878E-01	.2825E-01	.2341E-01
.99000	.5465E-02	.9366E-02	.1269E-01	.1247E-01	.1035E-01

AZIMUTH ANGLE=135.0 DEGREES

R/R1:	.8500E+00	.9500E+00
X/C		
.05000	.5492E+00	.4092E+00
.10000	.3982E+00	.2862E+00
.20000	.2603E+00	.1969E+00
.30000	.2029E+00	.1551E+00
.40000	.1660E+00	.1281E+00
.50000	.1424E+00	.1076E+00
.70000	.9411E-01	.7447E-01
.90000	.5074E-01	.3995E-01
.95000	.3455E-01	.2785E-01
.99000	.1524E-01	.1232E-01

AZIMUTH ANGLE=150.0 DEGREES

R/R1:	.8500E+00	.9500E+00
X/C		
.05000	.6243E+00	.4875E+00
.10000	.4341E+00	.3405E+00
.20000	.2953E+00	.2337E+00
.30000	.2301E+00	.1837E+00
.40000	.1881E+00	.1514E+00
.50000	.1585E+00	.1269E+00
.70000	.1064E+00	.8751E-01
.90000	.5614E-01	.4679E-01
.95000	.3809E-01	.3259E-01
.99000	.1679E-01	.1441E-01

AZIMUTH ANGLE=165.0 DEGREES

R/R1:	.8500E+00	.9500E+00
X/C		
.05000	.6561E+00	.5579E+00
.10000	.4559E+00	.3890E+00
.20000	.3098E+00	.2560E+00
.30000	.2410E+00	.2083E+00
.40000	.1968E+00	.1711E+00
.50000	.1636E+00	.1431E+00
.70000	.1109E+00	.9804E-01
.90000	.5839E-01	.5215E-01
.95000	.4052E-01	.3628E-01
.99000	.1787E-01	.1603E-01

AZIMUTH ANGLE=180.0 DEGREES

R/R1:	.3300E+00	.6000E+00	.7500E+00	.8500E+00	.9500E+00
X/C					
.05000	.1373E+00	.4698E+00	.5780E+00	.6639E+00	.5988E+00
.10000	.9468E-01	.3254E+00	.4009E+00	.4608E+00	.4167E+00
.20000	.6333E-01	.2198E+00	.2715E+00	.3124E+00	.2840E+00
.30000	.4853E-01	.1700E+00	.2106E+00	.2425E+00	.2216E+00
.40000	.3964E-01	.1390E+00	.1715E+00	.1976E+00	.1814E+00
.50000	.3198E-01	.1141E+00	.1421E+00	.1640E+00	.1512E+00
.70000	.2108E-01	.7650E-01	.9580E-01	.1107E+00	.1030E+00
.90000	.1088E-01	.3988E-01	.5019E-01	.5811E-01	.5449E-01
.95000	.7446E-02	.2761E-01	.3478E-01	.4029E-01	.3786E-01
.99000	.3266E-02	.1215E-01	.1532E-01	.1776E-01	.1671E-01

AZIMUTH ANGLE=195.0 DEGREES

R/R1:	.3300E+00	.6000E+00	.7500E+00	.8500E+00	.9500E+00
X/C					
.05000	.8270E-01	.3957E+00	.5546E+00	.6590E+00	.6036E+00
.10000	.5636E-01	.2738E+00	.3842E+00	.4567E+00	.4193E+00
.20000	.3683E-01	.1844E+00	.2594E+00	.3068E+00	.2848E+00
.30000	.2756E-01	.1422E+00	.2007E+00	.2391E+00	.2215E+00
.40000	.2164E-01	.1152E+00	.1629E+00	.1949E+00	.1808E+00
.50000	.1730E-01	.9496E-01	.1347E+00	.1609E+00	.1502E+00
.70000	.1084E-01	.6338E-01	.9031E-01	.1080E+00	.1018E+00
.90000	.5271E-02	.3289E-01	.4708E-01	.5643E-01	.5356E-01
.95000	.3685E-02	.2274E-01	.3250E-01	.3903E-01	.3716E-01
.99000	.1596E-02	.1000E-01	.1435E-01	.1721E-01	.1638E-01

AZIMUTH ANGLE=210.0 DEGREES

R/R1:	.3300E+00	.6000E+00	.7500E+00	.8500E+00	.9500E+00
X/C					
.05000	.3325E-01	.3154E+00	.5179E+00	.6308E+00	.5838E+00
.10000	.2174E-01	.2178E+00	.3582E+00	.4366E+00	.4049E+00
.20000	.1298E-01	.1462E+00	.2411E+00	.2943E+00	.2741E+00
.30000	.8756E-02	.1124E+00	.1860E+00	.2272E+00	.2125E+00
.40000	.6092E-02	.9068E-01	.1505E+00	.1842E+00	.1730E+00
.50000	.4216E-02	.7452E-01	.1241E+00	.1520E+00	.1433E+00
.70000	.1767E-02	.4941E-01	.8275E-01	.1016E+00	.9654E-01
.90000	.3945E-03	.2548E-01	.4291E-01	.5284E-01	.5055E-01
.95000	.1845E-03	.1759E-01	.2967E-01	.3655E-01	.3503E-01
.99000	.5036E-04	.7726E-02	.1304E-01	.1608E-01	.1543E-01

AZIMUTH ANGLE=225.0 DEGREES

R/R1:	.3300E+00	.6000E+00	.7500E+00	.8500E+00	.9500E+00
X/C					
.05000	.1153E-01	.2573E+00	.4538E+00	.5811E+00	.5629E+00
.10000	.5494E-02	.1776E+00	.3135E+00	.4017E+00	.3898E+00
.20000	.2409E-02	.1187E+00	.2105E+00	.2702E+00	.2630E+00
.30000	.3737E-03	.9089E-01	.1620E+00	.2081E+00	.2033E+00
.40000	-.8762E-03	.7306E-01	.1308E+00	.1683E+00	.1650E+00
.50000	-.1675E-02	.5980E-01	.1076E+00	.1386E+00	.1363E+00
.70000	-.2354E-02	.3934E-01	.7141E-01	.9228E-01	.9129E-01
.90000	-.1839E-02	.2013E-01	.3687E-01	.4777E-01	.4754E-01
.95000	-.1376E-02	.1587E-01	.2947E-01	.3301E-01	.3290E-01
.99000	-.6412E-03	.6084E-02	.1119E-01	.1451E-01	.1446E-01

AZIMUTH ANGLE=240.0 DEGREES

R/R1:	.3300E+00	.6000E+00	.7500E+00	.8500E+00	.9500E+00
X/C					
.05000	.1097E-01	.2183E+00	.3932E+00	.5402E+00	.5571E+00
.10000	.5158E-02	.1489E+00	.2714E+00	.3731E+00	.3852E+00
.20000	.2253E-02	.9924E-01	.1820E+00	.2504E+00	.2592E+00
.30000	.3058E-03	.7579E-01	.1398E+00	.1925E+00	.1998E+00
.40000	-.8893E-03	.6076E-01	.1127E+00	.1554E+00	.1616E+00
.50000	-.1652E-02	.4991E-01	.9251E-01	.1278E+00	.1332E+00
.70000	-.2295E-02	.3247E-01	.6123E-01	.8476E-01	.8874E-01
.90000	-.1756E-02	.1653E-01	.3152E-01	.4372E-01	.4598E-01
.95000	-.1335E-02	.1138E-01	.2175E-01	.3019E-01	.3178E-01
.99000	-.6222E-03	.4483E-02	.9549E-02	.1326E-01	.1397E-01

AZIMUTH ANGLE=255.0 DEGREES

R/R1:	.3300E+00	.6000E+00	.7500E+00	.8500E+00	.9500E+00
X/C					
.05000	.8709E-02	.1742E+00	.3699E+00	.5274E+00	.5600E+00
.10000	.5002E-02	.1199E+00	.2552E+00	.3640E+00	.3868E+00
.20000	.2012E-02	.8002E-01	.1710E+00	.2440E+00	.2597E+00
.30000	.5272E-03	.6116E-01	.1312E+00	.1874E+00	.1998E+00
.40000	-.3870E-03	.4909E-01	.1057E+00	.1511E+00	.1613E+00
.50000	-.9771E-03	.4010E-01	.8674E-01	.1240E+00	.1327E+00
.70000	-.1505E-02	.2630E-01	.5733E-01	.8207E-01	.8806E-01
.90000	-.1207E-02	.1341E-01	.2947E-01	.4224E-01	.4546E-01
.95000	-.9067E-03	.9233E-02	.2033E-01	.2915E-01	.3139E-01
.99000	-.4238E-03	.4046E-02	.8923E-02	.1280E-01	.1379E-01

AZIMUTH ANGLE=270.0 DEGREES

R/R1:	.3300E+00	.6000E+00	.7500E+00	.8500E+00	.9500E+00
X/C					
.05000	-.2495E-02	.1362E+00	.3689E+00	.5222E+00	.5545E+00
.10000	-.2053E-02	.9403E-01	.2545E+00	.3603E+00	.3828E+00
.20000	-.1816E-02	.6311E-01	.1706E+00	.2414E+00	.2568E+00
.30000	-.1729E-02	.4852E-01	.1310E+00	.1853E+00	.1973E+00
.40000	-.1660E-02	.3916E-01	.1056E+00	.1493E+00	.1591E+00
.50000	-.1579E-02	.3218E-01	.8705E-01	.1225E+00	.1307E+00
.70000	-.1327E-02	.2134E-01	.5732E-01	.8103E-01	.8657E-01
.90000	-.9248E-03	.1101E-01	.2949E-01	.4166E-01	.4460E-01
.95000	-.5934E-03	.7600E-02	.2034E-01	.2875E-01	.3078E-01
.99000	-.2689E-03	.3333E-02	.8931E-02	.1262E-01	.1352E-01

AZIMUTH ANGLE=285.0 DEGREES

R/R1:	.3300E+00	.6000E+00	.7500E+00	.8500E+00	.9500E+00
X/C					
.05000	-.3895E-02	.1273E+00	.3577E+00	.5047E+00	.5475E+00
.10000	-.3692E-02	.8861E-01	.2470E+00	.3482E+00	.3778E+00
.20000	-.3221E-02	.5997E-01	.1658E+00	.2334E+00	.2532E+00
.30000	-.2022E-02	.4649E-01	.1274E+00	.1791E+00	.1944E+00
.40000	-.1470E-02	.3783E-01	.1028E+00	.1444E+00	.1567E+00
.50000	-.7504E-03	.3134E-01	.8490E-01	.1185E+00	.1286E+00
.70000	-.1158E-03	.2110E-01	.5603E-01	.7835E-01	.8504E-01
.90000	.1322E-03	.1105E-01	.2889E-01	.4030E-01	.4374E-01
.95000	.1239E-03	.7654E-02	.1994E-01	.2780E-01	.3018E-01
.99000	.6579E-04	.3371E-02	.8759E-02	.1220E-01	.1325E-01

AZIMUTH ANGLE=300.0 DEGREES

R/R1:	.3300E+00	.6000E+00	.7500E+00	.8500E+00	.9500E+00
X/C					
.05000	-.9034E-03	.1350E+00	.3588E+00	.5122E+00	.5818E+00
.10000	.5135E-03	.1156E+00	.2478E+00	.3534E+00	.4012E+00
.20000	.1656E-02	.7841E-01	.1664E+00	.2367E+00	.2685E+00
.30000	.2574E-02	.6089E-01	.1280E+00	.1816E+00	.2059E+00
.40000	.2990E-02	.4963E-01	.1034E+00	.1463E+00	.1657E+00
.50000	.3198E-02	.4118E-01	.8501E-01	.1200E+00	.1359E+00
.70000	.3085E-02	.2782E-01	.5644E-01	.7932E-01	.8963E-01
.90000	.2075E-02	.1460E-01	.2914E-01	.4077E-01	.4599E-01
.95000	.1515E-02	.1012E-01	.2012E-01	.2812E-01	.3171E-01
.99000	.6942E-03	.4462E-02	.8840E-02	.1234E-01	.1391E-01

AZIMUTH ANGLE=315.0 DEGREES

R/R1: X/C	.3300E+00	.6000E+00	.7500E+00	.8500E+00	.9500E+00
.05000	.1223E-01	.2427E+00	.4365E+00	.6102E+00	.6939E+00
.10000	.1006E-01	.1681E+00	.3020E+00	.4206E+00	.4780E+00
.20000	.8872E-02	.1135E+00	.2029E+00	.2813E+00	.3193E+00
.30000	.8437E-02	.8790E-01	.1558E+00	.2155E+00	.2443E+00
.40000	.8096E-02	.7140E-01	.1256E+00	.1733E+00	.1963E+00
.50000	.7698E-02	.6904E-01	.1031E+00	.1420E+00	.1606E+00
.70000	.6463E-02	.5953E-01	.6824E-01	.9350E-01	.1055E+00
.90000	.4016E-02	.2069E-01	.3512E-01	.4790E-01	.5394E-01
.95000	.2689E-02	.1432E-01	.2424E-01	.3302E-01	.3716E-01
.99000	.1309E-02	.6803E-02	.1084E-01	.1448E-01	.1629E-01

AZIMUTH ANGLE=330.0 DEGREES

R/R1: X/C	.3300E+00	.6000E+00	.7500E+00	.8500E+00	.9500E+00
.05000	.2001E-01	.3259E+00	.5845E+00	.7937E+00	.8521E+00
.10000	.1801E-01	.2253E+00	.4107E+00	.5442E+00	.5864E+00
.20000	.1511E-01	.1515E+00	.2785E+00	.3683E+00	.3909E+00
.30000	.1187E-01	.1163E+00	.2133E+00	.2778E+00	.2986E+00
.40000	.1101E-01	.9451E-01	.1715E+00	.2230E+00	.2394E+00
.50000	.1021E-01	.7785E-01	.1404E+00	.1822E+00	.1954E+00
.70000	.8279E-02	.5136E-01	.9244E-01	.1195E+00	.1279E+00
.90000	.5027E-02	.2683E-01	.4732E-01	.6099E-01	.6513E-01
.95000	.3500E-02	.1856E-01	.3261E-01	.4200E-01	.4482E-01
.99000	.1628E-02	.8150E-02	.1430E-01	.1841E-01	.1964E-01

AZIMUTH ANGLE=345.0 DEGREES

R/R1: X/C	.3300E+00	.6000E+00	.7500E+00	.8500E+00	.9500E+00
.05000	.3421E-01	.3361E+00	.7519E+00	.9542E+00	.9542E+00
.10000	.2526E-01	.2604E+00	.5176E+00	.6427E+00	.6561E+00
.20000	.1912E-01	.1736E+00	.3453E+00	.4281E+00	.4366E+00
.30000	.1635E-01	.1371E+00	.2638E+00	.3268E+00	.3328E+00
.40000	.1451E-01	.1107E+00	.2116E+00	.2618E+00	.2663E+00
.50000	.1299E-01	.9067E-01	.1729E+00	.2136E+00	.2170E+00
.70000	.9998E-02	.5997E-01	.1133E+00	.1396E+00	.1416E+00
.90000	.5852E-02	.3084E-01	.5775E-01	.7098E-01	.7180E-01
.95000	.4159E-02	.2128E-01	.3976E-01	.4883E-01	.4937E-01
.99000	.1868E-02	.9342E-02	.1742E-01	.2139E-01	.2161E-01

Sample Airfoil Data

Printed below is a sample print of typical airfoil data to illustrate the previously described input format.

1127

	0.	.2	.3	.4	.5	.6	.7	.75	.8
	.9	1.							
-39.	-1.18	-1.18	-1.18	-1.18	-1.18	-1.18	-1.18	-1.18	-1.18
	-1.18	-1.18							
-21.	-.8	-.8	-.81	-.83	-.85	-.85	-.85	-.71	-.68
	-.64	-.64							
-16.5	-1.007	-1.007	-.944	-.960	-.965	-.965	-.965	-.795	-.760
	-.70	-.70							
-15.	-1.19	-1.19	-1.09	-1.055	-.99	-.98	-.98	-.83	-.79
	-.72	-.72							
-14.	-1.333	-1.333	-1.22	-1.096	-1.	-.97	-.97	-.84	-.805
	-.73	-.73							
-13.	-1.334	-1.334	-1.28	-1.12	-1.	-.96	-.96	-.85	-.815
	-.735	-.735							
-12.	-1.255	-1.255	-1.26	-1.13	-1.	-.947	-.94	-.85	-.82
	-.74	-.74							
-11.	-1.161	-1.161	-1.19	-1.12	-.994	-.930	-.923	-.85	-.81
	-.74	-.74							
-10.	-1.055	-1.055	-1.01	-1.082	-.985	-.910	-.900	-.845	-.805
	-.73	-.73							
-8.	-.844	-.844	-.88	-.907	-.922	-.87	-.84	-.82	-.77
	-.695	-.695							
-6.	-.633	-.633	-.66	-.684	-.741	-.77	-.75	-.77	-.72
	-.593	-.593							
-4.	-.46	-.46	-.46	-.4805	-.52	-.5657	-.6401	-.7244	-.53
	-.396	-.396							
-2.	-.25	-.25	-.25	-.2399	-.27	-.282	-.3274	-.3605	-.3469
	-.1399	-.1399							
0.	0.	0.	0.	0.	0.	0.	0.	0.	0.
	0.	0.							
2.	.23	.23	.23	.2403	.25	.271	.3245	.3417	.3676
	.1245	.1245							
4.	.45	.45	.45	.4916	.51	.5731	.6252	.6368	.5428
	.45	.45							
6.	.70	.70	.70	.7224	.75	.7967	.7367	.7169	.6430
	.593	.593							
8.	.89	.89	.89	.9416	.89	.8711	.7513	.7071	.70
	.695	.695							
10.	1.08	1.08	1.08	1.0333	.93	.8802	.8600	.845	.805
	.73	.73							
11.	1.161	1.161	1.19	1.1200	.994	.93	.923	.85	.81
	.74	.74							
12.	1.255	1.255	1.26	1.1305	1.0000	.947	.940	.85	.82
	.74	.74							
13.	1.334	1.334	1.28	1.12	1.	.96	.96	.85	.815
	.735	.735							
14.	1.33	1.33	1.22	1.096	1.	.97	.97	.84	.805
	.73	.73							
15.	1.19	1.19	1.09	1.055	.99	.98	.98	.83	.79
	.72	.72							
16.5	1.007	1.007	.944	.96	.965	.965	.965	.795	.76
	.7	.7							
21.	.8	.8	.81	.83	.85	.85	.85	.71	.68
	.64	.64							
39.	1.18	1.18	1.18	1.18	1.18	1.18	1.18	1.18	1.18
	1.18	1.18							

REFERENCES

1. Van Holten, Th.: The Computation of Aerodynamic Loads on Helicopter Blades in Forward Flight, Using the Method of the Acceleration Potential. Report VTH-189, Technische Hogeschool Delft, Netherlands, March 1975.

2. Pierce, G. Alvin and Vaidyanathan, Anand R.: Helicopter Rotor Loads Using a Matched Asymptotic Expansion Technique, NASA CR-165742, May 1981.

3. Pierce, G. Alvin and Vaidyanathan, Anand R.: Helicopter Rotor Loads Using Discretized Matched Asymptotic Expansions, NASA CR-166092, May 1983.

APPENDIX A

LISTING OF PROGRAM ASYMP1

```
      PROGRAM MAIN(INPUT,OUTPUT,TAPE5=INPUT,TAPE6=OUTPUT,
     1AFDATA,TAPE1=AFDATA)
C
C   CALCULATION OF THE UNSTEADY AIRLOADS ON A HELICOPTER ROTOR BLADE IN
C   FORWARD FLIGHT. THE METHOD USES AN ACCELERATION POTENTIAL DESCRIPTION
C   OF THE FLOW FIELD AND A MATCHED ASYMPTOTIC EXPANSION TECHNIQUE TO
C   OBTAIN A SOLUTION CORRECT TO O(1/(AR*AR)).
C   REF.1 - TH. VAN HOLTEN, REPORT VTH-189,TECHNISCHE HOGESCHOOL,DELFT,
C   NETHERLANDS.
C   REF.2 - G.A.PIERCE ET AL, NASA CR 165742, MAY 1981.
C   FOR IDENTIFICATION OF PROGRAM STEPS, REFER USER'S MANUAL.
C
      REAL MU,LAM,MCL,MINF,MLOC
      DIMENSION R80(5),XOUT(10),P800(24),A(59,59),B(59,1),
     1IPIVOT(59),PMIN(20),FI1(5),FI2(5),G0(5),GC(5,5),GS(5,5),F1(24),
     2F2(24),F3(24),FLT1(24),FLT2(24),FMT(24),COL(24),GST(24,5),WK(59),
     3OGS2(24,5),FL1(24,5),FL2(24,5),FM(24,5),XCP(24,5),
     4POUT(5,10),POIP(24,5)
      DIMENSION CL(50,20),MCL(20),ACL(50)
      COMMON/MAIN1/NL,PI
      YL(XL,XL1,XL2,YL1,YL2)=YL1+(XL-XL1)*(YL2-YL1)/(XL2-XL1)
      DATA NSP,NHM,NAZ,NCOF,NCOFP,DMAX/5,5,11,59,60,0.5/
      DATA XOUT/.05,.1,.2,.3,.4,.5,.7,.9,.95,.99/
      PI=4.*ATAN(1.)
C
C   PROGRAM STEP 1.
C   READ AND WRITE INPUT DATA AND ASSOCIATED QUANTITIES.
C
      READ(5,*)RO,AR,NB,TW,MU,ALR,CT,MINF
      READ(5,*)N1,N2,N3,N4
      IF(N1 .EQ. 1)READ(5,*)THC
      IF(N2 .EQ. 0)READ(5,*)GAMA
      IF(N2 .EQ. 1)READ(5,*)A0
      IF(N3 .EQ. 1)READ(5,*)A1
      IF(N4 .EQ. 1)READ(5,*)B1
      READ(5,*)(R80(I),I=1,NSP)
      READ(5,*)DP1D,DP2D,UTMIN,NAFD
C
C   NAFD=0 -- AIRFOIL TABLES NOT USED.
C   NAFD=1 -- AIRFOIL TABLES USED.
C
      IF(NAFD .EQ. 0)GO TO 8
      READ(1,1)NXL,NZL
    1 FORMAT(30X,2I2)
      READ(1,2)(MCL(I),I=1,NXL)
    2 FORMAT(7X,9F7.0)
      NL1=NXL/9
      NL2=NL1+1
      DO 3 I=1,NZL
      DO 3 J=1,NL2
      J1=(J-1)*9+1
      J2=J*9
      IF(J1 .GT. NXL)GO TO 3
      IF(J2 .GT. NXL)J2=NXL
      IF(J .EQ. 1)READ(1,4)ACL(I),(CL(I,J3),J3=J1,J2)
    4 FORMAT(F7.0,9F7.0)
      IF(J .GT. 1)READ(1,5)(CL(I,J3),J3=J1,J2)
    5 FORMAT(7X,9F7.0)
    3 CONTINUE
```

```
    8  CONTINUE
       DP1=DP1D*PI/180.
       DP2=DP2D*PI/180.
       WRITE(6,10)
   10  FORMAT(1H1)
       WRITE(6,20)RO,AR,NB,TW,MU,ALR,MINF
   20  FORMAT(//6X,"ROOT RADIUS/TIP RADIUS=",F10.5//6X,"ASPECT RATIO=",
      1F10.5//6X,"NUMBER OF BLADES=",I2//6X,
      2"LINEAR TWIST(ROOT TO TIP)=",F10.5,1X,"DEGREES"//6X,
      3"FORWARD SPEED/TIP SPEED=",F10.5//6X,
      4"ROTOR INCIDENCE(FORWARD TILT POSITIVE)=",F10.5,1X,"DEGREES"//6X,
      5"FREESTREAM MACH NUMBER=",F10.5)
       TW=TW*PI/180.
       ALR=ALR*PI/180.
       IF(N1 .EQ. 0)THC=0.
       IF(N2 .EQ. 0)A0=0.
       IF(N3 .EQ. 0)A1=0.
       IF(N4 .EQ. 0)B1=0.
       WRITE(6,30)CT
   30  FORMAT(/6X,"THRUST COEFFICIENT=",F10.5)
       IF(N1 .EQ. 1)WRITE(6,40)THC
   40  FORMAT(/6X,"PITCH ANGLE AT BLADE ROOT=",F10.5,1X,"DEGREES")
       IF(N2 .EQ. 0)WRITE(6,50)GAMA
   50  FORMAT(/6X,"FLAPPING INERTIA COEFFICIENT=",F10.5)
       IF(N2 .EQ. 1)WRITE(6,60)A0
   60  FORMAT(/6X,"CONING ANGLE=",F10.5,1X,"DEGREES")
       IF(N3 .EQ. 1)WRITE(6,70)A1
   70  FORMAT(/6X,"FLAPPING COEFFICIENT, A1=",F10.5,1X,"DEGREES")
       IF(N4 .EQ. 1)WRITE(6,80)B1
   80  FORMAT(/6X,"FLAPPING COEFFICIENT, B1=",F10.5,1X,"DEGREES")
       THC=THC*PI/180.
       A0=A0*PI/180.
       A1=A1*PI/180.
       B1=B1*PI/180.
       LAM=MU*ALR+SQRT(.5*(-MU*MU+SQRT(MU*MU*MU*MU+CT*CT)))
       WRITE(6,90)LAM,UTMIN,DP1D,DP2D
   90  FORMAT(/6X,"TOTAL INFLOW RATIO=",F10.5//6X,"MINIMUM UT=",F10.5,
      1"(ZERO LIFT CONDITION APPLIED BELOW THIS VALUE)"//6X,
      2"NORMAL AZIMUTH INTERVAL=",F10.5,1X,"DEGREES"//6X,
      3"REDUCED AZIMUTH INTERVAL=",F10.5,1X,"DEGREES")
       SLOR=1.
       CL0=0.
       IF(NAFD .EQ. 0)WRITE(6,91)
   91  FORMAT(/6X,"AIRFOIL DATA TABLES NOT USED")
       IF(NAFD .EQ. 1)WRITE(6,92)
   92  FORMAT(/6X,"AIRFOIL DATA TABLES USED")
C
C  CALCULATE QUANTITIES NEEDED FOR TRAJECTORY SEGMENT ADJACENT TO THE
C  COLLOCATION POINT.
C
       ETA1P=ALOG((3.+SQRT(5.))/2.)
       CF1=COSH(.5*ETA1P)/SINH(.5*ETA1P)
       CF2=.5*CF1-ETA1P
       CF3=.25*CF1-SINH(ETA1P)
       EX1=EXP(-ETA1P)
       CF4=.5-EX1
       CF5=-.5*ETA1P-.5*EX1+.25*EX1*EX1+3./8.
       L=1
C
C  PROGRAM STEP 2.
```

```
C   START OUTER LOOP FOR COLLOCATION. THIS LOOP SETS THE CURRENT AZIMUTH
C   STATION.
C
      DO 100 J=1,NAZ
      P80=2.*J*PI/NAZ
      PBO(J)=360.*J/NAZ
      CP1=COS(P80)
      SP1=SIN(PBO)
      CP2=COS(2.*P80)
      SP2=SIN(2.*P80)
C
C   START INNER LOOP FOR COLLOCATION. THIS LOOP SETS THE CURRENT RADIAL
C   LOCATION.
C
      DO 100 I=1,NSP
      DO 110 M=1,NCOF
      A(L,M)=0.
 110  CONTINUE
      B(L,1)=0.
      ZBO=2.*(RBO(I)-.5*(1.+RO))/(1.-RO)
      SQZ=SQRT(1.-ZBO*ZBO)
      UT=RBO(I)+MU*SP1
C
C   PROGRAM STEP 3.
C   TEST THE TANGENTIAL VELOCITY AT THE COLLOCATION POINT, TO DECIDE
C   WHETHER NORMAL VELOCITY BOUNDARY CONDITION OR ZERO LIFT CONDITION
C   SHOULD BE APPLIED.
C
      IF(UT .GT. UTMIN)GO TO 120
      WRITE(6,130)RBO(I),PBO(J),UT
 130  FORMAT(/6X,"R=",F8.3,1X,"PSI=",F8.3,"DEGREES",1X,"UT=",
     1F8.3,1X,"ZERO LIFT CONDITION APPLIED")
      GO TO 140
 120  DP=(1.-RO)/(2.*AR*UT)
      PLIM=PBO-(2.+RBO(I)*CP1)/SQRT(MU*MU+LAM*LAM)
      IF(NAFO .EQ. 0)GO TO 133
C
C   PROGRAM STEP 4.
C   CALCULATE LIFT CURVE SLOPE FROM DATA TABLES FOR THE CURRENT
C   COLLOCATION POINT, USING THE LOCAL INCIDENCE AND MACH NUMBER.
C
      MLOC=UT*MINF/MU
      ALOC=THC-TW*(RBO(I)-RO)/(1.-RO)+B1*CP1-A1*SP1
     1-(MU*A0*CP1+LAM)/UT
      ALOC=ALOC*180./PI
      CALL TABSCH(MCL,NXL,MLOC,IMCL1,IMCL2,INT)
      IF(INT .EQ. -1)IMCL1=IMCL2=1
      IF(INT .EQ. 1)IMCL1=IMCL2=NXL
      CALL TABSCH(ACL,NZL,ALOC,IACL1,IACL2,INT)
      IF(INT .EQ. 0)GO TO 131
      IF(INT .EQ. -1)GO TO 132
      IACL1=NXL-1
      IACL2=NXL
      GO TO 131
 132  IACL1=1
      IACL2=2
 131  SLC1=(CL(IACL2,IMCL1)-CL(IACL1,IMCL1))/(ACL(IACL2)
     1-ACL(IACL1))
      CLO1=CL(IACL1,IMCL1)-SLC1*ACL(IACL1)
      SLC1=SLC1*180./PI
```

```
      SLC2=(CL(IACL2,IMCL2)-CL(IACL1,IMCL2))/(ACL(IACL2)
     1-ACL(IACL1))
      CLC2=CL(IACL1,IMCL2)-SLC2*ACL(IACL1)
      SLC2=SLC2*180./PI
      IF(IMCL1 .EQ. IMCL2)SLCR=SLC1/(2.*PI)
      IF(IMCL1 .NE. IMCL2)SLCR=YL(MLOC,MCL(IMCL1),MCL(IMCL2),
     1SLC1,SLC2)/(2.*PI)
      IF(IMCL1 .EQ. IMCL2)CLO=CLO1
      IF(IMCL1 .NE. IMCL2)CLO=YL(MLOC,MCL(IMCL1),MCL(IMCL2),
     1CLO1,CLO2)
  133 CONTINUE
C
C  CALCULATE THE CONTRIBUTION TO THE INDUCED VELOCITY FROM THE
C  TRAJECTORY SEGMENT ADJACENT TO THE COLLOCATION POINT, AND ADD TO
C  COEFFICIENT MATRIX ELEMENT. ALTERNATIVELY, SET UP THE ZERO LIFT
C  CONDITION.
C
  140 DO 150 I1=1,NSP
      IF(I1 .GT. 1)GO TO 160
      IF(UT .LE. UTMIN)GO TO 170
      IF(SLCR .EQ. 0.)GO TO 151
      W1=-AR*(1.+ZBO)*CF1/UT+MU*CP1*CF2/(UT*UT)-(2.*AR*(1.+ZBO)-
     1FUN3(RO,AR,RBO(I),1))/UT
      W2=(1.-RO)*(1.+ZBO)*CF2/(2.*UT*UT)-(1.-RO)*MU*CP1*CF3/(2.*AR*
     1UT*UT*UT)
      W3=(1.-RO)*(1.-RO)*(1.+ZBO)*CF3/(8.*AR*UT*UT*UT)
      W1=W1-AR*(1.+ZBO)*(1.-SLCR)/(SLCR*UT)
      GO TO 180
  151 W1=AR*(1.+ZBO)
      W2=W3=0.
      GO TO 180
  170 W1=AR*(1.+ZBO)-FUN3(RO,AR,RBO(I),1)
      W2=0.
      W3=0.
      GO TO 180
  160 NL=I1-1
      IF(UT .LE. UTMIN)GO TO 190
      POS=PNM(I1-1,0,ZBO)
      P1S=PNM(I1-1,1,ZBO)
      PO=FUN3(RO,AR,RBO(I),3)
      IF(SLCR .EQ. 0.)GO TO 152
      W1=-AR*SQZ*P1S*CF1/(2.*PI*UT)-MU*CP1*NL*(NL+1.)*POS*CF2/(2.*PI
     1*UT*UT)+MU*MU*CP1*CP1*NL*(NL+1.)*P1S*CF3/(4.*PI*AR*SQZ*UT
     2*UT*UT)-(AR*SQZ*P1S+PO/2.)/(PI*UT)
      W2=(1.-RO)*SQZ*P1S*CF2/(4.*PI*UT*UT)+(1.-RO)*MU*CP1*NL*(NL+1.)
     1*POS*CF3/(4.*PI*AR*UT*UT*UT)
      W3=(1.-RO)*(1.-RO)*SQZ*P1S*CF3/(16.*PI*AR*UT*UT*UT)
      W1=W1-AR*SQZ*P1S*(1.-SLCR)/(2.*PI*SLCR*UT)
      GO TO 180
  152 W1=AR*SQZ*P1S/(2.*PI)
      W2=W3=0.
      GO TO 160
  190 W1=(AR*SQZ*PNM(I1-1,1,ZBO)+FUN3(RO,AR,RBO(I),3))/(2.*PI)
      W2=0.
      W3=0.
  180 M=(I1-1)*NAZ+1
      A(L,M)=A(L,M)+W1
      DO 150 I2=1,NHM
      M=M+1
      A(L,M)=A(L,M)+(W1+I2*I2*W3)*COS(I2*PBO)-I2*W2*SIN(I2*PBO)
```

```
      M=M+1
      A(L,M)=A(L,M)+(W1+I2*I2*W3)*SIN(I2*PB0)+I2*W2*COS(I2*PB0)
  150 CONTINUE
      IF(UT .GT. UTMIN)GO TO 200
      M=NSP*NAZ+1
      A(L,M)=A(L,M)+(1.-R0)*(2.*MU*CP1)/(4.*AR)+(1.-R0)*(1.-R0)
     1*(-1.)/(16.*AR*AR)
      M=M+1
      A(L,M)=A(L,M)+(1.-R0)*(2.*MU*SP1+RB0(I))/(4.*AR)
      M=M+1
      A(L,M)=A(L,M)+(1.-R0)*(-2.*MU*SP2-2.*RB0(I)*CP1)/(4.*AR)+(1.-R0)
     1*(1.-R0)*(2.*SP1)/(16.*AR*AR)
      M=M+1
      A(L,M)=A(L,M)+(1.-R0)*(2.*MU*CP2-2.*RB0(I)*SP1)/(4.*AR)+(1.-R0)
     1*(1.-R0)*(-2.*CP1)/(16.*AR*AR)
      B(L,1)=B(L,1)-TW*(2.*MU*R0*CP1-MU*MU*SP2-4.*MU*RB0(I)*CP1)/(4.*AR)
     1-(1.-R0)*(-R0+4.*RB0(I)+4.*MU*SP1)*TW/(16.*AR*AR)
      L=L+1
      GO TO 100
  200 CONTINUE
      IF(SLOR .NE. 0.)GO TO 201
      B(L,1)=B(L,1)-UT*UT*CL0/(2.*PI)
      L=L+1
      GO TO 100
  201 B(L,1)=B(L,1)+UT*CL0/(2.*PI*SLOR)
C
C   PROGRAM STEP 5.
C   START CALCULATION OF THE INDUCED VELOCITY CONTRIBUTION THAT REQUIRES
C   INTEGRATION WITH AZIMUTH.
C   START LOOP FOR NUMBER OF BLADES.
C
      DO 210 IBL=1,NB
      DB=2.*PI*(IBL-1)/NB
C
C   CALL SUBROUTINE TO DETERMINE AZIMUTH POSITIONS AT WHICH TRAJECTORY
C   IS CLOSE TO A BLADE.
C
      IF(DP1 .NE. DP2)CALL DMIN(MU,LAM,DB,RB0(I),PB0,PLIM,DMAX,IMIN,
     1PMIN)
      J1=1
      K1=0
C
C   SET LOWER AND UPPER LIMITS FOR AZIMUTH SUB-INTERVAL.
C
      PB2=PB0
      IF(IBL .EQ. 1)PB1=PB0-DP
      IF(IBL .GT. 1)PB1=PB0-DP1
  220 CONTINUE
      G1=.5*(PB2+PB1)
      G2=.5*(PB2-PB1)
C
C   PROGRAM STEP 6.
C   START LOOP FOR 5-POINT GAUSS-CHEBYSCHEV INTEGRATION.
C
      DO 230 I1=1,5
      G=G1+G2*COS((2.*I1-1.)*PI/10.)
      FACT=SQRT((G-PB1)*(PB2-G))
      DO 230 M=1,NCOFP
      M1=(M-1)/NAZ+1
      M2=M-(M1-1)*NAZ
```

```
      IF(M1 .GT. NSP)GO TO 240
      M3=M2/2
      M4=M2-M3*2
      IF(M1 .GT. 1)GO TO 250
      IF(M2 .EQ. 1)FN=FUN2(RO,AR,TW,MU,LAM,RBO(I),PBO,DP,DB,G,1)
      GO TO 260
  250 NL=M1-1
      IF(M2 .EQ. 1)FN=FUN2(RO,AR,TW,MU,LAM,RBO(I),PBO,DP,DB,G,2)
  260 IF(M2 .EQ. 1)A(L,M)=A(L,M)+FN*FACT*PI/5.
      IF(M2 .GT. 1 .AND. M4 .EQ. 0)A(L,M)=A(L,M)+FN*COS(M3*(G+DB))
     1*FACT*PI/5.
      IF(M2 .GT. 1 .AND. M4 .GT. 0)A(L,M)=A(L,M)+FN*SIN(M3*(G+DB))
     1*FACT*PI/5.
      GO TO 230
  240 I2=M+2-(NSP*NAZ)
      FN=FUN2(RO,AR,TW,MU,LAM,RBO(I),PBO,DP,DB,G,I2)
      IF(M .LE. NCOF)A(L,M)=A(L,M)+FN*FACT*PI/5.
      IF(M .EQ. NCOFP)B(L,1)=B(L,1)+FN*FACT*PI/5.
  230 CONTINUE
C
C   PROGRAM STEP 7.
C   END OF LOOP FOR GAUSS-CHEBYSCHEV INTEGRATION.
C   REDEFINE UPPER AND LOWER LIMITS FOR THE NEXT AZIMUTH SUB-INTERVAL.
C   TEST TO SEE IF THE AZIMUTH LIMIT HAS BEEN REACHED. ALSO TEST TO SEE
C   IF THE TRAJECTORY IN THE NEXT SEGMENT IS CLOSE TO A BLADE, IN WHICH
C   CASE REDUCED SPACING MUST BE USED.
C
      PB2=PB1
      IF(PB2 .LE. PLIM)GO TO 210
      IF(DP1 .EQ. DP2)GO TO 270
      IF(J1 .GT. IMIN)GO TO 270
      IF(K1 .EQ. 0 .AND. PB2 .LE. (PMIN(J1)+PI/6.))GO TO 280
      IF(K1 .EQ. 1 .AND. PB2 .GT. (PMIN(J1)-PI/6.))GO TO 280
      IF(K1 .EQ. 1 .AND. PB2 .LE. (PMIN(J1)-PI/6.))GO TO 290
      IF(PB2 .GT. (PBO-PI/6.) .AND. IBL .EQ. 1)PB1=PB1-DP2
      IF(PB2 .LE. (PBO-PI/6.) .OR. IBL .GT. 1)PB1=PB1-DP1
      IF(K1 .EQ. 0 .AND. PB1 .LT. (PMIN(J1)+DP1))PB1=PMIN(J1)+DP1
      GO TO 220
  270 PB1=PB1-DP1
      GO TO 220
  280 PB1=PB1-DP2
      K1=1
      GO TO 220
  290 PB1=PB1-DP1
      K1=0
      J1=J1+1
      GO TO 220
  210 CONTINUE
C
C   PROGRAM STEP 8.
C   END OF LOOP FOR NUMBER OF BLADES.
C   SET UP THE COEFFICIENT MATRIX ELEMENTS CORRESPONDING TO THE
C   4 AUXILIARY UNKNOWNS, AND THE RIGHT HAND SIDE.
C
      M=NSP*NAZ+1
      A(L,M)=A(L,M)-UT-(1.-RO)*(2.*MU*CP1)*CF4/(2.*AR*UT)-
     1(1.-RO)*(1.-RO)*(-2.*MU*SP1)*CF5/(4.*AR*AR*UT*UT)
      M=M+1
      A(L,M)=A(L,M)+MU*CP1-(1.-RO)*(2.*MU*SP1+RBO(I))*CF4/(2.*AR*UT)
     1-(1.-RO)*(1.-RO)*(3.*MU*CP1)*CF5/(4.*AR*AR*UT*UT)
```

```
      M=M+1
      A(L,M)=A(L,M)+.5*MU*(1.-CP2)+RBO(I)*SP1-(1.-RO)*(-2.*MU*SP2
     1-2.*RBO(I)*CP1)*CF4/(2.*AR*UT)-(1.-RO)*(1.-RO)*(-4.*MU*CP2
     2+2.*RBO(I)*SP1-2.*MU*CP1*CP1)*CF5/(4.*AR*AR*UT*UT)
      M=M+1
      A(L,M)=A(L,M)-RBO(I)*CP1-.5*MU*SP2-(1.-RO)*(2.*MU*CP2-2.*RBO(I)
     1*SP1)*CF4/(2.*AR*UT)-(1.-RO)*(1.-RO)*(-4.*MU*SP2-2.*RBO(I)
     2*CP1-2.*MU*CP1*SP1)*CF5/(4.*AR*AR*UT*UT)
      B(L,1)=B(L,1)-MU*ALR-TW*(RBO(I)-RO)*UT/(1.-RO)-TW*(-2.*MU*RO*CP1
     1+MU*MU*SP2+4.*MU*RBO(I)*CP1)*CF4/(2.*AR*UT)-(1.-RO)*TW*
     2(2.*MU*RO*SP1+2.*MU*MU*CP2-4.*MU*RBO(I)*SP1+4.*MU*MU
     3*CP1*CP1)*CF5/(4.*AR*AR*UT*UT)
      L=L+1
  100 CONTINUE
C
C   PROGRAM STEP 9.
C   END OF COLLOCATION LOOP.
C   CALCULATE SPANWISE INTEGRALS NEEDED IN SUBSEQUENT STEPS.
C
      DO 300 I=1,NSP
      FI1(I)=0.
      FI2(I)=0.
  300 CONTINUE
      G1=.5*(1.+RO)
      G2=.5*(1.-RO)
      DO 310 I=1,10
      G=G1+G2*COS((2.*I-1.)*PI/20.)
      FACT=SQRT((G-RO)*(1.-G))
      DO 310 I1=1,NSP
      NL=I1-1
      IF(I1 .GT. 1)GO TO 320
      FI1(I1)=FI1(I1)+FACT*FUN3(RO,AR,G,1)*PI/10.
      FI2(I1)=FI2(I1)+FACT*FUN3(RO,AR,G,2)*PI/10.
      GO TO 310
  320 FI1(I1)=FI1(I1)+FACT*FUN3(RO,AR,G,3)*PI/10.
      FI2(I1)=FI2(I1)+FACT*FUN3(RO,AR,G,4)*PI/10.
  310 CONTINUE
C
C   PROGRAM STEP 10.
C   SET UP THE EXTRA 4 EQUATIONS NEEDED TO CLOSE THE SYSTEM.
C
      DO 330 I=1,4
      DO 340 M=1,NCOF
      A(L,M)=0.
  340 CONTINUE
      B(L,1)=0.
      IF(I .EQ. 1 .AND. N1 .EQ. 1)GO TO 350
      IF(I .EQ. 2 .AND. N2 .EQ. 1)GO TO 360
      IF(I .EQ. 3 .AND. N3 .EQ. 1)GO TO 370
      IF(I .EQ. 4 .AND. N4 .EQ. 1)GO TO 380
      IF(I .LE. 2)I1=1
      IF(I .GT. 2)I1=I-1
      IF(I .GT. 1)GO TO 390
C
C   THE FOLLOWING EQUATION SETS THE TOTAL BLADE LIFT,AVERAGED OVER
C   THE AZIMUTH, EQUAL TO THE THRUST COEFFICIENT.
C
      M=1
      A(L,M)=A(L,M)+(1.-RO)*(1.-RO)-(1.-RO)*FI1(1)/AR
      M=M+NAZ
```

```
      A(L,M)=A(L,M)+(1.-R0)*(1.-R0)/(3.*PI)
      DO 400 I2=2,NSP
      M=(I2-1)*NAZ+I1
      A(L,M)=A(L,M)+(1.-R0)*FI1(I2)/(2.*PI*AR)
  400 CONTINUE
      M=NSP*NAZ+1
      A(L,M)=A(L,M)-(1.-R0)*(1.-R0)*(1.-R0)*(1.-R0)/(16.*AR*AR*AR)
      M=M+1
      A(L,M)=A(L,M)+(1.-R0)*(1.-R0)*(1.-R0)*(1.+R0)/(8.*AR*AR)
      B(L,1)=B(L,1)+CT/NB-(1.-R0)*(1.-R0)*(1.-R0)*(2.+R0)*TW/(16.*AR*AR*
     1AR)
      L=L+1
      GO TO 330
C
C   THE NEXT THREE EQUATIONS (I=2,3,4) REPRESENT MOMENT EQUILIBRIUM
C   ABOUT THE HUB (ZEROTH HARMONIC, FIRST HARMONIC COSINE AND FIRST
C   HARMONIC SINE COMPONENTS).
  390 M=I1
      A(L,M)=A(L,M)-FI2(1)+AR*(.5*(1.-R0*R0)+(1.-R0)*(1.-R0)/6.)
      M=M+NAZ
      A(L,M)=A(L,M)+AR*(1.-R0*R0)/(6.*PI)
      M=M+NAZ
      A(L,M)=A(L,M)+AR*(1.-R0)*(1.-R0)/(10.*PI)
      DO 410 I2=2,NSP
      M=(I2-1)*NAZ+I1
      A(L,M)=A(L,M)+FI2(I2)/(2.*PI)
  410 CONTINUE
      M=NSP*NAZ+1
      IF(I .EQ. 2)A(L,M)=A(L,M)-(1.-R0)*(1.-R0)*(1.-R0)*(1.+R0)/(32.*
     1AR*AR)
      IF(I .EQ. 3)A(L,M)=A(L,M)+MU*(1.-R0)*(1.-R0*R0)/(4.*AR)
      M=M+1
      IF(I .EQ. 2)A(L,M)=A(L,M)+(1.-R0)*(1.-R0*P0*R0)/(12.*AR)
     1-2./GAMA
      IF(I .EQ. 4)A(L,M)=A(L,M)+(1.-R0)*(1.-R0*R0)*MU/(4.*AR)
      M=M+1
      IF(I .EQ. 3)A(L,M)=A(L,M)-(1.-R0)*(1.-R0*R0*R0)/(6.*AR)
      IF(I .EQ. 4)A(L,M)=A(L,M)+(1.-R0)*(1.-R0)*(1.-R0*R0)/(16.*AR*AR)
      M=M+1
      IF(I .EQ. 3)A(L,M)=A(L,M)-(1.-R0)*(1.-R0)*(1.-R0*R0)/(16.*AR*AR)
      IF(I .EQ. 4)A(L,M)=A(L,M)-(1.-R0)*(1.-R0*R0*R0)/(6.*AR)
      IF(I .EQ. 2)B(L,1)=B(L,1)-(1.-R0)*(1.-R0)*(1.-R0)*(1.-R0)*TW/(12.
     1*AR*AR)+R0*(1.-R0)*(1.-R0)*(1.+R0)*TW/(32.*AR*AR)
      IF(I .EQ. 3)B(L,1)=B(L,1)+MU*TW*(-R0*(1.-R0*R0)/4.+(1.-R0*R0*R0)/
     13.)/AR
      IF(I .EQ. 4)B(L,1)=B(L,1)-MU*TW*(1.-R0)*(1.-R0*R0)/(8.*AR*AR)
      L=L+1
      GO TO 330
C
C   THE FOLLOWING EQUATION SETS THE COLLECTIVE PITCH EQUAL TO THE
C   GIVEN VALUE.
C
  350 M=NSP*NAZ+1
      A(L,M)=1.
      B(L,1)=THC
      L=L+1
      GO TO 330
C
C   THE FOLLOWING EQUATION SETS THE CONING ANGLE EQUAL TO THE GIVEN
C   VALUE.
```

```
C
 360  M=NSP*NAZ+2
      A(L,M)=1.
      B(L,1)=A0
      L=L+1
      GO TO 330
C
C   THE FOLLOWING EQUATION SETS THE CYCLIC PITCH COEFFICIENT, A1,EQUAL
C   TO THE GIVEN VALUE.
C
 370  M=NSP*NAZ+3
      A(L,M)=1.
      B(L,1)=A1
      L=L+1
      GO TO 330
C
C   THE FOLLOWING EQUATION SETS THE CYCLIC PITCH COEFFICIENT, B1, EQUAL
C   TO THE GIVEN VALUE.
C
 380  M=NSP*NAZ+4
      A(L,M)=1.
      B(L,1)=B1
      L=L+1
 330  CONTINUE
C
C   PROGRAM STEP 11.
C   SOLVE THE SYSTEM OF SIMULTANEOUS EQUATIONS AND PRINT THE SOLUTION.
C
      CALL GELIM(NCOF,NCOF,A,1,B,IPIVOT,0,WK,IERR)
      IF(IERR .EQ. 1)GO TO 420
      L=1
      DO 430 I1=1,NSP
      GO(I1)=B(L,1)
      L=L+1
      DO 430 I2=1,NHM
      GC(I1,I2)=B(L,1)
      L=L+1
      GS(I1,I2)=B(L,1)
      L=L+1
 430  CONTINUE
      THC=B(NSP*NAZ+1,1)
      THCD=THC*180./PI
      A0=B(NSP*NAZ+2,1)
      A0D=A0*180./PI
      A1=B(NSP*NAZ+3,1)
      A1D=A1*180./PI
      B1=B(NSP*NAZ+4,1)
      B1D=B1*180./PI
      WRITE(6,10)
      WRITE(6,440)
 440  FORMAT(//6X,"SOLUTION FOR COEFFICIENTS"/6X,25(1H-)//6X,
     1"(GO(I),I=1,NSP)")
      WRITE(6,450)(GO(I),I=1,NSP)
 450  FORMAT(/6X,5(E10.4,1X))
      WRITE(6,460)
 460  FORMAT(//6X,"(GC(I,J),J=1,NHM),I=1,NSP)"//)
      DO 470 I=1,NSP
      WRITE(6,450)(GC(I,J),J=1,NHM)
 470  CONTINUE
      WRITE(6,480)
```

```
 480  FORMAT(//6X,"(GS(I,J),J=1,NHM),I=1,NSP"//)
      DO 490 I=1,NSP
      WRITE(6,450)(GS(I,J),J=1,NHM)
 490  CONTINUE
      WRITE(6,500)THCD,A0D,A1D,B1D
 500  FORMAT(//6X,"PITCH ANGLE AT BLADE ROOT=",F10.5,"DEGREES"//6X,
     1"CONING ANGLE=",F10.5,1X,"DEGREES"//6X,
     2"FLAPPING COEFFICIENT, A1=",F10.5,1X,"DEGREES"//6X,
     3"FLAPPING COEFFICIENT, B1=",F10.5,1X,"DEGREES")
C
C  PROGRAM STEP 12.
C  START LOOP FOR AZIMUTH STATIONS AT WHICH OUTPUT QUANTITIES ARE
C  CALCULATED.
C
      CTCAL=0.
      CMXCAL=0.
      CMYCAL=0.
      DO 510 I=1,24
      PSID(I)=15.*(I-1.)
      PSI=(I-1.)*PI/12.
      CP1=COS(PSI)
      SP1=SIN(PSI)
      CP2=COS(2.*PSI)
      SP2=SIN(2.*PSI)
      FI(I)=-THC-TW*RO/(1.-RO)-2.*B1*CP1+(2.*A1+4.*MU*TW/(1.-RO))*SP1
      F2(I)=CP1*(2.*MU*TW*RO/(1.-RO)+2.*MU*THC)+2.*MU*A0*SP1
     1+2.*MU*B1*CP2-(2.*MU*A1+MU*MU*TW/(1.-RO))*SP2
      F3(I)=A0-CP1*(4.*MU*TW/(1.-RO)+2.*A1)-2.*B1*SP1
      FG1=GD(1)
      FG2=GD(2)
      FG3=GD(3)
      FN1=0.
      FN2=0.
      DO 520 I1=2,5
      FN1=FN1+FI1(I1)*GD(I1)
      FN2=FN2+FI2(I1)*GD(I1)
      DO 520 I2=1,NHM
      CI2=COS(I2*PSI)
      SI2=SIN(I2*PSI)
      IF(I1 .GT. 2)GO TO 530
      FG1=FG1+GC(1,I2)*CI2+GS(1,I2)*SI2
      FG2=FG2+GC(2,I2)*CI2+GS(2,I2)*SI2
      FG3=FG3+GC(3,I2)*CI2+GS(3,I2)*SI2
 530  FN1=FN1+FI1(I1)*(GC(I1,I2)*CI2+GS(I1,I2)*SI2)
      FN2=FN2+FI2(I1)*(GC(I1,I2)*CI2+GS(I1,I2)*SI2)
 520  CONTINUE
      FLT1(I)=-PI*(1.-RO)*FI1(1)*FG1/AR+PI*(1.-RO)*(1.-RO)*FG1+(1.-RO)*
     1(1.-RO)*FG2/3.+(1.-RO)*FN1/(2.*AR)+PI*(1.-RO)*(1.-RO)*(1.-RO)
     2*F2(I)/(4.*AR*AR)+PI*(1.-RO)*(1.-RO)*(1.-RO*RO)*F3(I)/(8.*
     3AR*AR)+PI*(1.-RO)*(1.-RO)*(1.-RO)*(1.-RO)*(F1(I)+2.*TW*(1.+RO)
     4/(1.-RO))/(16.*AR*AR*AR)
      FLT2(I)=FLT1(I)/(CT*PI/NB)
      FMT(I)=-PI*(1.-RO)*FI2(1)*FG1/AR+PI*(1.-RO)*(.5*(1.-RO*RO)+(1.-RO)
     1*(1.-RO)/6.)*FG1+(1.-RO)*(1.-RO*RO)*FG2/6.+(1.-RO)*(1.-RO)
     2*(1.-RO)*FG3/10.+(1.-RO)*FN2/(2.*AR)+PI*(1.-RO)*(1.-RO)*
     3(1.-RO*RO)*F2(I)/(8.*AR*AR)+PI*(1.-RO)*(1.-RO)*(1.-RO)*(1.-RO*RO*RO)
     4*F3(I)/(12.*AR*AR)+PI*(1.-RO)*(1.-RO)*(1.-RO)*(1.-RO)*(1.-RO*RO)*F1(I)
     5/(32.*AR*AR*AR)+PI*TW*(1.-RO)*(1.-RO)*(1.-RO*RO*RO)/(12.*AR
     6*AR*AR)
      COL(I)=FMT(I)/FLT1(I)
```

```
      CTCAL=CTCAL+FLT1(I)/24.
      CMXCAL=CMXCAL+FMT(I)*SP1/24.
      CMYCAL=CMYCAL-FMT(I)*CP1/24.
C
C  START LOOP FOR RADIAL STATIONS AT WHICH OUTPUT QUANTITIES ARE
C  CALCULATED.
C
      DO 510 I1=1,NSP
      F23=F2(I)+RBO(I1)*F3(I)
      ZB=2.*(RBO(I1)-.5*(1.+RO))/(1.-RO)
      UT=RBO(I1)+MU*SP1
      SQZ=SQRT(1.-ZB*ZB)
      PN0=PUN3(RO,AR,RBO(I1),1)
      PN1=0.
      PN2=0.
      PN3=0.
      DO 540 I2=2,5
      NL=I2-1
      PN1=PNM(I2-1,1,ZB)
      PN2=PUN3(RO,AR,RBO(I1),3)
      PN1=PN1+GC(I2)*PN1
      PN2=PN2+GC(I2)*PN2
      PN3=PN3+GC(I2)*NL*(NL+1.)*PN1
      DO 540 I3=1,NHM
      CI3=COS(I3*PBO)
      SI3=SIN(I3*PBO)
      PN1=PN1+PN1*(GC(I2,I3)*CI3+GS(I2,I3)*SI3)
      PN2=PN2+PN2*(GC(I2,I3)*CI3+GS(I2,I3)*SI3)
      PN3=PN3+NL*(NL+1.)*PN1*(GC(I2,I3)*CI3+GS(I2,I3)*SI3)
 540  CONTINUE
      GST(I,I1)=AR*((1.+ZB)*FG1+SQZ*PN1/(2.*PI))
      PDIP(I,I1)=-PNO*FG1+PN2/(2.*PI)
      DGS2(I,I1)=-AR*PN3/(2.*PI*SQZ)
      FL1(I,I1)=(1.-RO)*PI*(PDIP(I,I1)+GST(I,I1)+(1.-RO)*F23/
     1(4.*AR)+(1.-RO)*(1.-RO)*(F1(I)+4.*TW*RBO(I1)/(1.-RO))/
     2(16.*AR*AR))/AR
      FL2(I,I1)=FL1(I,I1)/(CT*PI/NB)
      FM(I,I1)=GST(I,I1)+(2.*DGS2(I,I1)+(1.-RO)*(1.-RO)*(F1(I)+4.*TW
     1*RBO(I1)/(1.-RO)))/(32.*AR*AR)
      FM(I,I1)=FM(I,I1)*PI*(1.-RO)*(1.-RO)/(4.*AR*AR)
      FM(I,I1)=FM(I,I1)+(1.-RO)*FL1(I,I1)/(4.*AR)
      XCP(I,I1)=.25+FM(I,I1)*AR/(FL1(I,I1)*(1.-RO))
 510  CONTINUE
      CTCAL=CTCAL*NB/PI
      CMXCAL=CMXCAL*NB/PI
      CMYCAL=CMYCAL*NB/PI
      WRITE(6,541)CTCAL,CMXCAL,CMYCAL
 541  FORMAT(//6X,"COMPUTED THRUST COEFFICIENT=",E10.4//6X,
     1"COMPUTED MOMENT COEFFICIENT ABOUT ROTOR X-AXIS=",E10.4//6X,
     2"COMPUTED MOMENT COEFFICIENT ABOUT ROTOR Y-AXIS=",E10.4)
C
C  PRINT OUTPUT IN TABULAR FORM.
C
      WRITE(6,10)
      WRITE(6,550)
 550  FORMAT(//6X,"TABLE 1 - SECTIONAL LIFT/(RHO*(OMEGA**2)*(R1**3))"/6X
     1,49(1H-)//)
      WRITE(6,560)(RBO(I),I=1,NSP)
 560  FORMAT(//12X,"R/R1:  ",5(E10.4,1X))
      WRITE(6,570)
```

```
570   FORMAT(//7X,"PSI")
      DO 580 I=1,24
      WRITE(6,590)PBOD(I),(FL1(I,I1),I1=1,NSP)
590   FORMAT(/6X,F5.1,8X,5(E10.4,1X))
580   CONTINUE
      WRITE(6,10)
      WRITE(6,600)
600   FORMAT(//6X,"TABLE 2 - SECTIONAL LIFT*R1/THRUST PER BLADE"/6X,
     144(1H-)//)
      WRITE(6,560)(RBO(I),I=1,NSP)
      WRITE(6,570)
      DO 610 I=1,24
      WRITE(6,590)PBOD(I),(FL2(I,I1),I1=1,NSP)
610   CONTINUE
      WRITE(6,10)
      WRITE(6,620)
620   FORMAT(//6X,"TABLE 3 - SECTIONAL PITCHING MOMENT/(RHO*(OMEGA**2)*(
     1R1**4))"/6X,60(1H-)/16X,"(ABOUT QUARTER-CHORD)"//)
      WRITE(6,560)(RBO(I),I=1,NSP)
      WRITE(6,570)
      DO 630 I=1,24
      WRITE(6,590)PBOD(I),(FM(I,I1),I1=1,NSP)
630   CONTINUE
      WRITE(6,10)
      WRITE(6,640)
640   FORMAT(//6X,"TABLE 4 - CENTER OF PRESSURE LOCATION FROM LEADING ED
     1GE(FRACTION OF CHORD)"/6X,74(1H-)//)
      WRITE(6,560)(RBO(I),I=1,NSP)
      WRITE(6,570)
      DO 650 I=1,24
      WRITE(6,590)PBOD(I),(XCP(I,I1),I1=1,NSP)
650   CONTINUE
      WRITE(6,10)
      WRITE(6,660)
660   FORMAT(//6X,"TABLE 5 - TOTAL BLADE LIFT, MOMENT ABOUT HUB AND RADI
     1AL CENTER OF LIFT"/6X,70(1H-)//6X,
     2"TOTAL BLADE LIFT/(RHO*(OMEGA**2)*(R1**4))"/6X,
     3"TOTAL BLADE LIFT/THRUST PER BLADE"/6X,
     4"MOMENT ABOUT HUB/(RHO*(OMEGA**2)*(R1**5))"/6X,
     5"RADIAL CENTER OF LIFT/R1"//7X,"PSI",8X,"TOTAL BLADE LIFT",
     65X,"MOMENT",5X,"CENTER"/38X,"ABOUT HUB",4X,"OF LIFT")
      DO 670 I=1,24
      WRITE(6,680)PBOD(I),FLT1(I),FLT2(I),FMT(I),COL(I)
680   FORMAT(/6X,F5.1,5X,4(E10.4,1X))
670   CONTINUE
      WRITE(6,10)
      WRITE(6,690)
690   FORMAT(//6X,"TABLE 6 -SURFACE PRESSURE DIFFERENTIAL/(RHO*(OMEGA**2
     1)*(R1**2))"/6X,64(1H-)//)
      DO 700 I=1,24
      WRITE(6,710)PBOD(I)
710   FORMAT(/6X,"AZIMUTH ANGLE=",F5.1,1X,"DEGREES"/6X,27(1H-))
      WRITE(6,560)(RBO(I1),I1=1,NSP)
      WRITE(6,720)
720   FORMAT(11X,"X/C")
      DO 730 I1=1,NSP
      F23=F2(I)+RBO(I1)*F3(I)
      DO 740 I2=1,10
      CCH=2.*XOUT(I2)-1.
      SCH=SQRT(1.-CCH*CCH)
```

```
      POUT(I1,I2)=-GST(I,I1)*SCH/(1.+CCH)+2.*SCH*(PDIP(I,I1)+2.*GST
     1(I,I1))+DGS2(I,I1)*SCH*SCH/(4.*AR*AR)+F23*(1.-RJ)*SCH/(2.*AR)
     2+(F1(I)+4.*TW*RB0(I1)/(1.-RJ))*(1.-R0)*(1.-R0)*(1.-RJ)*
     3SCH*(1.+CCH)/(8.*AR*AR)
      POUT(I1,I2)=2.*POUT(I1,I2)
  740 CONTINUE
  730 CONTINUE
      DO 750 I2=1,10
      WRITE(6,755)XOUT(I2),(POUT(I1,I2),I1=1,NSP)
  755 FORMAT(6X,F8.5,5X,5(E10.4,1X))
  750 CONTINUE
      IPG=3
      IREM=I-(I/IPG)*IPG
      IF(IREM .EQ. 0)WRITE(6,10)
  700 CONTINUE
      STOP
C
C  PRINT ERROR MESSAGE IF COEFFICIENT MATRIX IS SINGULAR.
C
  420 WRITE(6,760)
  760 FORMAT(/6X,"COEFFICIENT MATRIX IS SINGULAR")
      STOP
      END
      SUBROUTINE DMIN(MU,LAM,DB,RB0,PB0,PLIM,DMAX,I,P)
C
C  CALCULATION OF AZIMUTH POSITIONS AT WHICH TRAJECTORY IS DIRECTLY
C  OVER A BLADE, WITHIN A DISTANCE DMAX.
C
      REAL MU,LAM
      DIMENSION P(20)
      Y(X,X1,X2,Y1,Y2)=Y1+(Y2-Y1)*(X-X1)/(X2-X1)
      I=0
      P1=0.
      XB1=0.
      P2=-0.2
   10 XB2=RB0*SIN(P2+DB)+MU*SIN(P2+PB0+DB)*P2
      IF(P1 .NE. 0.)GO TO 20
   30 P1=P2
      IF(P1 .LE. PLIM)RETURN
      P2=P2-0.2
      XB1=XB2
      GO TO 10
   20 TEST=XB1*XB2
      IF(TEST .GT. 0.)GO TO 30
      PC=Y(0.,XB1,XB2,P1,P2)
      XBC=RB0*SIN(PC+DB)+MU*SIN(PC+PB0+DB)*PC
      RBC=RB0*COS(PC+DB)+MU*COS(PC+PB0+DB)*PC
      D=SQRT(XBC*XBC+LAM*LAM*PC*PC+(RBC-RB0)*(RBC-RB0))
      IF(D .GT. DMAX)GO TO 30
      I=I+1
      P(I)=PC
      GO TO 30
      END
      SUBROUTINE TRAJ(R0,AR,MU,LAM,RB0,PB0,DB,PB,ZS)
C  THIS SUBROUTINE CALCULATES THE PARAMETERS FOR THE LINEARISED
C  TRAJECTORY CORRESPONDING TO A GIVEN COLLOCATION POINT.
      REAL MU,LAM
      COMMON/TRAJ1/R,SX,CX,SHP,CHP,ST,CT,SHE,CHE,SP,CP
      XB=RB0*SIN(PB+DB-PB0)+MU*(PB-PB0)*SIN(PB+DB)
      YB=LAM*(PB-PB0)
```

```
      ZB=-.5*(1.+RO)+RBO*COS(PB+DB-PBO)+MU*(PB-PBO)*COS(PB+DB)
      R=SQRT(XB*XB+YB*YB)
      SX=YB/R
      CX=XB/R
      XS=2.*XB/(1.-RO)
      YS=2.*YB/(1.-RO)
      ZS=2.*ZB/(1.-RO)
      RS=2.*R/(1.-RO)
      R1=SQRT(RS*RS+(1.+ZS)*(1.+ZS))
      R2=SQRT(RS*RS+(1.-ZS)*(1.-ZS))
      CHP=(R1+R2)/2.
      SHP=SQRT(CHP*CHP-1.)
      CT=ZS/CHP
      ST=RS/SHP
      R3=SQRT((XS*AR-1.5)*(XS*AR-1.5)+YS*YS*AR*AR)
      R4=SQRT((XS*AR+.5)*(XS*AR+.5)+YS*YS*AR*AR)
      CHE=(R3+R4)/2.
      IF(CHE .LE. 1.)CHE=ABS((R4-R3)/2.)
      SHE=SQRT(CHE*CHE-1.)
      CP=(XS*AR-.5)/CHE
      SP=AR*YS/SHE
      RETURN
      END
      FUNCTION FUN1(RO,AR,I)
C  THIS SUBPROGRAM RETURNS THE VALUES OF VARIOUS FUNCTIONS REQUIRED
C  IN FUNCTION FUN2.
      COMMON/MAIN1/N,PI
      COMMON/TRAJ1/R,SX,CX,SHP,CHP,ST,CT,SHE,CHE,SP,CP
      GO TO (10,20,30,40,50,60),I
   10 F1=SHP*SHP*(CHP-CT)
      F2=(CHP-CT)*(CHP-CT)
      F3=(CHP-CT)*(CHP+CT)
      F4=(SHP*SHP*CT*CT-CHP*CHP*ST*ST)/F1-ST*ST*(CHP+CT)/F2
      FUN1=-2.*(SX*SX*F4/F3+CX*CX/F1)/(1.-RO)
      RETURN
   20 PN1=PNM(N,1,CT)
      PN2=PNM(N,2,CT)
      QN1=QNM(N,1,CHP)
      QN2=QNM(N,2,CHP)
      F1=1./(ST*SHP)
      F2=SX*SX/(SHP*SHP+ST*ST)
      FUN1=(F1*PN1*QN1+F2*(ST*CHP*PN1*QN2-CT*SHP*PN2*QN1))/(PI*(1.-RO))
      RETURN
   30 F1=SHP*SHP+ST*ST
      F2=F1*SHP*SHP
      F3=CHP/F1-CHP*CHP*CHP*ST*ST/F2
      F3=F3-2.*CHP*ST*ST*(CHP*CHP+CT*CT)/(F1*F1)
      F3=F3*SX*SX/F1
      FUN1=2.*(F3+CX*CX*CHP/F2)/(1.-RO)
      RETURN
   40 FUN1=(1.-RO)*(CX*CX-SX*SX)/(R*R)
      RETURN
   50 F1=SHE*SHE*CP*CP+CHE*CHE*SP*SP
      F2=(CHE+CP)*(CHE+CP)
      FUN1=2.*AR*(SHE*CP+SHE*CHE*(CP*CP-SP*SP))/((1.-RO)*F1*F2)
      RETURN
   60 F1=SHE*SHE*CP*CP+CHE*CHE*SP*SP
      F2=SHE*CP*CP-CHE*SP*SP
      FUN1=2.*AR*(CHE-SHE)*F2/((1.-RO)*F1)
      RETURN
```

```
      END
      FUNCTION FUN2(RO,AR,TW,MU,LAM,RBO,PBO,DP,DB,X,I)
C  THIS SUBPROGRAM SETS UP THE INTEGRAND FOR THE INTEGRATION REQUIRED
C  FOR THE INDUCED VELOCITY IN THE MAIN PROGRAM.
      REAL MU,LAM
      COMMON/MAIN1/N,PI
      COMMON/FUN21/F1,F2,F3,F4,F5,F6,ZBS
      P=X+DB
      IF(I .EQ. 2)GO TO 20
      IF(I .GT. 2)GO TO 40
      CALL TRAJ(RO,AR,MU,LAM,RBO,PBO,DB,X,ZS)
      ZBS=ZS
      F1=FUN1(RO,AR,1)
      F3=FUN1(RO,AR,3)
      F4=FUN1(RO,AR,4)
      F5=FUN1(RO,AR,5)
      F6=FUN1(RO,AR,6)
      FUN2=-F1
      IF(ABS(ZBS) .GT. 1.)GO TO 10
      FUN2=FUN2-(1.+ZBS)*F4/2.
   10 IF(DB .EQ. 0. .AND. X .GT. (PBO-DP))RETURN
      IF(ABS(ZBS) .GT. 1.)RETURN
      FUN2=FUN2+AR*(1.+ZBS)*F5
      RETURN
   20 F2=FUN1(RO,AR,2)
      FUN2=-F2
      IF(ABS(ZBS) .GT. 1.)GO TO 30
      PN1=PNM(N,1,ZBS)
      FUN2=FUN2-PN1*SQRT(1.-ZBS*ZBS)*F4/(4.*PI)
   30 IF(DB .EQ. 0. .AND. X .GT. (PBO-DP))RETURN
      IF(ABS(ZBS) .GT. 1.)RETURN
      FUN2=FUN2+AR*SQRT(1.-ZBS*ZBS)*PN1*F5/(2.*PI)
      RETURN
   40 ITEST=I-2
      ZB=(1.-RO)*ZBS/2.
      RB=ZB+.5*(1.+RO)
      GO TO (50,60,70,80,90),ITEST
   50 FN2=2.*MU*COS(P)
      FN3=0.
      GO TO 100
   60 FN2=2.*MU*SIN(P)
      FN3=1.
      GO TO 100
   70 FN2=-2.*MU*SIN(2.*P)
      FN3=-2.*COS(P)
      GO TO 100
   80 FN2=2.*MU*COS(2.*P)
      FN3=-2.*SIN(P)
      GO TO 100
   90 FN2=-TW*(2.*MU*COS(P)+MU*MU*SIN(2.*P))/(1.-RO)
      FN3=4.*MU*TW*COS(P)/(1.-RO)
  100 FUN2=-(1.-RO)*F3*(FN2+RB*FN3)/(4.*AR*AR)
      FUN2=FUN2+(1.-RO)*(1.-RO)*FN3*F1/(8.*AR*AR)
      IF(ABS(ZBS) .GT. 1.)GO TO 110
      FUN2=FUN2+(1.-RO)*(FN2+RB*FN3)*F4/(8.*AR*AR)
  110 IF(DB .EQ. 0. .AND. X .GT. (PBO-DP))RETURN
      IF(ABS(ZBS) .GT. 1.)RETURN
      FUN2=FUN2-(1.-RO)*(FN2+RB*FN3)*F6/(2.*AR)
      RETURN
      END
```

```
      FUNCTION FUN3(RO,AR,X,I)
C   THIS SUBPROGRAM SETS UP THE INTEGRAND FOR SOME SPANWISE INTEGRALS
C   REQUIRED IN THE MAIN PROGRAM.
      COMMON/MAIN1/N,PI
      ZBS=2.*(X-.5*(1.+RO))/(1.-RO)
      R1=SQRT(1./(16.*AR*AR)+.25*(1.+ZBS)*(1.+ZBS))
      R2=SQRT(1./(16.*AR*AR)+.25*(1.-ZBS)*(1.-ZBS))
      CHP1=R1+R2
      SHP1=SQRT(CHP1*CHP1-1.)
      CT1=ZBS/CHP1
      ST1=1./(2.*AR*SHP1)
      IF(I .LE. 2)GO TO 10
      PN1=PNM(N,1,CT1)
      QN1=QNM(N,1,CHP1)
      GO TO 20
   10 F1=ST1/(SHP1*(CHP1-CT1))
      IF(I .EQ. 1)FUN3=F1
      IF(I .EQ. 2)FUN3=X*F1
      RETURN
   20 F2=PN1*QN1
      IF(I .EQ. 3)FUN3=F2
      IF(I .EQ. 4)FUN3=X*F2
      RETURN
      END
      FUNCTION PNM(N,M,X)
C   CALCULATION OF ASSOCIATED LEGENDRE FUNCTIONS PNM.
C   RANGE: 0 .LE. N .LE. 4, 0 .LE. M .LE. 3, ABS(X) .LT. 1.
      IF(N .LT. 1 .OR. N .GT. 4)GO TO 10
      IF(M .LT. 0 .OR. M .GT. 3)GO TO 20
      IF(ABS(X) .GE. 1.)GO TO 30
      SX=SQRT(1.-X*X)
      IF(M .EQ. 1)GO TO 40
      IF(M .EQ. 2)GO TO 50
      IF(M .EQ. 3)GO TO 180
      GO TO (60,70,80,90),N
   60 PNM=X
      RETURN
   70 PNM=.5*(3.*X*X-1.)
      RETURN
   80 PNM=.5*(5.*X*X*X-3.*X)
      RETURN
   90 PNM=(35.*X*X*X*X-30.*X*X+3.)/8.
      RETURN
   40 GO TO (100,110,120,130),N
  100 PNM=SX
      RETURN
  110 PNM=3.*X*SX
      RETURN
  120 PNM=.5*SX*(15.*X*X-3.)
      RETURN
  130 PNM=.5*SX*(35.*X*X*X-15.*X)
      RETURN
   50 GO TO (140,150,160,170),N
  140 PNM=0.
      RETURN
  150 PNM=3.*SX*SX
      RETURN
  160 PNM=15.*X*SX*SX
      RETURN
  170 PNM=.5*SX*SX*(105.*X*X-15.)
```

```
      RETURN
  160 GO TO (190,200,210,220),N
  190 PNM=0.
      RETURN
  200 PNM=0.
      RETURN
  210 PNM=15.*SX*SX*SX
      RETURN
  220 PNM=105.*X*SX*SX*SX
      RETURN
   10 WRITE(6,11)N
   11 FORMAT(6X,*N=*,I5,1X,*INVALID N IN PNM*)
      STOP
   20 WRITE(6,21)M
   21 FORMAT(6X,*M=*,I5,1X,*INVALID M IN PNM*)
      STOP
   30 WRITE(6,31)X
   31 FORMAT(6X,*X=*,E10.4,1X,*INVALID X IN PNM*)
      STOP
      END
      FUNCTION QNM(N,M,X)
C  CALCULATION OF ASSOCIATED LEGENDRE FUNCTIONS QNM.
C  RANGE: 1 .LE. N .LE. 4, 1 .LE. M .LE. 2, ABS(X) .GT. 1.
C  ASYMPTOTIC EXPANSIONS USED FOR X .GT. 3.
      IF(N .LT. 1 .OR. N .GT. 4)GO TO 10
      IF(M .LT. 1 .OR. M .GT. 2)GO TO 20
      IF(ABS(X) .LE. 1.)GO TO 30
      SX=SQRT(X*X-1.)
      ALX=ALOG((X+1.)/(X-1.))
      X2=X*X
      X3=X2*X
      X4=X3*X
      X5=X4*X
      X6=X5*X
      X7=X6*X
      X8=X7*X
      X9=X8*X
      X10=X9*X
      X11=X10*X
      X12=X11*X
      IF(M .EQ. 2)GO TO 40
      GO TO (50,60,70,80),N
   50 IF(X .GT. 3.)GO TO 51
      QNM=SX*(.5*ALX-X/(SX*SX))
      RETURN
   51 QNM=-SX*(2./(3.*X3)+4./(5.*X5)+6./(7.*X7)+8./(9.*X9))
      RETURN
   60 IF(X .GT. 3.)GO TO 61
      QNM=SX*(1.5*X*ALX-(3.*X2-1.)/(2.*SX*SX)-1.5)
      RETURN
   61 QNM=-SX*(2./(5.*X4)+4./(7.*X6)+2./(3.*X8)+8./(11.*X10))
      RETURN
   70 IF(X .GT. 3.)GO TO 71
      QNM=SX*((15.*X2-3.)*ALX/4.-(5.*X3-3.*X)/(2.*SX*SX)-5.*X)
      RETURN
   71 QNM=-SX*(8./(35.*X5)+8./(21.*X7)+16./(33.*X9)+10./(13.*X11))
      RETURN
   80 IF(X .GT. 3.)GO TO 81
      QNM=SX*((35.*X3-15.*X)*ALX/4.-(35.*X4-30.*X2+3.)/(8.*SX*SX)
     1-105.*X2/8.+55./24.)
```

```
      RETURN
   81 QNM=-SX*(8./(63.*X6)+8./(33.*X8)+48./(143.*X10))
      RETURN
   40 GO TO (90,100,110,120),N
   90 IF(X .GT. 3.)GO TO 91
      QNM=2./(SX*SX)
      RETURN
   91 QNM=SX*SX*(2./X4+4./X6+6./X8+8./X10)
      RETURN
  100 IF(X .GT. 3.)GO TO 101
      QNM=SX*SX*(1.5*ALX-6.*X/(SX*SX)+X*(3.*X2-1.)/(SX*SX*SX*SX))
      RETURN
  101 QNM=SX*SX*(8./(5.*X5)+24./(7.*X7)+16./(3.*X9)+80./(11.*X11))
      RETURN
  110 IF(X .GT. 3.)GO TO 111
      QNM=SX*SX*(15.*X*ALX/2.-(15.*X2-3.)/(SX*SX)+X*(5.*X3-3.*X)
     1/(SX*SX*SX*SX)-5.)
      RETURN
  111 QNM=SX*SX*(8./(7.*X6)+3./(3.*X8)+48./(11.*X10)+110./(13.*X12))
      RETURN
  120 IF(X .GT. 3.)GO TO 121
      QNM=SX*SX*((105.*X2-15.)*ALX/4.-(35.*X3-15.*X)/(SX*SX)
     1+X*(35.*X4-30.*X2+3.)/(4.*SX*SX*SX*SX)-105.*X/4.)
      RETURN
  121 QNM=SX*SX*(16./(21.*X7)+64./(33.*X9)+480./(143.*X11))
      RETURN
   10 WRITE(6,11)N
   11 FORMAT(6X,*N=*,I5,1X,*INVALID N IN QNM*)
      STOP
   20 WRITE(6,21)M
   21 FORMAT(6X,*M=*,I5,1X,*INVALID M IN QNM*)
      STOP
   30 WRITE(6,31)X
   31 FORMAT(6X,*X=*,E10.4,1X,*INVALID X IN QNM*)
      STOP
      END
      SUBROUTINE TABSCH(X,N,XT,I1,I2,INT)
C
C  GIVEN AN APRAY X, TO LOCATE THE POSITION OF A VALUE XT.
C  IF INT=0, XT LIES BETWEEN X(I1) AND X(I2).
C  IF INT=1, XT IS GREATER THAN X(N).
C  IF INT=-1, XT IS LESS THAN X(1).
C
      DIMENSION X(N)
      I1=0
      I2=0
      NM=N-1
      DO 10 I=1,NM
      IF(XT .GE. X(I) .AND. XT .LE. X(I+1))GO TO 20
   10 CONTINUE
      IF(XT .LT. X(1))GO TO 30
      IF(XT .GT. X(N))GO TO 40
   20 INT=0
      IF(XT .EQ. X(I))GO TO 21
      IF(XT .EQ. X(I+1))GO TO 22
      I1=I
      I2=I+1
      RETURN
   21 I1=I2=I
      RETURN
```

```
22   I1=I2=I+1
     RETURN
30   INT=-1
     RETURN
40   INT=1
     RETURN
     END
```

APPENDIX B

LISTING OF PROGRAM ASYMP2

```
      PROGRAM MAIN(INPUT,OUTPUT,TAPE5=INPUT,TAPE6=OUTPUT,
     1AFDATA,TAPE1=AFDATA)
C
C   COMPUTATION OF THE UNSTEADY AIRLOADS ON A HELICOPTER ROTOR BLADE IN
C   FORWARD FLIGHT, USING A SIMPLIFIED VERSION OF THE ASYMPTOTIC APPROACH
C   PROPOSED BY VAN HOLTEN. THE DIPOLE STRENGTH DISTRIBUTION ALONG THE
C   BLADE IS APPROXIMATED BY A PIECEWISE CONSTANT OR PIECEWISE QUADRATIC
C   REPRESENTATION. THE HELICAL TRAJECTORY OF THE FREESTREAM FLUID
C   PARTICLE RELATIVE TO THE BLADE IS APPROXIMATED BY SUCCESSIVE STRAIGHT
C   LINE SEGMENTS.
C   FOR IDENTIFICATION OF PROGRAM STEPS, REFER USER'S MANUAL.
C
      REAL MU,LAM,MCL,MINF,MLOC
      DIMENSION R(6),RBO(5),DR(5),X(6),FX1(5),FX2(5),P1(5),P2(5),IP(5),
     1FG(5),WK(59),BT(4),GF(4,5),PMIN(20),GO(5),GC(5,5),GS(5,5),G(24,5),
     2A(59,59),B(59,1),IPIVOT(59),PBOD(24),FLT1(24),FLT2(24),
     3FMT(24),COL(24),GL(5),GR(5),FL1(24,5),FL2(24,5),FM(24,5),
     4XCP(24,5),XOUT(10),F23(24,5),POUT(5,10)
      DIMENSION CL(50,20),MCL(20),ACL(50)
      COMMON/MAIN1/XBI,XBS,YBS,RBI,RBS
      YL(XL,XL1,XL2,YL1,YL2)=YL1+(XL-XL1)*(YL2-YL1)/(XL2-XL1)
      DATA X/-1.,-.9,-.6,0.,.5,1./
      DATA NSP,NHM,NAZ,NCOF,DMAX/5,5,11,59,0.5/
      DATA XOUT/.05,.1,.2,.3,.4,.5,.7,.9,.95,.99/
      PI=4.*ATAN(1.)
C
C   PROGRAM STEP 1.
C   READ AND WRITE INPUT DATA AND ASSOCIATED QUANTITIES.
C
      READ(5,*)RO,AR,NB,TW,MU,ALR,CT,MINF
      READ(5,*)N1,N2,N3,N4
      IF(N1 .EQ. 1)READ(5,*)THC
      IF(N2 .EQ. 0)READ(5,*)GAMA
      IF(N2 .EQ. 1)READ(5,*)A0
      IF(N3 .EQ. 1)READ(5,*)A1
      IF(N4 .EQ. 1)READ(5,*)B1
      READ(5,*)(R(I),I=2,6)
C
C   ISEL .EQ. 0 -- PIECEWISE CONSTANT REPRESENTATION.
C   ISEL .EQ. 1 -- PIECEWISE QUADRATIC REPRESENTATION.
C
      READ(5,*)DP10,DP20,UTMIN,ISEL,NAFD
C
C   NAFD=0 -- AIRFOIL TABLES NOT USED.
C   NAFD=1 -- AIRFOIL TABLES USED.
C
      IF(NAFD .EQ. 0)GO TO 8
      READ(1,1)NXL,NZL
    1 FORMAT(30X,2I2)
      READ(1,2)(MCL(I),I=1,NXL)
    2 FORMAT(7X,9F7.0)
      NL1=NXL/9
      NL2=NL1+1
      DO 3 I=1,NZL
      DO 3 J=1,NL2
      J1=(J-1)*9+1
      J2=J*9
      IF(J1 .GT. NXL)GO TO 3
      IF(J2 .GT. NXL)J2=NXL
```

```
      IF(J .EQ. 1)READ(1,4)ACL(I),(CL(I,J3),J3=J1,J2)
    4 FORMAT(F7.3,9F7.0)
      IF(J .GT. 1)READ(1,5)(CL(I,J3),J3=J1,J2)
    5 FORMAT(7X,9F7.0)
    3 CONTINUE
    8 CONTINUE
      DP1=DP1D*PI/180.
      DP2=DP2D*PI/180.
      WRITE(6,9)
    9 FORMAT(1H1)
      WRITE(6,10)RO,AR,NB,TW,MU,ALR,MINF
   10 FORMAT(//6X,"ROOT RADIUS/TIP RADIUS= RO/R1 =",F10.5//6X,
     1"ASPECT RATIO=",F10.5//6X,"NUMBER OF BLADES=",I2//6X,
     2"LINEAR TWIST (ROOT TO TIP) =",F10.5,1X,"DEGREES"//6X,
     3"FORWARD SPEED/TIP SPEED=",F10.5//6X,
     4"ROTOR INCIDENCE (FORWARD TILT POSITIVE) =",F10.5,1X,
     5"DEGREES"//6X,"FREESTREAM MACH NUMBER=",F10.5)
      R(1)=RO
      TW=TW*PI/180.
      ALR=ALR*PI/180.
      IF(N1 .EQ. 0)THC=0.
      IF(N2 .EQ. 0)A0=0.
      IF(N3 .EQ. 0)A1=0.
      IF(N4 .EQ. 0)B1=0.
      WRITE(6,11)CT
   11 FORMAT(//6X,"THRUST COEFFICIENT=",F10.5)
      IF(N1 .EQ. 1)WRITE(6,12)THC
   12 FORMAT(//6X,"PITCH ANGLE AT BLADE ROOT=",F10.5,1X,"DEGREES")
      IF(N2 .EQ. 0)WRITE(6,13)GAMA
   13 FORMAT(//6X,"FLAPPING INERTIA COEFFICIENT=",F10.5)
      IF(N2 .EQ. 1)WRITE(6,14)A0
   14 FORMAT(//6X,"CONING ANGLE=",F10.5,1X,"DEGREES")
      IF(N3 .EQ. 1)WRITE(6,15)A1
   15 FORMAT(//6X,"FLAPPING COEFFICIENT, A1=",F10.5,1X,"DEGREES")
      IF(N4 .EQ. 1)WRITE(6,16)B1
   16 FORMAT(//6X,"FLAPPING COEFFICIENT, B1=",F10.5,1X,"DEGREES")
      THC=THC*PI/180.
      A0=A0*PI/180.
      A1=A1*PI/180.
      B1=B1*PI/180.
      LAM=MU*ALR+SQRT(.5*(-MU*MU+SQRT(MU*MU*MU*MU+CT*CT)))
      WRITE(6,20)LAM,UTMIN,DP1D,DP2D
   20 FORMAT(//6X,"TOTAL INFLOW RATIO=",F10.5//6X,
     1"MINIMUM UT=",F10.5,"(ZERO LIFT CONDITION APPLIED BELOW THIS VALUE
     2)"//6X,"NORMAL AZIMUTH SPACING=",F10.5,1X,"DEGREES"//6X,
     3"REDUCED AZIMUTH SPACING=",F10.5,1X,"DEGREES")
      IF(ISEL .EQ. 0)WRITE(6,30)
   30 FORMAT(//6X,"PIECEWISE CONSTANT APPROXIMATION OF SPANWISE DIPOLE ST
     1RENGTH VARIATION"/6X,70(1H*)/)
      IF(ISEL .NE. 0)WRITE(6,40)
   40 FORMAT(//6X,"PIECEWISE QUADRATIC APPROXIMATION OF SPANWISE DIPOLE S
     1TRENGTH VARIATION"/6X,71(1H*)/)
      SLOR=1.
      CL0=0.
      IF(NAFD .EQ. 0)WRITE(6,41)
   41 FORMAT(//6X,"AIRFOIL DATA TABLES NOT USED")
      IF(NAFD .EQ. 1)WRITE(6,42)
   42 FORMAT(//6X,"AIRFOIL DATA TABLES USED")
C
C  CALCULATE QUANTITIES NEEDED FOR TRAJECTORY SEGMENT ADJACENT TO
```

```
C   THE BLADE AT THE COLLOCATION POINT.
C
      ETA1P=ALOG((3.+SQRT(5.))/2.)
      CF1=COSH(.5*ETA1P)/SINH(.5*ETA1P)
      CF2=.5-EXP(-ETA1P)
      CF3=ETA1P-.5*CF1
C
C   CALCULATE QUANTITIES NEEDED FOR NEAR FIELD REPRESENTATION.
C
      DO 50 I=1,5
      T1=ACOS(X(I))
      T2=ACOS(X(I+1))
      FX1(I)=(T2-T1-(SIN(T2)-SIN(T1)))/(X(I+1)-X(I))
      FX2(I)=-((T2-T1)/2.-(SIN(2.*T2)-SIN(2.*T1))/4.)/(X(I+1)-X(I))
      FX2(I)=FX2(I)*(1.-R0)/(2.*AR)
   50 CONTINUE
      DO 60 I=1,NSP
      RBO(I)=(R(I)+R(I+1))/2.
      DR(I)=R(I+1)-R(I)
   60 CONTINUE
      IF(ISEL .EQ. 0)GO TO 70
C
C   FOR PIECEWISE QUADRATIC REPRESENTATION, DETERMINE VALUES AT THE ENDS
C   OF THE SEGMENTS IN TERMS OF THE CENTRAL VALUES.
C
      NSP1=NSP-1
      DO 80 I=1,NSPM
      BT(I)=3.*(1./DR(I)+1./DR(I+1))
      IF(I .EQ. 1)GO TO 80
      BT(I)=BT(I)-1./(BT(I-1)*DR(I)*DR(I))
   80 CONTINUE
      DO 90 I=1,NSPM
      DO 90 J=1,NSP
      GF(I,J)=0.
      IF(J .EQ. I .OR. J .EQ. (I+1))GF(I,J)=GF(I,J)+4./BT(I)
      IF(I .EQ. 1)GO TO 90
      GF(I,J)=GF(I,J)-GF(I-1,J)/(BT(I)*DR(I))
   90 CONTINUE
      DO 100 I=2,NSPM
      I1=NSP-I
      DO 100 J=1,NSP
      GF(I1,J)=GF(I1,J)-GF(I1+1,J)/(BT(I1)*DR(I1+1))
  100 CONTINUE
C
C   PROGRAM STEP 2.
C   BEGIN SETTING UP THE SYSTEM OF SIMULTANEOUS EQUATIONS.
C
   70 L=1
      DO 110 J=1,NAZ
C
C   SET THE AZIMUTH STATION FOR THE CURRENT COLLOCATION POINT.
C
      PBO=2.*J*PI/NAZ
      PBOO(J)=360.*J/NAZ
      CP1=COS(PBO)
      SP1=SIN(PBO)
      CP2=COS(2.*PBO)
      SP2=SIN(2.*PBO)
      DO 110 I=1,NSP
C
```

```
C   SET THE RADIAL STATION FOR THE CURRENT COLLOCATION POINT.
C
      UT=RBC(I)+MU*SP1
      DO 115 M=1,NCOF
      A(L,M)=0.
  115 CONTINUE
C
C   PROGRAM STEP 3.
C   TEST THE TANGENTIAL VELOCITY AT THE COLLOCATION POINT, TO DECIDE
C   WHETHER NORMAL VELOCITY BOUNDARY CONDITION OR ZERO LIFT CONDITION
C   SHOULD BE APPLIED.
C
      IF(UT .GT. UTMIN)GO TO 120
      WRITE(6,130)RBO(I),PBOD(J),UT
  130 FORMAT(/6X,"R=",F8.3,1X,"PSI=",F8.3,"DEGREES",1X,
     1"UT=",F8.3,1X,"ZERO LIFT CONDITION APPLIED")
      B(L,1)=0.
      GO TO 140
  120 DP=1.5*(1.-RO)/(2.*AR*UT)
      PLIM=-(2.+RBO(I)*CP1)/SQRT(MU*MU+LAM*LAM)
      IF(NAFO .EQ. 0)GO TO 133
C
C   PROGRAM STEP 4.
C   CALCULATE LIFT CURVE SLOPE FROM DATA TABLES FOR THE CURRENT
C   COLLOCATION POINT, USING THE LOCAL INCIDENCE AND MACH NUMBER.
C
      MLOC=UT*MINF/MU
      ALOC=THC-TW*(RBO(I)-RO)/(1.-RO)+B1*CP1-A1*SP1
     1-(MU*AO*CP1+LAM)/UT
      ALOC=ALOC*180./PI
      CALL TABSCH(MCL,NXL,MLOC,IMCL1,IMCL2,INT)
      IF(INT .EQ. -1)IMCL1=IMCL2=1
      IF(INT .EQ. 1)IMCL1=IMCL2=NXL
      CALL TABSCH(ACL,NZL,ALOC,IACL1,IACL2,INT)
      IF(INT .EQ. 0)GO TO 131
      IF(INT .EQ. -1)GO TO 132
      IACL1=NXL-1
      IACL2=NXL
      GO TO 131
  132 IACL1=1
      IACL2=2
  131 SLC1=(CL(IACL2,IMCL1)-CL(IACL1,IMCL1))/(ACL(IACL2)
     1-ACL(IACL1))
      CLO1=CL(IACL1,IMCL1)-SLC1*ACL(IACL1)
      SLC1=SLC1*180./PI
      SLC2=(CL(IACL2,IMCL2)-CL(IACL1,IMCL2))/(ACL(IACL2)
     1-ACL(IACL1))
      CLO2=CL(IACL1,IMCL2)-SLC2*ACL(IACL1)
      SLC2=SLC2*180./PI
      IF(IMCL1 .EQ. IMCL2)SLCR=SLC1/(2.*PI)
      IF(IMCL1 .NE. IMCL2)SLCR=YL(MLOC,MCL(IMCL1),MCL(IMCL2),
     1SLC1,SLC2)/(2.*PI)
      IF(IMCL1 .EQ. IMCL2)CLO=CLO1
      IF(IMCL1 .NE. IMCL2)CLO=YL(MLOC,MCL(IMCL1),MCL(IMCL2),
     1CLO1,CLO2)
  133 CONTINUE
      IF(SLCR .EQ. 0.)GO TO 134
      T1=-(CF1+(1.-SLCR)/SLCR)/UT
      T2=MU*CP1*CF3*(1.-RO)/(2.*AR*UT*UT*DR(I))
      T3=-(1.-RO)*CF3/(2.*AR*UT*UT)
```

```
      B(L,1)=-MU*ALR-UT*TW*(RBO(I)-RO)/(1.-RO)+UT*CLO/(2.*PI*SLCR)
      GO TO 140
  134 T1=1.
      T2=T3=0.
      B(L,1)=-UT*UT*CLO/(2.*PI)
  140 CONTINUE
C
C   SET UP THE CONTRIBUTION TO THE COEFFICIENT MATRIX OF THE TRAJECTORY
C   SEGMENT ADJACENT TO THE BLADE. ALTERNATIVELY, SET UP THE ZERO LIFT
C   CONDITION.
C
      DO 150 M=1,NCOF
      M1=(M-1)/NAZ+1
      M2=M-(M1-1)*NAZ
      IF(M1 .EQ. (NSP+1))GO TO 160
      M3=M2/2
      M4=M2-M3*2
      WT1=0.
      WT2=0.
      WT3=0.
      IF(UT .LE. UTMIN)GO TO 170
      IF(M1 .EQ. I)WT1=T1
      IF(M1 .EQ. I)WT3=T3
      IF(ISEL .EQ. 0)GO TO 180
      IF(I .LT. NSP)WT2=WT2+T2*GF(I,M1)/DR(M1)
      IF(I .GT. 1)WT2=WT2-T2*GF(I-1,M1)/DR(M1)
      GO TO 180
  170 IF(M1 .EQ. I)WT1=1.
  180 IF(M2 .EQ. 1)A(L,M)=WT1+WT2
      IF(M2 .GT. 1 .AND. M4 .EQ. 0)A(L,M)=(WT1+WT2)*COS(M3*PBO)
     1-M3*WT3*SIN(M3*PBO)
      IF(M2 .GT. 1 .AND. M4 .GT. 0)A(L,M)=(WT1+WT2)*SIN(M3*PBO)
     1+M3*WT3*COS(M3*PBO)
      GO TO 150
  160 IF(SLCR .EQ. 0.)GO TO 150
      IF(UT .GT. UTMIN)WT=-(1.-RO)*CF2/(2.*AR*UT)
      IF(UT .LE. UTMIN)WT=-(1.-RO)/(4.*AR)
      IF(M2 .EQ. 1)A(L,M)=WT*(2.*MU*CP1)
      IF(M2 .EQ. 2)A(L,M)=WT*(2.*MU*SP1+RBO(I))
      IF(M2 .EQ. 3)A(L,M)=WT*(-2.*MU*SP2-2.*RBO(I)*CP1)
      IF(M2 .EQ. 4)A(L,M)=WT*(2.*MU*CP2-2.*RBO(I)*SP1)
  150 CONTINUE
      IF(SLCR .EQ. 0.)GO TO 191
      B(L,1)=B(L,1)-WT*TW*(2.*MU*RO*CP1-MU*MU*SP2-4.*MU*CP1*RBO(I))/
     1(1.-RO)
      IF(UT .GT. UTMIN)GO TO 190
  191 L=L+1
      GO TO 110
C
C   PROGRAM STEP 5.
C   START LOOP FOR NUMBER OF BLADES.
C
  190 DO 200 IBL=1,NB
      IBLD=IBL
      DB=2.*PI*(IBL-1)/NB
C
C   CALL SUBROUTINE TO DETERMINE AZIMUTH POSITIONS ALONG THE TRAJECTORY
C   AT WHICH THE TRAJECTORY IS CLOSE TO A BLADE.
C
      IF(DP1 .NE. DP2)CALL DMIN(MU,LAM,DB,RBO(I),PBO,PLIM,DMAX,
```

```
     1IMIN,PMIN)
C
C   DEFINE THE AZIMUTH INTERVAL FOR THE FIRST TRAJECTORY SEGMENT.
C
      J1=1
      K1=0
      PB2=0.
      IF(IBL .EQ. 1)PB1=-DP
      IF(IBL .GT. 1)PB1=-DP1
  210 CONTINUE
      DO 220 I1=1,5
      FG(I1)=0.
  220 CONTINUE
      FCNF=0.
      FTHNF=0.
      FA0NF=0.
      FA1NF=0.
      FB1NF=0.
C
C   PROGRAM STEP 6.
C   CALCULATE SLOPE AND INTERCEPT COMPONENTS FOR CURRENT TRAJECTORY
C   SEGMENT.
C
      XB1=RB0(I)*SIN(PB1+DB)+MU*PB1*SIN(PB1+PB0+DB)
      XB2=RB0(I)*SIN(PB2+DB)+MU*PB2*SIN(PB2+PB0+DB)
      RB1=RB0(I)*COS(PB1+DB)+MU*PB1*COS(PB1+PB0+DB)
      RB2=RB0(I)*COS(PB2+DB)+MU*PB2*COS(PB2+PB0+DB)
      XBS=(XB2-XB1)/(PB2-PB1)
      XBI=XB1-XBS*PB1
      IF(PB2 .EQ. 0. .AND. (DB .EQ. 0. .OR. DB .EQ. PI))XBI=0.
      RBS=(RB2-RB1)/(PB2-PB1)
      RBI=RB1-RBS*PB1
      YBS=LAM
      NSPP=NSP+1
C
C   START CALCULATION OF FAR FIELD CONTRIBUTION.
C
      DO 230 I1=1,NSPP
      I2=I1-1
      CALL FFINT(PB1,PB2,R(I1),ISEL,FG1,FG2,FG3)
      IF(I1 .EQ. 1)GO TO 240
      IF(ISEL .EQ. 0)GO TO 250
      FF1=-(1.-RO)*(FG1-FG1M)/(4.*AR*DR(I2)*DR(I2))
      FF2=-(1.-RO)*(R(I1)*FG1-R(I2)*FG1M)/(4.*AR*DR(I2)*DR(I2))
      FF3=-(1.-RO)*(FG2-FG2M)/(4.*AR*DR(I2)*DR(I2))
      FF4=-(1.-RO)*(FG3-FG3M)/(4.*AR*DR(I2)*DR(I2))
      T1M=(-2.*(RB0(I2)+R(I1))+2.*RBI)*FF1+2.*FF2+2.*RBS*FF3-2.*FF4
      T1=(8.*RB0(I2)-4.*RBI)*FF1-4.*FF2-4.*RBS*FF3+4.*FF4
      T1P=(-2.*(RB0(I2)+R(I2))+2.*RBI)*FF1+2.*FF2+2.*RBS*FF3-2.*FF4
      DO 260 I3=1,NSP
      IF(I2 .NE. 1)FG(I3)=FG(I3)+T1M*GF(I2-1,I3)/DR(I3)
      IF(I3 .EQ. I2)FG(I3)=FG(I3)+T1
      IF(I2 .NE. NSP)FG(I3)=FG(I3)+T1P*GF(I2,I3)/DR(I3)
  260 CONTINUE
      GO TO 240
  250 FG(I2)=FG(I2)-(1.-RO)*(FG1-FG1M)/(4.*AR)
  240 FG1M=FG1
      FG2M=FG2
      FG3M=FG3
  230 CONTINUE
```

```
C
C   END CALCULATION OF FAR FIELD CONTRIBUTION.
C   CALL SUBROUTINE TO DIVIDE CURRENT TRAJECTORY SEGMENT INTO SUB-
C   SEGMENTS ALIGNED WITH SPANWISE SEGMENTS ALONG THE BLADE.
C
      CALL SUBIVL(RB1,RB2,PB1,PB2,R,IP,P1,P2)
      CB1=COS(PB2+PB0+DB)
      CB2=COS(2.*(PB2+PB0+DB))
      SB1=SIN(PB2+PB0+DB)
      SB2=SIN(2.*(PB2+PB0+DB))
      FC=TW*(2.*MU*R0*CB1-MU*MU*SB2-4.*MU*RB2*CB1)/(1.-R0)
      FTH=2.*MU*CB1
      FA0=2.*MU*SB1+RB2
      FA1=-2.*MU*SB2-2.*RB2*CB1
      FB1=2.*MU*CB2-2.*RB2*SB1
C
C   START CALCULATION OF COMMON PART AND NEAR FIELD CONTRIBUTIONS. IN
C   THE FOLLOWING LOOP, THE FIRST PASS CALCULATES THE COMMON PART, AND
C   THE SECOND PASS THE NEAR FIELD.
C
      DO 270 I1=1,2
      IF(I1 .EQ. 2 .AND. IBL .EQ. 1 .AND. PB2 .EQ. 0.)GO TO 280
      DO 270 I2=1,NSP
      FG1=0.
      FG2=0.
      FG3=0.
      FG4=0.
      IF(IP(I2) .EQ. 0)GO TO 270
      IF(I1 .EQ. 2)GO TO 290
      CALL CPINT(P1(I2),P2(I2),ISEL,FG1,FG2,FG3)
      IF(ISEL .EQ. 0)GO TO 300
      FG1=-(1.-R0)*FG1/(2.*AR*DR(I2)*DR(I2))
      FG2=-(1.-R0)*FG2/(2.*AR*DR(I2)*DR(I2))
      FG3=-(1.-R0)*FG3/(2.*AR*DR(I2)*DR(I2))
      GO TO 310
  300 FG(I2)=FG(I2)-(1.-R0)*FG1/(2.*AR)
      GO TO 270
  290 DO 320 I3=1,6
      CALL NFINT(P1(I2),P2(I2),(1.-R0)*X(I3)/(2.*AR),ISEL,FN1,FN2,FN3)
      IF(I3 .EQ. 1)GO TO 330
      FG4=FG4+FX2(I3-1)*(FN1-FN1M)/PI
      IF(ISEL .EQ. 0)GO TO 340
      FG1=FG1+FX1(I3-1)*(FN1-FN1M)/(PI*DR(I2)*DR(I2))
      FG2=FG2+FX1(I3-1)*(FN2-FN2M)/(PI*DR(I2)*DR(I2))
      FG3=FG3+FX1(I3-1)*(FN3-FN3M)/(PI*DR(I2)*DR(I2))
      GO TO 330
  340 FG(I2)=FG(I2)+FX1(I3-1)*(FN1-FN1M)/PI
  330 FN1M=FN1
      FN2M=FN2
      FN3M=FN3
  320 CONTINUE
      IF(ISEL .EQ. 0)GO TO 270
  310 T1M=2.*((RBI-R(I2+1))*(RBI-RB0(I2))*FG1+(2.*RBI-RB0(I2)
     1-R(I2+1))*RBS*FG2+RBS*RBS*FG3)
      T1=-4.*((RBI-R(I2))*(RBI-R(I2+1))*FG1+(2.*RBI-R(I2)-R(I2+1))
     1*RBS*FG2+RBS*RBS*FG3)
      T1P=2.*((RBI-R(I2))*(RBI-RB0(I2))*FG1+(2.*RBI-RB0(I2)-R(I2))
     1*RBS*FG2+RBS*RBS*FG3)
      DO 350 I3=1,NSP
      IF(I2 .GT. 1)FG(I3)=FG(I3)+T1M*GF(I2-1,I3)/DR(I3)
```

```
      IF(I3 .EQ. I2)FG(I3)=FG(I3)+T1
      IF(I2 .NE. NSP)FG(I3)=FG(I3)+T1P*GF(I2,I3)/DK(I3)
  350 CONTINUE
      IF(I1 .EQ. 1)GO TO 270
      FCNF=FCNF+FG4*FC
      FTHNF=FTHNF+FG4*FTH
      FA0NF=FA0NF+FG4*FA0
      FA1NF=FA1NF+FG4*FA1
      FB1NF=FB1NF+FG4*FB1
  270 CONTINUE
  280 CONTINUE
C
C   ADD THE CONTRIBUTIONS, CALCULATED FOR THE CURRENT TRAJECTORY SEGMENT,
C   TO THE COEFFICIENT MATRIX ELEMENTS
C
      DO 360 M=1,NCOF
      M1=(M-1)/NAZ+1
      M2=M-(M1-1)*NAZ
      IF(M1 .EQ. (NSP+1))GO TO 370
      M3=M2/2
      M4=M2-M3*2
      IF(M2 .EQ. 1)A(L,M)=A(L,M)+FG(M1)
      IF(M2 .GT. 1 .AND. M4 .EQ. 0)A(L,M)=A(L,M)+FG(M1)
     1*COS(M3*(PB2+PB0+DB))
      IF(M2 .GT. 1 .AND. M4 .GT. 0)A(L,M)=A(L,M)+FG(M1)
     1*SIN(M3*(PB2+PB0+DB))
      GO TO 360
  370 IF(M2 .EQ. 1)A(L,M)=A(L,M)+FTHNF
      IF(M2 .EQ. 2)A(L,M)=A(L,M)+FA0NF
      IF(M2 .EQ. 3)A(L,M)=A(L,M)+FA1NF
      IF(M2 .EQ. 4)A(L,M)=A(L,M)+FB1NF
  360 CONTINUE
      B(L,1)=B(L,1)-FCNF
C
C   PROGRAM STEP 7.
C   REDEFINE THE AZIMUTH INTERVAL, FOR THE NEXT TRAJECTORY SEGMENT.
C   TEST TO SEE IF THE FINAL SEGMENT HAS BEEN CALCULATED. ALSO TEST
C   TO SEE IF THE NEXT SEGMENT IS CLOSE TO A BLADE, IN WHICH CASE
C   REDUCED SPACING IS TO BE USED.
C
      PB2=PB1
      IF(PB2 .LE. PLIM)GO TO 200
      IF(DP1 .EQ. DP2)GO TO 380
      IF(J1 .GT. IMIN)GO TO 380
      IF(K1 .EQ. 0 .AND. PB2 .LE. (PMIN(J1)+DP1))GO TO 390
      IF(K1 .EQ. 1 .AND. PB2 .GT. (PMIN(J1)-DP1))GO TO 390
      IF(K1 .EQ. 1 .AND. PB2 .LE. (PMIN(J1)-DP1))GO TO 400
      IF(PB2 .GT. (-3.*DP1) .AND. IBL .EQ. 1)PB1=PB1-DP2
      IF(PB2 .LE. (-3.*DP1) .OR. IBL .GT. 1)PB1=PB1-DP1
      IF(K1 .EQ. 0 .AND. PB1 .LT. (PMIN(J1)+DP1))PB1=PMIN(J1)+DP1
      GO TO 210
  380 PB1=PB1-DP1
      GO TO 210
  390 PB1=PB1-DP2
      K1=1
      GO TO 210
  400 PB1=PB1-DP1
      K1=0
      J1=J1+1
      GO TO 210
```

```
C
C   PROGRAM STEP 8. END OF LOOP FOR NUMBER OF BLADES.
C
 200  CONTINUE
C
C   SET UP THE ELEMENTS CORRESPONDING TO THE 4 AUXILIARY UNKNOWNS.
C
      M=NSP*NAZ+1
      A(L,M)=A(L,M)-UT
      M=M+1
      A(L,M)=A(L,M)+MU*CP1
      M=M+1
      A(L,M)=A(L,M)+RBO(I)*SP1+.5*MU*(1.-CP2)
      M=M+1
      A(L,M)=A(L,M)-RBO(I)*CP1-.5*MU*SP2
      L=L+1
C
C   PROGRAM STEP 9. END OF COLLOCATION LOOP.
C
 110  CONTINUE
C
C   PROGRAM STEP 10.
C   SET UP THE EXTRA 4 EQUATIONS NEEDED TO CLOSE THE SYSTEM.
C
      DO 410 I=1,4
      DO 420 M=1,NCOF
      A(L,M)=0.
 420  CONTINUE
      B(L,1)=0.
      IF(I .EQ. 1 .AND. N1 .EQ. 1)GO TO 430
      IF(I .EQ. 2 .AND. N2 .EQ. 1)GO TO 440
      IF(I .EQ. 3 .AND. N3 .EQ. 1)GO TO 450
      IF(I .EQ. 4 .AND. N4 .EQ. 1)GO TO 460
      IF(I .LE. 2)I1=1
      IF(I .GT. 2)I1=I-1
      DO 470 M1=1,NSP
      IF(I .GT. 1)GO TO 480
      DO 490 M2=1,NSP
      M=(M2-1)*NAZ+I1
      IF(ISEL .EQ. 0)GO TO 500
      IF(M1 .NE. 1)A(L,M)=A(L,M)-DR(M1)*GF(M1-1,M2)/(6.*DR(M2))
      IF(M2 .EQ. M1)A(L,M)=A(L,M)-4.*DR(M1)/6.
      IF(M1 .LT. NSP)A(L,M)=A(L,M)-DR(M1)*GF(M1,M2)/(6.*DR(M2))
      GO TO 490
 500  IF(M2 .EQ. M1)A(L,M)=A(L,M)-DR(M1)
 490  CONTINUE
      GO TO 470
 480  DO 510 M2=1,NSP
      M=(M2-1)*NAZ+I1
      IF(ISEL .EQ. 0)GO TO 520
      IF(M1 .NE. 1)A(L,M)=A(L,M)-R(M1)*DR(M1)*GF(M1-1,M2)/(6.*DR(M2))
      IF(M2 .EQ. M1)A(L,M)=A(L,M)-4.*RBO(M1)*DR(M1)/6.
      IF(M1 .LT. NSP)A(L,M)=A(L,M)-R(M1+1)*DR(M1)*GF(M1,M2)/(6.*DR(M2))
      GO TO 510
 520  IF(M2 .EQ. M1)A(L,M)=A(L,M)-RBO(M1)*DR(M1)
 510  CONTINUE
 470  CONTINUE
      GO TO (530,540,550,560),I
 530  M=NSP*NAZ+2
      A(L,M)=(1.-RO)*(1.-RO*RO)/(8.*AR)
```

```
      B(L,1)=AR*CT/(NB*(1.-RO))
C
C   THE ABOVE EQUATION EQUATES THE TOTAL LIFT DUE TO ALL THE BLADES,
C   AVERAGED OVER THE AZIMUTH, TO THE THRUST COEFFICIENT.
C
      L=L+1
      GO TO 410
  430 M=NSP*NAZ+1
      A(L,M)=1.
      B(L,1)=THC
C
C   THE ABOVE EQUATION SETS THE COLLECTIVE PITCH TO THE GIVEN VALUE.
C
      L=L+1
      GO TO 410
  540 M=NSP*NAZ+2
      A(L,M)=(1.-RO)*(1.-RO*RO*RO)/(12.*AR)-2./GAMA
      B(L,1)=0.
C
C   THE ABOVE EQUATION REPRESENTS THE ZEROTH HARMONIC COMPONENT OF
C   MOMENT EQUILIBRIUM ABOUT THE HUB.
C
      L=L+1
      GO TO 410
  440 M=NSP*NAZ+2
      A(L,M)=1.
      B(L,1)=AO
C
C   THE ABOVE EQUATION SETS THE CONING ANGLE TO THE GIVEN VALUE.
C
      L=L+1
      GO TO 410
  550 M=NSP*NAZ+1
      A(L,M)=MU*(1.-RO)*(1.-RO*RO)/(4.*AR)
      M=M+2
      A(L,M)=-(1.-RO)*(1.-RO*RO*RO)/(6.*AR)
      B(L,1)=-TW*MU*(RO*(1.-RO*RO)-4.*(1.-RO*RO*RO)/3.)/(4.*AR)
C
C   THE ABOVE EQUATION REPRESENTS THE FIRST HARMONIC COSINE COMPONENT
C   OF MOMENT EQUILIBRIUM ABOUT THE HUB.
C
      L=L+1
      GO TO 410
  450 M=NSP*NAZ+3
      A(L,M)=1.
      B(L,1)=A1
C
C   THE ABOVE EQUATION SETS THE CYCLIC PITCH COEFFICIENT, A1, TO THE
C   GIVEN VALUE.
C
      L=L+1
      GO TO 410
  560 M=NSP*NAZ+2
      A(L,M)=MU*(1.-RO)*(1.-RO*RO)/(4.*AR)
      M=M+2
      A(L,M)=-(1.-RO)*(1.-RO*RO*RO)/(6.*AR)
      B(L,1)=0.
C
C   THE ABOVE EQUATION REPRESENTS THE FIRST HARMONIC SINE COMPONENT OF
C   MOMENT EQUILIBRIUM ABOUT THE HUB.
```

```
C
      L=L+1
      GO TO 410
 460  M=NSP*NAZ+4
      A(L,M)=1.
      B(L,1)=B1
C
C   THE ABOVE EQUATION SETS THE CYCLIC PITCH COEFFICIENT, B1, TO THE
C   GIVEN VALUE.
C
      L=L+1
 410  CONTINUE
C
C   PROGRAM STEP 11.
C   SOLVE THE SYSTEM OF SIMULTANEOUS EQUATIONS AND PRINT THE SOLUTION.
C
      CALL GELIM(NCOF,NCOF,A,1,B,IPIVOT,D,WK,IERR)
      IF(IERR .EQ. 1)GO TO 570
      L=1
      DO 580 I=1,NSP
      GC(I)=B(L,1)
      L=L+1
      DO 580 J=1,NHM
      GC(I,J)=B(L,1)
      L=L+1
      GS(I,J)=B(L,1)
      L=L+1
 580  CONTINUE
      THC=B(NSP*NAZ+1,1)
      THCD=THC*180./PI
      A0=B(NSP*NAZ+2,1)
      A0D=A0*180./PI
      A1=B(NSP*NAZ+3,1)
      A1D=A1*180./PI
      B1=B(NSP*NAZ+4,1)
      B1D=B1*180./PI
      WRITE(5,9)
      WRITE(6,590)
 590  FORMAT(6X,"SOLUTION FOR COEFFICIENTS"/6X,25(1H-)//6X,
     1"(GO(I),I=1,NSP)")
      WRITE(6,600)(GO(I),I=1,NSP)
 600  FORMAT(//6X,5(E10.4,1X))
      WRITE(6,610)
 610  FORMAT(//6X,"((GC(I,J),J=1,NHM),I=1,NSP)"//)
      DO 620 I=1,NSP
      WRITE(6,600)(GC(I,J),J=1,NHM)
 620  CONTINUE
      WRITE(6,630)
 630  FORMAT(//6X,"((GS(I,J),J=1,NHM),I=1,NSP)"//)
      DO 640 I=1,NSP
      WRITE(6,600)(GS(I,J),J=1,NHM)
 640  CONTINUE
      WRITE(6,650)THCD,A0D,A1D,B1D
 650  FORMAT(//6X,"PITCH ANGLE AT BLADE ROOT=",F10.5,1X,"DEGREES"//6X,
     1"CONING ANGLE=",F10.5,1X,"DEGREES"//6X,
     2"FLAPPING COEFFICIENT, A1=",F10.5,1X,"DEGREES"//6X,
     3"FLAPPING COEFFICIENT, B1=",F10.5,1X,"DEGREES")
C
C   PROGRAM STEP 12.
C   START LOOP FOR AZIMUTH STATIONS AT WHICH OUTPUT QUANTITIES ARE
```

```
C  CALCULATED.
C
      CTCAL=0.
      CMXCAL=0.
      CMYCAL=0.
      DO 670 I=1,24
      PBOD(I)=15.*(I-1)
      PBO=PBOD(I)*PI/180.
      CP1=COS(PBO)
      SP1=SIN(PBO)
      CP2=COS(2.*PBO)
      SP2=SIN(2.*PBO)
      F2=CP1*(2.*MU*TW*RO/(1.-RO)+2.*MU*THC)+2.*MU*AO*SP1+2.*MU*B1*CP2
     1-SP2*(MU*MU*TW/(1.-RO)+2.*MU*A1)
      F3=AO-CP1*(4.*MU*TW/(1.-RO)+2.*A1)-2.*B1*SP1
      GI1=0.
      GI2=0.
      DO 690 I1=1,NSP
      G(I,I1)=GO(I1)
      DO 690 I2=1,NHM
      G(I,I1)=G(I,I1)+GC(I1,I2)*COS(I2*PBO)+GS(I1,I2)*SIN(I2*PBO)
 690  CONTINUE
      DO 700 I1=1,NSP
      IF(ISEL .NE. 0)GO TO 710
      GI1=GI1+DR(I1)*G(I,I1)
      GI2=GI2+DR(I1)*RBO(I1)*G(I,I1)
      GO TO 700
 710  GI1=GI1+4.*DR(I1)*G(I,I1)/6.
      GI2=GI2+4.*DR(I1)*RBO(I1)*G(I,I1)/6.
      IF(I1 .EQ. 1)GL(I1)=0.
      IF(I1 .GT. 1)GL(I1)=GR(I1-1)
      GR(I1)=0.
      IF(I1 .EQ. NSP)GO TO 720
      DO 730 I2=1,NSP
      GR(I1)=GR(I1)+GF(I1,I2)*G(I,I2)/DR(I2)
 730  CONTINUE
 720  GI1=GI1+DR(I1)*(GL(I1)+GR(I1))/6.
      GI2=GI2+DR(I1)*(R(I1)*GL(I1)+R(I1+1)*GR(I1))/6.
 700  CONTINUE
      FLT1(I)=(1.-RO*RO)*AO/2.+CP1*(2.*MU*THC*(1.-RO)-2.*MU*TW
     1-A1*(1.-RO*RO))+SP1*(1.-RO)*(2.*MU*AO-B1*(1.+RO))
     2+2.*MU*B1*(1.-RO)*CP2-SP2*(2.*MU*A1*(1.-RO)+MU*MU*TW)
      FLT1(I)=-FLT1(I)*(1.-RO)/(4.*AR)
      FLT1(I)=-(FLT1(I)+GI1)*PI*(1.-RO)/AR
      FLT2(I)=FLT1(I)/(CT*PI/NB)
      FMT(I)=(1.-RO*RO*RO)*AO/3.+CP1*(MU*THC*(1.-RO*RO)-2.*A1*
     1(1.-RO*RO*RO)/3.+MU*TW*RO*(1.+RO)-4.*MU*TW*(1.+RO+RO*RO)/3.)
     2+SP1*(MU*AO*(1.-RO*RO)-2.*B1*(1.-RO*RO*RO)/3.)+CP2*MU*B1*
     3(1.-RO*RO)-SP2*(MU*A1*(1.-RO*RO)+MU*MU*TW*(1.+RO)/2.)
      FMT(I)=-FMT(I)*(1.-RO)/(4.*AR)
      FMT(I)=-(FMT(I)+GI2)*PI*(1.-RO)/AR
      COL(I)=FMT(I)/FLT1(I)
      CTCAL=CTCAL+FLT1(I)/24.
      CMXCAL=CMXCAL+FMT(I)*SP1/24.
      CMYCAL=CMYCAL-FMT(I)*CP1/24.
C
C  START LOOP FOR RADIAL STATIONS AT WHICH OUTPUT QUANTITIES ARE
C  CALCULATED.
C
      DO 740 I1=1,NSP
```

```
      IF(ISEL .EQ. 0)GO TO 780
      QC=2.*(GR(I1)+GL(I1)-2.*G(I,I1))/(DR(I1)*DR(I1))
      QB=(GR(I1)-GL(I1))/DR(I1)-2.*QC*RBO(I1)
      QA=G(I,I1)-RBO(I1)*QB-RBO(I1)*RBO(I1)*QC
      GOUT=QA+QB*RBO(I1)+QC*RBO(I1)*RBO(I1)
      GO TO 790
  780 GOUT=G(I,I1)
  790 F23(I,I1)=F2+RBO(I1)*F3
      FL1(I,I1)=-PI*(1.-RO)*(GOUT-(1.-RO)*F23(I,I1)/(4.*AR))/AR
      FL2(I,I1)=FL1(I,I1)/(CT*PI/NB)
      FM(I,I1)=-PI*(1.-RO)*(1.-RO)*F23(I,I1)/(16.*AR*AR*AR)
      XCP(I,I1)=.25+FM(I,I1)*AR/(FL1(I,I1)*(1.-RO))
  740 CONTINUE
  670 CONTINUE
      CTCAL=CTCAL*NB/PI
      CMXCAL=CMXCAL*NB/PI
      CMYCAL=CMYCAL*NB/PI
      WRITE(6,791)CTCAL,CMXCAL,CMYCAL
  791 FORMAT(//6X,"COMPUTED THRUST COEFFICIENT=",E10.4//6X,
     1"COMPUTED MOMENT COEFFICIENT ABOUT ROTOR X-AXIS=",E10.4//6X,
     2"COMPUTED MOMENT COEFFICIENT ABOUT ROTOR Y-AXIS=",E10.4)
C
C  PRINT ALL OUTPUT QUANTITIES IN TABULAR FORM.
C
      WRITE(6,9)
      WRITE(6,800)
  800 FORMAT(//6X,"TABLE 1 - SECTIONAL LIFT/(RHO*(OMEGA**2)*(R1**3))"/6X
     1,49(1H-)//)
      WRITE(6,810)(RBO(I),I=1,NSP)
  810 FORMAT(/12X,"R/R1:  ",5(E10.4,1X))
      WRITE(6,811)
  811 FORMAT(/7X,"PSI")
      DO 820 I=1,24
      WRITE(6,830)PBOD(I),(FL1(I,I1),I1=1,NSP)
  830 FORMAT(/6X,F5.1,6X,5(E10.4,1X))
  820 CONTINUE
      WRITE(6,9)
      WRITE(6,840)
  840 FORMAT(//6X,"TABLE 2 - SECTIONAL LIFT*R1/THRUST PER BLADE"/6X,
     144(1H-)//)
      WRITE(6,810)(RBO(I),I=1,NSP)
      WRITE(6,811)
      DO 850 I=1,24
      WRITE(6,830)PBOD(I),(FL2(I,I1),I1=1,NSP)
  850 CONTINUE
      WRITE(6,9)
      WRITE(6,860)
  860 FORMAT(//6X,"TABLE 3 - SECTIONAL PITCHING MOMENT/(RHO*(OMEGA**2)*(
     1R1**4))"/6X,60(1H-)/16X,"(ABOUT QUARTER-CHORD)"//)
      WRITE(6,810)(RBO(I),I=1,NSP)
      WRITE(6,811)
      DO 870 I=1,24
      WRITE(6,830)PBOD(I),(FM(I,I1),I1=1,NSP)
  870 CONTINUE
      WRITE(6,9)
      WRITE(6,880)
  880 FORMAT(//6X,"TABLE 4 - CENTER OF PRESSURE LOCATION FROM LEADING ED
     1GE(FRACTION OF CHORD)"/6X,74(1H-)//)
      WRITE(6,810)(RBO(I),I=1,NSP)
      WRITE(6,811)
```

```
      DO 890 I=1,24
      WRITE(6,830)PBOD(I),(XCP(I,I1),I1=1,NSP)
  890 CONTINUE
      WRITE(6,9)
      WRITE(6,900)
  900 FORMAT(//6X,"TABLE 5 - TOTAL BLADE LIFT, MOMENT ABOUT HUB AND RADI
     1AL CENTER OF LIFT"/6X,70(1H-)//6X,
     2"TOTAL BLADE LIFT/(RHO*(OMEGA**2)*(R1**4))"/6X,
     3"TOTAL BLADE LIFT/THRUST PER BLADE"/6X,
     4"MOMENT ABOUT HUB/(RHO*(OMEGA**2)*(R1**5))"/6X,
     5"RADIAL CENTER OF LIFT/R1"//7X,"PSI",8X,"TOTAL BLADE LIFT",
     55X,"MOMENT",5X,"CENTER"/38X,"ABOUT HUB",4X,"OF LIFT")
      DO 910 I=1,24
      WRITE(6,920)PBOD(I),FLT1(I),FLT2(I),FMT(I),COL(I)
  920 FORMAT(//6X,F5.1,5X,4(E10.4,1X))
  910 CONTINUE
      WRITE(6,9)
      WRITE(6,940)
  940 FORMAT(//6X,"TABLE 6 - SURFACE PRESSURE DIFFERENTIAL/(RHO*(OMEGA**
     12)*(R1**2))"/6X,64(1H-)//)
      DO 950 I=1,24
      WRITE(6,960)PBOD(I)
  960 FORMAT(//5X,"AZIMUTH ANGLE=",F5.1,1X,"DEGREES"/6X,27(1H-))
      WRITE(6,810)(RBO(I1),I1=1,NSP)
      WRITE(6,970)
  970 FORMAT(11X,"X/C")
      DO 980 I1=1,NSP
      DO 980 I2=1,10
      CCH=2.*XOUT(I2)-1.
      SCH=SQRT(1.-CCH*CCH)
      POUT(I1,I2)=-G(I,I1)*SCH/(1.+CCH)+F23(I,I1)*(1.-RO)*SCH/(2.*AR)
      POUT(I1,I2)=2.*POUT(I1,I2)
  980 CONTINUE
      DO 990 I2=1,10
      WRITE(6,991)XOUT(I2),(POUT(I1,I2),I1=1,NSP)
  991 FORMAT(6X,F8.5,5X,5(E10.4,1X))
  990 CONTINUE
      IREM=I-(I/3)*3
      IF(IREM .EQ. 0)WRITE(6,9)
  950 CONTINUE
      STOP
C
C   PRINT ERROR MESSAGE IF COEFFICIENT MATRIX IS SINGULAR.
C
  970 WRITE(6,930)
  930 FORMAT(6X,"COEFFICIENT MATRIX SINGULAR")
      STOP
      END
      SUBROUTINE DMIN(MU,LAM,DB,RBO,PBO,PLIM,DMAX,I,P)
C
C   CALCULATION OF AZIMUTH POSITIONS AT WHICH TRAJECTORY IS DIRECTLY
C   OVER A BLADE, WITHIN A DISTANCE DMAX.
C
      REAL MU,LAM
      DIMENSION P(20)
      Y(X,X1,X2,Y1,Y2)=Y1+(Y2-Y1)*(X-X1)/(X2-X1)
      I=0
      P1=0.
      XB1=0.
      P2=-0.2
```

```
   10  XB2=RB0*SIN(P2+DB)+MU*SIN(P2+PB0+DB)*P2
       IF(P1 .NE. 0.)GO TO 20
   30  P1=P2
       IF(P1 .LE. PLIM)RETURN
       P2=P2-0.2
       XB1=XB2
       GO TO 10
   20  TEST=XB1*XB2
       IF(TEST .GT. 0.)GO TO 30
       PC=Y(0.,XB1,XB2,P1,P2)
       XBC=RB0*SIN(PC+DB)+MU*SIN(PC+PB0+DB)*PC
       RBC=RB0*COS(PC+DB)+MU*COS(PC+PB0+DB)*PC
       D=SQRT(XBC*XBC+LAM*LAM*PC*PC+(RBC-RB0)*(RBC-RB0))
       IF(D .GT. DMAX)GO TO 30
       I=I+1
       P(I)=PC
       GO TO 30
       END
       SUBROUTINE SUBIVL(RB1,RB2,PB1,PB2,R,I,P1,P2)
C
C  DIVISION OF TRAJECTORY SEGMENT INTO SUB-SEGMENTS ALIGNED WITH BLADE
C  SPANWISE SEGMENTS.
C
       DIMENSION R(6),I(5),P1(5),P2(5)
       Y(X,X1,X2,Y1,Y2)=Y1+(Y2-Y1)*(X-X1)/(X2-X1)
       DO 10 J=1,5
       I(J)=0
       P1(J)=0.
       P2(J)=0.
   10  CONTINUE
       DO 20 J=1,5
       R1=R(J)
       R2=R(J+1)
       IF(RB1 .LE. R1 .AND. RB2 .LE. R1)GO TO 20
       IF(RB1 .GE. R2 .AND. RB2 .GE. R2)GO TO 20
       IF(RB1 .GE. R1 .AND. RB1 .LE. R2 .AND. RB2 .GE. R1
      1.AND. RB2 .LE. R2)GO TO 30
       IF(RB1 .LE. R2 .AND. RB2 .GT. R1)GO TO 40
       IF(RB1 .LT. R2 .AND. RB2 .GE. R2)GO TO 50
       IF(RB1 .GT. R1 .AND. RB2 .LE. R1)GO TO 60
       IF(RB1 .GE. R2 .AND. RB2 .LT. R2)GO TO 70
   30  I(J)=1
       P1(J)=PB1
       P2(J)=PB2
       RETURN
   40  I(J)=1
       P1(J)=Y(R1,RB1,RB2,PB1,PB2)
       IF(RB2 .GT. R2)P2(J)=Y(R2,RB1,RB2,PB1,PB2)
       IF(RB2 .LE. R2)P2(J)=PB2
       GO TO 20
   50  I(J)=1
       P2(J)=Y(R2,RB1,RB2,PB1,PB2)
       IF(RB1 .LT. R1)P1(J)=Y(R1,RB1,RB2,PB1,PB2)
       IF(RB1 .GE. R1)P1(J)=PB1
       GO TO 20
   60  I(J)=1
       P2(J)=Y(R1,RB1,RB2,PB1,PB2)
       IF(RB1 .GT. R2)P1(J)=Y(R2,RB1,RB2,PB1,PB2)
       IF(RB1 .LE. R2)P1(J)=PB1
       GO TO 20
```

```
   70   I(J)=1
        P1(J)=Y(R2,RB1,RB2,PB1,PB2)
        IF(RB2 .LT. R1)P2(J)=Y(R1,RB1,RB2,PB1,PB2)
        IF(RB2 .GE. R1)P2(J)=PB2
   20   CONTINUE
        RETURN
        END
        SUBROUTINE NFINT(P1,P2,X,ISEL,T1,T2,T3)
C
C   INTEGRATION OF NEAR FIELD PRESSURE GRADIENT.
C
        DIMENSION F0(2),F1(2),F2(2),F3(2)
        COMMON/MAIN1/XI,XS,YS,RI,RS
        D0=(X-XI)*(X-XI)
        D1=-2.*(X-XI)*XS
        D2=XS*XS+YS*YS
        Q=4.*D0*D2-D1*D1
        IF(Q .NE. 0.)SQ=SQRT(Q)
        DO 10 I=1,2
        IF(I .EQ. 1)P=P1
        IF(I .EQ. 2)P=P2
        DD=D0+D1*P+D2*P*P
        IF(Q .NE. 0.)F0(I)=2.*ATAN((D1+2.*D2*P)/SQ)/SQ
        IF(Q .EQ. 0.)F0(I)=-1./(D2*P)
        F1(I)=(ALOG(DD)-D1*F0(I))/(2.*D2)
        IF(ISEL .EQ. 0)GO TO 20
        F2(I)=(P-D1*F1(I)-D0*F0(I))/D2
        F3(I)=(P*P/2.-D1*F2(I)-D0*F1(I))/D2
        GO TO 10
   20   F2(I)=0.
        F3(I)=0.
   10   CONTINUE
        T1=(X-XI)*(F0(2)-F0(1))-XS*(F1(2)-F1(1))
        T2=(X-XI)*(F1(2)-F1(1))-XS*(F2(2)-F2(1))
        T3=(X-XI)*(F2(2)-F2(1))-XS*(F3(2)-F3(1))
        RETURN
        END
        SUBROUTINE CPINT(P1,P2,ISEL,T1,T2,T3)
C
C   INTEGRATION OF COMMON PART PRESSURE GRADIENT.
C
        DIMENSION F0(2),F1(2),F2(2),F3(2),F4(2)
        COMMON/MAIN1/XI,XS,YS,RI,RS
        R0=XI*XI
        R1=XI*XS
        R2=XS*XS+YS*YS
        Q=4.*XI*XI*YS*YS
        IF(Q .NE. 0.)SQ=SQRT(Q)
        DO 10 I=1,2
        IF(I .EQ. 1)P=P1
        IF(I .EQ. 2)P=P2
        RR=R0+2.*R1*P+R2*P*P
        IF(Q .EQ. 0. .AND. P .EQ. 0.)GO TO 20
        IF(Q .NE. 0.)T=2.*ATAN((2.*R1+2.*R2*P)/SQ)/SQ
        IF(Q .EQ. 0.)T=0.
        IF(Q .NE. 0.)F0(I)=2.*(R1+R2*P)/(Q*RR)+2.*R2*T/Q
        IF(Q .EQ. 0.)F0(I)=-1./(3.*R2*R2*P*P*P)
        F1(I)=(-1./(2.*RR)-R1*F0(I))/R2
        F2(I)=(-P/RR+R0*F0(I))/R2
        IF(ISEL .EQ. 0)GO TO 30
```

```
      F3(I)=(-R0*F1(I)-2.*R1*F2(I))/R2+(ALOG(RR)/2.-R1*T)/(R2*R2)
      IF(Q .EQ. 0.)F3(I)=ALOG(P*P)/(2.*R2*R2)
      F4(I)=(P*P*P/RR-4.*R1*F3(I)-3.*R0*F2(I))/R2
      GO TO 10
   20 F0(I)=0.
      F1(I)=0.
      F2(I)=0.
   30 F3(I)=0.
      F4(I)=0.
   10 CONTINUE
      DF0=F0(2)-F0(1)
      DF1=F1(2)-F1(1)
      DF2=F2(2)-F2(1)
      DF3=F3(2)-F3(1)
      DF4=F4(2)-F4(1)
      T1=R0*DF0+2.*R1*DF1+(XS*XS-YS*YS)*DF2
      T2=R0*DF1+2.*R1*DF2+(XS*XS-YS*YS)*DF3
      T3=R0*DF2+2.*R1*DF3+(XS*XS-YS*YS)*DF4
      RETURN
      END
      SUBROUTINE FFINT(P1,P2,R,ISEL,T1,T2,T3)
C
C  INTEGRATION OF FAR FIELD PRESSURE GRADIENT.
C
      DIMENSION F1(2),F2(2),F3(2)
      COMMON/MAIN1/XI,XS,YS,RI,RS
      R0=XI*XI
      R1=XI*XS
      R2=XS*XS+YS*YS
      D0=R0+(R-RI)*(R-RI)
      D1=R1-(R-RI)*RS
      D2=R2+RS*RS
      SD2=SQRT(D2)
      FN1=ABS(XI*YS)
      FN2=(R-RI)*R2+RS*R1
      FN3=D1*D1-D0*D2
      Q=4.*D2*FN1*FN1
      IF(Q .NE. 0.)SQ=SQRT(Q)
      DO 10 I=1,2
      IF(I .EQ. 1)P=P1
      IF(I .EQ. 2)P=P2
      F1(I)=0.
      F2(I)=0.
      F3(I)=0.
      XB=XI+XS*P
      YB=YS*P
      RB=RI+RS*P
      RR=XB*XB+YB*YB
      U=R-RB
      D=SQRT(RR+U*U)
      T=D1+D2*P+SD2*D
      G1=ALOG(T*T)/(2.*SD2)
      G2=(D-D1*G1)/D2
      IF(XI .EQ. 0. .AND. P .EQ. 0.)GO TO 20
      IF(XI .EQ. 0.)GO TO 30
      IF(ISEL .EQ. 0)GO TO 40
      G3=ATAN(2.*(T*(SD2+RS)-FN2)/SQ)-ATAN(2.*(T*(SD2-RS)+FN2)/SQ)
      G3=4.*SD2*G3/SQ
      G4=(ALOG((D-U)/(D+U))-2.*RS*G1-R1*G3)/R2
      G5=(-R0*G3-2.*R1*G4+2.*(R-RI)*G1-2.*RS*G2)/R2
```

```
      G6=(8.*SD2*FN3*(SD2*D-RS*U)/(T*RR)+8.*SD2*FN2*U/RR
     1+4.*D2*FN2*G3)/Q
      G7=(-2.*D/RR-R1*G6-RS*G3)/R2
      G8=(-R0*G6-2.*R1*G7+2.*G1+2.*(R-RI)*G3-2.*RS*G4)/R2
      G9=(-R0*G7-2.*R1*G8+2.*G2+2.*(R-RI)*G4-2.*RS*G5)/R2
      F1(I)=(2.*G1+(R-RI)*G3-RS*G4-YS*YS*G6)/2.
      F2(I)=(2.*G2+(R-RI)*G4-RS*G5-YS*YS*G9)/2.
      G10=2.*ATAN((2.*(SD2-RS)*T+2.*FN2)/SQ)/SQ
      G11=ALOG(ABS((SD2-RS)*T*T+2.*FN2*T-(SD2+RS)*FN3))
      G12=(-2.*R1*SD2*G10+G11-(SD2-RS)*G1)/R2
      G13=(P+2.*R0*(XS*XS-YS*YS)*SD2*G10/R2-2.*R1*G11/R2
     1+(2.*R1*D2-(SD2+RS)*FN2)*G1/(D2*(SD2+RS))+RS*D/D2)/R2
      F3(I)=P*ALOG(D+U)-R1*G12-XS*XS*G13+RS*G2
      GO TO 10
 40   F1(I)=RS*YS*(YS*D+SD2*YB)/(R2*SD2*T*D)-XS*XB*
     1(RS*D-SD2*U)/(R2*T*RR)-YS*YB*U*(1.-R1/T)/(U*R2*RR)
      F2(I)=0.
      F3(I)=0.
      GO TO 10
 30   IF(ISEL .EQ. 0)GO TO 50
      G14=(T-D1-SD2*ABS(R-RI))/(T-D1+SD2*ABS(R-RI))
      G14=ALOG(G14*G14)/2.
      F1(I)=(XS*XS-YS*YS)*(-D/P+D2*G1+D1*G14/ABS(R-RI))/(R2*R2)
     1+YS*YS*G1/R2
      F2(I)=(XS*XS-YS*YS)*(D+ABS(R-RI)*G14+D1*G1)/(R2*R2)
     1+YS*YS*G2/R2
      G15=(P+RS*D/D2)/R2-(R-RI)*G1/D2
      F3(I)=P*ALOG(D+U)-XS*XS*G15+RS*G2
      GO TO 10
 50   F1(I)=(XS*XS-YS*YS)*D/(R2*R2*(R-RI)*P)
     1+YS*YS*P/(R2*(R-RI)*D)
      F2(I)=0.
      F3(I)=0.
      GO TO 10
 20   IF(ISEL .EQ. 0)GO TO 60
      G16=ALOG(T/(2.*U*U))
      F1(I)=(XS*XS-YS*YS)*(D2*G1-D1*(1.-G16)/ABS(U))/(R2*R2)
     1+YS*YS*G1/R2
      F2(I)=(XS*XS-YS*YS)*(D1*G1+ABS(U)*(1.+G16))/(R2*R2)
     1+YS*YS*G2/R2
      G17=RS*D/(R2*D2)-U*G1/D2
      F3(I)=-XS*XS*G17+RS*G2
      GO TO 10
 60   F1(I)=-(XS*XS-YS*YS)*RS/(R2*R2*ABS(U))
      F2(I)=0.
      F3(I)=0.
 10   CONTINUE
      T1=F1(2)-F1(1)
      T2=F2(2)-F2(1)
      T3=F3(2)-F3(1)
      RETURN
      END
      SUBROUTINE TABSCH(X,N,XT,I1,I2,INT)
C
C  GIVEN AN ARRAY X, TO LOCATE THE POSITION OF A VALUE XT.
C  IF INT=0, XT LIES BETWEEN X(I1) AND X(I2).
C  IF INT=1, XT IS GREATER THAN X(N).
C  IF INT=-1, XT IS LESS THAN X(1).
C
      DIMENSION X(N)
```

```
      I1=0
      I2=0
      NM=N-1
      DO 10 I=1,NM
      IF(XT .GE. X(I) .AND. XT .LE. X(I+1))GO TO 20
   10 CONTINUE
      IF(XT .LT. X(1))GO TO 30
      IF(XT .GT. X(N))GO TO 40
   20 INT=0
      IF(XT .EQ. X(I))GO TO 21
      IF(XT .EQ. X(I+1))GO TO 22
      I1=I
      I2=I+1
      RETURN
   21 I1=I2=I
      RETURN
   22 I1=I2=I+1
      RETURN
   30 INT=-1
      RETURN
   40 INT=1
      RETURN
      END
```

1. Report No.	2. Government Accession No.	3. Recipient's Catalog No.
NASA CR-166093		

4. Title and Subtitle	5. Report Date
HELICOPTER ROTOR LOADS USING MATCHED ASYMPTOTIC EXPANSIONS: USER'S MANUAL	May 1983
	6. Performing Organization Code
7. Author(s)	8. Performing Organization Report No.
G. Alvin Pierce and Anand R. Vaidyanathan	
	10. Work Unit No.
9. Performing Organization Name and Address	11. Contract or Grant No.
Georgia Institute of Technology School of Aerospace Engineering Atlanta, Georgia 30332	NAS1-16817
	13. Type of Report and Period Covered
12. Sponsoring Agency Name and Address	Final Report
National Aeronautics and Space Adminstration Washington, DC 20546	14. Sponsoring Agency Code

15. Supplementary Notes

The contract research effort which led to the results in this report was financially supported by the Structures Laboratory, USARTL (AVRADCOM).
Langley Technical Monitor: John D. Berry Final Report

16. Abstract

Computer programs have been developed to implement the computational scheme arising from Van Holten's asymptotic method for calculating airloads on a helicopter rotor blade in forward flight, and a similar technique which is based on a discretized version of the method. The basic outlines of the two programs are presented, followed by separate descriptions of the input requirements and output format. Two examples illustrating job entry with appropriate input data and corresponding output are included. Appendices contain a sample table of lift coefficient data for the NACA 0012 airfoil and listings of the two programs.

17. Key Words (Suggested by Author(s))	18. Distribution Statement
Unsteady airloads, Helicopter rotor, Potential flow, Asymptotic expansion	Unclassified - Unlimited Subject Category 02

19. Security Classif. (of this report)	20. Security Classif. (of this page)	21. No. of Pages	22. Price
Unclassified	Unclassified	92	

For sale by the National Technical Information Service, Springfield, Virginia 22161